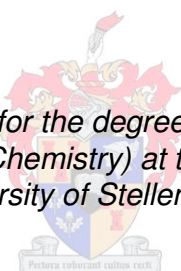


# Chemical characterisation of the aroma of honeybush (*Cyclopia*) species

by  
Joan Christel Cronje

*Dissertation presented for the degree of Doctor of Philosophy  
(Chemistry) at the  
University of Stellenbosch*



Promoter: Dr. Maritha le Roux  
Co-promoter: Prof. B.V. Burger  
Faculty of Science  
Department of Chemistry and Polymer Science

December 2010

# Declaration

By submitting this thesis/dissertation electronically, I declare that the entirety of the work contained therein is my own, original work, and that I have not previously in its entirety or in part submitted it for obtaining any qualification.

December 2010

.....

## ABSTRACT

Honeybush tea, also known as “South Africa’s sweetest tea”, is a herbal tea made from the leaves and twigs of *Cyclopia* spp., indigenous to the fynbos biome in the Western and Eastern Cape provinces of South Africa. The pleasant sweet aroma and taste of fermented honeybush, its low tannin content and the absence of caffeine have led to widespread interest in the commercial cultivation and processing of honeybush tea since the mid-1990s. Although more than 20 species of honeybush grow in the wild, only a few species are commercially exploited for the manufacture of tea. Currently the more prominent species are *C. intermedia*, *C. subternata*, *C. genistoides*, and *C. sessiliflora*. The present research contributes to a comprehensive honeybush research programme being conducted at the Agricultural Research Council (ARC) Infruitec-Nietvoorbij in South Africa.

The first phase of the present study, using *C. genistoides* as representative species, was aimed at developing the necessary methodology for the analysis of extremely low concentrations of honeybush volatiles. A high-capacity headspace sample enrichment probe was applied successfully in conjunction with gas chromatography-mass spectrometry (GC-MS) to analyse the volatile organic compounds present in dry or infused unfermented and fermented honeybush.

A total number of 255 volatile compounds were identified in unfermented and fermented honeybush, the majority of which are terpenoids (138; 54%) comprising mostly terpenes, terpene ketones, terpene alcohols and terpene ethers. Of the other compound classes, the aldehydes are the largest group, followed by esters, hydrocarbons and ketones. The stereochemistry of the identified compounds was determined whenever possible. This is the most comprehensive chemical characterisation of the volatile compounds in a South African herbal plant reported to date.

A comparative study of green and fermented honeybush showed that the same compounds are, to a large extent, present in both, albeit in different relative concentrations.

Not all of the identified honeybush volatiles are necessarily odour-active compounds contributing to the overall typical honeybush aroma. An important aspect of this research was thus the identification of the 46 odour-active compounds in fermented honeybush by means of gas chromatography-olfactometry (GC-O), using detection frequency and aroma extract dilution analysis methods. Fifteen of these compounds, mainly terpenoids, were singled out as the most intense individual contributors to the honeybush aroma based on consideration of all the relevant GC-O data. The odours of certain compounds, i.e. (6*E*,8*Z*)-megastigma-4,6,8-trien-3-one, (6*E*,8*E*)-megastigma-4,6,8-trien-3-one, (7*E*)-megastigma-5,7,9-trien-4-one, 10-*epi*- $\gamma$ -eudesmol, *epi*- $\alpha$ -muurolol and *epi*- $\alpha$ -cadinol, were perceived by GC-O assessors as typically honeybush-like.

The quantitative GC-MS data of seven different *Cyclopia* samples (including four different species and variants thereof) were compared with respect to all the volatile components and particularly with respect to the odour-active compounds. Interesting variations were found in the concentrations of certain odour-active compounds in the various samples.

The quantitative data obtained for the odour-active honeybush volatiles and data obtained from the sensory analysis of eight *Cyclopia* samples (including four different species and variants thereof)

were subjected to statistical analysis and interesting associations between compounds with certain sensory aroma attributes were established.

The present study has made a major contribution to the scientific knowledge regarding one of South Africa's most popular indigenous herbal teas.

## OPSOMMING

Heuningbostee, wat ook bekend staan as “Suid-Afrika se soetste tee”, word gemaak van die blare en takkies van *Cyclopia* spp. wat inheems is en voorkom in die fynbosbloom van die Wes- en Oos-Kaapprovinsies van Suid-Afrika. Die aangename soet smaak en aroma van gefermenteerde heuningbos, die lae tannien-inhoud en die feit dat die tee kafeïenvry is, het gelei tot belangstelling in die kommersiële verbouing en prosessering van heuningbostee gedurende die 1990s. Meer as 20 heuningbosspesies kom in die natuur voor, maar slegs ‘n paar spesies word kommersieel verbou vir die vervaardiging van heuningbostee waarvan *C. intermedia*, *C. subternata*, *C. genistoides* en *C. sessiliflora* tans die belangrikste spesies is. Die navorsing maak deel uit van ‘n omvattende heuningbos navorsingsprogram wat onder leiding staan van die Landbounavorsingsraad Infruitec-Nietvoorbij in Suid-Afrika.

In die eerste fase van die huidige studie is die nodige analitiese metodologie ontwikkel vir die monsterneming en analise van die vlugtige organiese verbindings wat in uiters lae konsentrasies in heuningbos voorkom, deur van ‘n verteenwoordigende spesie, *C. genistoides*, gebruik te maak. ‘n Sogenaamde “sample enrichment probe” (SEP) is ontwikkel en suksesvol in kombinasie met gaschromatografie-massaspektrometrie (GC-MS) aangewend vir die analise van die vlugtige verbindings aanwesig in die bodamp van sowel droë plantmateriaal as infusies van ongefermenteerde en gefermenteerde heuningbos.

‘n Totaal van 255 vlugtige verbindings is geïdentifiseer, waarvan die meeste hoofsaaklik terpenoïede is (138, 54%) en terpenoïede, terpeenketone, terpeenalkohole en terpeeneters insluit. Die ander verbindingsgroepe, waarvan die aldehyede die grootste groep is, sluit in esters, koolwaterstowwe en ketone. Indien haalbaar, is die stereochemie van die geïdentifiseerde verbindings ook bepaal. Hierdie studie is die mees omvattende chemiese karakterisering van die vlugtige verbindings in ‘n Suid-Afrikaanse kruieplant wat tot dusver onderneem is.

‘n Vergelykende studie het getoon dat ongefermenteerde en gefermenteerde heuningbos tot ‘n groot mate dieselfde verbindings, hoewel in verskillende relatiewe konsentrasies, bevat.

Nie al die geïdentifiseerde vlugtige verbindings in heuningbos is noodwendig aroma-aktiewe verbindings wat ‘n bydrae tot die algehele tipiese heuningbosaroma lewer nie en daarom was die identifisering van die 46 aroma-aktiewe verbindings in gefermenteerde heuningbos deur gebruik te maak van gaschromatografie-olfaktometrie (GC-O) deur middel van deteksiefrekwensie en aroma ekstrak verdunningsanalise, ‘n belangrike aspek van die navorsing. Na oorweging van al die tersaaklike GC-O data is 15 van hierdie verbindings, hoofsaaklik terpenoïede, uitgesonder as die verbindings wat die belangrikste bydrae tot die heuningbosaroma lewer. Die reuke van sekere van die verbindings, nl. (6*E*,8*Z*)-megastigma-4,6,8-triën-3-oon, (6*E*,8*E*)-megastigma-4,6,8-triën-3-oon, (7*E*)-megastigma-5,7,9-triën-4-oon, 10-*epi*- $\gamma$ -eudesmol, *epi*- $\alpha$ -muurolol, en *epi*- $\alpha$ -cadinol, is deur sommige van die GC-O paneellede as tipies heuningbosagtig beskryf.

Die kwantitatiewe GC-MS data van sewe verskillende *Cyclopia* monsters (insluitende vier verskillende spesies en variante daarvan) is vergelyk met betrekking tot al die vlugtige verbindings,

asook veral met betrekking tot die aroma-aktiewe verbindings. Interessante variasies in die konsentrasies van sekere aroma-aktiewe verbindings is in die verskillende monsters waargeneem.

Die kwantitatiewe data van die aroma-aktiewe heuningbosverbindings en data verkry uit die sensoriese analise van agt *Cyclopia* monsters (insluitende vier verskillende spesies en variante daarvan), is onderwerp aan statistiese analises waaruit interessante assosiasies tussen verbindings met sekere sensoriese aroma-eienskappe waargeneem is.

Hierdie studie lewer 'n groot bydrae tot die wetenskaplike kennis aangaande een van Suid-Afrika se mees populêre inheemse kruietees.

## ACKNOWLEDGEMENTS

I would like to sincerely thank the following people for the very important part they played in helping me to complete this study.

- My supervisor, dr. le Roux for all her guidance and assistance during this study; for all her kindness, motivation and for her friendship over the past few years.
- My co-supervisor, prof. Burger for whom I have great admiration—for all prof's help, guidance and advice.
- To my good friend, Marlize. Thank you for your friendship over these past few years—it was an honor and privilege to share the lab with you.
- To Dr. Lizette Joubert for providing me with all the honeybush samples used in the study and for her input and advice during the writing of the thesis.
- To dr. Nina Muller for all her assistance and help with the sensory tests as well as with the interpretation of the statistical data and advice during the writing of the thesis.
- To Me Booyse who did the all the statistical processing.
- To the dr. Ferreira, Prof Green and dr. De Villiers for proofreading my script.
- To my whole family, especially my mom and dad for all the years of support; for believing in me and always encouraging me to be the best I can be—I would not have come this far without all your support and love.
- My heavenly Father for always being at my side and giving me the strength to see this through—in my own strength I would not have been able to accomplish this.

# CONTENTS

DECLARATION	2
ABSTRACT	3
OPSOMMING	5
ACKNOWLEDGEMENTS	7
TABLE OF CONTENTS	9
LIST OF FIGURES	17
LIST OF TABLES	29
ABBREVIATIONS	30



## CHAPTER 1

### INTRODUCTION AND OBJECTIVES

1.1 HONEYBUSH	32
1.1.1 Introduction	32
1.1.2 Botanical description and geographical distribution	32
1.1.3 The honeybush industry	35
1.1.4 Honeybush processing	35
1.1.5 Chemical composition	36
1.1.6 Biological properties	37
1.1.6.1 Antioxidant properties of honeybush extracts and individual polyphenolic compounds	37
1.1.6.2 Antimutagenic/anticancer properties	37
1.1.6.3 Phyto-oestrogenic properties	38
1.1.6.4 Antimicrobial and antiviral properties	38
1.2 AROMA COMPOUNDS IN NATURAL PRODUCTS	38
1.2.1 The importance of smell	38
1.2.2 General overview of aroma compounds	39
1.2.3 Terpenoids	40
1.2.3.1 Introduction to terpenoids	40
1.2.3.2 The role of terpenoids in nature	46
1.2.3.3 Uses of terpenoids	48
1.3 OBJECTIVES	48
1.4 REFERENCES	49

## CHAPTER 2

### SELECTION OF APPROPRIATE ANALYTICAL METHODS

2.1	SAMPLE PREPARATION AND SAMPLING METHODS	54
2.1.1	Sampling of honeybush infusions vs dry plant material	54
2.1.2	Enrichment of headspace volatiles by a sample enrichment probe technique	55
2.1.3	Increased-capacity sample enrichment probe extraction technique	57
2.1.4	Conventional sample extraction	60
2.2	ANALYTICAL TECHNIQUES	61
2.2.1	Gas chromatography-mass spectrometry	61
2.2.2	Gas chromatography-high-resolution mass spectrometry	62
2.2.3	Enantioselective gas chromatography-mass spectrometry	62
2.2.4	Gas chromatography-olfactometry and gas chromatography-mass spectrometry-olfactometry	62
2.3	REFERENCES	64

## CHAPTER 3

### CHEMICAL CHARACTERISATION OF THE VOLATILE COMPOUNDS PRESENT IN HONEYBUSH (*Cyclopia*)

3.1	IDENTIFICATION METHODS	66
3.2	STRUCTURE DETERMINATION OF HONEYBUSH VOLATILES	67
3.2.1	Saturated and unsaturated aliphatic hydrocarbons	67
3.2.2	Aromatic hydrocarbons	69
3.2.3	Saturated and unsaturated aliphatic alcohols	71

3.2.4	Phenols	73
3.2.5	Saturated and unsaturated aliphatic aldehydes	73
3.2.6	Aromatic aldehydes	76
3.2.7	Furans	78
3.2.8	Saturated and unsaturated aliphatic carboxylic acids	81
3.2.9	Saturated and unsaturated aliphatic ketones	82
3.2.10	Ketones with an aromatic moiety	87
3.2.11	Saturated and unsaturated aliphatic esters	88
3.2.12	Aromatic esters	92
3.2.13	Saturated and unsaturated lactones	93
3.2.14	Ethers	97
3.2.15	Other compounds	98
3.2.16	Terpenoids	100
3.2.16.1	Terpenes	100
3.2.16.2	Terpene alcohols	114
3.2.16.3	Terpene aldehydes	125
3.2.16.4	Terpene ketones	128
3.2.16.5	Terpene esters	144
3.2.16.6	Terpene ethers	146
3.2.16.7	Terpene lactones	157
3.2.17	Unidentified compounds	158
<b>3.3</b>	<b>SUMMARY</b>	<b>165</b>
<b>3.4</b>	<b>REFERENCES</b>	<b>253</b>

## CHAPTER 4

# OLFACTOMETRY: IDENTIFICATION OF THE ODOUR-ACTIVE COMPOUNDS PRESENT IN THE AROMA OF FERMENTED HONEYBUSH

4.1	GAS CHROMATOGRAPHY-OLFACTOMETRY	259
4.1.1	Detection frequency	260
4.1.2	Dilution to threshold: Aroma extract dilution analysis	261
4.1.3	Direct intensity methods	262
4.2	IDENTIFICATION OF ODOUR-ACTIVE HONEYBUSH VOLATILES	263
4.3	REFERENCES	271

## CHAPTER 5

# QUANTITATIVE ANALYSIS OF THE COMPOUNDS PRESENT IN HONEYBUSH

5.1	QUANTITATIVE METHODS	276
5.1.1	Relative quantification	276
5.1.2	Absolute quantification	276
5.2	COMPARATIVE STUDIES	276
5.2.1	Green (unfermented) vs fermented honeybush	276
5.2.2	Comparison of seven <i>Cyclopia</i> samples	289
5.3	REFERENCES	304

## CHAPTER 6

### SENSORY AROMA ATTRIBUTES OF HONEYBUSH TEA

6.1	INTRODUCTION	306
6.2	RESULTS AND DISCUSSION	307
6.2.1	Sensory aroma attributes of honeybush tea, using univariate analyses	307
6.2.1.1	Honeybush aroma	309
6.2.1.2	Sweet aroma	309
6.2.1.3	Plant-like, rooibos, lemon and Earl Grey aroma	309
6.2.2	Sensory aroma attributes of honeybush tea, using multivariate analyses	310
6.3	SUMMARY	312
6.4	REFERENCES	313

## CHAPTER 7

### STATISTICAL DATA ANALYSIS: CORRELATION OF CHEMICAL AND SENSORY DATA OF HONEYBUSH SAMPLES

7.1	INTRODUCTION	314
7.2	PRINCIPAL COMPONENT ANALYSIS OF HONEYBUSH DATA	314
7.2.1	Principal component analysis based on concentration data	314
7.2.2	Principal component analysis based on combined concentration and sensory data	316
7.2.3	Principal component analysis based on combined 'odour-activity value' and sensory data	324
7.3	SUMMARY	325

7.4 REFERENCES	326
----------------	-----

## CHAPTER 8

### EXPERIMENTAL

8.1 GENERAL	328
8.2 SAMPLE PREPARATION METHODS	328
8.2.1 Collection, fermentation and drying of honeybush plant material	328
8.2.2 Preparation of honeybush infusions	329
8.3 SAMPLING METHODS	329
8.3.1 Enrichment of headspace volatiles by the sample enrichment probe technique	329
8.3.1.1 Sample enrichment probe sampling of dry honeybush plant material	329
8.3.1.2 Sample enrichment probe sampling of honeybush infusions	330
8.3.2 Increased-capacity sample enrichment probe	330
8.3.3 Conventional sample extraction	330
8.4 ANALYTICAL TECHNIQUES	331
8.4.1 Gas chromatography	331
8.4.2 Gas chromatography-mass spectrometry	331
8.4.3 Gas chromatography-time-of-flight-high-resolution mass spectrometry	332
8.4.4 Enantioselective gas chromatographic-mass spectrometric analyses with $\beta$ -cyclodextrin columns as chiral selectors	332
8.4.5 Gas chromatographic-mass spectrometric retention index determination	332
8.4.6 Quantitative gas chromatography and gas chromatography-mass spectrometry	332

8.4.7	Gas chromatography-olfactometry	335
8.4.7.1	Detection frequency method	336
8.4.7.2	Dilution to threshold method: aroma extract dilution analysis	336
8.4.8	Gas chromatography-mass spectrometry-olfactometry	336
8.4.9	Nuclear magnetic resonance spectrometry	337
<b>8.5</b>	<b>REFERENCE COMPOUNDS</b>	<b>337</b>
8.5.1	Commercial standards	337
8.5.2	Synthetic standards	337
8.5.2.1	2,6,6-Trimethylcyclohex-2-enone	337
a.	<i>2-Bromo-2,6,6-trimethylcyclohexanone</i>	337
b.	<i>2,6,6-Trimethylcyclohex-2-enone</i>	338
8.5.2.2	( <i>E,E</i> )- and ( <i>Z,E</i> )-3,5-Octadien-2-one	338
8.5.2.3	5,6-Epoxy- $\beta$ -ionone	338
8.5.2.4	Hexyl tiglate	339
8.5.2.5	Benzyl tiglate	339
8.5.2.6	3,4-Dehydro- $\beta$ -ionone	340
8.5.2.7	Octan-5-olide	341
8.5.2.8	Hexahydrofarnesylacetone	341
8.5.2.9	Nerol oxide	342
8.5.2.10	(+)- <i>p</i> -Menth-1-en-9-al	343
8.5.2.11	<i>cis</i> - and <i>trans</i> -Dehydroxy linalool oxide	343
<b>8.6</b>	<b>SENSORY ANALYSIS</b>	<b>344</b>
<b>8.7</b>	<b>STATISTICAL METHODS</b>	<b>345</b>
8.7.1	Univariate analysis of data	345
8.7.2	Multivariate statistical techniques	345
<b>8.8</b>	<b>REFERENCES</b>	<b>346</b>
	<b>ADDENDUM 1</b>	<b>348</b>

## CHAPTER 9

### CONCLUSION

9.1 SUMMARY OF RESULTS	349
9.2 RECOMMENDATIONS	350



## LIST OF FIGURES

Fig. 1.1:	<i>Cyclopia subternata</i> (top left), <i>C. genistoides</i> (top right) and <i>C. intermedia</i> bushes.	33
Fig. 1.2:	The flat-leaved shape of the leaves of <i>C. intermedia</i> (left) and <i>C. subternata</i> (middle), compared with the narrow-leaved shape of <i>C. genistoides</i> (right).	33
Fig. 1.3:	Production area of rooibos tea ( <i>Aspalathus linearis</i> ) and natural distribution of <i>Cyclopia</i> species and bush tea ( <i>Athrixia phylicoides</i> ). Key: (1) <i>Cyclopia genistoides</i> ; (2) <i>Cyclopia sessiliflora</i> ; (3) <i>Cyclopia subternata</i> ; (4) <i>Cyclopia intermedia</i> ; (5) <i>Aspalathus linearis</i> ; (6) <i>Athrixia phylicoides</i> (Map supplied by ARC Infruitec-Nietvoorbij; Joubert <i>et al.</i> 2008a).	34
Fig. 2.1:	SEP installed in GC injector cap.	56
Fig. 2.2:	SEP installed for sampling headspace volatiles from dry, fermented honeybush.	56
Fig. 2.3:	Volatile compounds in dry, fermented honeybush analysed by HS- <b>SPME</b> -GC-MS.	57
Fig. 2.4:	Volatile compounds in dry, fermented honeybush analysed by HS- <b>SEP</b> -GC-MS.	57
Fig. 2.5:	High-capacity sample enrichment device comprising coiled PDMS tubing (left) and installed for sampling headspace volatiles from dry fermented honeybush material (right).	58
Fig. 2.6:	TIC of VOCs extracted from the headspace of a standard honeybush infusion over a period of 42 h by means of a high-capacity SEP.	58
Fig. 2.7:	TIC of VOCs extracted from the headspace of dry honeybush plant material over a period of 48 h by means of a high-capacity SEP.	59
Fig. 2.8:	TIC of VOCs extracted from the headspace of dry, finely ground honeybush plant material over a period of five days by means of a high-capacity SEP.	59
Fig. 2.9:	TIC obtained by GC-MS analysis of a DCM extract of dry honeybush plant material.	60
Fig. 2.10:	TIC obtained by HS-SEP-GC-MS analysis of unfermented honeybush infusion.	61

Fig. 2.11:	TIC obtained by HS-SEP-GC-MS analysis of fermented honeybush infusion.	61
Fig. 2.12:	Evaluator assessing the column effluent at the sniffing port of the GC-O apparatus.	63
Fig. 3.1:	TIC obtained by HS-SEP-GC-MS analysis of unfermented honeybush.	178
Fig. 3.2a:	TIC obtained by HS-SEP-GC-MS analysis of fermented honeybush (0–25 min).	178
Fig. 3.2b:	TIC obtained by HS-SEP-GC-MS analysis of fermented honeybush (25–32 min).	179
Fig. 3.2c:	TIC obtained by HS-SEP-GC-MS analysis of fermented honeybush (32–34.8 min).	179
Fig 3.2d:	TIC obtained by HS-SEP-GC-MS analysis of fermented honeybush (34.8–37 min).	179
Fig. 3.2e:	TIC obtained by HS-SEP-GC-MS analysis of fermented honeybush (37–51 min).	180
Fig. 3.2f:	TIC obtained by HS-SEP-GC-MS analysis of fermented honeybush (51–75min).	180
Fig. 3.3:	EI mass spectrum of undecane ( <b>C80</b> ).	181
Fig. 3.4:	EI mass spectrum of 5,5-dimethyl-2-ethyl-1,3-cyclopentadiene ( <b>C7</b> ).	181
Fig. 3.5:	EI mass spectrum of 1,3,6-octatriene ( <b>C12</b> ).	181
Fig. 3.6:	EI mass spectrum of 2,8-dimethyl-2,6-nonadiene ( <b>C67</b> ).	182
Fig. 3.7:	EI mass spectrum of 1,5,8-trimethyl-1,2-dihydronaphthalene ( <b>C189</b> ).	182
Fig. 3.8:	EI mass spectrum of 2,3-dihydro-1,1,5,6-tetramethyl-1 <i>H</i> -indene ( <b>C192</b> ).	182
Fig. 3.9:	EI mass spectrum of 2-(2-butenyl)-1,3,5-trimethylbenzene ( <b>C147</b> ).	183
Fig. 3.10:	EI mass spectrum of 1,3-dimethylnaphthalene ( <b>C213</b> ).	183
Fig. 3.11:	EI mass spectrum of 1-octanol ( <b>C65</b> ).	183
Fig. 3.12:	EI mass spectrum of ( <i>Z</i> )-2-penten-1-ol ( <b>C5</b> ).	184
Fig. 3.13:	EI mass spectrum of ( <i>Z</i> )-3-hexen-1-ol ( <b>C9</b> ).	184

Fig. 3.14:	El mass spectrum of 1-octen-3-ol ( <b>C31</b> ).	184
Fig. 3.15:	El mass spectrum of ( <i>E</i> )-2-decen-1-ol ( <b>C153</b> ).	185
Fig. 3.16:	El mass spectrum of benzyl alcohol ( <b>C55</b> ).	185
Fig. 3.17:	El mass spectrum of 2-phenylethanol ( <b>C79</b> ).	185
Fig. 3.18:	El mass spectrum of eugenol ( <b>C191</b> ).	186
Fig. 3.19:	El mass spectrum of hexanal ( <b>C6</b> ).	186
Fig. 3.20:	El mass spectrum of decanal ( <b>C124</b> ).	186
Fig. 3.21:	El mass spectrum of ( <i>E</i> )-2-nonenal ( <b>C108</b> ).	187
Fig. 3.22:	El mass spectrum of ( <i>Z</i> )-4-heptenal ( <b>C15</b> ).	187
Fig. 3.23:	El mass spectrum of 2-butyl-2-octenal ( <b>C202</b> ).	187
Fig. 3.24:	El mass spectrum of ( <i>E,E</i> )-2,4-heptadienal ( <b>C41</b> ).	188
Fig. 3.25:	El mass spectrum of ( <i>E,E</i> )-2,4-decadienal ( <b>C171</b> ).	188
Fig. 3.26:	El mass spectrum of ( <i>E,Z</i> )-2,6-nonadienal ( <b>C101</b> ).	188
Fig. 3.27:	El mass spectrum of ( <i>E,E,E</i> )-2,4,6-nonatrienal ( <b>C155</b> ).	189
Fig. 3.28:	El mass spectrum of benzaldehyde ( <b>C25</b> ).	189
Fig. 3.29:	El mass spectrum of <i>p</i> -anisaldehyde ( <b>C141</b> ).	189
Fig. 3.30:	El mass spectrum of a dimethylbenzaldehyde ( <b>C114</b> ).	190
Fig. 3.31:	El mass spectrum of 2,3,4-trimethylbenzaldehyde ( <b>C166</b> ).	190
Fig. 3.32:	El mass spectrum of 2-pentylfuran ( <b>C35</b> ).	190
Fig. 3.33:	El mass spectrum of (2 <i>Z</i> )-2-(2-pentenyl)furan ( <b>C40</b> ).	191
Fig. 3.34:	El mass spectrum of 2-acetylfuran ( <b>C19</b> ).	191
Fig. 3.35:	El mass spectrum of 6-methyl-(5-methylfuran-2-yl)heptan-2-one ( <b>C215</b> ).	191
Fig. 3.36:	El mass spectrum of 5-methyl-2-furancarboxaldehyde ( <b>C28</b> ).	192
Fig. 3.37:	El mass spectrum of 5-methoxy-6,7-dimethylbenzofuran ( <b>C223</b> ).	192

Fig. 3.38:	El mass spectrum of 3-methylbutanoic acid ( <b>C11</b> ).	192
Fig. 3.39:	El mass spectrum of ( <i>R</i> )-2-methylbutanoic acid ( <b>C13</b> ).	193
Fig. 3.40:	El mass spectrum of nonanoic acid ( <b>C159</b> ).	193
Fig. 3.41:	El mass spectrum of tiglic acid ( <b>C20</b> ).	193
Fig. 3.42:	El mass spectrum of 6-methyl-2-heptanone ( <b>C27</b> ).	194
Fig. 3.43:	El mass spectrum of 6-methyl-5-hepten-2-one ( <b>C32</b> ).	194
Fig. 3.44:	El mass spectrum of ( <i>E</i> )-3-octen-2-one ( <b>C53</b> ).	194
Fig. 3.45:	El mass spectrum of ( <i>E</i> )-3-nonen-2-one ( <b>C95</b> ).	195
Fig. 3.46:	El mass spectrum of 3,5,7-nonatrien-2-one ( <b>C145</b> ).	195
Fig. 3.47:	El mass spectrum of ( <i>Z,E</i> )-3,5-octadien-2-one ( <b>C63</b> ).	195
Fig. 3.48:	El mass spectrum of (3 <i>E</i> )-6-methyl-3,5-heptadien-2-one ( <b>C74</b> ).	196
Fig. 3.49:	El mass spectrum of 3,4,4-trimethyl-2-cyclopenten-1-one ( <b>C81</b> ).	196
Fig. 3.50:	El mass spectrum of 4,8-dimethyl-3,7-nonadien-2-one ( <b>C154</b> ).	196
Fig. 3.51:	El mass spectrum of acetophenone ( <b>C60</b> ).	197
Fig. 3.52:	El mass spectrum of 1-(2,3,6-trimethylphenyl)-3-buten-2-one ( <b>C273</b> ).	197
Fig. 3.53:	El mass spectrum of methyl hexanoate ( <b>C22</b> ).	197
Fig. 3.54:	El mass spectrum of pentyl acetate ( <b>C21</b> ).	198
Fig. 3.55:	El mass spectrum of phenylmethyl acetate ( <b>C109</b> ).	198
Fig. 3.56:	El mass spectrum of 2-phenylethyl acetate ( <b>C142</b> ).	198
Fig. 3.57:	El mass spectrum of isopropyl myristate ( <b>C298</b> ).	199
Fig. 3.58:	El mass spectrum of 3-hydroxy-2,4,4-trimethylpentyl 2-methylpropa- noate ( <b>C201</b> ).	199
Fig. 3.59:	El mass spectrum of ( <i>Z</i> )-3-hexenyl isovalerate ( <b>C140</b> ).	199
Fig. 3.60:	El mass spectrum of ( <i>Z</i> )-3-hexenyl ( <i>E</i> )-2-methyl-2-butenolate ( <b>C175</b> ).	200
Fig. 3.61:	El mass spectrum of hexyl tiglate ( <b>C179</b> ).	200

Fig. 3.62:	El mass spectrum of benzyl tiglate ( <b>C237</b> ).	200
Fig. 3.63:	El mass spectrum of ( <i>Z</i> )-3-hexenyl benzoate ( <b>C261</b> ).	201
Fig. 3.64:	El mass spectrum of hexyl benzoate ( <b>C263</b> ).	201
Fig. 3.65:	El mass spectrum of $\gamma$ -butyrolactone ( <b>C16</b> ).	201
Fig. 3.66:	El mass spectrum of hexan-4-olide ( <b>C54</b> ).	202
Fig. 3.67:	El mass spectrum of 2-hexen-4-olide ( <b>C49</b> ).	202
Fig. 3.68:	El mass spectrum of nonan-4-olide ( <b>C186</b> ).	202
Fig. 3.69:	El mass spectrum of ( <i>R</i> )-octan-5-olide ( <b>C152</b> ).	203
Fig. 3.70:	El mass spectrum of ( <i>S</i> )-( <i>Z</i> )-7-decen-5-olide ( <b>C229</b> ).	203
Fig. 3.71:	El mass spectrum of bovolide ( <b>C245</b> ).	203
Fig. 3.72:	El mass spectrum of 4-vinylanisole ( <b>C100</b> ).	204
Fig. 3.73:	El mass spectrum of 3,7,7-trimethyl-1-penta-1,3-dienyl-2-oxabicyclo[3.2.0]hept-3-ene ( <b>C291</b> ).	204
Fig. 3.74:	El mass spectrum of benzothiazole ( <b>C127</b> ).	204
Fig. 3.75:	El mass spectrum of <i>N</i> -methyl-2-formylpyrrole ( <b>C37</b> ).	205
Fig. 3.76:	El mass spectrum of 3,4-dimethyl-2,5-furandione ( <b>C48</b> ).	205
Fig. 3.77:	El mass spectrum of 2-ethyl-3-methylmaleimide ( <b>C130</b> ).	205
Fig. 3.78:	El mass spectrum of $\alpha$ -pinene ( <b>C23</b> ).	206
Fig. 3.79:	El mass spectrum of myrcene ( <b>C38</b> ).	206
Fig. 3.80:	El mass spectrum of ( <i>Z</i> )- $\beta$ -ocimene ( <b>C56</b> ).	206
Fig. 3.81:	El mass spectrum of allo-ocimene ( <b>C93</b> ).	207
Fig. 3.82:	El mass spectrum of (6 <i>E</i> )-2,6-dimethyl-2,6-octadiene ( <b>C43</b> ).	207
Fig. 3.83:	El mass spectrum of terpinolene ( <b>C71</b> ).	207
Fig. 3.84:	El mass spectrum of $\gamma$ -terpinene ( <b>C61</b> ).	208
Fig. 3.85:	El mass spectrum of limonene ( <b>C52</b> ).	208

Fig. 3.86:	El mass spectrum of <i>p</i> -cymene ( <b>C50</b> ).	208
Fig. 3.87:	El mass spectrum of <i>p</i> -cymenene ( <b>C69</b> ).	209
Fig. 3.88:	El mass spectrum of $\delta$ -cadinene ( <b>C247</b> ).	209
Fig. 3.89:	El mass spectrum of $\gamma$ -cadinene ( <b>C244</b> ).	209
Fig. 3.90:	El mass spectrum of $\alpha$ -muurolene ( <b>C240</b> ).	210
Fig. 3.91:	El mass spectrum of $\alpha$ -copaene ( <b>C205</b> ).	210
Fig. 3.92:	El mass spectrum of $\beta$ -selinene ( <b>C235</b> ).	210
Fig. 3.93:	El mass spectrum of ( <i>E</i> )-caryophyllene ( <b>C216</b> ).	211
Fig. 3.94:	El mass spectrum of 9- <i>epi</i> -( <i>E</i> )-caryophyllene ( <b>C226</b> ).	211
Fig. 3.95:	El mass spectrum of $\alpha$ -humulene ( <b>C221</b> ).	211
Fig. 3.96:	El mass spectrum of <i>trans</i> -calamenene ( <b>C246</b> ).	212
Fig. 3.97:	El mass spectrum of $\alpha$ -calacorene ( <b>C252</b> ).	212
Fig. 3.98:	El mass spectrum of cadalene ( <b>C290</b> ).	212
Fig. 3.99:	El mass spectrum of $\beta$ -bourbonene ( <b>C208</b> ).	213
Fig. 3.100:	El mass spectrum of 4,6,8-megastigmatriene ( <b>C197</b> ).	213
Fig. 3.101:	El mass spectrum of linalool ( <b>C76</b> ).	213
Fig. 3.102:	El mass spectrum of hotrienol ( <b>C78</b> ).	214
Fig. 3.103:	El mass spectrum of dihydrolinalool ( <b>C94</b> ).	214
Fig. 3.104:	El mass spectrum of ( <i>E</i> )-ocimenol ( <b>C113</b> ).	214
Fig. 3.105:	El mass spectrum of geraniol ( <b>C148</b> ).	215
Fig. 3.106:	El mass spectrum of ( <i>E</i> )-nerolidol ( <b>C260</b> ).	215
Fig. 3.107:	El mass spectrum of ( <i>R</i> )- $\beta$ -citronellol ( <b>C137</b> ).	215
Fig. 3.108:	El mass spectrum of <i>cis-p</i> -2-menthen-1-ol ( <b>C86</b> ).	216
Fig. 3.109:	El mass spectrum of terpinen-4-ol ( <b>C118</b> ).	216
Fig. 3.110:	El mass spectrum of $\alpha$ -terpineol ( <b>C121</b> ).	216

Fig. 3.111:	El mass spectrum of <i>p</i> -cymen-8-ol ( <b>C120</b> ).	217
Fig. 3.112:	El mass spectrum of limonen-10-ol ( <b>C160</b> ).	217
Fig. 3.113:	El mass spectrum of $\alpha$ -fenchol ( <b>C85</b> ).	217
Fig. 3.114:	El mass spectrum of camphene hydrate ( <b>C98</b> ).	218
Fig. 3.115:	El mass spectrum of 2-chloro-1,7,7-trimethylbicyclo[2.2.1]heptane ( <b>C111</b> ).	218
Fig. 3.116:	El mass spectrum of borneol ( <b>C112</b> ).	218
Fig. 3.117:	El mass spectrum of 10- <i>epi</i> - $\gamma$ -eudesmol ( <b>C278</b> ).	219
Fig. 3.118:	El mass spectrum of $\beta$ -eudesmol ( <b>C286</b> ).	219
Fig. 3.119:	El mass spectrum of 7- <i>epi</i> - $\alpha$ -eudesmol ( <b>C289</b> ).	219
Fig. 3.120:	El mass spectrum of <i>epi</i> - $\alpha$ -cadinol ( <b>C284</b> ).	220
Fig. 3.121:	El mass spectrum of <i>epi</i> - $\alpha$ -muurolol ( <b>C285</b> ).	220
Fig. 3.122:	El mass spectrum of <i>epi</i> - $\alpha$ -bisabolol ( <b>C292</b> ).	220
Fig. 3.123:	El mass spectrum of $\beta$ -cyclositral ( <b>C129</b> ).	221
Fig. 3.124:	El mass spectrum of safranal ( <b>C122</b> ).	221
Fig. 3.125:	El mass spectrum of 2,6,6-trimethyl-1-cyclohexene-1-acetaldehyde ( <b>C146</b> ).	221
Fig. 3.126:	El mass spectrum of (+)- <i>p</i> -menth-1-en-9-al ( <b>C125</b> ).	222
Fig. 3.127:	El mass spectrum of neral ( <b>C139</b> ).	222
Fig. 3.128:	El mass spectrum of lilac aldehyde ( <b>C97</b> ).	222
Fig. 3.129:	El mass spectrum of 2,2,6-trimethylcyclohexanone ( <b>C51</b> ).	223
Fig. 3.130:	El mass spectrum of 2,6,6-trimethylcyclohex-2-enone ( <b>C59</b> ).	223
Fig. 3.131:	El mass spectrum of 4-ketoisophorone ( <b>C92</b> ).	223
Fig. 3.132:	El mass spectrum of 2,2,6-trimethyl-1,4-cyclohexanedione ( <b>C104</b> ).	224
Fig. 3.133:	El mass spectrum of 4-acetyl-1-methylcyclohexene ( <b>C89</b> ).	224
Fig. 3.134:	El mass spectrum of 1-(1,4-dimethyl-3-cyclohexen-1-yl)ethanone ( <b>C99</b> ).	224

Fig. 3.135:	El mass spectrum of 3-thujanone ( <b>C84</b> ).	225
Fig. 3.136:	El mass spectrum of carvenone ( <b>C143</b> ).	225
Fig. 3.137:	El mass spectrum of 6,10-dimethyl-2-undecanone ( <b>C209</b> ).	225
Fig. 3.138:	El mass spectrum of geranylacetone ( <b>C220</b> ).	226
Fig. 3.139:	El mass spectrum of ( <i>E,E</i> )-pseudoionone ( <b>C266</b> ).	226
Fig. 3.140:	El mass spectrum of hexahydrofarnesylacetone ( <b>C299</b> ).	226
Fig. 3.141:	El mass spectrum of ( <i>E</i> )- $\beta$ -damascenone ( <b>C204</b> ).	227
Fig. 3.142:	El mass spectrum of ( <i>E</i> )- $\beta$ -ionone ( <b>C234</b> ).	227
Fig. 3.143:	El mass spectrum of ( <i>R</i> )- $\alpha$ -ionone ( <b>C217</b> ).	227
Fig. 3.144:	El mass spectrum of ( <i>E</i> )- $\beta$ -damascone ( <b>C212</b> ).	228
Fig. 3.145:	El mass spectrum of 5,6-epoxy- $\beta$ -ionone ( <b>C232</b> ).	228
Fig. 3.146:	El mass spectrum of 2,3-dehydro- $\alpha$ -ionone ( <b>C203</b> ).	228
Fig. 3.147:	El mass spectrum of 3,4-dehydro- $\gamma$ -ionone ( <b>C218</b> ).	229
Fig. 3.148:	El mass spectrum of 2,3-dehydro- $\gamma$ -ionone ( <b>C222</b> ).	229
Fig. 3.149:	El mass spectrum of 3,4-dehydro- $\beta$ -ionone ( <b>C230</b> ).	229
Fig. 3.150:	El mass spectrum of 4-(2,6,6-trimethyl-1,3-cyclohexadien-1-yl)- 2-butanone ( <b>C214</b> ).	230
Fig. 3.151:	El mass spectrum of $\beta$ -oplophenone ( <b>C274</b> ).	230
Fig. 3.152:	El mass spectrum of (6 <i>Z</i> ,8 <i>E</i> )-megastigma-4,6,8-trien-3-one ( <b>C262</b> ).	230
Fig. 3.153:	El mass spectrum of (6 <i>E</i> ,8 <i>E</i> )-megastigma-4,6,8-trien-3-one ( <b>C277</b> ).	231
Fig. 3.154:	El mass spectrum of (7 <i>E</i> )-megastigma-5,7,9-trien-4-one ( <b>C295</b> ).	231
Fig. 3.155:	El mass spectrum of geranyl formate ( <b>C164</b> ).	231
Fig. 3.156:	El mass spectrum of geranyl acetate ( <b>C206</b> ).	232
Fig. 3.157:	El mass spectrum of $\alpha$ -terpinyl acetate ( <b>C188</b> ).	232
Fig. 3.158:	El mass spectrum of geranyl propanoate ( <b>C228</b> ).	232



Fig. 3.159:	El mass spectrum of 2,6,6-trimethyl-2-vinyltetrahydropyran ( <b>C29</b> ).	233
Fig. 3.160:	El mass spectrum of <i>cis</i> -dehydroxylinalool oxide ( <b>C45</b> ).	233
Fig. 3.161:	El mass spectrum of <i>trans</i> -arbusculone ( <b>C62</b> ).	233
Fig. 3.162:	El mass spectrum of <i>trans</i> -linalool oxide ( <b>C68</b> ).	234
Fig. 3.163:	El mass spectrum of <i>trans</i> -pyranoid linalool oxide ( <b>C116</b> ).	234
Fig. 3.164:	El mass spectrum of <i>cis</i> -rose oxide ( <b>C91</b> ).	234
Fig. 3.165:	El mass spectrum of nerol oxide ( <b>C106</b> ).	235
Fig. 3.166:	El mass spectrum of cabreuva oxide B ( <b>C225</b> ).	235
Fig. 3.167:	El mass spectrum of oxo-edulan ( <b>C227</b> ).	235
Fig. 3.168:	El mass spectrum of dill ether isomer 1 ( <b>C119</b> ).	236
Fig. 3.169:	El mass spectrum of theaspirane isomer 2 ( <b>C173</b> ).	236
Fig. 3.170:	El mass spectrum of vitispirane ( <b>C157</b> ).	236
Fig. 3.171:	El mass spectrum of 2,5,-epoxy-megastigma-6,8-diene ( <b>C182</b> ).	237
Fig. 3.172:	El mass spectrum of calamenene-1,11-epoxide ( <b>C236</b> ).	237
Fig. 3.173:	El mass spectrum of $\beta$ -dihydroagarofuran ( <b>C239</b> ).	237
Fig. 3.174:	El mass spectrum of dihydroagarofuran isomer ( <b>C258</b> ).	238
Fig. 3.175:	El mass spectrum of $\alpha$ -agarofuran ( <b>C253</b> ).	238
Fig. 3.176:	El mass spectrum of dihydroactinidiolide ( <b>C243</b> ).	238
Fig. 3.177:	El mass spectrum of component <b>C66</b> .	239
Fig. 3.178:	El mass spectrum of component <b>C73</b> .	239
Fig. 3.179:	El mass spectrum of component <b>C144</b> .	239
Fig. 3.180:	El mass spectrum of component <b>C151</b> .	240
Fig. 3.181:	El mass spectrum of component <b>C156</b> .	240
Fig. 3.182:	El mass spectrum of component <b>C162</b> .	240
Fig. 3.183:	El mass spectrum of component <b>C168</b> .	241

Fig. 3.184:	El mass spectrum of component <b>C169</b> .	241
Fig. 3.185:	El mass spectrum of component <b>C172</b> .	241
Fig. 3.186:	El mass spectrum of component <b>C178</b> .	242
Fig. 3.187:	El mass spectrum of component <b>C183</b> .	242
Fig. 3.188:	El mass spectrum of component <b>C180</b> .	242
Fig. 3.189:	El mass spectrum of component <b>C207</b> .	243
Fig. 3.190:	El mass spectrum of component <b>C254</b> .	243
Fig. 3.191:	El mass spectrum of component <b>C255</b> .	243
Fig. 3.192:	El mass spectrum of component <b>C267</b> .	244
Fig. 3.193:	El mass spectrum of component <b>C269</b> .	244
Fig. 3.194:	El mass spectrum of component <b>C268</b> .	244
Fig. 3.195:	El mass spectrum of component <b>C275</b> .	245
Fig. 3.196:	El mass spectrum of component <b>C279</b> .	245
Fig. 3.197:	El mass spectrum of component <b>C280</b> .	245
Fig. 3.198:	El mass spectrum of component <b>C282</b> .	246
Fig. 3.199:	El mass spectrum of component <b>C18</b> .	246
Fig. 3.200:	El mass spectrum of component <b>C77</b> .	246
Fig. 3.201:	El mass spectrum of component <b>C87</b> .	247
Fig. 3.202:	El mass spectrum of component <b>C88</b> .	247
Fig. 3.203:	El mass spectrum of component <b>C102</b> .	247
Fig. 3.204:	El mass spectrum of component <b>C117</b> .	248
Fig. 3.205:	El mass spectrum of component <b>C123</b> .	248
Fig. 3.206:	El mass spectrum of component <b>C133</b> .	248
Fig. 3.207:	El mass spectrum of component <b>C134</b> .	249
Fig. 3.208:	El mass spectrum of component <b>C136</b> .	249

Fig. 3.209:	El mass spectrum of components <b>C165</b> and <b>C185</b> .	249
Fig. 3.210:	El mass spectrum of component <b>C174</b> .	250
Fig. 3.211:	El mass spectrum of component <b>C181</b> .	250
Fig. 3.212:	El mass spectrum of component <b>C187</b> .	250
Fig. 3.213:	El mass spectrum of component <b>C224</b> .	251
Fig. 3.214:	El mass spectrum of component <b>C238</b> .	251
Fig. 3.215:	El mass spectrum of component <b>C250</b> .	251
Fig. 3.216:	El mass spectrum of component <b>C251</b> .	252
Fig. 3.217:	El mass spectrum of component <b>C281</b> .	252
Fig. 5.1	Quantitative comparison of the volatile compounds with highest concentrations (area %) present in the headspace of green and fermented <i>Cyclopia intermedia</i> .	287
Fig. 5.2:	Comparison of the concentrations (area %) of the 10 most abundant compounds in the headspace of green (left) and fermented (right) <i>Cyclopia intermedia</i> .	288
Fig. 5.3:	Comparison of the VOCs identified by HS-SEP-GC-MS analysis in seven <i>Cyclopia</i> samples (area % >0.1%).	293
Fig. 5.4a–p:	Comparison of the relative concentrations (area %) of the most intense odour-active compounds identified in seven <i>Cyclopia</i> samples.	296
Fig. 6.1:	Sensory aroma attributes of eight honeybush samples.	308
Fig. 6.2:	Presentation (spider web) of the sensory aroma attributes of eight honeybush samples.	309
Fig. 6.3:	PCA bi-plots indicating the association between sensory aroma attributes (loadings) and products 1–8 (scores): (a) based on overall means, (b) based on product × replicate means. [G(a): <i>C. genistoides</i> (a) (Albertinia); G(b): <i>C. genistoides</i> (b) (Pearly Beach); GxI: <i>C. genistoides</i> × <i>C. intermedia</i> ; I: <i>C. intermedia</i> ; L: <i>C. longifolia</i> ; S(a): <i>C. subternata</i> (a) (Bredasdorp); S(b): <i>C. subternata</i> (b) (Genadendal; – flower); S(c): <i>C. subternata</i> (c) (Genadendal; + flower)].	311

- Fig. 6.4: DA plot indicating the overall discrimination between products using a spectrum of aroma attributes.  
 [G(a): *C. genistoides*(a) (Albertinia); G(b): *C. genistoides*(b) (Pearly Beach); Gxl: *C. genistoides* × *C. intermedia*; I: *C. intermedia*; L: *C. longifolia*; S(a): *C. subternata*(a) (Bredasdorp); S(b): *C. subternata*(b) (Genadendal; – flower); S(c): *C. subternata*(c) (Genadendal; + flower)] 312
- Fig. 7.1: PCA loadings and scores plots of the relative concentrations of the odour-active compounds in eight honeybush samples: (a) loadings plot; (b) scores plot. [G(a): *C. genistoides*(a) (Albertinia); G(b): *C. genistoides*(b) (Pearly Beach); Gxl: *C. genistoides* × *C. intermedia*; I: *C. intermedia*; L: *C. longifolia*; S(a): *C. subternata*(a) (Bredasdorp); S(b): *C. subternata*(b) (Genadendal; – flower); S(c): *C. subternata*(c) (Genadendal; + flower)]. 316
- Fig. 7.2: Loadings plot (a), scores plot (two-dimensional map) (b) and bi-plot (c) resulting from PCA utilising the relative concentrations of the aroma-active compounds and the sensory aroma attributes obtained during sensory analysis of honeybush samples. [G(a): *C. genistoides*(a) (Albertinia); G(b): *C. genistoides*(b) (Pearly Beach); Gxl: *C. genistoides* × *C. intermedia*; I: *C. intermedia*; L: *C. longifolia*; S(a): *C. subternata*(a) (Bredasdorp); S(b): *C. subternata*(b) (Genadendal; – flower); S(c): *C. subternata*(c) (Genadendal; + flower)]. 318
- Fig. 7.3: Loadings plot (a) and scores plot (b) constructed by PCA using the relative 'OAV's and sensory aroma attributes obtained during sensory analysis of honeybush samples. [G(a): *C. genistoides*(a) (Albertinia); G(b): *C. genistoides*(b) (Pearly Beach); Gxl: *C. genistoides* × *C. intermedia*; I: *C. intermedia*; L: *C. longifolia*; S(a): *C. subternata*(a) (Bredasdorp); S(b): *C. subternata*(b) (Genadendal; – flower); S(c): *C. subternata*(c) (Genadendal; + flower)]. 324

## LIST OF TABLES

Table 1.1:	Classification of terpenoids.	42
Table 1.2:	Main categories and some families of terpenoids.	43
Table 3.1:	The most abundant ions in the mass spectra of components <b>C278</b> and <b>C283</b> .	123
Table 3.2:	Ions common to the mass spectra of components <b>C203</b> , <b>C218</b> , <b>C222</b> and <b>C230</b> .	139
Table 3.3:	Compound classes of VOCs identified by HS-GC-MS analysis in honeybush ( <i>Cyclopia</i> ).	165
Table 3.4:	VOCs identified by GC-MS analysis in honeybush ( <i>Cyclopia</i> ). (Odour-active compounds are listed in bold type <sup>a</sup> ).	166
Table 3.5:	Enantiomeric composition of chiral components of the headspace volatiles of honeybush tea as determined by enantioselective GC-MS analysis.	176
Table 4.1:	Odour-active compounds identified in fermented honeybush ( <i>C. subternata</i> ) aroma by means of GC-O-analysis.	265
Table 4.2:	The most intense odour-active compounds identified in honeybush ( <i>C. subternata</i> ) aroma by means of GC-O analysis.	270
Table 5.1:	VOCs, identified by HS-GC-MS analysis in green(unfermented) and fermented honeybush, <i>Cyclopia intermedia</i> .	278
Table 5.2:	Comparison of the odour-active compounds identified in seven <i>Cyclopia</i> samples.	291
Table 6.1:	Sensory aroma attributes of eight honeybush samples.	308
Table 6.2:	Summary of the main and minor sensory aroma attributes associated with eight samples of honeybush tea.	310
Table 7.1:	Correlation of components (squared cosine values >0.5) with axes F1 or F2.	315
Table 7.2:	Correlation of odour-active compounds with the respective sensory aroma attributes determined by PCA.	319
Table 7.3:	Most intense odour-active compounds and their association with the aroma attributes.	325

Table 8.1:	Composition of standard solutions of reference compounds used for quantitation of honeybush aroma constituents.	333
Table 8.2:	Honeybush samples tested by sensory panel.	344
Table 8.3:	Descriptors for the respective sensory aroma attributes.	345

## ABBREVIATIONS

AEDA	Aroma extract dilution analysis
ANOVA	Analysis of variance
ARC	Agricultural Research Council
°C	Degrees Celsius
CDCl <sub>3</sub>	Deuteriochloroform
DA	Discriminant analysis
DCM	Dichloromethane
DF	Detection frequency
DMAPP	Dimethylallyl diphosphate
DXP	1-Deoxy- <i>D</i> -xylulose-5-phosphate
EAD	Electroantennographic detector
EI	Electron impact
FD	Flavour dilution
FID	Flame ionisation detector
GC	Gas chromatograph Gas chromatography Gas chromatographic
GC-HRMS	Gas chromatography-high resolution mass spectrometry Gas chromatographic-high resolution mass spectrometric
GC-LRMS	Gas chromatography-low resolution mass spectrometry Gas chromatographic-low resolution mass spectrometric
GC-MS	Gas chromatography-mass spectrometry Gas chromatographic-mass spectrometric
GC-MS-O	Gas chromatography-mass spectrometry-olfactometry Gas chromatograph-mass spectrometer-olfactometer Gas chromatographic-mass spectrometric-olfactometric
GC-O	Gas chromatography-olfactometry Gas chromatographic-olfactometric
GC-TOF-HRMS	Gas chromatography-time-of-flight-high-resolution mass spectrometry Gas chromatographic-time-of-flight-high-resolution mass spectrometric

Gas chromatograph-time-of-flight-high-resolution mass spectrometer

h	Hour
HCSP	High-capacity sorption probe
HPLC	High-pressure liquid chromatography
HRMS	High-resolution mass spectrometry High-resolution mass spectrometric High-resolution mass spectrum/spectra
HS-GC-MS	Headspace gas chromatography-mass spectrometry Headspace gas chromatographic-mass spectrometric
HS-SEP-GC-MS	Headspace sample enrichment probe-gas chromatography-mass spectrometry
HS-SPME-GC-MS	Headspace solid-phase microextraction-gas chromatography-mass spectrometry
i.d.	Inner diameter
IPP	Isoprenyl diphosphate
LC-MS	Liquid-chromatography mass spectrometry
LECUS	Laboratory for Ecological Chemistry, Stellenbosch University
LRMS	Low-resolution mass spectrum/spectra
LSD	Least significant difference
MEP	2C-Methyl- <i>D</i> -erythritol-4-phosphate
MS	Mass spectrometer Mass spectrometry Mass spectrometric
NMR	Nuclear magnetic resonance spectrometry
OAV	Odour activity value
PCA	Principal component analysis
PDMS	Polydimethylsiloxane
RFA	Relative flavour activity
RI	Retention index
SBSE	Stir bar sorbtive extraction
SEP	Sample enrichment probe
SEP-GC-MS	Sample enrichment probe-gas chromatography-mass spectrometry
SPACE	Solid-phase aroma concentrate extraction
SPME	Solid-phase microextraction
SPME-GC-MS	Solid-phase microextraction-gas chromatography-mass spectrometry
TIC	Total ion chromatogram
VOCs	Volatile organic compounds

## CHAPTER 1

# INTRODUCTION AND OBJECTIVES

## 1.1 HONEYBUSH

### 1.1.1 Introduction

The leaves and twigs of various *Cyclopia spp.* (family Fabaceae; tribe Podalyrieae), endemic to the Cape fynbos biome in the Western and Eastern Cape provinces of South Africa, are used to make a sweet honey-like herbal infusion, known as honeybush tea. Colonists in the early Cape colony not only enjoyed honeybush as a herbal tea (Greenish, 1881; Kies, 1951; Marloth, 1913: 9, 1925: 69–72; Smith *et al.*, 1966: 247), but also realised its medicinal value (Bowie, 1830; Kobert, 1906: 748, 1029; Marloth, 1925: 69–72; Rood, 1994: 51; Van Wyk *et al.*, 1997: 290; Watt and Breyer-Brandwijk, 1932: 70), probably from observing the local inhabitants who were assumed to be familiar with the uses of the tea for many centuries (Du Toit *et al.*, 1998). Gradually, the medicinal value of the tea became less important and was enjoyed only as a herbal tea for everyday use. Today, however, with the increasing demand for the use of natural products against the health problems facing modern-day society, its medicinal value is one of the reasons renewed interest is being shown in the honeybush industry. The honeybush industry has come a long way since its early and very slow start. This can be attributed to an ongoing research programme that focuses on various aspects such as the determination of appropriate and sustainable cultivation practices; the improvement of honeybush through breeding, selection and evaluation; the identification and documentation of the health-promoting properties of honeybush and development of value-added products; the establishment of guidelines for the sustainable harvesting of natural stands; and lastly, the training of commercial and emerging farmers in production techniques (Agricultural Research Council [ARC], 2008).

### 1.1.2 Botanical description and geographical distribution

The name *Cyclopia* was mentioned in botanical literature that dates back to 1705, but it was not until 1825 that the specific species referred to in this document was classified and named *Cyclopia genistoides* (Kies, 1951). Today, more than 20 species of *Cyclopia* have been described (Bond and Goldblatt, 1984: 285–286; Kies, 1951; Schutte, 1995) and they are divided into two groups (reseeders or resprouters), depending on which fire-survival strategy they utilise (Joubert *et al.*, 2008a). Normally, bushes in natural veld grow up to 1.5 m high but, depending on the species, they can reach up to 3 m (Bond and Goldblatt, 1984: 285–286). The difference in height of the bushes of the three species *C. subternata*, *C. genistoides* and *C. intermedia* are illustrated in Fig.1.1.



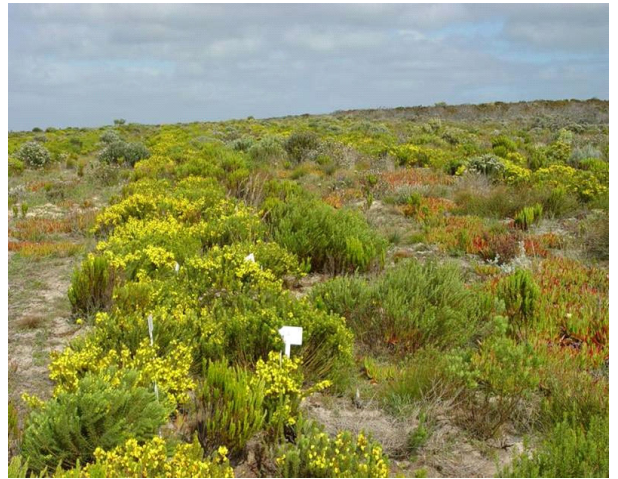


Fig. 1.1: *Cyclophia subternata* (top left), *C. genistoides* (top right) and *C. intermedia* bushes.

The shape and size of leaves differ between species and vary from pubescent, narrow-leaved species to flat-leaved species (Bond and Goldblatt, 1984: 285–286; Kies, 1951) as illustrated by the photos of the leaves of *C. intermedia*, *C. subternata* and *C. genistoides* in Fig. 1.2.



Fig. 1.2: The flat-leaved shape of the leaves of *C. intermedia* (left) and *C. subternata* (middle), compared with the narrow-leaved shape of *C. genistoides* (right).

The stems of the plants are woody and a relatively low leaf-to-stem mass ratio exists (Du Toit *et al.*, 1998). The plants have hard-shelled seeds that require scarification prior to planting due to their tendency to germinate poorly (Du Toit *et al.*, 1998; Welgemoed, 1993). Characteristic of the genus is the trifoliate arrangement of the leaves and the presence of deep yellow flowers with indented calyxes (Du Toit *et al.*, 1998; Levyns, 1920: 147; Marloth, 1925: 69–72). Flowering of the species usually occurs from September to October, with the exception of *C. sessiliflora* which flowers during late autumn or early winter (May and June) (Du Toit *et al.*, 1998). *Cyclopia* species grow in the fynbos biome of South Africa, mainly localised in the coastal and mountainous areas of the Western and Eastern Cape provinces (Fig. 1.3) (Du Toit *et al.*, 1998; Schutte, 1995). Four species, *C. intermedia*, *C. subternata*, *C. sessiliflora* and *C. genistoides*, are currently the most important species utilised for commercialisation (ARC, 2008). They grow under diverse conditions (Bond and Goldblatt, 1984: 285–286). The bushes normally prefer to grow on the shady and cooler southern slopes of mountain ranges, with the exception of *C. genistoides* that can also be found in flat and sandy coastal areas (Du Toit *et al.*, 1998; Joubert *et al.*, 2008a).

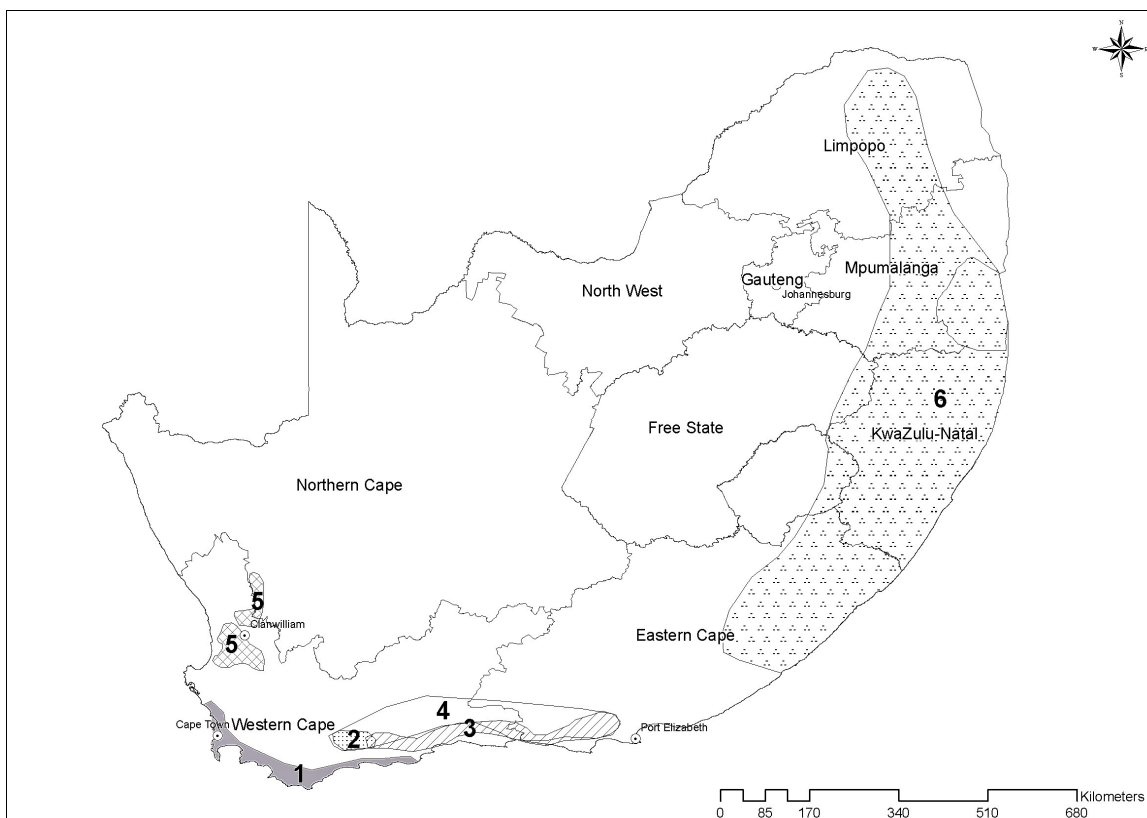


Fig. 1.3: Production area of roibos tea (*Aspalathus linearis*) and natural distribution of *Cyclopia* species and bush tea (*Athrixia phyllicoides*). Key: (1) *Cyclopia genistoides*; (2) *Cyclopia sessiliflora*; (3) *Cyclopia subternata*; (4) *Cyclopia intermedia*; (5) *Aspalathus linearis*; (6) *Athrixia phyllicoides* (Map supplied by ARC Infruitec-Nietvoorbij; Joubert *et al.* 2008a).

### 1.1.3 The honeybush industry

Although the use of honeybush tea has such a long history, it has never become as popular as rooibos tea. After World War II, no active marketing of honeybush tea took place and eventually consumption thereof declined to such a point that processing was largely discontinued except for some activity in the Langkloof area (De Lange, 2002; Joubert *et al.*, 2008a). Only in the 1990s did the honeybush industry attract renewed interest when the commercial success of rooibos led to the initiation of projects by the National Botanical Institute (Kirstenbosch) and the ARC of South Africa to investigate the commercial cultivation, processing and health-promoting properties of honeybush, which was necessary to provide a solid foundation for a successful honeybush industry (Joubert *et al.*, 2008a). After initial propagation and cultivation trials had been carried out by dr. Hannes de Lange of the National Botanical Institute of South Africa, *C. subternata* (a reseeder) and *C. genistoides* (a resprouter) were selected for commercial cultivation. Seedlings or cuttings can be used for propagation and currently more than 200 ha are under cultivation in areas spanning from the Overberg in the southern part of the Cape province to the Langkloof in the Eastern Cape province (Joubert *et al.*, 2008a). Although *C. intermedia* is the most important species in terms of market shares, it is mostly harvested from natural fynbos areas and private farms with only a few hectares under cultivation. The fact that farmers are not using more of their land for the cultivation of *C. intermedia* can be ascribed to the fact that this species grows very slowly and cannot be harvested annually (ARC, 2008; Joubert *et al.*, 2008a). Honeybush is exported as conventional, organic and green tea; most of the tea is exported in bulk quantities and then repackaged under various brand names (ARC, 2008). Although honeybush is mainly sold as a herbal tea, extracts are also produced for the food, beverage and cosmetic industries (ARC, 2008). In 2009 the Netherlands and Germany were the major export markets for conventional honeybush tea (export data for 2009 provided by South African Rooibos Council) and although the honeybush industry is still very small (<300 tons per annum) it is supported by an active horticultural research programme which involves the investigation of nutrient requirements, soil preparation techniques, harvesting practises and plant improvement (selection and cross-breeding), as well as product research (ARC, 2008).

### 1.1.4 Honeybush processing

The processing of honeybush involves the shredding of fresh shoots, fermentation\*, drying, sieving and bulk packaging. During the fermentation process oxidative and other chemical changes take place in the plant material, which leads to the browning of the leaves, in order to produce a red-brown infusion with a characteristic sweet flavour (ARC, 2008). Traditionally honeybush material was fermented in heaps (so-called heap fermentation), but this process yielded a product of poor microbial quality, because extensive mould and bacterial growth took place (Du Toit *et al.*, 1999). Heap fermentation did not allow for effective control over the production process, and the demand for

---

\* High-temperature oxidation known as fermentation in the industry.

tea of higher quality and export regulations requiring very low levels of microbial contaminants led to the implementation of high-temperature fermentation and drying under controlled conditions (Du Toit and Joubert, 1998a; Du Toit and Joubert, 1998b; Du Toit *et al.*, 1999). Research has shown that temperatures higher than 60 °C are essential to obtain a product of good microbial and sensory quality (Du Toit *et al.*, 1998a; Du Toit and Joubert, 1999) and that the addition of water before fermentation improves the uniformity of the colour of the dried product and improves the release of tea solids when preparing the infusion (Du Toit and Joubert, 1998b). The plant material is harvested in summer to late autumn before flowering can occur. This is because flowering places the plants under unnecessary stress and it was found not to contribute significantly to the characteristic sweet, honey-like flavour of the tea as was traditionally believed (Du Toit and Joubert, 1999). Batch rotary fermentation, which was initially developed for rooibos fermentation (Joubert and Müller, 1997) but is now also utilised by the honeybush industry, takes place at 70 °C for 60 h or 80–85 °C for 18 h (Joubert *et al.*, 2008a). After fermentation, the plant material is dried in a rotary drier under controlled conditions or in the sun on drying racks. The dried material is then sieved into different size categories ranging from a coarse cut to dust (<40 mesh) (ARC, 2008). Unfermented honeybush is also commercially produced *via* a steam-treatment process that inhibits enzyme activity which is responsible for the browning of the leaves (ARC, 2008; De Beer and Joubert, 2002; Joubert *et al.*, 2010). Unfermented honeybush tea does not have the characteristic sweet flavour of the traditional tea, but it has higher antioxidant activity (ARC, 2008).

### 1.1.5 Chemical composition

Honeybush is caffeine-free and has a low tannin content (Greenish, 1881; Marloth, 1925: 69–72; Terblanche, 1982). A cup of honeybush tea contains fluoride (0.59 µg/ml) and calcium (20.5 µg/ml), but no specific information on the content of the different *Cyclopia* species is available (Joubert *et al.*, 2008a; Touyz and Smit, 1982). *Cyclopia* species are a good source of polyphenols, which have the ability to act as antioxidants *in vivo* or *in vitro* (Joubert *et al.*, 2009), and have anticarcinogenic and phyto-oestrogenic properties (Joubert *et al.*, 2008a). The polyphenolic composition of *Cyclopia* species such as *C. intermedia* (fermented) and *C. subternata* (unfermented) has been thoroughly investigated (Ferreira *et al.*, 1998; Kamara *et al.*, 2003, 2004) and some polyphenols have also been identified by reversed-phase high-pressure liquid chromatography (HPLC) and liquid chromatography-mass spectrometry (LC-MS) in *C. genistoides* and *C. sessiliflora* (Joubert *et al.*, 2008b; De Beer and Joubert, 2010). All species analysed thus far contain the three major polyphenolic compounds, namely mangiferin and isomangiferin (xanthones), as well as hesperidin (a flavanone) (Joubert *et al.*, 2008a). Although hesperetin and isosakuranetin are present in a number of species, including *C. intermedia* and *C. subternata* (De Nysschen *et al.*, 1996), isosakuranetin was not detected in several extracts of *C. intermedia*, *C. subternata*, *C. sessiliflora* and *C. genistoides* analysed by means of LC-MS (Joubert *et al.*, 2008b). Qualitative and quantitative differences have been observed in the polyphenolic composition of different *Cyclopia* species

(Joubert *et al.*, 2003; Joubert *et al.*, 2008a), and even two samples of honeybush (*C. genistoides* from Overberg and West Coast) were found to exhibit quantitative differences in their polyphenolic composition (Joubert *et al.*, 2003). Fermentation of the honeybush plant material is responsible for a decrease in the total polyphenolic content and this is attributed to the decrease in the xanthone and flavonoid content (Joubert *et al.*, 2008a, 2008b).

## **1.1.6 Biological properties**

### **1.1.6.1 Antioxidant properties of honeybush extracts and individual polyphenolic compounds**

Polyphenolic compounds such as those present in honeybush species act as antioxidants due to their radical scavenging abilities (Joubert *et al.*, 2008b) and this is considered one of the most important health-promoting properties of honeybush tea. The antioxidant activity of the extracts of a number of unfermented and fermented *Cyclopia* species has been investigated (Du Toit *et al.*, 2001; Ivanova *et al.*, 2005; Joubert *et al.*, 2008b; Lindsey *et al.*, 2002; Steenkamp *et al.*, 2004). As mentioned above, unfermented honeybush extracts have a higher total polyphenolic content than the fermented extracts, and therefore they exhibit higher antioxidant activity. It is difficult to single out one specific species that exhibits the highest antioxidant activity because the determination of antioxidant activity not only depends on the assay used, but also on the sample set, since variation in the composition exists between samples of the same species (Joubert *et al.*, 2008a). Comparative studies on the antioxidant activity of individual polyphenolic compounds such as mangiferin and the other *Cyclopia* polyphenols have been conducted, and mangiferin was found to be one of the most active antioxidants of the polyphenols (Hubbe, 2000; Hubbe and Joubert, 2000; Joubert *et al.*, 2008b).

### **1.1.6.2 Antimutagenic/anticancer properties**

Another attractive health property of honeybush is its potential antimutagenic properties. Flavonoids (polyphenolic compounds) are thought to play an important role in chemoprevention since they have the ability to modulate carcinogen action in cells by affecting the cell's oxidative status and level of xenobiotic metabolising enzymes in order to inhibit and/or reduce the binding of reactive carcinogenic metabolites to macromolecules such as proteins and DNA (Giuseppe and O'Brien, 2004; Moon *et al.*, 2006). Honeybush extracts proved effective against carcinogens by interfering with the activation process of these carcinogens (Marnewick *et al.*, 2000). Honeybush extracts also changed the activity of carcinogen metabolising enzymes, which resulted in the effective protection against carcinogen tissue interaction *via* the removal of reactive mutagenic metabolites *in vivo* (Marnewick *et al.*, 2003). The antimutagenic properties of tea extracts of unfermented and fermented rooibos and honeybush as well as black tea and oolong tea were investigated in order to compare and establish their different protective properties (Joubert *et al.*, 2006; Van der Merwe, 2004; Van der Merwe *et al.*, 2006). Black tea exhibited the highest protective properties followed by oolong ≈ green

≈ fermented rooibos > unfermented rooibos ≈ unfermented honeybush > fermented honeybush. The contribution of individual polyphenols against certain antimutagens was also considered, and polyphenols such as hesperidin, eriocitrin, mangiferin, hesperitin and eriodictyol exhibited moderate antimutagenic properties (Joubert *et al.*, 2008a; Van der Merwe *et al.*, 2006). Unfermented and fermented honeybush tea of *C. intermedia* inhibited the promotion of skin cancer tumours (Marnewick *et al.*, 2005) and honeybush tea of the same species also showed cancer modulating properties towards liver and oesophagus cancer (Marnewick, 2004; Sissing, 2008). In a recent study, the modulating and chemoprotective properties of unfermented and fermented rooibos (*Aspalathus linearis*) and honeybush (*Cyclopia intermedia*), as well as green and black teas, against a potent liver cancer promoter (fumonisin B<sub>1</sub>) were investigated in rats. The study showed that the teas exhibited varying protective effects against different oxidative parameters and cancer promoting activity induced by fumonisin B<sub>1</sub> (Marnewick *et al.*, 2009).

#### **1.1.6.3 Phyto-oestrogenic properties**

Phyto-oestrogens are polyphenolic non-steroidal secondary metabolites produced by plants. They possess a similar structure and function as the endogenous human hormone, oestrogen (Dixon, 2004). Recent scientific interest in these metabolites relates to their potential to modulate oestrogen signalling and therefore they can be considered as alternatives for the treatment of menopausal symptoms and steroid-dependent cancers such as breast, prostate, endometrial and colon cancer (Cornwell *et al.*, 2004; Usui, 2006). The presence of phyto-oestrogens in honeybush suggests that extracts thereof may be used for the preparation of a phyto-oestrogenic nutraceutical (Verhoog *et al.*, 2007a, 2007b). Consequently, the phyto-oestrogenicity of different extracts of *Cyclopia* species as well as of individual polyphenolic compounds were screened, and showed promising phyto-oestrogenic activity (Verhoog *et al.*, 2007a, 2007b). Extracts of *C. genistoides* and *C. subternata* with enhanced phyto-oestrogenicity were also prepared and compared with specific commercial nutraceutical products and found to possess comparable efficiency and potency (Mfenyana, 2008; Mfenyana *et al.*, 2008).

#### **1.1.6.4 Antimicrobial and antiviral properties**

Honeybush also possesses antimicrobial and antiviral properties, as shown in some studies where extracts prepared of unfermented and fermented honeybush were able to inhibit the growth of *E. coli* and a certain plant pathogen (*Bortrytis cinerea*) (Coetzee *et al.*, 2008).

## **1.2 AROMA COMPOUNDS IN NATURAL PRODUCTS**

### **1.2.1 The importance of smell**

Living organisms have five senses (sight, hearing, taste, smell and touch) with which they are able to gather information about their environment in order to survive. The senses of smell and taste

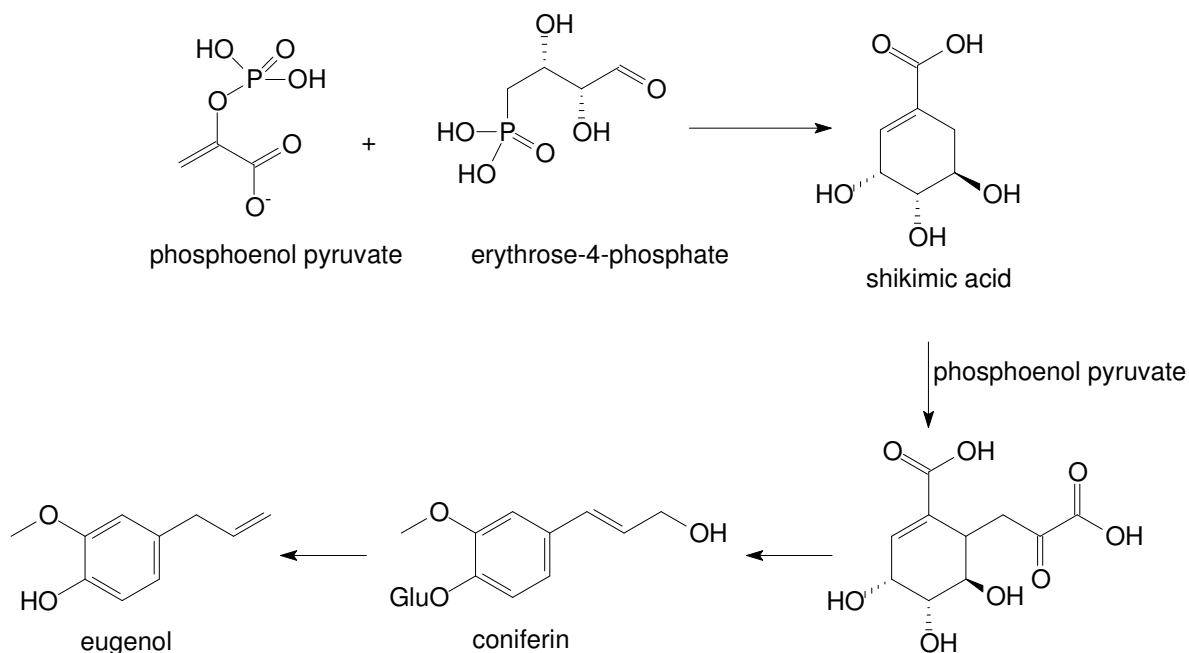
specifically provide organisms with information about changes in the chemical composition of their environment, which could either present them with a threat or an opportunity (Sell, 2006: 229–230). The sense of smell is thought to be one of the oldest senses and was probably present in very primitive species (Sell, 2006: 229–230). Most animal species use their chemical senses (taste and smell) as the dominant medium through which they obtain information about their surroundings, whereas diurnal birds and aquatic animals are more dependent on their hearing, and humans and a few primates rely mostly on vision (Sell, 2006: 24–31). Humans have lost, and are still losing, active olfactory genes at a greater rate than any other primate due to our development into a civilised race that is no longer dependent on smell for survival (Sell, 2006: 229–230). However, smell does play an important role in our enjoyment of food. The tongue can only distinguish between sweet, salt, sour, bitter and umami (savory or monosodium glutamate taste), which means that our total taste experience is in fact made possible, and enhanced, by our sense of smell (Sell, 2006: 24–31). The mechanism involved in the sense of smell is not yet fully understood, but what is known is that the sense of smell is directly related to the part of the brain that is responsible for memory and emotion (Sell, 2006: 1), and this is one of the reasons why people have been fascinated by the sense of smell for centuries.

*“Smell is a potent wizard that transports you across thousands of miles and all the years you have lived.”* Helen Keller

## **1.2.2 General overview of aroma compounds**

A variety of chemicals are biosynthesised by all living organisms and the compounds are grouped as primary or secondary metabolites. Primary metabolites are compounds that are present in all species, and include proteins, carbohydrates, lipids and nucleic acids (Sell, 2003: 1–2). Secondary metabolites, also known as “natural products”, are divided into terpenoids, alkaloids, shikimates and polyketides, based on the route followed to produce these compounds. Secondary metabolites may be common to a number of species or may be produced only by a specific organism (Sell, 2003: 1–2). Most odorous compounds belong to the terpenoid compound class and to a lesser extent to the shikimates and polyketides, whereas very few odorous materials are derived from the alkaloid family (Sell, 2006: 24–31). Green plants and photosynthetic algae produce glucose during an energetically unfavourable process known as photosynthesis by utilising carbon dioxide, water and sunlight as energy source. The glucose produced by the plant can be broken down to the enol form of pyruvic acid, either by the plant itself or by any other species that obtains the glucose by eating the plant. In the pyruvic acid the enolic hydroxy group is protected as a phosphate ester. From this phosphoenol pyruvate, two metabolic pathways lead to the formation of shikimic acid and acetyl coenzyme-A. Aldol-type reactions of esters with acetyl coenzyme-A are responsible for the biosynthesis of lipids and polyketides, and addition of phosphoenol pyruvate to erythrose-4-phosphate yields shikimic acid after a number of steps (Sell, 2006: 24–31). Many odorous materials

contain the 3,4,5-trihydroxy skeleton of shikimic acid and the compound eugenol is derived from shikimic acid, as shown in the following scheme (Sell, 2006: 24–31):



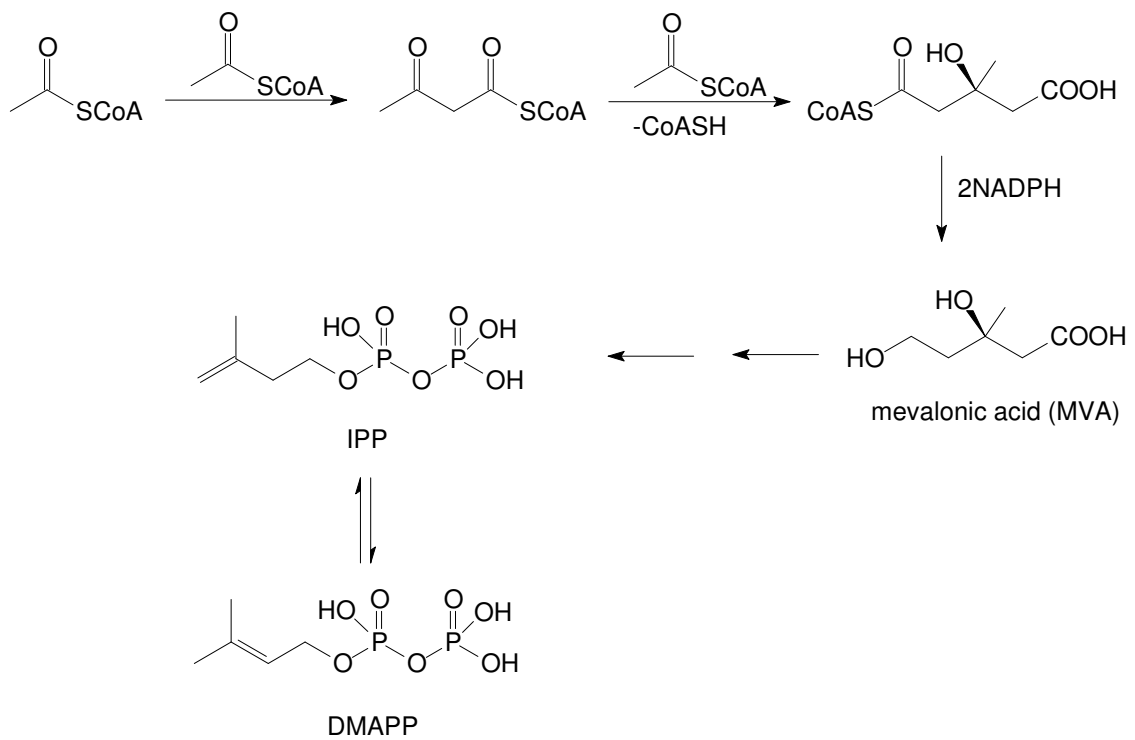
For a compound to be deemed odorous, it should have certain molecular properties such as surface activity, low polarity, some water solubility, a high vapour pressure and high lipophilicity (Ohloff, 1994: 9). As already mentioned, most odorous compounds are terpenoids. In the present study most of the compounds identified in honeybush aroma do indeed belong to this compound class, hence terpenoids will be discussed in more detail in the next section.

## 1.2.3 Terpenoids

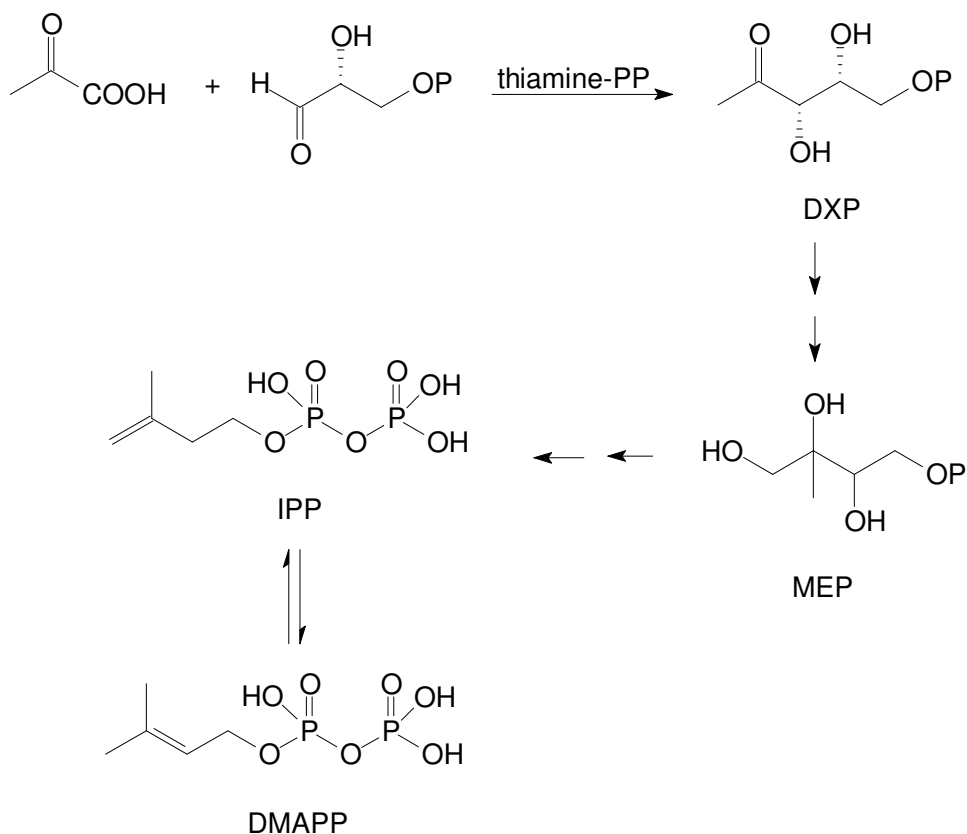
### 1.2.3.1 Introduction to terpenoids

Terpenoids contain carbon backbones made up of isoprene (2-methylbuta-1,3-diene) units, and because isoprene is a five-carbon molecule the number of carbons in any terpenoid is usually a multiple of five. Some terpenoids deviate from this trend when carbon atoms have been lost through chemical or biochemical processes, but it will still be evident from their overall structure that they are nonetheless terpenoids (Sell, 2003: 1–6). As already discussed in § 1.2.2, glucose is broken down to phosphoenolpyruvate in plants or other organisms, and hydrolysis thereof yields free pyruvate which is attacked at the carbonyl moiety by the thiol group of coenzyme-A. After decarboxylation, acetyl coenzyme-A is produced, which in turn is converted through a series of reactions to the two isomeric building blocks of terpenoids, i.e. isopentenyl- and prenyl pyrophosphate (Sell, 2003: 25–28). These two isomeric compounds are also known as isoprenyl diphosphate (IPP) and dimethylallyl diphosphate (DMAPP), and their formation from three molecules of acetyl coenzyme-A through mevalonic acid is shown in the scheme below (Berger, 2007: 45–47):





Approximately 10 years ago, a second pathway leading to the formation of IPP and DMAPP was discovered. It involves the condensation of glyceraldehyde phosphate and pyruvate to afford 1-deoxy-*D*-xylulose-5-phosphate (DXP) which, through a series of reactions, leads to the formation of 2C-methyl-*D*-erythritol-4-phosphate (MEP) and ultimately the same two building blocks of terpenoids (IPP and DMAPP) (Berger, 2007: 45–47; Rohdich *et al.*, 2005):



Hydrolysis or coupling of these two isomeric building blocks is responsible for the formation of hemiterpenoids and monoterpenoids (*via* the formed geranyl pyrophosphate monoterpenoid precursor), respectively. If additional isopentenyl compounds couple to geranyl pyrophosphate, then these coupled units lead to the formation of sesquiterpenoids and other higher terpenoids (Sell, 2006: 24–31). Terpenoids are classified according to the number of isoprene units in their structures, as seen in Table 1.1.

Table 1.1: Classification of terpenoids

<b>Name</b>	<b>No. of isoprene units</b>	<b>No. of carbon atoms</b>
Hemiterpenoids	1	5
Monoterpenoids	2	10
Sesquiterpenoids	3	15
Diterpenoids	4	20
Sesterterpenoids	5	25
Triterpenoids	6	30
Tetraterpenoids	8	40
Polyisoprenoids	>8	>40
Steroids	8	40
Carotenoids	8	40

The most common way in which isoprene units connect is in a head-to-tail fashion. Tail-to-tail connections are less common and normally observed in steroids and carotenoids (Sell, 2003: 1–6). With the aid of appropriate enzymes, known as terpene cyclases, terpenoid pyrophosphates can undergo numerous reactions, including cyclisation, oxidation, rearrangement, reduction and hydration, which are responsible for the formation of numerous different terpenoid compounds (Berger, 2007: 45–47; Sell, 2006: 24–31), making terpenoids one of the most diverse groups of natural compounds. Therefore, terpenoids are not only classified according to their number of isoprene units, but also according to their different skeleton structures, i.e. cyclic, acyclic, or even bi- or tricyclic, etc. They are usually named after one of the principal members of a specific family that is usually the most common or the first to have been discovered (Sell, 2003: 1–6). Table 1.2 lists some important terpenoid families under each main category of terpenoids (Berger, 2007: 47–64; Connolly and Hill, 1991).

Table 1.2: Main categories and some families of terpenoids

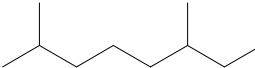
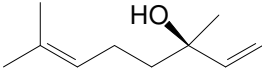
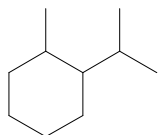
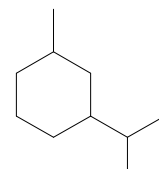
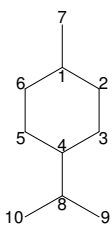
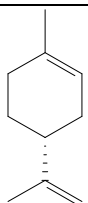
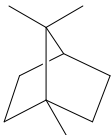
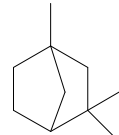
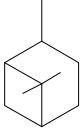
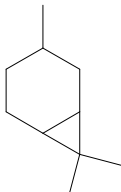
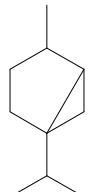
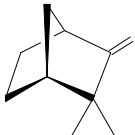
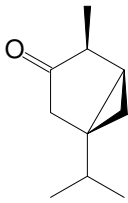
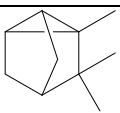
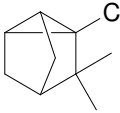
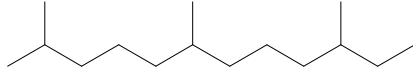
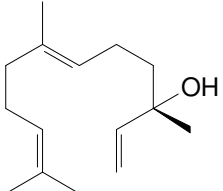
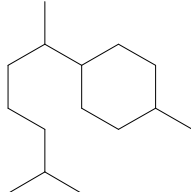
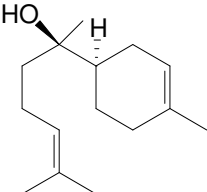
	Terpenoid family	Skeleton	Examples
Monoterpenoids	Acyclic monoterpenoids	 2,6-Dimethyloctane	 ( <i>R</i> )-Linalool
	Monocyclic monoterpenoids	The menthanes    <i>o</i> -Menthane <i>m</i> -Menthane <i>p</i> -Menthane	 ( <i>R</i> )-Limonene
	Bicyclic monoterpenoids	   Camphane    Fenchane    Pinane   Carane    Thujane	 (+) - Camphene  (+) - 3 - Thujanone
	Tricyclic monoterpenoids	 Tricyclene	 Tricyclal
Sesquiterpenoids	Acyclic sesquiterpenoids	 2,6,10-Trimethyldodecane	 ( <i>S</i> )-( <i>E</i> )-Nerolidol
	Monocyclic sesquiterpenoids: bisabolanes	 Bisabolane	 (+) - $\alpha$ - Bisabolol

Table 1.2: *contd.*

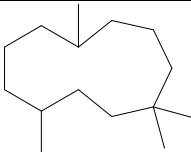
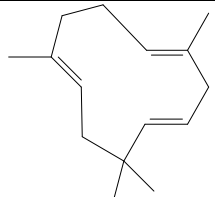
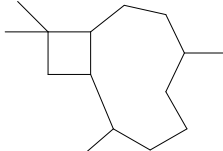
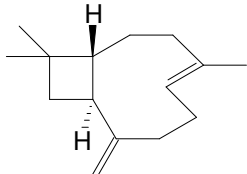
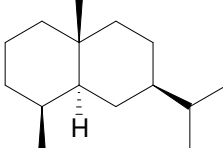
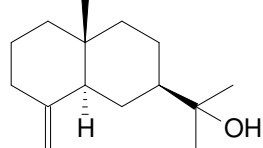
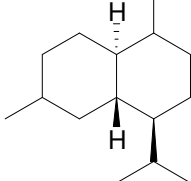
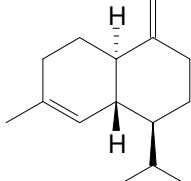
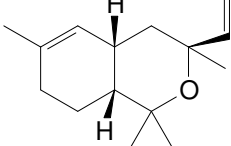
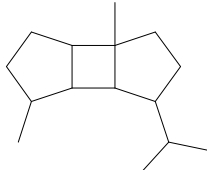
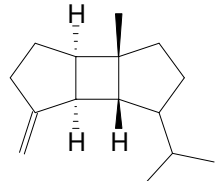
Terpenoid family	Skeleton	Examples
Monocyclic sesquiterpenoids: humulanes	 Humulane	 $\alpha$ -Humulene
Bicyclic sesquiterpenoids: caryophyllanes	 Caryophyllane	 $\beta$ -Caryophyllene
Bicyclic sesquiterpenoids: eudesmanes	 Eudesmane	 $\beta$ -Eudesmol
Bicyclic sesquiterpenoids: cadinanes	 Cadinane	 $\gamma$ -Cadinene
Miscellaneous cyclohexane sesquiterpenoids		 Cabreuva oxide B
Tricyclic sesquiterpenes: bourbonanes	 Bourbonane	 $\beta$ -Bourbonene

Table 1.2: *contd.*

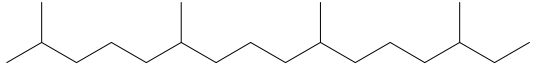
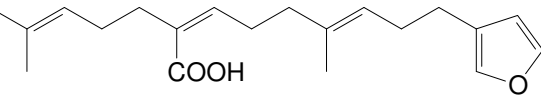
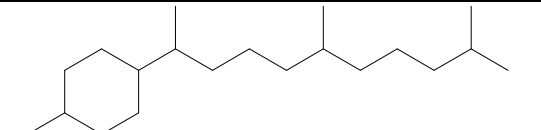
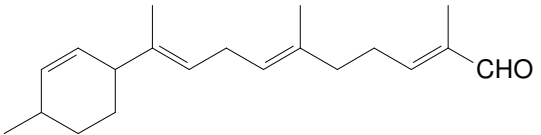
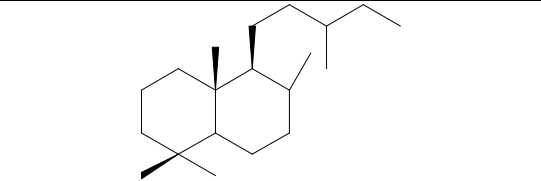
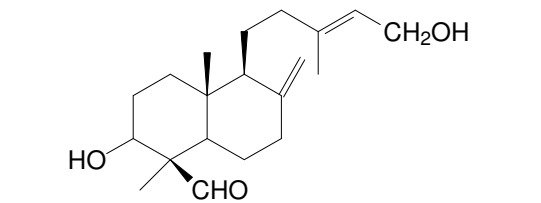
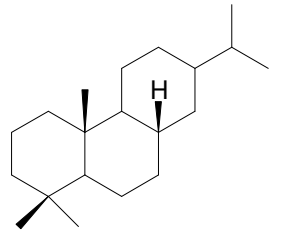
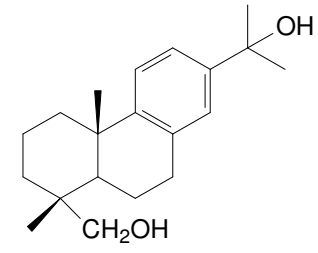
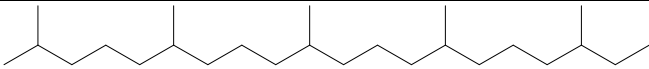
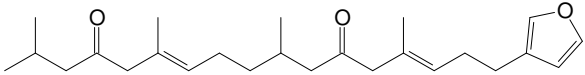
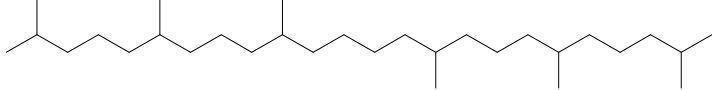
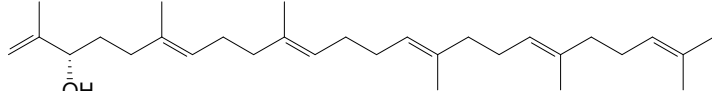
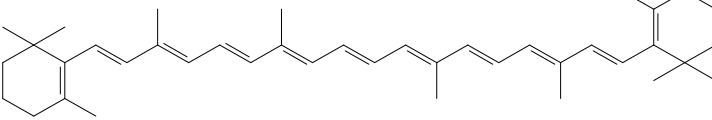
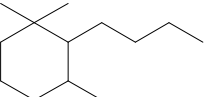
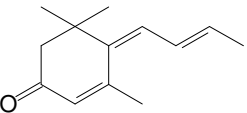
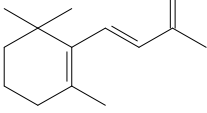
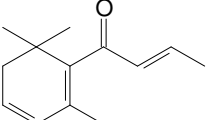
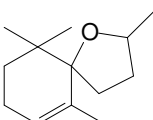
Terpenoid family	Skeleton	Examples
Diterpenoids	Acyclic diterpenoids: phytanes	 <p>Phytane</p> <p>e.g.</p>  <p>Centipedic acid</p>
	Monocyclic diterpenoids: prenylbisabolanes	 <p>Prenylbisabolane</p> <p>e.g.</p>  <p>16-Hellicallenal</p>
Diterpenoids	Bicyclic diterpenoids: labdanes	 <p>Labdane</p> <p>e.g.</p>  <p>3<math>\alpha</math>-Hydroxyisoagatholal</p>
	Tricyclic diterpenoids: abietanes	 <p>Abietane</p>  <p>8,11,13-Abietatriene-15,18-diol</p>

Table 1.2: *contd.*

Terpenoid family	Skeleton	Examples	
Sesterterpenoids	Acyclic sesterterpenoids:		
	Acyclic sesterterpenoid skeleton	e.g.	
			
	Idiadione		
Triterpenoids	Acyclic triterpenoids:		
	Linear triterpenoid skeleton	e.g.	
			
	(S)-3-Isosqualenol (all double bonds <i>E</i> )		
Tetraterpenoids	Tetraterpenoids:	Carotenoids:	
			
		β-Carotene	
		C <sub>13</sub> -Carotenoid-derived compounds:	
			
		Megastigmane skeleton	
			
		4,6,8-Megastigmatrien-3-one	β-Ionone
			
	β-Damascenone	Theaspirane	

### 1.2.3.2 The role of terpenoids in nature

When plants, animals and microorganisms produce metabolites such as terpenoids, it places them under a metabolic load, which almost invariably means that there is a reason for the

metabolites to be synthesised. The role that terpenoids play in living organisms can be grouped into three categories, i.e. functional, defence and communication (Sell, 2003: 6–13).

Functional terpenoids play an important role in the metabolic processes of the organism in which they are produced, and include Vitamin A (retinol), which is the precursor for the pigment in the eyes that detects light and is responsible for the sense of sight. Other examples include Vitamin E, which acts as antioxidant and protects cells against oxidative damage. Vitamin D is responsible for regulating calcium metabolism and is vital for the maintenance and building of bones. In plant leaves, the pigment chlorophyll plays a vital role during the process of photosynthesis that produces glucose in plants (Sell, 2003: 6–13).

Plants and animals use terpenoids to protect themselves against predators that threaten to damage or eat them. The shrub *Commiphora abyssinica* produces a resin that contains antibacterial and antifungal compounds, one of which is an eudesmane derivative, known to seal a wound and prevent bacteria and fungi from entering and further damaging the plant. This plant resin has a very pleasant odour and has been used as a perfume ingredient, known as myrrh (Sell, 2003: 6–13). Plants produce some terpenoids which render them inedible to insects. Warburganal is such a compound, produced by plants belonging to the genus *Warburgia*. This compound has two formyl functions, one of which is  $\alpha,\beta$ -unsaturated, and therefore is capable of undergoing triple alkylation of nucleophilic materials such as the nitrogen atoms of proteins and nucleic acids. This property not only makes warburganal a skin sensitiser but also a carcinogen (Sell, 2003: 6–13).

Finally, terpenoids are used by organisms as chemical messengers, either in communication between different parts of the same organism, in which case the messenger is referred to as a hormone, or as chemicals known as semiochemicals, which carry signals between different organisms. Semiochemicals are subdivided into two further classes, i.e. pheromones, involved in the transmission of information between members of the same species, or allelochemicals, used for communication between members of different species (Sell, 2003: 6–13). Pheromones can carry a vast array of information; some organisms make use of only one or two pheromones whereas others, such as the social insects (e.g. bees, ants and termites), use many chemical signals to organise their intricate social lives. Sex pheromones are widespread among organisms and play an important role during mating. Insects also make use of trail, alarm, aggregation, dispersal and social pheromones. Allelochemicals are subdivided as allomones, which benefit the sender of the signal, kairomones, which benefit the receiver, or synomones, which benefit both the sender and the receiver (Sell, 2003: 6–13). Camphor and *d*-limonene are examples of allomones, because they protect the trees that produce them against attack from insects. Myrcene can be classified as a kairomone since it attracts the female bark beetles to the ponderosa pine that produces it. Geraniol, present in the scents of many flowers, for example roses, is classified as a synomone. It benefits both the plant being pollinated by the insects that it attracts and the insects in turn are rewarded with nectar (Sell, 2003: 6–13).

### 1.2.3.3 Uses of terpenoids

Many of the commercial uses of terpenoids reflect their natural functions, e.g. those that possess biological activity in nature can be used as commercial drugs or pest control agents. The odorous terpenoids are used in the fragrance industry as ingredients in a variety of cosmetics, toiletries and other household products, and they can also be used as flavourants in foods and beverages. Some terpenoids have unique and attractive physical and chemical properties which are put to use for purposes that do not reflect the original role for which they were produced in nature, e.g. rubber, a polymer of isoprene produced by the rubber tree as a defensive secretion, is widely used for its elastic properties (Sell, 2003: 6–13).

## 1.3 OBJECTIVES

Although more than 20 species of honeybush grow in the wild, only a few species are commercially exploited for the manufacturing of tea, the more prominent species presently being *Cyclopia intermedia*, *C. subternata*, *C. sessiliflora* and *C. genistoides*. This study forms part of an ongoing research programme at the ARC Infruitec-Nietvoorbij aimed at furthering the establishment and commercialisation of a prominent and secure honeybush industry, comparable to the very successful rooibos tea industry in South Africa.

This is the first time research aimed at the complete chemical characterisation of honeybush aroma has been undertaken. Apart from its potential scientific contribution to the honeybush research programme and honeybush industry, the research was also initiated because honeybush is such an interesting indigenous herbal plant with such unique flavour properties.

The main broad goal of this study was the chemical characterisation of all the volatile organic compounds present in unfermented and fermented honeybush with special emphasis on the identification of the odour-active volatile organic compounds present in fermented honeybush. In order to achieve this goal, the following objectives were formulated at the outset of the study:

- development of the analytical methodology necessary for the sampling and analysis of extremely low concentrations of honeybush volatile compounds;
- chemical characterisation of all the volatile organic compounds in unfermented and fermented honeybush, using mainly gas chromatography-mass spectrometry as primary analytical technique;
- quantification and comparison of the volatile organic compounds in unfermented and fermented honeybush of a representative species, *C. intermedia*, in order to identify significant qualitative and quantitative differences;



- identification of the odour-active compounds in fermented honeybush by means of gas chromatography-olfactometry;
- quantification and comparison of the volatile organic compounds in seven honeybush samples, with special emphasis on the odour-active compounds;
- establishment of sensory aroma attributes for eight different honeybush samples and combination of these attributes with the quantitative data for the aroma-active compounds by means of statistical analytical methods.

## 1.4 REFERENCES

- Agricultural Research Council. 2008. Website of honeybush research programme. ARC, South Africa [Online]. Available: <http://www.arc.agric.za/home.asp?pid=4053> [2010, 5 February].
- Berger, R.G. 2007. Flavours and fragrances: Chemistry, bioprocessing and sustainability. Springer, Berlin, Heidelberg.
- Bond P., Goldblatt, P. 1984. Plants of the Cape flora. A descriptive catalogue. CTP Book Printers, Cape Town, South Africa.
- Bowie, J. 1830. Sketches of the botany of South Africa. *South African Quarterly Journal* **1**, 27–36.
- Coetzee, G., Marx, I.J., Pengilly, M., Bushula, V.S., Joubert, E., Bloom, M. 2008. Effect of rooibos and honeybush tea extracts against *Botrytis cinerea*. *S. Afr. J. Enol. Vitic.* **29**, 33–38.
- Connolly, J.D., Hill, R.A. 1991. Dictionary of terpenoids, Vols. I, II and III. Chapman & Hall, Cambridge, London.
- Cornwell, T., Cohick, W., Raskin, I. 2004. Dietary phytoestrogens and health. *Phytochemistry* **65**, 995–1016.
- De Beer, D., Joubert, E. 2010. Development of HPLC method for *Cyclopia subternata* phenolic compound analysis and application to other *Cyclopia* spp. *J. Food Compos. Anal.* **23**, 289–297.
- De Beer, S.W., Joubert, E. 2002. Preparation of tea-like beverages. SA patent no. 2002/2802.
- De Lange, H. 2002. Geskiedenis en ontwikkeling van heuningbostee. SAHTA publication no. 6.
- De Nysschen, A.M., Van Wyk, B.-E., Van Heerden, F.R., Schutte, A.L. 1996. The major phenolic compounds in the leaves of *Cyclopia* species (Honeybush tea). *Biochem. Syst. Ecol.* **24**, 243–246.
- Dixon, R.A. 2004. Phytoestrogens. *Annu. Rev. Plant Biol.* **55**, 225–261.
- Du Toit, J., Joubert, E. 1998a. Effect of drying conditions on the quality of honeybush tea (*Cyclopia*). *J. Food Process Preserv.* **22**, 493–507.
- Du Toit, J., Joubert, E. 1998b. The effect of pre-treatment on the fermentation of honeybush tea (*Cyclopia maculata*). *J. Sci. Food Agric.* **76**, 537–545.

- Du Toit, J., Joubert, E. 1999. Optimization of the fermentation parameters of honeybush tea (*Cyclopia*). *J. Food Qual.* **22**, 241–256.
- Du Toit, J., Joubert E., Britz, T.J. 1998. Honeybush tea—a rediscovered indigenous South African herbal tea. *J. Sustain. Agric.* **12**, 67–84.
- Du Toit, J., Joubert, E., Britz, T.J. 1999. Identification of microbial contaminants present during the curing of honeybush tea (*Cyclopia*). *J. Sci. Food Agric.* **79**, 2040–2044.
- Du Toit, R., Volstedt, Y., Apostolides, Z. 2001. Comparison of the antioxidant content of fruits, vegetables and teas as vitamin C equivalents. *Toxicology* **166**, 63–69.
- Ferreira, D. Kamara, B.I., Brandt, E.V., Joubert, E. 1998. Phenolic compounds from *Cyclopia intermedia* (honeybush tea). *J. Agric. Food. Chem.* **46**, 3406–3410.
- Giuseppe, G., O'Brien, P.J. 2004. Serial Review: Flavonoids and isoflavones (phytoestrogens): Absorption, metabolism, and bioactivity. *Free Radic. Biol. Med.* **37**, 287–303.
- Greenish, H.G. 1881. Cape tea. *The Pharmaceutical Journal and Transactions* **11**, 549–551.
- Hubbe, M.H. 2000. Evaluation of the antioxidant and free radical scavenging activities of honeybush tea (*Cyclopia*). MSc (Biochemistry) thesis, Stellenbosch University, Stellenbosch, South Africa.
- Hubbe, M.H., Joubert, E. in: Johnson, I.T., Fenwick, G.R. (Eds.). 2000. Dietary anticarcinogens and antimutagens. Chemical and biological aspects: Proceedings of the Food and Cancer Prevention III Meeting, 5–8 September 1999, Royal Chemical Society, UK, pp. 242–244.
- Ivanova, D., Gerova, D., Chervenko, T., Yankova, T. 2005. Polyphenols and antioxidant capacity of Bulgarian medicinal plants. *J. Ethnopharmacol.* **96**, 145–150.
- Joubert, E., Gelderblom, W.C.A., De Beer, D. 2009. Phenolic contribution of South African herbal teas to healthy diet. *Nat. Prod. Commun.* **4**, 701–718.
- Joubert, E., Gelderblom W.C.A., Louw, A., De Beer, D. 2008a. South African herbal teas: *Aspalathus linearis*, *Cyclopia* spp. and *Athrixia phylloides*—a review. *J. Ethnopharmacol.* **119**, 376–412.
- Joubert, E., Manley, E., Maicu, C., De Beer, D. 2010. Effect of pre-drying treatments and storage on color and phenolic composition of green honeybush (*Cyclopia subternata*) herbal tea. *J. Agric. Food Chem.* **58**, 338–344.
- Joubert, E., Müller, R. 1997. A small-scale rotary fermentation unit for rooibos tea. *Int. J. Food Sci. Tech.* **32**, 135–139.
- Joubert, E., Otto, F., Grüner, S., Weinrich, B. 2003. Reversed-phase HPLC determination of mangiferin, isomangiferin and hesperidin in *Cyclopia* and the effect of harvesting date on the phenolic composition of *C. genistoides*. *Eur. Food Res. Technol.* **216**, 270–273.
- Joubert, E. Richards, E.S., Van der Merwe, J.D., de Beer, D., Manley, M., Gelderblom, W.C.A. 2008b. Effect of species variation and processing on phenolic composition and *in vitro* antioxidant activity of aqueous extracts of *Cyclopia* spp. (honeybush tea). *J. Agric. Food Chem.* **56**, 954–963.
- Joubert, E. Van der Merwe, J.D., Gelderblom, W.C.A., Manley, M. 2006. Implication of CYP450 stabilization in the evaluation of *in vitro* antimutagenicity of the herbal teas, *Cyclopia* spp.

- (honeybush) and *Aspalathus linearis* (rooibos) and selected polyphenols. In: Polyphenols Communications 2006: Abstracts of XXXIIIrd International Conference on Polyphenols, 22–25 August, Winnipeg, Manitoba, Canada, pp. 505–506.
- Kamara, B.I., Brandt, E.V., Ferreira, D., Joubert, E. 2003. Polyphenols from honeybush tea (*Cyclopia intermedia*). *J. Agric. Food Chem.* **51**, 3874–3879.
- Kamara, B.I., Brand, D.J., Brandt, E.V., Joubert, E. 2004. Phenolic metabolites from honeybush tea (*Cyclopia subternata*). *J. Agric. Food Chem.* **52**, 5391–5395.
- Kies, P. 1951. Revision of the genus *Cyclopia* and notes on some other sources of bush tea. *Bothalia* **6**, 161–176.
- Kobert, R. 1906. Lehrbuch der intoxicationen, 2<sup>nd</sup> ed., ii (2), (as cited by Watt and Breyer-Brandwijk, 1932).
- Levyns, M.R. 1920. A guide to the flora of the Cape Peninsula. Juta and Co. (Ltd.), Cape Town.
- Lindsey, K.L., Motsei, M.L., Jäger, A.K. 2002. Screening of South African food plants for antioxidant activity. *J. Food Sci.* **67**, 2129–2131.
- Marloth, R. 1913. The chemistry of South African plants and plant products. Cape Chemical Society, Cape Town.
- Marloth, R. 1925. The flora of South Africa with synoptical tables of the genera of the higher plants. Darter Bros & Co, Cape Town.
- Marnewick, J.L. 2004. Chemopreventive properties of two South African herbal teas, rooibos tea (*Aspalathus linearis*) and honeybush tea (*Cyclopia intermedia*) utilizing different short-term *in vivo* and *in vitro* carcinogenesis models. PhD (Biochemistry) thesis, University of Stellenbosch, Stellenbosch, South Africa.
- Marnewick, J.L., Gelderblom, W.C.A., Joubert, E. 2000. An investigation on the antimutagenic properties of South African herbal teas. *Mutat. Res.* **471**, 157–166.
- Marnewick, J.L., Joubert, E., Joseph, S., Swanevelder, S., Swart, P., Gelderblom, W.C.A. 2005. Inhibition of tumour promotion in mouse skin by extracts of rooibos (*Aspalathus linearis*) and honeybush (*Cyclopia intermedia*), unique South African herbal teas, *Cancer Lett.* **224**, 193–202.
- Marnewick, J.L., Joubert, E., Swart, P., Van der Westhuizen, F., Gelderblom, W.C.A. 2003. Modulation of hepatic drug metabolizing enzymes and oxidative status by green and black (*Camillia sinensis*), rooibos (*Aspalathus linearis*) and honeybush (*Cyclopia intermedia*) teas in rats. *J. Agric. Food Chem.* **51**, 8113–8119.
- Marnewick, J.L., Van der Westhuizen, F.H., Joubert, E., Swanevelder, S., Swart, P., Gelderblom, W.C.A. 2009. Chemoprotective properties of rooibos (*Aspalathus linearis*), honeybush (*Cyclopia intermedia*) herbal and green and black (*Camillia sinensis*) teas against cancer promotion induced by fumonisin B<sub>1</sub> in rat liver. *Food Chem. Toxicol.* **47**, 220–229.
- Mfenyana, C. 2008. Selective extraction of *Cyclopia* for enhanced *in vitro* phyto-oestrogenicity. MSc (Biochemistry) thesis, Stellenbosch University, Stellenbosch, South Africa.

- Mfenyana, C., De Beer, E., Joubert, E., Louw, A. 2008. Selective extraction of *Cyclopia* for enhanced benchmarking against commercial phytoestrogen extracts. *J. Steroid Biochem. Mol. Biol.* **112**, 74–86.
- Moon, Y.J., Wang, X., Morris, M.E. 2006. Dietary flavonoids: Effects on xenobiotic and carcinogen metabolism. *Toxicol. in Vitro* **20**, 187–210.
- Ohloff, G. Scent and Fragrances. 1994. The fascination of odors and their chemical perspectives. Springer-Verlag, Berlin, Germany.
- Rohdich, F., Bacher, A., Eisenreich, W. 2005. Isoprenoid biosynthetic pathways as anti-infective drug targets. *Biochem. Soc. Trans.* **33**, 785–791.
- Rood, B. 1994. Uit die veldapteek. Tafelberg-Uitgewers Bpk, Cape Town, South Africa.
- Schutte, A.L. 1995. A taxonomic study of the tribes Podalyrieae and Liparieae (Fabaceae). PhD dissertation, Rand Afrikaans University, Johannesburg, South Africa.
- Sell, E. 2003. A fragrant introduction to terpenoid chemistry. The Royal Society of Chemistry, Cambridge, United Kingdom.
- Sell, E. 2006. The chemistry of fragrances. From perfumer to consumer. The Royal Society of Chemistry, Cambridge, United Kingdom.
- Smith, C.A., Philips, E.P., Van Hoepen, E. 1966. Common names of South African plants. Botanical Survey Memoir No. 35. The Government Printer, Pretoria, South Africa.
- Steenkamp, A., Fernandes, A.C., Van Rensburg, C.E.J. 2004. Antioxidant scavenging potential of South African export herbal teas. *S. Afr. J. Bot.* **70**, 660–663.
- Sissing, 2008. Investigation into the cancer modulating properties of *Aspalathus linearis* (rooibos), *Cyclopia intermedia* (honeybush) and *Sutherlandia frutescens* (cancer bush) in oesophageal carcinogenesis. MSc (Physiology) thesis, University of the Western Cape, Belville, South Africa.
- Terblanche, S.E. 1982. Report on honeybush tea. Department of Biochemistry, University of Port Elizabeth, Port Elizabeth, South Africa.
- Touyz, L.Z.G., Smit, A.A. 1982. Herbal tea infusions—their acidity, fluoride and calcium concentrations. *J. Dent. Assoc. S. Afr.* **37**, 737–739.
- Usui, T. 2006. Pharmaceutical prospects of phytoestrogens. *Endocr. J.* **53**, 7–20.
- Van der Merwe, J.D. 2004. A comparative study on protection of *Cyclopia* spp. (honeybush), *Aspalathus linearis* (rooibos) and *Camillia sinensis* teas against aflatoxin B1 induced mutagenesis in the Salmonella mutagenicity assay: Possible mechanisms involved. MSc (Food Science) thesis, Stellenbosch University, Stellenbosch, South Africa.
- Van der Merwe, J.D., Joubert, E., Richards, E.S., Manley, M., Snijman, P.W., Marnewick, J.L., Gelderblom, W.C.A. 2006. A comparative study on the antimutagenic properties of aqueous extracts of *Aspalathus linearis* (rooibos), different *Cyclopia* spp. (honeybush) and *Camillia sinensis* teas. *Mutat. Res.* **611**, 42–53.
- Van Wyk, B.-E., Van Oudtshoorn, B., Gericke, N. 1997. Medicinal plants of South Africa. Briza Publications, Pretoria, South Africa.

- Verhoog, N.J.D., Joubert, E., Louw, A. 2007a. Evaluation of the phyto-oestrogenic activity of *Cyclopia genistoides* (honeybush) methanol extracts and relevant polyphenols. *J. Agric. Food Chem.* **55**, 4371–4381.
- Verhoog, N.J.D., Joubert, E., Louw, A. 2007b. Screening of four *Cyclopia* (honeybush) species for putative phyto-oestrogenic activity by oestrogen receptor binding assays. *S. Afr. J. Sci.* **103**, 13–21.
- Watt, J.M., Breyer-Brandwijk, M.G. 1932. The medicinal and poisonous plants of Southern Africa. E & S Livingstone, Edinburgh, UK.
- Welgemoed, Z. 1993. Heuningtee straks kommersieel verbou. *Landbouweekblad* **792**, 52–55.

## CHAPTER 2

# SELECTION OF APPROPRIATE ANALYTICAL METHODS

## 2.1 SAMPLE PREPARATION AND SAMPLING METHODS

The experimental details of the methods used in this study are given in Chapter 8. Only certain methods and aspects thereof are discussed in this chapter. The purpose of this chapter is to discuss the rationale behind the choice of selected sample preparation, sampling and analytical techniques used in this study.

### 2.1.1 Sampling of honeybush infusions vs dry plant material

Initially, dry plant material was used to investigate the volatile organic compounds (VOCs) present in honeybush by headspace gas chromatography-mass spectrometry (HS-GC-MS) analysis. Although previous studies on the differences in the volatiles from extracted dry tea leaves and from extracted infusions revealed anomalous behaviour (Schuh and Schieberle, 2006; Wright *et al.*, 2007) and showed that the effect of infusion and holding temperatures on the volatile profile of tea headspace samples are compound-dependent (Wright *et al.*, 2007), it was established in the present study that HS-GC-MS analysis of infused honeybush gave approximately the same qualitative and relative quantitative results as those obtained with the dry material. Honeybush infusions were therefore used as alternative to dry honeybush plant material in subsequent analyses.

A distinct advantage of the use of infusions proved to be their use in gas chromatography-olfactometry (GC-O) analysis where the highest possible concentrations of the volatile components, and controlled quantitative dilutions were required. Furthermore, the analysis of an infusion compared to dry honeybush was expected to produce a more realistic aroma profile of honeybush tea as it is normally consumed and savoured.

Infusions of two different strengths were prepared and are referred to as standard and concentrated infusions, respectively. Standard infusions were used in all qualitative and quantitative gas chromatography-mass spectrometry (GC-MS) analyses, except the initial comparative analyses of unfermented and fermented dry honeybush material of the species *Cyclopia genistoides*. Concentrated infusions were prepared specifically for GC-O, gas chromatography-mass spectrometry-olfactometry (GC-MS-O), and gas chromatography-high-resolution mass spectrometry (GC-HRMS) analyses. These analytical methods were greatly facilitated by sampling higher concentrations of volatiles present in concentrated infusions. The use of concentrated infusions in the case of GC-O analysis using the aroma extract dilution analysis (AEDA) method was particularly successful. The AEDA method, used for the identification of individual odour-active compounds that contribute to the aroma of a certain product, involves the stepwise dilution of a sample until none of

the individual odours can be detected in the final dilution (Acree *et al.*, 1984; Acree, 1993). The use of concentrated infusions made it possible to carry out an adequate and significant number of dilutions for the calculation of flavour dilution (FD) factors for the individual odour-active compounds in honeybush (Chapter 4).

### **2.1.2 Enrichment of headspace volatiles by a sample enrichment probe technique**

A high-capacity sample enrichment probe (SEP) (Burger *et al.*, 2006), developed in the Laboratory for Ecological Chemistry (LECUS) for research on the aroma constituents of herbal teas derived from different South African plant species, was used in this study as an alternative to existing sampling techniques such as solid-phase microextraction (SPME) (Arthur and Pawliszyn, 1990; Risticvic *et al.*, 2009; Vas and Vékey, 2004), stir bar sorptive extraction (SBSE) (Baltussen *et al.*, 1999), extraction by high-capacity sorption probe (HCSP) (Pettersson *et al.*, 2004), and solid-phase aroma concentrate extraction (SPACE) (Ishikawa *et al.*, 2004).

SPME is a convenient solvent-free extraction method that does not normally require cryofocussing of the desorbed volatiles and thus does not require additional expensive instrumentation when operated in the non-automated mode. This popular technique has been applied successfully over more than two decades in analyses of a wide variety of sample types, including food and beverages (Kataoka *et al.*, 2000; Wardencki *et al.*, 2004). Satisfactory quantitation of volatile flavour components has been achieved under specific sampling conditions in many studies (Holt, 2001; Steffen and Pawliszyn, 1996), however relatively low enrichment factors, due to the often unfavourable phase ratio between the fibre and sample (Baltussen *et al.*, 1999; Smith, 2003), and reportedly low precision (Wardencki *et al.*, 2004), are disadvantages of the SPME technique. While the sensitivity of SBSE, HCSP and SPACE is much higher than that of SPME, these techniques require cryotrapping or cryofocussing of the analyte bands. Due to the automation of the three stages of SBSE and HCSP analyses, *viz.* introduction of the stir bar or HCSP into a thermal desorption unit, cryofocussing of the desorbed volatiles and subsequent gas chromatographic (GC) analysis, these techniques are relatively complex and require expensive instrumentation.

The SEP (Figs. 2.1 and 2.2) affords a sample enrichment method in which the simplicity of SPME and the high capacity of SBSE are combined and which is, although not as sophisticated as these methods, a versatile and sensitive method that can be used by untrained personnel for exploratory work in situations that do not require automated high sample throughput. As in the case of SPME, SEP analysis does not involve organic solvents and requires no cryofocussing. The reproducibility, repeatability and accuracy of the SEP method have been established and reported (Burger *et al.*, 2006, 2010 [submitted for publication]).

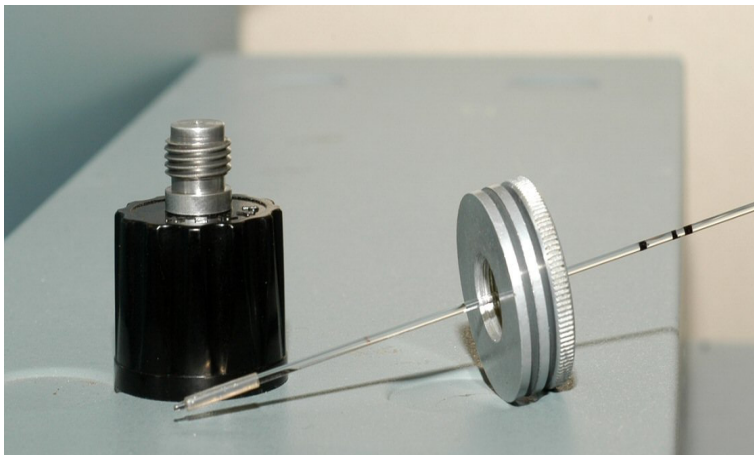


Fig 2.1: SEP installed in a GC injector cap.



Fig. 2.2: SEP installed for sampling headspace volatiles from dry, fermented honeybush.

The effectiveness of this technique in the analysis of samples containing only trace amounts of volatile constituents has been demonstrated by an exploratory comparison of the results of solid-phase microextraction-gas chromatography-mass spectrometry (SPME-GC-MS) and sample enrichment probe-gas chromatography-mass spectrometry (SEP-GC-MS) analyses of the aroma of dry, fermented plant material of *Aspalathus linearis*, known as rooibos tea (Burger *et al.*, 2006). In spite of a long sample enrichment period of 24 h, only some of the peaks visible in the higher retention-time range of the total ion chromatogram (TIC) of the material enriched by SPME gave mass spectra that contained useful diagnostic information. In contrast, sample enrichment for 24 h in the case of a SEP-GC-MS analysis gave more than 140 library searchable or interpretable mass spectra. In the present study, comparison of the results of headspace solid-phase microextraction-gas chromatography-mass spectrometry (HS-SPME-GC-MS) (Fig. 2.3) and headspace sample enrichment probe-gas chromatography-mass spectrometry (HS-SEP-GC-MS) (Fig. 2.4) analyses confirmed that the much higher capacity of the SEP produced results that were clearly superior and the latter was therefore selected as the method of choice for the analysis of honeybush volatiles.



Sample: HBS GENISTOIDES SPME 5h(2) P275(PS089) 40-280 @ 2C/min

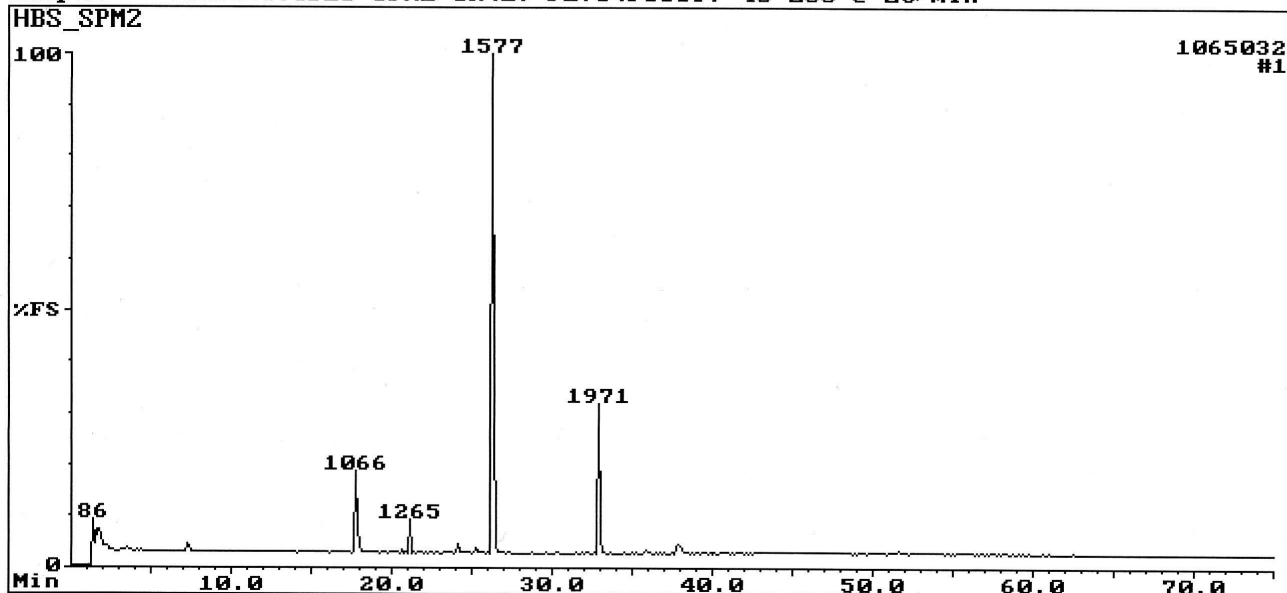


Fig. 2.3: Volatile compounds in dry, fermented honeybush analysed by HS-SPME-GC-MS.

Sample: HBS GENISTOIDES GE 5h SEP(3) P275(PS089) 40-280 @ 2C/min

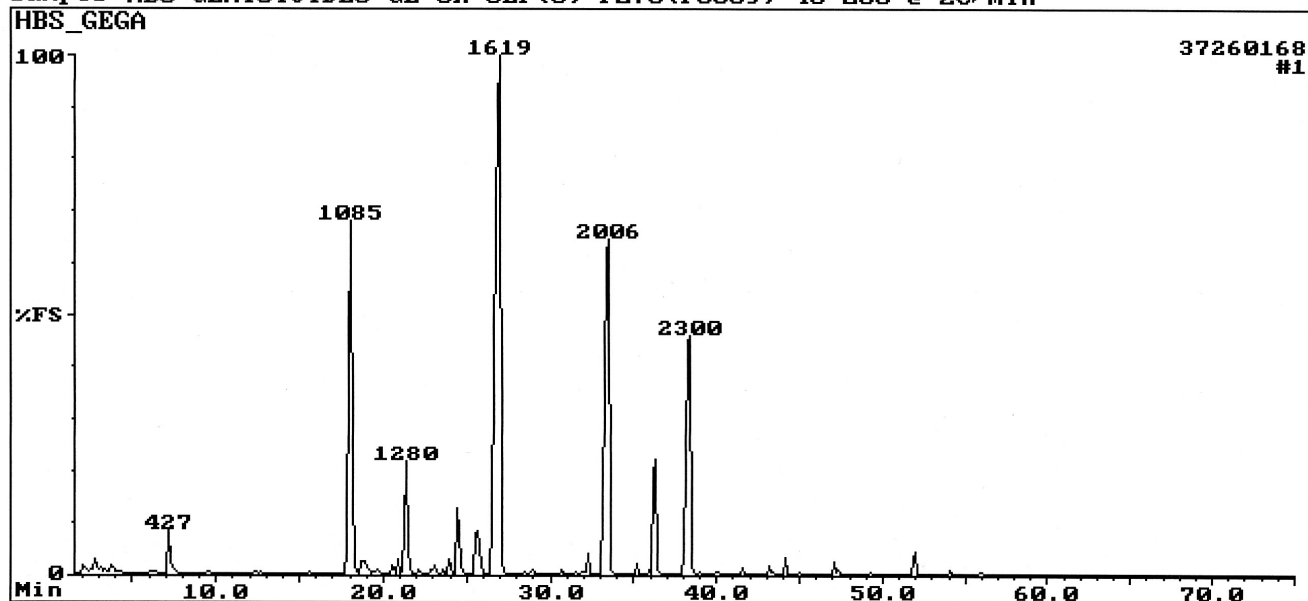


Fig. 2.4: Volatile compounds in dry, fermented honeybush analysed by HS-SEP-GC-MS.

### 2.1.3 Increased-capacity sample enrichment probe extraction technique

An attempt was made to improve the enrichment of headspace volatiles by manufacturing a high-capacity sample enrichment device (Fig. 2.5), which contained 1 m polydimethylsiloxane (PDMS) tubing, compared to 3 cm used in conventional SEPs. The adsorbed headspace volatiles were extracted from the PDMS rubber with dichloromethane (DCM) prior to GC-MS analysis, as described in § 8.3.2. It was hoped that this technique would simplify the GC-O experiments, since it is easier to analyse portions of the same extract instead of having to prepare a separate infusion for each analysis.



Fig. 2.5: High-capacity sample enrichment device comprising coiled PDMS tubing (left) and installed for sampling headspace volatiles from dry fermented honeybush material (right).

Chromatograms of the headspace volatiles extracted from a standard honeybush infusion and dry honeybush plant material (coarse and finely ground) by means of the high-capacity SEP are shown in Figs. 2.6, 2.7 and 2.8, respectively.

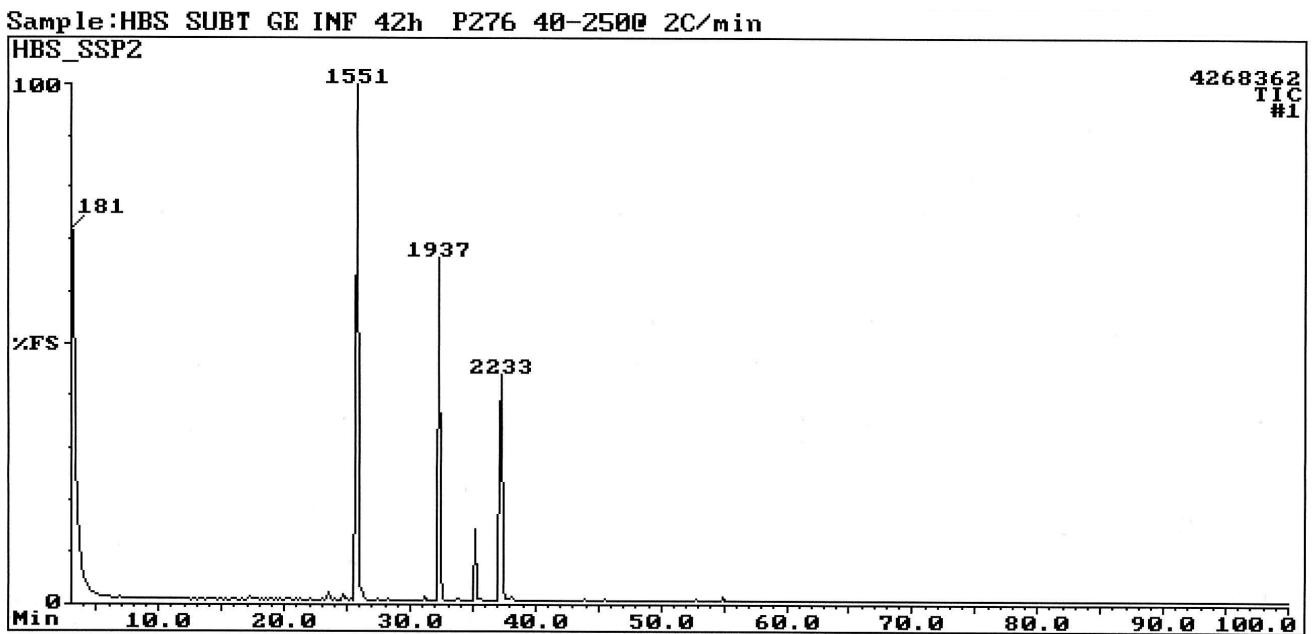


Fig. 2.6: TIC of VOCs extracted from the headspace of a standard honeybush infusion over a period of 42 h by means of a high-capacity SEP.

Sample:HBS SUBT GE 48h P276 40-2500 2C/min

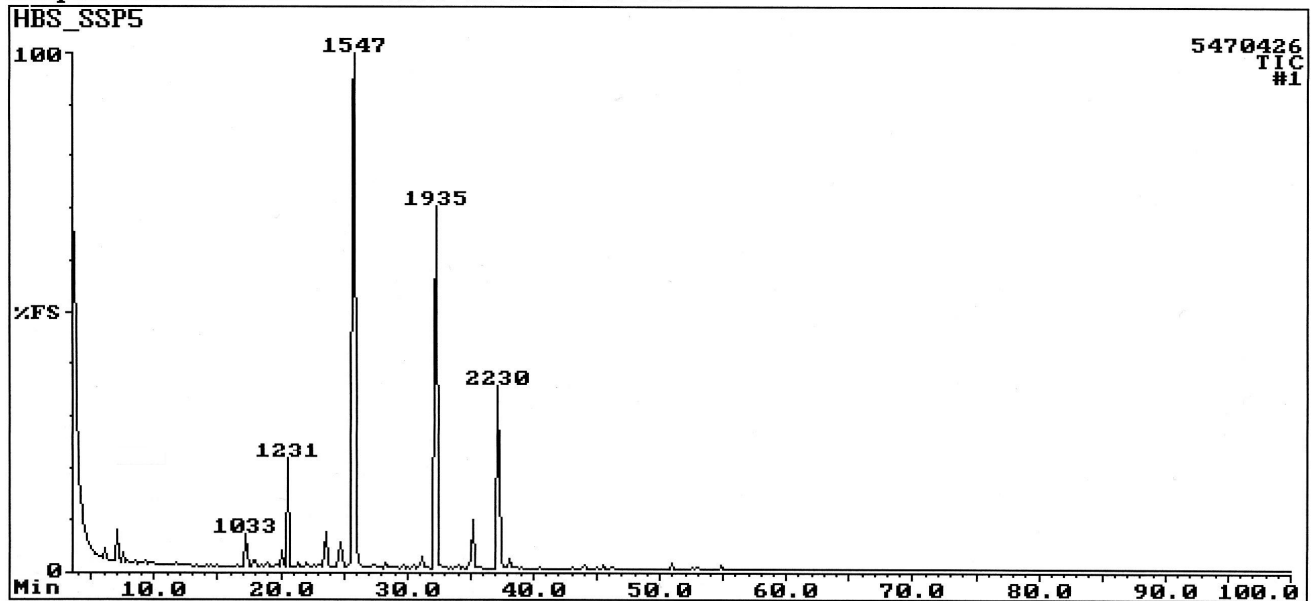


Fig. 2.7: TIC of VOCs extracted from the headspace of dry honeybush plant material over a period of 48 h by means of a high-capacity SEP.

Sample:HBS SUBT GE Ekstr.P128-2 (PS089) 40-28C @ 2C/min

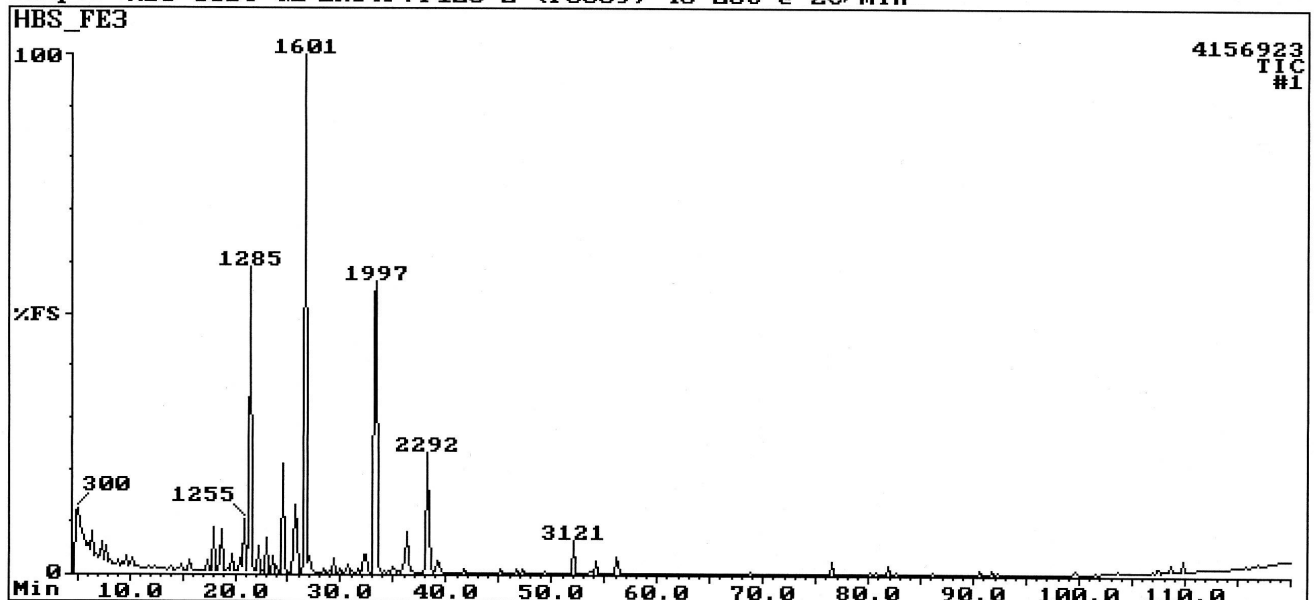


Fig. 2.8: TIC of VOCs extracted from the headspace of dry, finely ground honeybush plant material over a period of five days by means of a high-capacity SEP.

The extraction of the VOCs from the headspace of the standard honeybush infusion was not very successful. Only the volatile compounds present in very high concentrations were extracted.

During the long extraction period water droplets formed on the surface of the PMDS rubber and probably hindered the efficient adsorption of the organic volatiles to some extent. More peaks were observed in the chromatogram obtained by sampling dry plant material (Fig. 2.7), but this analysis was still not better than analyses obtained by direct SEP sampling of the headspace of an infusion. When extending the sampling period from 48 h to five days and using finely ground plant material more peaks were observed (Fig. 2.8) than in the previous two extractions with the high-capacity SEP. However, the results were still not that much better than those obtained by direct SEP sampling of the headspace of an infusion, probably because the effectiveness of the extraction is determined by the rate of the release of the volatiles from the plant material and not by the rate of sorption of the volatiles in the rubber. The standard SEP method was therefore preferred to the cumbersome extraction of headspace volatiles by means of the increased-capacity SEP. Furthermore, the most volatile compounds will be lost during the concentration of the extract.

#### 2.1.4 Conventional solvent extraction

Solvent extraction of dry honeybush plant material was examined as a possible sampling method before headspace SEP sampling was finally chosen as the preferred sampling method for use in this study. This method proved to be unsuccessful however, since very few VOCs were successfully extracted, and a large number of high boiling compounds dominated the chromatogram (Fig. 2.9). These non-volatile compounds were considered irrelevant to this study in which only volatile compounds that can contribute to the aroma of the sample are of importance. The analysis of these high boiling compounds also required long analysis times and additional high-temperature conditioning that was time consuming and possibly also detrimental to the GC columns used.

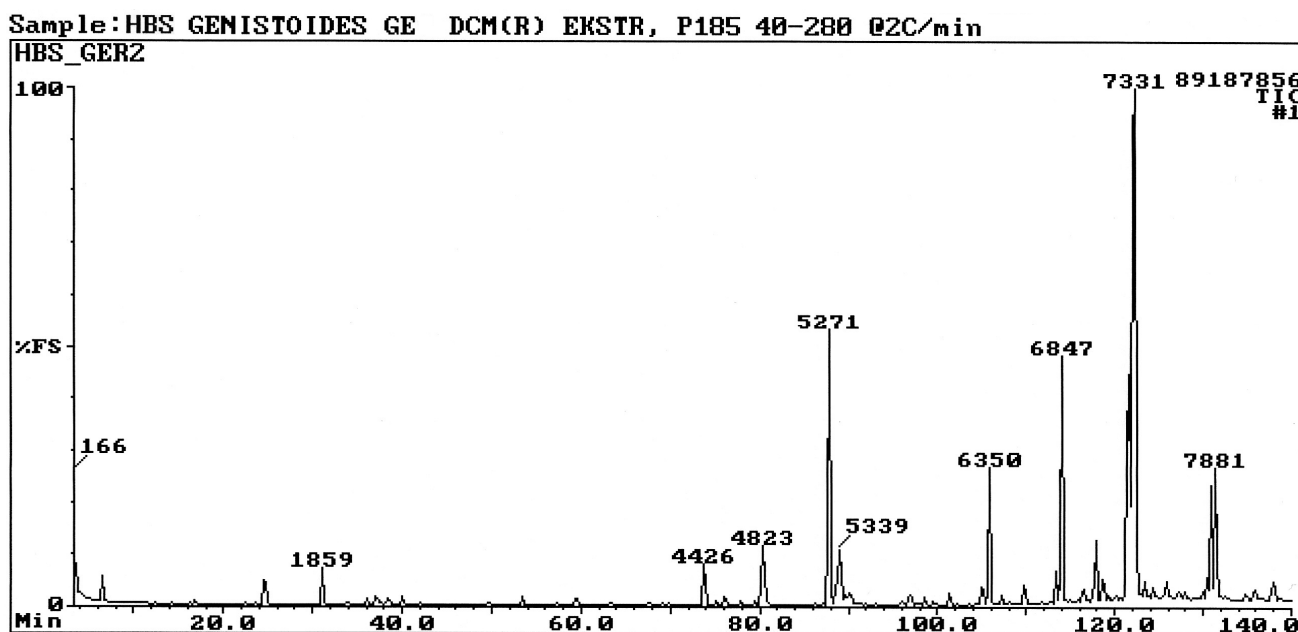


Fig. 2.9: TIC obtained by GC-MS analysis of a DCM extract of dry honeybush plant material.

## 2.2 ANALYTICAL TECHNIQUES

### 2.2.1 Gas chromatography-mass spectrometry

The VOCs in unfermented (green) and fermented samples of *C. genistoides*, as well as in fermented samples of various *Cyclopia* species, were successfully analysed under the conditions and with the columns specified in Chapter 8 (§ 8.4.2). Typical examples of TICs obtained by GC-MS analysis of infusions of unfermented and fermented honeybush are presented in Figs. 2.10 and 2.11.

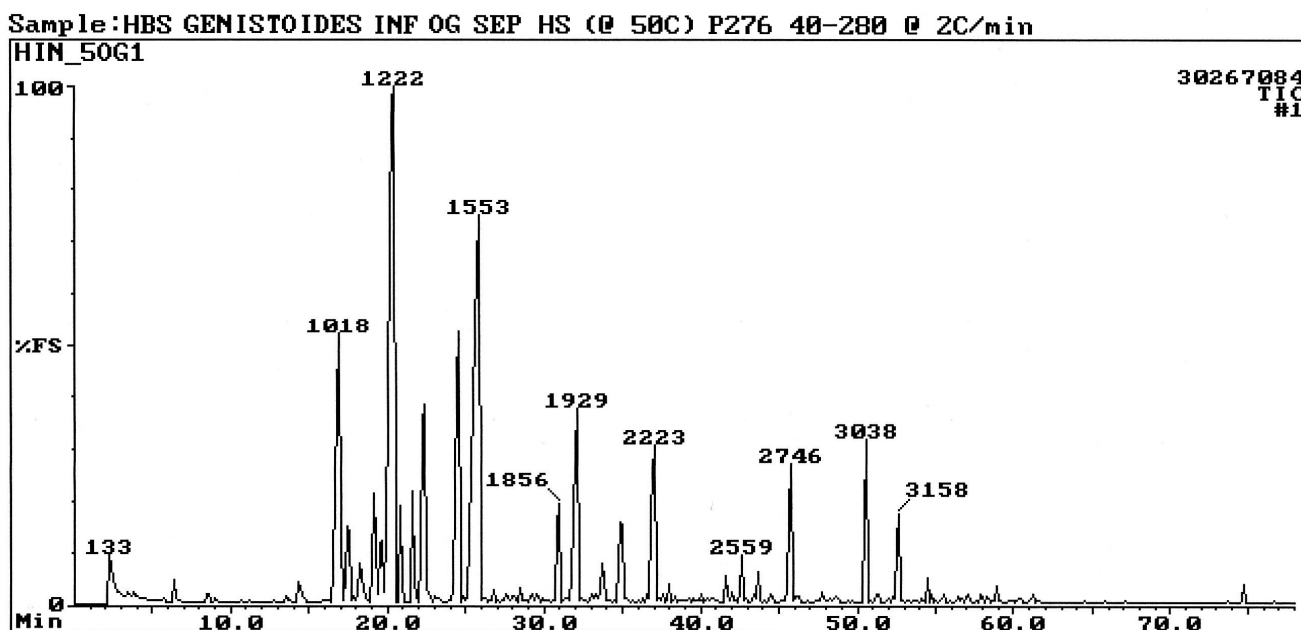


Fig. 2.10: TIC obtained by HS-SEP-GC-MS analysis of unfermented honeybush infusion.

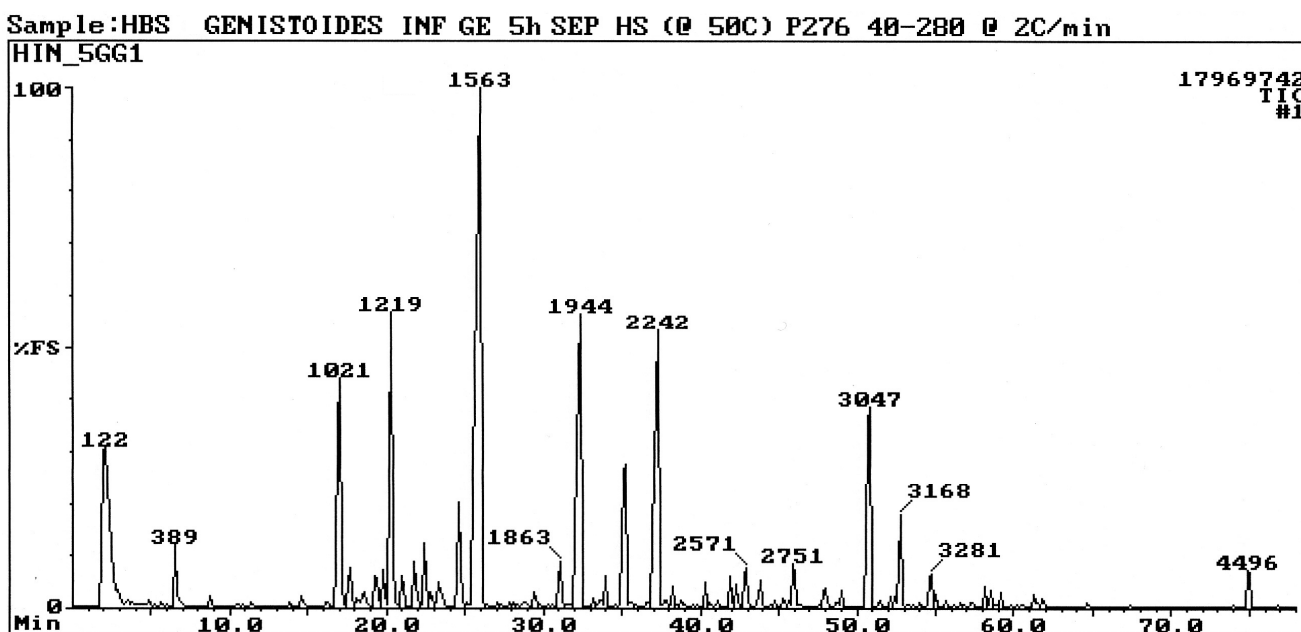


Fig. 2.11: TIC obtained by HS-SEP-GC-MS analysis of fermented honeybush infusion.

## 2.2.2 Gas chromatography-high-resolution mass spectrometry

GC separation of the constituents of complex mixtures in conjunction with high-resolution mass spectrometry (HRMS) is a powerful analytical tool with which the elemental composition of molecular ions as well as other important diagnostic ions in the mass spectra of analytes can be determined. The gas chromatograph-time-of-flight-high-resolution mass spectrometer (GC-TOF-HRMS) that became available during the later stages of the present investigation also proved more sensitive than the quadrupole instruments that were initially used. Although the information obtained with this instrument was used mainly to confirm the qualitative information that had already been obtained with the quadrupole instruments, it also furnished invaluable information on the presence and composition of molecular ions that could previously not be detected in the mass spectra of some of the constituents present in trace concentrations in the samples that were analysed. The high data acquisition rate of the instrument also allowed deconvolution of overlapping peaks in the TIC. This made high quality mass spectral information available and it was thus possible to identify compounds for which the online mass spectral libraries could not suggest feasible candidate structures, and which would otherwise have remained unidentified. In high-resolution analyses with this instrument, mass differences of less than 5 mDa between the observed mass and the mass calculated for a specific ion were considered acceptable.

For the purpose of GC-HRMS analysis headspace volatiles were sampled by both SPME and SEP. A combination of shorter and longer SPME and SEP enrichment times were used to obtain analyses in which as many as possible of the molecular ions and diagnostic ions could be detected and their masses measured accurately to obtain reliable elemental compositions of the particular ions.

## 2.2.3 Enantioselective gas chromatography-mass spectrometry

Because LECUS has a wide range of enantioselective GC columns available, enantioselective GC was the method of choice for the determination of the absolute configuration of the chiral constituents of the honeybush samples. The best results were obtained with glass columns coated with OV-1701-OH containing suitably derivatised  $\beta$ -cyclodextrins as chiral selectors. OV-1701-OH is a moderately polar stationary phase from which even the lower carboxylic acids elute as reasonably sharp peaks and the higher acids as peaks with the peak widths of apolar compounds. Details of the columns and conditions used during these analyses are given in § 8.4.4.

## 2.2.4 Gas chromatography-olfactometry and gas chromatography-mass spectrometry-olfactometry

A conventional GC was converted for GC-O use by installing a glass effluent splitter, a humidified air conduit, and a glass sniffing port (see Fig. 2.12). Details of the instrumentation and the

methodology used are given in § 8.4.7. The specific GC-O methods used in this study are discussed in Chapter 4.



Fig. 2.12: Evaluator assessing the column effluent at the sniffing port of the GC-O apparatus.

A GC-MS-O became available for use only later in the present study. It was used to confirm the results obtained by GC-O analysis.

## 2.3 REFERENCES

- Acree, T.E., Barnard, J., Cunningham, D.G. 1984. A procedure for the sensory analysis of gas chromatographic effluents. *Food Chem.* **14**, 273–286.
- Acree, T.E. in: Acree, T.E., Teranishi, R. (Eds.). 1993. Flavor science: Sensible principles and techniques. American Chemical Society, Washington DC, pp. 1–22.
- Arthur, C.L., Pawliszyn, J. 1990. Solid-phase microextraction with thermal desorption using fused silica optical fibres. *Anal. Chem.* **62**, 2145–2148.
- Baltussen, E., Sandra, P., David, F., Cramers, C. 1999. Stir bar sorptive extraction (SBSE), a novel extraction technique for aqueous samples: Theory and principles. *J. Microcolumn Sep.* **11**, 737–747.
- Burger, B.V., le Roux, M., Marx, B., Herbert, S.A., Amakali, K.T. 2010. Improved performance of second-generation sample enrichment probe (SEP) for sorptive analysis of volatile organic compounds. Submitted for publication in *J. Chromatogr. A*.
- Burger, B.V., Marx, B., le Roux, M., Burger, W.J.G. 2006. Simplified analysis of organic compounds in headspace and aqueous samples by high-capacity sample enrichment probe. *J. Chromatogr. A* **1121**, 259–267.
- Du Toit, J., Joubert, E. 1999. Optimization of the fermentation parameters of honeybush tea (*Cyclopia*). *J. Food Qual.* **22**, 241–256.
- Holt, R.U. 2001. Mechanisms effecting analysis of volatile flavour components by solid-phase microextraction and gas chromatography. *J. Chromatogr. A* **937**, 107–114.
- Ishikawa, M., Ito, O., Ishizaki, S., Kurobayashi, Y., Fujita, A. 2004. Solid-phase aroma concentrate extraction (SPACE<sup>TM</sup>): A new headspace technique for more sensitive analysis of volatiles. *Flavour Fragr. J.* **19**, 183–187.
- Kataoka, H., Lord, H.L., Pawliszyn, J. 2000. Application of solid-phase microextraction in food analysis. *J. Chromatogr. A* **880**, 35–62.
- Pettersson, J., Kloskowski, A., Zaniol, C., Roeraade, J. 2004. Automated high-capacity sorption probe for extraction of aqueous samples followed by gas-chromatographic analysis. *J. Chromatogr. A* **1033**, 339–347.
- Risticvic, S., Niri, V.H., Vuckovic, D., Pawliszyn, J. 2009. Recent developments in solid-phase microextraction. *Anal. Bioanal. Chem.* **393**, 781–795.
- Schuh, C., Schieberle, P. 2006. Characterization of the key aroma compounds in the beverage prepared from Darjeeling black tea: Quantitative differences between tea leaves and infusion. *J. Agric. Food Chem.* **54**, 916–924.
- Smith, R.M. 2003. Before the injection—modern methods of sample preparation for separation techniques. *J. Chromatogr. A* **1000**, 3–27.
- Steffen, A., Pawliszyn, J. 1996. Analysis of flavor volatiles using headspace solid-phase microextraction. *J. Agric. Food Chem.* **44**, 2187–2193.



- Vas, G., Vékey, K. 2004. Solid-phase microextraction: A powerful sample preparation tool prior to mass spectrometric analysis. *J. Mass Spectrom.* **39**, 233–254.
- Wardencki, W., Michulec M., Curylo, J. 2004. A review of theoretical and practical aspects of solid-phase microextraction in food analysis. *Int. J. Food Sci. Tech.* **39**, 703–717.
- Wright, J., Wulfert, F., Hort, J., Taylor, A.J. 2007. Effect of preparation conditions on release of selected volatiles in tea headspace. *J. Agric. Food Chem.* **55**, 1445–1453.

## CHAPTER 3

# CHEMICAL CHARACTERISATION OF THE VOLATILE COMPOUNDS PRESENT IN HONEYBUSH (*Cyclopia*)

### 3.1 IDENTIFICATION METHODS

During the present study the identification of volatile constituents of honeybush species was primarily based on their electron impact (EI) mass spectra as tentative starting point. The interpretation of the mass spectra of the majority of volatile constituents present in unfermented and fermented honeybush was facilitated by initial computerised library searches using online and offline reference libraries of mass spectrometric (MS) data (Adams, 2004; NBS, 1990; NIST, 2005).

As far as practically possible, the identification of constituents was confirmed by GC-MS retention time comparison with authentic, commercially available synthetic compounds, compounds that were available from previous LECUS research projects, or compounds that were synthesised during the course of the present investigation. Solutions of the synthetic compounds in DCM were prepared either individually or as mixtures. In the discussions below where retention time comparison is mentioned, it implies that the MS properties of the compounds under discussion were also taken into consideration. Retention indices (RIs) (relative to C<sub>5</sub>–C<sub>18</sub> *n*-alkanes) (Kovats, 1958; Van den Dool and Kratz, 1963) were also determined to confirm the identification of the constituents under investigation. Molecular formulae mentioned in the discussions of mass spectra were determined by GC-HRMS analysis, which supplied important information on the accurate masses and elemental compositions of molecular ions and ion fragments of those constituents that proved difficult to identify by means of gas chromatography-low resolution electron impact mass spectrometry (GC-LRMS) and RI data only.

The interpretation of the mass spectra of constituents that were relatively easy to identify, and of which MS fragmentation patterns are available in the literature, is discussed only very briefly. Detailed discussions of MS fragmentation mechanisms are only included in this chapter in those cases where no mass spectral library data and/or no reference compounds were available and discussion of the relevant mass spectrum was therefore necessary to prove a point or support the tentative identification of a component. In some cases short discussions of the identification processes leading up to the final characterisation of certain components are included for the sake of interest. However, the mass spectra of the terpenoids are generally discussed in greater detail, since terpenoids constitute the largest group of compounds identified in honeybush. Many of the terpenoids were found to be odour-active, and the identification of terpenoids proved to be the most interesting and the greatest challenge in this research project. Although many studies have been conducted by

LECUS on complex mixtures of volatile compounds, e.g. semiochemicals this is the first study in which such a large number of terpenoids have been encountered and successfully identified.

Mass spectra obtained in GC-MS analyses of both unfermented and fermented honeybush, with both the apolar column A (Figs. 3.1 and 3.2, respectively) as well as polar column B, were used for identification purposes. The peaks in the TIC (Fig. 3.2) of the honeybush volatiles are numbered from C1 to C299 and these numbers are used when reference is made to a component under discussion. The TICs and the individual mass spectra of the components are given at the end of this chapter in order to avoid undue fragmentation of the text. A complete list of all the volatile compounds identified in honeybush is tabulated in Table 3.4 and the representative compound classes are summarised in Table 3.3.

The determination of the absolute configuration of the 94 chiral compounds present in the aroma of *Cyclopia* species proved difficult, mainly because most of these compounds are terpenoids, and only a limited range of reference samples of the terpenes in question are commercially available. In cases where only one of the enantiomers was available as reference compound only one peak was observed in an enantioselective GC-MS analysis of a terpenoid with one stereogenic centre, and without published information on the enantioselective resolution of the racemic compound it was impossible to determine the absolute configuration of the natural constituent. With the exception of the conversion of certain commercially available terpenoids to appropriate derivatives, it was not possible to synthesise the majority of these chiral compounds due to time constraints. Furthermore, many of these chiral compounds were not identified as odour-active in the GC-O analyses. Some were also present in the material under investigation in such low concentrations that they were not observed in analyses using enantioselective columns, probably due to the low programming rate that had to be used for optimal resolution, or to overlapping by other constituents. Information that was nevertheless obtained from enantioselective GC-MS analyses of available reference compounds is briefly discussed, and summarised in Table 3.5.

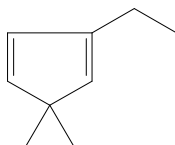
## 3.2 STRUCTURE DETERMINATION OF HONEYBUSH VOLATILES

### 3.2.1 Saturated and unsaturated aliphatic hydrocarbons

The mass spectra of saturated unbranched hydrocarbons consist of clusters of peaks, 14 mass units ( $\text{CH}_2$ ) apart, exhibiting decreasing intensities with increasing fragment mass (Pasto and Johnson, 1969: 266). The most abundant ions in these clusters are of the general formulae  $[\text{C}_n\text{H}_{2n+1}]^+$  ( $m/z$  29, 43, 57, 71, ...) and to a lesser extent  $[\text{C}_n\text{H}_{2n-1}]^+$  ( $m/z$  27, 41, 55, ...), with abundance maxima around C-3 or C-4. The molecular ion is usually present, but is normally of low abundance (McLafferty and Tureček, 1993: 226). The EI mass spectra of components **C46**, **C80**, **C126**, **C170**, **C211**, **C241**, **C276** (Fig. 3.3), **C296** and **C297** all exhibit these characteristic clusters of ions. These components have molecular ions at  $m/z$  142, 156, 170, 184, 198, 226, 240 and 254, respectively, and were identified as the alkanes **decane**, **undecane**, **dodecane**, **tridecane**, **tetradecane**,

**pentadecane, hexadecane, heptadecane and octadecane.** The identification of these components was confirmed by retention time comparison with the corresponding commercially available alkanes.

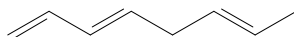
An elemental composition of  $C_9H_{14}$  was determined for the molecular ion present at  $m/z$  122 in the EI mass spectrum of component **C7** (Fig. 3.4), indicating that this component is a hydrocarbon with three degrees of unsaturation, i.e. three double bonds or a cyclic structure with two double bonds. An online library search (NIST) suggested **2-ethyl-5,5-dimethyl-1,3-cyclopentadiene** with a correlation factor of 81%.



2-Ethyl-5,5-dimethyl-1,3-cyclopentadiene

The main fragmentation process observed for methyl-substituted cyclopentadienes is loss of a methyl radical followed by further decomposition of the  $[M - CH_3]$  species (Budzikiewicz *et al.*, 1967: 64; Harrison *et al.*, 1965).

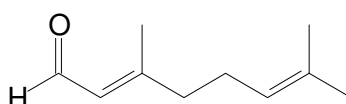
The mass spectrum of component **C12** (Fig. 3.5) has a base peak at  $m/z$  79 and molecular ion at  $m/z$  108. The online library search (NBS) predicted with 91% certainty that **C12** could be **1,3,6-octatriene**.



1,3,6-Octatriene

The elemental composition of  $C_8H_{12}$  obtained for **C12** by HRMS provided further evidence that it should be a compound with three degrees of unsaturation. Alkene ions have a strong tendency to isomerise *via* the migration of the double bond, and this phenomenon might explain the formation of the ion at  $m/z$  79 ( $C_6H_7^+$ ) when migration of the double bond affords the loss of an ethyl group (McLafferty and Tureček, 1993: 230).

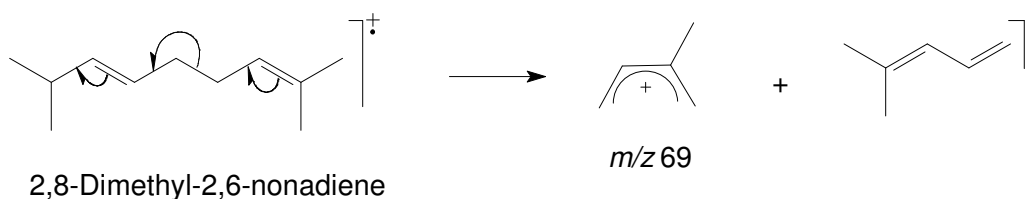
Component **C67** (Fig. 3.6) has a base peak at  $m/z$  69 and molecular ion at  $m/z$  152 ( $C_{11}H_{20}^+$ ). Although the NIST and NBS libraries predicted geranial as a possible candidate, this is not correct, since it has a molecular formula of  $C_{11}H_{16}O$ . Component **C67** should however be a similar compound, in order to afford so many of the ions also present in the mass spectrum of geranial.



Geranial

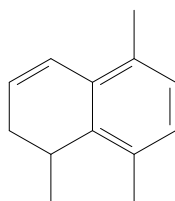
**2,8-Dimethyl-2,6-nonadiene** was considered to be the best possible candidate structure. Losses of methyl, ethyl and isopropyl groups result in the formation of the ions at  $m/z$  137 ( $C_{10}H_{17}^+$ ), 123

( $C_9H_{15}^+$ ) and 109 ( $C_8H_{13}^+$ ). The base peak at  $m/z$  69 ( $C_5H_9^+$ ) is formed by cleavage of the bi-allylic bond:



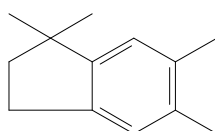
### 3.2.2 Aromatic hydrocarbons

In the mass spectrum of component **C189** (Fig. 3.7) the only ions with abundances of approximately 20% and higher appear in the upper mass range at  $m/z$  115, 128, 141, 142, 157 (base peak) and 172 ( $M^+$ ). HRMS gave  $C_{13}H_{16}$  as the elemental composition of **C189**, which corresponds to that of **1,5,8-trimethyl-1,2-dihydronaphthalene**, suggested by two different online library searches (NBS and NIST), with a correlation factor of 87%. Loss of one or two methyl groups from the molecular ion affords the ions at  $m/z$  157 ( $C_{12}H_{13}^+$ ) and  $m/z$  142 ( $C_{11}H_{10}^+$ ), respectively.



1,5,8-Trimethyl-1,2-dihydronaphthalene

The mass spectrum of component **C192** (Fig. 3.8) contains ions at  $m/z$  174, 159 and 144, i.e. two mass units higher than the ions at  $m/z$  172, 157 and 142 observed in the mass spectrum of **C189**, suggesting that **C192** might be a similar compound but with one double bond fewer. Two online library searches (NBS and NIST) presented **2,3-dihydro-1,1,5,6-tetramethyl-1H-indene** as the most likely candidate structure for **C192** (86% and 74% correlation respectively).

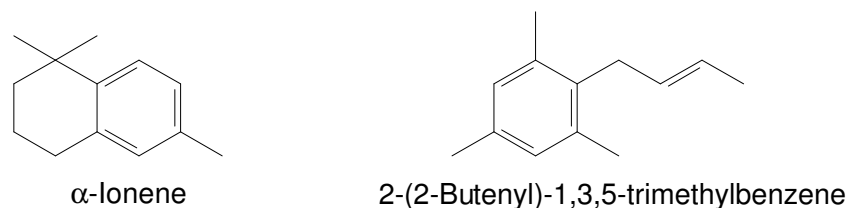


2,3-Dihydro-1,1,5,6-tetramethyl-1H-indene

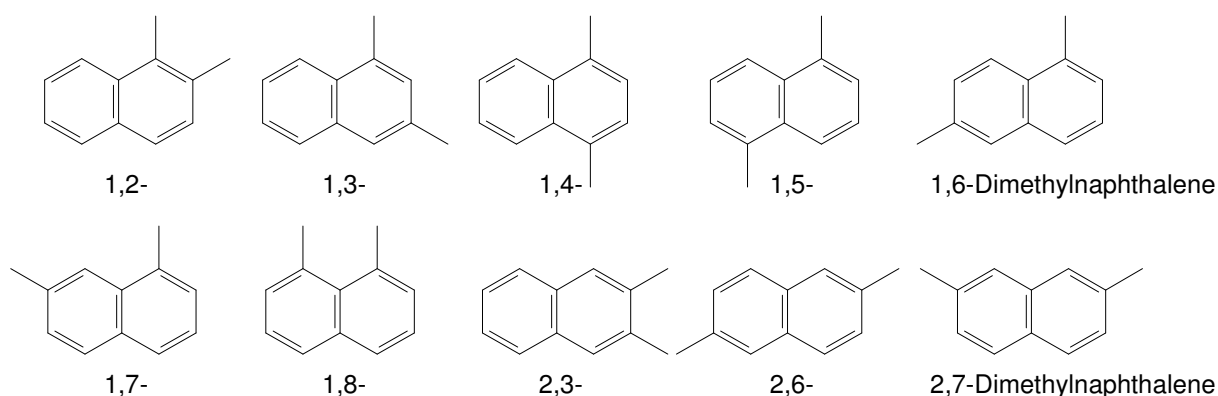
The loss of one, two or three methyl groups is responsible for the formation of the ions at  $m/z$  159 ( $C_{12}H_{15}^+$ ), 144 ( $C_{11}H_{12}^+$ ) and 129 ( $C_{10}H_9^+$ ), respectively.

Components **C147** (Fig. 3.9) and **C193** have mass spectra similar to that of **C192**, and also have the same elemental composition ( $C_{13}H_{18}$ ) as **C192**. An online library search (NIST) suggested that both components could be  $\alpha$ -ionene. Component **C193** was tentatively identified as  $\alpha$ -ionene,

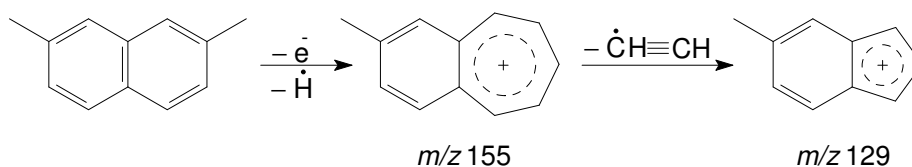
based on the agreement with available RI data (Gomez *et al.*, 1993) and **C147** was identified as **2-(2-butenyl)-1,3,5-trimethylbenzene** based on the similarities between its mass spectrum and the mass spectrum available in the NIST library. The ions at  $m/z$  159 and 144 form in the same way as already discussed for **C192**.



The mass spectrum of component **C213** (Fig. 3.10) has characteristic ions of high intensity in the upper mass range of the spectrum at  $m/z$  115, 128, 141 and 156 ( $M^+$ ,  $C_{12}H_{12}^+$ ). According to its mass spectrum this component could be any one of the following dimethyl naphthalenes:



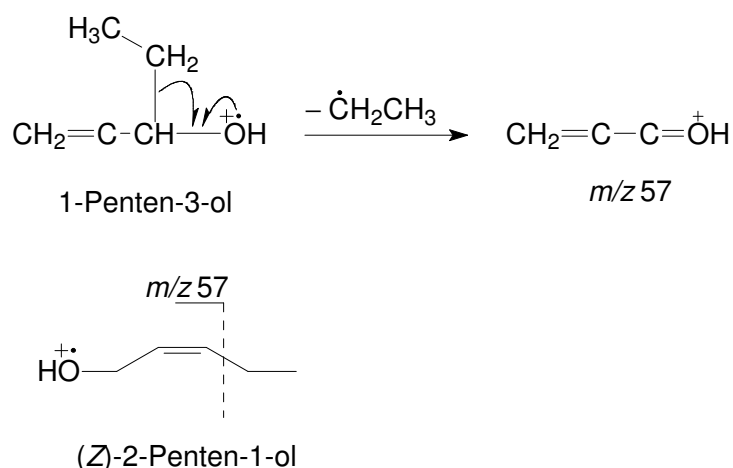
The RIs available in the NIST library for 2,6-dimethylnaphthalene and 2,7-dimethylnaphthalene were closest to the RI obtained for **C213**, and these two isomers were therefore considered the most likely possibilities. However, the RI obtained for commercially available 2,6-dimethylnaphthalene was lower than the RI of **C213**, and therefore 2,6-dimethylnaphthalene was eliminated as possible candidate. 2,7-Dimethylnaphthalene was also eliminated since its RI (Lai and Song, 1995) is very close to that of 2,6-dimethylnaphthalene. According to RI data (Lai and Song, 1995) the most likely remaining candidate was **1,3-dimethylnaphthalene** and therefore **C213** was tentatively identified as this compound. An important fragmentation of alkylated polycyclic aromatics, such as naphthalenes, involves the elimination of acetylene after the loss of a hydrogen atom as illustrated for 2,7-dimethylnaphthalene in the following scheme, and affords the ions present at  $m/z$  155 ( $C_{12}H_{11}^+$ ) and  $m/z$  129 ( $C_{10}H_9^+$ ) in the mass spectrum of **C213** (Budzikiewicz *et al.*, 1967: 87).



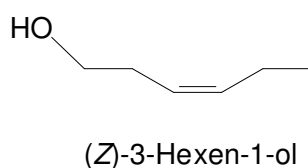
### 3.2.3 Saturated and unsaturated aliphatic alcohols

Components **C4**, **C10** and **C65** have EI mass spectra (Fig 3.11) containing two series of characteristic ions at  $m/z$  41, 55, 69, ... and  $m/z$  43, 57, 71, ..., corresponding to the general formulae  $[C_nH_{2n-1}]^+$  and  $[C_nH_{2n+1}]^+$ , which are typically found in the mass spectra of unbranched 1-alkanols and 1-alkenes (Budzikiewicz *et al.*, 1967: 94–102; Dolejs *et al.*, 1968; McLafferty, 1973: 113–116). A library search (NBS) suggested that **C4**, **C10** and **C65** could be **1-pentanol**, **1-hexanol** and **1-octanol** (94%, 93% and 91% correlation, respectively) and this was confirmed by retention time comparison with the corresponding commercially available alcohols.

Components **C1** and **C5** (Fig. 3.12) have very similar mass spectra with, a base peak at  $m/z$  57. A library search (NBS) suggested that **C1** and **C5** could be **1-penten-3-ol** and **(Z)-2-penten-1-ol** (86% and 87% correlation), respectively. This was confirmed by retention time comparison with the commercially available compounds. In the case of 1-penten-3-ol the ion at  $m/z$  57 is formed *via*  $\alpha$ -cleavage of the bond  $\beta$  to the oxygen atom, whereas for **(Z)-2-penten-1-ol** (a 1-alkanol) the same ion is preferably formed by loss of an ethyl group (McLafferty and Tureček, 1993: 241):

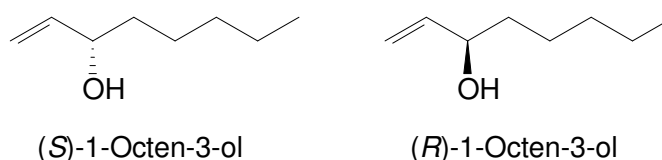


The EI mass spectrum of component **C9** (Fig. 3.13) has a molecular ion at  $m/z$  100, two mass units lower than that of 1-hexanol, suggesting that this component could be a hexenol. The NBS library suggested that this component could be **(Z)-3-hexen-1-ol** (95% correlation), which was confirmed by retention time comparison with commercially available **(Z)-3-hexen-1-ol**.

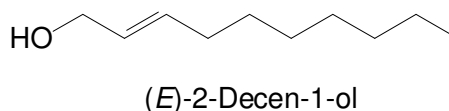


The EI mass spectrum of component **C31** (Fig. 3.14), does not contain any detectable molecular ion, but a molecular mass of 128 Da was assumed, based on logical fragmentations and the RI of this component. A library search (NBS) suggested **1-octen-3-ol** as the best possible

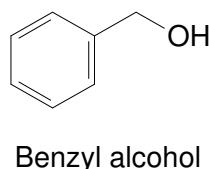
candidate structure (92% correlation) and GC-MS comparison with commercially available 1-octen-3-ol confirmed this identification. The enantiomers of 1-octen-3-ol were resolved on chiral column D coated with the stationary phase OV-1701-OH containing heptakis(2,3-di-*O*-acetyl-6-*O*-tert-butyltrimethylsilyl)- $\beta$ -cyclodextrin as chiral selector ( $R_s$  value of 1.5). The (*S*)-enantiomer of 1-octen-3-ol elutes before its (*R*)-enantiomer from a column containing an equivalent enantioselective phase (Maas *et al.*, 1994b). Enantioselective analysis of honeybush material established the presence of both enantiomers in a ratio of 38:62 (*S*:*R*).



The EI mass spectrum of component **C153** (Fig. 3.15) has prominent ions at  $m/z$  43, 57, 69, 82, 95 and 109. The NBS library suggested undecanal as the best candidate structure, but retention time comparison with this aldehyde revealed that **C153** could not be undecanal. However, a manual NIST library search using the mentioned prominent ions, gave (*E*)-2-decen-1-ol as possible candidate structure. Component **C153** was subsequently identified as this alcohol by retention time comparison with the commercially available compound.



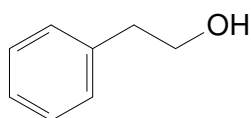
The EI mass spectrum of component **C55** (Fig. 3.16) has prominent ions at  $m/z$  77 and  $m/z$  79 (base peak) and at  $m/z$  107 and  $m/z$  108 ( $M^+$ ). An NBS library search suggested that the component could be **benzyl alcohol** (82% correlation). This was confirmed by retention time comparison with the commercially available compound.



The formation of significant ions in the mass spectrum of benzyl alcohol is discussed in detail in the literature (Budzikiewicz *et al.*, 1967: 119–120; Ethiel *et al.*, 1961; Meyerson *et al.*, 1959).

The EI mass spectrum of component **C79** (Fig. 3.17) has prominent ions at  $m/z$  91 (base peak), 92 and 122 ( $M^+$ ), which are characteristic of 2-phenylethanol and some of its derivatives (Budzikiewicz *et al.*, 1967: 124–125). Retention time comparison with commercially available 2-phenylethanol confirmed the identity of **C79** as **2-phenylethanol**.

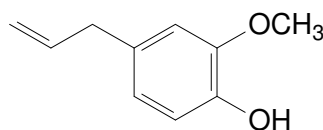




2-Phenylethanol

### 3.2.4 Phenols

Characteristic aromatic ions at  $m/z$  77 and 91 occur in the mass spectrum of component **C191** (Fig. 3.18). The molecular ion is also the base peak at  $m/z$  164. The assumption that **C191** could be **eugenol** was confirmed by an online library search (90% correlation) and by retention time comparison with commercially available eugenol.

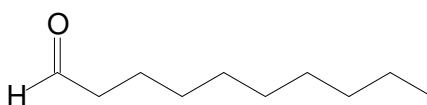


Eugenol

The formation of many of the ions in the mass spectrum of **C191** can be explained in terms of the fragmentation patterns of aromatic and benzyl alkyl ethers (Budzikiewicz *et al.*, 1967: 237–248).

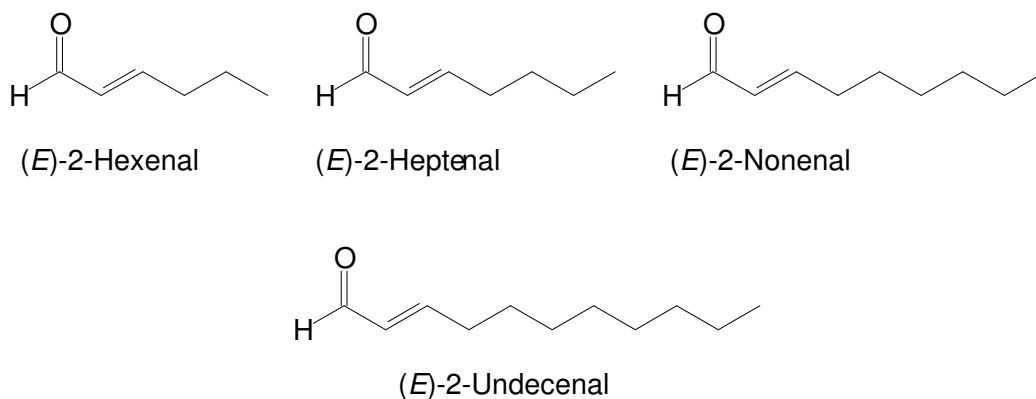
### 3.2.5 Saturated and unsaturated aliphatic aldehydes

In the EI mass spectra of components **C2**, **C6** (Fig. 3.19) and **C17** abundant ions occur at  $m/z$  44, which led to the assumption that these components could possibly be unsaturated, unbranched aldehydes having four to seven carbon atoms (Budzikiewicz *et al.*, 1967: 131). According to NBS library searches, **C2**, **C6** and **C17** could be **pentanal**, **hexanal** and **heptanal** (93%, 97% and 87% correlation) and this was confirmed by retention time comparison with the corresponding commercially available compounds. A number of components have mass spectra similar to the mass spectra of the three aldehydes already mentioned, the major difference being the absence of a prominent ion at  $m/z$  44. This led to the conclusion that these components must be aliphatic aldehydes with more than seven carbon atoms. Components **C39**, **C75**, **C124** (Fig. 3.20), **C167**, **C210** and **C242** were identified as **octanal**, **nonanal**, **decanal**, **undecanal**, **dodecanal** and **tridecanal** after examination of their mass spectra and confirmation by retention time comparison with the corresponding commercially available compounds.

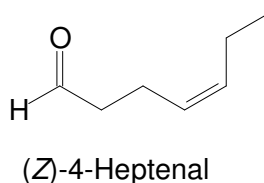


Decanal

The EI mass spectra of components **C8**, **C26**, **C108** (Fig. 3.21) and **C196** have similar prominent ions at  $m/z$  41, 55, 69, 70, 83 and 97. The molecular mass of **C8** is 98 Da, which is two mass units lower than that of hexanal (100 Da), suggesting that **C8** could be a monounsaturated hexenal. This component was tentatively identified as (*E*)-2-hexenal based on the NBS library search (90% correlation). This was confirmed by retention time comparison with the commercially available compound. Using the same arguments, **C26**, **C108** and **C196** were identified as (*E*)-2-heptenal, (*E*)-2-nonenal and (*E*)-2-undecenal. This was confirmed by retention time comparison with the corresponding commercially available compounds.

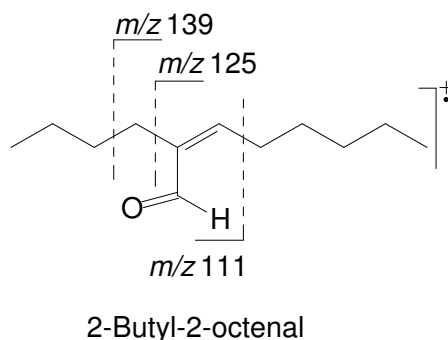


Component **C15** (Fig. 3.22) elutes much earlier than (*E*)-2-heptenal, and just before heptanal. Its mass spectrum displays similar ions to that of (*E*)-2-heptenal, but with apparent differences in the abundances of some of the ions. It was assumed that this component could be a monounsaturated aldehyde. Although no molecular ion was observed the molecular mass was believed to be 112 Da, since the ion at  $m/z$  97, if taken as the molecular mass, could not provide for any sensible fragmentations that would explain the other ions in the mass spectrum. (*Z*)-2-Heptenal was excluded as a possibility, due to differences in the relative abundances of the ions in the mass spectrum of this compound and that of **C15**, as well as to the shorter retention time of **C15**. The only reasonable conclusion was that the double bond was in a different position. The library search (NBS) suggested a monounsaturated aldehyde with the double bond at C-4 (80% correlation). Component **C15** was then identified as (*Z*)-4-heptenal by retention time comparison with commercially available (*Z*)-4-heptenal.



Component **C202** (Fig. 3.23) elutes earlier than dodecanal and has a molecular mass (182 Da) two mass units lower than dodecanal, which indicated that this component is a dodecenal. Although most of the ions typically found in the mass spectra of unsaturated aldehydes occur at  $m/z$  41, 55,

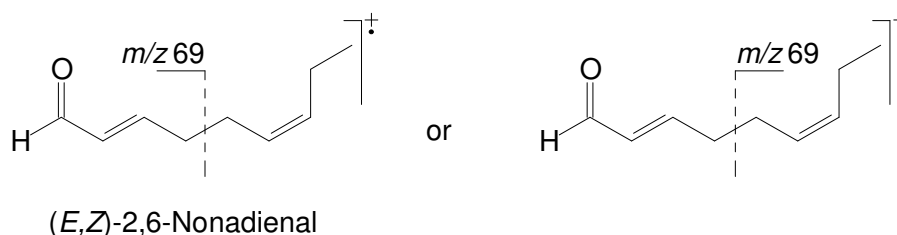
69, 70, 83 and 97, this mass spectrum also contains prominent ions at  $m/z$  111, 125 and 139, distinguishing it from the other unsaturated aldehydes found thus far. An NBS library search identified **C202** as **2-butyl-2-octenal** (80% correlation), and although the compound was not available for retention time comparison the elemental composition ( $C_{12}H_{22}O$ ) determined by means of HRMS analysis was also in accordance with the structure proposed by the library search. The ions at  $m/z$  111 ( $C_7H_{11}O^+$ ), 125 ( $C_8H_{13}O^+$ ) and 139 ( $C_9H_{15}O^+$ ) could be produced by relatively simple cleavage reactions involving the loss of different alkyl fragments to give the following oxygen-containing ions:



The three components **C33**, **C41** (Fig. 3.24) and **C171** (Fig. 3.25) have similar mass spectra with a base peak at  $m/z$  81. Taking into account the molecular mass (110 Da) and retention time of **C41**, this component was assumed to be an unsaturated aldehyde with two double bonds. One of the unique features of the spectra of these components is the absence of an ion at  $m/z$  44, indicating that no McLafferty rearrangement is possible as in saturated aldehydes. The presence of an  $[M - 44]^+$  ion indicates that these components have no substitution in the  $\alpha$ -position (Budzikiewicz *et al.*, 1967: 132). Therefore, it is possible that one of the double bonds might be present at C-2. According to a computerised library search (NBS), **C33** and **C41** are geometric isomers of 2,4-heptadienal. Fortunately the commercially available (*E,E*)-2,4-heptadienal contained (*E,Z*)-2,4-heptadienal as impurity. Retention time comparison revealed that **C33** and **C41** are indeed the two isomers (*E,Z*)-2,4-heptadienal and (*E,E*)-2,4-heptadienal, respectively. Component **C171** was identified as (*E,E*)-2,4-decadienal after inspection of its mass spectrum following results of a computerised library search. This was confirmed by retention time comparison with the commercially available compound.

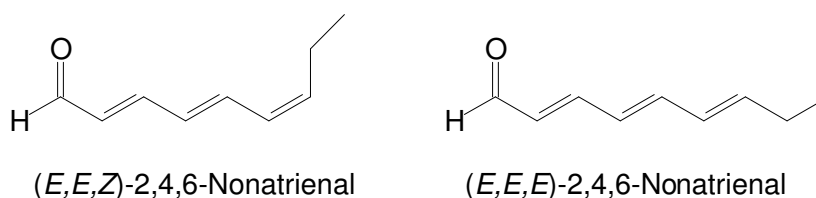
Some of the characteristic ions occurring in the mass spectra of aldehydes can be seen in the mass spectrum of component **C101** (Fig. 3.26) at  $m/z$  41 (base peak), 69 and 70, but no molecular ion was initially visible in the mass spectrum. Once again, the absence of a McLafferty rearrangement ion at  $m/z$  44 indicated the possible presence of a double bond at C-2, but the absence of a base peak at  $m/z$  81 suggested that this component differed from the three aldehydes discussed above. The retention time of this component indicated that it could be a  $C_9$ -aldehyde, since it elutes earlier than (*E*)-2-nonenal, and before decanal. A computerised library search suggested that **C101** could be (*E,Z*)-2,6-nonadienal (88% correlation), which was confirmed by retention time

comparison with the commercially available compound. Normally, the ion at  $m/z$  69 can be either an oxygen-containing fragment or an alkene fragment:



Interestingly, according to the HRMS data obtained for **C101**, the cleavage that leads to an ion with the charge on the oxygen-containing fragment predominates; the ion with nominal mass  $m/z$  69 consists almost exclusively of  $C_4H_5O^+$ . After the identity of **C101** had been established the molecular ion at  $m/z$  138 was detected in the higher mass range of the mass spectrum.

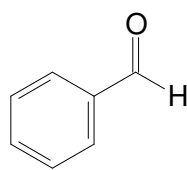
Components **C149** and **C155** (Fig. 3.27) were assumed to be geometrical isomers since their mass spectra are identical, with a base peak at  $m/z$  79 and molecular ion at  $m/z$  136. A computerised library search suggested that these components might be butenyl cyclohexenes with molecular formula  $C_{10}H_{16}$ , but HRMS analysis gave a molecular formula of  $C_9H_{12}O$ , which meant that the components had either four double bonds or three double bonds and a ring. By comparing the published mass spectra of a number of 2,4,6-nonatrienal isomers, of which the (E,E,Z)-isomer has been identified as the character impact aroma compound in oat flakes (Schuh and Schieberle, 2005), with the mass spectra of **C149** and **C155** it was possible to tentatively identify these components as two isomers of 2,4,6-nonatrienal. This identification was also in agreement with the results of the HRMS analysis. In order to assign the stereochemistry of **C149** and **C155**, (E,E,E)-2,4,6-nonatrienal was synthesised (Buttery, 1975). The synthesis produced two isomers: the target compound (E,E,E)-2,4,6-nonatrienal as the major product and a minor product thought to be the (E,E,Z) isomer. The retention times of these two synthesised isomers were in agreement with the retention times of **C149** and **C155**, and these two components were identified as (E,E,Z)-2,4,6-nonatrienal (tentatively) and (E,E,E)-2,4,6-nonatrienal, respectively.



### 3.2.6 Aromatic aldehydes

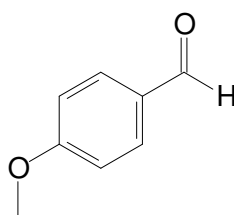
The EI mass spectrum of component **C25** (Fig. 3.28) has prominent ions at  $m/z$  50, 51, 77 (base peak), 78, 105 and 106 ( $M^+$ ). The latter two ions appear in the mass spectrum with almost the same relative abundance, indicating that **C25** could be **benzaldehyde** (Budzikiewicz *et al.*, 1967:

162–163). This was confirmed by retention time comparison with commercially available benzaldehyde.



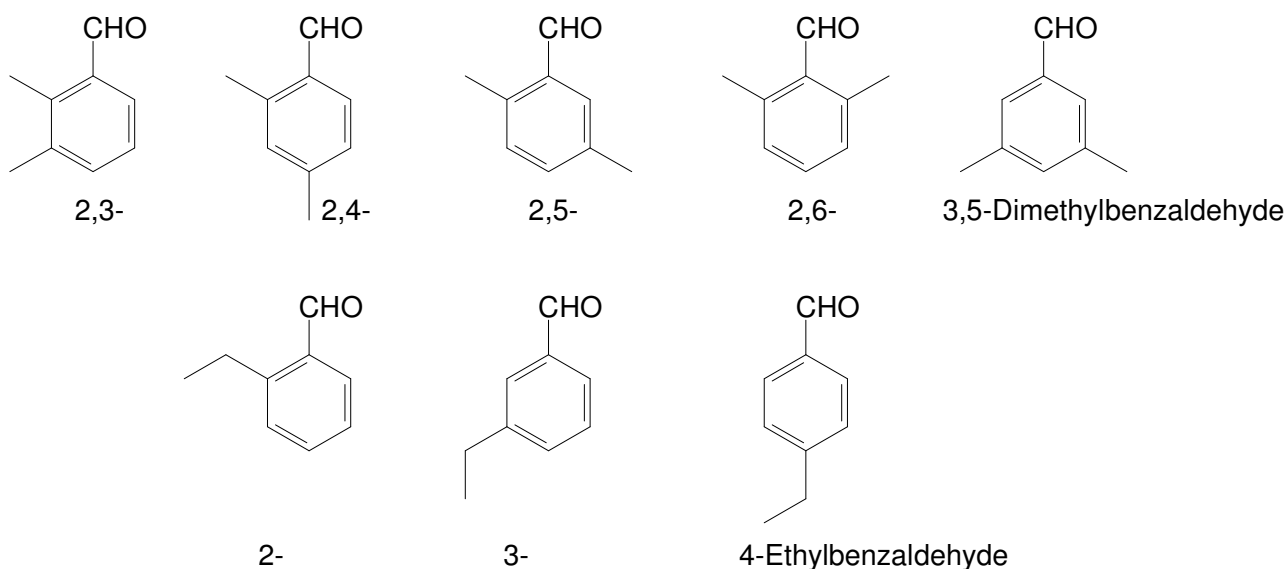
Benzaldehyde

The EI mass spectrum of component **C141** (Fig. 3.29) contains a pair of ions at  $m/z$  135 (base peak) and 136 ( $M^+$ ) with a relative abundance similar to the pair of ions at  $m/z$  105 and 106 in the mass spectrum of benzaldehyde. The same phenomenon can also be seen in the EI mass spectra of components **C114** and **C166**, in which each contains a pair of ions at  $m/z$  133 (base peak) and 134 ( $M^+$ ), and at  $m/z$  147 and 148 ( $M^+$ ), respectively. It was therefore assumed that **C141**, **C114** and **C166** are substituted benzaldehydes. The online library search (NBS) gave *m*- or *p*-methoxy benzaldehyde as possible structures for **C141** (85% and 78% correlation). Component **C141** was identified by retention time comparison as ***p*-methoxy benzaldehyde (*p*-anisaldehyde)**. The RI available for *m*-methoxy benzaldehyde (Adams, 2004) is much lower than that of **C141**.



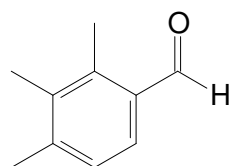
*p*-Anisaldehyde

Component **C114** (Fig. 3.30) has a molecular formula of  $C_9H_{10}O$  and was identified as 3,4-dimethyl benzaldehyde by an online NBS library search (84% correlation), but retention time comparison with the commercially available compound proved that this identification was not correct. The following dimethyl- and ethyl-substituted benzaldehydes were also considered as possible candidate structures:



The mass spectra of 3-ethyl- and 4-ethylbenzaldehyde contain a relatively prominent ion at  $m/z$  119 (NIST) which is not observed in the mass spectrum of **C114**, and these aldehydes were therefore not considered as possible structures. Of all the remaining compounds, RIs (DB-5 equivalent column) for only 2,4-dimethylbenzaldehyde and 2-ethylbenzaldehyde were found in the literature, and the RI of the latter compound was found to be the closest to that of **C114** (Flamini *et al.*, 2004; Elmore *et al.*, 2005). However, GC-MS analysis proved that the natural compound was not 2-ethylbenzaldehyde either. This meant that **C114** could possibly be any one of the above **dimethylbenzaldehydes**. This component could eventually not be identified.

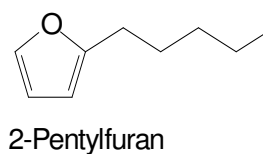
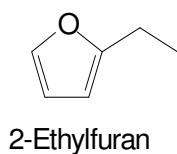
Since the molecular mass of component **C166** (148 Da) (Fig. 3.31) is 14 mass units higher than the molecular mass of **C114** it was assumed that it could be a trimethyl-substituted benzaldehyde. The online NBS library search suggested two different trimethyl-substituted benzaldehydes, but it was difficult to establish which one was the exact match on account of the many different possible substitution positions of the methyl groups on the aromatic ring. The substitution could be (2,3,4), (2,3,5), (2,3,6), (2,4,5), (2,4,6) or (3,4,5). By comparing the RI of **C166** with the published RIs of 2,3,4- and 2,3,6-trimethylbenzaldehyde (Adams, 2004) it was evident that **C166** must be **2,3,4-trimethylbenzaldehyde**.



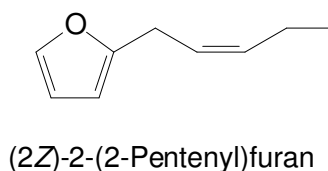
2,3,4-Trimethylbenzaldehyde

### 3.2.7 Furans

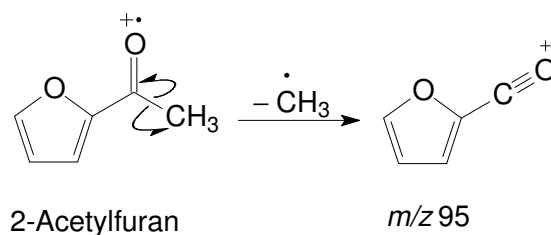
The EI mass spectra of components **C3** and **C35** (Fig. 3.32) both have base peaks at  $m/z$  81 and molecular ions at  $m/z$  96 and 138, respectively. Library searches (NBS) tentatively gave **2-ethylfuran** and **2-pentylfuran** as the most likely candidate structures (86% and 92% correlation) and this was confirmed by retention time comparison with the commercially available compounds.



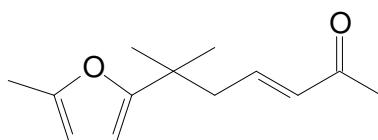
The EI mass spectrum of component **C40** (Fig. 3.33) has prominent ions at  $m/z$  39, 53, 68 ( $C_5H_8^+$ ), 79 ( $C_6H_7^+$ ), 94 ( $C_6H_6O^+$ ), 107 ( $C_7H_7O^+$ ), 121 ( $C_8H_9O^+$ ) and 136 ( $M^+$ ,  $C_9H_{12}O^+$ ). This component has two hydrogen atoms fewer than 2-pentylfuran ( $C_9H_{14}O$ ). This led to the assumption that **C40** might be an unsaturated 2-pentylfuran. An online library search (NBS) did not provide any logical suggestions for **C40** but, using the relative abundances of the ions in the mass spectrum, a manual NIST library search was performed and **(2Z)-2-(2-pentenyl)furan** was found as possible candidate structure. The elution order of the components further supports the identification of **C40** as (2Z)-2-(2-pentenyl)furan, since the unsaturated compound is expected to elute from column A later than the saturated one.



The EI mass spectrum of component **C19** (Fig. 3.34) has a molecular ion at  $m/z$  110 and other significant ions at  $m/z$  95 (base peak), 67, 53 and 39. Except for the molecular ion and the base peak all of these ions were recognised as those typically found in the spectra of substituted furans. Since the molecular mass of **C19** is 14 mass units higher than that of previously identified 2-ethylfuran it was reasonable to assume that **C19** might be 2-propylfuran. However, the base peak would then have been expected at  $m/z$  81 instead of  $m/z$  95. Thus, these findings suggested a furan with a functional group other than a normal alkyl group as substituent. An online library search (NBS) gave **2-acetylfuran** as possible candidate structure for **C19** (87% correlation), and this was confirmed by retention time comparison with commercially available 2-acetylfuran. Due to the presence of the acetyl group the loss of the alkyl radical gives rise to an abundant ion at  $m/z$  95 (base peak), which is also observed when other functional groups, such as esters, are conjugated with the furan nucleus (Budzikiewicz *et al.*, 1967: 617–618):

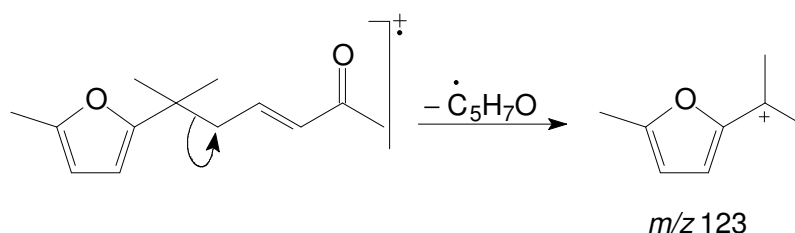


The mass spectra of components **C215** (Fig. 3.35) and **C219** have base peaks at  $m/z$  123 and molecular ions at  $m/z$  208 and 206, respectively. Considering the relative retention times of these components and the difference observed in their molecular masses it was assumed that they are structurally similar, but **C219** has an additional double bond. Online NBS library searches did not provide any acceptable suggestions as to possible structures for **C215** and **C219**. An offline NIST library search was conducted by entering the relative abundances of the prominent ions present in the mass spectrum of **C215** and this gave **6-methyl-(5-methylfuran-2-yl)heptan-2-one** as a possible structure for **C215**. The elemental composition of **C215** ( $C_{13}H_{20}O_2$ ) was in agreement with this suggestion, while the elemental composition of **C219** ( $C_{13}H_{18}O_2$ ) confirmed its similarity to **C215**, as well as the presence of a double bond in the molecule. The mass spectrum of a natural furan, identified in lavender absolute and extracts of prunes, spinach leaves and green and black tea (*Thea sinensis* L.) (Näf *et al.*, 1997), was found to be exactly the same as that of **C219** found in the honeybush aroma. This furan has the same structure as **C215** except for a double bond at position 3 of the ketone moiety. Based on these grounds, **C219** was identified as **(E)-6-methyl-6-(5-methylfuran-2-yl)hept-3-en-2-one**.



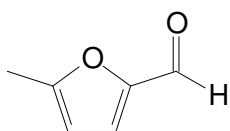
(E)-6-Methyl-6-(5-methylfuran-2-yl)hept-3-en-2-one

A base peak at  $m/z$  43 ( $CH_3CO^+$ ) is characteristic of branched and unbranched methyl ketones (Budzikiewicz *et al.*, 1967: 134). However, in the case of **C215** and **C219** the base peak is present at  $m/z$  123 ( $C_8H_{11}O^+$ ). The formation of this ion can possibly be explained as follows:



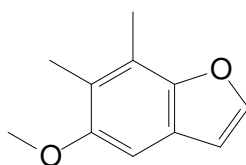
The EI mass spectrum of component **C28** (Fig. 3.36) contains an abundant molecular ion at  $m/z$  110 and an  $[M - 1]^+$  ion of almost equal abundance. An online NBS library search gave **5-methyl-2-furancarboxaldehyde** as the best possible candidate structure for **C28** (75% correlation). This was confirmed by retention time comparison with the commercially available material.





5-Methyl-2-furancarboxaldehyde

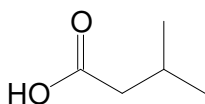
The EI mass spectrum of component **C223** (Fig. 3.37) has a base peak at  $m/z$  161 and molecular ion at  $m/z$  176 ( $C_{11}H_{12}O_2^+$ ). The molecular formula is in accordance with the suggestion given by online NBS and NIST library searches, namely **5-methoxy-6,7-dimethylbenzofuran** (64 and 75% correlation, respectively). When the conjugation of a furan ring is extended to a benzofuran system it has an effect on the stability of the molecular ion, which is usually the base peak in the spectra of simple methylbenzofurans (Budzikiewicz *et al.*, 1967: 622; Grigg *et al.*, 1966). Although the molecular ion in the mass spectrum of **C223** is not the base peak it has a high abundance (85%).



5-Methoxy-6,7-dimethylbenzofuran

### 3.2.8 Saturated and unsaturated aliphatic carboxylic acids

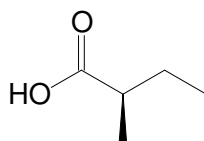
Component **C11** was assumed to be an aliphatic acid on account of the presence in its EI mass spectrum (Fig. 3.38) of a prominent ion at  $m/z$  60 (base peak), which is typically present in the mass spectra of aliphatic acids, and is formed by McLafferty rearrangement (Budzikiewicz *et al.*, 1967: 214–216; Macoll, 1988). According to an online computerised library search **C11** could be **3-methylbutanoic acid** (80% correlation). Retention time comparison with commercially available 3-methylbutanoic acid confirmed this identification.



3-Methylbutanoic acid

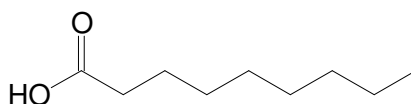
The mass spectrum of component **C13** (Fig. 3.39) contains a base peak at  $m/z$  74 ( $C_3H_6O_2^+$ ) and an ion at  $m/z$  45 ( $CO_2H^+$ ), which is characteristic of carboxylic acids with a low molecular mass (Budzikiewicz *et al.*, 1967: 214–216). An online library search suggested that **C13** might be **2-methylbutanoic acid** (88% correlation), which was confirmed by retention time comparison with the commercially available compound. Pure enantiomers available for 2-methylbutanoic acid were used to establish that the (*S*)-(+)-enantiomer elutes before its (*R*)-enantiomer from the enantioselective

column C, coated with the stationary phase OV-1701-OH containing heptakis(2,3-di-*O*-methyl-6-*O*-tert-butyldimethylsilyl)- $\beta$ -cyclodextrin as chiral selector, with an  $\alpha$ -value of 1.01. In the honeybush samples, 2-methylbutanoic acid was present as the pure (*R*)-(-)-enantiomer.



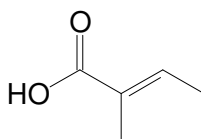
(*R*)-2-Methylbutanoic acid

The EI mass spectra of components **C44**, **C159** (Fig. 3.40) and **C264** were all characterised by the presence of a prominent ion at  $m/z$  60 ( $C_2H_4O_2^+$ ), and were identified as **hexanoic, nonanoic and dodecanoic acid** (correlation factors >80%) by performing an online library search with their respective mass spectra and confirming their identities by retention time comparison with the corresponding commercially available compounds.



Nonanoic acid

The EI mass spectrum of component **C20** (Fig. 3.41) has an abundant ion at  $m/z$  55 and base peak at  $m/z$  100 ( $M^+$ ,  $C_5H_8O_2^+$ ). This component was identified by the NBS library as **tiglic acid** (77% correlation) and confirmed by retention time comparison with the commercially available compound.



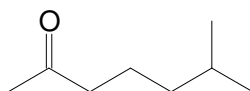
Tiglic acid

Due to the presence of the double bond in the  $\alpha$ -position the mass spectrum does not contain the typical  $m/z$  74 ion formed by a McLafferty rearrangement.

### 3.2.9 Saturated and unsaturated aliphatic ketones

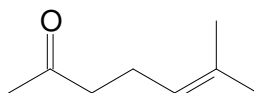
The EI mass spectra of components **C14**, **C27** (Fig. 3.42), **C72** and **C161** have a prominent ion at  $m/z$  43 ( $CH_3CO^+$ ), which in most cases is the base peak. It is also a characteristic ion in the mass spectra of branched and unbranched methyl ketones. The occurrence of a prominent ion at  $m/z$  58

indicates that these methyl ketones have side chains of three or more carbon atoms and that branching can only be beyond C-3 (Budzikiewicz *et al.*, 1967: 134–138; McLafferty and Tureček, 1993: 247–249). Components **C14**, **C27**, **C72** and **C161** were identified as **2-heptanone**, **6-methyl-2-heptanone**, **2-nonanone** and **2-undecanone** by means of an online NBS library search (correlation factors >80%) and by retention time comparison with the commercially available compounds.



6-Methyl-2-heptanone

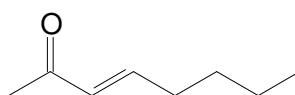
The EI mass spectrum of component **C32** (Fig. 3.43) has a base peak at  $m/z$  43 and molecular ion at  $m/z$  126. According to the literature a prominent  $[M - 58]^+$  ion is characteristic of olefinic ketones with at least four carbon atoms between the carbonyl group and the double bond (Dias *et al.*, 1972; Fenselau *et al.*, 1970). Since the  $[M - 58]^+$  ion at  $m/z$  68 is of a low intensity in the mass spectrum of **C32** it was concluded that this component could be an olefinic ketone that contains fewer than four carbon atoms between the carbonyl group and the double bond. According to the online NBS mass spectral library **C32** could be **6-methyl-5-hepten-2-one** (97% correlation). Retention time comparison with the corresponding commercially available material confirmed that this was indeed correct.



6-Methyl-5-hepten-2-one

The prominent ion at  $m/z$  108 is formed by the loss of water from the molecular ion, which probably takes place only after the double bond has migrated to a more favourable position (Dias *et al.*, 1972). The ion present at  $m/z$  58 forms *via* McLafferty rearrangement as mentioned for saturated ketones and formation of the ion at  $m/z$  68 proceeds *via* a similar mechanism but with charge retention on the alkyl fragment (McLafferty and Tureček, 1993: 247–249). Structurally, 6-methyl-5-hepten-2-one shows some resemblance to acyclic terpenoid compounds, but its mass spectrum is more characteristic of unsaturated ketones.

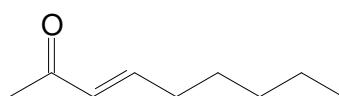
According to the EI mass spectrum of component **C53** (Fig. 3.44) its molecular mass is 126 Da and, since it has the same molecular mass as 6-methyl-5-hepten-2-one, it was assumed that it could also be a methyl octenone. The mass spectrum of **C53** does not have a very abundant ion at  $m/z$  68 (the  $[M - 58]^+$  ion), suggesting that this component is also an olefinic ketone with fewer than four carbon atoms present between the carbonyl group and the double bond (Dias *et al.*, 1972; Fenselau *et al.*, 1970). An online library search (NBS) suggested that **C53** could be (**E**)-**3-octen-2-one** (90% correlation).



(*E*)-3-Octen-2-one

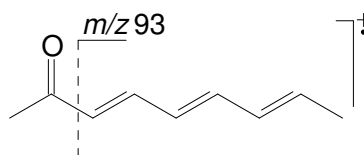
A characteristic fragmentation reaction occurring in  $\alpha,\beta$ -unsaturated aldehydes, ketones and esters affords the nonallylic loss of  $\delta$ -alkyl radicals. This reaction proceeds *via* a  $\gamma$ -H rearrangement, analogous to photoenolisation in solution chemistry, to give a more stable dienol ion (McLafferty and Tureček, 1993: 145–146). After cleavage of this newly formed allylic bond the ion loses the  $\delta$ -alkyl group. In the EI mass spectrum of **C53** this ion appears at  $m/z$  97 ( $C_6H_9O^+$ ). Component **C53** was identified as (*E*)-3-octen-2-one by retention time comparison with the corresponding commercially available compound.

The EI mass spectrum of component **C95** (Fig. 3.45) is similar to that of (*E*)-3-octen-2-one and its molecular mass (140 Da) is 14 mass units higher than that of (*E*)-3-octen-2-one, indicating that it might be 3-nonen-2-one. As in the case of (*E*)-3-octen-2-one, the low intensity of the  $[M - 58]^+$  ion at  $m/z$  82 is indicative of an olefinic ketone with fewer than four carbon atoms between the carbonyl group and the double bond. An online library search (85% correlation), followed by retention time comparison, resulted in identification of **C95** as (*E*)-3-nonen-2-one.



(*E*)-3-Nonen-2-one

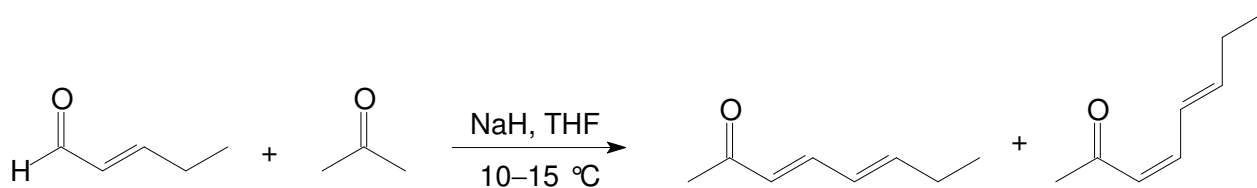
Since the EI mass spectrum of component **C145** (Fig. 3.46) contains a prominent ion at  $m/z$  43 ( $CH_3CO^+$ ), typically present in the mass spectra of methyl ketones, it was assumed that, according to its molecular formula ( $C_9H_{12}O$ ), this component might be a methyl ketone with three degrees of unsaturation. An online library search (NBS) gave **3,5,7-nonatrien-2-one** as possible candidate structure (75% correlation). The ion at  $m/z$  93 ( $C_7H_9^+$ ) is formed by cleavage of the bond between C-2 and C-3:



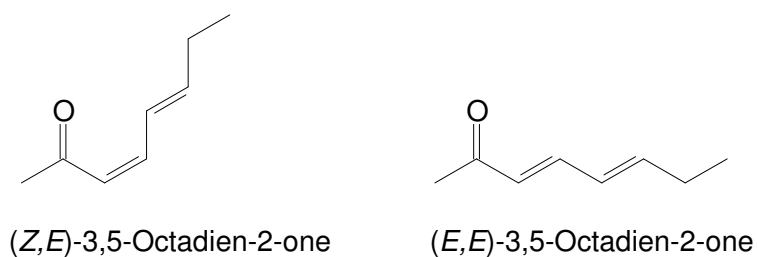
3,5,7-Nonatrien-2-one

Since the EI mass spectra of components **C63** (Fig. 3.47) and **C70** contain the same ions with similar relative abundances it was assumed that they are geometrical isomers. The molecular mass of these two geometrical isomers is two mass units lower than that of (*E*)-3-octen-2-one. HRMS gave an elemental composition of  $C_8H_{12}O$  for the molecular ion at  $m/z$  124, which indicates that these two

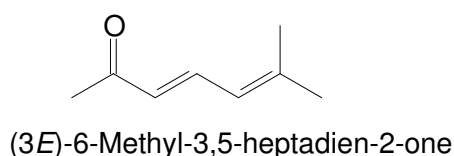
components have two degrees of unsaturation. An online NBS library search suggested 3,5-octadien-2-one as possible candidate structure for these components (correlation >92%). The (*Z,E*)- and (*E,E*)-isomers of 3,5-octadien-2-one were synthesised according to the following reaction scheme (Heydanek and McGorin, 1981):



Comparison of the retention times of the synthesised compounds with those of the natural components proved that **C63** and **C70** were indeed (*Z,E*)-3,5-octadien-2-one and (*E,E*)-3,5-octadien-2-one.

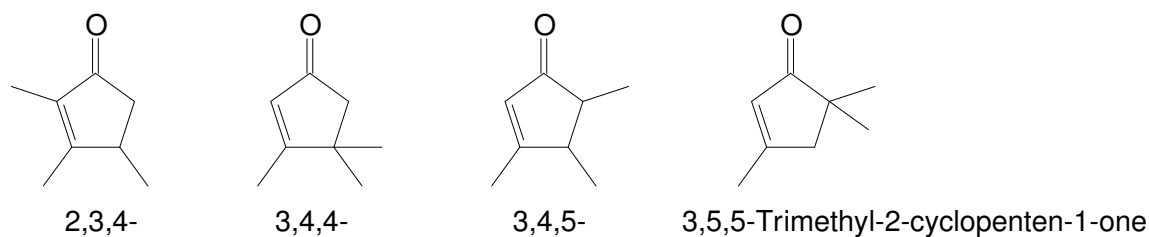


Component **C74** has the same molecular mass (124 Da) as the two isomers of 3,5-octadien-2-one and the same prominent ions occur in its mass spectrum (Fig. 3.48), but with different relative abundances. For instance, **C74** has a base peak at  $m/z$  109 instead of at  $m/z$  95, as observed for the 3,5-octadien-2-ones. This implies that loss of a methyl group from the molecular ion rather than loss of an ethyl group is more favourable for **C74**. (*3E*)-6-Methyl-3,5-heptadien-2-one was proposed as a possible structure by an online library search (93% correlation) and this structure was confirmed by comparison with commercially available (*3E*)-6-methyl-3,5-heptadien-2-one.

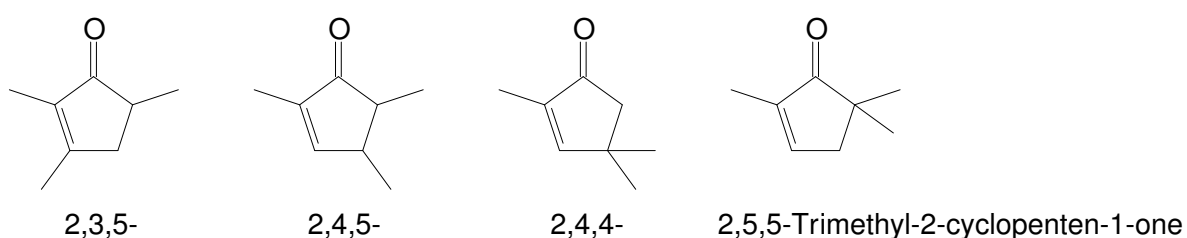


At first it was thought that component **C74** could be the (*Z*)-isomer of 6-methyl-3,5-heptadien-2-one and that component **C81** (Fig. 3.49) could be the (*E*)-isomer, since the mass spectra of these components are quite similar and they have the same molecular formulae ( $C_8H_{12}O$ ). However, as stated above, **C74** was identified as the (*E*)-isomer by retention time comparison with the commercially available material. This meant that **C81** should necessarily be a different compound since the (*Z*)-isomer is expected to elute earlier than the (*E*)-isomer from the apolar column A. Examination of the mass spectrum of **C81** revealed that it does not have such an abundant ion at  $m/z$  43 as (*3E*)-6-methyl-3,5-heptadien-2-one, implying that this component might not be a methyl ketone.

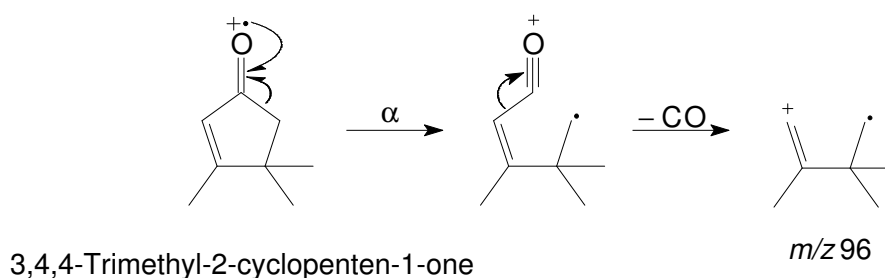
Even assuming **C81** to be a heptadienone with the carbonyl group at C-3 or C-4, the mass spectrum would be markedly different. An online NIST library search gave several 2-cyclopentenones as possible candidate structures:



Other possibilities not included in the NIST library are the following:

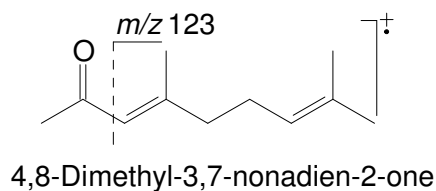


The mass spectrum of **C81** has a correlation factor of 80% with the library mass spectrum of 3,4,4-trimethyl-2-cyclopenten-1-one. Based on this information, **C81** was tentatively identified as **3,4,4-trimethyl-2-cyclopenten-1-one**. The loss of any one of the three methyl groups from the molecular ion could be responsible for the formation of the base peak at  $m/z$  109 ( $C_7H_9O^+$ ). Not very clear in the low-resolution mass spectrum (LRMS) of **C81**, but clearly seen in the HRMS, is the presence of an ion at  $m/z$  96 ( $C_7H_{12}^+$ ), formed by the loss of a CO molecule from the molecular ion:

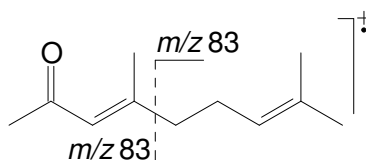


The EI mass spectrum of component **C154** (Fig. 3.50) has prominent ions at  $m/z$  41, 43, 69 (base peak), 83, 123, 151 and 166 ( $M^+$ ,  $C_{11}H_{18}O^+$ ). An online library search (NBS) did not give any structures that could be reconciled with the retention time of **C154**. However, a manual NIST library search, based on the relative abundances of the prominent ions listed above, gave **4,8-dimethyl-3,7-nonadien-2-one** as the best possible candidate structure. The ions present at  $m/z$  43 ( $CH_3CO^+$ ) and 151 ( $C_{10}H_{15}O^+$ ) are oxygen-containing fragments resulting from simple  $\alpha$ -cleavage reactions

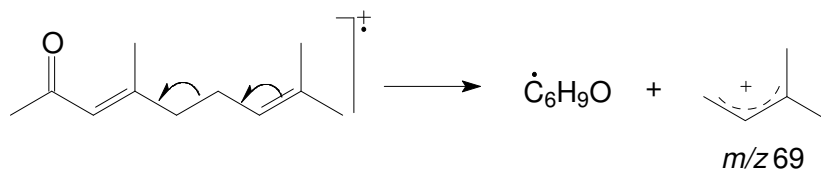
(Budzikiewicz *et al.*, 1967: 134–138). Such an  $\alpha$ -cleavage, with charge retention on the alkyl fragment, could be responsible for the formation of the ion at  $m/z$  123 ( $C_9H_{15}^+$ ):



An  $[M - 58]^+$  ion of low intensity at  $m/z$  108 confirms the fact that **C154** is an olefinic ketone with fewer than 4 carbon atoms between the carbonyl group and the double bond (Dias *et al.*, 1972; Fenselau *et al.*, 1970). The ion at  $m/z$  83 can be either an oxygen-containing fragment ( $C_5H_7O^+$ ) or an alkyl fragment ( $C_6H_{11}^+$ ):

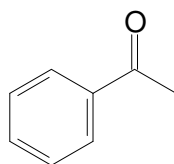


According to HRMS data, only the oxygen-containing ion ( $C_5H_7O^+$ ) is formed. The base peak at  $m/z$  69 is formed by cleavage of the allylic bond:



### 3.2.10 Ketones with an aromatic moiety

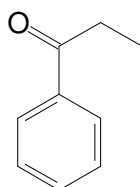
The EI mass spectrum of component **C60** (Fig. 3.51) is characteristic of acetophenone (Budzikiewicz *et al.*, 1967: 163; Meyerson and Rylander, 1957) and this was also suggested by an online library search as the best possible candidate structure (76% correlation). The identity of **C60** as **acetophenone** was confirmed by retention time comparison with the commercially available compound.



Acetophenone

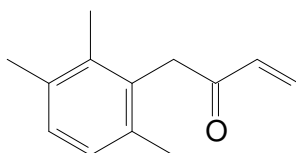
Components **C107** and **C108** [(*E*)-2-nonenal] were found to coelute in GC-MS analyses, which made it very difficult to obtain a pure mass spectrum for **C107**. It was however possible to see which

ions did not belong to the mass spectrum of (*E*)-2-nonenal and, as a result, prominent ions at  $m/z$  51, 77, 105 (base peak) and 134 (molecular mass) could be identified as ions belonging to the mass spectrum of **C107**. These ions are similar to those observed in the mass spectrum of acetophenone, and since the molecular mass of **C107** is 14 mass units higher than that of acetophenone it was assumed that this component might be an aromatic ketone with an additional methylene group. HRMS analysis gave an elemental composition of  $C_9H_{10}O$  for **C107**, which is in accordance with this assumption. The identification of **C107** as **propiophenone** was confirmed by retention time comparison with the commercially available compound.



Propiophenone

The elemental composition determined by HRMS for the molecular ion in the EI mass spectrum of component **C273** (Fig. 3.52) is  $C_{13}H_{16}O$  (188.1234). Online library searches (NBS and NIST) suggested that **C273** might be **1-(2,3,6-trimethylphenyl)-3-buten-2-one** (70% and 77% correlation), which is in agreement with its molecular composition.



1-(2,3,6-Trimethylphenyl)-3-buten-2-one

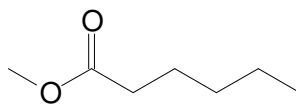
The base peak at  $m/z$  173 ( $C_{12}H_{13}O^+$ ) could be formed by the loss of any one of the three methyl groups, whereas loss of two methyl groups can account for the formation of the ion at  $m/z$  158 ( $C_{11}H_{10}O^+$ ). The ion at  $m/z$  145 is a  $C_{11}H_{13}^+$  ion, which is possibly formed by the loss of a methyl group followed by elimination of CO. The ions at  $m/z$  77 and 91 are  $C_6H_5^+$  and  $C_7H_7^+$  ions, typically found in mass spectra of aromatic molecules. Component **C273** was tentatively identified as 1-(2,3,6-trimethylphenyl)-3-buten-2-one.

### 3.2.11 Saturated and unsaturated aliphatic esters

The EI mass spectra of components **C22** (Fig. 3.53), **C90**, **C132**, **C177** and **C248** have base peaks at  $m/z$  74, which is a characteristic ion in the mass spectra of methyl esters of  $\alpha$ -unbranched  $C_6$ – $C_{26}$  carboxylic acids (Budzikiewicz *et al.*, 1967: 176). These components were identified as **methyl hexanoate**, **methyl octanoate**, **methyl nonanoate**, **methyl decanoate** and **methyl**



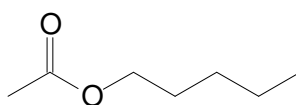
**dodecanoate** by online library searches (NBS) of their respective mass spectra (correlation >80%) and retention time comparison with the corresponding commercially available compounds.



Methyl hexanoate

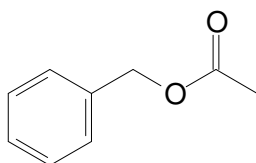
The mass spectra of methyl esters have been discussed in detail by Budzikiewicz (1967: 174–183), as well as by McLafferty and Tureček (1993: 252–255).

In the EI mass spectrum of component **C21** (Fig. 3.54) a significant ion appears at  $m/z$  61 ( $C_2H_5O_2^+$ ) (21%), which is characteristic of alkyl acetates (Mo, 1994: 87). The ion is formed by rearrangement of two hydrogen atoms followed by cleavage of the alkyl–oxygen bond (Beynon *et al.*, 1961; Sharkey *et al.*, 1959). The precise mechanism involved in the rearrangement of the two hydrogen atoms is not fully understood, and different mechanisms have been proposed (Benz and Biemann, 1964; Black *et al.*, 1964; Djerassi and Fenselau, 1964; McLafferty, 1959). **Pentyl acetate** was proposed as the structure of **C21** following an online library search (NBS) (87% correlation) and the identification was confirmed by retention time comparison with the commercially available material.



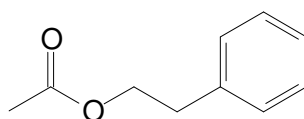
Pentyl acetate

An online library search (NBS) gave **benzyl acetate** as a possible candidate structure (82% correlation) for component **C109** (Fig. 3.55) and this was confirmed by retention time comparison with the commercially available compound.



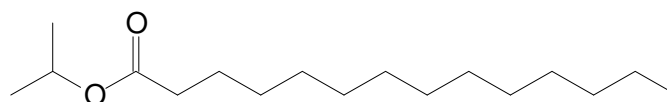
Benzyl acetate

Component **C142** (Fig. 3.56) was identified by an NBS online library search as **2-phenylethyl acetate** (89% correlation) and this was confirmed by retention time comparison with the commercially available compound.



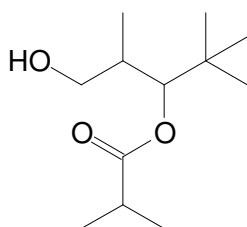
2-Phenylethyl acetate

The mass spectrum of component **C298** (Fig. 3.57) has a prominent ion at  $m/z$  102 ( $C_5H_{10}O_2^+$ ), which commonly occurs in the mass spectra of  $\alpha$ -methylsubstituted ethyl esters,  $\alpha$ -ethylsubstituted methyl esters, unsubstituted propyl esters, and isopropyl esters, and is formed by a McLafferty rearrangement. In the mass spectra of  $\alpha$ -methylsubstituted ethyl esters and unsubstituted propyl esters the ion at  $m/z$  102 can even be the base peak, which does not apply in the case of **C298**.  $\alpha$ -Methylsubstituted ethyl esters have a prominent ion at  $m/z$  87, which is easily formed from the ion at  $m/z$  102 by the loss of a methyl radical (Budzikiewicz *et al.*, 1967: 183). The low intensity of the ion at  $m/z$  87 in the mass spectrum of **C298** thus indicates that the ester is not branched in the carboxylic acid function and, as suggested by the online library search (84% correlation), **C298** could be **isopropyl myristate**. This was confirmed by comparison with the commercially available compound.

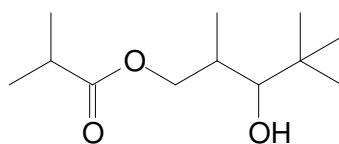


Isopropyl myristate

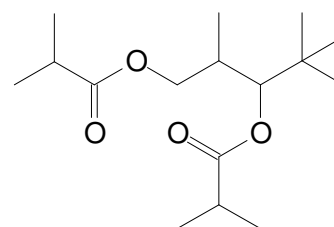
The EI mass spectra of components **C190**, **C201** (Fig. 3.58) and **C270** contain a base peak at  $m/z$  71 ( $C_4H_7O^+$ ), and these components were respectively identified as **1-(2-hydroxy-1-methylethyl)-2,2-dimethylpropyl 2-methylpropanoate**, **3-hydroxy-2,4,4-trimethylpentyl 2-methylpropanoate** and **1-[2-(isobutyryloxy)-1-methylethyl]-2,2-dimethylpropyl 2-methylpropanoate**, based on the good agreement with the NBS library (correlation >80%).



Component 190



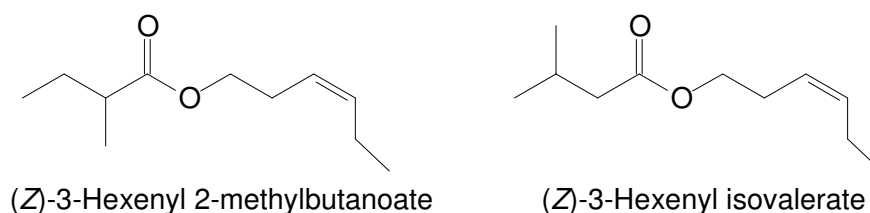
Component 201



Component 270

The ions at  $m/z$  173 ( $C_9H_{17}O_3^+$ ) and 243 ( $C_{13}H_{23}O_4^+$ ) in the mass spectra of the three esters are not their molecular ions, but are formed when  $\alpha$ -cleavage at the carbonyl group results in the loss of the isopropyl moiety. It is interesting to note that these three compounds are mono-esters (**C190** and **C201**) and a di-ester (**C270**) of the same glycol.

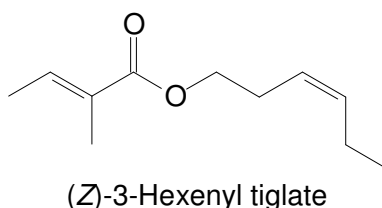
The mass spectra of components **C138** and **C140** (Fig. 3.59) are similar; they contain prominent ions at  $m/z$  57, 67, 82, 85 and 103 which only slightly differs with regard to their relative abundances. Clearly the ion at  $m/z$  103 cannot be the molecular ion because the retention times of these components cannot be reconciled with such a low molecular mass. An online library search (NBS) gave 3-hexenyl propanoate as possible candidate structure, but after inspection of the mass spectrum of 3-hexenyl propanoate it was possible to detect slight differences between the mass spectrum of this propanoate and those of **C138** and **C140**, and therefore this compound was not considered a likely candidate. A manual NIST library search using the relative abundances of the prominent ions in the mass spectrum gave two possible esters, i.e. 3-hexenyl valerate and 3-hexenyl isovalerate. At a later stage it was also possible to conduct a NIST online library search, which also gave these two esters as the best possible candidate structures. Since these two possible candidates are unsaturated compounds, and bearing in mind the similarity of their mass spectra, it was assumed that **C138** and **C140** could be geometrical isomers of one of these two basic structures. It has been found that (*Z*)-3-hexenyl valerate elutes much later than (*Z*)-3-hexenyl isovalerate (ESO, 2006) and therefore it was assumed that **C138** and **C140** could possibly be (*Z*)- and (*E*)-3-hexenyl isovalerate. Commercially available (**Z**)-3-hexenyl isovalerate was found to be gas chromatographically identical to **C140** rather than to **C138**. Since **C138** could not be the (*E*)-isomer of 3-hexenyl isovalerate, the compound (*Z*)-3-hexenyl 2-methylbutanoate, known to elute just before (*Z*)-3-hexenyl isovalerate (Fernández *et al.*, 2000; Radulovic *et al.*, 2008), was considered as a possibility. The commercially available compound was used as reference to identify **C138** as (**Z**)-3-hexenyl 2-methylbutanoate.



It is not surprising that the molecular ions of **C138** and **C140** were not observed in their mass spectra, since the molecular ion peak of RCOOR' generally has a low abundance when R' is larger than butyl (McLafferty and Tureček, 1993: 255).

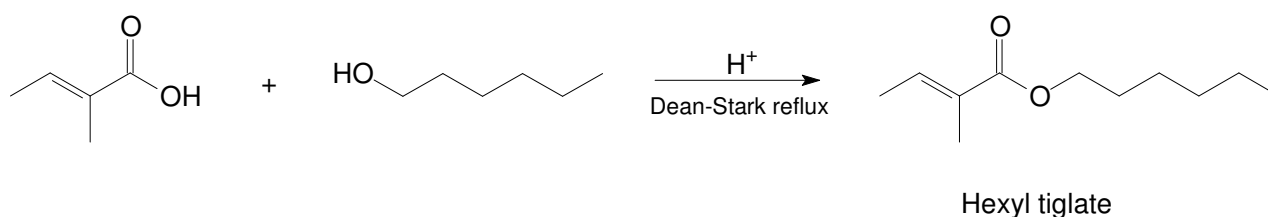
The mass spectrum of component **C175** (Fig. 3.60) shares some similar features with those of the 3-hexenyl esters. Four prominent ions appear at  $m/z$  55, 67, 82 and 83, two of which correspond to ions present in the mass spectra of the hexenyl esters. It also has an ion of much lower intensity at  $m/z$  101, with no other ions of higher mass that could possibly be the molecular ion. If the molecular mass is assumed to be 182 Da then **C175** could be an ester similar to the 3-hexenyl esters, but with an additional double bond. Online library searches (NBS and NIST) did not propose any likely candidate structures for the identification of **C175**, but by manually entering the relative abundances of the ions into the Spectral Database for Organic Compounds (National Institute of AIST, 2010), (**Z**)-

**3-hexenyl (*E*)-2-methyl-2-butenoate [(*Z*)-3-hexenyl tiglate]** was identified as an acceptable structure for **C175**.

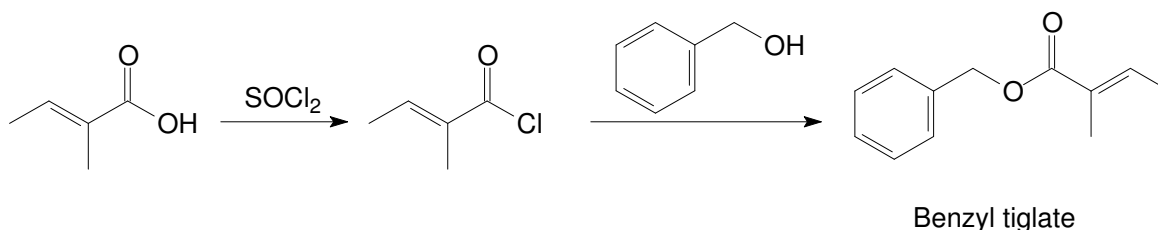


The identity of this component was confirmed by comparison of the commercially available compound with **C175** in the usual manner.

The mass spectrum of component **C179** (Fig. 3.61), with prominent ions at  $m/z$  55, 83 and 101, also closely resembles the mass spectra of the unsaturated esters discussed above. Published MS and RI data for hexyl tiglate (Adams, 2004) corresponded to the data obtained for **C179**. Hexyl tiglate was synthesised according to the reaction shown below, and served to confirm that the identification of **C179** as **hexyl tiglate** was indeed correct.

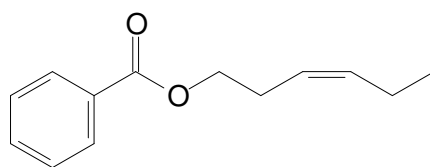


The mass spectrum of component **C237** (Fig. 3.62) has prominent ions at  $m/z$  55, 65, 77, 83, 91 (base peak), 145, 172 and 190 ( $M^+$ ,  $C_{12}H_{14}O_2^+$ ) and these ions were used in a manual NIST library search to identify **C237** as **benzyl tiglate**. Benzyl tiglate was prepared as illustrated in the scheme below and retention time comparison with the synthesised compound proved that the identification was correct:



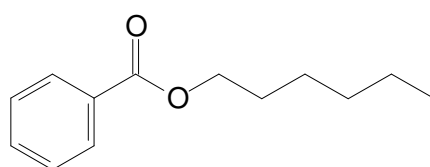
### 3.2.12 Aromatic esters

The mass spectra of components **C259** and **C261** (Fig. 3.63) are identical and an online library search (NBS) gave (*Z*)-3-hexenyl benzoate as the best possible candidate structure for both components (87% correlation). (***Z*-3-Hexenyl benzoate**) is commercially available and its retention time matched that of **C261**. The commercial product also contains some of the (*E*)-isomer, which, according to elution order data, elutes before the (*Z*)-isomer (Binder and Flath, 1989; Toda *et al.*, 1983). The retention time of (***E*-3-hexenyl benzoate**) was found to be the same as that of **C259**.



(Z)-3-Hexenyl benzoate

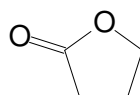
Since the EI mass spectrum of component **C263** (Fig. 3.64) shows some similarity to the mass spectra of the 3-hexenyl benzoate esters (**C259** and **C261**), and because its molecular mass is only two mass units higher than the molecular mass of these esters, it was assumed that it might be a similar ester without a double bond. An online NBS library search proposed **hexyl benzoate** as the best possible candidate (72% correlation) and retention time comparison with the commercially available compound supported this identification.



Hexyl benzoate

### 3.2.13 Saturated and unsaturated lactones

The mass spectrum of component **C16** (Fig. 3.65) has a base peak at  $m/z$  42 (base peak) and molecular ion at  $m/z$  86. The NBS library predicted with more than 85% certainty that **C16** could be  **$\gamma$ -butyrolactone**:

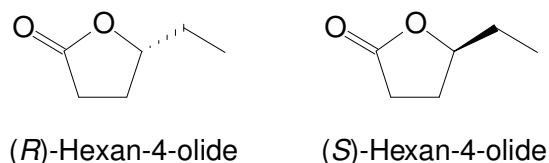


$\gamma$ -Butyrolactone

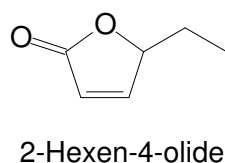
Confirmation of the identity of **C16** was obtained by retention time comparison with the commercially available material. The prominent  $[M - 44]$  ion at  $m/z$  42 is formed by elimination of carbon dioxide from the molecular ion and is most significant for lactones with fewer than seven or eight carbon atoms (Budzikiewicz *et al.*, 1967: 205–206; Friedman and Long, 1953; McFadden *et al.*, 1965).

The EI mass spectrum of component **C54** (Fig. 3.66) has a prominent ion at  $m/z$  85 ( $C_4H_5O_2^+$ ), which is also the base peak, and characteristic of  $\gamma$ -substituted  $\gamma$ -lactones ( $\gamma$ -substituted butanolides). Given the high intensity of this ion in comparison to all the other ions present in the mass spectrum it was safe to assume that this lactone is unbranched. Only a small percentage of the total ion current is usually carried by the molecular ion of  $\gamma$ -lactones, which sometimes complicates their identification (Budzikiewicz *et al.*, 1967: 205–206). In this instance however, a molecular ion of low intensity is present at  $m/z$  114 ( $C_6H_{10}O_2^+$ ), which led to the assumption that **C54** might be **hexan-4-olide**. This

was confirmed by retention time comparison with the commercially available material.  $\alpha$ -Cleavage of the bond adjacent to the ether–oxygen of the lactone affords the loss of the alkyl fragment and explains the presence of the ion at  $m/z$  85 (Budzikiewicz *et al.*, 1967: 205–206). According to published data, the (*R*)-enantiomer of this  $\gamma$ -lactone elutes before the (*S*)-enantiomer from an enantioselective column equivalent to column D (Maas *et al.*, 1994b). Enantioselective analysis of the honeybush material gave a high  $R_s$  value of 9.4 and both enantiomers were present in a ratio of 52:48 (*R*:*S*).

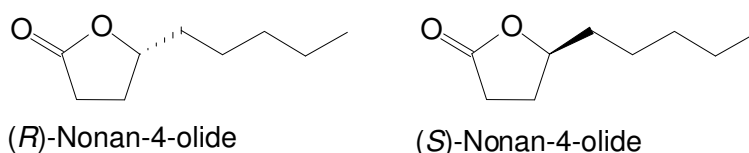


The EI mass spectrum of component **C49** (Fig. 3.67) has prominent ions at  $m/z$  55, 83 (base peak) and 112 ( $M^+$ ,  $C_6H_8O_2$ ). The molecular mass and base peak are two mass units lower than those of hexan-4-olide (**C54**) and in agreement with those of 2-hexen-4-olide, suggested by the online NBS library search, with a correlation factor of 87%. Therefore, **C49** was tentatively identified as **2-hexen-4-olide**.

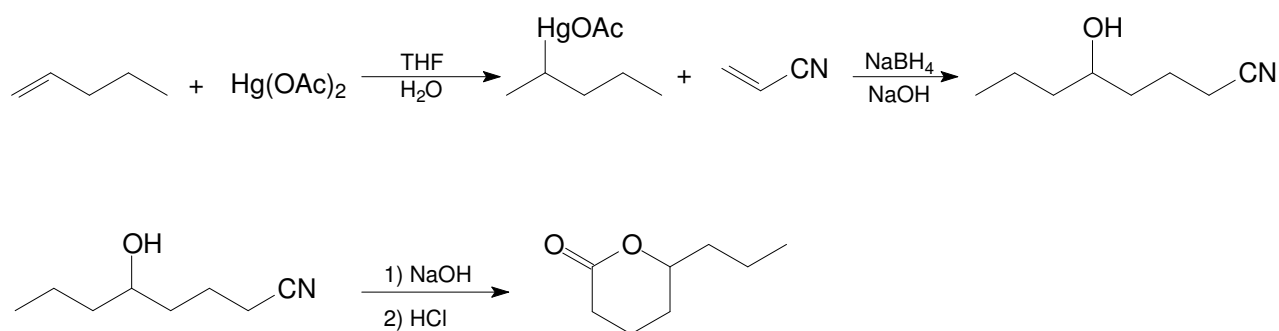


The base peak at  $m/z$  83 represents a  $C_4H_3O_2^+$  ion and is possibly formed by the same  $\alpha$ -cleavage reaction that is responsible for the formation of the corresponding ion at  $m/z$  85 present in the mass spectrum of the saturated lactone (**C54**). Two enantiomers of **C49** were observed in the chromatogram of the enantioselective analysis of honeybush samples on an enantioselective column equivalent to column D, and had a similar  $R_s$  value to that obtained for hexan-4-olide (**C54**). The two enantiomers were present as a racemate.

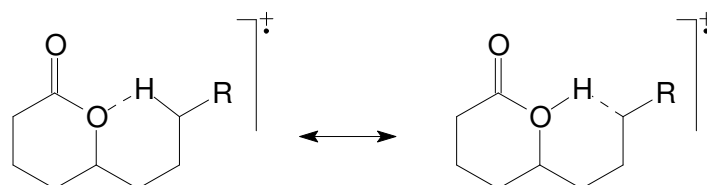
The EI mass spectrum of component **C186** (Fig. 3.68) also has a base peak at  $m/z$  85, similar to **C54**. It is evident from the few prominent ions in the mass spectrum that **C186** is unbranched, and it was therefore identified as nonan-4-olide, and later confirmed by an online library search (85% correlation) and by retention time comparison with the commercially available compound. Similar to the  $\gamma$ -lactone (**C54**) discussed previously, the (*R*)-enantiomer of nonan-4-olide elutes before its (*S*)-enantiomer from an enantioselective column equivalent to column D (Maas *et al.*, 1994b). A relatively high  $R_s$  value of 2.7 was determined experimentally and **C186** was finally identified as (*R*)- and (*S*)-**nonan-4-olide**, present in a ratio of 51:49.



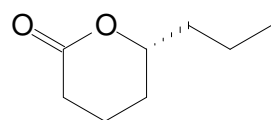
The mass spectra of components **C152** (Fig. 3.69) and **C233** are similar with respect to their most prominent ions, but they do have different even-mass ions at  $m/z$  124 and 152, respectively. Molecular ions could not be detected in their mass spectra. The prominent ion at  $m/z$  99 is characteristic of  $\delta$ -lactones and forms *via* the same reaction that is responsible for the formation of the base peak at  $m/z$  85 for  $\gamma$ -lactones (Budzikiewicz *et al.*, 1967: 205–206). Online library searches (NBS) suggested that **C152** and **C233** could be **octan-5-olide** and **decan-5-olide**, respectively (96% and 80% correlation), and **C233** was identified as the mentioned lactone by retention time comparison with the commercially available compound. Octan-5-olide was synthesised according to the following scheme (Giese *et al.*, 1984) and **C152** was subsequently identified as this lactone by retention time comparison with the synthesised compound.



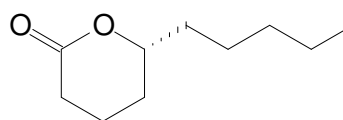
The even-mass ions present in the mass spectra of **C152** and **C233** at  $m/z$  124 ( $C_8H_{12}O^+$ ) and 152 ( $C_{10}H_{16}O^+$ ) are formed by the loss of water from their respective molecular ions. This type of fragmentation is not observed for the smaller lactones, but only becomes more significant as the chain length of the alkyl group increases to three or more carbon atoms, since this length presumably permits a favourable six-membered configuration, allowing for the transfer of a hydrogen atom (McFadden *et al.*, 1965):



The (*S*)-enantiomers of octan-5-olide and decan-5-olide elute before their (*R*)-enantiomers from an enantioselective column D-equivalent (Maas *et al.*, 1994b) ( $R_s$  values of respectively 1.23 and 1.29) and **C152** and **C233** were finally identified as both the (*R*)-enantiomers of **octan-** and **decan-5-olide**, respectively.

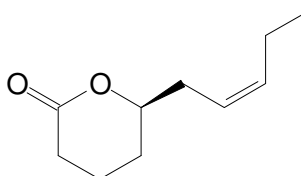


(*R*)-Octan-5-olide



(*R*)-Decan-5-olide

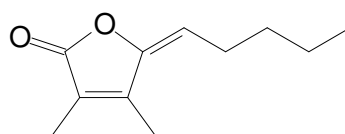
The mass spectrum of component **C229** (Fig. 3.70) has ions at  $m/z$  42, 55, 71 and 99 (base peak), which are characteristic of  $\delta$ -substituted  $\delta$ -lactones, as well as other significant ions at  $m/z$  108, 150 and 168 ( $M^+$ ). The molecular mass is two mass units lower than that of decan-5-olide, which suggests that **C229** is possibly a decen-5-olide. An online NBS library search suggested 7-decen-5-olide (70% correlation). After exploring the literature, it was found that the (*Z*)-isomer of this unsaturated lactone predominates in nature, and is referred to as jasmine lactone. It occurs in products such as gardenia flowers, jasmine, osmanthus, tea and tuberose (Leffingwell, 1999). When commercially available jasmine absolute oil (Morocco) was analysed by GC-MS the retention time of the jasmine lactone was found to be identical to that of **C229**, hence this component was identified as (*Z*)-7-decen-5-olide. According to the literature only (*R*)-(*Z*)-7-decen-5-olide is present in jasmine absolute and its optical antipode in tuberose (Leffingwell, 1999). The (*R*)-enantiomer was observed in the jasmine absolute oil when analysed on the enantioselective column D, but its retention time were shorter than the retention time of the enantiomer present in the honeybush samples. It was therefore deduced that **C229** should be (**S**)-(**Z**)-7-decen-5-olide.



(*S*)-(*Z*)-7-Decen-5-olide

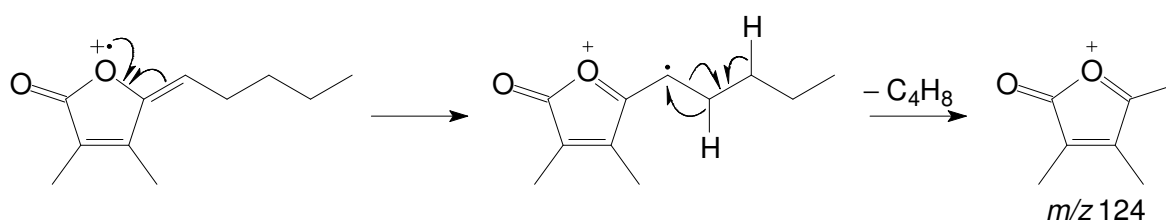
Online library searches (NBS and NIST) did not propose any acceptable candidate structures for component **C245** (Fig. 3.71). HRMS analysis gave an elemental composition of  $C_{11}H_{16}O_2$  for this component, which was entered into the Spectral Database for Organic Compounds (National Institute of AIST, 2010) and the mass spectrum of **2,3-dimethyl-2,4-nonadien-4-olide** was found to correspond to that of **C245**. This compound is also known as **bovolide**, and was originally used as artificial flavour additive in tobacco products (Schumacher and Roberts, 1966; Sigrist, 2002). Bovolide was first identified in butter and the chosen name was given to the compound in order to denote its bovine origin (Boldingh and Taylor, 1962; Lardelli *et al.*, 1966; Sigrist, 2002) This lactone was later also found in various types of tea (Horita and Hara, 1984; Horita and Hara, 1985; Kawakami *et al.*, 1986; Kawakami *et al.*, 1987; Kawakami *et al.*, 1995; Kawakami and Shibamoto, 1991; Owuor and Obanda, 1999), as well as in other natural products (Sigrist, 2002).





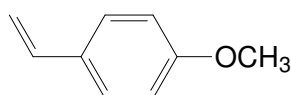
Bovolide

The ions at  $m/z$  165 ( $C_{10}H_{13}O_2^+$ ) and 162 ( $C_{11}H_{14}O^+$ ) in the mass spectrum of **C245** are formed by the loss of any one of the methyl groups present in the molecule and by loss of water from the molecular ion, respectively. The ion present at  $m/z$  137 ( $C_8H_9O_2^+$ ) is probably formed by the loss of a  $C_3H_7$  fragment that is part of the alkyl side chain. Hydrogen transfer prior to cleavage of the bond adjacent to the double bond in the alkyl side chain can explain the formation of the ion at even-mass  $m/z$  124 ( $C_7H_8O_2^+$ ):



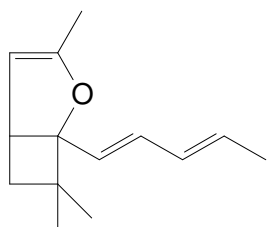
### 3.2.14 Ethers

An online library search (NBS) proposed **4-vinylanisole** as possible candidate structure for component **C100** (Fig. 3.72) (92% correlation) and this structure was confirmed by retention time comparison with the available commercial compound. Formation of the most prominent ions in the mass spectrum of **C100** can be explained by the fragmentation reactions of aromatic ethers (Budzikiewicz *et al.*, 1967: 237–247).



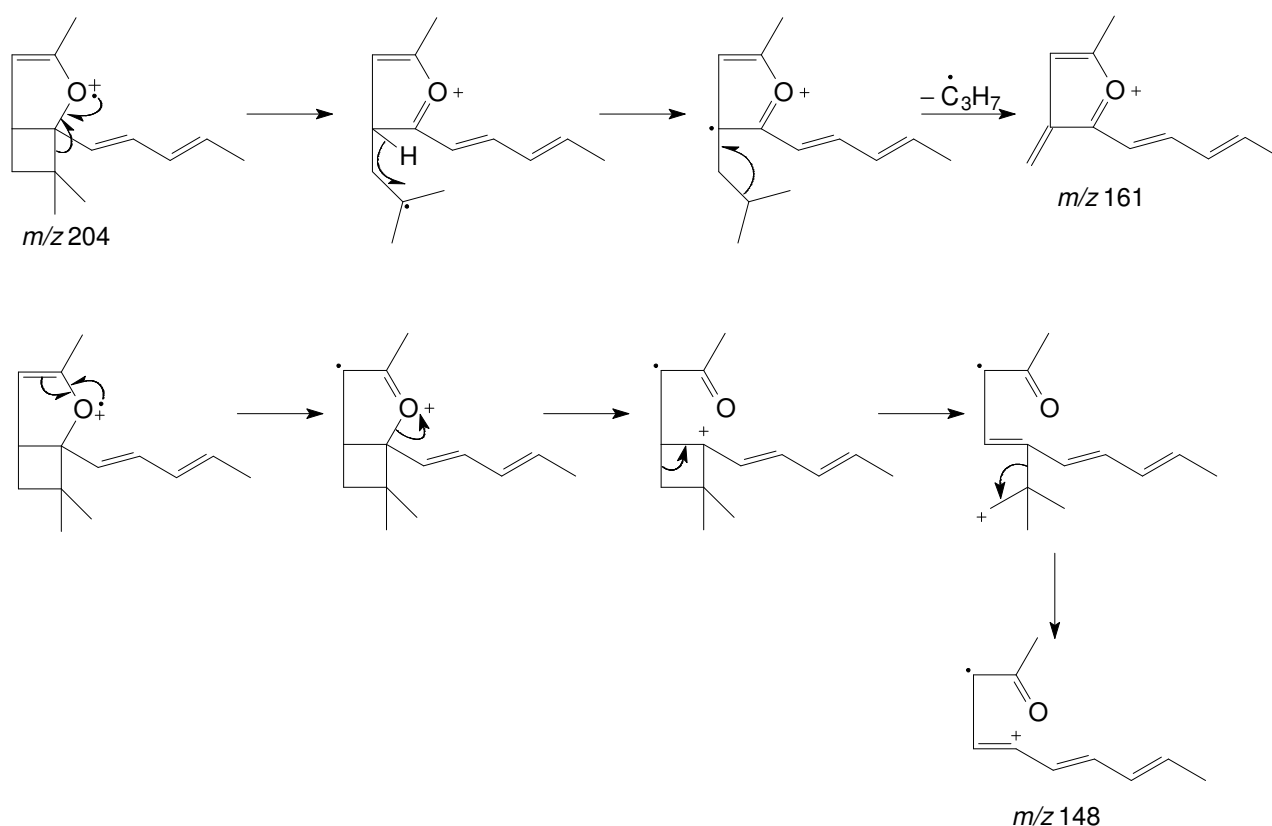
4-Vinylanisole

The mass spectra of components **C291** (Fig. 3.73) and **C294** are identical. They have prominent ions in the higher mass range at  $m/z$  133 ( $C_9H_9O^+$ ), 148 (base peak;  $C_{10}H_{12}O^+$ ), 161 ( $C_{11}H_{13}O^+$ ), 189 ( $C_{13}H_{17}O^+$ ;  $[M - CH_3]^+$ ) and 204 ( $M^+$ ,  $C_{14}H_{20}O^+$ ). Online library searches (NBS and NIST) were carried out on the mass spectra of these components, but only the NIST library suggested a candidate with a mass spectrum similar to the mass spectra of **C291** and **C294** (80% correlation), namely 3,7,7-trimethyl-1-penta-1,3-dienyl-2-oxabicyclo[3.2.0]hept-3-ene.



3,7,7-Trimethyl-1-penta-1,3-dienyl-2-oxabicyclo[3.2.0]hept-3-ene

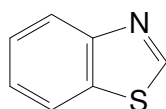
In the following scheme, a mechanism is proposed to explain the formation of the ions at  $m/z$  161 and 148:



Components **C291** and **C294** were tentatively identified as two **geometrical isomers** of **3,7,7-trimethyl-1-penta-1,3-dienyl-2-oxabicyclo[3.2.0]hept-3-ene**.

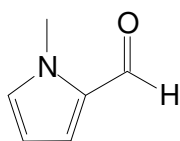
### 3.2.15 Other compounds

Component **C127** (Fig. 3.74) was tentatively identified by an online NBS library search as **benzothiazole** (75% correlation) and this was confirmed by retention time comparison with the commercially available compound. The mass spectra of thiazole and methylthiazoles are dominated by the molecular ions (base peaks) and by fragments formed by cleavage of the 1,2 and 3,4 bonds (Budzikiewicz *et al.*, 1967: 634–637; Clarke *et al.*, 1966).



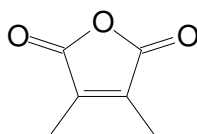
Benzothiazole

An online NBS library search predicted that component **C37** (Fig. 3.75) might be **2-formyl-1-methylpyrrole** (80% correlation) and this was confirmed by retention time comparison with the commercially available compound. The mass spectra of acylpyrroles display strong  $[M - 1]$  peaks, similar to benzaldehyde, since they have the tendency to form acylium ions (Budzikiewicz *et al.*, 1964a; Budzikiewicz *et al.*, 1967: 602–604). This explains the formation of the prominent ion at  $m/z$  108 ( $C_6H_6NO^+$ ) in the mass spectrum of **C37**.



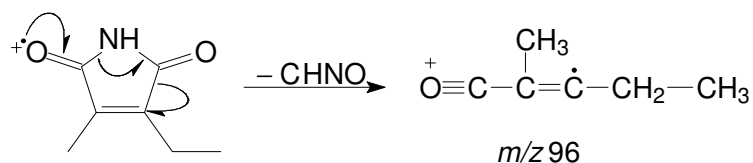
2-Formyl-1-methylpyrrole

An online library search (NBS) gave **3,4-dimethyl-2,5-furandione (dimethylmaleic anhydride)** as best possible candidate structure (94% correlation) for component **C48** (Fig. 3.76) and this was confirmed by retention time comparison with the corresponding commercially available compound.



Dimethylmaleic anhydride

The mass spectrum of component **C130** (Fig. 3.77) has a molecular ion at  $m/z$  139 ( $C_7H_9NO_2^+$ ) and the best candidate structure suggested for this component by the NIST library was **2-ethyl-3-methylmaleimide** (80% correlation). Losses of a methyl and a CHO group from the molecular ion are responsible for the formation of the ions at  $m/z$  124 ( $C_6H_6NO_2^+$ ) and 110 ( $C_6H_8NO^+$ ), respectively. The formation of the ion at  $m/z$  96 ( $C_6H_8O^+$ ) can be explained by the following mechanism, which is also responsible for the formation of similar ions in the mass spectra of imides (Budzikiewicz *et al.*, 1967: 364):



2-Ethyl-3-methylmaleimide

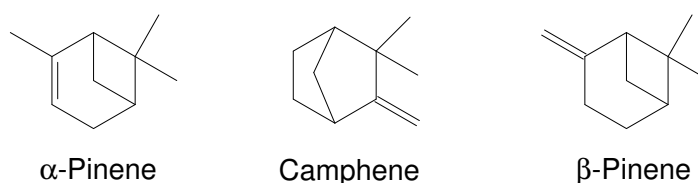
The published RI of this compound (Miyazawa *et al.*, 2008) is in good agreement with that of **C130** and provides further evidence that the component is indeed 2-ethyl-3-methylmaleimide.

### 3.2.16 Terpenoids

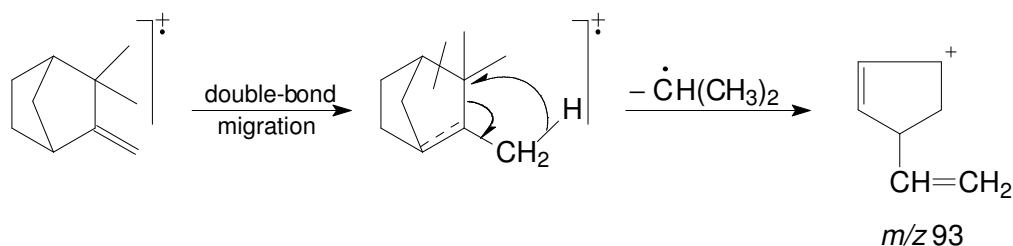
The carbon skeletons of terpenoid compounds are constructed of one or more units of 2-methylbuta-1,3-diene (isoprene) and therefore contain multiples of five carbon atoms. Honeybush contains a number of compounds with structures that, although they do not adhere to this rule, nevertheless have some structural characteristics of the terpenoids. For this reason, compounds with an irregular terpenoid structure of this type will also be discussed in this section. These compounds with fewer than the usual number of carbon atoms could be degradation products of the original terpenoid from which carbon atoms have been lost through chemical or biochemical processes. The carotenoid-derived compounds, also known as norisoprenoids, such as  $\beta$ -ionone, typically have 9, 11, 13 and 15 carbon atoms and are examples of compounds of this type.

#### 3.2.16.1 Terpenes

The mass spectra of components **C23** (Fig. 3.78), **C24** and **C30** all have in common a base peak at  $m/z$  93 and a molecular mass of 136 Da. The mass spectra of nine bicyclic monoterpenes ( $C_{10}H_{16}$ ), with the exception of  $\beta$ -fenchene, display a base peak at  $m/z$  93 ( $[M - 43]^+$ ) (Budzikiewicz *et al.*, 1964b: 148; Ryhage and Von Sydow, 1963; Thomas and Willhalm, 1964). Isotopic  $^{13}C$ -labelling of camphene suggests that the loss of 43 mass units can be ascribed to the predominant expulsion of the *gem*-dimethyl group together with one more hydrogen atom (Friedman and Wolf, 1958). This fragmentation is not necessarily favoured by the stability of the  $C_7H_9^+$  ion, but is rather caused by the ease with which these monoterpenes expel a  $C_3H_7$  fragment (Budzikiewicz *et al.*, 1964b: 148). After subjecting the individual mass spectra of **C23**, **C24**, and **C30** to online NBS library searches,  $\alpha$ -pinene, camphene and  $\beta$ -pinene were proposed as candidates (correlation >80%) and these structures were confirmed by retention time comparison with the corresponding commercially available compounds.

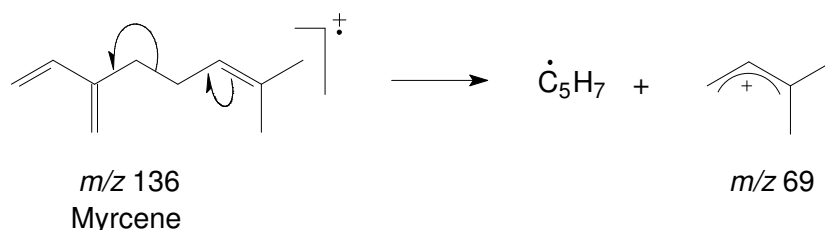


The formation of the ion at  $m/z$  93 in the mass spectrum of camphene is illustrated in the following scheme:

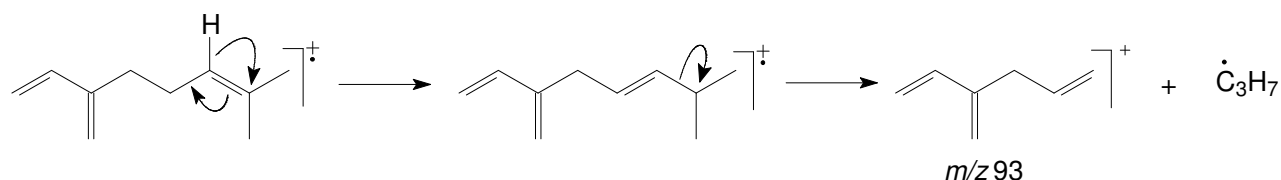


Both  $\alpha$ -pinene and camphene were resolved on enantioselective column C with  $R_s$  values of 2.4 and 1.3, respectively. The (-)-enantiomer of  $\alpha$ -pinene elutes before the (+)-enantiomer, but the order is reversed for camphene from an enantioselective column equivalent to column C (Maas *et al.*, 1994a; Filippi *et al.*, 2006). The enantioselective analysis of honeybush material established the presence of both the (-)- and (+)-enantiomers of  $\alpha$ -pinene and camphene in a ratio of 82:18 and 85:15, respectively. The concentration of  $\beta$ -pinene in the honeybush samples is very low and this component was not detected in any of the chiral analyses.

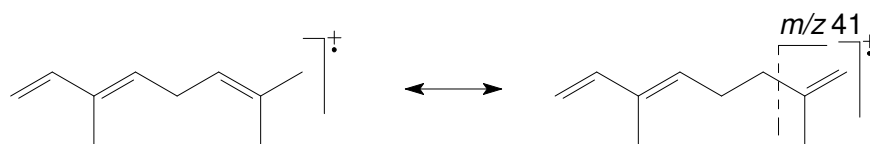
The mass spectrum of component **C38** (Fig. 3.79) has prominent ions at  $m/z$  41 (base peak), 69, 91, 93, 121 and 136 ( $M^+$ ) and it was assumed that this component might be a terpenoid, since this combination of ions is characteristic of the mass spectra of terpenoids. An online NBS library search identified **myrcene** as possible candidate with a correlation factor of 95% and retention time comparison of **C38** with commercially available myrcene proved this identification to be correct. The ion at  $m/z$  69 ( $C_5H_9^+$ ) is formed by cleavage of the bi-allylic bond (McLafferty and Tureček, 1993: 230):



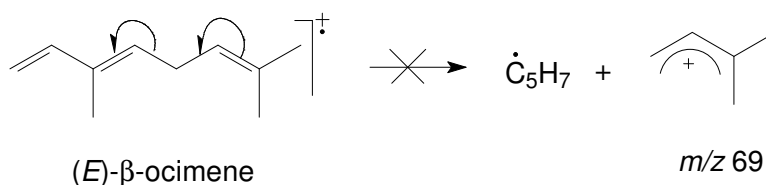
The double bonds of unsaturated hydrocarbons have the tendency to migrate when the compounds are subjected to conditions in the ion source of the mass spectrometer and this probably explains the formation of the ion at  $m/z$  93 ( $C_7H_9^+$ ) in the mass spectrum of **C38**:



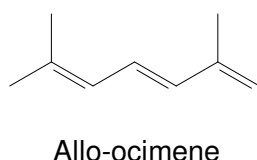
Loss of two hydrogen atoms or a hydrogen molecule from the ion at  $m/z$  93 explains the presence of the ion at  $m/z$  91. Rearrangement of the double bonds in myrcene, as illustrated below, accounts for the formation of the base peak at  $m/z$  41 ( $C_3H_5^+$ ):



The mass spectra of components **C56** (Fig. 3.80) and **C58** are identical, and in many ways also similar to the mass spectrum of myrcene. The most obvious difference between the mass spectrum of **C56** and that of myrcene is the much lower intensity of the ion at  $m/z$  69 in the former mass spectrum. The mass spectra of alkenes (and especially polyenes) are usually not affected by the position of double bonds unless the double bonds are substituted or could give rise to benzylic or allylic cleavages. In the mass spectrum of **C56** the low intensity of the ion at  $m/z$  69 can be ascribed to the fact that the cleaved bond is vinylic, in contrast to the doubly allylic bond in myrcene (McLafferty and Tureček, 1993: 230). Based on these arguments and the results of online library searches (correlation >94%), components **C56** and **C58** were identified as (**Z**)- and (**E**)- **$\beta$ -ocimene**, respectively, and this was confirmed by retention time comparison with the corresponding commercially available compounds:

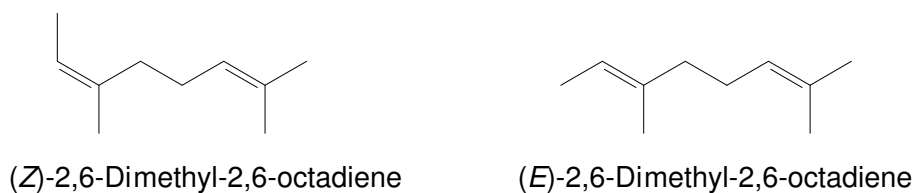


The mass spectrum of component **C93** (Fig. 3.81) displays the same group of ions that are characteristic of terpenes, such as the ones already mentioned, but with different relative abundances. Again, these differences in the abundances of the ions reflect directly on the positions of the double bonds in the compound. Component **C93** was tentatively identified as **allo-ocimene** [(**4E,6Z**)-2,6-dimethyl-2,4,6-octatriene] by an online NBS library search (86% correlation) and its identity was confirmed by retention time comparison with the commercially available compound.

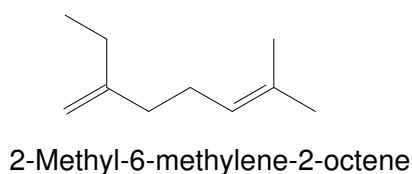


The mass spectra of components **C34**, **C43** (Fig. 3.82) and **C57** are mutually similar. They contain a base peak at  $m/z$  69, which suggests that the double bonds in these components are arranged in a similar manner as in myrcene (bi-allylic bond). The molecular mass (138 Da) suggests however that these components should contain one double bond fewer than myrcene. The NBS library suggested that **C34** and **C43** could be (**Z**)- and (**E**)-2,6-dimethyl-2,6-octadiene, respectively

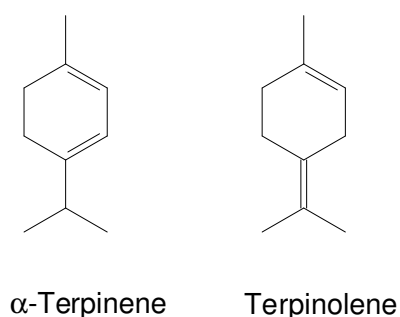
(correlation >90%), and this was confirmed by retention time comparison with the commercially available compounds.



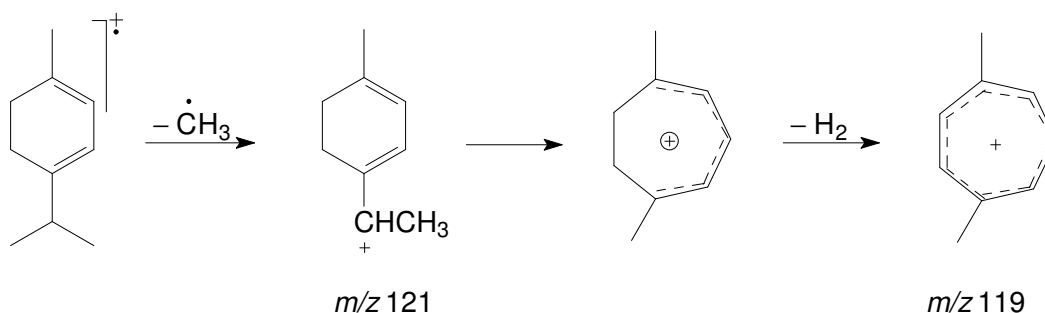
An online library search did not propose any acceptable candidate structures for component **C57**. The relative abundances of the ions in its mass spectrum were therefore used in a manual library search (NIST), which gave **2-methyl-6-methylene-2-octene** as possible structure for this component.



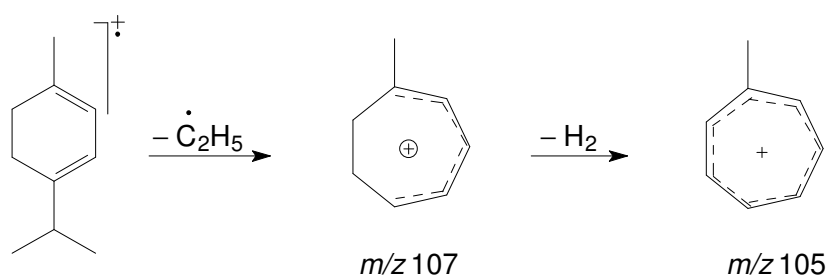
The mass spectra of components **C47** and **C71** (Fig. 3.83) are strikingly similar. They have very abundant ions at  $m/z$  93, 121 and a molecular ion at  $m/z$  136. Online library searches (NBS) gave an indication that these components could be cyclic terpenes, but were not conclusive. By comparing the RIs of these components with those found in the literature (Adams, 2004), **C47** and **C71** were identified as  **$\alpha$ -terpinene** and **terpinolene**, respectively, and this was confirmed by retention time comparison with the commercially available compounds.



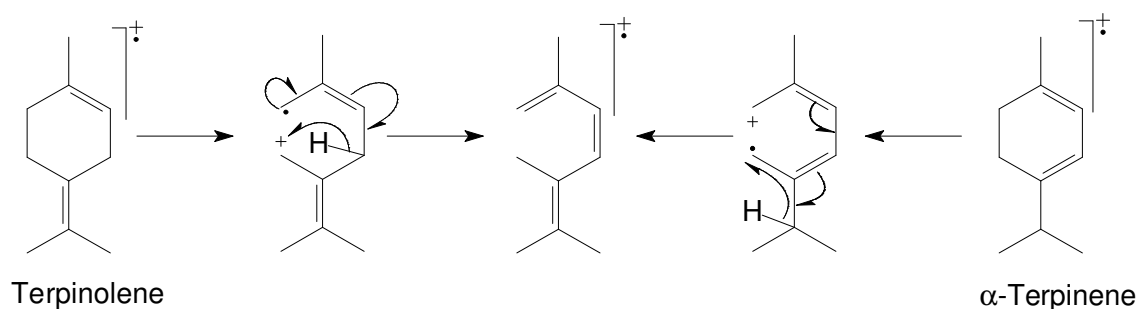
Loss of a methyl group from the molecular ion accounts for the formation of the ion at  $m/z$  121 ( $C_9H_{13}^+$ ) in the mass spectra of both of these components. This ion rearranges to form a  $C_7$  cyclic molecule, which can lose a hydrogen molecule to give the ion at  $m/z$  119 ( $C_9H_{11}^+$ ), as illustrated for  $\alpha$ -terpinene (Thomas and Willhalm, 1964):



Formation of the ions at  $m/z\ 107$  ( $C_8H_{11}^+$ ) and  $105$  ( $C_8H_9^+$ ) proceeds *via* the formation of a methylcycloheptane, which is converted to the ion at  $m/z\ 105$  by the loss of a hydrogen molecule (Thomas and Willhalm, 1964):

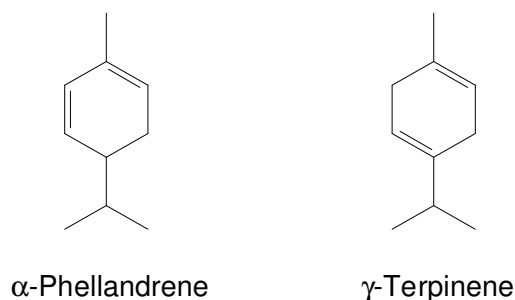


In these cyclic isomers cleavage of the allylic bond is followed by an energetically favourable hydrogen transfer, which leads to the formation of a linear conjugated triene ion, similar to the allocimene molecular ion (**C93**), and which might explain the similarity observed in the mass spectra of these components (Budzikiewicz *et al.*, 1964b: 146–147; Thomas and Willhalm, 1964):

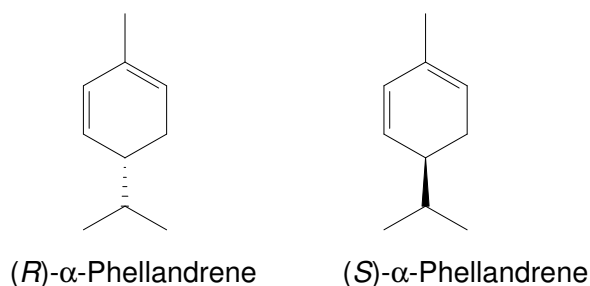


The mass spectra of components **C42** and **C61** (Fig. 3.84) are similar. They contain the same prominent ions observed in the mass spectra of the previous two cyclic dienes, but have different relative abundances. By comparing the RI of **C42** with RIs available in the literature (Adams, 2004)  **$\alpha$ -phellandrene** was identified as possible candidate structure. This was confirmed by retention time comparison with the commercially available compound. Component **C61** was identified as  **$\gamma$ -terpinene** by an online library search (NBS) (93% correlation) and retention time comparison with the commercially available compound.

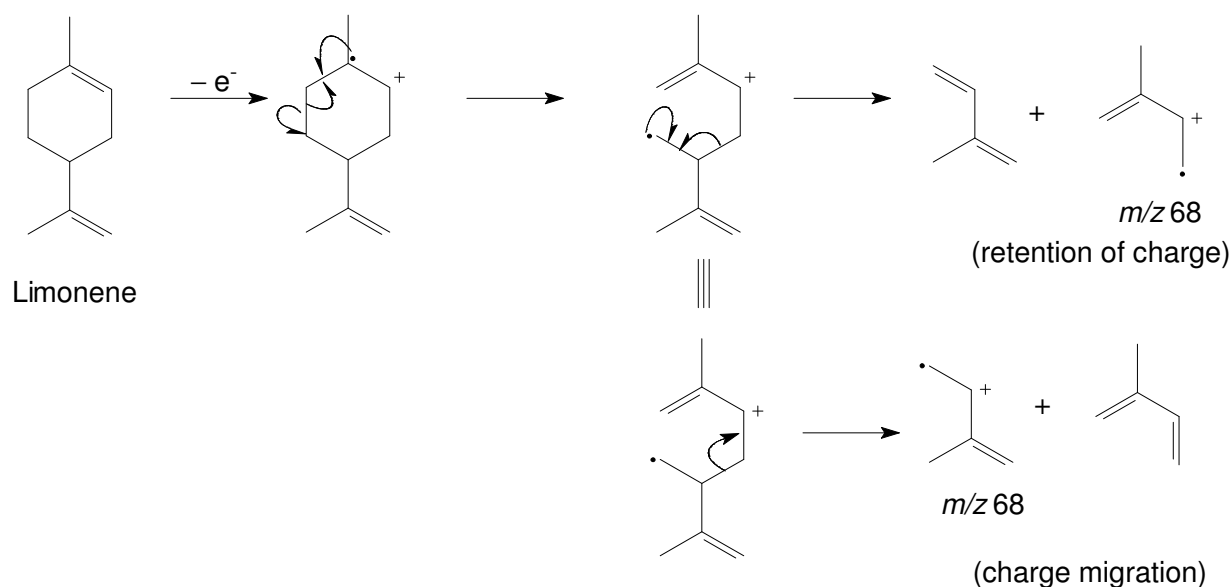




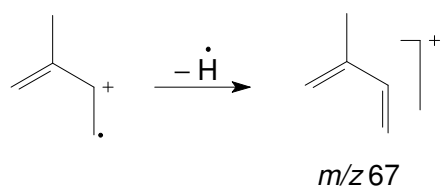
In  $\alpha$ -phellandrene and  $\gamma$ -terpinene allylic cleavage and simple hydrogen migration cannot take place to form a conjugated triene. This explains the differences observed in the mass spectra of these two cyclic dienes compared to the previous two dienes ( $\alpha$ -terpinene and terpinolene) (Budzikiewicz *et al.*, 1964b: 146–147). Another significant ion appearing in the mass spectra of all these cyclic dienes, is the  $[M - 2]^+$  ion, which is generated by thermal decomposition. The driving force of this is the formation of an aromatic ring upon expulsion of two hydrogen atoms (Budzikiewicz *et al.*, 1964b: 146–147; Ryhage and Von Sydow, 1963). The intensity of this ion is highest in the cyclic dienes, such as  $\alpha$ -phellandrene,  $\gamma$ -terpinene and  $\alpha$ -terpinene, where both the double bonds are endo-cyclic, and it is less prominent for terpinolene, which has one exo-cyclic double bond. The (*R*)-enantiomer of  $\alpha$ -phellandrene elutes before its (*S*)-enantiomer from an enantioselective column equivalent to column C (Kreck *et al.*, 2002). The enantiomers of  $\alpha$ -phellandrene were resolved on this column ( $\alpha$ -value of 1.01) and enantioselective analysis of the honeybush material established that both enantiomers are present in a ratio of 20:80 (*R*:*S*).



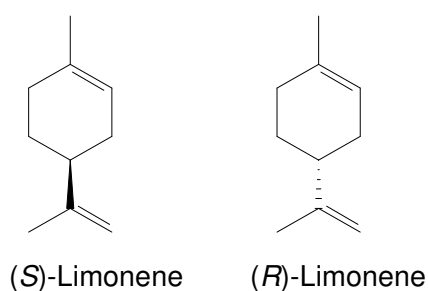
The mass spectrum of component **C52** (Fig. 3.85) contains many of the prominent ions present in the cyclic dienes already discussed, such as  $m/z$  77, 79, 93, 121 and 136 ( $M^+$ ), but also has a prominent ion at  $m/z$  67 and a base peak at  $m/z$  68. It was assumed that **C52** might also be a cyclic diene, but with the double bonds arranged in a manner that would allow a rearrangement, which would explain the formation of the ion with even mass at  $m/z$  68. This rearrangement will only be possible if one of the double bonds is exo-cyclic in the  $C_3$  moiety, as in the case of terpinolene (**C71**). The mass spectrum of **C52** does not contain an  $[M - 2]^+$  ion, which further proves that one of the double bonds is exo-cyclic. Component **C52** was identified by an online library search as **limonene** (97% correlation) and its identity was confirmed by retention time comparison with the commercially available compound. The base peak at  $m/z$  68 ( $C_5H_8^+$ ) is formed by a retro-Diels-Alder rearrangement (McLafferty and Tureček, 1993: 70):



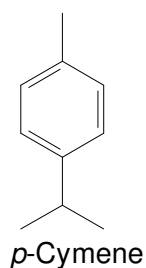
The formation of the ion at  $m/z$  67 ( $C_5H_7^+$ ) can be explained in terms of an expulsion of a hydrogen atom from the ion at  $m/z$  68:



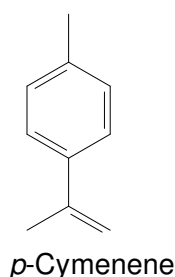
Pure commercially available enantiomers of limonene were used to determine that the (*S*)-enantiomer elutes before the (*R*)-enantiomer from the enantioselective column C ( $R_s$  value of 3.1). Enantioselective analysis of the honeybush material established the presence of both enantiomers in a ratio of 26:74 (*S*:*R*).



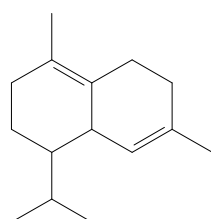
The molecular mass of component **C50** (Fig 3.86) is two mass units lower than the masses of the cyclic dienes discussed thus far, indicating that this component might contain an additional double bond. An online NIST library search of the mass spectrum of **C50** gave *p*-cymene as the most likely candidate structure (82% correlation). The retention times of **C50** and commercially available *p*-cymene were also found to be identical. The base peak at  $m/z$  119 ( $C_9H_{11}^+$ ) is formed by the loss of a methyl group from the molecular ion, whereas the ions present at  $m/z$  65 ( $C_5H_5^+$ ), 77 ( $C_6H_5^+$ ) and 91 ( $C_7H_7^+$ , tropylium ion) are ions typically associated with aromatic molecules.



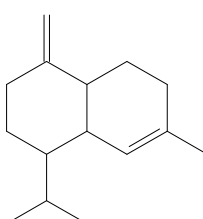
The mass spectrum of component **C69** (Fig. 3.87) has a molecular ion at  $m/z$  132, which indicates that this component has one double bond more than *p*-cymene. Loss of a methyl group yet again explains the base peak at  $m/z$  117. Ions characteristic of aromatic systems are present at  $m/z$  65, 77 and 91. This compound was tentatively identified as ***p*-cymenene** by comparing the RI of this compound with published RI data (Adams, 2004) and further confirmation was obtained by retention time comparison with the commercially available compound.



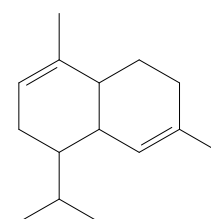
The mass spectra of components **C247** (Fig. 3.88), **C244** (Fig. 3.89) and **C240** (Fig. 3.90) contain a molecular ion at  $m/z$  204 ( $C_{15}H_{24}^+$ ) and the same prominent ions, although with different relative abundances, indicating that these components are structurally related. Online NBS library searches gave the following three candidate structures with correlation factors of 74%, 98% and 94%, respectively.



C247 :  $\delta$ -Cadinene



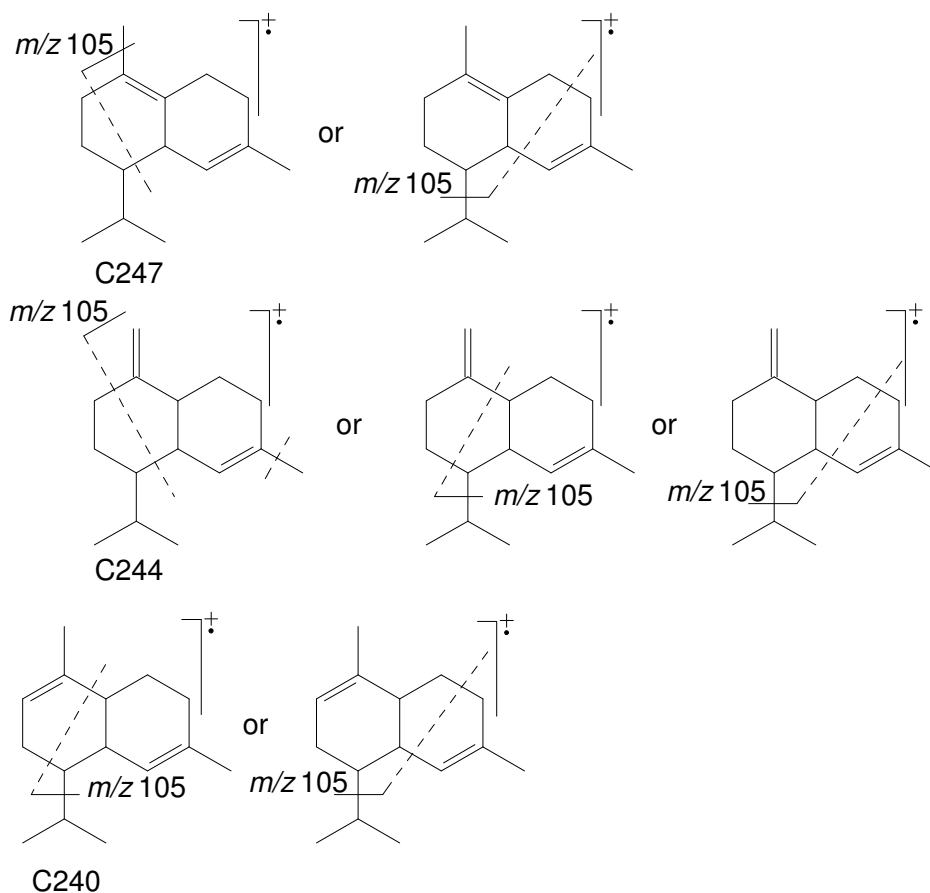
C244:  $\gamma$ -Cadinene



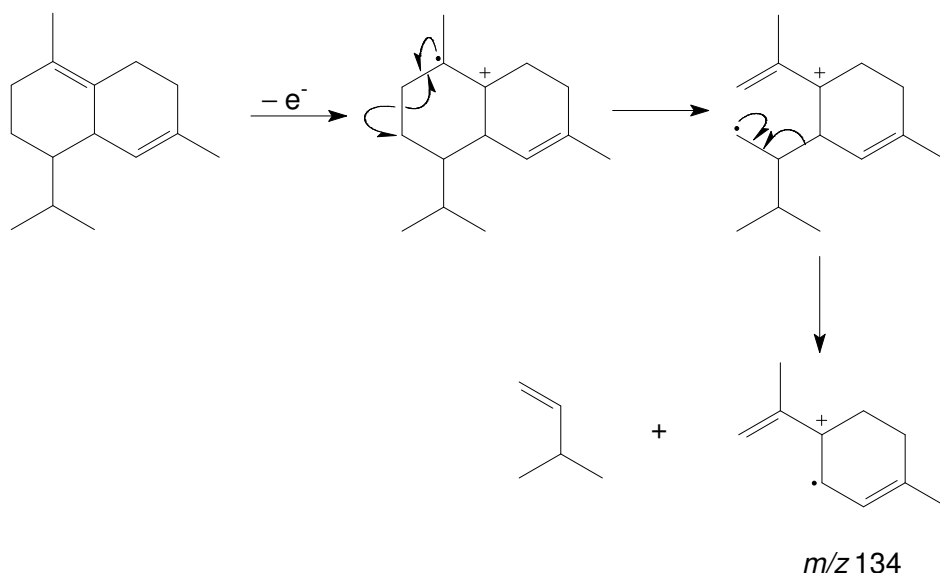
C240:  $\alpha$ -Muurolene

The RIs of these components are in agreement with the specific RIs obtained in the literature (Adams, 2004). For **C247** and **C244** a base peak appears at  $m/z$  161 ( $C_{12}H_{17}^+$ ), which can be ascribed to the loss of the isopropyl moiety or possibly the loss of a  $C_2H_4$  moiety together with a methyl group. For **C240** the base peak is at  $m/z$  105 ( $C_8H_9^+$ ) instead of  $m/z$  161. Although the

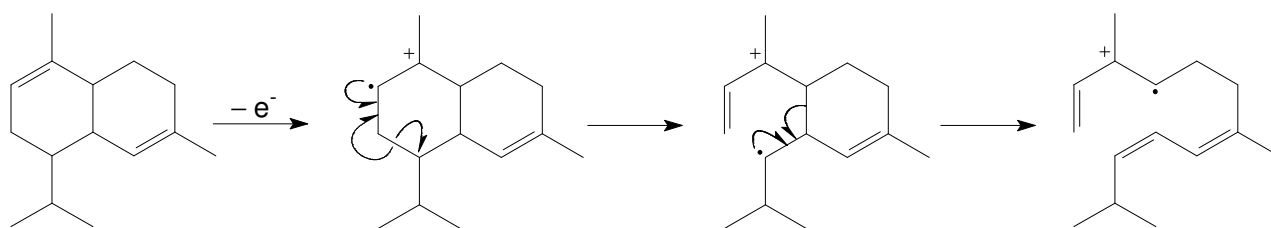
following are not proposed as mechanisms, the formation of the ion at  $m/z$  105 can be schematically illustrated as follows:



The formation of the ion at  $m/z$  105 is more favourable in **C240** than in **C247** and **C244** since it involves the cleavage of both a vinylic and an allylic bond in both scenarios, whereas in the case of both **C247** and **C244** it is possible in only one of the scenarios. Another important difference observed between the mass spectra of these components is the presence of an ion with even mass at  $m/z$  134 ( $C_{10}H_{14}^+$ ), which is more abundant in the mass spectrum of **C247** than in those of **C240** and **C244**, and could be formed by a retro-Diels-Alder rearrangement:

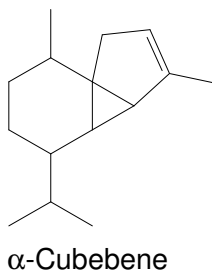


The respective positions of the double bonds in **C240** and **C244** impair the formation of the ion at  $m/z$  134 through a retro-Diels-Alder rearrangement as illustrated for **C240**:



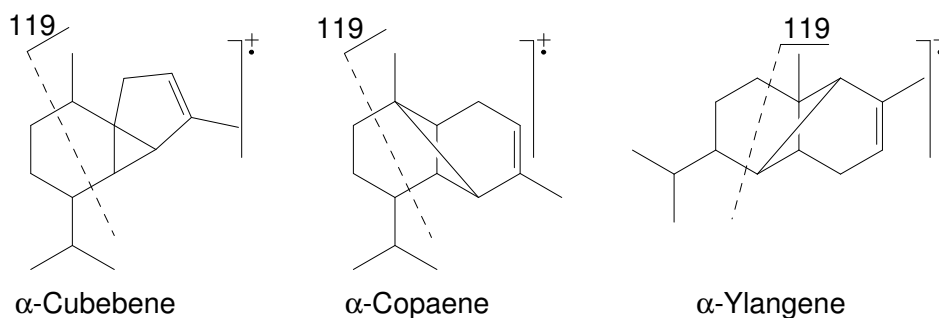
Based on the discussion above, **C247**, **C244** and **C240** were tentatively identified as  **$\delta$ -cadinene**,  **$\gamma$ -cadinene** and  **$\alpha$ -muurolene**, respectively.

The mass spectra of components **C194**, **C200** and **C205** (Fig. 3.91) are very similar. They contain many of the prominent ions also present in the mass spectra of the two cadinenes and  $\alpha$ -muurolene. Online NBS library searches suggested the same structure for both **C194** and **C205** (correlation >90%).

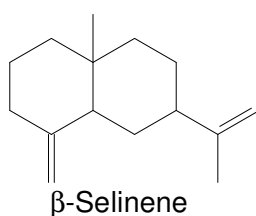


The RI of  **$\alpha$ -cubebene** (Adams, 2004) was found to correspond to that of **C194**, whereas the RI of  **$\alpha$ -copaene** (Adams, 2004), of which the mass spectrum is similar to that of  $\alpha$ -cubebene, corresponds to that of **C205**. Identification of **C194** and **C205** as  $\alpha$ -cubebene and  $\alpha$ -copaene, respectively, was confirmed by retention time comparison with the commercially available compounds. Component

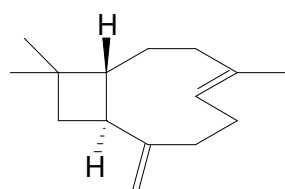
**C200** was identified as  **$\alpha$ -ylangene**, based on the good agreement between its RI and mass spectral data with  $\alpha$ -ylangene (Adams, 2004). The ion at  $m/z$  119 ( $C_9H_{11}^+$ ) might form by the loss of a  $C_6H_{13}$  fragment, schematically illustrated as follows:



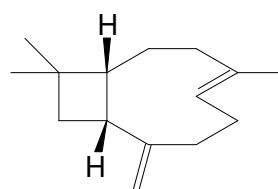
The mass spectrum of component **C235** (Fig. 3.92) has a large number of prominent ions at  $m/z$  41, 53, 55 ( $C_4H_7^+$ ), 67 ( $C_5H_7^+$ ), 77, 79 ( $C_6H_7^+$ ), 81, 91, 93, 105, 107 ( $C_8H_{11}^+$ ), 121 ( $C_9H_{13}^+$ ), 133 ( $C_{10}H_{13}^+$ ), 147 ( $C_{11}H_{15}^+$ ), 161, 175, 189 and 204 ( $M^+$ ), all appearing with relatively high abundances, resulting in a very complex mass spectrum. Ions were also observed in the mass spectrum at  $m/z$  128, 143, 158 and 173, which did not seem to fit into the general pattern of the majority of the ions in the mass spectrum. It was ascertained that these ions do in fact belong to component **C236** which elutes very closely to **C235**, and which was identified as calamenene-1,11-epoxide (§ 3.2.16.6). In the same manner **C235** was tentatively identified as  **$\beta$ -selinene** (Adams, 2004).



The mass spectra of components **C216** (Fig. 3.93) and **C226** (Fig. 3.94) have many of the same prominent ions observed in the mass spectra of the  $C_{15}H_{24}$  compounds discussed thus far and they also have the same elemental composition. An online NBS library search presented (***E***-**caryophyllene**) as the most likely candidate structure (93% correlation) for **C216** and this identification was confirmed by retention time comparison with the commercially available compound. Component **C226** was identified as **9-*epi*-(*E*)-caryophyllene** by comparing its mass spectrum and RI with published data (Adams, 2004).

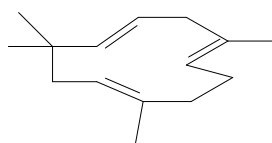


(*E*)-Caryophyllene



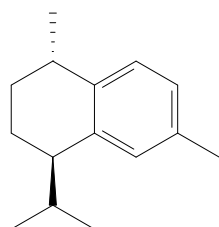
9-*epi*-(*E*)-Caryophyllene

The mass spectrum of component **C221** (Fig. 3.95) has a base peak at  $m/z$  93 and molecular ion at  $m/z$  204. This component was tentatively identified by an online library search (NBS, 94% correlation) as  **$\alpha$ -humulene** and this was later confirmed by retention time comparison with the commercially available compound.

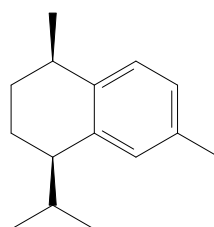


$\alpha$ -Humulene

The mass spectrum of component **C246** (Fig. 3.96) has a base peak at  $m/z$  159 ( $C_{12}H_{15}^+$ ) and molecular ion at  $m/z$  202. An online library search presented **calamenene** as the best possible candidate structure (87% correlation). The methyl and isopropyl groups can be either *cis* or *trans* (Adams, 2004).



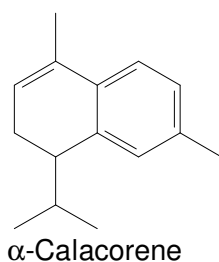
*trans*-Calamenene



*cis*-Calamenene

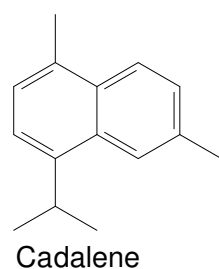
These two diastereomers have different retention indices, and the RI of **C246** corresponds to that of ***trans*-calamenene** (Adams, 2004). The base peak in its mass spectrum is formed by the loss of the isopropyl group.

The mass spectrum of component **C252** (Fig. 3.97) has prominent ions at  $m/z$  142, 157 (base peak) and 200 ( $M^+$ ). Its elemental composition was determined as  $C_{15}H_{20}$ , which led to the assumption that this component might be similar to *trans*-calamenene, probably with an additional double bond. An online library search did not present any candidate structures that could be used to identify this component, but by using the relative abundances of the significant ions in a manual library search  **$\alpha$ -calacorene** was obtained as possible candidate.



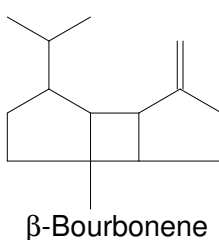
The published RI of  $\alpha$ -calacorene (Adams, 2004) was found to correspond to that of **C252**. The ion at  $m/z$  157 ( $C_{12}H_{13}^+$ ) is formed by the loss of an isopropyl group. The consecutive loss of an isopropyl and methyl group from the molecular ion could explain the formation of the ion at  $m/z$  142 ( $C_{11}H_{10}^+$ ). Component **C252** was tentatively identified as  $\alpha$ -calacorene.

The molecular mass of component **C290** (Fig. 3.98) is two mass units lower than the molecular mass of  $\alpha$ -calacorene, which means that this component has one double bond more than  $\alpha$ -calacorene and two double bonds more than calamenene. Prominent ions appear at  $m/z$  183 (base peak), 168 and 153. The online NBS library suggested that **C290** might be **cadalene** (89% correlation).



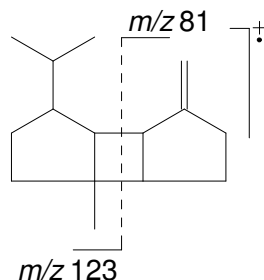
This suggestion given by the library search was in accordance with the elemental composition of  $C_{15}H_{18}$  and RI comparison with published data (Adams, 2004) also supported this. The ion at  $m/z$  183 ( $C_{14}H_{15}^+$ ) is formed by loss of any one of the methyl groups present in the molecule, and the additional loss of one and two methyl groups, respectively, is responsible for the formation of the ions at  $m/z$  168 ( $C_{13}H_{12}^+$ ) and 153 ( $C_{12}H_9^+$ ). Component **C290** was therefore tentatively identified as cadalene

The mass spectrum of component **C208** (Fig. 3.99) has prominent ions at  $m/z$  80, 81 (base peak), 123, 161 and a very weak molecular ion at  $m/z$  204, which was only observed in the mass spectrum obtained with HRMS analysis. An online library search (NBS) presented  **$\beta$ -bourbonene** (90% correlation) as best possible candidate structure for **C208**.

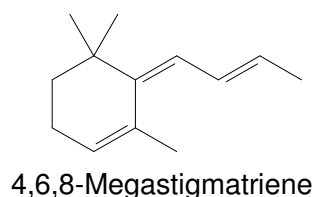




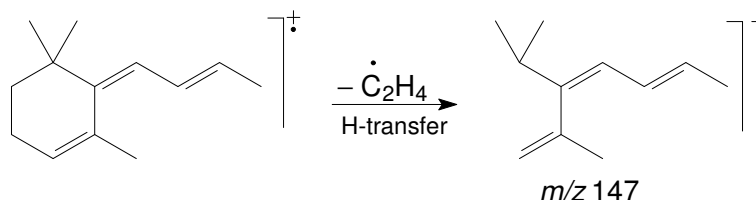
The RI for this compound (Adams, 2004) is in accordance with that of **C208**. The ion at  $m/z$  161 ( $C_{12}H_{17}^+$ ) is formed by the loss of the isopropyl group, whereas the ion at  $m/z$  123 ( $C_9H_{15}^+$ ) most likely consists of the  $C_5$  ring moiety containing the isopropyl group, but when formed should proceed with the transfer of hydrogen atoms. Retention of the charge on the other  $C_5$  moiety could explain the ion at  $m/z$  81 ( $C_6H_9^+$ ). This process is accompanied by hydrogen transfer, but when no hydrogen transfer takes place the ion at  $m/z$  80 ( $C_6H_8^+$ ) is formed:



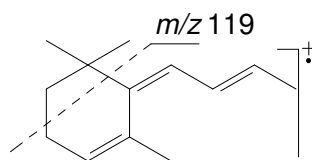
The mass spectrum of component **C197** (Fig. 3.100) has a base peak at  $m/z$  105 and molecular ion at  $m/z$  176. Online NBS and NIST library searches gave **4,6,8-megastigmatriene** as possible candidate structure (80% correlation).



Loss of any one of the methyl groups from the molecular ion is responsible for the formation of the ion at  $m/z$  161 ( $C_{12}H_{17}^+$ ). The ion at  $m/z$  147 ( $C_{11}H_{15}^+$ ) could be formed by the loss of the  $C_2H_4$  moiety of the six-membered ring, accompanied by a hydrogen transfer to afford this  $[M - 29]^+$  ion:



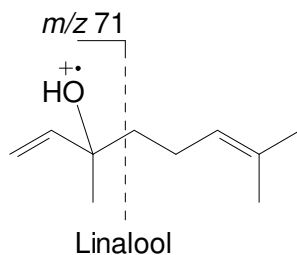
Loss of the  $C_2H_4$  moiety without hydrogen transfer, accompanied by the loss of a methyl group, accounts for the formation of the ion at  $m/z$  133 ( $C_{10}H_{13}^+$ ). The  $C_9H_{11}^+$  ion ( $m/z$  119) could possibly be formed when the following allylic and vinylic bonds are cleaved as schematically illustrated below:



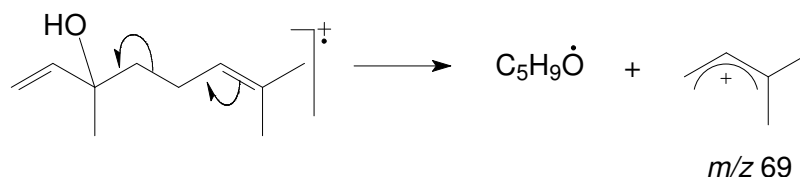
The formation of the ion at  $m/z$  105 (C<sub>8</sub>H<sub>9</sub><sup>+</sup>) can be explained in terms of the loss of the same C<sub>4</sub>H<sub>8</sub> moiety as shown above, but without hydrogen transfer and with the additional loss of a methyl group.

### 3.2.16.2 Terpene alcohols

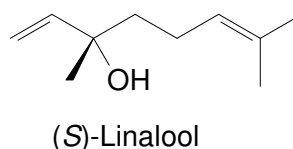
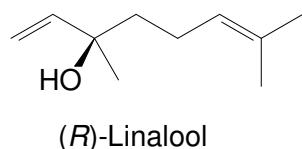
In the EI mass spectrum of component **C76** (Fig. 3.101) two ions appear in the high mass range at  $m/z$  136 (C<sub>10</sub>H<sub>16</sub><sup>+</sup>) and 139 (C<sub>9</sub>H<sub>15</sub>O<sup>+</sup>), respectively. Initially it was uncertain whether either one of them was the molecular ion. According to the online NBS library search **C76** could be **linalool** (96% correlation) and this was confirmed by retention time comparison with the commercially available compound. Linalool has a molecular mass of 154 Da, and therefore the ions at  $m/z$  136 and 139 are formed by the loss of a methyl group and the elements of water, respectively. The ion at  $m/z$  121 (C<sub>9</sub>H<sub>13</sub><sup>+</sup>) is formed by the consecutive loss of both these groups. The base peak at  $m/z$  71 (C<sub>4</sub>H<sub>7</sub>O<sup>+</sup>) is formed by an  $\alpha$ -cleavage reaction, typically occurring in alcohols, with resultant loss of the largest alkyl fragment:



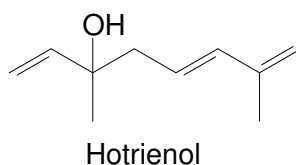
Cleavage of the allylic bond leads to the formation of the ion at  $m/z$  69 (C<sub>5</sub>H<sub>9</sub><sup>+</sup>):



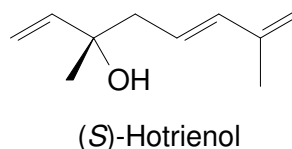
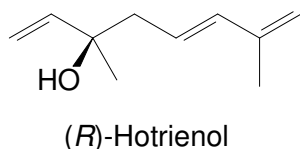
Loss of a C<sub>3</sub>H<sub>7</sub> fragment as well as a molecule of water explains the presence of the ion at  $m/z$  93 (C<sub>7</sub>H<sub>9</sub><sup>+</sup>). The even-mass ion at  $m/z$  80 (C<sub>6</sub>H<sub>8</sub><sup>+</sup>) is formed by loss of a C<sub>4</sub>H<sub>9</sub> fragment and water, which is accompanied by the transfer of a hydrogen atom. The whole process prior to the formation of the ion most probably involves the rearrangement of the double bonds. The enantiomers of linalool were resolved on enantioselective column D ( $R_s$  value of 1.6). The (*R*)-enantiomer of linalool elutes before its (*S*)-enantiomer from an enantioselective column equivalent to column D (Maas *et al.*, 1994b). The enantioselective analysis of honeybush samples established the presence of both enantiomers of linalool in a ratio of 53:47 (*R*:*S*).



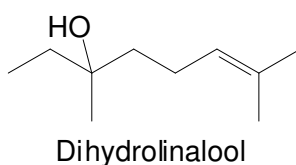
The mass spectrum of component **C78** (Fig. 3.102) has prominent ions at  $m/z$  43, 67, 71 (base peak), 82, 91, 119 and 134. The online library search did not suggest any likely candidate structures for **C78**, but when the relative abundances of the prominent ions were manually entered into the NIST library **hotrienol** was tentatively suggested.



HRMS analysis gave results in accordance with the suggested identity of **C78**. For example, the elemental composition of the ion at  $m/z$  134 was reported as  $C_{10}H_{14}^+$   $[M - H_2O]^+$ . The loss of a molecule of water followed by the loss of a methyl group explains the formation of the ion at  $m/z$  119 ( $C_9H_{11}^+$ ). According to Luan *et al.* (2004) the enantiomers of hotrienol can be resolved on an enantioselective column equivalent to column C. The (*R*)-enantiomer elutes before its (*S*)-enantiomer from this column and the enantioselective analysis of honeybush material established the presence of both enantiomers of hotrienol in a ratio of 38:62.

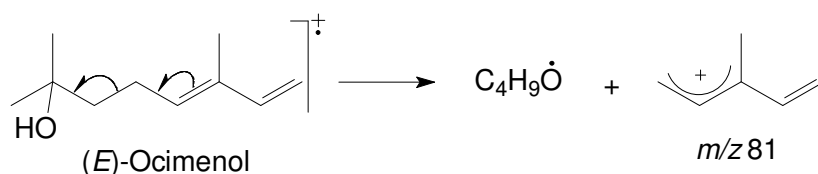


Based on the molecular masses of components eluting close to component **C94** it was assumed that the ion with the highest mass at  $m/z$  138 in its mass spectrum (Fig. 3.103) could not be the molecular ion, but that its molecular mass should rather be 156 Da  $[138 + H_2O]$ . The elemental composition of the ion at  $m/z$  138 was determined as  $C_{10}H_{18}$ , and after inclusion of the elements of water the elemental composition of **C94** becomes  $C_{10}H_{20}O$ . An NBS online library search presented **dihydrolinalool** as the best possible candidate structure for **C94** (80% correlation).

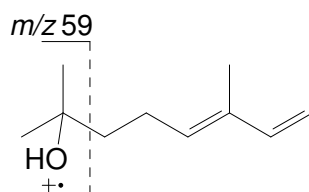


This compound has one double bond fewer than linalool (**C76**) and many of the prominent ions, such as  $m/z$  123 [ $M - 18 - 15$ ]<sup>+</sup>, 95 [ $M - 18 - 43$ ]<sup>+</sup>, 81 [ $M - 18 - C_4H_9$ ]<sup>+</sup>, 73 [ $\alpha$ -cleavage with resultant loss of the largest alkyl group] and 69 [cleavage of the allyl bond], are formed in the same way as already discussed for linalool. The base peak at  $m/z$  109 ( $C_8H_{13}^+$ ) is formed by the loss of a water molecule as well as the ethyl group attached to the tertiary alcohol. The reported RI (Adams, 2004) for dihydrolinalool is in agreement with the RI of **C94** and it was concluded that this component is indeed dihydrolinalool.

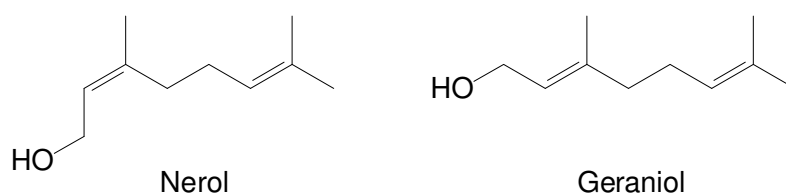
Although the ions with the highest mass in the mass spectra of both components **C103** and **C113** (Fig. 3.104) appear at  $m/z$  136 it seemed unlikely that the molecular mass of these two components could be 136 Da, considering their retention times. Online library searches (NBS) suggested that these components might be (**Z**)- and (**E**)-ocimanol, respectively (80% correlation), with a molecular mass of 154 Da, in which case the ions at  $m/z$  136, mentioned above, are formed by the loss of a water molecule from the molecular ions of the two ocimenols. The formation of the ions at  $m/z$  121 and 93 has already been discussed (cf. component **C76**). Cleavage of the allylic bond in ocimanol leads to the formation of the ion at  $m/z$  81 ( $C_6H_9^+$ ):



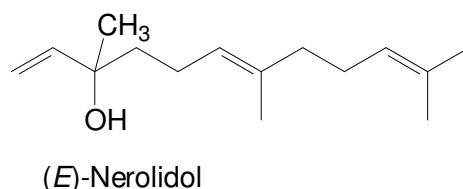
The same  $\alpha$ -cleavage reaction responsible for the formation of the ion at  $m/z$  71 in the mass spectrum of linalool leads to the formation of the ion at  $m/z$  59 ( $C_3H_7O^+$ ) in the mass spectrum of ocimanol:



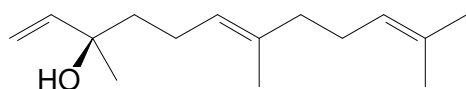
The mass spectra of components **C135** and **C148** (Fig. 3.105) are identical. They have a base peak at  $m/z$  69 and molecular ion at  $m/z$  154. Online library searches (NBS) suggested **nerol** and **geraniol** as possible candidate structures for **C135** and **C148**, respectively (93% and 94% correlation) and this was confirmed by retention time comparison with the commercially available compounds.



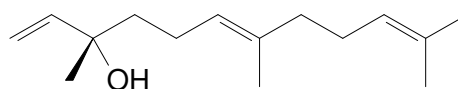
The ion with the highest mass in the mass spectrum of component **C260** (Fig. 3.106) appears at  $m/z$  204. An online library search (NBS) suggested that **C260** could be  $\beta$ -farnesene (91% correlation), which has a molecular mass of 204 Da. Component **C260**, however, elutes much later than  $\beta$ -farnesene (Adams, 2004). This led to the conclusion that **C260** must have a somewhat higher molecular mass. The online library search also suggested nerolidol (222 Da) (88% correlation) as another possible candidate structure. Retention time comparison with the commercially available compound proved that **C260** was in fact (*E*)-nerolidol. The ion at  $m/z$  204 ( $C_{15}H_{24}^+$ ) is therefore the  $[M - 18]^+$  ion.



The enantiomers of (*E*)-nerolidol were resolved on enantioselective column C with a resolution of 1.2. The (*R*)-enantiomer of (*E*)-nerolidol elutes before its (*S*)-enantiomer from a column equivalent to column C (Mathias and Mosandl, 2004), and it was established that both of these enantiomers were present in the honeybush samples in a ratio of 41:59 (*R*:*S*).

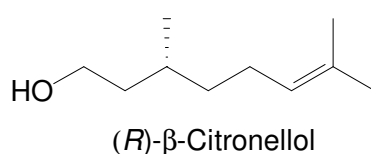


(*R*)-(*E*)-Nerolidol

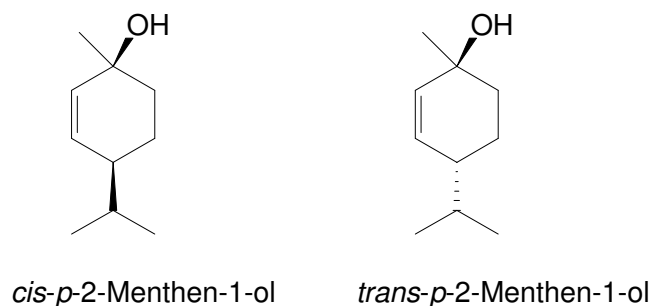


(*S*)-(*E*)-Nerolidol

The mass spectrum of component **C137** is contaminated by some of the prominent ions of the neighbouring component **C138**. However, **C137** has an abundant ion at  $m/z$  69 as well as other less abundant ions at  $m/z$  95, 109, 123 and 138 that do not belong to the mass spectrum of **C138**. It was assumed that **C137** might be  $\beta$ -citronellol, the RI and mass spectral data (Adams, 2004) of which are in good agreement with those of **C137**. Retention time comparison with commercially available  $\beta$ -citronellol confirmed that **C137** was indeed  $\beta$ -citronellol. A better mass spectrum was obtained for **C137** in an analysis done on the polar column B (Fig. 3.107), and  $[M - H_2O]^+$ ,  $[M - H_2O - CH_3]^+$  and  $[M - H_2O - C_3H_7]^+$  ions could be observed at  $m/z$  138, 123 and 109, respectively. The enantiomers of  $\beta$ -citronellol were resolved on enantioselective column D ( $\alpha$ -value of 1.00). The (*S*)-enantiomer of  $\beta$ -citronellol elutes before its (*R*)-enantiomer from an enantioselective column equivalent to column D (Maas *et al.*, 1994b) and it was found that only the (*R*)-enantiomer is present in the honeybush samples.

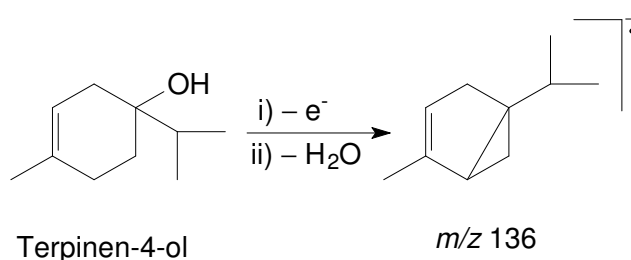


The mass spectra of components **C86** (Fig. 3.108) and **C96** are similar. Both have molecular ions at  $m/z$  154. Online library searches (NBS) presented *p*-2-menthen-1-ol as a possible candidate structure for both of these components (90% correlation) and the elemental composition of  $C_{10}H_{18}O$  determined for these two components was in agreement with this suggestion. Comparison of their RIs with those of *cis-p*-2-menthen-1-ol and *trans-p*-2-menthen-1-ol (Adams, 2004), confirmed these assignments.

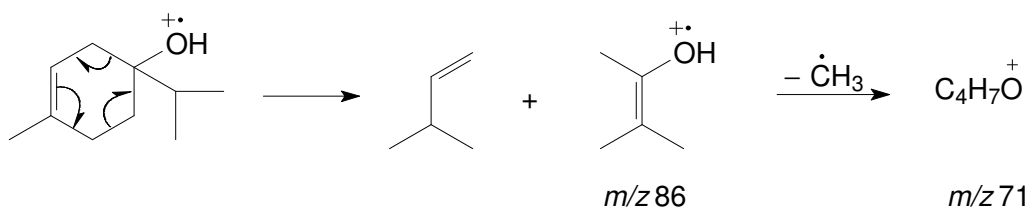


The ion at  $m/z$  139 ( $C_9H_{15}O^+$ ) in the mass spectra of **C86** and **C96** is formed by the loss of a methyl group, whereas loss of a molecule of water is responsible for the formation of the ion at  $m/z$  136 ( $C_{10}H_{16}^+$ ). Loss of both water and the methyl group is responsible for the presence of the ion at  $m/z$  121 ( $C_9H_{13}^+$ ). The elimination of the isopropyl group from the molecular ion gives the ion at  $m/z$  111 ( $C_7H_{11}O^+$ ), and loss of this group plus water gives the ion at  $m/z$  93 ( $C_7H_9^+$ ). Components **C86** and **C96** were tentatively identified as *cis*- and *trans-p*-2-menthen-1-ol.

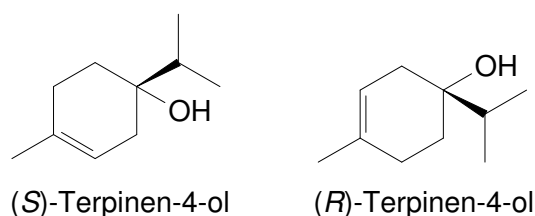
The mass spectrum of component **C118** (Fig. 3.109) has a base peak at  $m/z$  71 and a molecular ion at  $m/z$  154, with the same elemental composition ( $C_{10}H_{18}O$ ) as the previous two components. An online library search tentatively gave **terpinen-4-ol** as possible candidate (94% correlation). This tentative identification was confirmed by retention time comparison with the commercially available compound. Many of the prominent ions, such as those present at  $m/z$  139 ( $[M - 15]^+$ ), 136 ( $[M - 18]^+$ ), 111 ( $[M - C_3H_7]^+$ ) and 93 ( $[M - 18 - C_3H_7]^+$ ), are formed in the same way as in the case of *cis*- and *trans-p*-2-menthen-1-ol (**C86** and **C96**). In saturated cyclic alcohols the elimination of water involves loss of the hydroxyl group accompanied by a hydrogen atom either from C-3 or C-4 (Budzikiewicz *et al.*, 1967: 111). Since terpinen-4-ol has no hydrogen atoms at C-1 and two hydrogen atoms at C-6 it can be concluded that these are the ones involved in the elimination of water:



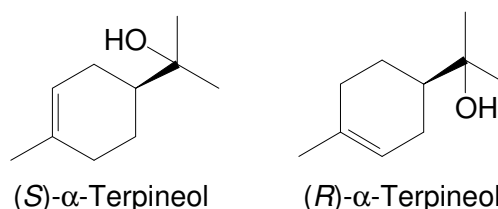
A retro-Diels-Alder rearrangement produces the  $C_5H_{10}O^+$  fragment at  $m/z$  86, with the additional loss of a methyl group, resulting in the  $C_4H_7O^+$  ion at  $m/z$  71, which is the base peak in the mass spectrum of **C118**:



The two enantiomers of terpinen-4-ol were resolved on enantioselective column D with a resolution of 2.5. The (*S*)-enantiomer elutes before the (*R*)-enantiomer from an enantioselective column equivalent to column D (Maas *et al.*, 1994b). Enantioselective analysis of the honeybush samples established the presence of both enantiomers in a ratio of 40:60 (*R*:*S*).

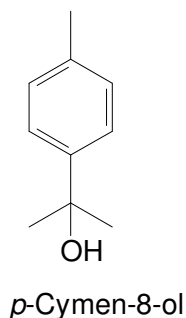


The retention time of component **C121** was not reconcilable with the ion of highest mass at  $m/z$  139 in its mass spectrum (Fig. 3.110). Furthermore, two ions three mass units apart typically result from the loss of a molecule of water and a methyl group from the molecular ion. It was therefore concluded that **C121** has a molecular mass of 154 Da. An online library search suggested  **$\alpha$ -terpineol** as possible candidate structure for **C121** (92% correlation) and retention time comparison with commercially available  $\alpha$ -terpineol confirmed this tentative identification. The (*S*)-enantiomer of  $\alpha$ -terpineol elutes before its (*R*)-enantiomer with  $R_s = 1.4$  from an enantioselective column equivalent to column D (Mathias and Mosandl, 2004). Enantioselective analysis of the honeybush samples established the presence of both enantiomers in a ratio of 38:62 (*S*:*R*).

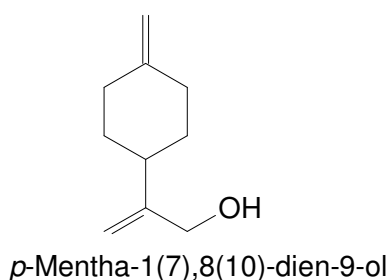


The EI mass spectrum of component **C120** (Fig. 3.111) contains ions typically present in the mass spectra of some aromatic compounds at  $m/z$  65, 77, and 91. Other prominent ions occur at  $m/z$  43 (base peak) 117, 132, 135 and 150 ( $M^+$ ). This component was thought to be ***p*-cymen-8-ol**, as

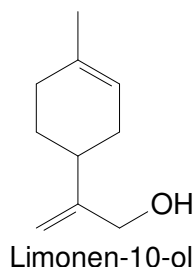
suggested by the online library search (78% correlation), and this identification was confirmed by retention time comparison with the commercially available compound.



The mass spectrum of component **C160** (Fig. 3.112) has an abundant ion at  $m/z$  91 and molecular ion at  $m/z$  152 ( $C_{10}H_{16}O^+$ ). An online NBS library search suggested *p*-mentha-1(7),8(10)-dien-9-ol as the most likely candidate structure.



Inspection of the mass spectrum, however, revealed differences in the relative abundances of some of the ions, which led to the conclusion that **C160** might be a monoterpene, but not this specific one. The mass spectrum of menthadienol has an abundant ion at  $m/z$  93 instead of  $m/z$  91, and the ions at  $m/z$  67 and 106 are not as prominent as in the mass spectrum of **C160**. The published mass spectrum and RI data of **limonen-10-ol** (Adams, 2004) correspond to those of **C160**:

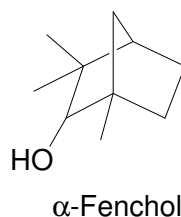


The ion at  $m/z$  134 ( $C_{10}H_{14}^+$ ) represents the  $[M - 18]^+$  ion. Loss of water and a methyl group gives the ion at  $m/z$  119 ( $C_9H_{11}^+$ ), whereas loss of water and a  $C_3H_7$  fragment results in the ion at  $m/z$  91 ( $C_7H_7^+$ ). Component **C160** was tentatively identified as limonen-10-ol.

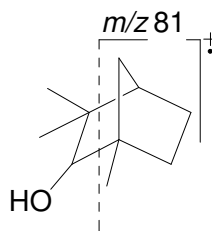
A molecular ion was observed at  $m/z$  154 ( $C_{10}H_{18}O^+$ ) in the HRMS of component **C85**, although this ion could not be detected in its LRMS (Fig. 3.113). An online library search indicated that **C85**



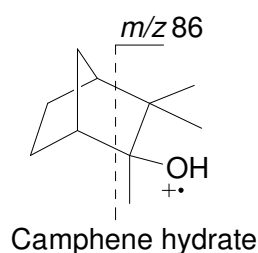
might be fenchol (71% correlation). Comparing the RI of the natural material with those of  $\alpha$ - and  $\beta$ -fenchol (Adams, 2004), it was concluded that **C85** could be  **$\alpha$ -fenchol**. The  $[M - 18]^+$  and  $[M - 18 - 15]^+$  ions appear at  $m/z$  136 and 121. The ion at  $m/z$  111 ( $C_7H_{11}O^+$ ) is formed by the loss of a  $C_2H_4$  fragment as well as a methyl group.



The ion at  $m/z$  107 ( $C_8H_{11}^+$ ) is formed by the loss of water and the same  $C_2H_4$  fragment mentioned above; in this case, however, in conjunction with the transfer of an additional hydrogen atom. The base peak at  $m/z$  81 ( $C_6H_9^+$ ) is formed by the loss of a  $C_4H_9O$  fragment, which also proceeds with the transfer of a hydrogen atom:

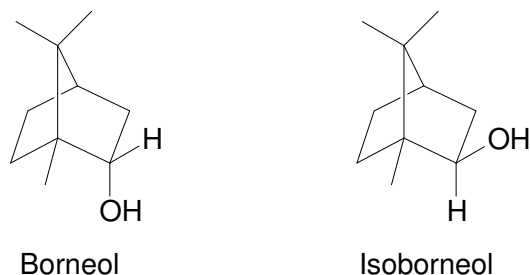


Component **C98** (Fig. 3.114) has the same elemental composition ( $C_{10}H_{18}O$ ) as **C85**, but no acceptable suggestions as to the possible identity of **C98** were obtained by online library searches. The relative abundances of the ions present in the mass spectrum of **C98** were used in a manual NIST library search, which produced **camphene hydrate** as possible candidate. The published RI available for camphene hydrate (Adams, 2004) corresponds to the RI of **C98**. The ions at  $m/z$  139, 136 and 121 are characteristic of the terpene alcohols discussed thus far and are formed in the same manner. According to HRMS analysis, the composition of the even-mass ion at  $m/z$  96 is  $C_7H_{12}^+$ , but its formation is not yet fully understood. Another prominent ion with even mass appears at  $m/z$  86 ( $C_5H_{10}O^+$ ). Schematically, the formation of this ion could be rationalised as follows:



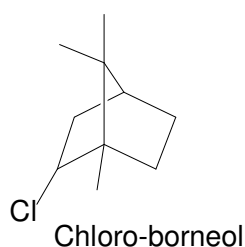
The base peak at  $m/z$  71, which is also an oxygen-containing fragment ( $C_4H_7O^+$ ), is possibly formed by the loss of a methyl group from the  $m/z$  86 ion.

The mass spectra of components **C105**, **C111** (Fig. 3.115) and **C112** (Fig. 3.116) all have a base peak at  $m/z$  95 and all of the other ions are present in abundances lower than 30%. The mass spectra of **C105** and **C112** contain the familiar  $[M - \text{CH}_3]^+$ ,  $[M - \text{H}_2\text{O}]^+$  and  $[M - \text{H}_2\text{O} - \text{CH}_3]^+$  ions and hence it was assumed that these components have a molecular mass of 154 Da. An online library search gave borneol as the best candidate structure for **C112** (80% correlation). Since two isomers of borneol with the same mass spectrum exist, i.e. borneol and isoborneol, it was thought that **C105** and **C112** might be these two isomers. Retention time analysis of the commercially available isomers proved that **C105** and **C112** are indeed **isoborneol** and **borneol**, respectively.



Pure (+)- and (-)-borneol were used to determine the order of elution of the enantiomers of borneol from enantioselective column C: a  $R_s$  value of 1.5 was obtained. It was found that only the (+)-enantiomer of borneol is present in honeybush. According to an enantioselective GC-MS analysis on column C, the commercial sample of isoborneol contained two enantiomers. No information on the elution order of the isoborneol enantiomers could be found in the literature, and the pure enantiomers are not commercially available. It was therefore not possible to assign the absolute configuration of the isoborneol present in the honeybush material investigated.

The mass spectrum of component **C111** does not have an ion at  $m/z$  139 that is typically present in the mass spectra of terpene alcohols, but the two ions at  $m/z$  157 and 159 are present in the spectrum in the isotopic ratio of 3:1, which indicates that **C111** contains one chloride atom. This conclusion is supported by the elemental composition of the ion at  $m/z$  157,  $\text{C}_9\text{H}_{14}\text{Cl}$ . An online library search suggested that **C111** might be **2-chloro-1,7,7-trimethylbicyclo[2.2.1]heptane (chloro-borneol)** (88% agreement), which means that this component has a molecular mass of 172 Da ( $\text{C}_{10}\text{H}_{17}\text{Cl}$ ) and that the ion at  $m/z$  157 represents the  $[M - \text{CH}_3]^+$  ion. The loss of hydrogen chloride (HCl) from the molecular ion is responsible for the formation of the ion at  $m/z$  136 ( $\text{C}_{10}\text{H}_{16}^+$ ) and the additional loss of a methyl group accounts for the ion at  $m/z$  121 ( $\text{C}_9\text{H}_{13}^+$ ).

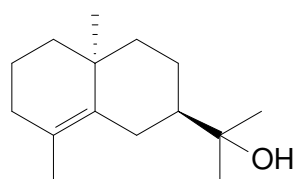


The EI mass spectra of components **C278** (Fig. 3.117) and **C283** are identical. The most prominent ions in their mass spectra are tabulated in Table 3.1:

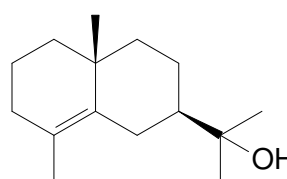
Table 3.1: The most abundant ions in the mass spectra of components **C278** and **C283**

Ion ( <i>m/z</i> )	Elemental composition	Ion ( <i>m/z</i> )	Elemental composition	Ion ( <i>m/z</i> )	Elemental composition
222 [M] <sup>+</sup>	C <sub>15</sub> H <sub>26</sub> O <sup>+</sup>	119	C <sub>9</sub> H <sub>11</sub> <sup>+</sup>	55	C <sub>4</sub> H <sub>7</sub> <sup>+</sup>
204 [M – H <sub>2</sub> O] <sup>+</sup>	C <sub>15</sub> H <sub>24</sub> <sup>+</sup>	105	C <sub>8</sub> H <sub>9</sub> <sup>+</sup>	43	C <sub>3</sub> H <sub>7</sub> <sup>+</sup>
189 [M – H <sub>2</sub> O – CH <sub>3</sub> ] <sup>+</sup>	C <sub>14</sub> H <sub>21</sub> <sup>+</sup>	91	C <sub>7</sub> H <sub>7</sub> <sup>+</sup>	41	C <sub>3</sub> H <sub>5</sub> <sup>+</sup>
161	C <sub>12</sub> H <sub>17</sub> <sup>+</sup>	81	C <sub>6</sub> H <sub>9</sub> <sup>+</sup>		
149	C <sub>11</sub> H <sub>17</sub> <sup>+</sup>	67	C <sub>5</sub> H <sub>7</sub> <sup>+</sup>		
133	C <sub>10</sub> H <sub>13</sub> <sup>+</sup>	59	C <sub>3</sub> H <sub>7</sub> O <sup>+</sup>		

Components **C278** and **C283** were identified as **10-*epi*- $\gamma$ -eudesmol** and  **$\gamma$ -eudesmol**, two diastereoisomers of  $\gamma$ -eudesmol, based on the good agreement between their mass spectra and RIs and the corresponding data available for these two components in the literature (Adams, 2004).

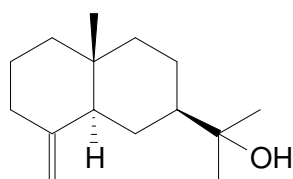


C278: 10-*epi*- $\gamma$ -Eudesmol

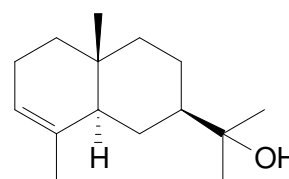


C283:  $\gamma$ -Eudesmol

Although the mass spectra of components **C286** (Fig. 3.118) and **C287** are fairly weak, they have the same characteristic base peak at *m/z* 59, which is also present in the mass spectra of compounds such as  $\alpha$ -terpineol, 10-*epi*- $\gamma$ -eudesmol and  $\gamma$ -eudesmol. This suggests that they contain the same tertiary alcohol function that undergoes  $\alpha$ -cleavage to give the ion at *m/z* 59. This observation simplified the process of comparing the mass spectra of **C286** and **C287** with published mass spectra.  **$\beta$ -Eudesmol** and  **$\alpha$ -eudesmol** were considered as possible candidate structures because they furthermore also have RIs corresponding to those published by Adams (2004).



$\beta$ -Eudesmol

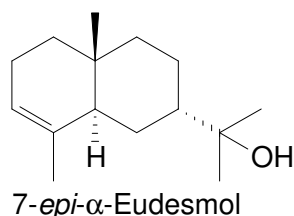


$\alpha$ -Eudesmol

The molecular ions of these two components, expected at *m/z* 222, were not detected. The [M – H<sub>2</sub>O]<sup>+</sup> and [M – H<sub>2</sub>O – CH<sub>3</sub>]<sup>+</sup> ions were however observed at *m/z* 204 and 189, respectively. Retention

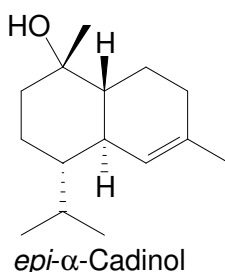
time comparison of **C286** with commercially available  $\beta$ -eudesmol proved that this component had been correctly identified.

Component **C289** (Fig. 3.119) was identified as a stereoisomer of  $\alpha$ -eudesmol based on the good agreement between the mass spectrum and RI of **C289** and the corresponding data available for **7-*epi*- $\alpha$ -eudesmol** in the literature (Adams, 2004).



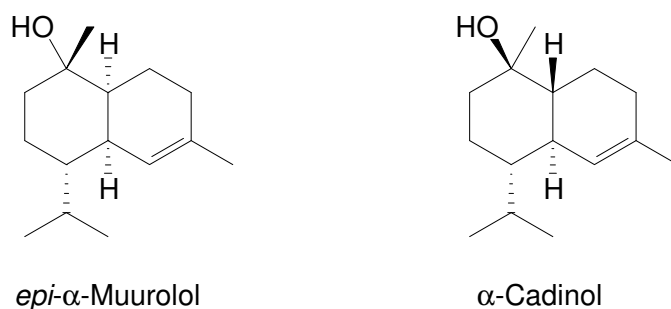
The molecular ion of **C289** ( $C_{15}H_{26}O^+$ ) could only be detected in its HRMS at  $m/z$  222. Component **C289** has the same elemental composition as **7-*epi*- $\alpha$ -eudesmol**. The ions at  $m/z$  204 ( $C_{15}H_{24}^+$ ), 189 ( $C_{14}H_{21}^+$ ) and 161 ( $C_{12}H_{17}^+$ ) (base peak) are the characteristic  $[M - H_2O]^+$ ,  $[M - H_2O - CH_3]^+$  and  $[M - H_2O - C_3H_7]^+$  ions. The presence of the ion at  $m/z$  59 ( $C_3H_7O^+$ ), once again, provides additional evidence that **C289** probably contains the tertiary alcohol group present in all the other eudesmol compounds.

Component **C284** (Fig. 3.120) was identified as ***epi*- $\alpha$ -cadinol** by comparison of its mass spectral and RI data with literature data (Adams, 2004).

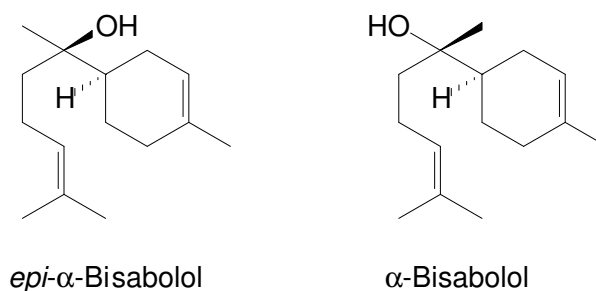


*Epi*- $\alpha$ -cadinol has a molecular mass of 222 Da and although the molecular ion was not observed in the LRMS, it was present in the HRMS with an expected elemental composition of  $C_{15}H_{26}O$ . The ions at  $m/z$  204 and 189 are the familiar  $[M - H_2O]^+$  and  $[M - H_2O - CH_3]^+$  ions. The base peak at  $m/z$  161 ( $C_{12}H_{17}^+$ ) is formed by the loss of water and a  $C_3H_7$  fragment, which in this case is probably the isopropyl group on the ring.

The mass spectra of components **C285** (Fig. 3.121) and **C288** are very similar and both have a molecular ion at  $m/z$  222 ( $C_{15}H_{26}O^+$ ), which is the same as that of **C284** (*epi*- $\alpha$ -cadinol). The RI and mass spectral data of **C285** and **C288** showed good agreement with published data for ***epi*- $\alpha$ -muurolol** and  **$\alpha$ -cadinol** (Adams, 2004).



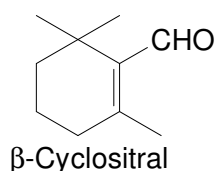
The mass spectra and RIs of components **C292** (Fig. 3.122) and **C293** compared well with the corresponding data for *epi*- $\alpha$ -bisabolol and  $\alpha$ -bisabolol (Adams, 2004).



Molecular ions were not detected at  $m/z$  222 in their mass spectra due to the ease with which these compounds lose a molecule of water to form the ion at  $m/z$  204 ( $C_{15}H_{24}^+$ ). As in the case of **C284**, the loss of water and a  $C_3H_7$  fragment affords the ion at  $m/z$  161 ( $C_{12}H_{17}^+$ ). Cleavage of the allylic bond with charge retention on the oxygen-containing fragment, followed by the loss of water, gives the ion at  $m/z$  134 ( $C_{10}H_{14}^+$ ), while the ion at  $m/z$  69 ( $C_5H_9^+$ ) is formed by cleavage of the allylic bond as in the mass spectra of some of the simpler terpene alcohols such as linalool (**C76**).

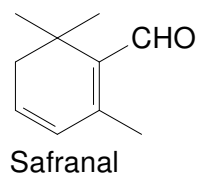
### 3.2.16.3 Terpene aldehydes

The mass spectrum of component **C129** (Fig. 3.123) has prominent ions in its higher mass range at  $m/z$  109 ( $C_7H_9O^+$ ), 123 ( $C_9H_{15}^+$ ), 137 (base peak,  $C_9H_{13}O^+$ ) and 152 ( $M^+$ ,  $C_{10}H_{16}O^+$ ). An online library search suggested that **C129** could be  $\beta$ -cyclosital (92% correlation), which was confirmed by retention time comparison with the commercially available compound.



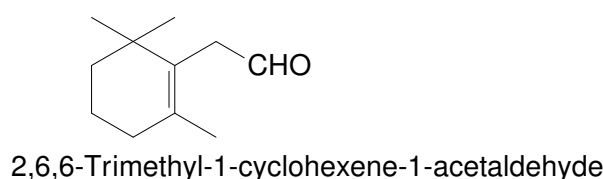
Loss of any one of the methyl groups from the molecule could account for the formation of the ion at  $m/z$  137 ( $C_9H_{13}O^+$ ), while the ion at  $m/z$  123 ( $C_9H_{15}^+$ ) is formed from the molecular ion by the loss of 29 mass units, equivalent to the aldehyde moiety.

The mass spectrum of component **C122** (Fig. 3.124) has a molecular ion at  $m/z$  150 ( $C_{10}H_{14}O^+$ ) and prominent ions at  $m/z$  107 (base peak,  $C_7H_7O^+$ ), 121 ( $C_9H_{13}^+$ ) and 135 ( $C_9H_{11}O^+$ ), i.e. all at two mass units lower than the prominent ions in the mass spectrum of  $\beta$ -cyclositral (**C129**) at  $m/z$  109, 123 and 137. This suggests that **C122** might have a structure similar to  $\beta$ -cyclositral, but with an additional double bond. In the mass spectrum of **C122** the ion at  $m/z$  107 ( $[M - 43]^+$ ) is the base peak instead of the  $[M - CH_3]^+$  ion as in the case of  $\beta$ -cyclositral. Another interesting difference is that the mass spectrum of **C122** has a more prominent ion at  $m/z$  91 ( $C_7H_7^+$ ) than that of  $\beta$ -cyclositral. An online NBS library search gave **safranal** as best possible candidate structure for **C122** (83% correlation).



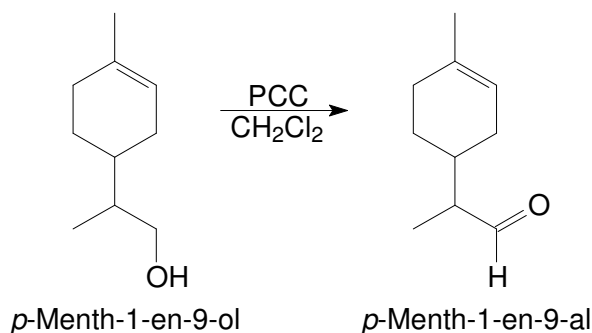
The identification of **C122** as safranal was confirmed by retention time comparison with the commercially available compound. The ion at  $m/z$  91 is possibly a tropylium ion, which would form more readily in the case of safranal than in  $\beta$ -cyclositral since there are already two double bonds present in the ring.

The mass spectrum of component **C146** (Fig. 3.125) shows some resemblance to the spectra of  $\beta$ -cyclositral and safranal, since they contain similar prominent ions in the higher mass range. In the mass spectrum of **C146** the molecular ion appears at  $m/z$  166 ( $C_{11}H_{18}O^+$ ), which is 14 mass units higher than that of  $\beta$ -cyclositral, and since the loss of a methyl group is also responsible for the formation of the base peaks in **C146** and  $\beta$ -cyclositral it was assumed that **C146** might be more closely related to  $\beta$ -cyclositral than to safranal. The relative abundances of the most prominent ions were used in a manual NIST library search which gave **2,6,6-trimethyl-1-cyclohexene-1-acetaldehyde** as the most probable candidate structure.

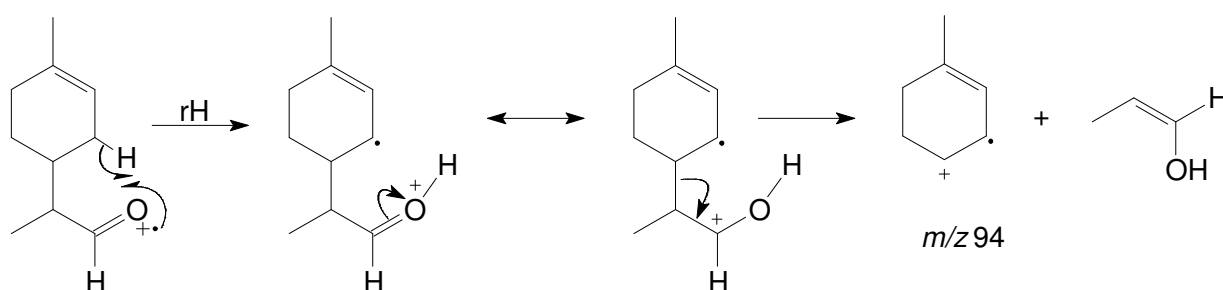


The identification of **C146** as 2,6,6-trimethyl-1-cyclohexene-1-acetaldehyde was confirmed by retention time comparison with the commercially available compound.

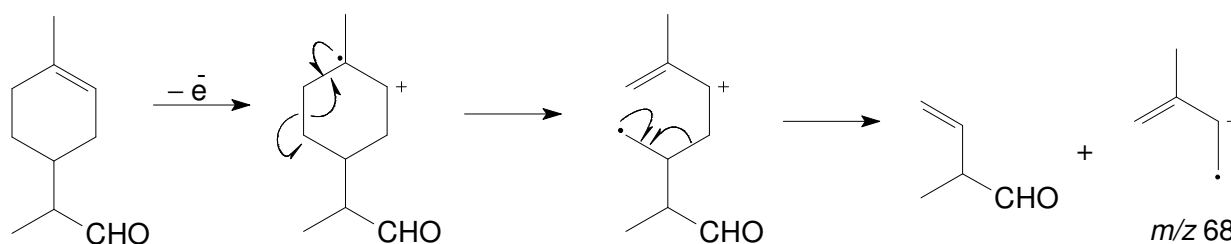
The mass spectra of components **C125** (Fig. 3.126) and **C128** are identical and prominent ions occur at  $m/z$  79 and 94 (base peak). Online NBS library searches gave *p*-menth-1-en-9-al as best possible candidate structure (90% correlation). (+)-(4*R*,8*R*)- and (+)-(4*R*,8*S*)-*p*-Menth-1-en-9-al were synthesised by oxidising the corresponding *p*-menth-1-en-9-ol diastereomers.



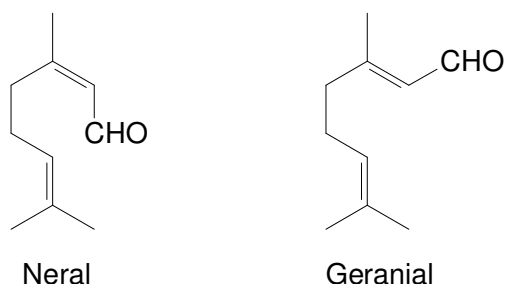
Retention time comparison with the synthesised compounds proved that **C125** and **C128** were indeed correctly identified as **(+)-(4*R*,8*R*)-** and **(+)-(4*R*,8*S*)-*p*-menth-1-en-9-al**, respectively. The formation of the ion at  $m/z$  94 ( $\text{C}_7\text{H}_{10}^+$ ) proceeds *via* the transfer of a  $\gamma$ -hydrogen atom followed by cleavage of the  $\beta$ -bond (McLafferty and Tureček, 1993: 246–249):



The ion at  $m/z$  79 ( $\text{C}_6\text{H}_7^+$ ) is formed from the ion at  $m/z$  94 by the additional loss of a methyl group, while the ion at  $m/z$  68 ( $\text{C}_5\text{H}_8^+$ ) is formed in the following manner:

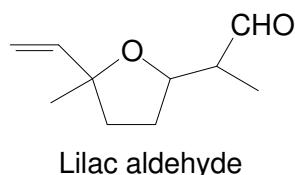


The mass spectra of components **C139** (Fig. 3.127) and **C150** are identical, with a base peak at  $m/z$  69 ( $\text{C}_5\text{H}_9^+$ ) and significant ions in the higher mass range at  $m/z$  119 ( $[\text{M} - \text{CH}_3 - \text{H}_2\text{O}]^+$ ), 134 ( $[\text{M} - \text{H}_2\text{O}]^+$ ), 137 ( $[\text{M} - \text{CH}_3]^+$ ) and 152 ( $\text{M}^+$ ,  $\text{C}_{10}\text{H}_{16}\text{O}^+$ ). An online library search gave geranial as the most likely candidate structure for both components (90% and 97% correlation). Components **C139** and **C150** were identified as **neral** (*Z*-isomer) and **geranial** (*E*-isomer), respectively, by retention time comparison with the corresponding commercially available compounds.

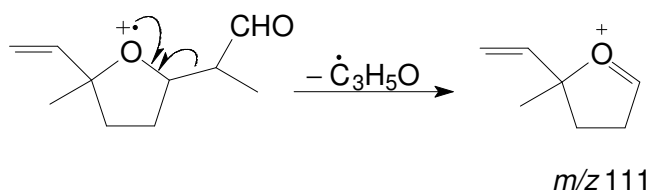


Cleavage of the bi-allylic bond with charge retention on either the oxygen-containing fragment or the alkyl fragment results in the ions at  $m/z$  84 ( $C_5H_8O^+$ ) and  $m/z$  69 ( $C_5H_9^+$ ), respectively.

Since the mass spectra of components **C97** (Fig. 3.128) and **C110** are identical it was assumed that they are isomers of the same compound. A manual NIST library search using the relative abundances of the most prominent ions ( $m/z$  43, 55, 67, 71, 93, 111 and 153) presented lilac aldehyde, 2-(5-methyl-5-vinyltetrahydro-furan-2-yl)propanal, as the best possible candidate structure:



The molecular ion that was expected at  $m/z$  168 was only detected in mass spectra obtained by HRMS analysis. It has an elemental composition of  $C_{10}H_{16}O_2$ , in agreement with the structure of lilac aldehyde. An online NIST library search carried out later in this study gave lilac aldehyde with a correlation factor of 80%. Loss of a methyl group from the molecular ion explains the formation of the ion at  $m/z$  153 ( $C_9H_{13}O^+$ ). The favoured mechanism for the loss of an oxygen-containing fragment leading to the formation of the ion at  $m/z$  111 ( $C_7H_{11}O^+$ ) is by loss of the fragment containing the aldehyde moiety:



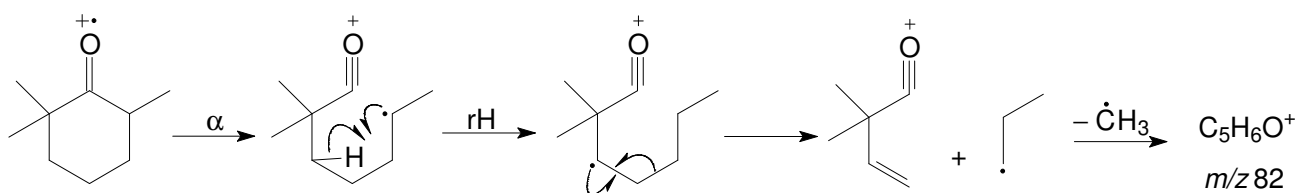
Components **C97** and **C110** were identified as two **diastereomers** of **lilac aldehyde**, based on the good agreement obtained with the NIST library searches and by investigation of their mass spectra.

#### 3.2.16.4 Terpene ketones

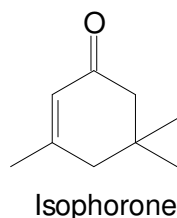
An online NBS library search indicated that component **C51** (Fig. 3.129) could be **2,2,6-trimethylcyclohexanone** (83% correlation) and this tentative identification was confirmed by retention time comparison with the commercially available compound. The mass spectrum of a structurally related compound, 3,3,5-trimethylcyclohexanone, has ions at  $m/z$  56 ( $C_4H_8^+$ ) and 69



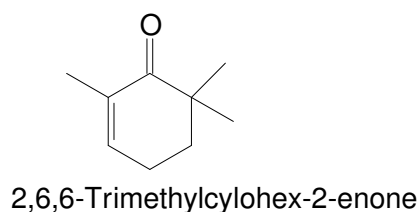
( $C_4H_5O^+$ ) in common with the mass spectrum of **C51**. The formation of these ions is discussed by McLafferty and Tureček (1993: 184, 251). Formation of the base peak at  $m/z$  82 ( $C_5H_6O^+$ ) in the mass spectrum of **C51** thus probably proceeds as follows:



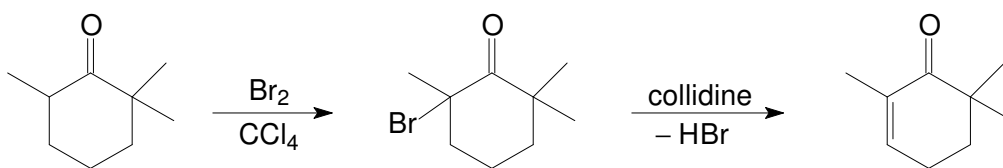
The mass spectra of components **C59** (Fig. 3.130) and **C82** are identical. They have molecular ions at  $m/z$  138, two mass units lower than that of 2,2,6-trimethylcyclohexanone, which led to the assumption that these components could be unsaturated trimethylcyclohexenones. Online library searches (NBS) suggested that both these components could be **3,5,5-trimethyl-2-cyclohexen-1-one (isophorone)** (correlation >80%).



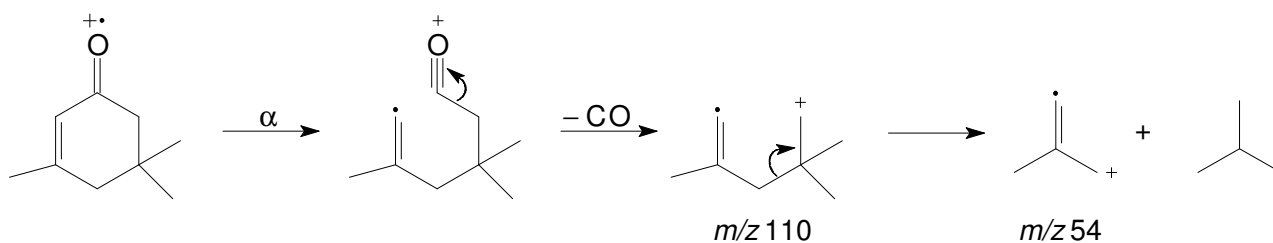
According to GC-MS analysis **C82** has the same retention time as commercially available isophorone. The possibility that **C59** could be **2,6,6-trimethylcyclohex-2-enone** was investigated.



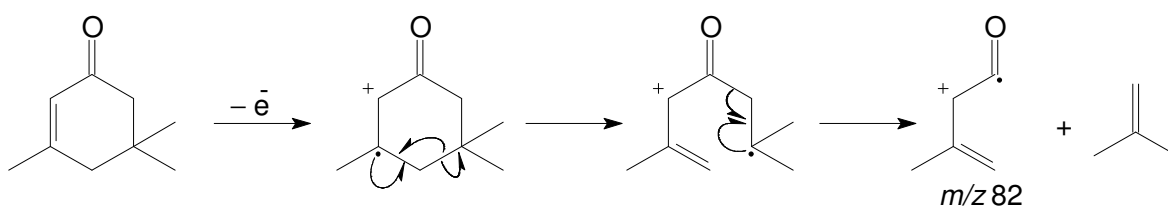
A mass spectrum of this compound (Ramalho *et al.*, 1999) proved to be the same as that of isophorone. 2,6,6-Trimethylcyclohex-2-enone was synthesised according to the following reaction scheme (Tietze and Eicher, 1981: 261–262):



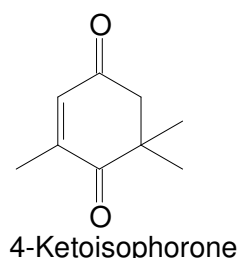
Component **C59** was identified as 2,6,6-trimethylcyclohex-2-enone by retention time comparison with the synthesised compound. Loss of any one of the three methyl groups results in the formation of the ion at  $m/z$  123 ( $C_8H_{11}O^+$ ) in the mass spectra of these components.  $\alpha$ -Cleavage followed by loss of a CO molecule, gives the ion at  $m/z$  110 ( $C_8H_{14}^+$ ), as illustrated below for isophorone. The formation of the ion at  $m/z$  54 ( $C_4H_6^+$ ) can be rationalised as follows:



Expulsion of a methyl group from the ion at  $m/z$  110 may be responsible for the ion at  $m/z$  95 ( $C_7H_{11}^+$ ). The base peak at  $m/z$  82 ( $C_5H_6O^+$ ) most likely forms to some extent in the same manner as already illustrated for 2,2,6-trimethylcyclohexanone, but could possibly also form according to the following fragmentation mechanism, as formulated for isophorone:



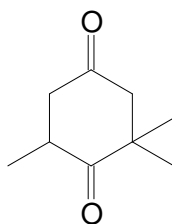
Interestingly, most of the ions with high abundances in the EI mass spectrum of component **C92** (Fig. 3.131) have even masses and occur at  $m/z$  68 (base peak), 96 and 152 ( $M^+$ ,  $C_9H_{12}O_2^+$ ). Using the relative abundances of the ions, a manual NIST library search was carried out. It gave **4-ketoisophorone** as candidate structure for **C92**, which was confirmed by retention time comparison with the commercially available compound.



As in the mass spectra of the above-mentioned ketones, loss of a methyl group takes place easily and is responsible for the formation of the ion at  $m/z$  137 ( $C_8H_9O_2^+$ ) in the EI mass spectrum of **C92**.  $\alpha$ -Cleavage, followed by loss of a CO group gives the ion at  $m/z$  124 ( $C_8H_{12}O^+$ ) in a manner similar to the formation of the ion at  $m/z$  110 in the mass spectrum of 2,6,6-trimethylcyclohex-2-enone (**C59**).

The ion at  $m/z$  96 ( $C_5H_4O_2^+$ ) is formed by a similar fragmentation as the one shown for the formation of  $m/z$  82 in isophorone (**C82**). The base peak at  $m/z$  68 ( $C_4H_4O^+$ ) is possibly formed by the loss of an alkyl fragment from the ion at  $m/z$  124, while the ion at  $m/z$  40 ( $C_3H_4^+$ ) is possibly formed by the further loss of a carbonyl group from the ion at  $m/z$  68.

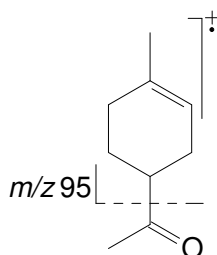
The mass spectrum of component **C104** (Fig. 3.132) shows some resemblance to the mass spectrum of 2,6,6-trimethylcyclohexanone (**C51**) discussed earlier. An online NBS library search suggested **2,2,6-trimethyl-1,4-cyclohexanedione** as possible candidate structure (82% correlation).



2,2,6-Trimethyl-1,4-cyclohexanedione

The formation of the most important ions in the mass spectrum of **C104** could be rationalised in terms of the compound being 2,2,6-trimethyl-1,4-cyclohexanedione. The  $[M - 15]^+$  ion at  $m/z$  139 ( $C_8H_{11}O_2^+$ ) is prominent, due to the loss of any one of the three methyl groups. The ions at  $m/z$  83 ( $C_5H_7O^+$ ), 69 ( $C_4H_5O^+$ ) and 56 ( $C_4H_8^+$ ) are formed by similar reactions to the ones shown for the structurally related compound 3,3,5-trimethylcyclohexanone (McLafferty and Tureček, 1993: 184, 251).

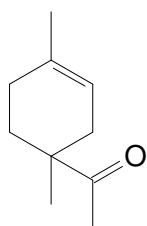
The mass spectrum of component **C89** (Fig. 3.133) has prominent ions at  $m/z$  43 (base peak), 67, 79, 95, 105, 123 and 138 ( $M^+$ ,  $C_9H_{14}O^+$ ). The relative abundances of these ions were used in a manual library search (NIST), which gave **4-acetyl-1-methylcyclohexene (limona ketone)** as the best candidate structure. The ions at  $m/z$  123 ( $C_8H_{11}O^+$ ) and 105 ( $C_8H_9^+$ ) represent  $[M - CH_3]^+$  and  $[M - CH_3 - H_2O]^+$  fragments. The ion at  $m/z$  95 ( $C_7H_{11}^+$ ) is formed by loss of the acetyl moiety from the molecular ion:



4-Acetyl-1-methylcyclohexene

The base peak at  $m/z$  43 is formed by charge retention on the acetyl moiety. Retention time comparison with the commercially available compound proved that the identification of **C89** as 4-acetyl-1-methylcyclohexene was indeed correct.

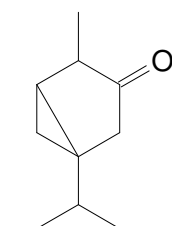
Online library searches (NBS and NIST) predicted that component **C99** (Fig. 3.134) could be **1-(1,4-dimethyl-3-cyclohexen-1-yl)ethanone** (75% and 82% correlation) and this was also in agreement with the elemental composition,  $C_{10}H_{16}O$ , of this component.



1-(1,4-Dimethyl-3-cyclohexen-1-yl)ethanone

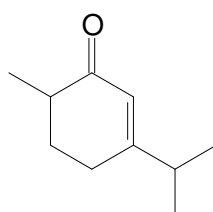
The structure of 1-(1,4-dimethyl-3-cyclohexen-1-yl)ethanone is similar to that of 4-acetyl-1-methylcyclohexene except for the presence of an additional methyl group on the ring. Ions resulting from the fragmentations similar to those observed in the mass spectrum of 4-acetyl-1-methylcyclohexene are also present in the mass spectrum of **C99**, but are present at masses 14 mass units higher than those in the latter spectrum. These ions include those at  $m/z$  137 ( $[M - CH_3]^+$ ), 134 ( $[M - H_2O]^+$ ), 119 ( $[M - CH_3 - H_2O]^+$ ) and 109 ( $[M - \text{acetyl-moiety}]^+$ ). The ion at  $m/z$  43 ( $C_2H_3O^+$ ) is formed in a similar manner as already discussed for 4-acetyl-1-methylcyclohexene (**C89**).

The mass spectrum of component **C84** (Fig. 3.135) has a molecular ion at  $m/z$  152 with elemental composition  $C_{10}H_{16}O^+$ , corresponding to that of the compound **3-thujanone**, proposed by an online NBS library search (87% correlation). This identification was confirmed by retention time comparison with the commercially available compound.



3-Thujanone

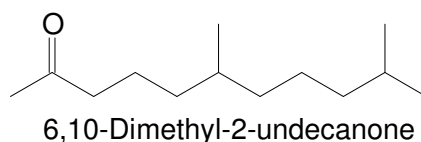
Component **C143** (Fig. 3.136) has the same elemental composition ( $C_{10}H_{16}O$ ) as 3-thujanone. An online library search (NBS) predicted that **C143** could be **carvenone** (90% correlation) and its RI is in agreement with the RI of carvenone (Adams, 2004).



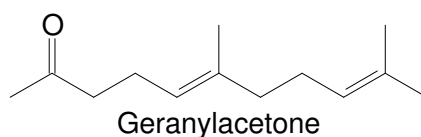
Carvenone

The ion at  $m/z$  110 ( $C_7H_{10}O^+$ ) is formed by a similar fragmentation to the one responsible for the formation of the ion at  $m/z$  82 in the mass spectrum of isophorone (**C82**). The base peak at  $m/z$  95 ( $C_6H_7O^+$ ) could possibly be formed by further loss of a methyl group from the ion at  $m/z$  110. Component **C143** was tentatively identified as carvenone.

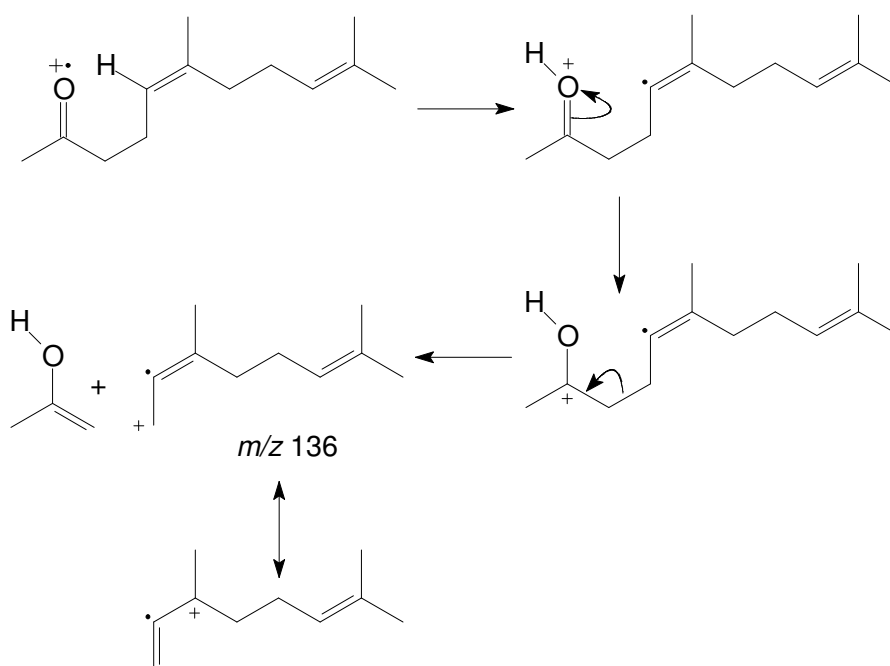
The ions with the highest masses in the LRMS of component **C209** (Fig. 3.137) occur at  $m/z$  180 ( $C_{13}H_{24}^+$ ) and  $m/z$  183 ( $C_{12}H_{23}O^+$ ), but in the HRMS an additional ion at  $m/z$  198 ( $C_{13}H_{26}O^+$ ) is also visible, and this was assumed to be the molecular ion. Component **C209** has a base peak at  $m/z$  43 and a prominent ion at  $m/z$  58 that are characteristic of methyl ketones containing an alkyl group with three or more carbon atoms, with or without branching occurring beyond C-3 (Budzikiewicz *et al.*, 1967: 134–138). An online NBS library search suggested that this component could be **6,10-dimethyl-2-undecanone** (89% correlation) and this identification was confirmed by retention time comparison in the usual manner.



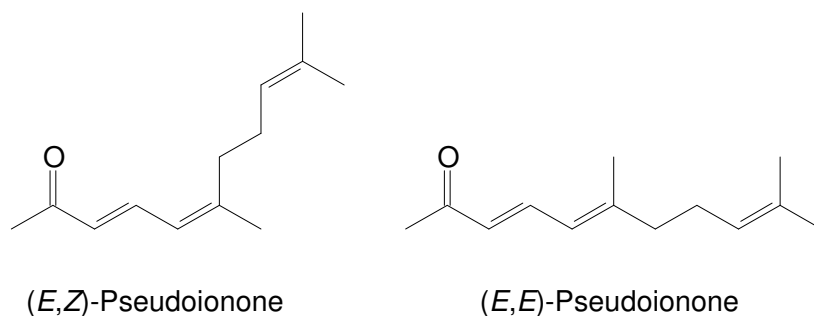
A molecular ion of low abundance is present in the mass spectrum of component **C220** (Fig. 3.138) at  $m/z$  194 ( $C_{13}H_{22}O^+$ ). The molecular formula of **C220** contains four hydrogen atoms fewer than 6,10-dimethyl-2-undecanone (**C209**), which suggests that it contains two double bonds. Another difference observed between the two mass spectra is the low abundance of the ion at  $m/z$  58 in the mass spectrum of **C220**. This indicates that **C220** could possibly be branched at C-3 or that the double bond is present in a position that renders the McLafferty rearrangement less favourable. An online library search (NBS) gave **geranylacetone** as the best possible candidate structure (96% correlation) and this identification was confirmed by retention time comparison with the commercially available compound.



As suggested, the McLafferty rearrangement ion at  $m/z$  58 is indeed less abundant in geranylacetone since its formation requires the rearrangement of the  $\gamma$ -hydrogen atom from a vinyl bond, unless migration of the double bond occurs. However, should this  $\beta$ -cleavage-reaction take place with retention of the charge on the alkyl fragment then delocalisation of the double bond is possible, which leads to the stability of the ion at  $m/z$  136 (McLafferty and Tureček, 1993: 249):



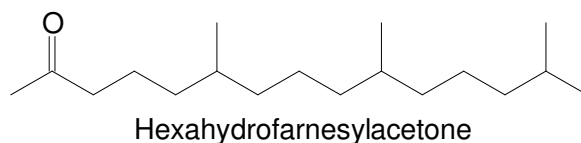
The mass spectra of components **C249** and **C266** (Fig. 3.139) are identical, indicating that these components could be geometrical isomers. Molecular formulae of  $C_{13}H_{20}O$  suggest that these components are similar to geranylacetone, but probably contain an additional double bond. The NBS library indicated with a correlation factor of 97% that these components could be pseudoionone isomers. Commercial pseudoionone was available for retention time analysis, but without any indication of the isomeric composition of the sample or whether it had been synthesised or isolated from natural material. However, the retention times of the two isomers present in the highest concentrations corresponded to those of **C249** and **C266** and it was assumed that if the material had been synthesised, the thermodynamically favoured isomers (***E,Z*-pseudoionone** and (***E,E*-pseudoionone** would probably have been produced.



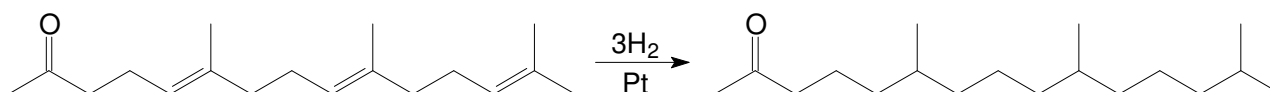
The ions at  $m/z$  177 ( $C_{12}H_{17}O^+$ ) and 149 ( $C_{10}H_{13}O^+$ ) in the spectra of these isomers are formed by loss of a methyl and isopropyl group, respectively. The base peak at  $m/z$  69 ( $C_5H_9^+$ ) is formed by cleavage of the bi-allylic bond.

In the LRMS of component **C299** (Fig. 3.140) the ion with the highest mass occurs at  $m/z$  250, but in the HRMS a molecular ion was present at  $m/z$  268 ( $C_{18}H_{36}O^+$ ), which means that the ion at  $m/z$

250 is formed by the loss of the elements of water. The mass spectrum of **C299** has a base peak at  $m/z$  43 and a characteristic even-mass ion at  $m/z$  58, which is also present in the mass spectrum of 6,10-dimethyl-2-undecanone (**C209**). The online library search (NBS) suggested **hexahydrofarnesylacetone** as possible candidate structure for **C299** (97% correlation).

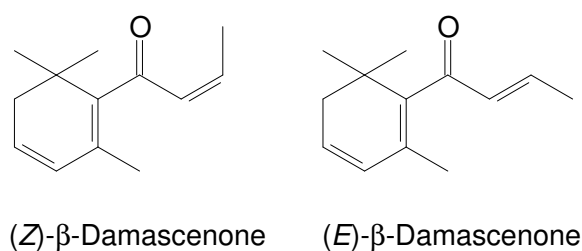


Hexahydrofarnesylacetone was synthesised by catalytic hydrogenation of farnesylacetone. Under the specific reaction conditions used only the three double bonds were reduced and the carbonyl group was left intact:

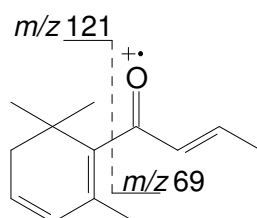


Component **C299** was identified as hexahydrofarnesylacetone by retention time comparison with the synthesised compound.

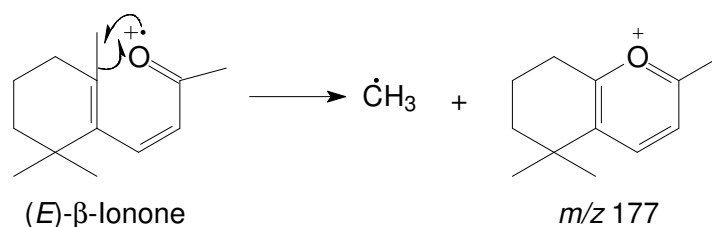
The mass spectra of components **C195** and **C204** (Fig. 3.141) are identical and have molecular ions at  $m/z$  190 ( $C_{13}H_{18}O^+$ ). The most likely candidate structure found in an online library search (NBS) was  $\beta$ -damascenone (81% correlation). An authentic sample of (*E*)- $\beta$ -damascenone, which contains a small amount of the (*Z*)-isomer, was used to confirm that **C195** and **C204** are (*Z*)- $\beta$ -damascenone and (*E*)- $\beta$ -damascenone, respectively.



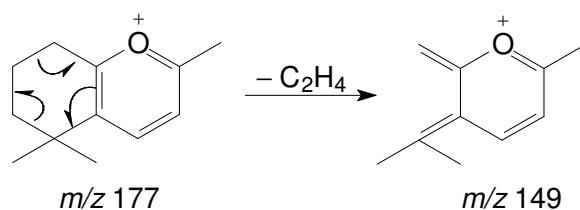
The ion at  $m/z$  175 ( $C_{12}H_{15}O^+$ ) in the spectra of these isomers is formed by the loss of a methyl group. The ions at  $m/z$  121 ( $C_9H_{13}^+$ ) and 69 ( $C_4H_5O^+$ ) are formed by  $\alpha$ -cleavage with charge retention on either the alkyl- or oxygen-containing fragments, respectively:



A unique feature of the mass spectrum of component **C234** (Fig. 3.142) is that only two ions, namely those at  $m/z$  177 (base peak) and  $m/z$  43, have abundances higher than 25%. The molecular ion is present at  $m/z$  192 ( $C_{13}H_{20}O^+$ ). An online NBS library search gave (*E*)- $\beta$ -ionone as possible candidate structure (correlation factor of 88%) and this identification was confirmed by retention time comparison with commercially available (*E*)- $\beta$ -ionone. The base peak at  $m/z$  177 ( $C_{12}H_{17}O^+$ ) is formed by a displacement reaction that takes place at the carbonyl group (McLafferty and Tureček, 1993: 250–251, 302):

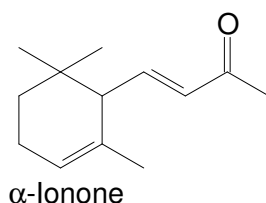


A retro-Diels-Alder rearrangement is expected to give a relatively prominent ion at  $m/z$  164, but this is not the case in the mass spectrum of **C234**, because of the favoured competing displacement reaction illustrated above (McLafferty and Tureček, 1993: 250–251, 302). Loss of water and a methyl group from the molecular ion is responsible for the presence of the ion at  $m/z$  159 ( $C_{12}H_{15}^+$ ). The ion at  $m/z$  149 ( $C_{10}H_{13}O^+$ ) is possibly formed from the ion at  $m/z$  177 by a retro-Diels-Alder-type rearrangement (Budzikiewicz *et al.*, 1964b: 265):

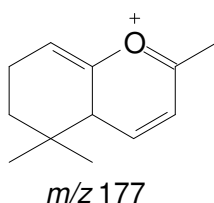


The mass spectrum of component **C217** has a molecular ion at  $m/z$  192 ( $C_{13}H_{20}O^+$ ) and a relatively prominent ion at  $m/z$  43 (Fig. 3.143), indicating that this component could be a methyl ketone similar to  $\beta$ -ionone. An online NBS library search gave  $\alpha$ -ionone as most likely candidate structure (82% correlation) and this was confirmed by retention time comparison with the commercially available compound.

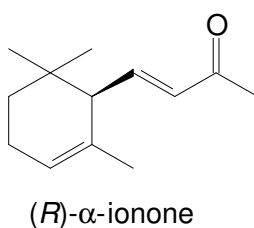




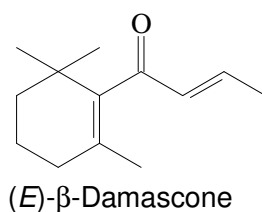
As discussed above, in the case of  $\beta$ -ionone a stable ion is formed at  $m/z$  177 (base peak) as the result of a displacement reaction at the carbonyl group, but in the case of  $\alpha$ -ionone the product is less stable and therefore this ion has a much lower abundance:



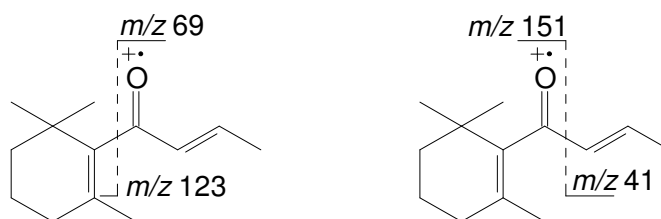
$\beta$ -ionone does not undergo a retro-Diels-Alder rearrangement in the ion source because of the favoured competing displacement reaction, but since the latter reaction is less favourable in  $\alpha$ -ionone, a product of a retro-Diels-Alder rearrangement is present at  $m/z$  136 ( $C_9H_{12}O^+$ ) in the mass spectrum of  $\alpha$ -ionone, as illustrated by McLafferty and Tureček (1993: 250–251, 302). The base peak at  $m/z$  121 ( $C_8H_9O^+$ ) is possibly formed from the ion at  $m/z$  136 by loss of a methyl group. The (*R*)-enantiomer of  $\alpha$ -ionone elutes before its (*S*)-enantiomer ( $R_s = 2.14$ ) from an enantioselective column equivalent to column D (Junge and König, 2003). Enantioselective analysis of the honeybush samples established the presence of only the (*R*)-enantiomer.



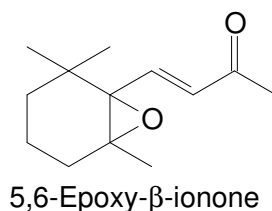
The EI-mass spectrum of component **C212** (Fig. 3.144) is somewhat similar to that of (*E*)- $\beta$ -ionone (**C234**). For example, it also contains ions at  $m/z$  192 ( $M^+$ ) and 177 (base peak). There are however also significant differences between these two mass spectra, such as the much higher abundances of the ions at  $m/z$  41, 69 and 123, and a much less abundant ion at  $m/z$  43 in the mass spectrum of **C212**. The latter indicated that **C212** might not be a methyl ketone. This conclusion was in fact confirmed when a manual library search suggested (**E**)- $\beta$ -damascone as best possible candidate structure.



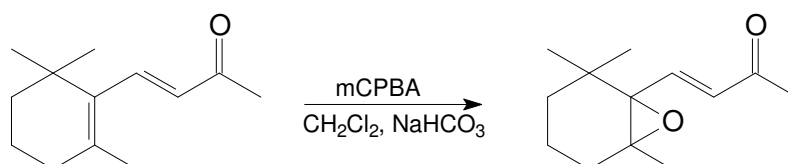
This identification was confirmed by retention time comparison with commercially available material. The ion at  $m/z$  177 ( $C_{12}H_{17}O^+$ ) is formed by the loss of a methyl group as in the case of (E)- $\beta$ -ionone. The ions at  $m/z$  69 ( $C_4H_5O^+$ ), 151 ( $C_{10}H_{15}O^+$ ), 123 ( $C_9H_{15}^+$ ) and 41 ( $C_3H_5^+$ ) are formed by  $\alpha$ -cleavage reactions:



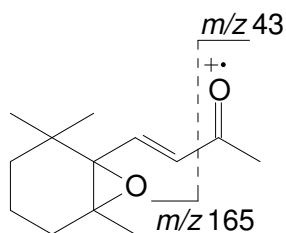
Most of the ions present in the mass spectrum of component **C232** (Fig. 3.147) have an abundance of 20% or less, except for the two ions at  $m/z$  43 (73%) and 123 (100%). An online library search suggested that **C232** could be **5,6-epoxy- $\beta$ -ionone** (75% correlation).



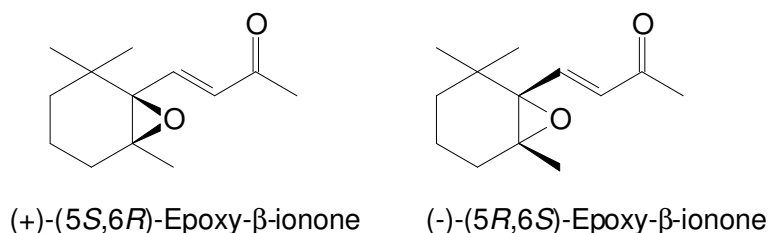
No molecular ion was observed in the mass spectrum of **C232**, but magnification of the higher mass range revealed a molecular ion at  $m/z$  208 ( $C_{13}H_{20}O_2^+$ ), which corresponds to the molecular mass of 5,6-epoxy- $\beta$ -ionone. This compound was synthesised according to the following reaction scheme and **C232** was positively identified by retention time comparison:



The ion at  $m/z$  193 ( $C_{12}H_{17}O_2^+$ ) in the mass spectrum of **C232** is formed by the loss of any one of the three methyl groups, and the ions at  $m/z$  165 ( $C_{11}H_{17}O^+$ ) and  $m/z$  43 ( $C_2H_3O^+$ ) are formed by  $\alpha$ -cleavage at the carbonyl group:



The two isomers of 5,6-epoxy- $\beta$ -ionone were resolved on enantioselective column D ( $\alpha$ -value of 1.00). 5,6-Epoxy- $\beta$ -ionone is present as a racemate in the honeybush samples analysed.

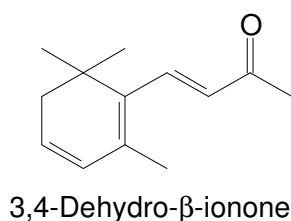


Components **C203** (Fig. 3.146), **C218** (Fig. 3.147), **C222** (Fig. 3.148) and **C230** (Fig. 3.149) have the ions listed in Table 3.2 in common. Although the ions occur in different relative abundances in the four mass spectra all the spectra have a base peak at  $m/z$  43, which is characteristic of methyl ketones.

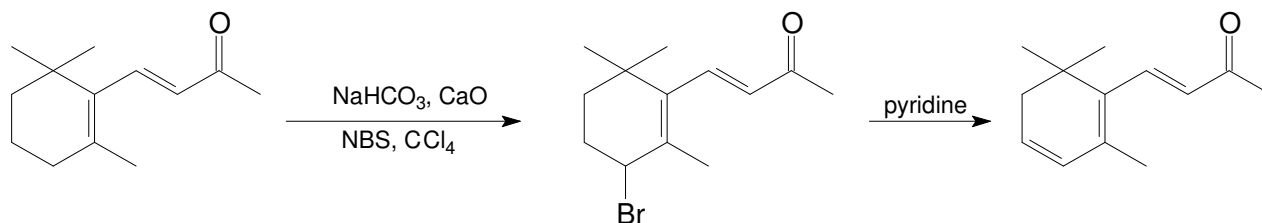
Table 3.2: Ions common to the mass spectra of components **C203**, **C218**, **C222** and **C230**

Ion ( $m/z$ )	Elemental composition	Ion ( $m/z$ )	Elemental composition	Ion ( $m/z$ )	Elemental composition
190 [M] <sup>+</sup>	C <sub>13</sub> H <sub>18</sub> O <sup>+</sup>	119	C <sub>9</sub> H <sub>11</sub> <sup>+</sup>	77	C <sub>6</sub> H <sub>5</sub> <sup>+</sup>
175 [M - CH <sub>3</sub> ] <sup>+</sup>	C <sub>12</sub> H <sub>15</sub> O <sup>+</sup>	115	C <sub>9</sub> H <sub>7</sub> <sup>+</sup>	65	C <sub>5</sub> H <sub>5</sub> <sup>+</sup>
157 [M - CH <sub>3</sub> - H <sub>2</sub> O] <sup>+</sup>	C <sub>12</sub> H <sub>13</sub> <sup>+</sup>	105	C <sub>8</sub> H <sub>9</sub> <sup>+</sup>	55	C <sub>4</sub> H <sub>7</sub> <sup>+</sup>
147 [M - C <sub>2</sub> H <sub>3</sub> O] <sup>+</sup>	C <sub>11</sub> H <sub>15</sub> <sup>+</sup>	91	C <sub>7</sub> H <sub>7</sub> <sup>+</sup>	43	C <sub>2</sub> H <sub>3</sub> O <sup>+</sup>
131	C <sub>10</sub> H <sub>11</sub> <sup>+</sup>	79	C <sub>6</sub> H <sub>7</sub> <sup>+</sup>		

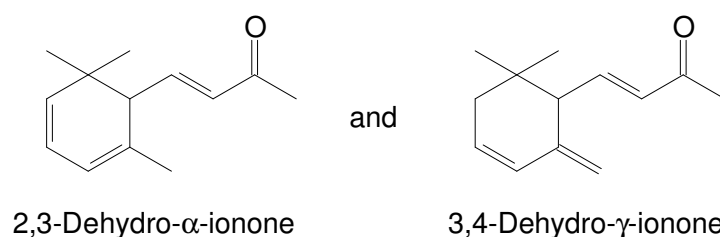
Online NBS library searches did not provide any useful diagnostic information on these components. However, a manual NIST library search, using the relative abundances of the ions present in the mass spectrum of **C230**, gave **3,4-dehydro- $\beta$ -ionone** as a possible candidate structure.



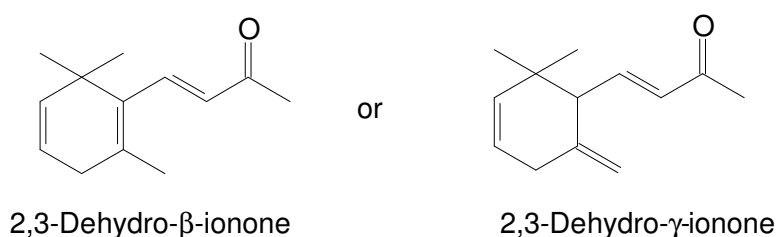
3,4-Dehydro- $\beta$ -ionone was synthesised according to the following reaction scheme and the synthesised compound was used to confirm the identity of **C230**:



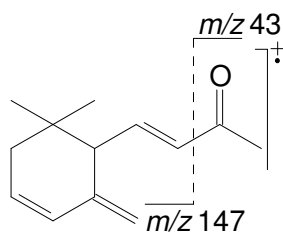
On account of the similarity between the mass spectra of **C203**, **C218**, **C222** and **C230** it was assumed that **C203**, **C218** and **C222** might be other dehydro-ionone isomers. Constructing mass spectra from published mass spectral data of the following two dehydro-ionone compounds (Serra *et al.*, 2006; Yamazaki *et al.*, 1988) facilitated the identification of **C203** and **C218** as **2,3-dehydro- $\alpha$ -ionone** and **3,4-dehydro- $\gamma$ -ionone**, respectively.



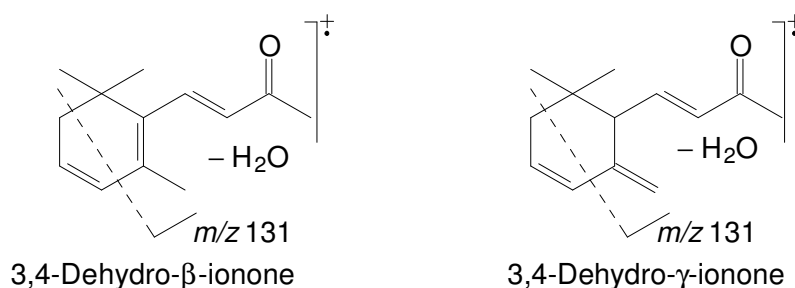
Component **C222** was more difficult to characterise, but since it was expected to have a structure similar to the dehydro-ionones discussed thus far, only 2,3-dehydro- $\beta$ -ionone and 2,3-dehydro- $\gamma$ -ionone remained as possibilities.



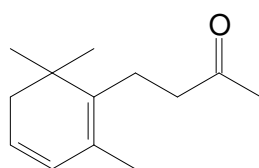
2,3-Dehydro- $\beta$ -ionone was eliminated as a possibility when it was found that **C222** eluted as two distinct peaks from enantioselective column C, and therefore it must contain a stereogenic centre, which is only present in the  $\gamma$ -ionone. Thus, **C222** was identified as **2,3-dehydro- $\gamma$ -ionone**. In all four of these components the ions at  $m/z$  147 ( $C_{11}H_{15}^+$ ) and 43 (base peak,  $C_2H_3O^+$ ) are formed by  $\alpha$ -cleavage at the carbonyl group:



3,4-Dehydro- $\beta$ -ionone and 3,4-dehydro- $\gamma$ -ionone have a more abundant ion at  $m/z$  131 ( $C_{10}H_{11}^+$ ) than the other two dehydro-ionones. This could be explained by the fact that one of their double bonds has the same position in the ring, which leads to the same fragmentation in these two components. In the overall process, shown schematically, two bonds are cleaved, a hydrogen atom is transferred, and the fragments lose a molecule of water:

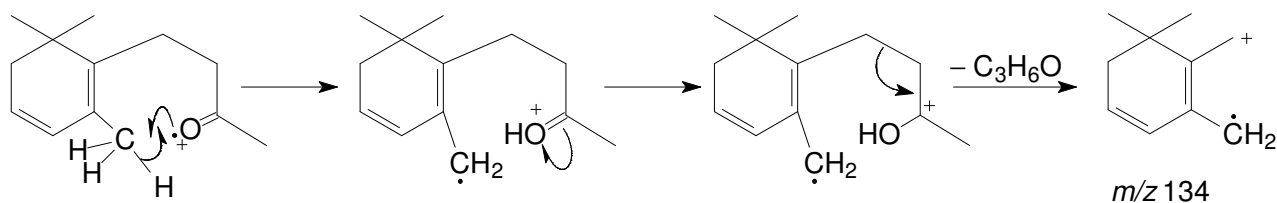


Except for the base peak present at  $m/z$  119, all the other ions in the mass spectrum of component **C214** (Fig. 3.150) have abundances lower than 30%. Component **C214** was identified as **4-(2,6,6-trimethyl-1,3-cyclohexadien-1-yl)-2-butanone** by using the relative abundances of the most significant ions in a manual library search.



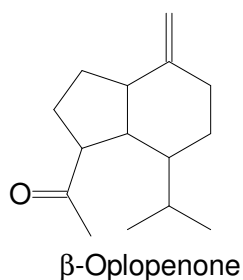
4-(2,6,6-Trimethyl-1,3-cyclohexadien-1-yl)-2-butanone

The ion at  $m/z$  177 ( $C_{12}H_{17}O^+$ ) in the compound's mass spectrum is a  $[M - CH_3]^+$  ion. A possible mechanism for the formation of the ion at  $m/z$  134 ( $C_{10}H_{14}^+$ ) can be formulated as follows:

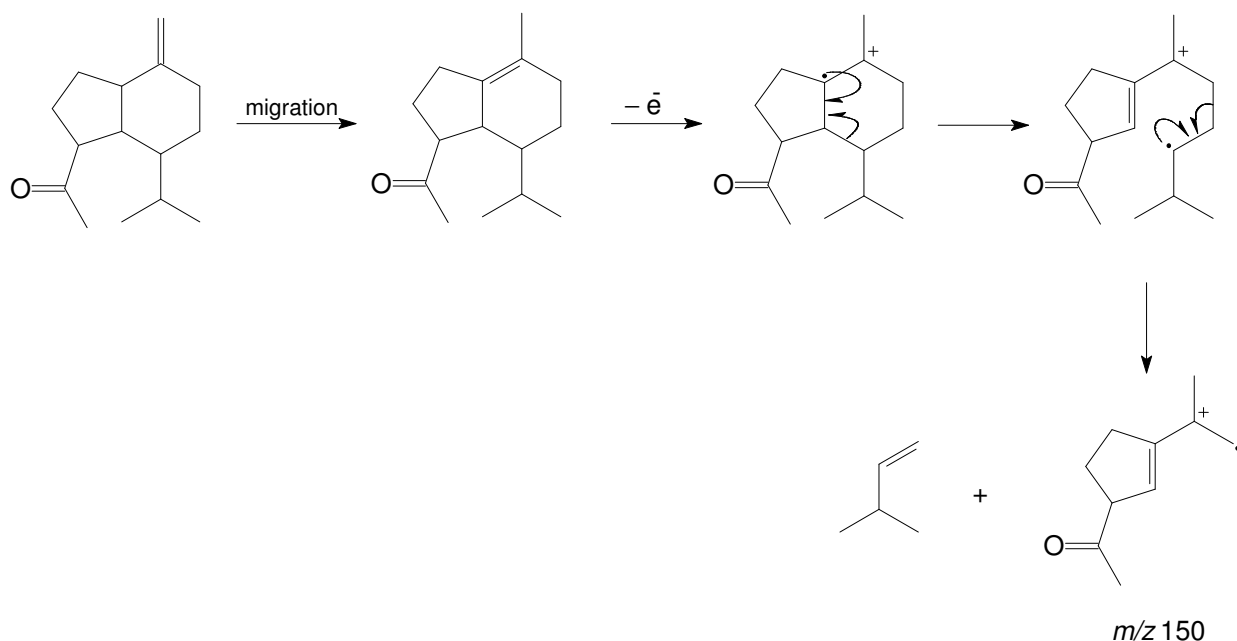


The ion at  $m/z$  119 ( $C_9H_{11}^+$ ) is possibly formed by the loss of a methyl group from the ion at  $m/z$  134.

The mass spectrum of component **C274** (Fig. 3.151) has a molecular ion at  $m/z$  220 ( $C_{15}H_{24}O^+$ ), and the presence of a base peak at  $m/z$  43 ( $C_2H_3O^+$ ) led to the conclusion that **C274** might also be a methyl ketone. The mass spectral and RI data of  **$\beta$ -Oploponone** (Adams, 2004) were in agreement with those of **C274**.

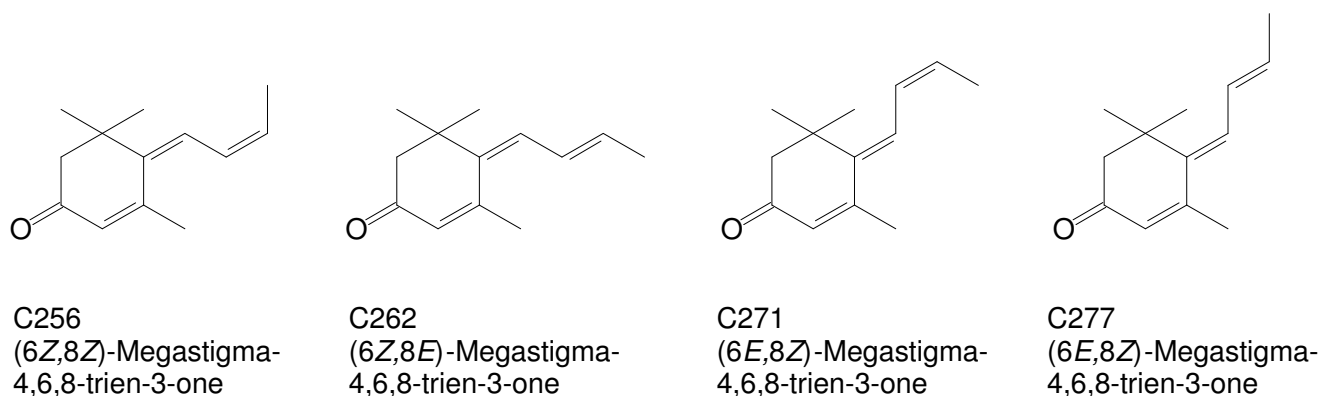


The ion at  $m/z$  205 ( $C_{14}H_{24}O^+$ ) in the mass spectrum of **C274** is formed by loss of a methyl group and the ions at  $m/z$  202 and  $m/z$  187 represent the  $[M - H_2O]^+$  and  $[M - H_2O - CH_3]^+$  ions, respectively. The even-mass ion at  $m/z$  150 ( $C_{10}H_{14}O^+$ ) is possibly formed by a retro-Diels-Alder rearrangement, preceded by the migration of the double bond to the six-membered ring:

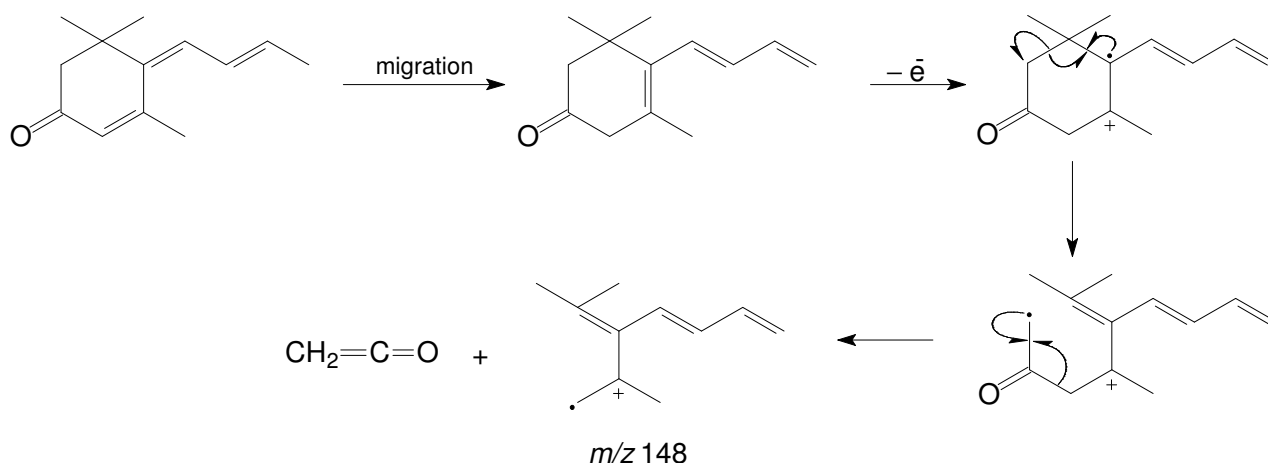


The mass spectra of components **C256**, **C262** (Fig. 3.152), **C271** and **C277** (Fig. 3.153) all contain prominent ions at  $m/z$  65 ( $C_5H_5^+$ ), 69 ( $C_4H_5O^+$ ), 77 ( $C_6H_5^+$ ), 91 ( $C_7H_7^+$ ), 105 ( $C_8H_9^+$ ), 119 ( $C_9H_{11}^+$ ), 133 ( $C_{10}H_{13}^+$ ), 147 ( $C_{11}H_{15}^+$ ), 148 ( $C_{11}H_{16}^+$ ), 175 ( $C_{12}H_{15}O^+$ ) and 190 ( $M^+$ ,  $C_{13}H_{18}O^+$ ), with only small variations in their relative abundances. Although the molecular ions of these four components have the same elemental composition as those of the dehydro-ionones discussed earlier, their mass spectra do not have a base peak at  $m/z$  43, indicating that they could not be methyl ketones. The relative abundances of the most abundant ions in the mass spectra were used in a manual NIST library search, which gave megastigmatrienone as best possible candidate

structure. **Four isomers of megastigma-4,6,8-trien-3-one** exist and their mass spectral data (Takazawa *et al.*, 1982) were found to corresponded to those of **C256**, **C262**, **C271** and **C277**.



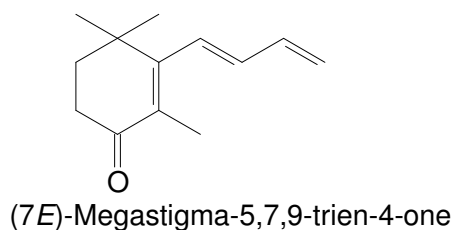
The even-mass ion at  $m/z$  148 in their mass spectra is possibly formed by a retro-Diels-Alder rearrangement after the migration of the double bonds to more favourable positions:



The ion at  $m/z$  147 is formed in the same manner as the ion at  $m/z$  148, but needs to proceed with the transfer of an additional hydrogen atom. The ion at  $m/z$  133 is possibly formed by loss of a methyl group from the ion at  $m/z$  148. None of these megastigma-4,6,8-trien-3-ones were commercially available for retention time and mass spectral comparison with the natural substances. Because compounds with *Z* configuration elute at lower retention times than their (*E*)-isomers from apolar columns, it was concluded that the four isomeric megastigma-4,6,8-trien-3-ones are eluted from column A in the order in which they are listed above.

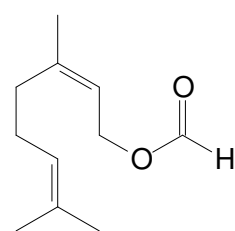
The mass spectrum of component **C295** (Fig. 3.154) contains the same prominent ions as the mass spectra of the four isomers of megastigma-4,6,8-trien-3-one. Although this component occurs in the honeybush samples in very low concentrations it was identified by GC-MS-O analysis as one of the odour-active components of honeybush tea and it has a typical honeybush aroma. 7(*E*)-Megastigma-5,7,9-trien-4-one, with olfactory properties described by Demole and Enggist (1974) and Ohloff (1994: 166–167) as tea-like, spicy and resembling dried fruit, has a mass spectrum (Kaiser and Lamparsky, 1978b) that is similar to the mass spectra of the four megastigma-4,6,8-trien-3-ones

discussed above. Component **C295** was tentatively identified as **(7E)-megastigma-5,7,9-trien-4-one**.

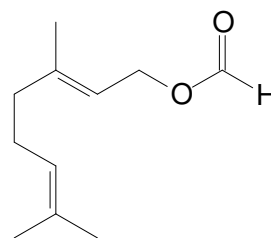


### 3.2.16.5 Terpene esters

The LRMS of components **C158** and **C164** (Fig. 3.155) have the same prominent ions at  $m/z$  41, 69 (base peak), 93, 121 and 136. It was clear that the ion at  $m/z$  136 could not be the molecular ion of these components, and a molecular ion at  $m/z$  182 ( $C_{11}H_{18}O_2^+$ ) could in fact be detected by HRMS analysis. This molecular formula corresponded to the formulae of the possible structures suggested by an online NBS library search, i.e. the two isomers neryl formate (*Z*-isomer) and geranyl formate (*E*-isomer) (83% correlation). Retention time comparison with an authentic sample of this compound confirmed the identity of **C164** as **geranyl formate**. The RI of **C158** corresponded to the published RI of **neryl formate** (Adams, 2004).



Neryl formate

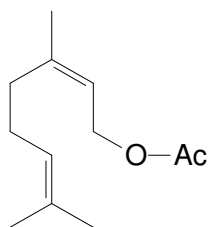


Geranyl formate

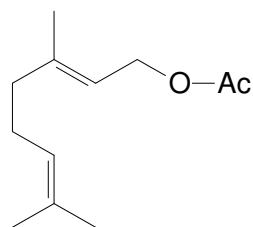
The ion at  $m/z$  136 ( $C_{10}H_{16}^+$ ) in the mass spectra of these components is formed by the loss of water and a CO group from the molecular ion, and the ions at  $m/z$  121 ( $C_9H_{13}^+$ ) and 93 ( $C_7H_9^+$ ) are formed from this ion by further loss of a methyl or  $C_3H_7$  group, respectively. The base peak at  $m/z$  69 ( $C_5H_9^+$ ) is formed by cleavage of the bi-allylic bond.

The mass spectra of components **C198** and **C206** (Fig. 3.156) are identical and not very different from the mass spectra of **C158** and **C164** discussed above. An online library search (NBS) suggested that these components could be **neryl acetate** and **geranyl acetate** (87% and 94% correlation) with a molecular mass of 196 Da, and this was confirmed by retention time comparison with the commercially available compounds.





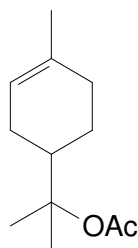
Neryl acetate



Geranyl acetate

The molecular ion is not visible in the mass spectra of these two compounds. The ion with the highest mass appears at  $m/z$  154 ( $C_{10}H_{18}O^+$ ), and is formed by the loss of the acetyl moiety, i.e.  $[M - 42]^+$ .

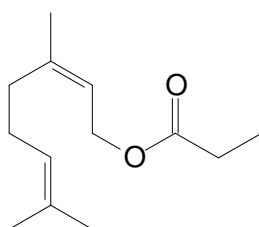
It was likewise unlikely that the ion with highest mass at  $m/z$  136 in the mass spectrum of component **C188** (Fig. 3.157) could be its molecular ion, since the compounds eluting at more or less the same retention time have molecular masses exceeding 136 Da. An ion at  $m/z$  136 could also be formed by the loss of the elements of acetic acid (60 Da) from a molecular ion at  $m/z$  196. The RI and mass spectral data of  $\alpha$ -terpinyl acetate (Adams, 2004) corresponded to those of **C188** and hence this component was tentatively identified as  **$\alpha$ -terpinyl acetate**.



$\alpha$ -Terpinyl acetate

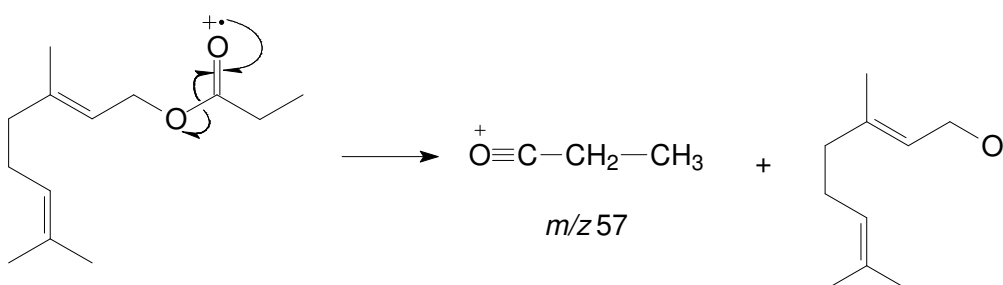
The ion at  $m/z$  136 ( $C_{10}H_{16}^+$ ) in the mass spectrum of **C188** is formed by the loss of the acetyl moiety plus the elements of water. The ion at  $m/z$  121 ( $C_9H_{13}^+$ ) is formed from the ion at  $m/z$  136 by the additional loss of a methyl group.

The mass spectrum of component **C228** (Fig. 3.158) has many of the ions that are present in the mass spectra of the terpene esters discussed thus far. The ion at  $m/z$  57 is significant however, since it is much more prominent in the mass spectrum of this component than in any of the spectra of the other terpene esters. By comparing the RI and mass spectral data of geranyl propanoate (Adams, 2004) with those of **C228**, this component was identified as **geranyl propanoate**.



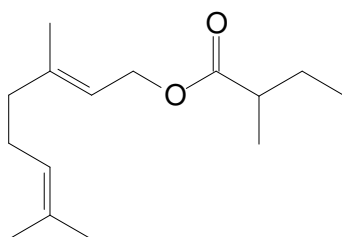
Geranyl propanoate

The ion with the highest mass in the mass spectrum of this component occurs at  $m/z$  136 ( $C_{10}H_{16}^+$ ) and is the result of the loss of 74 mass units from the molecular ion. The significant ion at  $m/z$  57 ( $C_3H_5O^+$ ) is formed by the following  $\alpha$ -cleavage reaction:



The  $m/z$  57 ion is not prominent in the mass spectra of terpene esters with a carboxylic acid moiety of fewer than three carbon atoms, because the above reaction results in the formation of a prominent ion at  $m/z$  43 in such terpene esters.

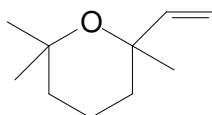
The mass spectrum of component **C272** is very similar to that of geranyl propanoate (**C228**) and also has a prominent ion at  $m/z$  57. Comparison of RI and mass spectral data (Adams, 2004) led to the identification of **C272** as **geranyl 2-methylbutanoate**.



Geranyl 2-methylbutanoate

### 3.2.16.6 Terpene ethers

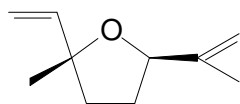
The results of an online library search indicated that component **C29** (Fig. 3.159) could be **2,6,6-trimethyl-2-vinyltetrahydropyran** (94% correlation).



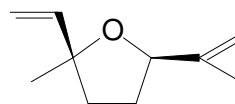
2,6,6-Trimethyl-2-vinyltetrahydropyran

Although the molecular ion of **C29** was not detectable in the LRMS it was visible in the HRMS. Its elemental composition of  $C_{10}H_{18}O$  corresponded to that of the structure suggested by the library search. The formation of the prominent ions in the mass spectrum of this compound has been discussed by McLafferty and Tureček (1993: 263).

The mass spectra of components **C36** and **C45** (Fig. 3.160) are identical. There is a base peak at  $m/z$  67 and molecular ion at  $m/z$  152 ( $C_{10}H_{16}O^+$ ). Online library searches (NBS and NIST) did not provide any useful diagnostic information but it was found that the RIs and mass spectra of **C36** and **C45** corresponded to those of *trans*-dehydroxylinalool oxide and *cis*-dehydroxylinalool oxide (Adams, 2004). At a later stage, when an online Wiley library search (Wiley 275) could be performed, *trans*- and *cis*-dehydroxylinalool oxide were obtained as possible candidate structures with 93% correlation factors.

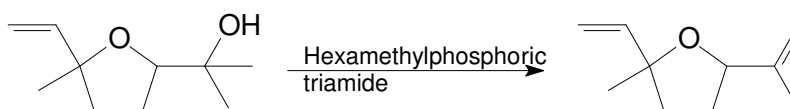


*trans*-Dehydroxylinalool oxide



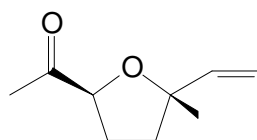
*cis*-Dehydroxylinalool oxide

*Trans*- and *cis*-dehydroxylinalool oxide were prepared from *trans*- and *cis*-linalool oxide as follows:



Comparison of the retention times of the synthesised *trans*- and *cis*-dehydroxylinalool oxides with those of **C36** and **C45** proved that these components had indeed been correctly identified. Enantioselective analysis of honeybush samples established that all four stereoisomers of dehydroxylinalool oxide are present in honeybush tea. The four isomers were resolved on enantioselective column C with  $R_s$  values ranging from 2.6 to 16.4. According to Berger (2007: 381), the order of elution of the stereoisomers of linalool oxide from an enantioselective column equivalent to column C is: *trans* ( $2R$ ,  $5R$ ); *cis* ( $2R$ ,  $5S$ ); *trans* ( $2S$ ,  $5S$ ); *cis* ( $2S$ ,  $5R$ ). Although the structures of linalool oxide and dehydroxylinalool oxide are similar, it would be risky to assume that the elution order of the dehydroxylinalool oxide enantiomers could be the same.

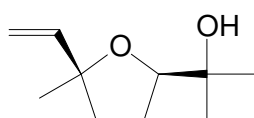
Component **C62** (Fig. 3.161) was tentatively identified as *trans*-arbusculone based on the good agreement between its mass spectral and RI data and those available for *trans*-arbusculone (Adams, 2004).



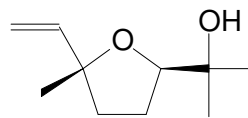
*trans*-Arbusculone

The ion at  $m/z$  111 ( $C_7H_{11}O^+$ ) in the mass spectrum of this component is formed by loss of the acetate group *via* an  $\alpha$ -cleavage reaction. Further loss of water from this ion affords the ion at  $m/z$  93 ( $C_7H_9^+$ ).

The mass spectra of components **C64** and **C68** (Fig. 3.162) are identical. They have base peaks at  $m/z$  59 and ions with highest mass at  $m/z$  155. Molecular masses of 170 Da for these components were inferred from the presence in their mass spectra of ions at  $m/z$  155 [ $M - CH_3$ ] and  $m/z$  137 [ $M - H_2O - CH_3$ ]. An online NBS library search indicated that these components were both linalool oxide isomers (86% correlation) and this was confirmed by retention time comparison with commercially available *cis*- and *trans*-linalool oxide.

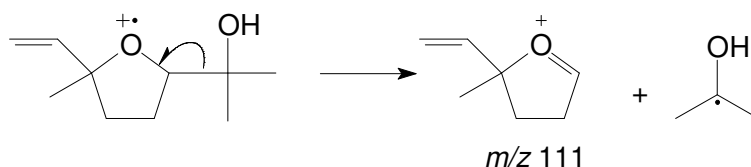


*cis*-Linalool oxide

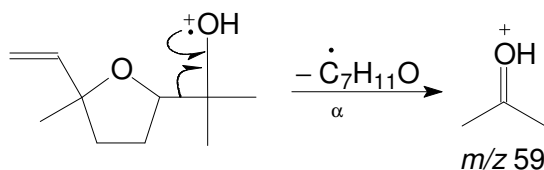


*trans*-Linalool oxide

The  $C_9H_{13}O^+$  ion at  $m/z$  137 in their mass spectra is formed by the loss of water and a methyl group. Loss of the alcohol-containing R-group *via*  $\alpha$ -cleavage is responsible for the formation of the ion at  $m/z$  111 ( $C_7H_{11}O^+$ ) (Budzikiewicz *et al.*, 1964b: 270–271):

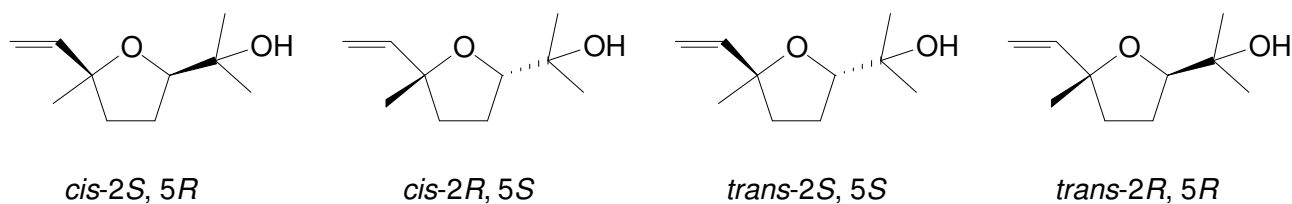


The base peak at  $m/z$  59 ( $C_3H_7O^+$ ) is formed by  $\alpha$ -cleavage at the tertiary alcohol group:

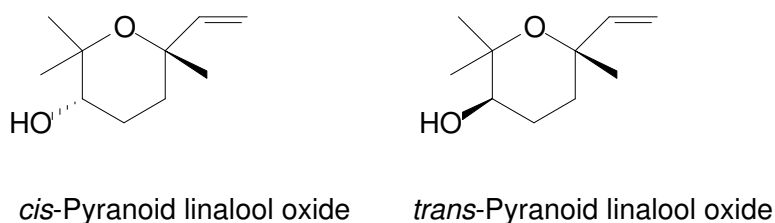


The four enantiomers of linalool oxide were resolved on enantioselective column C with  $R_s$  values ranging from 1.15 to 11.4. According to Berger (2007: 381) the four enantiomers of linalool oxide elute from an enantioselective column equivalent to column C in the order: *trans* (2*R*, 5*R*); *cis* (2*R*,

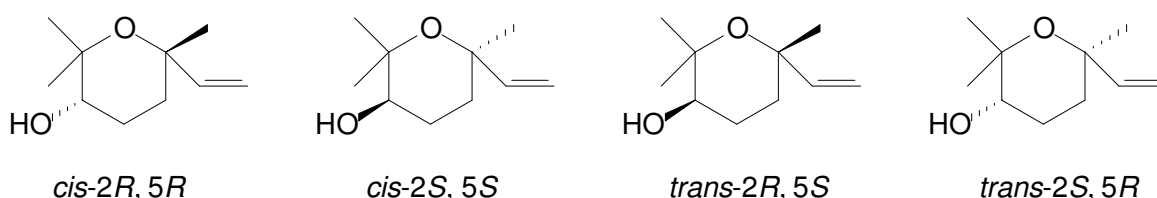
5S); *trans* (2S, 5S); *cis* (2S, 5R). All four of the enantiomers of linalool oxide are present in honeybush tea in a ratio of 23:39:20:18.



The two components **C115** and **C116** (Fig. 3.163) have identical mass spectra and molecular ions at  $m/z$  170 ( $C_{10}H_{18}O_2^+$ ). They were identified by online library (NBS) searches as the two diastereomers of pyranoid linalool oxide (93% correlation) and this was confirmed by retention time comparison with an authentic sample of *cis*-pyranoid- and *trans*-pyranoid linalool oxide.

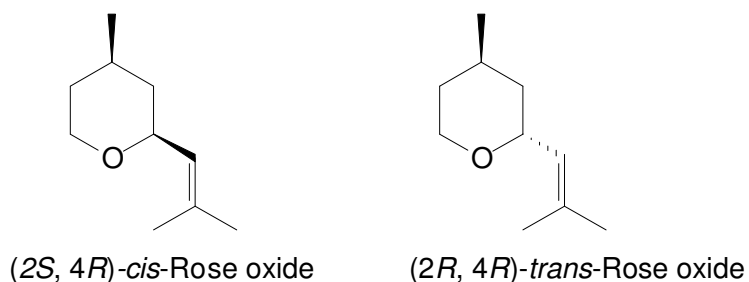


The ions at  $m/z$  155 ( $C_9H_{15}O_2^+$ ) and 137 ( $C_9H_{13}O^+$ ) in their mass spectra represent  $[M - CH_3]^+$  and  $[M - CH_3 - H_2O]^+$  ions formed in a similar manner as the ions at  $m/z$  139 and 121 in the mass spectrum of 2,6,6-trimethyl-2-vinyltetrahydropyran (**C29**) (McLafferty and Tureček, 1993: 263). The ions at  $m/z$  68 ( $C_5H_8^+$ ) and  $m/z$  43 ( $C_2H_3O^+$ ) are also formed according to mechanisms similar to those formulated for 2,6,6-trimethyl-6-vinyltetrahydropyran (**C29**) (McLafferty and Tureček 1993: 263). The four enantiomers of pyranoid linalool oxide were resolved on enantioselective column C with  $R_s$  values ranging from 2.2 to 7.3. The order of elution from an enantioselective column equivalent to column C is: *trans* (2S, 5R); *cis* (2S, 5S); *trans* (2R, 5S); *cis* (2R, 5R) (Weinert *et al.*, 1998). Enantioselective GC analysis of honeybush samples established the presence of all four isomers in the tea in a ratio of 20:22:31:27.

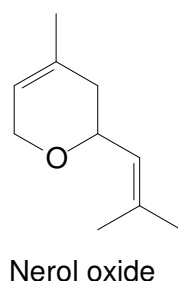


The EI mass spectra of components **C83** (Fig. 3.164) and **C91** appear to be the same, which indicates that these two components could be isomers. Molecular ions are present at  $m/z$  154 ( $C_{10}H_{18}O^+$ ) and the  $[M - CH_3]^+$  ion at  $m/z$  139 ( $C_9H_{15}O^+$ ) is the base peak. An online library search

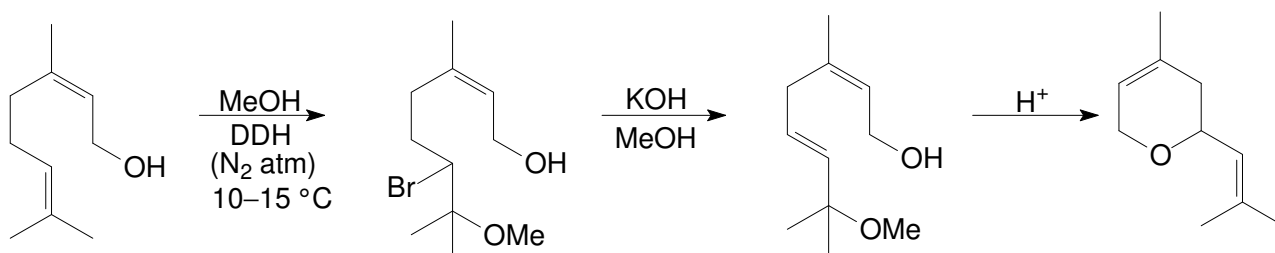
gave rose oxide as possible candidate structure (correlation factor >90%). This identification was confirmed by retention time comparison with commercially available *cis*- and *trans*-rose oxide. The four enantiomers of rose oxide were resolved on enantioselective column D ( $\alpha$ -values of 1.01 and 1.00). The order of elution from an enantioselective column equivalent to column D is: (+)-(2*R*,4*S*)-*cis*; (-) (2*S*,4*R*)-*cis*; (-)-(2*R*,4*R*)-*trans*; (+)-(2*S*,4*S*)-*trans* (Maas *et al.*, 1994b; Wüst *et al.*, 1997). Enantioselective GC analysis of honeybush samples established the presence in honeybush tea of only the *cis*- and *trans* isomers of (-) rose oxide in a ratio of 70:30.



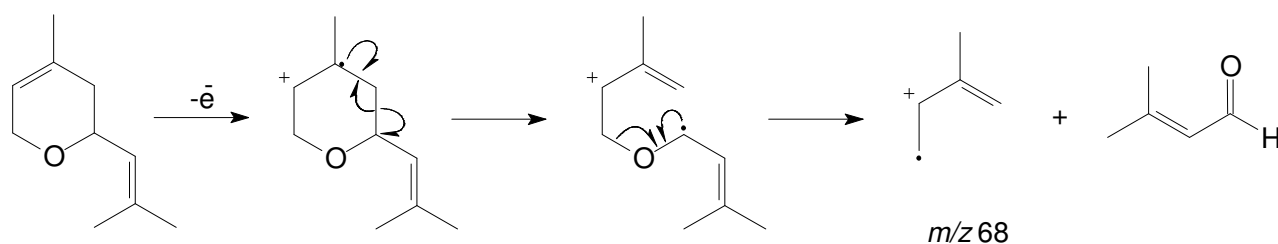
The EI mass spectrum of component **C106** (Fig. 3.165) has many prominent ions in the lower mass range and only a few ions in the higher mass range at  $m/z$  109, 137 and 152 ( $M^+$ ). The elemental composition of  $C_{10}H_{16}O$  of **C106** suggested that this compound could be similar to rose oxide, but that it contains an additional double bond. Online library searches did not provide any useful diagnostic information, but it was found that the RI and mass spectrum of **C106** correspond to those of **nerol oxide** (Adams, 2004).



The identity of **C106** as nerol oxide was confirmed by synthesising the compound according to the following reaction scheme and comparing its retention time with that of **C106**:

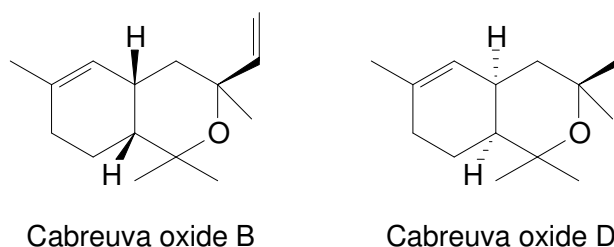


As a result of the presence of the double bond in the ring the loss of the  $\alpha$ -alkyl substituent (to produce a cyclic oxonium ion) is less favourable than a retro-Diels-Alder decomposition of the ring, which is responsible for the formation of the base peak at  $m/z$  68 ( $C_5H_8^+$ ) (Budzikiewicz *et al.*, 1967: 253–254):

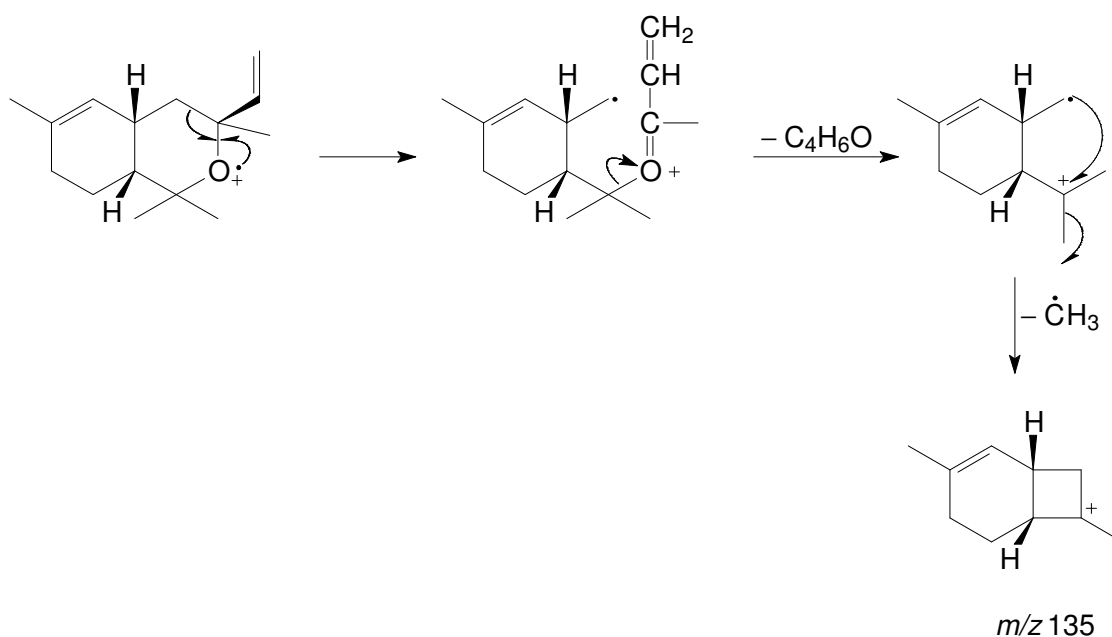


The enantiomers of nerol oxide could not be resolved on any of the  $\beta$ -cyclodextrin-type enantioselective columns available in our laboratory. However, all essential oils such as rose oil, geranium oil and the essential oils of several other plant species contain racemic nerol oxide (Wüst and Mosandl, 1999; Ohloff *et al.*, 1980; Kaiser, 1984), and it was therefore assumed that it is most likely also present as a racemate in the honeybush samples

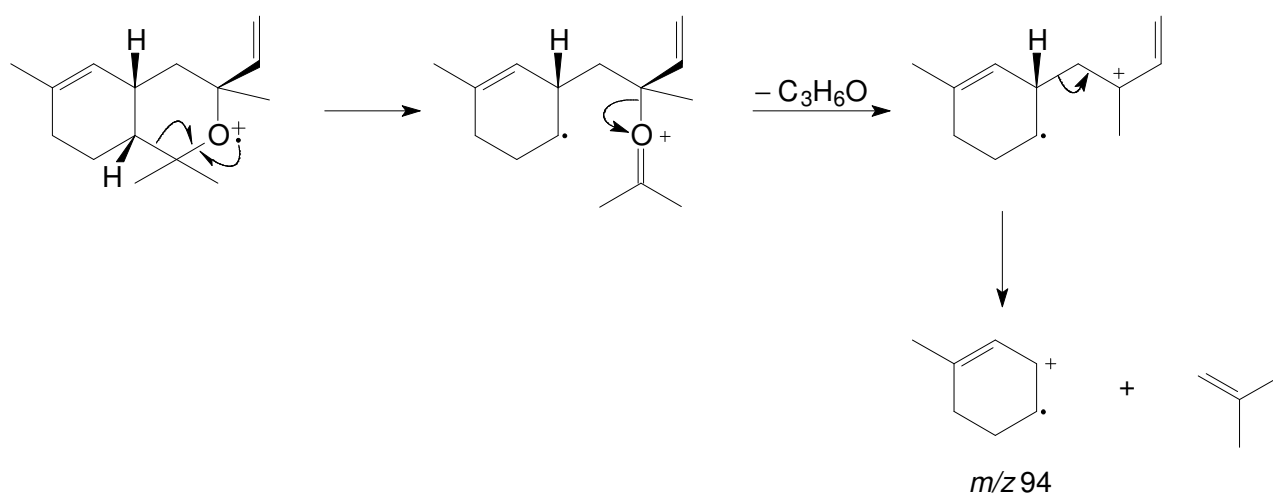
The mass spectra of components **C225** (Fig. 3.166) and **C231** are similar, and most of the ions, including the molecular ion at  $m/z$  220 ( $C_{15}H_{24}O^+$ ), have relative abundances lower than 50%. The base peak is at  $m/z$  94. Components **C225** and **C231** were identified as two isomers of cabreuva oxide by comparing their mass spectra and RIs with those of **cabreuva oxide B** and **cabreuva oxide D** (Adams, 2004):



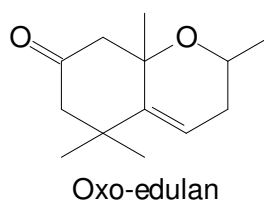
The ion at  $m/z$  135 ( $C_{10}H_{15}^+$ ) in the spectra of these two compounds is formed by the cleavage of a bond  $\alpha$  to the ether oxygen atom, followed by the expulsion of an oxygen-containing fragment:



As shown in the following mechanism, the formation of the base peak at  $m/z$  94 ( $C_7H_{10}^+$ ) is also initiated by the cleavage of an  $\alpha$ -bond:



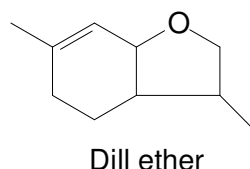
The relative abundances of the prominent ions in the mass spectrum of component **C227** (Fig. 3.167) at  $m/z$  43, 79, 91, 107, 109, 124, 151, 166, 193 (base peak) and 208 ( $M^+$ ,  $C_{13}H_{20}O_2^+$ ) were used in a manual NIST library search, which gave **oxo-edulan** ( $C_{13}H_{20}O_2$ ) as possible candidate structure. An online NIST library search, carried out later in this study, confirmed the proposed structure (74% correlation) and **C227** was therefore tentatively identified as oxo-edulan.



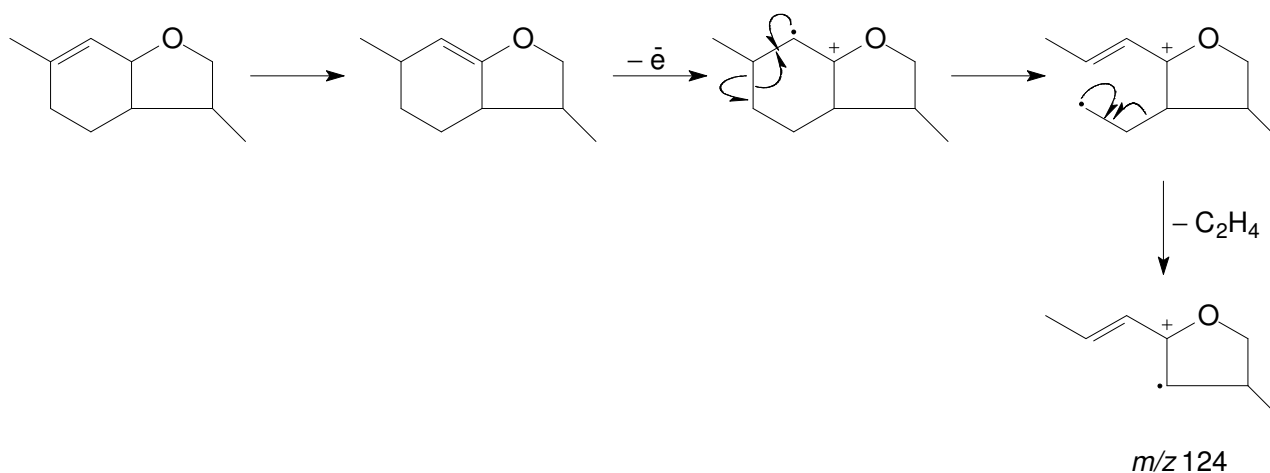


The base peak of the mass spectrum at  $m/z$  193 ( $C_{12}H_{17}O_2^+$ ) is formed by the facile loss of any one of the four methyl groups present in oxo-edulan.

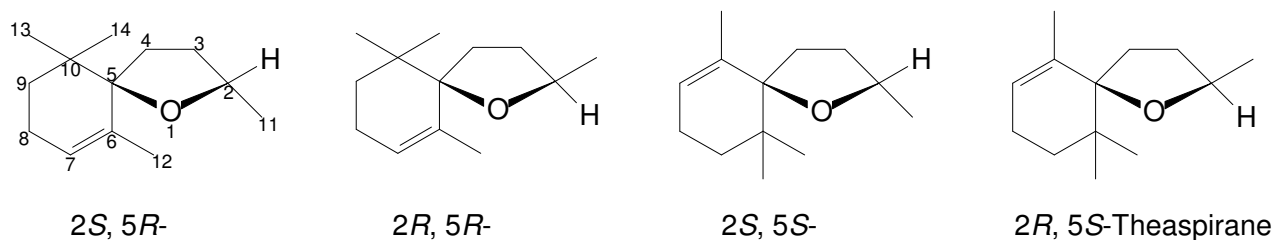
Components **C119** and **C131** were considered to be isomers since they have identical mass spectra (Fig. 3.168), with a molecular ion at  $m/z$  152 ( $C_{10}H_{16}O^+$ ) and a base peak at  $m/z$  137. An online NBS library search suggested **dill ether** as most acceptable candidate structure (80% correlation) for these two components.



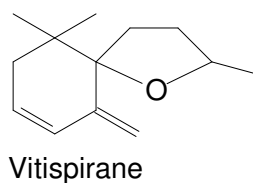
In the mass spectrum of tetrahydrofuran an abundant  $[M - 1]^+$  ion can be observed due the elimination of hydrogen from either the  $\alpha$ - or  $\beta$ -position (Budzikiewicz *et al.*, 1967: 252). Such an  $[M - 1]^+$  ion is observed in the mass spectra of **C119** and **C131** at  $m/z$  151 ( $C_{10}H_{15}O^+$ ), formed by an analogous elimination of hydrogen from the dill ether's tetrahydrofuran ring. The ion of even mass at  $m/z$  124 ( $C_8H_{12}O^+$ ) is formed by the loss of a  $C_2H_4$  fragment *via* a retro-Diels-Alder rearrangement, which is only possible after migration of the double bond in the ring:



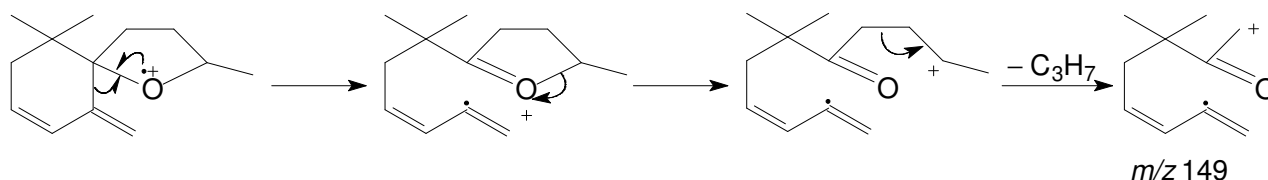
Components **C163** and **C173** (Fig. 3.169) have similar mass spectra with prominent ions at  $m/z$  82, 96, 109, 123, 138 (base peak), 161 and 179, and were thought to be isomers of the same compound. A manual library search, using the relative abundances of these ions, gave theaspirane as most acceptable candidate structure. Theaspirane has a molecular mass of 194 Da, which could not be detected in the LRMS, but was present in the HRMS. The components' elemental composition ( $C_{13}H_{22}O$ ) was also in agreement with the structure of theaspirane and further confirmation of the identity of **C163** and **C173** was achieved by retention time comparison with a commercially available mixture of **theaspirane** enantiomers. The four enantiomers of theaspirane were resolved on enantioselective column C, but their absolute configurations were not assigned since the pure enantiomers were not available for retention time comparison.



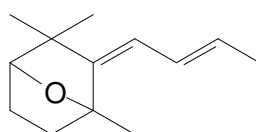
Component **C157** was identified as **vitispirane** on the basis of the good agreement between its mass spectrum (Fig. 3.170) and that of vitispirane (Eggers *et al.*, 2006).



The elemental composition ( $C_{13}H_{20}O$ ) of **C157** matches that of vitispirane. The ion at  $m/z$  177 ( $C_{12}H_{17}O^+$ ) is formed by loss of a methyl group from the molecular ion and the familiar  $[M - H_2O - CH_3]^+$  ion is present at  $m/z$  159 ( $C_{12}H_{15}^+$ ). Loss of a methyl and a methylene group is responsible for the formation of the ion at  $m/z$  163 ( $C_{11}H_{15}O^+$ ). The formation of the ion at  $m/z$  149 ( $C_{10}H_{13}O^+$ ) involves an  $\alpha$ -cleavage reaction as well as the transfer of an additional hydrogen atom:

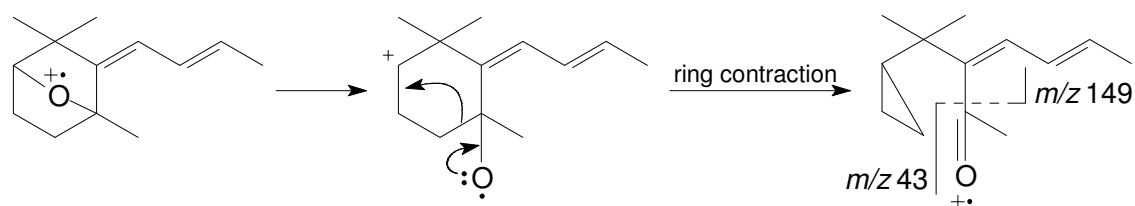


The mass spectra of components **C176**, **C182** (Fig. 3.171) and **C184** are practically identical. They contain the same prominent ions, including a base peak at  $m/z$  43 ( $C_2H_3O^+$ ), and molecular ion at  $m/z$  192 ( $C_{13}H_{20}O^+$ ). Based on the similarity of their mass spectral data and data published by Kaiser and Lamparsky (1978a), components **C176**, **C182** and **C184** were identified as three isomeric **2,5-epoxymegastigma-6,8-dienes**. Due to the presence of two stereogenic centres and two double bonds that can have either *E* or *Z* configuration, this compound theoretically has 16 stereoisomers.

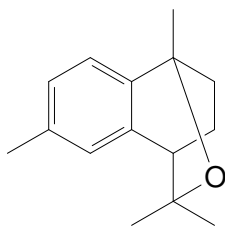


2,5-Epoxymegastigma-6,8-diene

Ring contraction of the epoxide affords a carbonyl derivative from which the base peak at  $m/z$  43 in the mass spectra of these components is formed. The ion at  $m/z$  149 ( $C_{11}H_{17}^+$ ), on the other hand, is formed by loss of this carbonyl moiety (Budzikiewicz *et al.*, 1967: 459–460):



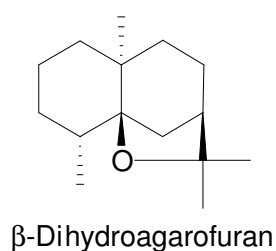
With the exception of the ion at  $m/z$  43, the only other prominent ions in the mass spectrum of component **C236** (Fig. 3.172) appear in the higher mass range at  $m/z$  115, 128, 143, 158, 173 188 and 201. It was assumed that the ion at  $m/z$  201 could not be the molecular ion. Component **C236** was identified as **calamenene-1,11-epoxide** due to the good agreement that exists between its mass spectrum and RI and those of calamenene-1,11-epoxide (Adams, 2004).



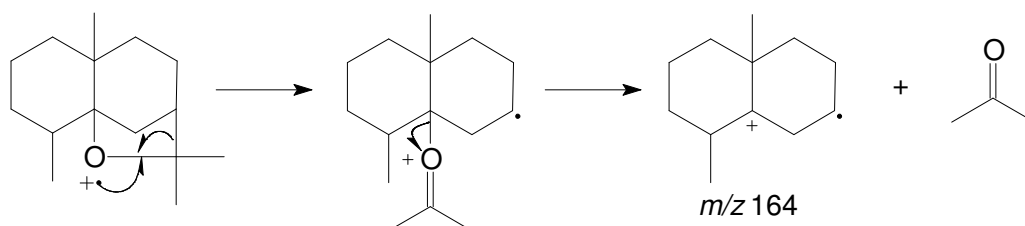
Calamenene-1,11-epoxide

Component **C236** has a molecular mass of 216 Da. The corresponding molecular ion with an elemental composition of  $C_{15}H_{20}O$  (the same as that of calamenene-1,11-epoxide) could only be observed in its HRMS. The ion at  $m/z$  201 ( $C_{14}H_{17}O^+$ ) in the spectrum is formed by loss of a methyl group from the molecular ion. The ion at  $m/z$  188 ( $C_{13}H_{16}O^+$ ) represents an  $[M - C_2H_4]^+$  fragment. The ion at  $m/z$  173 ( $C_{12}H_{13}O^+$ ) is formed by the loss of the isopropyl group, but only after opening of the epoxide ring and migration of a hydrogen atom to the hydrogen-depleted isopropyl group has occurred.

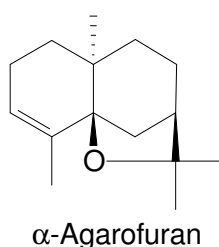
The mass spectra of components **C239** (Fig. 3. 173) and **C258** (Fig. 3.174) are similar. They have a molecular ion at  $m/z$  222 ( $C_{15}H_{26}O^+$ ) and a base peak at  $m/z$  207 ( $C_{14}H_{23}O^+$ ). Component **C239** was identified as  **$\beta$ -dihydroagarofuran** on the basis of the good agreement between its mass spectrum and the RI of the corresponding compound (Adams, 2004). The mass spectrum of **C258** is in agreement with the mass spectrum of *cis*-dihydroagarofuran (Adams, 2004), confirming that **C258** is indeed a compound of the same type as **C239**, but has a higher RI and was therefore tentatively identified as a **dihydroagarofuran isomer**, of which the configuration is not know.



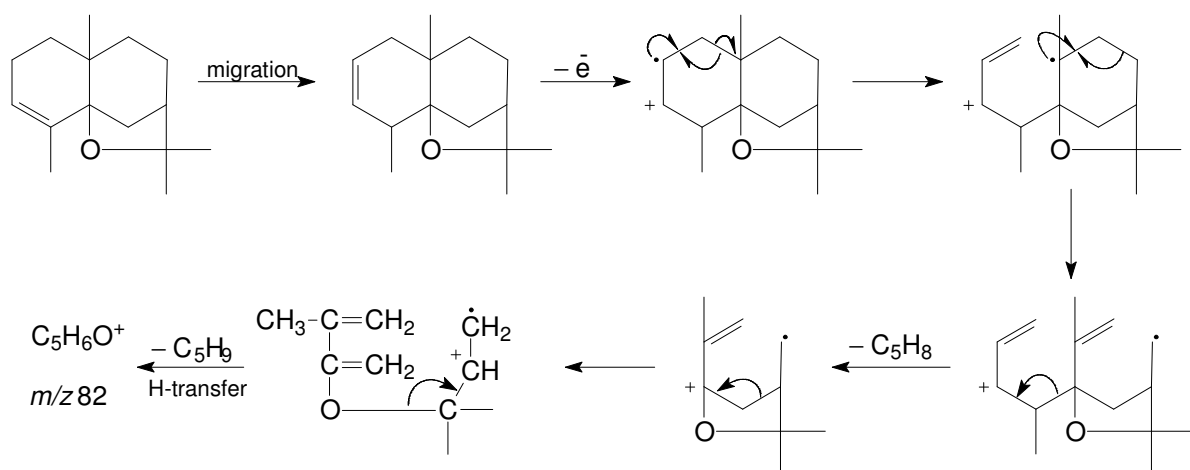
The ion at even-mass  $m/z$  164 ( $C_{12}H_{20}^+$ ) is formed by the loss of 58 mass units from the molecular ion:



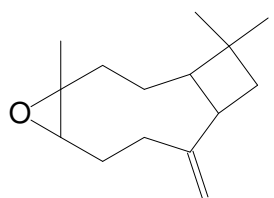
Component **C253** (Fig. 3.175) has a molecular ion at  $m/z$  220 ( $C_{15}H_{24}O^+$ ), which is two hydrogen atoms fewer than the elemental composition of the previous two compounds. This could be an indication that **C253** is a similar type of compound with an additional double bond. Component **C253** was identified as  $\alpha$ -agarofuran on account of the fact that its mass spectrum and RI very closely resemble those of  $\alpha$ -agarofuran (Adams, 2004).



The  $[M - 58]^+$  ion present in the mass spectra of the dihydroagarofurans at  $m/z$  164 appears at  $m/z$  162 ( $C_{12}H_{18}^+$ ) in the spectrum of **C253**, due to the presence of the double bond. The ion at even-mass  $m/z$  82 (base peak,  $C_5H_6O^+$ ) is probably formed *via* a retro-Diels-Alder rearrangement:



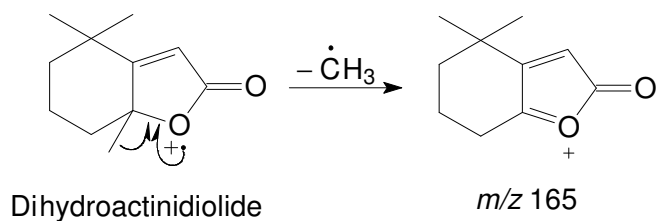
Component **C265** was identified by comparison of its mass spectrum and RI with those of caryophyllene oxide (Adams, 2004) and this structural assignment was confirmed by retention time comparison with an authentic sample of **caryophyllene oxide**.



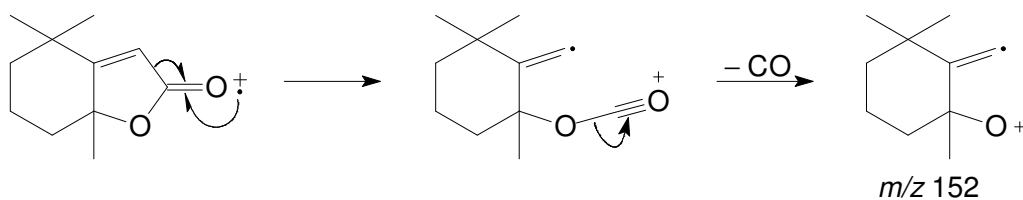
Caryophyllene oxide

### 3.2.16.7 Terpene lactones

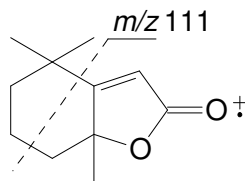
The mass spectrum of component **C243** (Fig. 3.176) has a base peak at  $m/z$  111 and a molecular ion at  $m/z$  180 ( $\text{C}_{11}\text{H}_{16}\text{O}^+$ ). An online NBS library search suggested **dihydroactinidiolide** (87% correlation) as candidate structure. The ion at  $m/z$  165 ( $\text{C}_{10}\text{H}_{13}\text{O}_2^+$ ) is formed by  $\alpha$ -cleavage of the ether–oxygen bond and the expulsion of a methyl group:



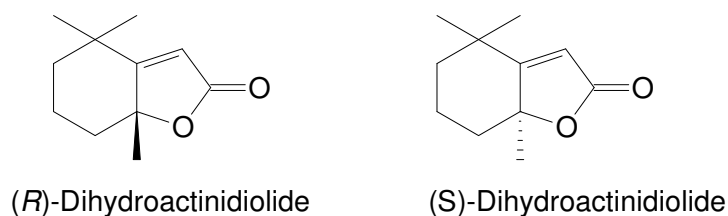
The ion at  $m/z$  152 ( $\text{C}_{10}\text{H}_{16}\text{O}^+$ ) is formed by loss of a CO group from the molecular ion:



Schematically, the formation of the base peak at  $m/z$  111 ( $C_6H_7O_2^+$ ) can be rationalised as follows. This fragmentation requires the transfer of a hydrogen atom:

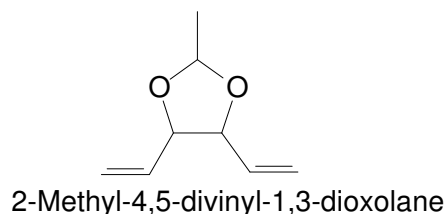


The enantiomers of dihydroactinidiolide were resolved on enantioselective column D ( $R_s$  value = 3.6). The (*R*)-enantiomer of dihydroactinidiolide elutes before its (*S*)-enantiomer from an enantioselective column equivalent to column D (Berger, 2007: 385–386) and the enantioselective analysis of honeybush samples established the presence of both enantiomers in a ratio of 52:48 (*R*:*S*).



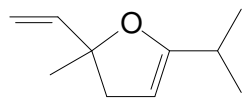
### 3.2.17 Unidentified compounds

The EI mass spectrum of component **C66** (Fig. 3.177) has prominent ions at  $m/z$  43 (base peak), 56, 69, 83, 98 and 140 ( $M^+$ ,  $C_8H_{12}O_2^+$ ). Although no acceptable candidate structures were suggested by any of the library searches it was assumed that **C66** might be related to 2,2-dimethyl-4,5-divinyl-1,3-dioxolane due to similarities in their mass spectra. The molecular mass of 2,2-dimethyl-4,5-divinyl-1,3-dioxolane is 14 mass units higher than that of **C66**, which could be tentatively identified as its monomethyl analogue **2-methyl-4,5-divinyl-1,3-dioxolane**.

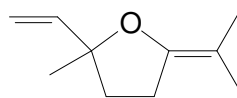


It was assumed that component **C73** (Fig. 3.178) could be related to *trans*- and *cis*-dehydroxylinalool oxide (**C36** and **C45**) since there is a marked resemblance between the mass spectra of these compounds. Component **C73** has the same molecular mass (152 Da), elemental composition ( $C_{10}H_{16}O$ ), base peak ( $m/z$  67) and other prominent ions at  $m/z$  137 and 123 as the dehydroxylinalool oxides. All four enantiomers of dehydroxylinalool oxide were observed in the enantioselective gas chromatogram, but only two isomers were present in the enantioselective gas

chromatogram of **C73**, which could indicate the presence of only one stereogenic centre in **C73**. The following compounds were considered as possible candidate structures for **C73**:

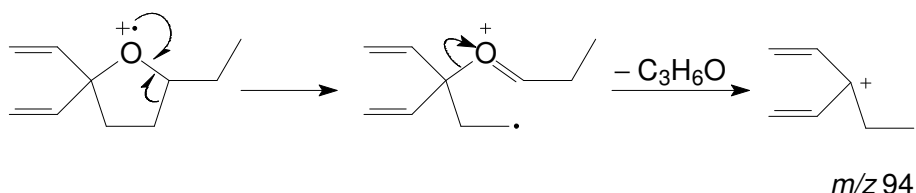


2,3-Dihydro-2-ethenyl-2-methyl-5-isopropylfuran

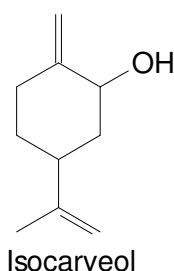


2-Ethenyltetrahydro-2-methyl-5-(1-methylethylidene)furan

Another compound, 2,2-diethenyltetrahydro-5-ethylfuran, was considered as probably the best candidate structure, since it is possible to explain the presence of the ion at  $m/z$  94 ( $C_7H_{10}^+$ ) in the mass spectrum of **C73** in terms of this structure, which is not possible with the two previously mentioned compounds:

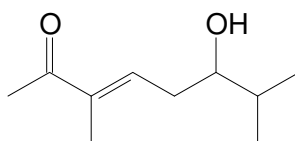


In the EI mass spectrum of component **C144** (Fig. 3.179) the prominent  $[M - H_2O]^+$  ion at  $m/z$  134 gives an indication that **C144** might contain an alcohol group. Both the NBS and NIST libraries proposed *cis*- or *trans*-carveol as possible candidate structures, but their mass spectra have a prominent peak at  $m/z$  84, which is formed by a retro-Diels-Alder rearrangement due to the double bond present in the ring, while this ion is not as prominent in the mass spectrum of **C144**. Therefore, it is proposed that **C144** could contain an exo-cyclic double bond instead of an endo-cyclic double bond as in isocarveol.



In the LRMS of component **C151** (Fig. 3.180) prominent ions are present at  $m/z$  43 ( $C_2H_3O^+$ ; base peak), 69 ( $C_5H_9^+$ ), 86 ( $C_5H_{10}O^+$ ), 109 ( $C_9H_{13}^+$ ), 127 ( $C_8H_{15}O^+$ ) and 170 ( $M^+$ ,  $C_{10}H_{18}O_2^+$ ). In the HRMS however, additional ions are present at  $m/z$  155 ( $[M - CH_3]^+$ ), 152 ( $[M - H_2O]^+$ ) and 137 ( $[M - H_2O - CH_3]^+$ ). Although the compound 2,3,6-trimethyl-7-octen-3-ol, proposed by the NIST library as a possible candidate structure, has a molecular formula of  $C_{11}H_{22}O$  its mass spectrum shows some

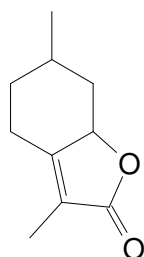
resemblance to that of **C151**, and this was used as argument in favour of 3,7-dimethyl-6-hydroxy-4-octen-2-one as a possible candidate structure for **C151**.



6-Hydroxy-3,7-dimethyl-4-octen-2-one

The EI mass spectrum of component **C156** (Fig. 3.181) has a base peak at  $m/z$  121 ( $C_7H_5O_2^+$ ), a molecular ion at  $m/z$  150 ( $C_9H_{10}O_2^+$ ), and other prominent ions at  $m/z$  65 ( $C_5H_5^+$ ) and 93 ( $C_7H_9^+$ ). The NBS library proposed three possible compounds, the mass spectra and molecular formulae of which matched those of **C156**, i.e. 3- or 4-ethoxybenzaldehyde and 4-hydroxypropiophenone. 2-Hydroxypropiophenone was also considered as a possibility, but retention time comparison revealed that not one of these compounds was a correct match for **C156**.

In the mass spectrum of component **C162** (Fig. 3.182) the molecular ion at  $m/z$  166 ( $C_{10}H_{14}O_2^+$ ) is also the base peak, and other prominent ions are present at  $m/z$  67 ( $C_5H_5^+$ ), 81 ( $C_6H_9^+$ ), 95 ( $C_7H_{11}^+$ ), 109 ( $C_8H_{13}^+$ ), 123 ( $C_8H_{11}O^+$ ), 137 ( $C_9H_{13}O^+$ ) and 151 ( $C_9H_{11}O_2^+$ ). Component **C162** was initially identified as mintlactone based on a manual NIST library search using these significant ions. Furthermore, the elemental composition of **C162** provided by HRMS analysis did not rule out mintlactone as a possibility. However, GC-MS analysis showed that the retention time of mintlactone did not match that of **C162**. This component remains unidentified, but it is expected to be a compound similar to mintlactone.



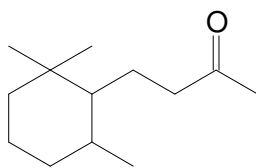
Mintlactone

The EI mass spectrum of component **C168** (Fig. 3.183) is very similar to the mass spectrum of **C156** discussed above, except for the presence of additional ions at  $m/z$  77 ( $C_6H_5^+$ ) and 107 ( $C_7H_7O^+$ ). Many of the compounds proposed by library searches for **C156** were therefore also candidate structures for **C168**, but none gave a positive match. From the type of compounds proposed by the mass spectral libraries it is evident that these two components are probably phenolic compounds.

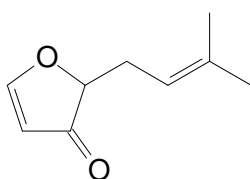
The EI mass spectrum of component **C169** (Fig. 3.184) contains the same prominent ions as the mass spectra of the dehydro-ionone compounds discussed in § 3.2.16.4 (**C203**, **C218**, **C222** and



**C230**), but with different abundances. It was therefore assumed that **C169** should have the same architecture (double bonds not indicated):

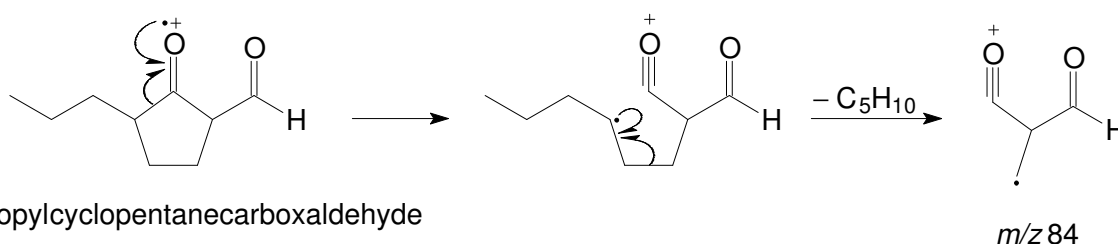


The mass spectrum of component **C172** (Fig. 3.185) has prominent ions at  $m/z$  41 (base peak), 69 ( $C_5H_9^+$ ) and 84 ( $C_4H_4O_2^+$ ), as well as a molecular ion at  $m/z$  152 ( $C_9H_{12}O_2^+$ ). It would be easier to formulate a cyclic candidate structure with this molecular formula having one stereogenic centre since the peaks of two enantiomers were observed in an enantioselective GC-MS analysis. The following is a possible candidate structure:

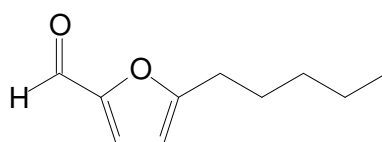


2-(3-Methyl-2-butenyl)-3(2*H*)-furanone

The EI mass spectrum of component **C178** (Fig. 3.186) has a base peak at  $m/z$  84 ( $C_4H_4O_2^+$ ) and a molecular ion at  $m/z$  154 ( $C_9H_{14}O_2^+$ ). The presence of  $[M - CHO]^+$  and  $[M - CO]^+$  ions at  $m/z$  125 and 126, respectively, led to the assumption that **C178** might contain an aldehyde and a ketone moiety, as proposed in the following compound, in which case the base peak at  $m/z$  84 could possibly be formed by the mechanism formulated below. The presence of a stereogenic centre is supported by the presence of the peaks of two enantiomers in an enantioselective GC-MS analysis.



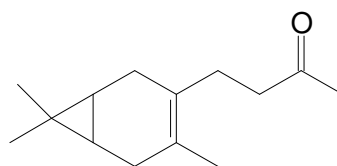
The EI mass spectrum of component **C183** (Fig. 3.187) has prominent ions at  $m/z$  53, 81, 109 (base peak) and 110, as well as a molecular ion at  $m/z$  166 ( $C_{10}H_{14}O_2$ ). The relative abundances of these ions were used in a manual library search and a very good correlation was obtained with the mass spectrum of 5-hexyl-2-furaldehyde. It is therefore possible that **C183** might be 5-pentyl-2-furaldehyde.



5-Pentyl-2-furaldehyde

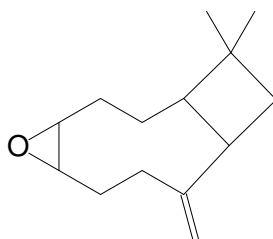
The EI mass spectrum of component **C199** has ions at  $m/z$  77 ( $C_6H_5^+$ ),  $m/z$  105 ( $C_7H_5O^+$ ) and  $m/z$  123 ( $C_7H_7O_2$ ) in common with the mass spectra of the aromatic esters discussed in § 3.2.12, which led to the assumption that **C199** might be a benzoate ester.

The mass spectra of components **C180** (Fig. 3.188) and **C207** (Fig. 3.189) are similar and show some resemblance to the mass spectrum of **C214**, which was identified as 4-(2,6,6-trimethyl-1,3-cyclohexadien-1-yl)-2-butanone. The mass spectra of **C180** and **C207** contain prominent  $[M - H_2O]^+$  and  $[M - H_2O - CH_3]^+$  ions, which might suggest the presence of an alcohol group, but would then not have the correct elemental composition. It is therefore possible that they might contain an epoxy group or that they might be carene-like compounds, the mass spectra of which also show some similarities to the mass spectra of **C180** and **C207**.



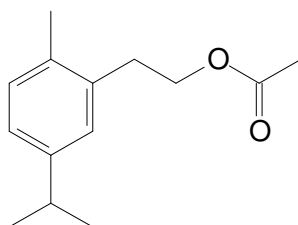
Carene-like compound

The mass spectra of components **C254** (Fig. 3.190) and **C257** are identical and therefore they could possibly be *E/Z*-isomers. Their mass spectra are very similar to that of caryophyllene oxide, which suggests that they might be similar compounds, but with the double bond in another position so as to afford geometrical isomerism.



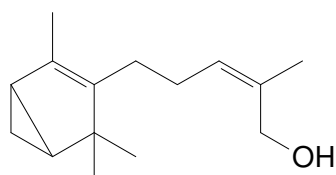
Caryophyllene oxide

The EI mass spectrum of component **C255** (Fig. 3.191) has prominent ions at  $m/z$  145 and 160 and ions at  $m/z$  77, 91 and 105, which are characteristic of aromatic compounds. The ion at  $m/z$  43 is usually characteristic of methyl ketones. The mass spectrum of 5-isopropyl-2-methylphenylethyl acetate (NIST) is quite similar to that of **C255** and it is therefore proposed that **C255** might be a similar type of compound.

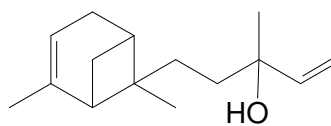


5-Isopropyl-2-methylphenylethyl acetate

The EI mass spectra of components **C267** (Fig. 3.192) and **C269** (Fig. 3.193) have certain ions in common with the mass spectra of bicycolaurencenol and bergamotol (Horsely *et al.*, 1981; NIST). Component **C267**, for example, has a base peak at  $m/z$  119, as does bicycolaurencenol. The ion at  $m/z$  132 in the mass spectrum of **C267** is also present in the mass spectrum of bergamotol. Component **C269**, on the other hand, has a base at  $m/z$  93, in common with the mass spectrum of bergamotol, but instead of an even-mass ion at  $m/z$  132 it has an ion at  $m/z$  134, in common with bicycolaurencenol. Based on this, **C267** and **C269** could tentatively be identified as the following two sesquiterpene alcohols that contain those parts of the sesquiterpene alcohols that are most likely responsible for the presence of the ions at  $m/z$  93, 119, 132 and 134 in their mass spectra:

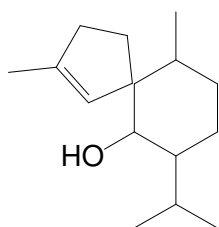


Component 267 (C<sub>15</sub>H<sub>24</sub>O)



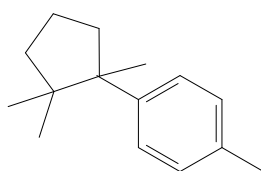
Component 269 (C<sub>15</sub>H<sub>24</sub>O)

Component **C268** (Fig. 3.194) and gleenol have practically identical mass spectra, except for the molecular mass of **C268**, which at  $m/z$  220 (C<sub>15</sub>H<sub>24</sub>O) is two mass units lower than that of gleenol (Adams, 2004), indicating the presence of an additional double bond in **C268**.



Gleenol

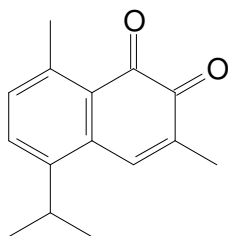
It was assumed that component **C275** (Fig. 3.195) may be similar to the compound cuparene, since their mass spectra are similar (Adams, 2004).



Cuparene

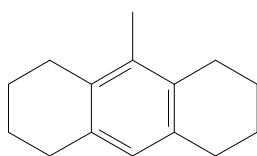
The EI mass spectrum of component **C279** (Fig. 3.196) is similar to that of *trans*-calamenene, discussed in § 3.2.16.1. The fact that **C279** elutes much later suggests that the ion with highest mass present at  $m/z$  202 might not be the molecular ion, but rather that this component has additional functional groups, such as hydroxyl groups, that could be responsible for its longer retention time.

Online library searches (NBS and NIST) gave the following dihydronaphthalenedione compound as the best possible candidate structure (60% and 78% correlation) for component **C280** (Fig. 3.197), but this implies that the ion at  $m/z$  200 ( $C_{15}H_{20}^+$ ) is not the molecular ion.



5-Isopropyl-3,8-dimethyl-1,2-naphthalenedione

If the ion at  $m/z$  200 is the molecular ion, then **C280** might be the following aromatic compound, as also suggested by the NIST library (74% correlation).



1,2,3,4,5,6,7,8-Octahydro-9-methylantracene

It is most likely that the ion with the highest mass ( $m/z$  204) in the mass spectrum of component **C282** (Fig. 3.198) is not the molecular ion, because the suggestions made by the online libraries are hydrocarbon sesquiterpene compounds that are supposed to elute earlier. It is therefore possible that **C282** might rather be a sesquiterpene alcohol.

### 3.3 SUMMARY

Table 3.3: Compound classes of VOCs identified by HS-GC-MS analysis in honeybush (*Cyclopia*)

Compound class	Total number of compounds
Hydrocarbons (saturated, unsaturated, aromatic)	16
Alcohols (saturated, unsaturated, aromatic)	10
Phenols	1
Aldehydes (saturated, unsaturated, aromatic)	25
Furans (saturated, unsaturated, substituted)	8
Carboxylic acids (saturated, unsaturated)	6
Ketones (saturated, unsaturated, aromatic)	16
Esters (saturated, unsaturated and aromatic)	20
Lactones (saturated, unsaturated)	8
Ethers	3
Other compounds	4
Terpenes	33
Terpene alcohols	30
Terpene aldehydes	9
Terpene ketones	31
Terpene esters	7
Terpene ethers	27
Terpene lactone	1

A total number of 255 compounds were identified, the majority of which are terpenoids (138). Within this group it is the terpenes, terpene ketones, terpene alcohols and terpene ethers that are the most prominent. Of the other compound classes, the aldehydes are the largest group, followed by esters, hydrocarbons and ketones.

Table 3.4: VOCs identified by GC-MS analysis in honeybush (*Cyclopia*). (Odour-active compounds are listed in bold type<sup>a</sup>)

No.	Compound name <sup>b</sup>	RI <sup>c</sup> Col A	RI <sup>d</sup> Col B	Identification method <sup>e</sup>	Molecular mass	Elemental composition	Deviation (mDa)
C1	1-Penten-3-ol	639	1133	A	86.0717	C <sub>5</sub> H <sub>10</sub> O	-1.5
C2	Pentanal	649	1000	A	86.0727	C <sub>5</sub> H <sub>10</sub> O	-0.5
C3	2-Ethylfuran	659	977	A	96.0561	C <sub>6</sub> H <sub>8</sub> O	-1.4
C4	1-Pentanol	739	1204	A	70.0772	C <sub>5</sub> H <sub>10</sub> [M – H <sub>2</sub> O]	-1.1
C5	( <i>Z</i> )-2-Penten-1-ol	743	1261	A	86.0732	C <sub>5</sub> H <sub>10</sub> O	0
C6	<b>Hexanal</b>	767	1054	A	82.0784	C <sub>6</sub> H <sub>10</sub> [M – H <sub>2</sub> O]	0.1
C7	2-Ethyl-5,5-dimethyl-1,3-cyclopentadiene	827	1545	B	122.1105	C <sub>9</sub> H <sub>14</sub>	0.9
C8	( <i>E</i> )-2-Hexenal	828	1160	A	98.0743	C <sub>6</sub> H <sub>10</sub> O	1.1
C9	( <i>Z</i> )-3-Hexen-1-ol	838	1316	A	100.0895	C <sub>6</sub> H <sub>12</sub> O	0.7
C10	1-Hexanol	852	1294	A	84.0947	C <sub>6</sub> H <sub>12</sub> [M – H <sub>2</sub> O]	0.8
C11	<b>3-Methylbutanoic acid</b>	857	1581	A	102.0656	C <sub>5</sub> H <sub>10</sub> O <sub>2</sub>	-2.5
C12	1,3,6-Octatriene <sup>f</sup>	863		B	108.0942	C <sub>8</sub> H <sub>12</sub>	0.3
C13	<b>(<i>R</i>)-2-Methylbutanoic acid</b>	866	1588	A	102.0650	C <sub>5</sub> H <sub>10</sub> O <sub>2</sub>	-3.1
C14	2-Heptanone	871	1105	A	114.1058	C <sub>7</sub> H <sub>14</sub> O	1.3
C15	( <i>Z</i> )-4-Heptenal	879	1167	A	112.0849	C <sub>7</sub> H <sub>12</sub> O	-3.9
C16	γ-Butyrolactone	881	1521	A	86.0367	C <sub>4</sub> H <sub>6</sub> O <sub>2</sub>	-0.1
C17	Heptanal	882	1107	A	114.1044	C <sub>7</sub> H <sub>14</sub> O	-0.1
C18	Component C18	883	1120		142.1009	C <sub>8</sub> H <sub>14</sub> O <sub>2</sub>	1.5
C19	2-Acetylfuran	891	1418	A	110.0371	C <sub>6</sub> H <sub>6</sub> O <sub>2</sub>	0.3
C20	Tiglic acid	890	1702	A	100.0508	C <sub>5</sub> H <sub>8</sub> O <sub>2</sub>	-1.6
C21	Pentyl acetate	902		A	70.0785	C <sub>5</sub> H <sub>10</sub> [M – 60]	0.2
C22	Methyl hexanoate	911		A	130.0937	C <sub>7</sub> H <sub>14</sub> O <sub>2</sub>	-1.5
C23	α-Pinene	923	1006	A	136.1260	C <sub>10</sub> H <sub>16</sub>	0.8
C24	Camphene	936	1037	A	136.1263	C <sub>10</sub> H <sub>16</sub>	1.1
C25	Benzaldehyde	936	1426	A	106.0416	C <sub>7</sub> H <sub>6</sub> O	-0.3
C26	( <i>E</i> )-2-Heptenal	938	1352	A	112.0909	C <sub>7</sub> H <sub>12</sub> O	2.1
C27	6-Methyl-2-heptanone	939	1221	A	128.1192	C <sub>8</sub> H <sub>16</sub> O	-0.9
C28	5-Methyl-2-furancarboxaldehyde	940	1582	A	110.0366	C <sub>6</sub> H <sub>6</sub> O <sub>2</sub>	-0.2
C29	2,2,6-Trimethyl-6-vinyltetrahydropyran <sup>f</sup>	960	1073	B	154.1364	C <sub>10</sub> H <sub>18</sub> O	0.6
C30	β-Pinene <sup>f</sup>	966	1114	A	136.1253	C <sub>10</sub> H <sub>16</sub>	0.1
C31	1-Octen-3-ol	969	1386	A	110.1093	C <sub>8</sub> H <sub>14</sub> [M – H <sub>2</sub> O]	-0.3
C32	<b>6-Methyl-5-hepten-2-one</b>	971	1269	A	126.1039	C <sub>8</sub> H <sub>14</sub> O	-0.6

Table 3.4: *contd.*

No.	Compound name <sup>b</sup>	RI <sup>c</sup> Col A	RI <sup>d</sup> Col B	Identification method <sup>e</sup>	Molecular mass	Elemental composition	Deviation (mDa)
C33	( <i>E,Z</i> )-2,4-Heptadienal	978	1384	A	110.0740	C <sub>7</sub> H <sub>10</sub> O	0.8
C34	(6 <i>Z</i> )-2,6-Dimethyl-2,6-octadiene	981	1069	A	138.1373	C <sub>10</sub> H <sub>18</sub>	-3.6
C35	2-Pentylfuran	981	1164	A	138.1043	C <sub>9</sub> H <sub>14</sub> O	-0.2
C36	<i>trans</i> -Dehydroxylinalool oxide (furanoid)	981	1150	A	152.1201	C <sub>10</sub> H <sub>16</sub> O	0
C37	2-Formyl-1-methylpyrrole	981	1521	A	109.0531	C <sub>6</sub> H <sub>7</sub> NO	0.3
C38	Myrcene	983	1116	A	136.1236	C <sub>10</sub> H <sub>16</sub>	-1.6
C39	Octanal	988	1221	A	110.1111	C <sub>8</sub> H <sub>14</sub>	1.3
C40	(2 <i>Z</i> )-2-(2-Pentenyl)furan	990	1229	B	136.0901	C <sub>9</sub> H <sub>12</sub> O	1.3
C41	( <i>E,E</i> )-2,4-Heptadienal	992	1409	A	110.0735	C <sub>7</sub> H <sub>10</sub> O	0.3
C42	α-Phellandrene	994	1135	A	136.1247	C <sub>10</sub> H <sub>16</sub>	0.5
C43	(6 <i>E</i> )-2,6-Dimethyl-2,6-octadiene	996	1089	A	138.1404	C <sub>10</sub> H <sub>18</sub>	-0.5
C44	Hexanoic acid	996	1766	A	87.0431	C <sub>4</sub> H <sub>7</sub> O <sub>2</sub> [M - C <sub>2</sub> H <sub>5</sub> ]	-1.5
C45	<i>cis</i> -Dehydroxylinalool oxide (furanoid)	997	1185	A	152.1208	C <sub>10</sub> H <sub>16</sub> O	0.7
C46	Decane	997	1020	A	142.1712	C <sub>10</sub> H <sub>22</sub>	-1.0
C47	α-Terpinene	1007	1118	A	136.1257	C <sub>10</sub> H <sub>16</sub>	0.5
C48	3,4-Dimethyl-2,5-furandione	1009	1630	A	126.0315	C <sub>6</sub> H <sub>6</sub> O <sub>3</sub>	-0.2
C49	2-Hexen-4-olide	1010	1652	B	112.0501	C <sub>6</sub> H <sub>8</sub> O <sub>2</sub>	-2.3
C50	<b>p-Cymene</b>	1013	1199	A	134.1085	C <sub>10</sub> H <sub>14</sub>	-1.1
C51	2,2,6-Trimethylcyclohexanone	1019	1235	A	140.1214	C <sub>9</sub> H <sub>16</sub> O	1.3
C52	Limonene	1019	1131	A	136.1266	C <sub>10</sub> H <sub>16</sub>	1.4
C53	( <i>E</i> )-3-Octen-2-one	1024	1333	A	126.1055	C <sub>8</sub> H <sub>14</sub> O	1.0
C54	Hexan-4-olide	1026	1593	A	114.0670	C <sub>6</sub> H <sub>10</sub> O <sub>2</sub>	-1.1
C55	Benzylalcohol	1025	1420	A	108.0582	C <sub>7</sub> H <sub>8</sub> O	0.7
C56	<b>(Z)-β-Ocimene</b>	1030	1181	A	136.1279	C <sub>10</sub> H <sub>16</sub>	2.7
C57	2-Methyl-6-methylene-2-octene	1039		B	–		
C58	( <i>E</i> )-β-Ocimene	1040	1193	A	136.1256	C <sub>10</sub> H <sub>16</sub>	0.4
C59	2,6,6-Trimethylcyclohex-2-enone	1042	1316	A	138.1047	C <sub>9</sub> H <sub>14</sub> O	0.2
C60	Acetophenone	1044	1548	A	120.0589	C <sub>8</sub> H <sub>8</sub> O	1.4
C61	<b>γ-Terpinene</b>	1049	1193	A	136.1260	C <sub>10</sub> H <sub>16</sub>	0.8
C62	<i>trans</i> -Arbusculone <sup>f</sup>	1054		B	139.0747	C <sub>8</sub> H <sub>11</sub> O <sub>2</sub> [M - CH <sub>3</sub> ]	-1.2
C63	( <i>Z,E</i> )-3,5-Octadien-2-one	1054	1438	A	124.0893	C <sub>8</sub> H <sub>12</sub> O	0.5
C64	<i>trans</i> -Linalool oxide (furanoid)	1061	1366	A	155.1076	C <sub>9</sub> H <sub>15</sub> O <sub>2</sub> [M - CH <sub>3</sub> ]	0.4

Table 3.4: *contd.*

No.	Compound name <sup>b</sup>	RI <sup>c</sup> Col A	RI <sup>d</sup> Col B	Identification method <sup>e</sup>	Molecular mass	Elemental composition	Deviation (mDa)
C65	1-Octanol	1062	1494	A	112.1226	C <sub>8</sub> H <sub>16</sub> [M – H <sub>2</sub> O]	–2.6
C66	Component C66	1066	1407	C	140.0843	C <sub>8</sub> H <sub>12</sub> O <sub>2</sub>	0.6
C67	2,8-Dimethyl-2,6-nonadiene <sup>f</sup>	1076		B	152.1574	C <sub>11</sub> H <sub>20</sub>	0.9
C68	<i>cis</i> -Linalool oxide (furanoid)	1076	1394	A	155.1072	C <sub>9</sub> H <sub>15</sub> O <sub>2</sub> [M – CH <sub>3</sub> ]	0
C69	<i>p</i> -Cymenene	1076	1343	A	132.0945	C <sub>10</sub> H <sub>12</sub>	0.6
C70	<b>(<i>E,E</i>)-3,5-Octadien-2-one</b>	1077	1491	A	124.0889	C <sub>8</sub> H <sub>12</sub> O	0.1
C71	<b>Terpinolene</b>	1079	1208	A	136.1272	C <sub>10</sub> H <sub>16</sub>	2
C72	2-Nonanone	1079	1320	A	142.1338	C <sub>9</sub> H <sub>18</sub> O	–2
C73	Component C73	1085	1256	C	152.1208	C <sub>10</sub> H <sub>16</sub> O	0.7
C74	(3 <i>E</i> )-6-Methyl-3,5-heptadien-2-one	1088	1509	A	124.0881	C <sub>8</sub> H <sub>12</sub> O	–0.7
C75	Nonanal	1093	1331	A	141.1314	C <sub>9</sub> H <sub>17</sub> O [M – 1]	3.5
C76	<b>Linalool</b>	1095	1489	A	154.1352	C <sub>10</sub> H <sub>18</sub> O	–0.6
C77	Component C77	1095	1499		156.1147	C <sub>9</sub> H <sub>16</sub> O <sub>2</sub>	–0.3
C78	Hotrienol	1096	1540	B	134.1125	C <sub>10</sub> H <sub>14</sub> [M – H <sub>2</sub> O]	2.9
C79	<b>2-Phenylethanol</b>	1098	1818	A	122.0729	C <sub>8</sub> H <sub>10</sub> O	–0.3
C80	Undecane	1100	1110	A	–		
C81	3,4,4-Trimethyl-2-cyclopenten-1-one	1101	1495	B	124.0902	C <sub>8</sub> H <sub>12</sub> O	1.4
C82	Isophorone	1102	1490	A	138.1042	C <sub>9</sub> H <sub>14</sub> O	–0.3
C83	(-)- <i>cis</i> -Rose oxide	1103	1282	A	154.1359	C <sub>10</sub> H <sub>18</sub> O	0.1
C84	3-Thujanone <sup>f</sup>	1104	1331	A	152.1201	C <sub>10</sub> H <sub>16</sub> O	0
C85	α-Fenchol <sup>f</sup>	1104		B	154.1365	C <sub>10</sub> H <sub>18</sub> O	0.7
C86	<i>cis</i> -2- <i>p</i> -Menthen-1-ol <sup>f</sup>	1110		B	154.1346	C <sub>10</sub> H <sub>18</sub> O	–1.2
C87	Component C87	1112	1572		–		
C88	Component C88	1113	1449		141.0910	C <sub>6</sub> H <sub>11</sub> N <sub>3</sub> O	0.5
C89	<b>4-Acetyl-1-methylcyclohexene<sup>f</sup></b>	1114	1457	A	138.1039	C <sub>9</sub> H <sub>14</sub> O	–0.6
C90	Methyl octanoate	1116	1321	A	158.1324	C <sub>9</sub> H <sub>18</sub> O <sub>2</sub>	1.7
C91	(-)- <i>trans</i> -Rose oxide	1119	1293	A	154.1366	C <sub>10</sub> H <sub>18</sub> O	0.8
C92	4-Ketoisophorone	1121	1592	A	152.0848	C <sub>9</sub> H <sub>12</sub> O <sub>2</sub>	1.1
C93	Allo-ocimene	1122	1101	A	136.1267	C <sub>10</sub> H <sub>16</sub>	1.5
C94	Dihydrolinalool <sup>f</sup>	1125	1474	B	138.1432	C <sub>10</sub> H <sub>18</sub> [M – H <sub>2</sub> O]	2.3
C95	( <i>E</i> )-3-Nonen-2-one	1126	1432	A	140.1199	C <sub>9</sub> H <sub>16</sub> O	–0.2
C96	<i>trans</i> -2- <i>p</i> -Menthen-1-ol <sup>f</sup>	1129		B	154.1391	C <sub>10</sub> H <sub>18</sub> O	3.3



Table 3.4: *contd.*

No.	Compound name <sup>b</sup>	RI <sup>c</sup> Col A	RI <sup>d</sup> Col B	Identification method <sup>e</sup>	Molecular mass	Elemental composition	Deviation (mDa)
C97	Lilac aldehyde isomer 1 <sup>f</sup>	1134	1513	B	168.1127	C <sub>10</sub> H <sub>16</sub> O <sub>2</sub>	-2.3
C98	Camphene hydrate <sup>f</sup>	1135	1502	B	154.1391	C <sub>10</sub> H <sub>18</sub> O	3.3
C99	1-(1,4-Dimethyl-3-cyclohexen-1-yl)ethanone <sup>f</sup>	1135		B	152.1212	C <sub>10</sub> H <sub>16</sub> O	1.1
C100	4-Vinylanisole	1135		A	–		
C101	<b>(E,Z)-2,6-Nonadienal</b>	1137	1501	A	138.1007	C <sub>9</sub> H <sub>14</sub> O	-3.8
C102	Component C102	1138			152.1228	C <sub>10</sub> H <sub>16</sub> O	2.7
C103	(Z)-Ocimenol	1142		B	136.1253	C <sub>10</sub> H <sub>16</sub> [M – H <sub>2</sub> O]	0.1
C104	2,2,6-Trimethyl-1,4-cyclohexanedione <sup>f</sup>	1142	1675	B	154.0987	C <sub>9</sub> H <sub>14</sub> O <sub>2</sub>	-0.7
C105	Isoborneol	1144		A	154.1346	C <sub>10</sub> H <sub>18</sub> O	-1.2
C106	Nerol oxide <sup>f</sup>	1144	1391	A	152.1199	C <sub>10</sub> H <sub>16</sub> O	-0.2
C107	Propiophenone	1144		A	134.0709	C <sub>9</sub> H <sub>10</sub> O	-2.3
C108	<b>(E)-2-Nonenal</b>	1145	1453	A	140.1204	C <sub>9</sub> H <sub>16</sub> O	0.3
C109	Benzyl acetate	1146	1634	A	150.0666	C <sub>9</sub> H <sub>10</sub> O <sub>2</sub>	-1.5
C110	Lilac aldehyde isomer 2 <sup>f</sup>	1149	1566	B	168.1116	C <sub>10</sub> H <sub>16</sub> O <sub>2</sub>	-3.4
C111	2-Chloro-1,7,7-trimethylbicyclo- [2.2.1]heptane <sup>f</sup>	1149		B	157.0793	C <sub>9</sub> H <sub>14</sub> Cl [M – CH <sub>3</sub> ]	0.9
C112	Borneol	1152		A	154.1390	C <sub>10</sub> H <sub>18</sub> O	3.2
C113	(E)-Ocimenol	1153		B	136.1227	C <sub>10</sub> H <sub>16</sub> [M – H <sub>2</sub> O]	-2.5
C114	A dimethylbenzaldehyde	1155	1622	A	134.0728	C <sub>9</sub> H <sub>10</sub> O	-0.4
C115	<i>cis</i> -Pyranoid linalool oxide	1158	1654	A	155.1086	C <sub>9</sub> H <sub>15</sub> O <sub>2</sub> [M – CH <sub>3</sub> ]	1.4
C116	<i>trans</i> -Pyranoid linalool oxide	1164	1687	A	155.1084	C <sub>9</sub> H <sub>15</sub> O <sub>2</sub> [M – CH <sub>3</sub> ]	1.2
C117	Component C117	1164	1909		142.0644	C <sub>7</sub> H <sub>10</sub> O <sub>3</sub>	1.4
C118	Terpinen-4-ol	1165	1516	A	154.1364	C <sub>10</sub> H <sub>18</sub> O	0.6
C119	Dill ether isomer 1 <sup>f</sup>	1171	1493	B	152.1189	C <sub>10</sub> H <sub>16</sub> O	-1.2
C120	<i>p</i> -Cymen-8-ol	1172	1763	A	150.1027	C <sub>10</sub> H <sub>14</sub> O	-1.8
C121	<b>α-Terpineol</b>	1181	1619	A	154.1366	C <sub>10</sub> H <sub>18</sub> O	0.8
C122	Safranal	1182	1542	A	150.1026	C <sub>10</sub> H <sub>14</sub> O	-1.9
C123	Component C123	1183	1649	A	136.1199	C <sub>10</sub> H <sub>16</sub>	-5.3
C124	Decanal	1194	1433	A	156.1537	C <sub>10</sub> H <sub>20</sub> O	2.3
C125	(+)- <i>p</i> -Menth-1-en-9-al	1198	1519	A	152.1217	C <sub>10</sub> H <sub>16</sub> O	1.6
C126	Dodecane	1199	1201	A	170.2035	C <sub>12</sub> H <sub>26</sub>	0
C127	Benzothiazole	1200		A	135.0143	C <sub>7</sub> H <sub>5</sub> NS	0

Table 3.4: contd.

No.	Compound name <sup>b</sup>	RI <sup>c</sup> Col A	RI <sup>d</sup> Col B	Identification method <sup>e</sup>	Molecular mass	Elemental composition	Deviation (mDa)
C128	<b>(+)-<i>p</i>-Menth-1-en-9-al</b>	1200	1519	A	152.1188	C <sub>10</sub> H <sub>16</sub> O	-1.3
C129	<b>β-Cyclositral</b>	1203	1522	A	152.1184	C <sub>10</sub> H <sub>16</sub> O	-1.7
C130	2-Ethyl-3-methylmaleimide	1211	2177	B	139.0636	C <sub>7</sub> H <sub>9</sub> NO <sub>2</sub>	0.3
C131	Dill ether isomer 2 <sup>f</sup>	1213		B	152.1213	C <sub>10</sub> H <sub>16</sub> O	1.2
C132	Methyl nonanoate	1215		A	172.1482	C <sub>10</sub> H <sub>20</sub> O <sub>2</sub>	1.9
C133	Component C133	1215	2301		120.0573	C <sub>8</sub> H <sub>8</sub> O	-0.2
C134	Component C134	1216			166.1373	C <sub>11</sub> H <sub>18</sub> O	1.5
C135	<b>Nerol</b>	1219	1727	A	154.1368	C <sub>10</sub> H <sub>18</sub> O	1
C136	Component C136	1223	1815	B	148.0886	C <sub>10</sub> H <sub>12</sub> O	-0.4
C137	( <i>R</i> )-β-Citronellol	1223	1702	A	156.1563	C <sub>10</sub> H <sub>20</sub> O	4.9
C138	( <i>Z</i> )-3-Hexenyl 2-methylbutanoate <sup>f</sup>	1223	1408	A	103.0770	C <sub>5</sub> H <sub>11</sub> O <sub>2</sub> [M - C <sub>6</sub> H <sub>9</sub> ]	1.1
C139	Neral	1225	1626	A	152.1176	C <sub>10</sub> H <sub>16</sub> O	-2.5
C140	( <i>Z</i> )-3-Hexenyl isovalerate	1228	1424	A	103.0729	C <sub>5</sub> H <sub>11</sub> O <sub>2</sub> [M - C <sub>6</sub> H <sub>9</sub> ]	-3.0
C141	<b><i>p</i>-Anisaldehyde</b>	1232	1936	A	136.0504	C <sub>8</sub> H <sub>8</sub> O <sub>2</sub>	-2
C142	2-Phenylethyl acetate	1238	1725	A	104.0616	C <sub>8</sub> H <sub>8</sub> [M - C <sub>2</sub> H <sub>4</sub> O <sub>2</sub> ]	-1.0
C143	Carvenone <sup>f</sup>	1239	1603	B	152.1220	C <sub>10</sub> H <sub>16</sub> O	1.9
C144	Component C144	1239		C	152.1189	C <sub>10</sub> H <sub>16</sub> O	-1.2
C145	3,5,7-Nonatrien-2-one	1241	1819	B	136.0887	C <sub>9</sub> H <sub>12</sub> O	-0.1
C146	2,6,6-Trimethyl-1-cyclohexene-1-acetaldehyde	1241	1520	A	166.1361	C <sub>11</sub> H <sub>18</sub> O	0.3
C147	2-(2-Butenyl)-1,3,5-trimethylbenzene <sup>f</sup>	1241		B	174.1411	C <sub>13</sub> H <sub>18</sub>	0.2
C148	<b>Geraniol</b>	1248	1783	A	154.1345	C <sub>10</sub> H <sub>18</sub> O	-1.3
C149	( <i>E,E,Z</i> )-2,4,6-nonatrienal	1253		A	136.0922	C <sub>9</sub> H <sub>12</sub> O	3.4
C150	<b>Geranial</b>	1255	1647	A	152.1207	C <sub>10</sub> H <sub>16</sub> O	0.6
C151	Component C151	1259	1766	C	170.1313	C <sub>10</sub> H <sub>18</sub> O <sub>2</sub>	0.6
C152	<b>(<i>R</i>)-Octan-5-olide</b>	1259	1864	A	142.0954	C <sub>8</sub> H <sub>14</sub> O <sub>2</sub>	-4.0
C153	( <i>E</i> )-2-Decen-1-ol	1260		A	—		
C154	4,8-Dimethyl-3,7-nonadien-2-one <sup>f</sup>	1261		B	166.1345	C <sub>11</sub> H <sub>18</sub> O	-1.3
C155	( <i>E,E,E</i> )-2,4,6-nonatrienal	1262	1800	A	136.0854	C <sub>9</sub> H <sub>12</sub> O	-3.4
C156	Component C156	1265		C	150.0658	C <sub>9</sub> H <sub>10</sub> O <sub>2</sub>	-2.3
C157	Vitispirane <sup>f</sup>	1268		B	192.1505	C <sub>13</sub> H <sub>20</sub> O	-0.9
C158	Neryl formate	1270	1596	B	182.1262	C <sub>11</sub> H <sub>18</sub> O <sub>2</sub>	-4.5
C159	Nonanoic acid	1272	2110	A	158.1292	C <sub>9</sub> H <sub>18</sub> O <sub>2</sub>	-1.5

Table 3.4: *contd.*

No.	Compound name <sup>b</sup>	RI <sup>c</sup> Col A	RI <sup>d</sup> Col B	Identification method <sup>e</sup>	Molecular mass	Elemental composition	Deviation (mDa)
C160	Limonen-10-ol <sup>f</sup>	1279		B	152.1183	C <sub>10</sub> H <sub>16</sub> O	-1.8
C161	2-Undecanone	1283	1529	A	170.1661	C <sub>11</sub> H <sub>22</sub> O	-1.0
C162	<b>Component 162</b>	1283	1790	C	166.0993	C <sub>10</sub> H <sub>14</sub> O <sub>2</sub>	-0.1
C163	Theaspirane isomer 1 <sup>f</sup>	1288		A	194.1656	C <sub>13</sub> H <sub>22</sub> O	-1.5
C164	<b>Geranyl formate</b>	1291	1630	A	182.1343	C <sub>11</sub> H <sub>18</sub> O <sub>2</sub>	3.6
C165	Component C165	1294			152.0879	C <sub>9</sub> H <sub>12</sub> O <sub>2</sub>	4.2
C166	2,3,4-Trimethylbenzaldehyde	1295		B	148.0875	C <sub>10</sub> H <sub>12</sub> O	-1.3
C167	Undecanal	1295		A	152.1571	C <sub>11</sub> H <sub>20</sub> [M - H <sub>2</sub> O]	0.6
C168	Component C168	1298		C	150.0676	C <sub>9</sub> H <sub>10</sub> O <sub>2</sub>	-0.5
C169	Component C169	1299	1637	C	190.1351	C <sub>13</sub> H <sub>18</sub> O	-0.7
C170	Tridecane	1299	1305	A	184.2228	C <sub>13</sub> H <sub>28</sub>	3.7
C171	<b>(E,E)-2,4-Decadienal</b>	1300	1721	A	152.1187	C <sub>10</sub> H <sub>16</sub> O	-1.4
C172	Component C172	1301	2022	C	152.0802	C <sub>9</sub> H <sub>12</sub> O <sub>2</sub>	-3.5
C173	Theaspirane isomer 2 <sup>f</sup>	1304		A	194.1646	C <sub>13</sub> H <sub>22</sub> O	-2.5
C174	Component C174	1311			192.1206	C <sub>12</sub> H <sub>16</sub> O <sub>2</sub>	5.6
C175	(Z)-3-Hexenyl (E)-2-methyl-2-butenolate	1312	1591	A	101.0620	C <sub>5</sub> H <sub>9</sub> O <sub>2</sub> [M - C <sub>6</sub> H <sub>9</sub> ]	1.7
C176	2,5-Epoxymegastigma-6,8-diene <sup>f</sup>	1315	1555	B	192.1532	C <sub>13</sub> H <sub>20</sub> O	1.8
C177	Methyl decanoate	1315		A	186.1592	C <sub>11</sub> H <sub>22</sub> O	-2.8
C178	<b>Component C178</b>	1317	1988	C	154.0981	C <sub>9</sub> H <sub>14</sub> O <sub>2</sub>	-1.3
C179	Hexyl tiglate	1320		A	184.1428	C <sub>11</sub> H <sub>20</sub> O <sub>2</sub>	-3.5
C180	Component C180 (carene-type comp.)	1323	1814	C	192.1486	C <sub>13</sub> H <sub>20</sub> O	-2.8
C181	Component C181	1326	1620		153.0925	C <sub>9</sub> H <sub>13</sub> O <sub>2</sub>	0.9
C182	2,5-Epoxymegastigma-6,8-diene <sup>f</sup>	1326	1550	B	192.1504	C <sub>13</sub> H <sub>20</sub> O	-1.0
C183	Component C183	1327		C	166.1001	C <sub>10</sub> H <sub>14</sub> O <sub>2</sub>	0.7
C184	2,5-Epoxymegastigma-6,8-diene <sup>f</sup>	1330	1526	B	192.1494	C <sub>13</sub> H <sub>20</sub> O	-2.0
C185	Component C185	1336			152.0829	C <sub>9</sub> H <sub>12</sub> O <sub>2</sub>	-0.8
C186	Nonan-4-olide	1337	1942	A	138.1078	C <sub>9</sub> H <sub>14</sub> O [M - H <sub>2</sub> O]	3.3
C187	Component C187	1337		A	180.1109	C <sub>11</sub> H <sub>16</sub> O <sub>2</sub>	-4.1
C188	α-Terpinyol acetate <sup>f</sup>	1337		B	136.1238	C <sub>10</sub> H <sub>16</sub> [M - C <sub>2</sub> H <sub>4</sub> O <sub>2</sub> ]	-1.4
C189	1,5,8-Trimethyl-1,2-dihydronaphthalene <sup>f</sup>	1338		B	172.1261	C <sub>13</sub> H <sub>16</sub>	0.9
C190	1-(2-Hydroxy-1-methylethyl)-2,2-dimethylpropyl 2-methylpropanoate <sup>f</sup>	1339	1780	B	173.1172	C <sub>9</sub> H <sub>17</sub> O <sub>3</sub> [M - C <sub>3</sub> H <sub>7</sub> ]	-0.6
C191	<b>Eugenol</b>	1340	2090	A	164.0824	C <sub>10</sub> H <sub>12</sub> O <sub>2</sub>	-1.3

Table 3.4: *contd.*

No.	Compound name <sup>b</sup>	RI <sup>c</sup> Col A	RI <sup>d</sup> Col B	Identification method <sup>e</sup>	Molecular mass	Elemental composition	Deviation (mDa)
C192	2,3-Dihydro-1,1,5,6-tetramethyl-1 <i>H</i> -indene	1340		B	174.1402	C <sub>13</sub> H <sub>18</sub>	-0.7
C193	α-Ionene	1343		A	174.1408	C <sub>13</sub> H <sub>18</sub>	-0.1
C194	α-Cubebene <sup>f</sup>	1345	1419	A	204.1870	C <sub>15</sub> H <sub>24</sub>	-0.8
C195	( <i>Z</i> )-β-Damascenone	1347		A	190.1360	C <sub>13</sub> H <sub>18</sub> O	0.2
C196	( <i>E</i> )-2-Undecenal	1350		A	150.1392	C <sub>11</sub> H <sub>18</sub> [M - H <sub>2</sub> O]	-1.7
C197	4,6,8-Megastigmatriene <sup>f</sup>	1352		A	176.1581	C <sub>13</sub> H <sub>20</sub>	1.6
C198	Neryl acetate	1353	1658	A	154.1391	C <sub>10</sub> H <sub>18</sub> O [M - C <sub>2</sub> H <sub>2</sub> O]	3.3
C199	Component C199 (a benzoate ester)	1357		C	123.0466	C <sub>7</sub> H <sub>7</sub> O <sub>2</sub>	2.0
C200	α-Ylangene <sup>f</sup>	1362	1426	B	204.1901	C <sub>15</sub> H <sub>24</sub>	2.3
C201	3-Hydroxy-2,4,4-trimethylpentyl 2-methylpropanoate <sup>f</sup>	1363	1790	B	173.1170	C <sub>9</sub> H <sub>17</sub> O <sub>3</sub> [M - C <sub>3</sub> H <sub>7</sub> ]	-0.8
C202	2-Butyl-2-octenal <sup>f</sup>	1364		B	182.1673	C <sub>12</sub> H <sub>22</sub> O	0.2
C203	<b>2,3-Dehydro-α-ionone<sup>f</sup></b>	1366	1729	B	190.1349	C <sub>13</sub> H <sub>18</sub> O	-0.9
C204	<b>(<i>E</i>)-β-Damascenone</b>	1369	1722	A	190.1364	C <sub>13</sub> H <sub>18</sub> O	0.6
C205	α-Copaene <sup>f</sup>	1369	1423	A	204.1882	C <sub>15</sub> H <sub>24</sub>	0.4
C206	Geranyl acetate	1372	1687	A	154.1382	C <sub>10</sub> H <sub>18</sub> O [M - C <sub>2</sub> H <sub>2</sub> O]	2.4
C207	Component C207 (carene-type comp.)	1376	1933	C	192.1543	C <sub>13</sub> H <sub>20</sub> O	2.9
C208	β-Bourbonene <sup>f</sup>	1377	1445	B	204.1900	C <sub>15</sub> H <sub>24</sub>	2.2
C209	6,10-Dimethyl-2-undecanone <sup>f</sup>	1395	1628	A	198.1983	C <sub>13</sub> H <sub>26</sub> O	-0.1
C210	Dodecanal	1398	1641	A	184.1815	C <sub>12</sub> H <sub>24</sub> O	-1.2
C211	Tetradecane	1399	1403	A	198.2341	C <sub>14</sub> H <sub>30</sub>	-0.7
C212	<b>(<i>E</i>)-β-Damascone</b>	1399	1718	A	192.1518	C <sub>13</sub> H <sub>20</sub> O	0.4
C213	1,3-Dimethylnaphthalene	1401	1901	A	156.0919	C <sub>12</sub> H <sub>12</sub>	-2.0
C214	4-(2,6,6-Trimethyl-1,3-cyclohexadien-1-yl)-2-butanone	1403		B	192.1483	C <sub>13</sub> H <sub>20</sub> O	-3.1
C215	6-Methyl-6-(5-methylfuran-2-yl)heptan-2-one	1410	1821	B	208.1471	C <sub>13</sub> H <sub>20</sub> O <sub>2</sub>	0.8
C216	( <i>E</i> )-Caryophyllene <sup>f</sup>	1411	1509	A	204.1854	C <sub>15</sub> H <sub>24</sub>	-2.4
C217	( <i>R</i> )-α-Ionone	1413	1755	A	192.1541	C <sub>13</sub> H <sub>20</sub> O	2.7
C218	3,4-Dehydro-γ-ionone <sup>f</sup>	1415	1847	B	190.1370	C <sub>13</sub> H <sub>18</sub> O	1.2
C219	( <i>E</i> )-6-Methyl-6-(5-methylfuran-2-yl)hept-3-en-2-one	1431	1888	B	206.1297	C <sub>13</sub> H <sub>18</sub> O <sub>2</sub>	-1.0
C220	Geranylacetone	1441	1784	A	194.1646	C <sub>13</sub> H <sub>22</sub> O	-2.5
C221	α-Humulene	1445	1577	A	204.1874	C <sub>15</sub> H <sub>24</sub>	-0.4
C222	<b>2,3-Dehydro-γ-ionone<sup>f</sup></b>	1450	1805	B	190.1367	C <sub>13</sub> H <sub>18</sub> O	0.9
C223	5-Methoxy-6,7-dimethylbenzofuran	1451	2039	B	176.0860	C <sub>11</sub> H <sub>12</sub> O <sub>2</sub>	2.3

Table 3.4: *contd.*

No.	Compound name <sup>b</sup>	RI <sup>c</sup> Col A	RI <sup>d</sup> Col B	Identification method <sup>e</sup>	Molecular mass	Elemental composition	Deviation (mDa)
C224	Component C224	1452			192.1485	C <sub>13</sub> H <sub>20</sub> O	-2.9
C225	Cabreuva oxide B <sup>f</sup>	1452	1623	B	220.1841	C <sub>15</sub> H <sub>24</sub> O	1.4
C226	9- <i>epi</i> -( <i>E</i> )-Caryophyllene <sup>f</sup>	1452	1602	B	204.1881	C <sub>15</sub> H <sub>24</sub>	0.3
C227	Oxo-edulan <sup>f</sup>	1463	1905	B	208.1439	C <sub>13</sub> H <sub>20</sub> O <sub>2</sub>	-2.4
C228	Geranyl propanoate	1464	1751	B	136.1222	C <sub>10</sub> H <sub>16</sub> [M - C <sub>3</sub> H <sub>6</sub> O <sub>2</sub> ]	-3.0
C229	<b>(S)-(Z)-7-Decen-5-olide</b>	1465	2151	A	168.1156	C <sub>10</sub> H <sub>16</sub> O <sub>2</sub>	0.6
C230	<b>3,4-Dehydro-β-ionone</b>	1467	1923	A	190.1362	C <sub>13</sub> H <sub>18</sub> O	0.4
C231	Cabreuva oxide D <sup>f</sup>	1468	1663	B	220.1821	C <sub>15</sub> H <sub>24</sub> O	-0.6
C232	5,6-Epoxy-β-ionone	1469	1911	A	208.1487	C <sub>13</sub> H <sub>20</sub> O <sub>2</sub>	2.4
C233	<b>(R)-Decan-5-olide</b>	1470	2099	A	170.1267	C <sub>10</sub> H <sub>18</sub> O <sub>2</sub>	-4.0
C234	<b>(E)-β-Ionone</b>	1471	1850	A	192.1512	C <sub>13</sub> H <sub>20</sub> O	-0.2
C235	β-Selinene <sup>f</sup>	1476		B	204.1870	C <sub>15</sub> H <sub>24</sub>	-0.8
C236	Calamenene-1,11-epoxide <sup>f</sup>	1477	1784	B	216.1516	C <sub>15</sub> H <sub>20</sub> O	0.2
C237	Benzyl tiglate	1480	2030	A	190.1022	C <sub>12</sub> H <sub>14</sub> O <sub>2</sub>	2.8
C238	Component C238	1485			168.1519	C <sub>11</sub> H <sub>20</sub> O	0.5
C239	β-Dihydroagarofuran <sup>f</sup>	1489	1616	B	222.1991	C <sub>15</sub> H <sub>26</sub> O	0.7
C240	α-Muurolene <sup>f</sup>	1492	1642	B	204.1895	C <sub>15</sub> H <sub>24</sub>	1.7
C241	Pentadecane	1499	1502	A	212.2508	C <sub>15</sub> H <sub>32</sub>	0.4
C242	Tridecanal	1499		A	180.1871	C <sub>13</sub> H <sub>24</sub> [M - H <sub>2</sub> O]	-0.7
C243	Dihydroactinidiolide	1499	2201	B	180.1159	C <sub>11</sub> H <sub>16</sub> O <sub>2</sub>	0.9
C244	γ-Cadinene <sup>f</sup>	1504	1667	B	204.1868	C <sub>15</sub> H <sub>24</sub>	-1.0
C245	<b>Bovolide</b>	1504	2065	B	180.1181	C <sub>11</sub> H <sub>16</sub> O <sub>2</sub>	3.1
C246	<i>trans</i> -Calamenene <sup>f</sup>	1511	1738	B	202.1735	C <sub>15</sub> H <sub>22</sub>	1.3
C247	δ-Cadinene <sup>f</sup>	1514	1672	B	204.1881	C <sub>15</sub> H <sub>24</sub>	0.3
C248	Methyl dodecanoate	1516		A	214.1928	C <sub>13</sub> H <sub>26</sub> O <sub>2</sub>	-0.5
C249	Pseudoionone isomer ( <i>E,Z</i> )	1516	1977	A	192.1496	C <sub>13</sub> H <sub>20</sub> O	-1.8
C250	Component C250	1522			210.1569	C <sub>13</sub> H <sub>22</sub> O <sub>2</sub>	-5.1
C251	Component C251	1523			202.1740	C <sub>15</sub> H <sub>22</sub>	1.8
C252	α-Calacorene <sup>f</sup>	1530	1814	B	200.1560	C <sub>15</sub> H <sub>20</sub>	-0.5
C253	α-Agarofuran <sup>f</sup>	1531	1773	B	220.1857	C <sub>15</sub> H <sub>24</sub> O	3.0
C254	Component C254	1537	1827	C	220.1816	C <sub>15</sub> H <sub>24</sub> O	-1.1
C255	Component C255	1540		C	218.1699	C <sub>15</sub> H <sub>22</sub> O	2.8

Table 3.4: *contd.*

No.	Compound name <sup>b</sup>	RI <sup>c</sup> Col A	RI <sup>d</sup> Col B	Identification method <sup>e</sup>	Molecular mass	Elemental composition	Deviation (mDa)
C256	(6 <i>Z</i> ,8 <i>Z</i> )-Megastigma-4,6,8-trien-3-one	1542	2068	B	190.1360	C <sub>13</sub> H <sub>18</sub> O	0.2
C257	Component C257	1543	1856	C	220.1787	C <sub>15</sub> H <sub>24</sub> O	-4.0
C258	Dihydroagarofuran isomer <sup>f</sup>	1545	1723	B	222.1951	C <sub>15</sub> H <sub>26</sub> O	-3.3
C259	( <i>E</i> )-3-Hexenyl benzoate	1546		A	123.0455	C <sub>7</sub> H <sub>7</sub> O <sub>2</sub> [M - C <sub>6</sub> H <sub>9</sub> ]	0.9
C260	( <i>E</i> )-Nerolidol	1554	2001	A	204.1890	C <sub>15</sub> H <sub>24</sub> [M - H <sub>2</sub> O]	1.2
C261	( <i>Z</i> )-3-Hexenyl benzoate	1554	2044	A	123.0435	C <sub>7</sub> H <sub>7</sub> O <sub>2</sub> [M - C <sub>6</sub> H <sub>9</sub> ]	-1.1
C262	(6 <i>Z</i> ,8 <i>E</i> )-Megastigma-4,6,8-trien-3-one	1560	2105	B	190.1347	C <sub>13</sub> H <sub>18</sub> O	-1.1
C263	Hexyl benzoate	1561		A	206.1331	C <sub>13</sub> H <sub>18</sub> O <sub>2</sub>	2.4
C264	Dodecanoic acid	1562		A	200.1784	C <sub>12</sub> H <sub>24</sub> O <sub>2</sub>	0.8
C265	Caryophyllene oxide <sup>f</sup>	1568		A	220.1856	C <sub>15</sub> H <sub>24</sub> O	2.9
C266	Pseudoionone isomer ( <i>E,E</i> )	1569	2069	A	192.1496	C <sub>13</sub> H <sub>20</sub> O	-1.8
C267	Component C267 (a sesquiterpene alcohol)	1581		C	220.1806	C <sub>15</sub> H <sub>24</sub> O	-2.1
C268	Component C268 (gleenol-type comp.)	1583		C	220.1828	C <sub>15</sub> H <sub>24</sub> O	0.1
C269	<b>Component C269</b> (bergamotol-type comp.)	1586		C	220.1837	C <sub>15</sub> H <sub>24</sub> O	1.0
C270	1-[2-(Isobutyryloxy)-1-methylethyl]-2,2-dimethylpropyl 2-methylpropanoate <sup>f</sup>	1586	1821	B	243.1606	C <sub>13</sub> H <sub>23</sub> O <sub>4</sub> [M - C <sub>3</sub> H <sub>7</sub> ]	1.0
C271	<b>(6<i>E</i>,8<i>Z</i>)-Megastigma-4,6,8-trien-3-one</b>	1591	2168	B	190.1369	C <sub>13</sub> H <sub>18</sub> O	1.1
C272	<b>Geranyl 2-methylbutanoate<sup>f</sup></b>	1591		B	136.1203	C <sub>10</sub> H <sub>16</sub> [M - C <sub>5</sub> H <sub>9</sub> O <sub>2</sub> ]	-4.9
C273	1-(2,3,6-Trimethylphenyl)-3-buten-2-one	1592		B	188.1234	C <sub>13</sub> H <sub>16</sub> O	3.3
C274	β-Oplopenone <sup>f</sup>	1592		B	220.1789	C <sub>15</sub> H <sub>24</sub> O	-3.8
C275	Component C275 (cuparene-type comp.)	1593		C	202.1702	C <sub>15</sub> H <sub>22</sub>	-2.0
C276	Hexadecane	1598	1604	A	226.2653	C <sub>16</sub> H <sub>34</sub>	-0.8
C277	<b>(6<i>E</i>,8<i>E</i>)-Megastigma-4,6,8-trien-3-one</b>	1604	2194	B	190.1355	C <sub>13</sub> H <sub>18</sub> O	-0.3
C278	<b>10-<i>epi</i>-γ-Eudesmol<sup>f</sup></b>	1605	2009	B	222.1977	C <sub>15</sub> H <sub>26</sub> O	-0.7
C279	Component C279 (calamenene-type comp.)	1605		C	202.1728	C <sub>15</sub> H <sub>22</sub>	0.6
C280	Component C280	1607		C	200.1551	C <sub>15</sub> H <sub>20</sub>	-1.4
C281	Component C281	1607			220.1863	C <sub>15</sub> H <sub>24</sub> O	3.6
C282	Component C282	1612		C	204.1883	C <sub>15</sub> H <sub>24</sub>	0.5
C283	γ-Eudesmol <sup>f</sup>	1617		B	222.1980	C <sub>15</sub> H <sub>26</sub> O	-0.4
C284	<b><i>epi</i>-α-Cadinol<sup>f</sup></b>	1628		B	222.1972	C <sub>15</sub> H <sub>26</sub> O	-1.2
C285	<b><i>epi</i>-α-Muurolol<sup>f</sup></b>	1629		B	222.1957	C <sub>15</sub> H <sub>26</sub> O	-2.7
C286	β-Eudesmol <sup>f</sup>	1634		A	-		

Table 3.4: *contd.*

No.	Compound name <sup>b</sup>	RI <sup>c</sup> Col A	RI <sup>d</sup> Col B	Identification method <sup>e</sup>	Molecular mass	Elemental composition	Deviation (mDa)
C287	$\alpha$ -Eudesmol <sup>f</sup>	1638		B	–		
C288	$\alpha$ -Cadinol <sup>f</sup>	1641		B	222.1954	C <sub>15</sub> H <sub>26</sub> O	–3.0
C289	7- <i>epi</i> - $\alpha$ -Eudesmol <sup>f</sup>	1644		B	222.1932	C <sub>15</sub> H <sub>26</sub> O	–5.2
C290	<b>Cadalene</b>	1659	2127	B	198.1388	C <sub>15</sub> H <sub>18</sub>	–2.1
C291	3,7,7-Trimethyl-1-penta-1,3-dienyl-2-oxabicyclo[3.2.0]hept-3-ene isomer 1 <sup>f</sup>	1661	2135	B	204.1536	C <sub>14</sub> H <sub>20</sub> O	2.2
C292	<i>epi</i> - $\alpha$ -Bisabolol <sup>f</sup>	1671		B	204.1884	C <sub>15</sub> H <sub>24</sub> [M – H <sub>2</sub> O]	0.6
C293	$\alpha$ -Bisabolol <sup>f</sup>	1673		B	204.1893	C <sub>15</sub> H <sub>24</sub> [M – H <sub>2</sub> O]	1.5
C294	3,7,7-Trimethyl-1-penta-1,3-dienyl-2-oxabicyclo[3.2.0]hept-3-ene isomer 2 <sup>f</sup>	1680	2168	B	204.1539	C <sub>14</sub> H <sub>20</sub> O	2.5
C295	<b>(7E)-Megastigma-5,7,9-trien-4-one</b>	1686		B	190.1342	C <sub>13</sub> H <sub>18</sub> O	–1.6
C296	Heptadecane	1700	1701	A	240.2846	C <sub>17</sub> H <sub>36</sub>	2.9
C297	Octadecane	1798	1802	A	254.2980	C <sub>18</sub> H <sub>38</sub>	0.6
C298	Isopropyl myristate	1817	2029	A	270.2528	C <sub>17</sub> H <sub>34</sub> O <sub>2</sub>	–3.1
C299	Hexahydrofarnesylacetone <sup>f</sup>	1834	2103	A	268.2732	C <sub>18</sub> H <sub>36</sub> O	–3.4

<sup>a</sup> Odour-active components are discussed in Chapter 4.

<sup>b</sup> In order of elution from apolar PS-089 column (DB-5 equivalent).

<sup>c</sup> RI, relative to C<sub>5</sub>–C<sub>18</sub> *n*-alkanes, on PS-089 column (DB-5 equivalent).

<sup>d</sup> RI, relative to C<sub>5</sub>–C<sub>18</sub> *n*-alkanes, on AT-1000 column (FFAP equivalent).

<sup>e</sup> Identification: A, comparison of mass spectrum and RI with those of an authentic synthetic standard; B, comparison of mass spectrum and RI with published MS and RI data; C, see § 3.2.17 for structure proposals.

<sup>f</sup> Stereochemistry not determined (see Table 3.5 for additional information on certain compounds).

Table 3.5: Enantiomeric composition of chiral components of the headspace volatiles of honeybush tea as determined by enantioselective GC-MS analysis

Component <sup>a</sup>	Compound	Enantiomeric ratio <sup>b</sup>
C1	1-Penten-3-ol (column C <sup>c</sup> )	Racemic (n=1)
C13	2-Methylbutanoic acid (column C)	0S:100R (n=5)
C23	α-Pinene (column C)	82(1S,5S):18(1R, 5R) (n=1)
C24	Camphene (column C)	15R:85S (n=1)
C29	2,2,6-Trimethyl-6-vinyltetrahydropyran (column C)	57:43 (n=2) <sup>d</sup>
C30	β-Pinene	– <sup>e</sup>
C31	1-Octen-3-ol (column D <sup>f</sup> )	38S:62R (n=3)
C36 & C45	Dehydroxylinalool oxide (furanoid) (column C)	35:21:20:20 (n=1) <sup>d</sup>
C42	α-Phellandrene (column C)	20R:80S (n=1)
C49	2-Hexen-4-olide (column D)	Racemic (n=3)
C51	2,2,6-Trimethylcyclohexanone (column C)	Racemic (n=2)
C52	Limonene (column C)	26S:74R (n=4)
C54	Hexan-4-olide (column D)	52R:48S (n=3)
C57	2-Methyl-6-methylene-2-octene	– <sup>e</sup>
C62	<i>trans</i> -Arbusculone	– <sup>d</sup>
C64 & C68	Linalool oxide (furanoid) (column C)	23(2R5R):39(2R5S):20(2S5S): 18(2S5R) (n=3)
C76	Linalool (column D)	53R:47S (n=4)
C78	Hotrienol (column C)	38R:62S (n=1)
C83 & C91	(-) Rose oxide (column D)	70(2S4R):30(2R4R) (n=2)
C84	3-Thujanone	– <sup>e</sup>
C85	α-Fenchol	– <sup>e</sup>
C86 & C96	<i>cis</i> - and <i>trans</i> -2- <i>p</i> -Menthen-1-ol	– <sup>e</sup>
C89	4-Acetyl-1-methylcyclohexene (column C)	40:60 (n=2) <sup>d</sup>
C94	Dihydrolinalool (column D)	20:80 (n=1) <sup>d</sup>
C97 & C110	Lilac aldehyde (1 and 2)	– <sup>d</sup>
C98	Camphene hydrate (column C)	– <sup>d</sup>
C99	1-(1,4-Dimethyl-3-cyclohexen-1-yl)ethanone	– <sup>e</sup>
C104	2,2,6-Trimethyl-1,4-cyclohexanedione (column D)	Racemic (n=1)
C105	Isoborneol (column C)	– <sup>d</sup>
C106	Nerol oxide	– <sup>g</sup>
C111	2-Chloro-1,7,7-trimethylbicyclo[2.2.1]heptane	– <sup>e</sup>
C112	Borneol (column C)	0(1S2R4S):100(1R2S4R) (n=2)
C115 & C116	Pyranoid linalool oxide (column C)	20(2S5R):22(2S5S):31(2R5S): 27(2R5R) (n=1)
C118	Terpinen-4-ol (column D)	40R:60S (n=4)
C119 & C131	Dill ether (1 and 2)	– <sup>d</sup>
C121	α-Terpineol (column D)	38S:62R (n=7)
C137	β-Citronellol (column D)	0S:100R (n=2)
C138	( <i>Z</i> )-3-Hexenyl 2-methylbutanoate (column C, D)	– <sup>d</sup>
C143	Carvenone (column D)	– <sup>d</sup>
C152	Octan-5-olide (column D)	0S:100R (n=5)
C157	Vitispirane (column D)	– <sup>d</sup>
C160	Limonen-10-ol	– <sup>e</sup>
C163 & C173	Theaspirane (isomers 1 and 2) (column C)	46:15:11:27 <sup>d</sup> (n=1)



Table 3.5: *contd.*

Component <sup>a</sup>	Compound	Enantiomeric ratio <sup>b</sup>
C176, C182 & C184	2,5-Epoxymegastigma-6,8-diene	— <sup>d</sup>
C186	Nonan-4-olide (column D)	51 <i>R</i> :49 <i>S</i> (n=2)
C188	α-Terpinyl acetate	— <sup>e</sup>
C189	1,5,8-Trimethyl-1,2-dihydronaphthalene (column C, D)	— <sup>d</sup>
C190	1-(2-Hydroxy-1-methylethyl)-2,2-dimethylpropyl 2-methylpropanoate (column C, D)	— <sup>d</sup>
C194	α-Cubebene (column C) 3-Hydroxy-2,4,4-trimethylpentyl 2-methylpropanoate (column C, D)	— <sup>d</sup>
C201	α-Ylangene (column C)	— <sup>d</sup>
C200	2,3-Dehydro-α-ionone (column C, D)	— <sup>d</sup>
C203	α-Copaene (column C)	— <sup>d</sup>
C205	β-Bourbonene	— <sup>d</sup>
C208	6,10-Dimethyl-2-undecanone	— <sup>g</sup>
C209	( <i>E</i> )-Caryophyllene (column C)	— <sup>d</sup>
C216	α-Ionone (column D)	100 <i>R</i> :0 <i>S</i> (n=3)
C217	3,4-Dehydro-γ-ionone (column C, D)	— <sup>d</sup>
C218	2,3-Dehydro-γ-ionone (column C)	33:67 (n=1) <sup>d</sup>
C222	Cabreuva oxide B (column C, D)	— <sup>d</sup>
C225	9- <i>epi</i> -( <i>E</i> )-Caryophyllene (column C, D)	— <sup>d</sup>
C226	Oxo-edulan (column C, D)	— <sup>d</sup>
C227	( <i>Z</i> )-7-Decen-5-olide (column D)	0 <i>R</i> :100 <i>S</i> (n=4)
C229	Cabreuva oxide D (column C, D)	— <sup>d</sup>
C231	5,6-Epoxy-β-ionone (column D)	Racemic (n=4)
C232	Decan-5-olide (column D)	0 <i>S</i> :100 <i>R</i> (n=5)
C233	β-Selinene	— <sup>e</sup>
C235	Calamenene-1,11-epoxide (column C, D)	— <sup>d</sup>
C236	β-Dihydroagarofuran (column C, D)	— <sup>d</sup>
C239	α-Muurolene (column C)	— <sup>d</sup>
C240	Dihydroactinidiolide (column D)	52 <i>R</i> :48 <i>S</i> (n=5)
C243	γ-Cadinene (column C, D)	— <sup>d</sup>
C244	<i>trans</i> -Calamenene (column C, D)	— <sup>d</sup>
C246	δ-Cadinene (column C, D)	— <sup>d</sup>
C247	α-Calacorene (column C, D)	— <sup>d</sup>
C252	α-Agarofuran (column C, D)	— <sup>d</sup>
C253	Dihydroagarofuran isomer (column C, D)	— <sup>d</sup>
C258	( <i>E</i> )-Nerolidol (column C)	41 <i>R</i> :59 <i>S</i> (n=2)
C260	Caryophyllene oxide (column C)	— <sup>d</sup>
C265	1-[2-(Isobutyryloxy)-1-methylethyl]-2,2-dimethylpropyl 2-methylpropanoate (column C)	— <sup>d</sup>
C270	Geranyl 2-methylbutanoate	— <sup>e</sup>
C272	β-Oplopenone	— <sup>e</sup>
C274	10- <i>epi</i> -γ-Eudesmol (column C, D)	— <sup>d</sup>
C278	γ-Eudesmol	— <sup>e</sup>
C283	<i>epi</i> -α-Cadinol	— <sup>e</sup>
C284	<i>epi</i> -α-Muurolol	— <sup>e</sup>
C285	β-Eudesmol	— <sup>e</sup>
C286	α-Eudesmol	— <sup>e</sup>
C287	α-Cadinol	— <sup>e</sup>
C288		

Table 3.5: *contd.*

Component <sup>a</sup>	Compound	Enantiomeric ratio <sup>b</sup>
C289	7- <i>epi</i> - $\alpha$ -Eudesmol	— <sup>e</sup>
C291 & C294	3,7,7-Trimethyl-1-penta-1,3-dienyl-2-oxabicyclo-[3.2.0]hept-3-ene (1 and 2)	— <sup>e</sup>
C292	<i>epi</i> - $\alpha$ -Bisabolol	— <sup>e</sup>
C293	$\alpha$ -Bisabolol	— <sup>e</sup>
C299	Hexahydrofarnesylacetone	— <sup>g</sup>

<sup>a</sup> In order of elution from PS-089 column (DB-5 equivalent).

<sup>b</sup> Ratios determined by integration of the base peaks in selected ion plots of the individual enantiomers. Enantiomers given in order of their elution from the respective enantioselective columns.

<sup>c</sup> Column C: OV-1701-OH containing 10% heptakis(2,3-di-*O*-methyl-6-*O*-*tert*-butyldimethylsilyl)- $\beta$ -cyclodextrin.

<sup>d</sup> Absolute configuration not determined; no information in the literature on enantiomeric resolution and elution order; no reference material and or pure enantiomers available.

<sup>e</sup> Compound not detected in enantioselective analysis.

<sup>f</sup> Column D: OV-1701-OH containing 10% heptakis(2,3-di-*O*-acetyl-6-*O*-*tert*-butyldimethylsilyl)- $\beta$ -cyclodextrin.

<sup>g</sup> Enantiomers not resolved on enantioselective columns C or D.

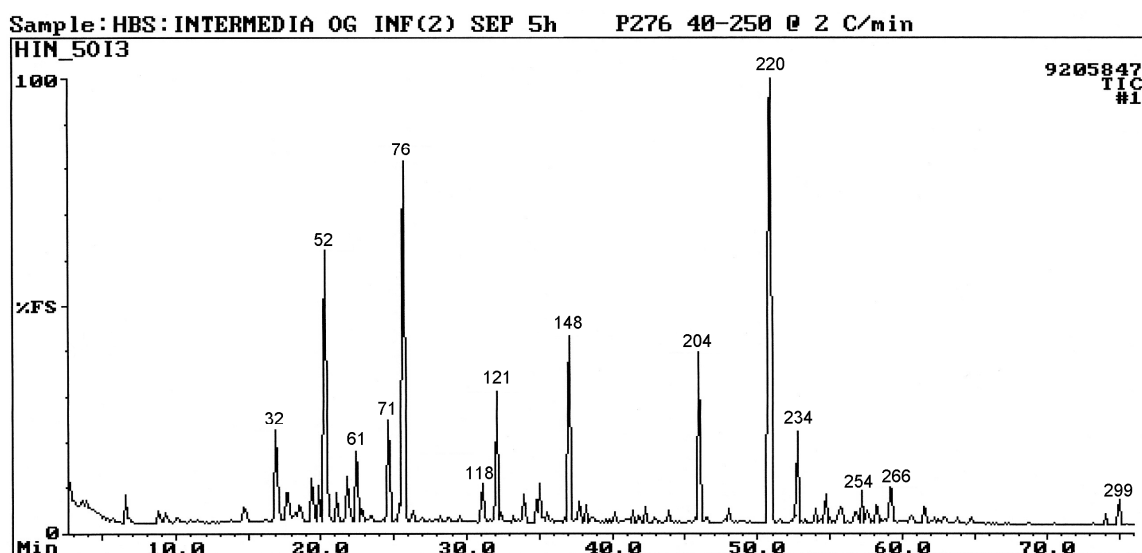


Fig. 3.1: TIC obtained by HS-SEP-GC-MS analysis of unfermented honeybush.

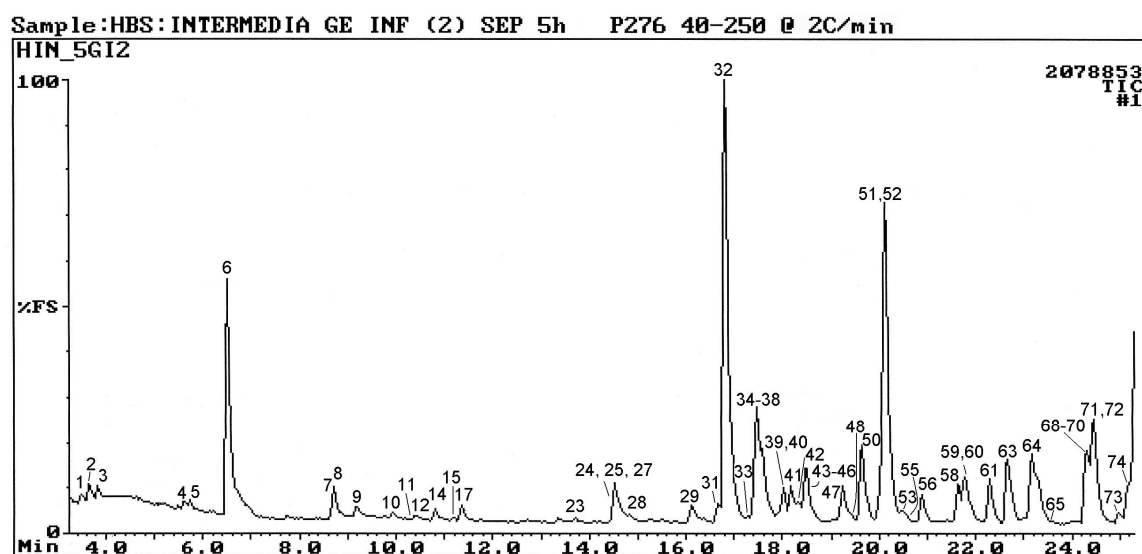


Fig. 3.2a: TIC obtained by HS-SEP-GC-MS analysis of fermented honeybush (0–25 min).

Sample:HBS:INTERMEDIA GE INF (2) SEP 5h P276 40-250 @ 2C/min

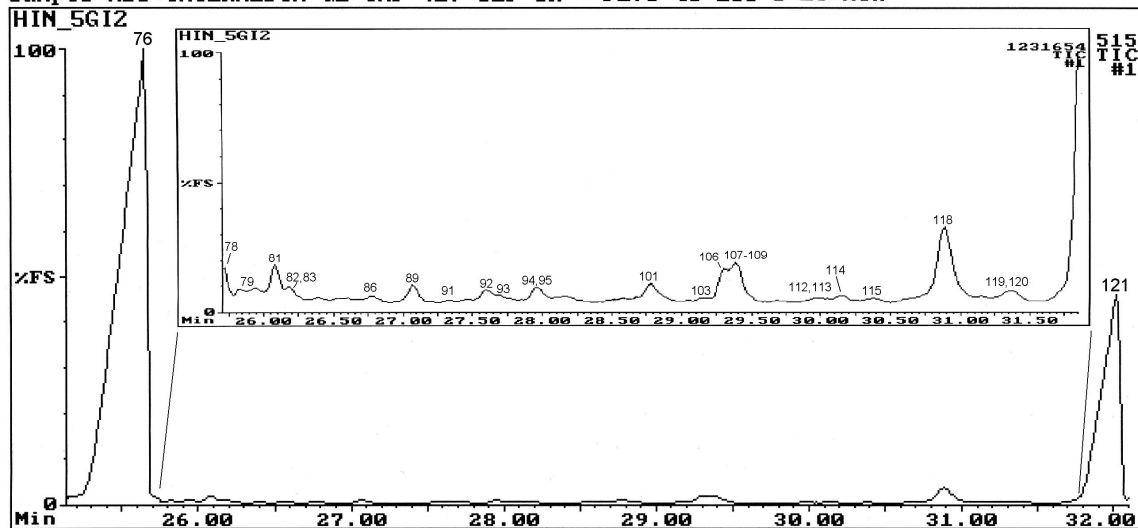


Fig. 3.2b: TIC obtained by HS-SEP-GC-MS analysis of fermented honeybush (25–32 min).

Sample:HBS:INTERMEDIA GE INF (2) SEP 5h P276 40-250 @ 2C/min

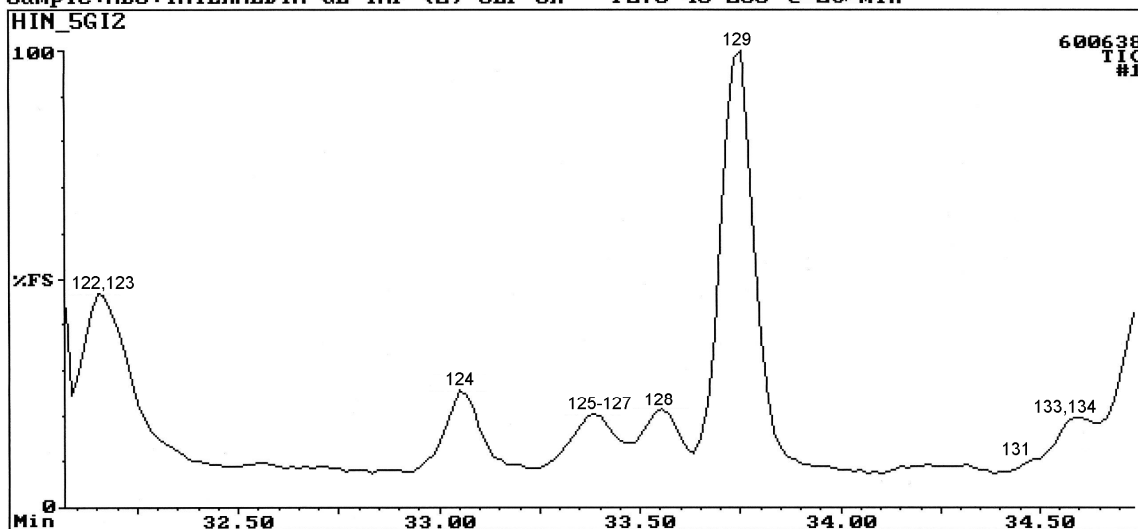


Fig. 3.2c: TIC obtained by HS-SEP-GC-MS analysis of fermented honeybush (32–34.8 min).

Sample:HBS:INTERMEDIA GE INF (2) SEP 5h P276 40-250 @ 2C/min

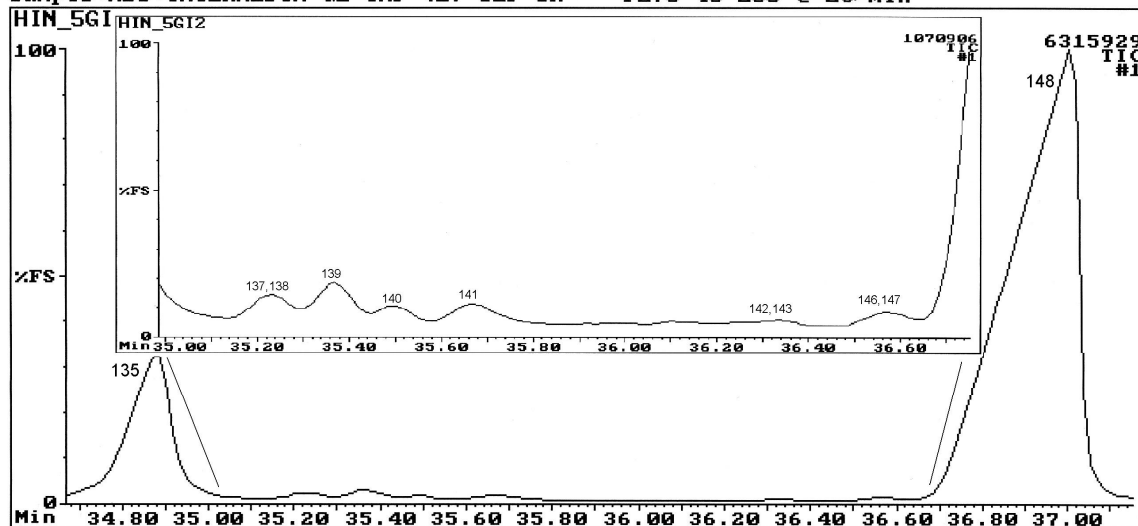


Fig. 3.2d: TIC obtained by HS-SEP-GC-MS analysis of fermented honeybush (34.8–37 min).

Sample:HBS:INTERMEDIA GE INF (2) SEP 5h P276 40-250 @ 2C/min

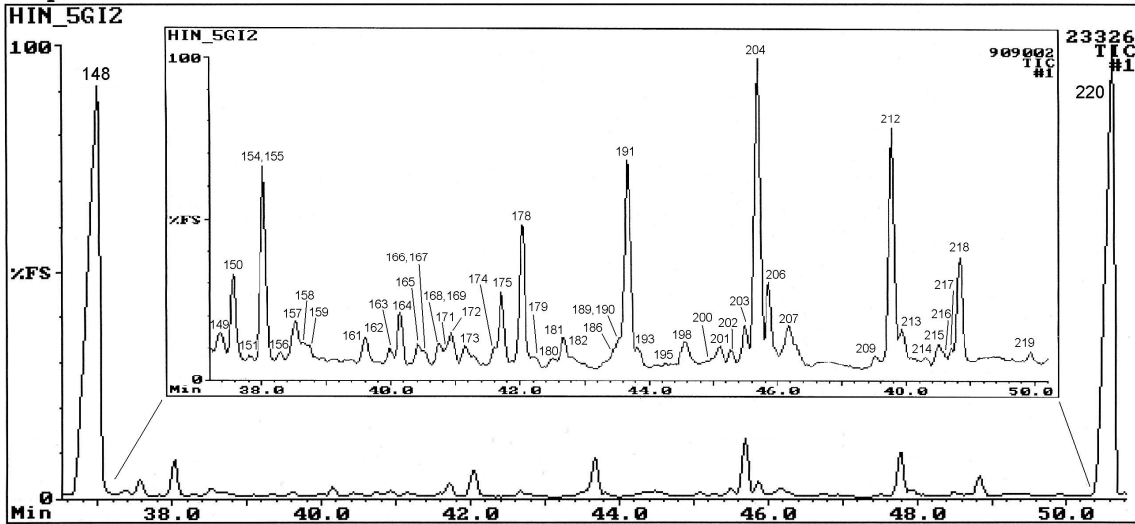


Fig. 3.2e: TIC obtained by HS-SEP-GC-MS analysis of fermented honeybush (37–51 min).

Sample:HBS:INTERMEDIA GE INF (2) SEP 5h P276 40-250 @ 2C/min

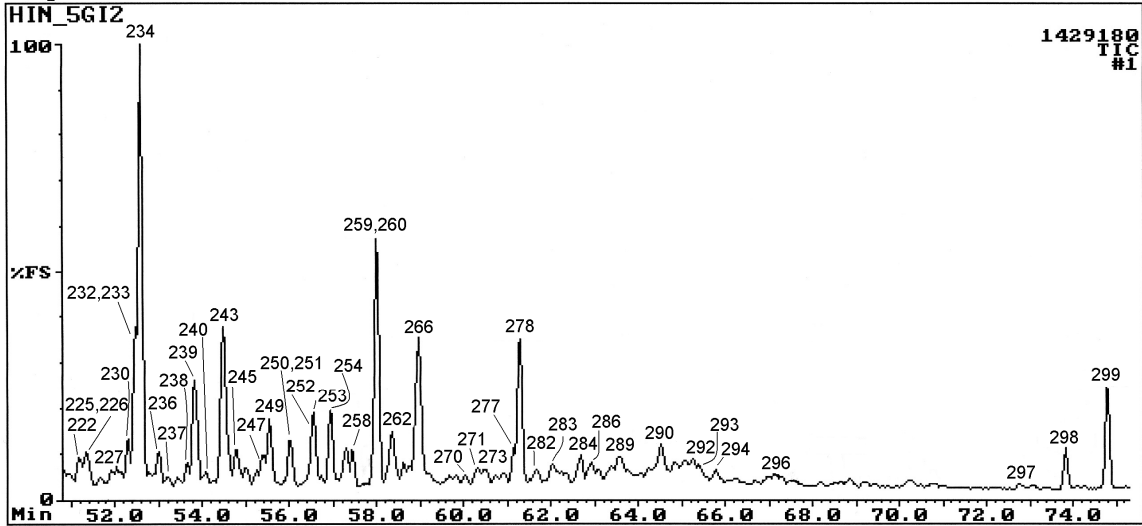


Fig. 3.2f: TIC obtained by HS-SEP-GC-MS analysis of fermented honeybush (51–75 min).

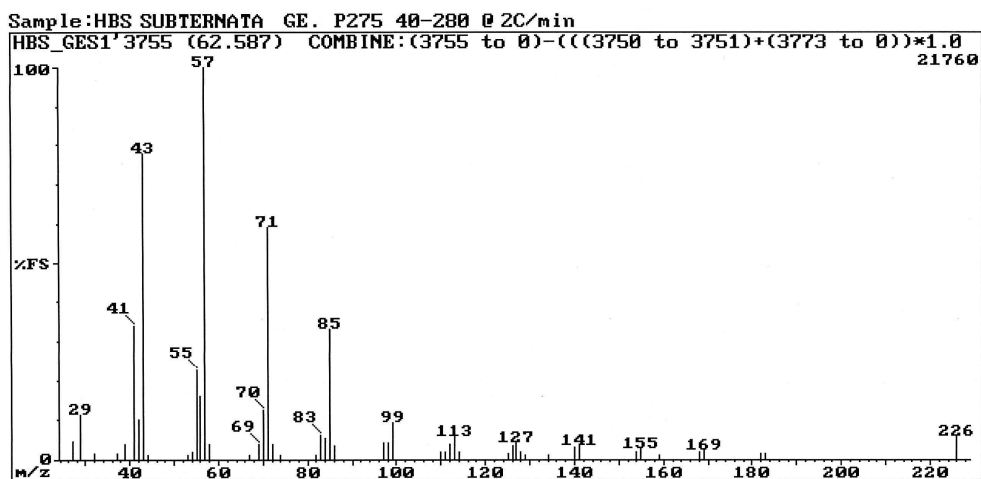


Fig. 3.3: EI mass spectrum of hexadecane (**C276**).

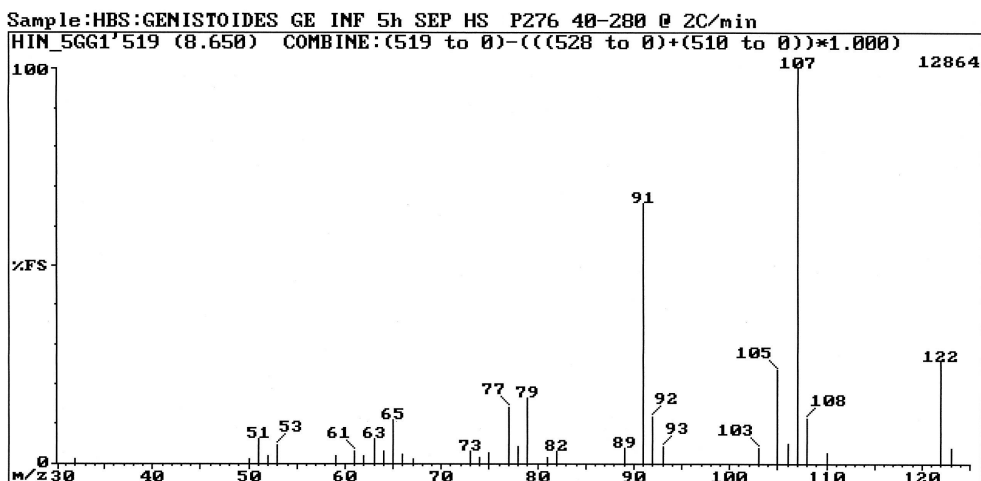


Fig. 3.4: EI mass spectrum of 2-ethyl-5,5-dimethyl-1,3-cyclopentadiene (**C7**).

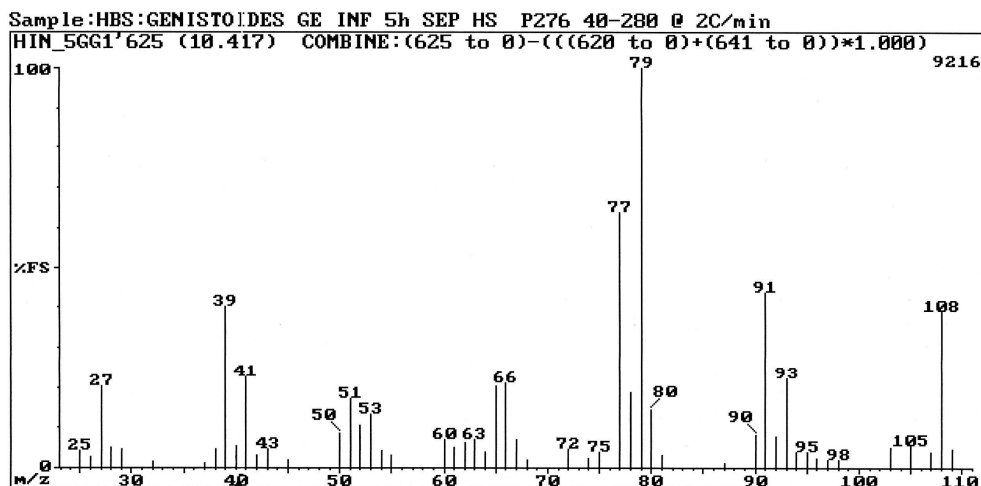


Fig. 3.5: EI mass spectrum of 1,3,6-octatriene (**C12**).

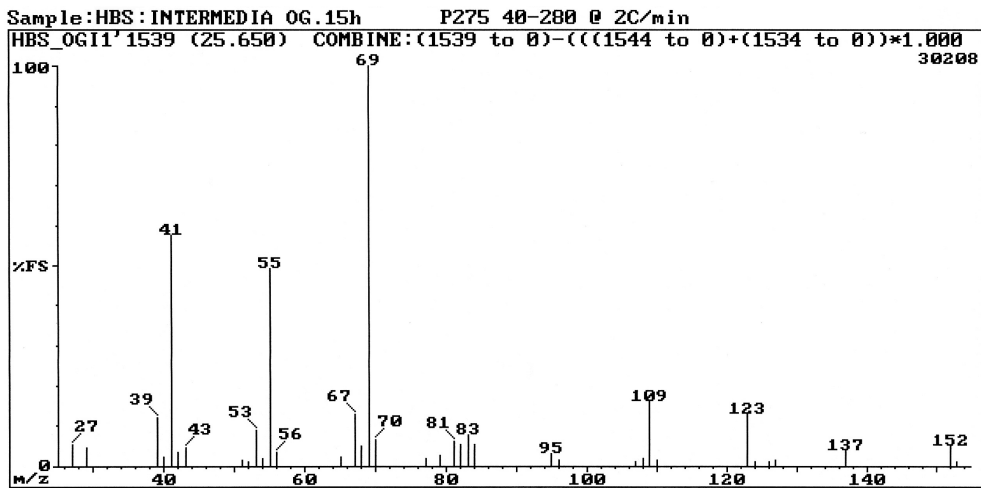


Fig. 3.6: EI mass spectrum of 2,8-dimethyl-2,6-nonadiene (C67).

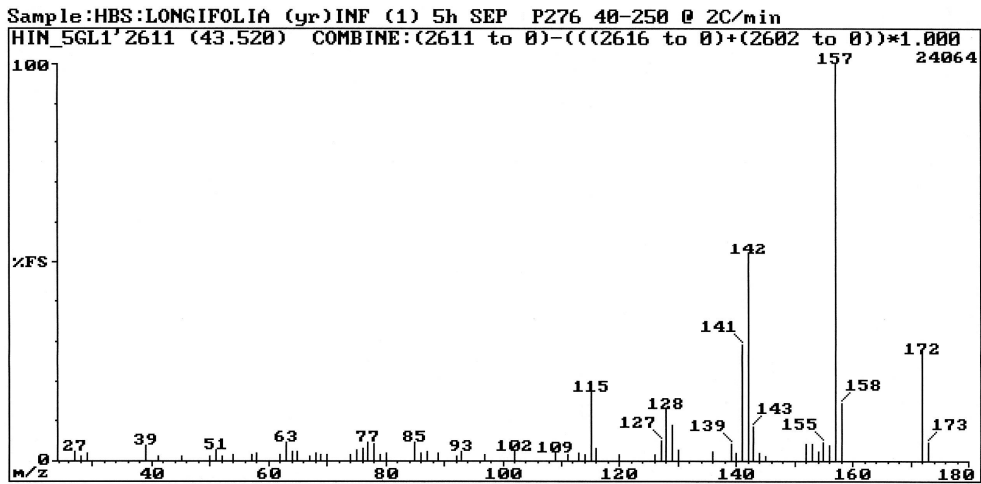


Fig. 3.7: EI mass spectrum of 1,5,8-trimethyl-1,2-dihydronaphthalene (C189).

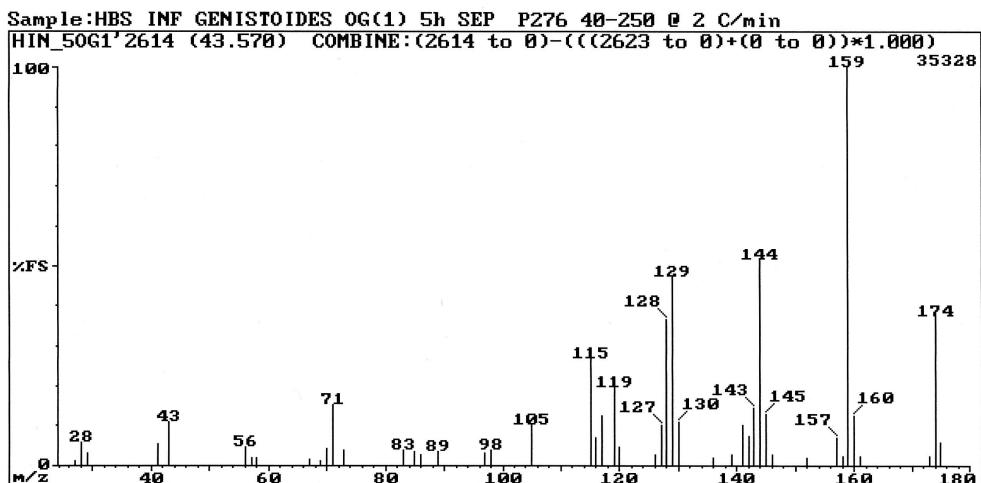


Fig. 3.8: EI mass spectrum of 2,3-dihydro-1,1,5,6-tetramethyl-1H-indene (C192).

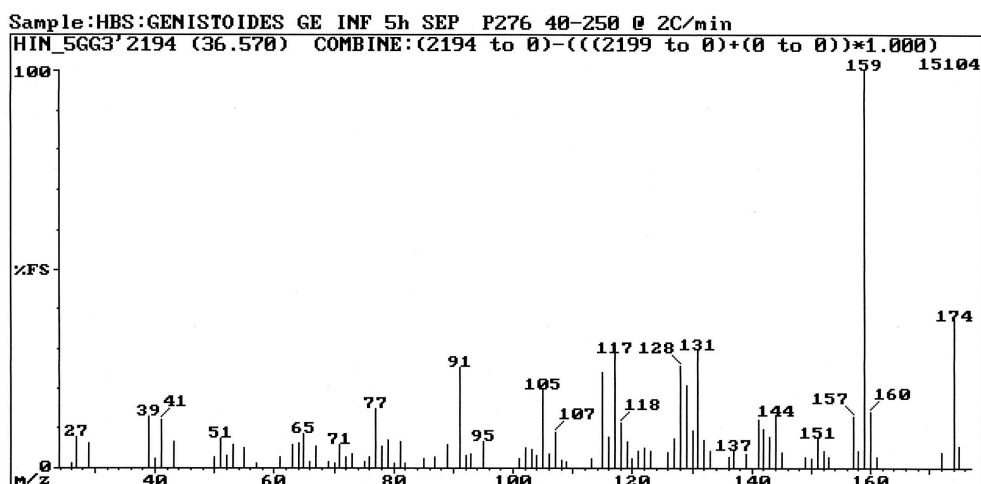


Fig. 3.9: EI mass spectrum of 2-(2-butenyl)-1,3,5-trimethylbenzene (**C147**).

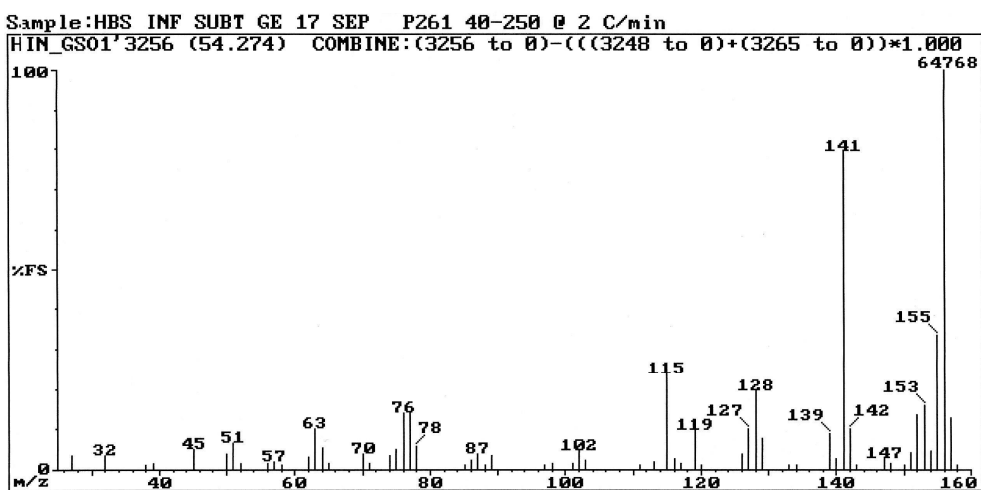


Fig. 3.10: EI mass spectrum of 1,3-dimethylnaphthalene (**C213**).

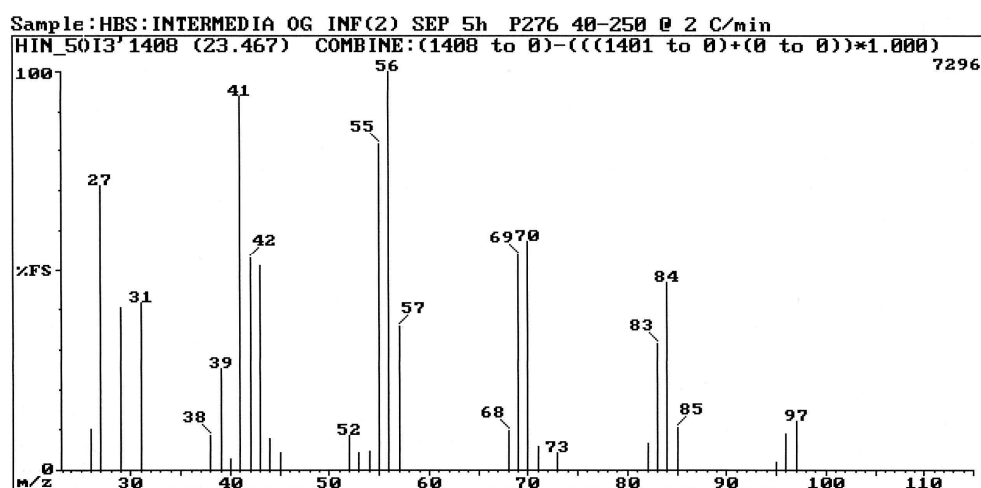


Fig. 3.11: EI mass spectrum of 1-octanol (**C65**).

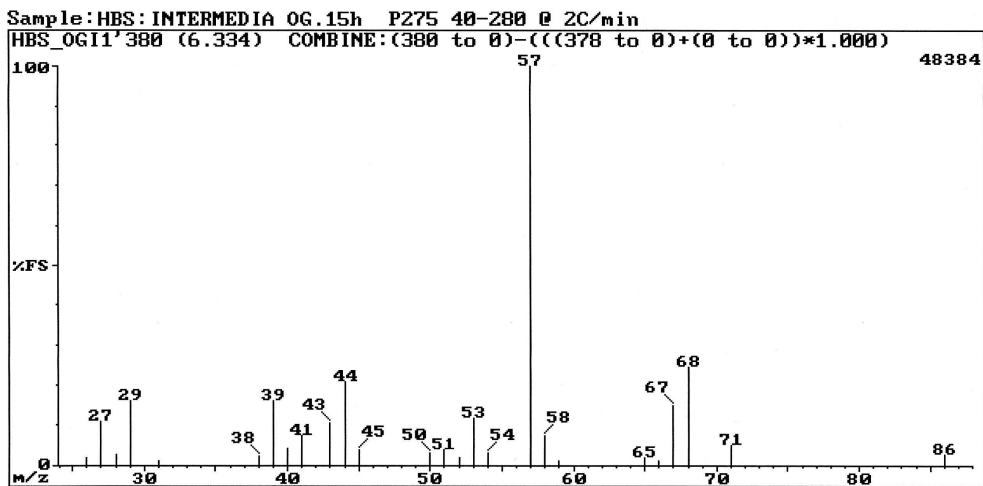


Fig. 3.12: El mass spectrum of (Z)-2-penten-1-ol (C5).

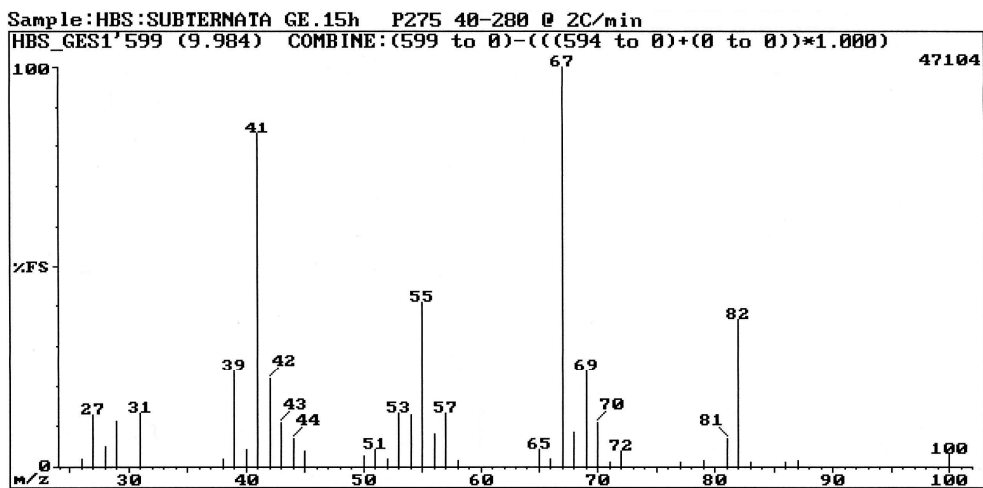


Fig. 3.13: El mass spectrum of (Z)-3-hexen-1-ol (C9).

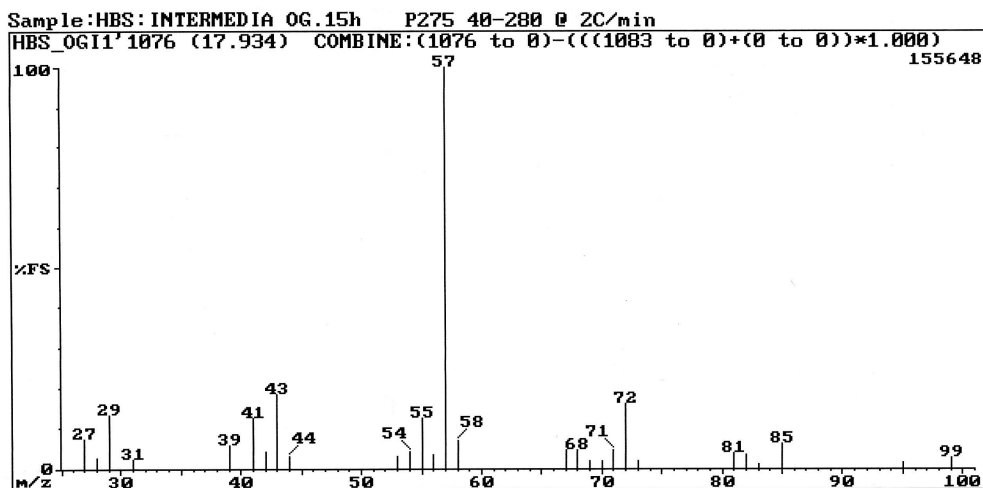


Fig. 3.14: El mass spectrum of 1-octen-3-ol (C31).



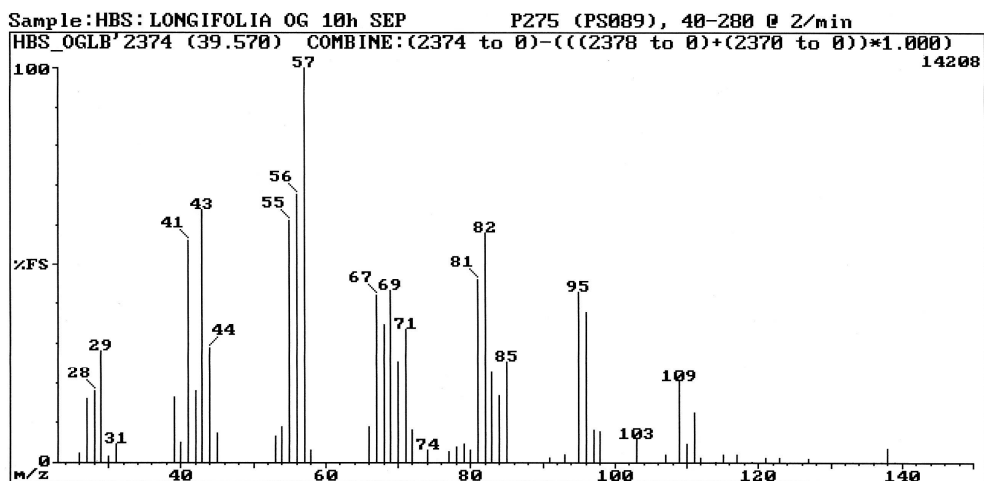


Fig. 3.15: El mass spectrum of (*E*)-2-decen-1-ol (C153).

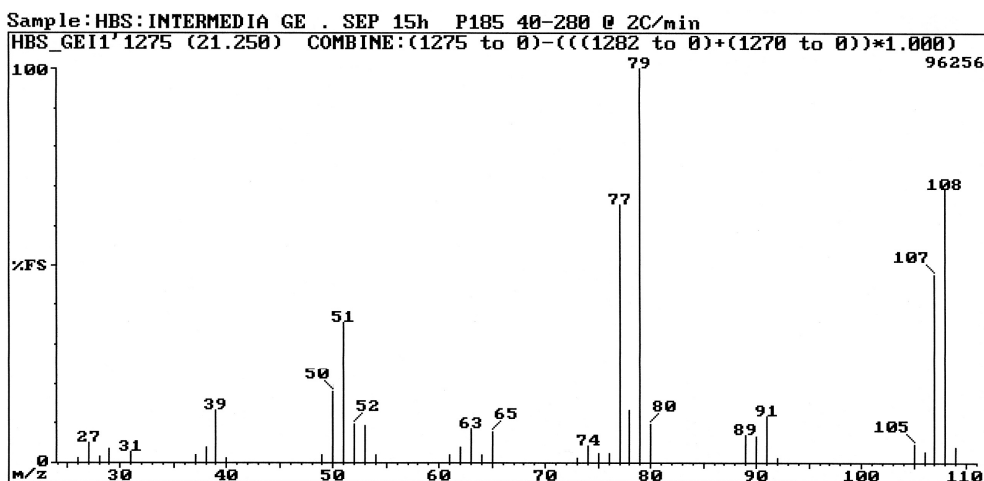


Fig. 3.16: El mass spectrum of benzyl alcohol (C55).

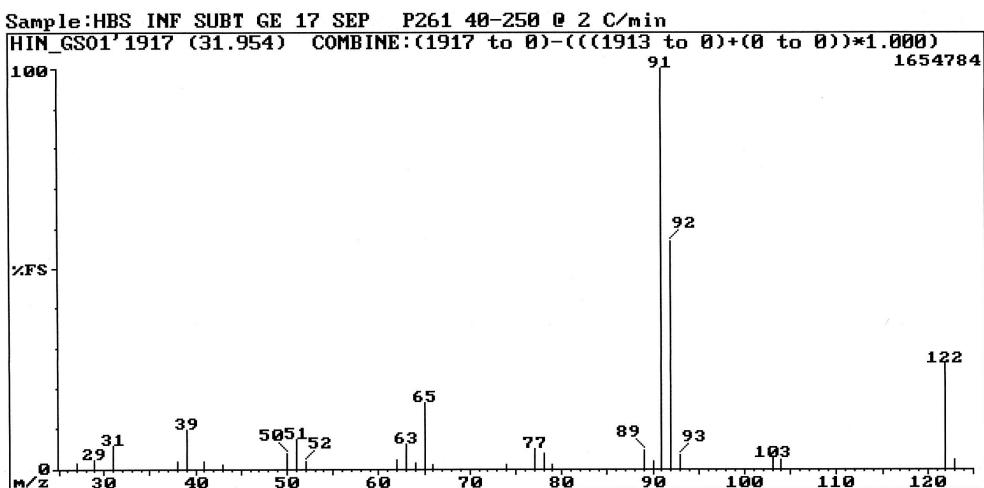


Fig. 3.17: El mass spectrum of 2-phenylethanol (C79).

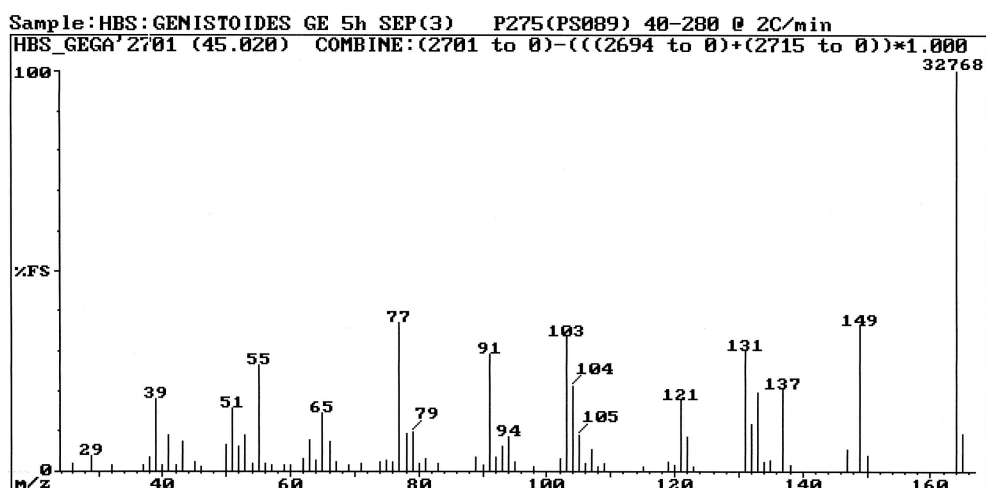


Fig. 3.18: El mass spectrum of eugenol (C191).

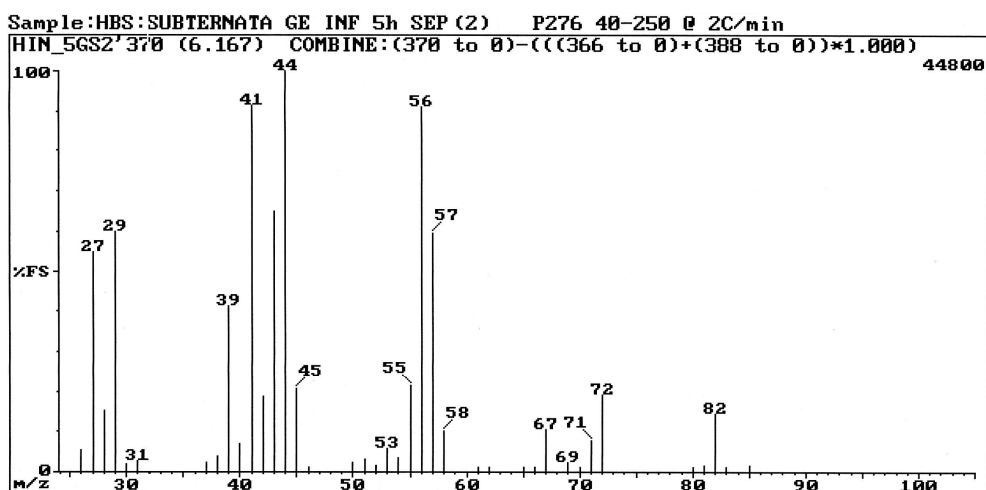


Fig. 3.19: El mass spectrum of hexanal (C6).

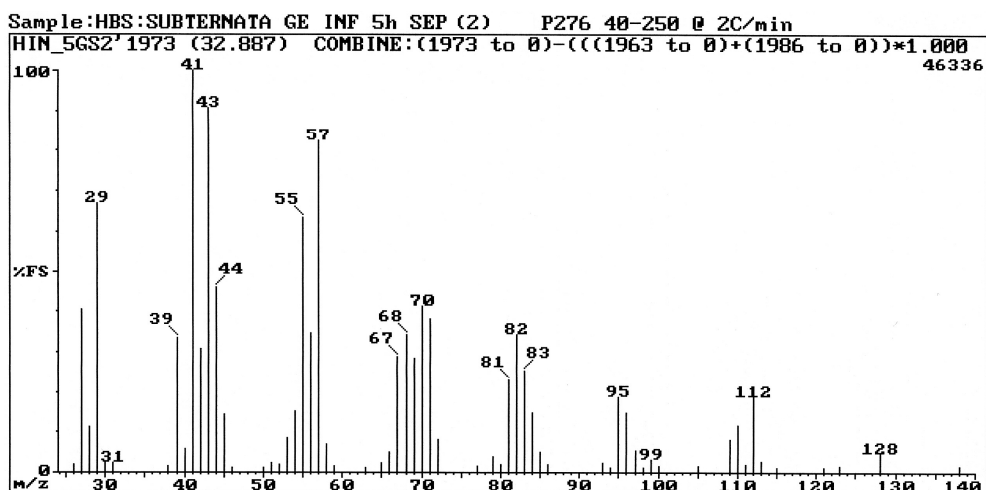


Fig. 3.20: El mass spectrum of decanal (C124).

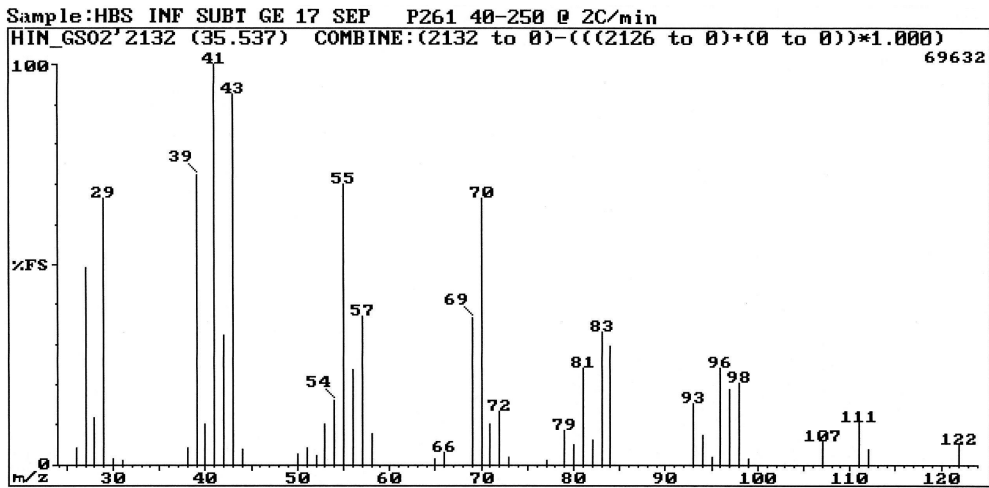


Fig. 3.21: EI mass spectrum of (*E*)-2-nonenal (**C108**).

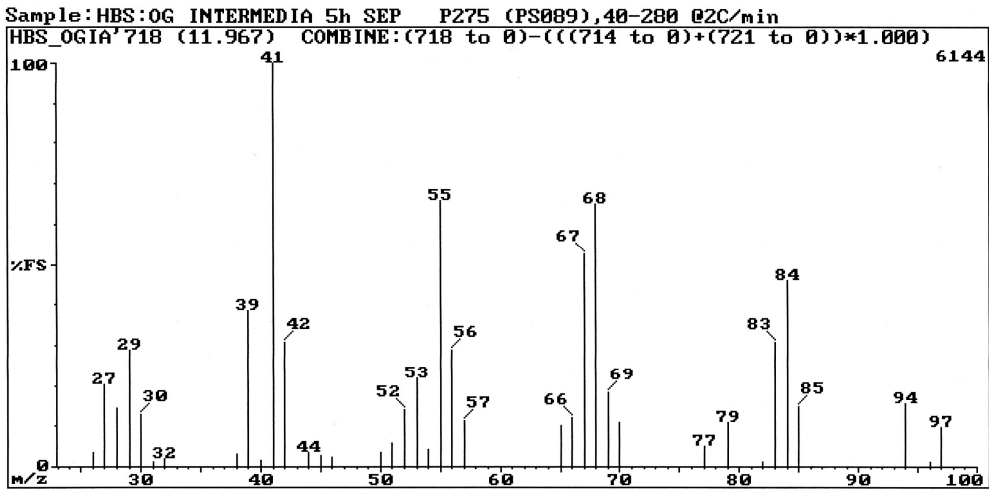


Fig. 3.22: EI mass spectrum of (*Z*)-4-heptenal (**C15**).

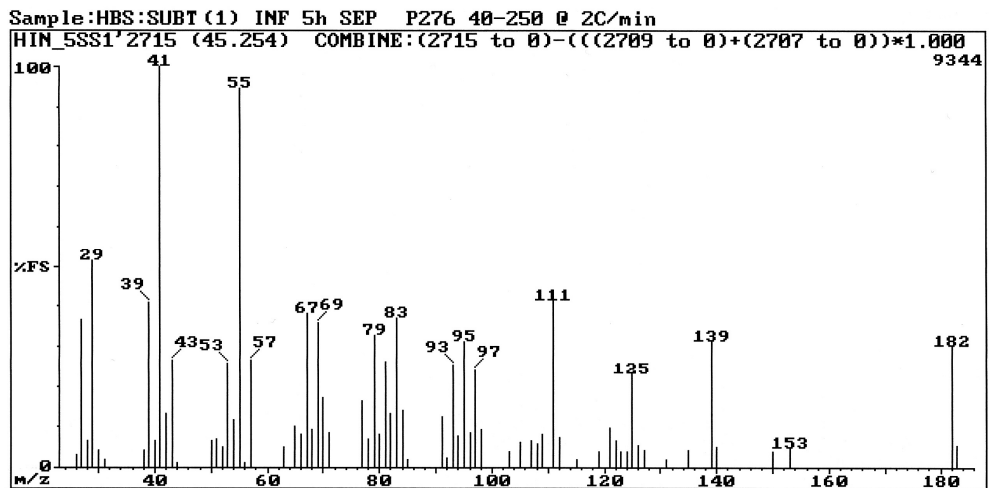


Fig. 3.23: EI mass spectrum of 2-butyl-2-octenal (**C202**).

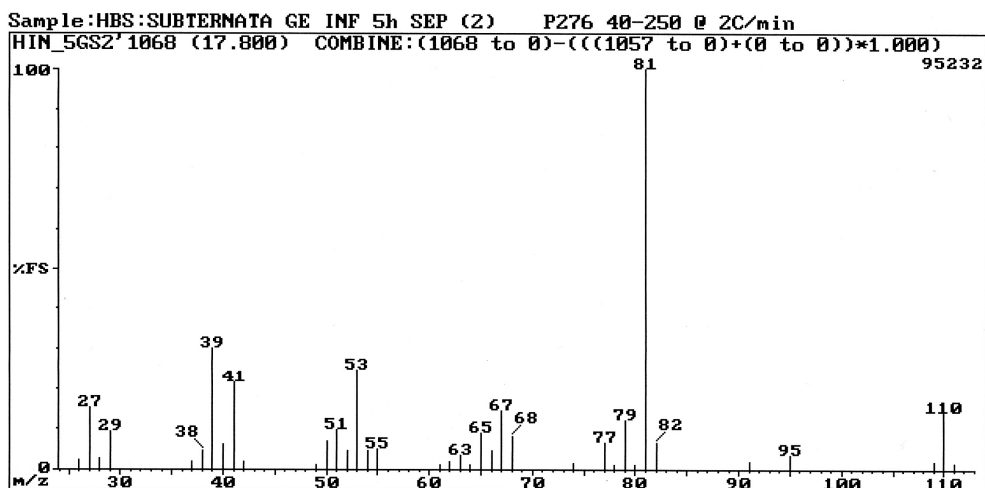


Fig. 3.24: EI mass spectrum of (*E,E*)-2,4-heptadienal (**C41**).

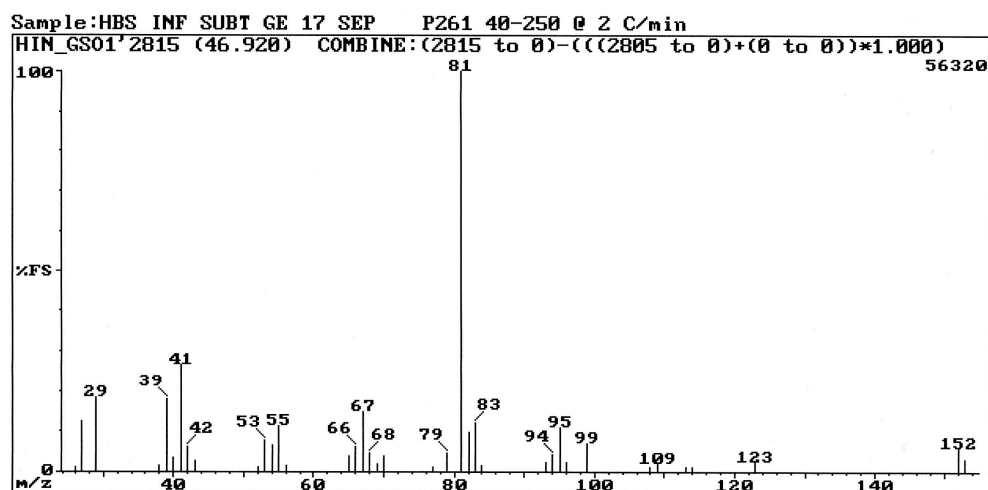


Fig. 3.25: EI mass spectrum of (*E,E*)-2,4-decadienal (**C171**).

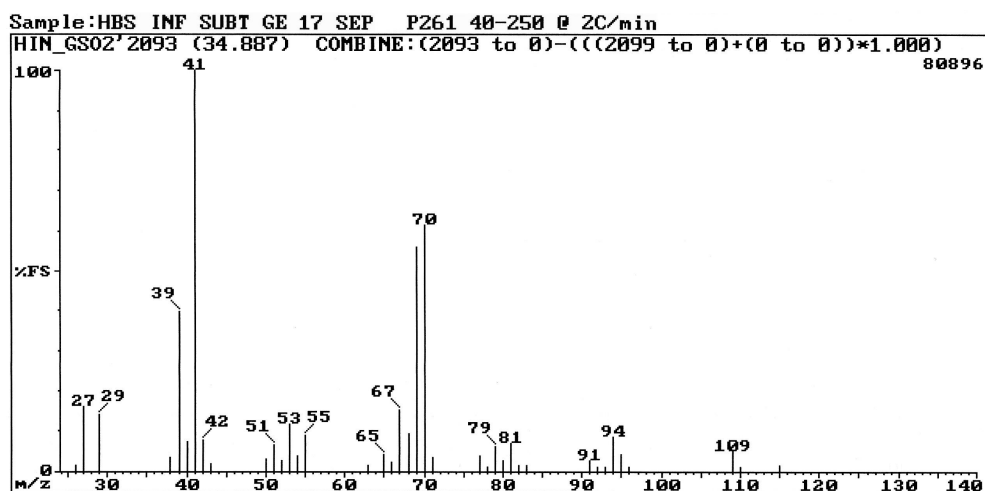


Fig. 3.26: EI mass spectrum of (*E,Z*)-2,6-nonadienal (**C101**).

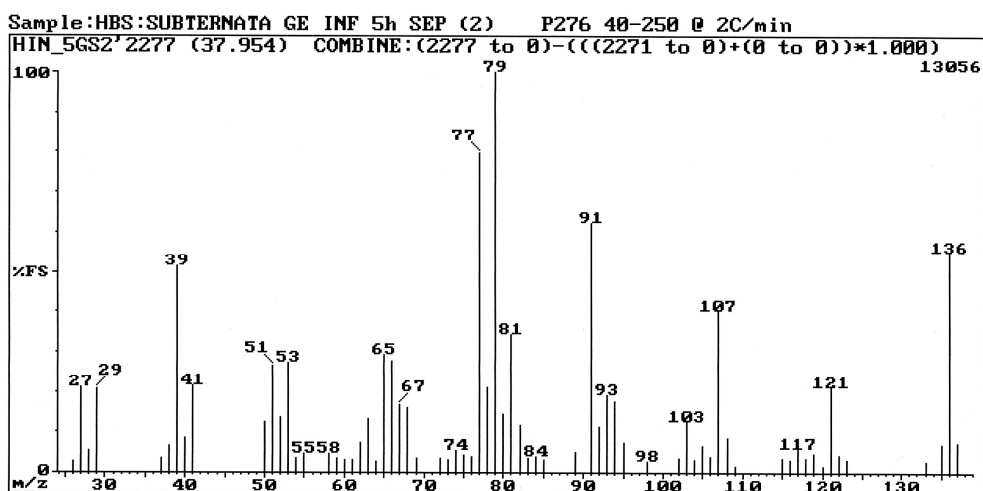


Fig. 3.27: EI mass spectrum of (*E,E,E*)-2,4,6-nonatrienal (**C155**).

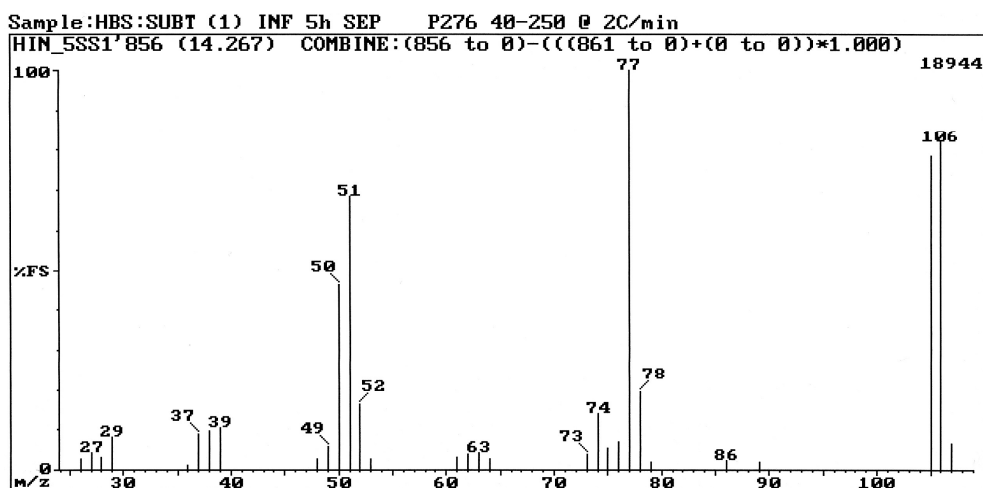


Fig. 3.28: EI mass spectrum of benzaldehyde (**C25**).

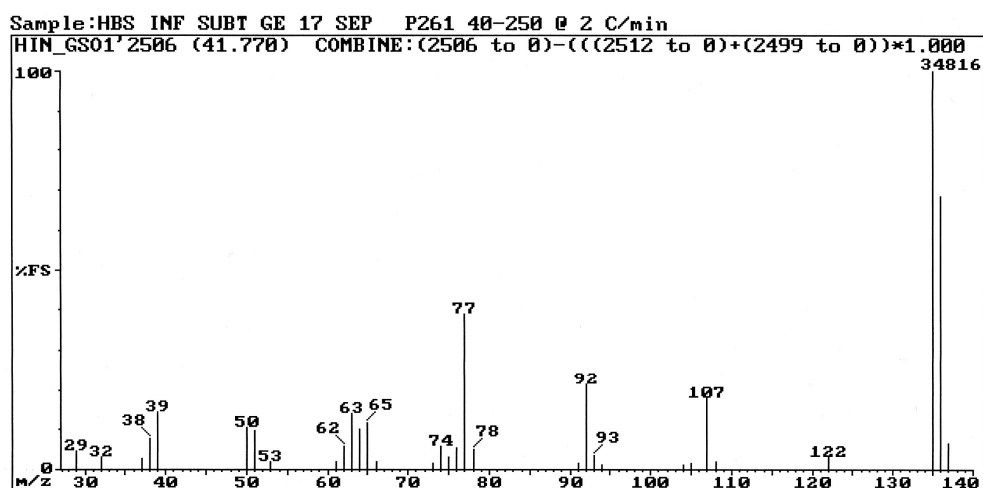


Fig. 3.29: EI mass spectrum of *p*-anisaldehyde (**C141**).

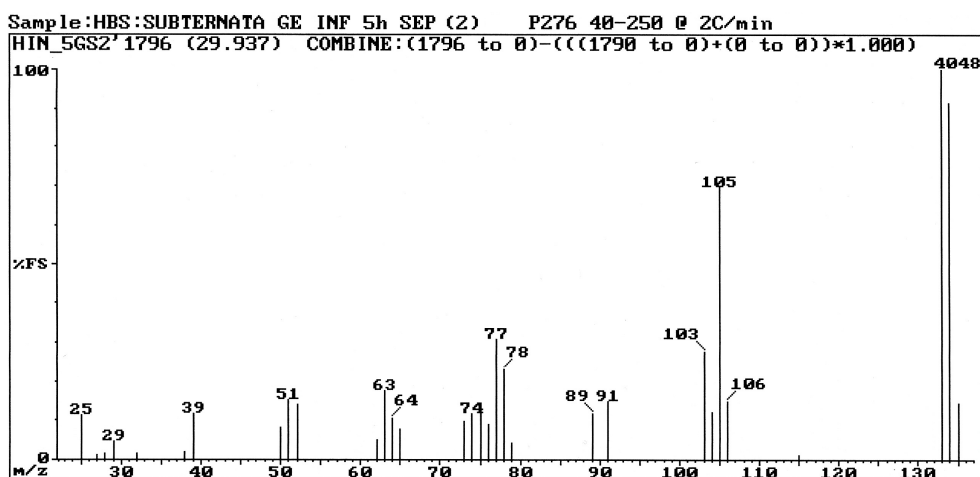


Fig. 3.30: EI mass spectrum of a dimethylbenzaldehyde (**C114**).

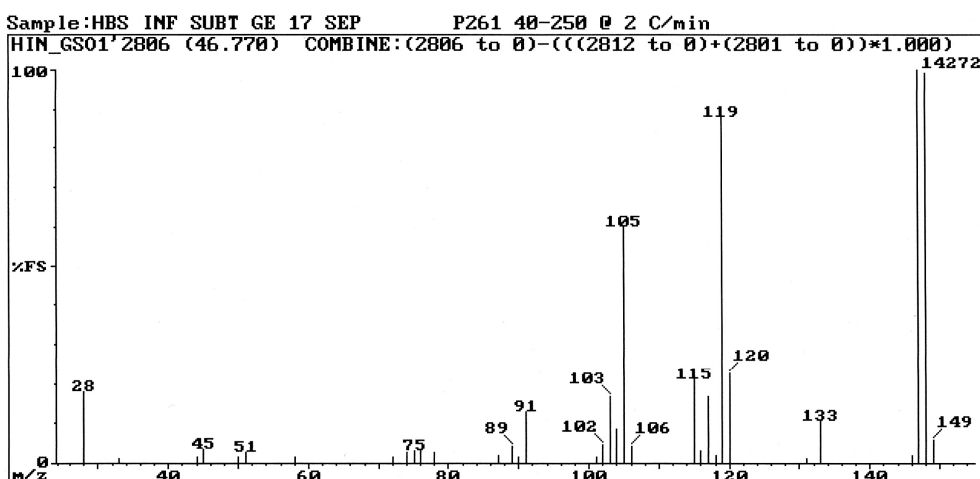


Fig. 3.31: EI mass spectrum of 2,3,4-trimethylbenzaldehyde (**C166**).

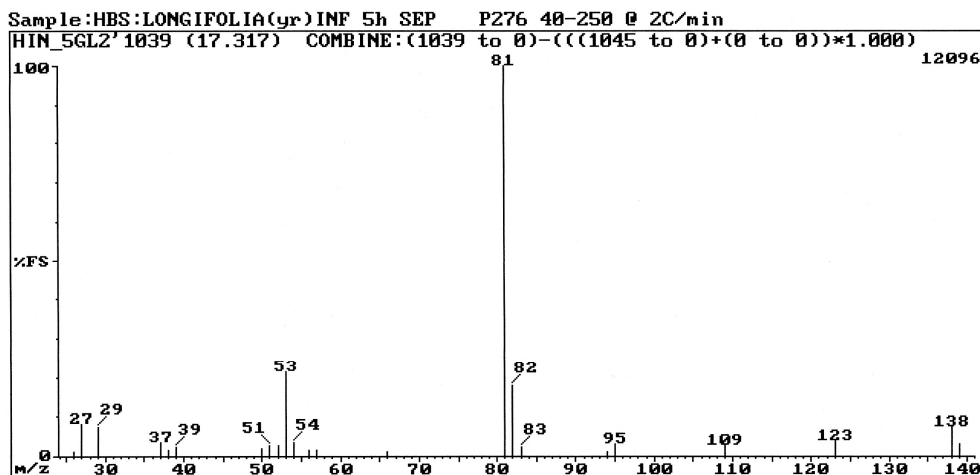


Fig. 3.32: EI mass spectrum of 2-pentylfuran (**C35**).

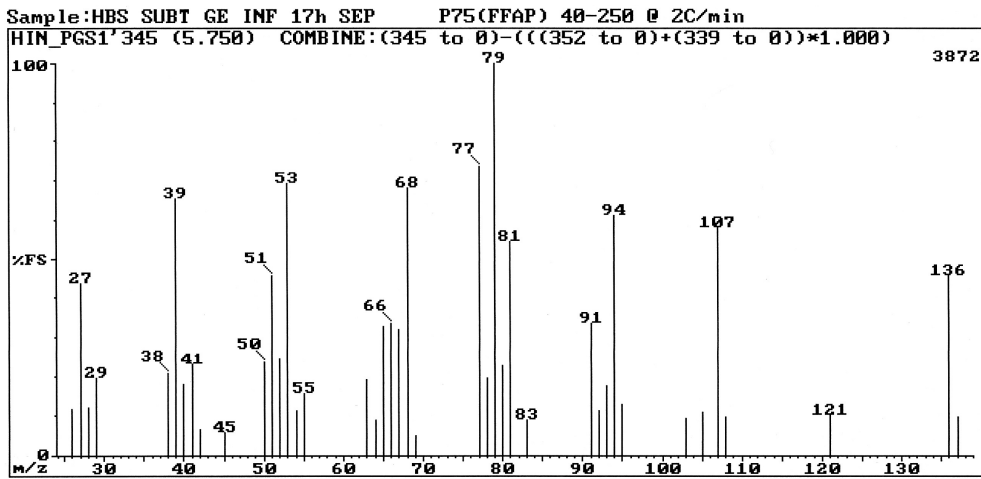


Fig. 3.33: El mass spectrum of (2Z)-2-(2-pentenyl)furan (C40).

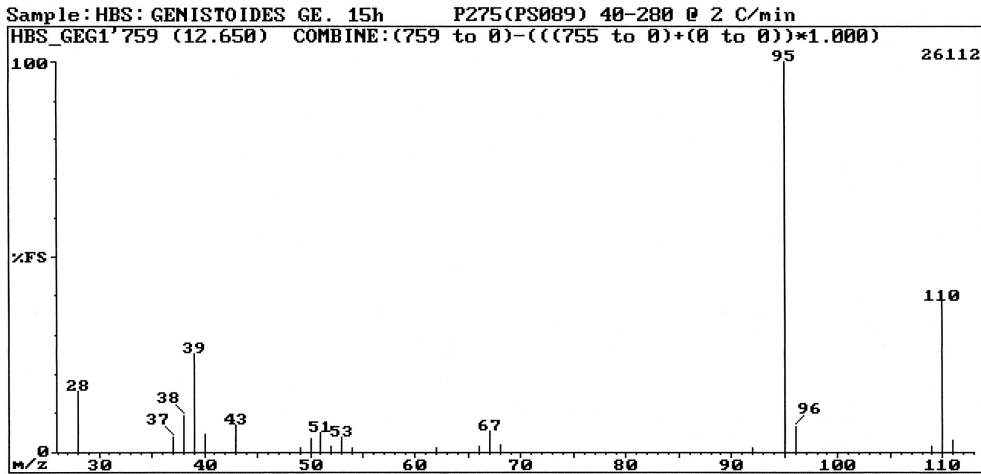


Fig. 3.34: El mass spectrum of 2-acetylfuran (C19).

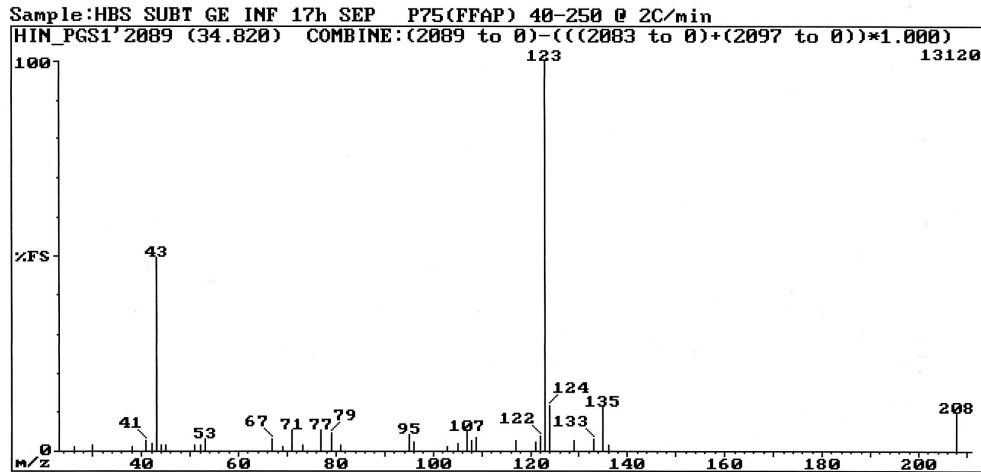


Fig. 3.35: El mass spectrum of 6-methyl-(5-methylfuran-2-yl)heptan-2-one (C215).

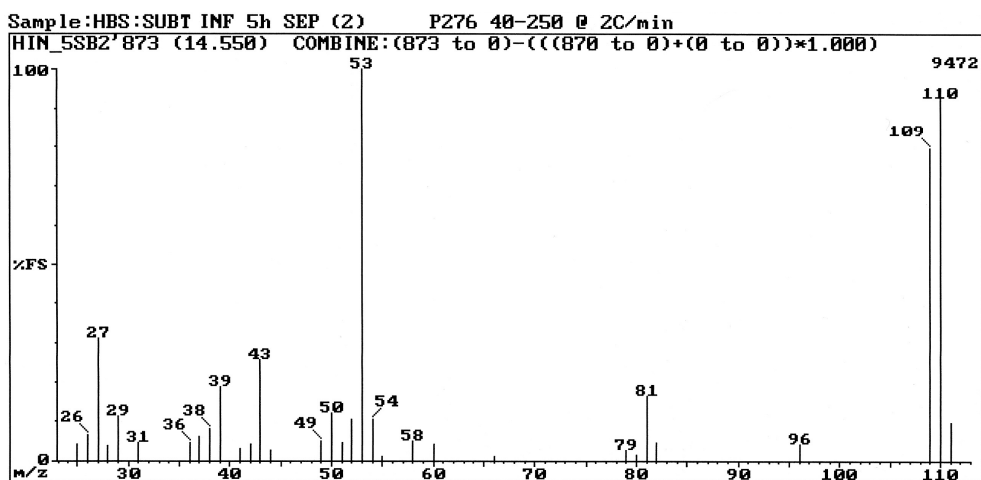


Fig. 3.36: El mass spectrum of 5-methyl-2-furancarboxaldehyde (C28).

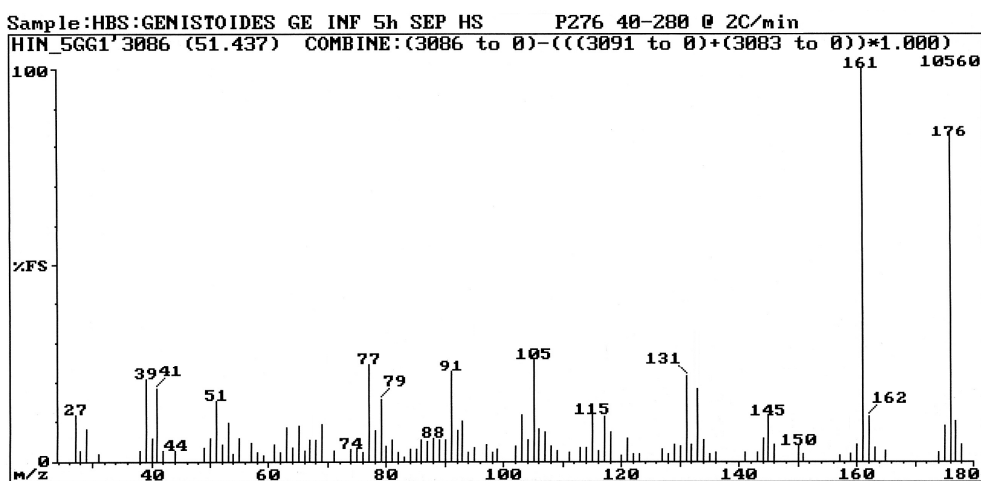


Fig. 3.37: El mass spectrum of 5-methoxy-6,7-dimethylbenzofuran (C223).

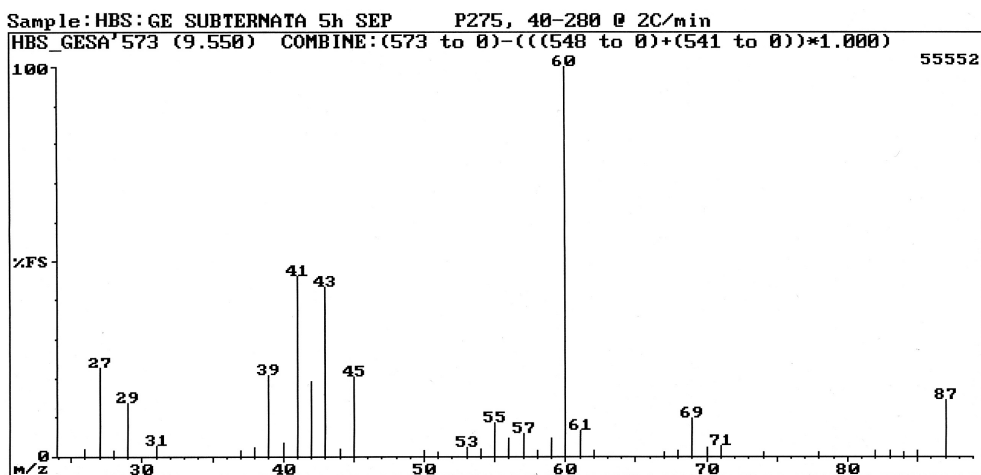


Fig. 3.38: El mass spectrum of 3-methylbutanoic acid (C11).



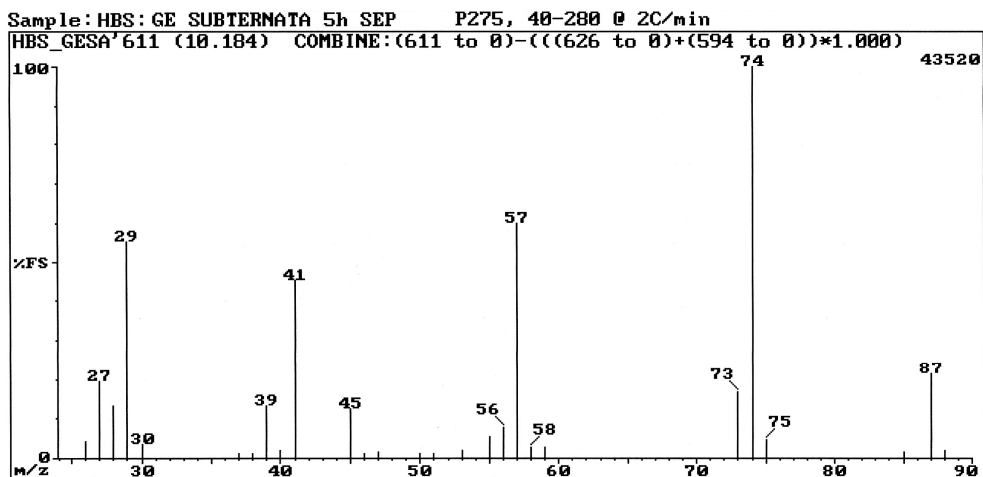


Fig. 3.39: EI mass spectrum of (*R*)-2-methylbutanoic acid (C13).

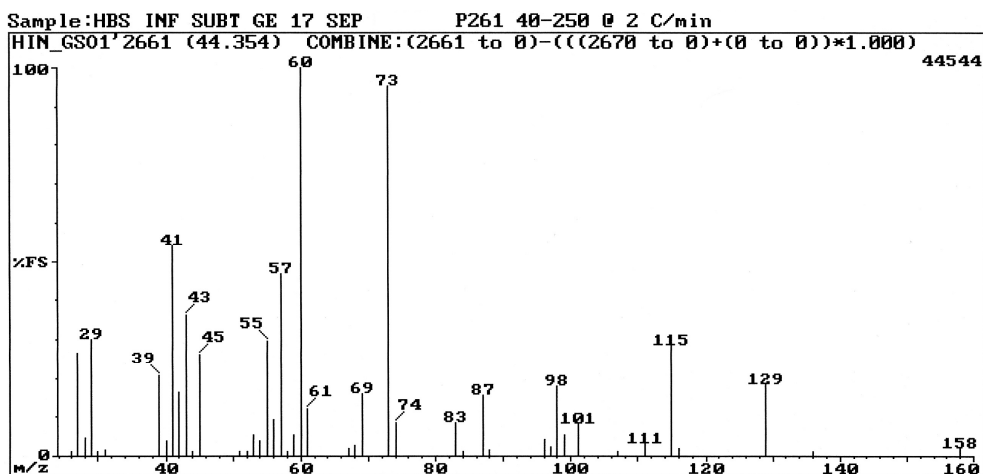


Fig. 3.40: EI mass spectrum of nonanoic acid (C15).

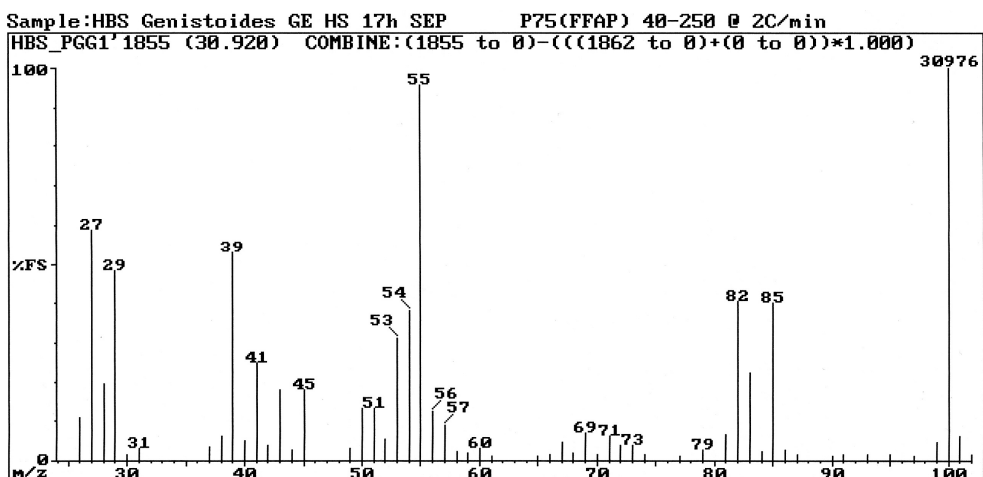


Fig. 3.41: EI mass spectrum of tiglic acid (C20).

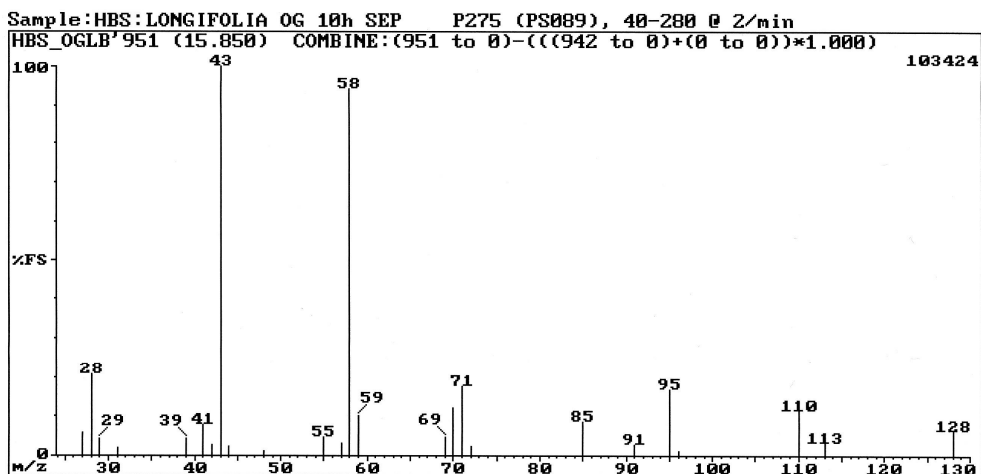


Fig. 3.42: EI mass spectrum of 6-methyl-2-heptanone (**C27**).

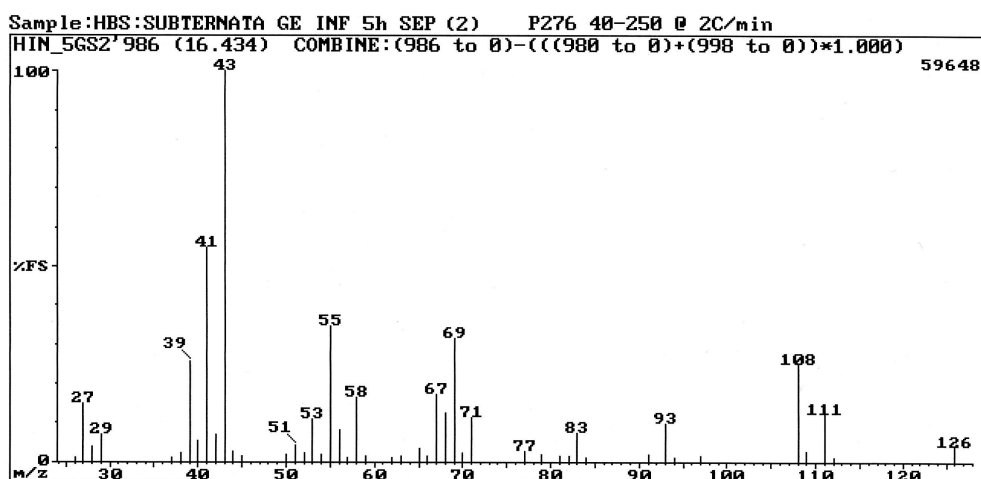


Fig. 3.43: EI mass spectrum of 6-methyl-5-hepten-2-one (**C32**).

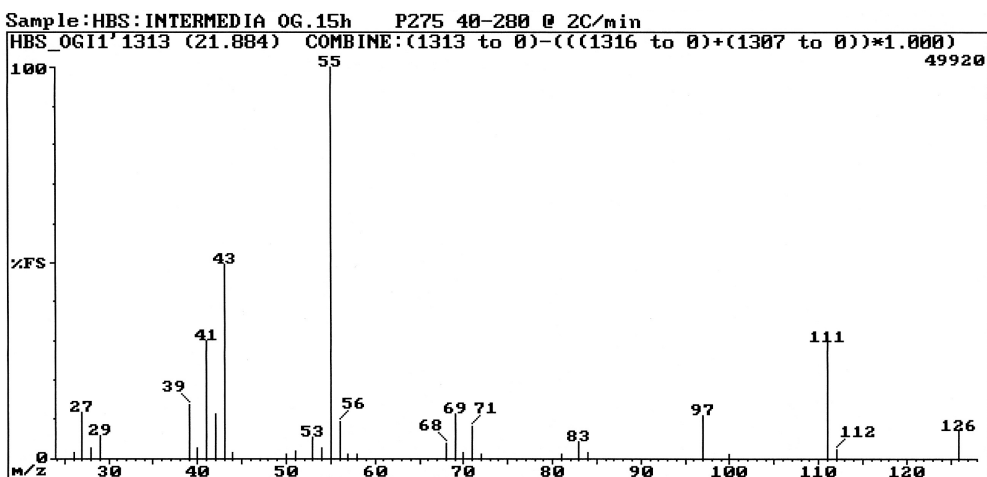


Fig. 3.44: EI mass spectrum of (*E*)-3-octen-2-one (**C53**).

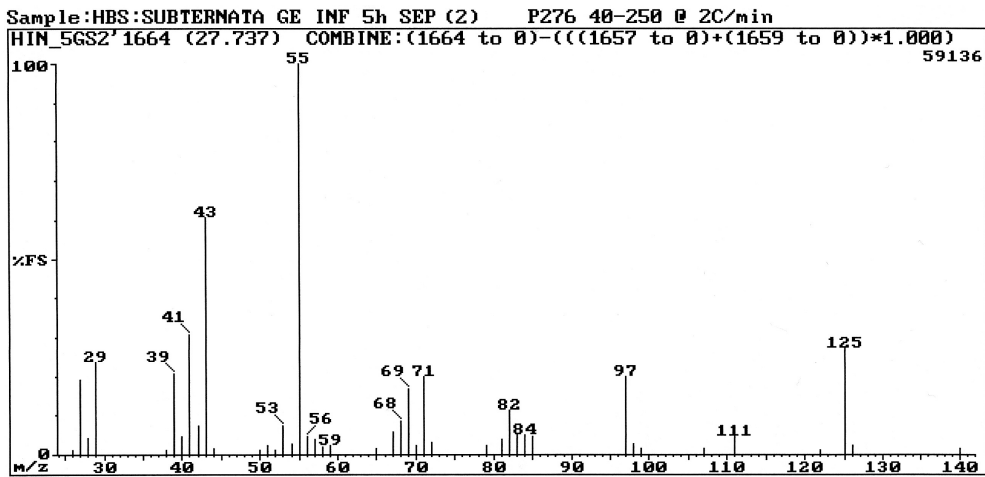


Fig. 3.45: EI mass spectrum of (*E*)-3-nonen-2-one (C95).

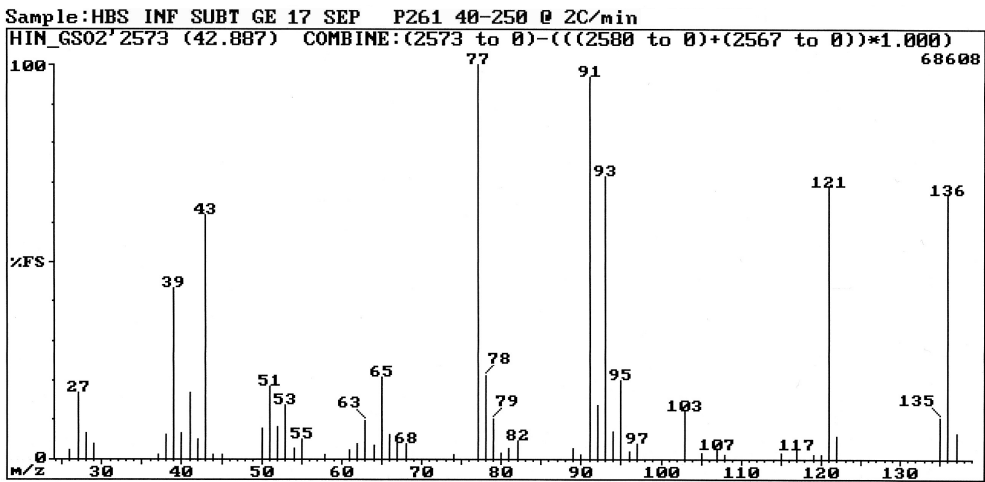


Fig. 3.46: EI mass spectrum of 3,5,7-nonatrien-2-one (C145).

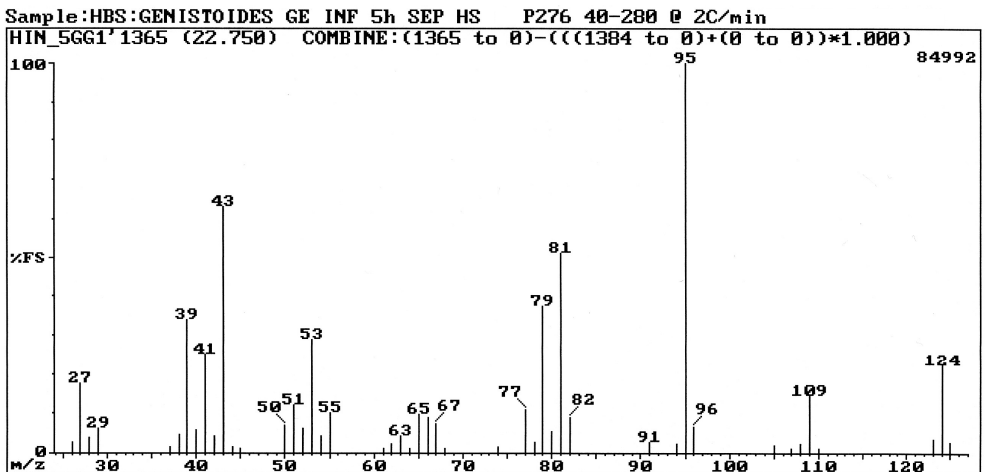


Fig. 3.47: EI mass spectrum of (*Z,E*)-3,5-octadien-2-one (C63).

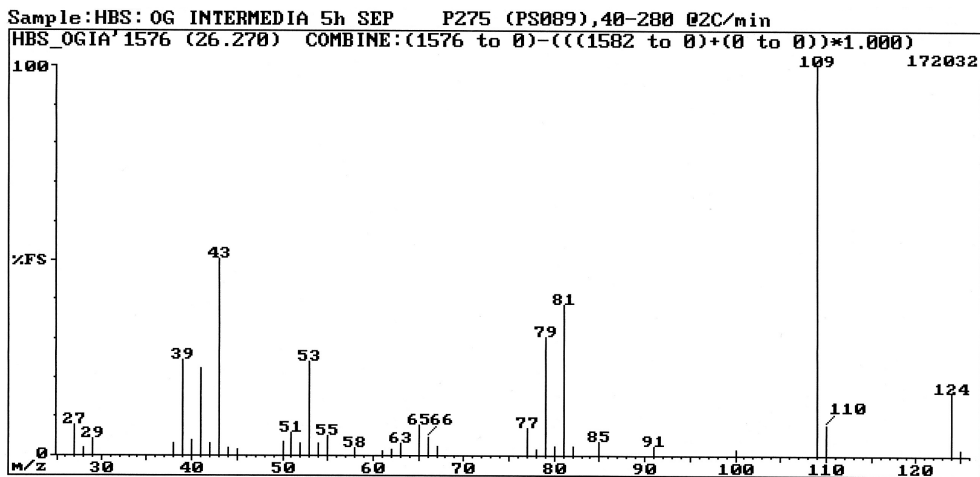


Fig. 3.48: EI mass spectrum of (3E)-6-methyl-3,5-heptadien-2-one (C74).

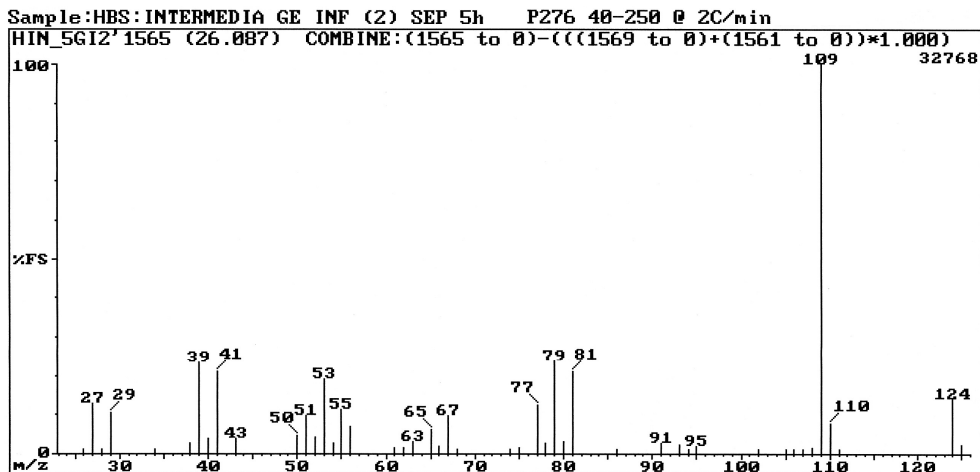


Fig. 3.49: EI mass spectrum of 3,4,4-trimethyl-2-cyclopenten-1-one (C81).

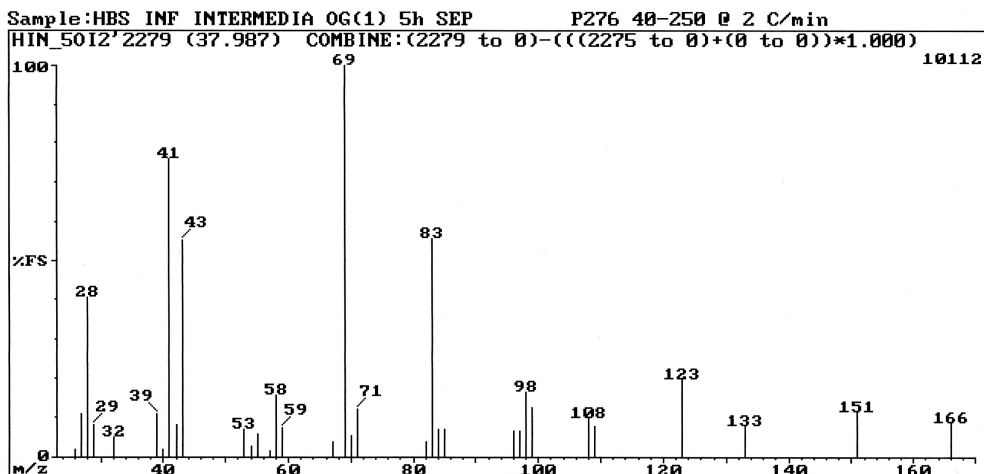


Fig. 3.50: EI mass spectrum of 4,8-dimethyl-3,7-nonadien-2-one (C154).

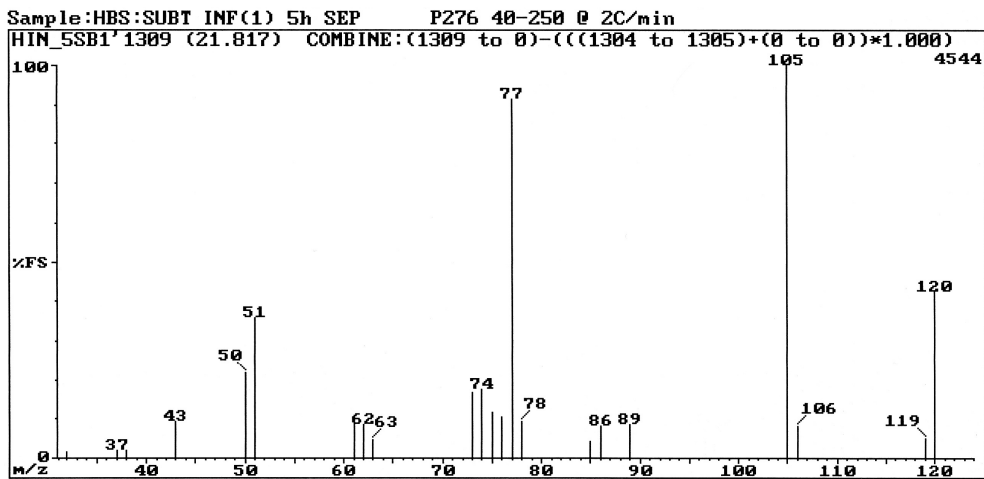


Fig. 3.51: El mass spectrum of acetophenone (C60).

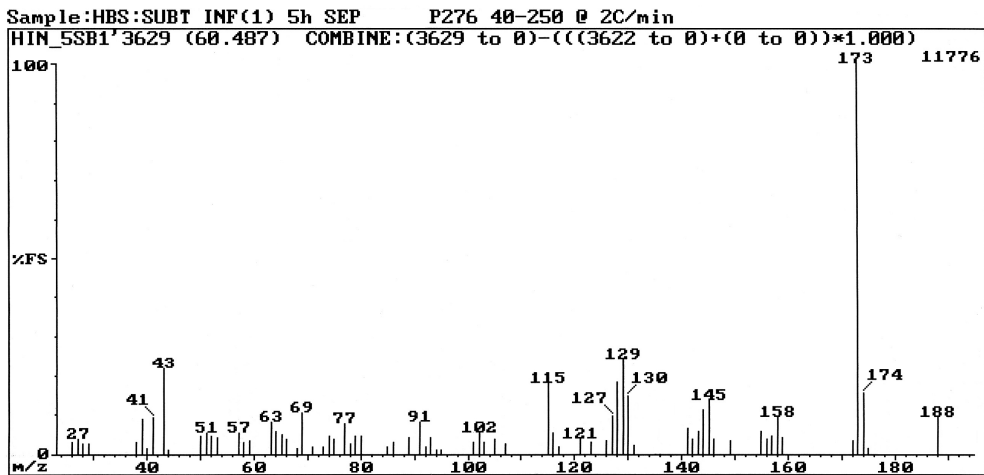


Fig. 3.52: El mass spectrum of 1-(2,3,6-trimethylphenyl)-3-buten-2-one (C273).

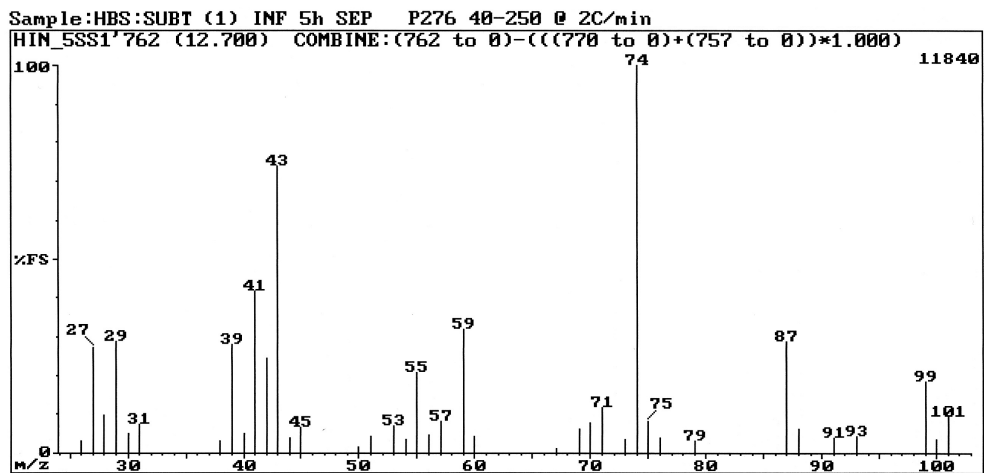


Fig. 3.53: El mass spectrum of methyl hexanoate (C22).

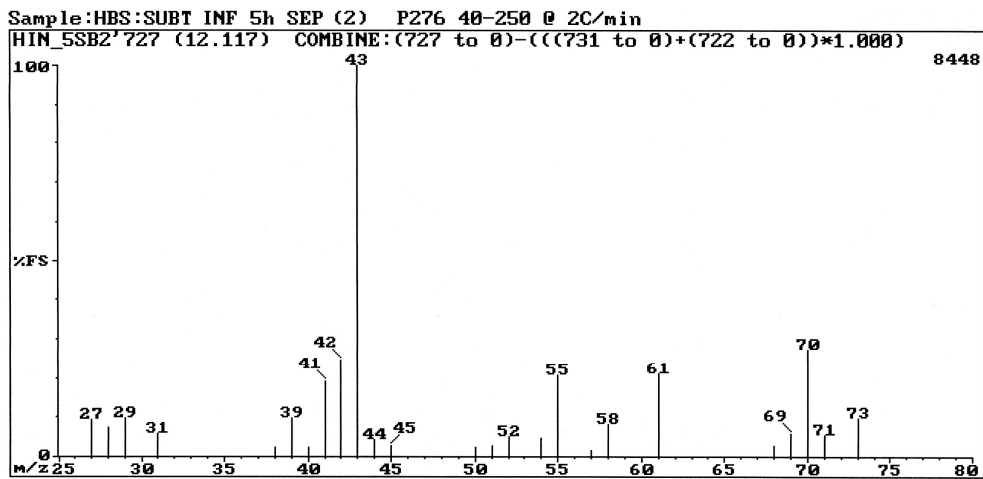


Fig. 3.54: EI mass spectrum of pentyl acetate (C21).

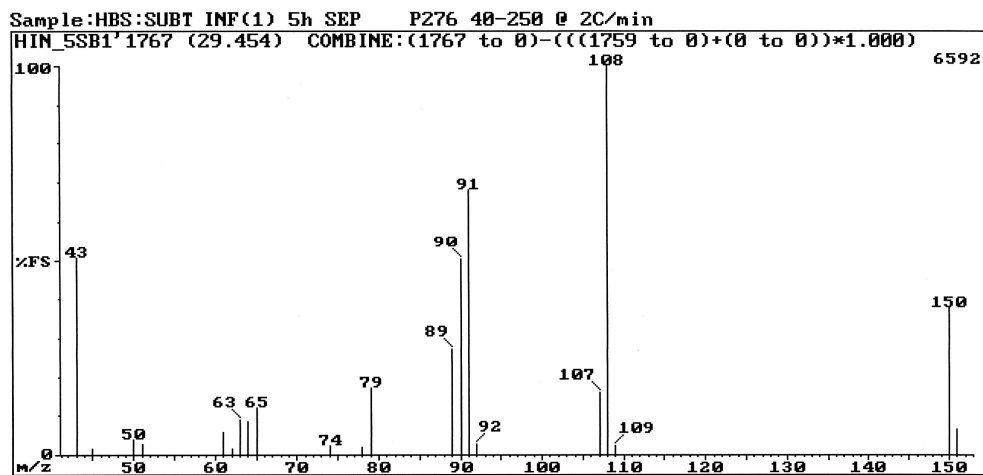


Fig. 3.55: EI mass spectrum of benzyl acetate (C109).

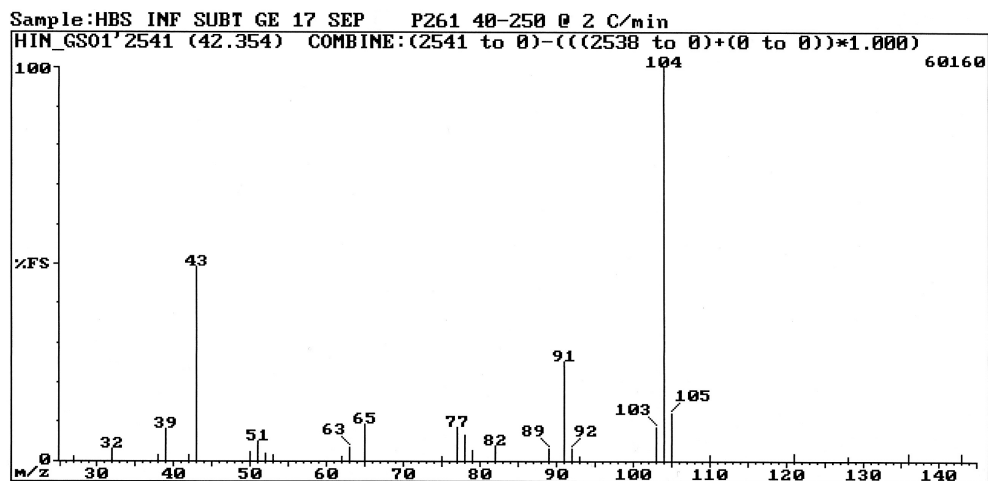


Fig. 3.56: EI mass spectrum of 2-phenylethyl acetate (C142).

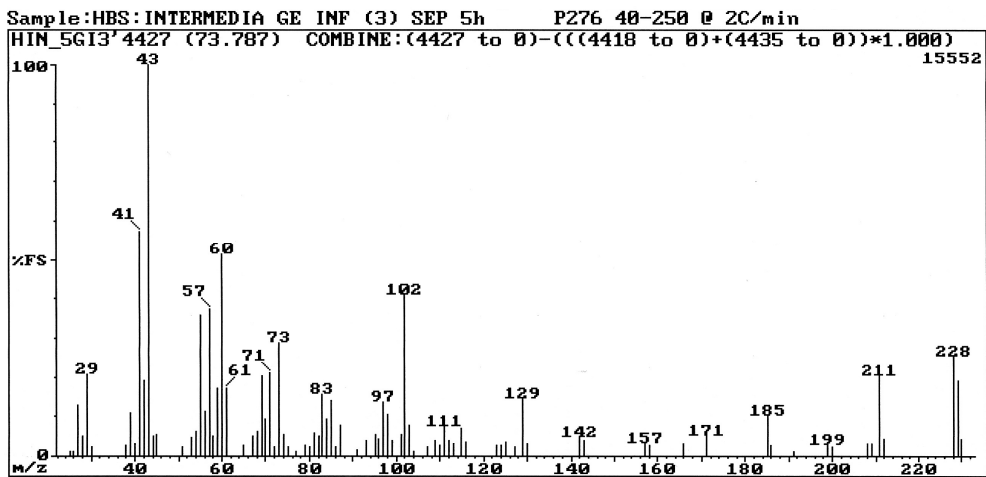


Fig. 3.57: EI mass spectrum of isopropyl myristate (C298).

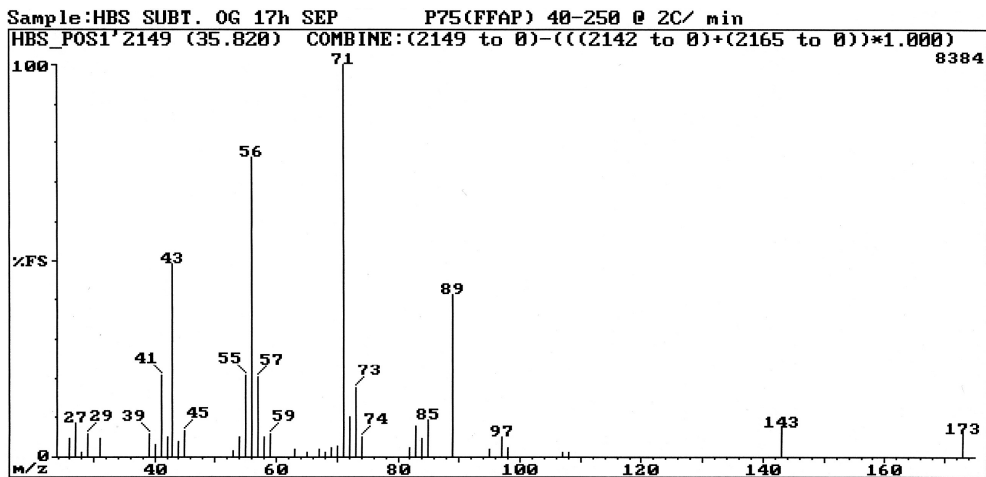


Fig. 3.58: EI mass spectrum of 3-hydroxy-2,4,4-trimethylpentyl 2-methylpropanoate (C201).

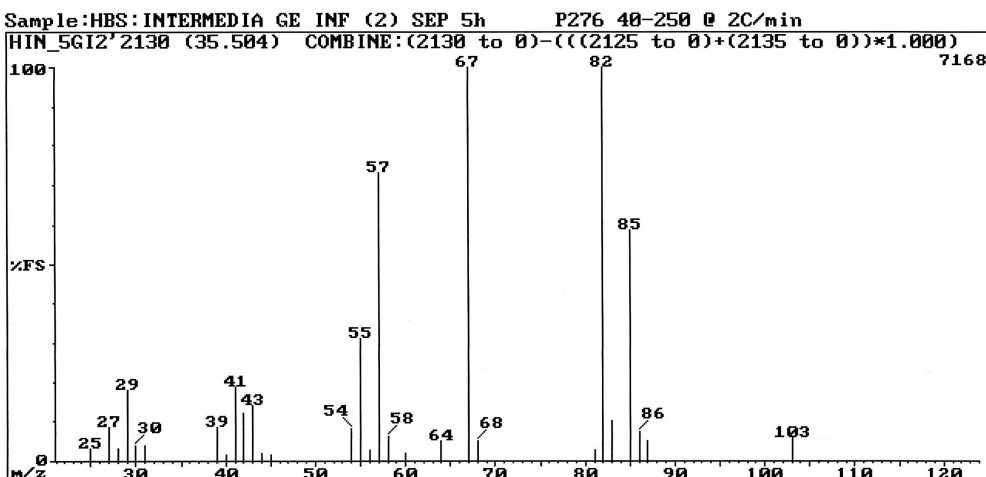


Fig. 3.59: EI mass spectrum of (Z)-3-hexenyl isovalerate (C140).

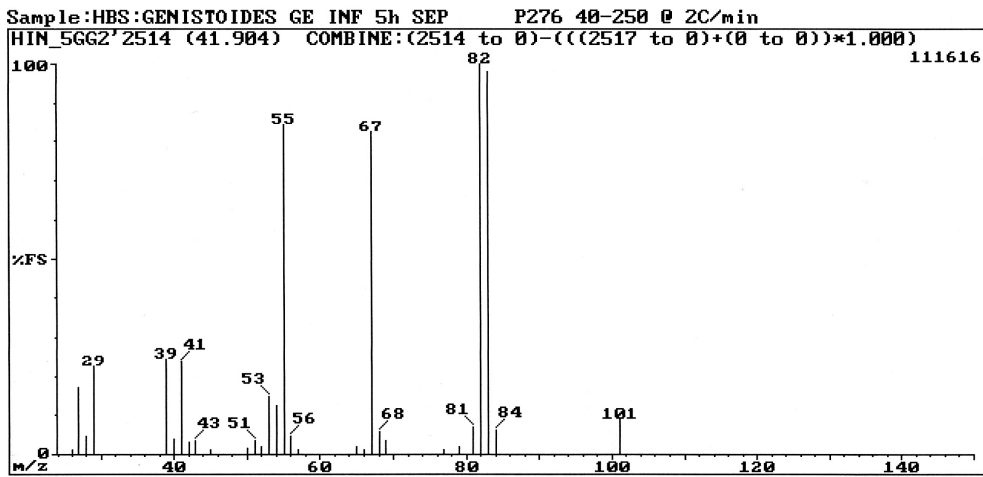


Fig. 3.60: El mass spectrum of (*Z*)-3-hexenyl (*E*)-2-methyl-2-butenolate (**C175**).

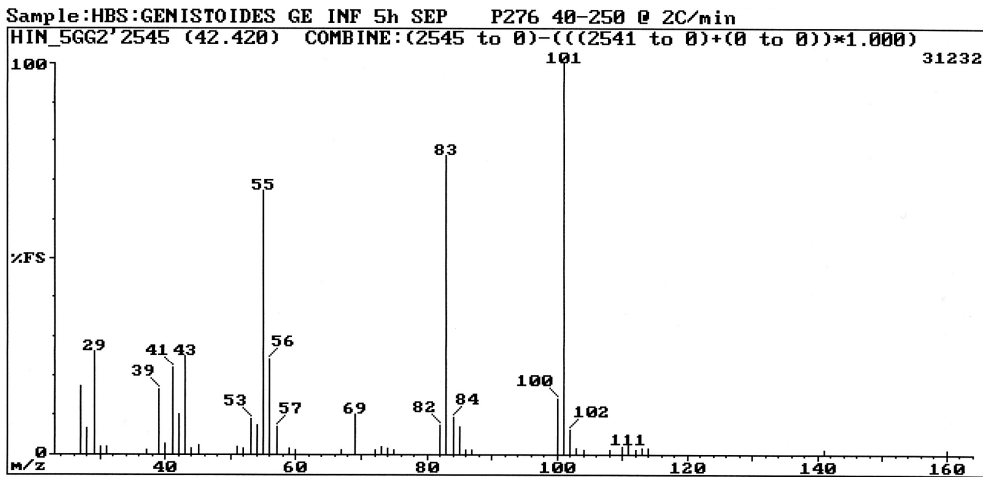


Fig. 3.61: El mass spectrum of hexyl tiglate (**C179**).

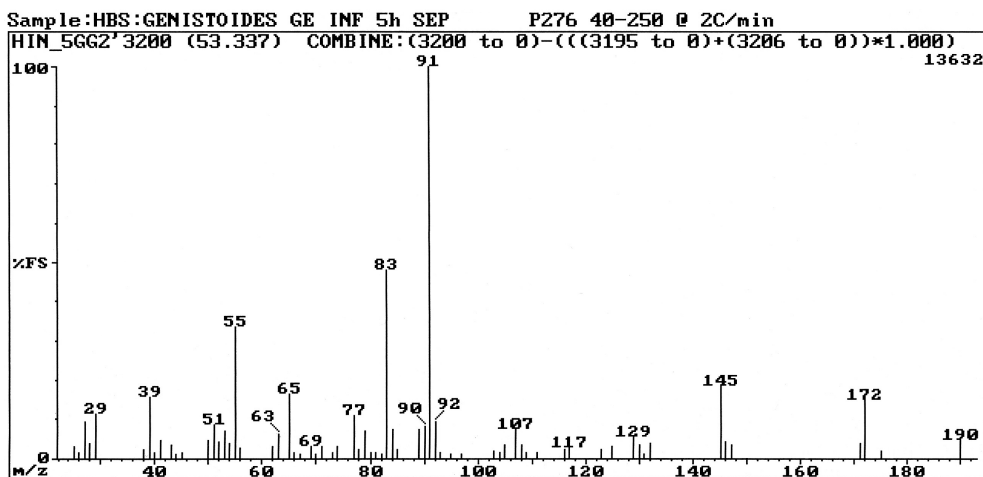


Fig. 3.62: El mass spectrum of benzyl tiglate (**C237**).



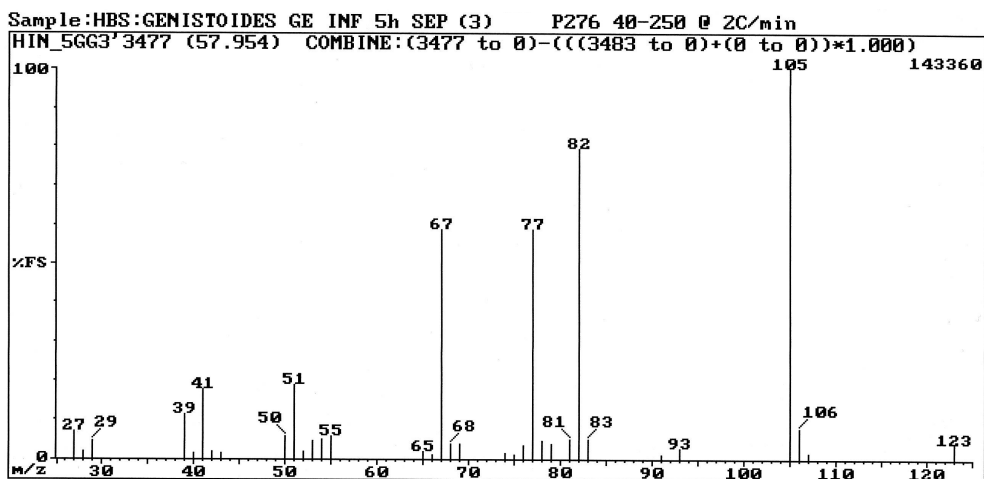


Fig. 3.63: El mass spectrum of (*Z*)-3-hexenyl benzoate (**C261**).

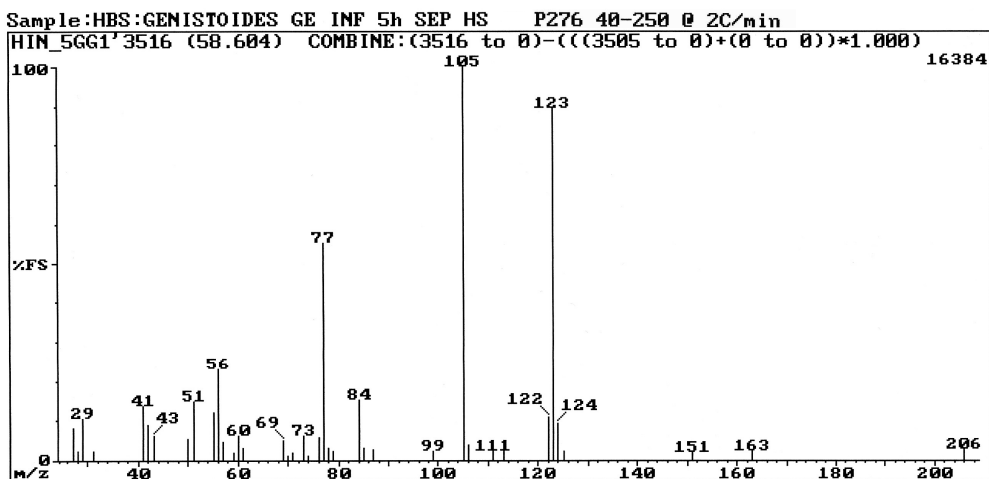


Fig. 3.64: El mass spectrum of hexyl benzoate (**C263**).

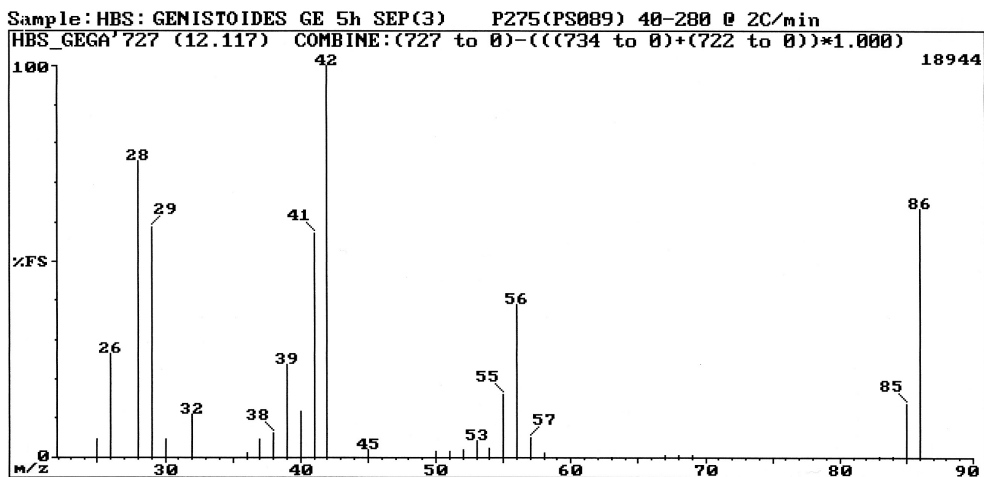


Fig. 3.65: El mass spectrum of  $\gamma$ -butyrolactone (**C16**).

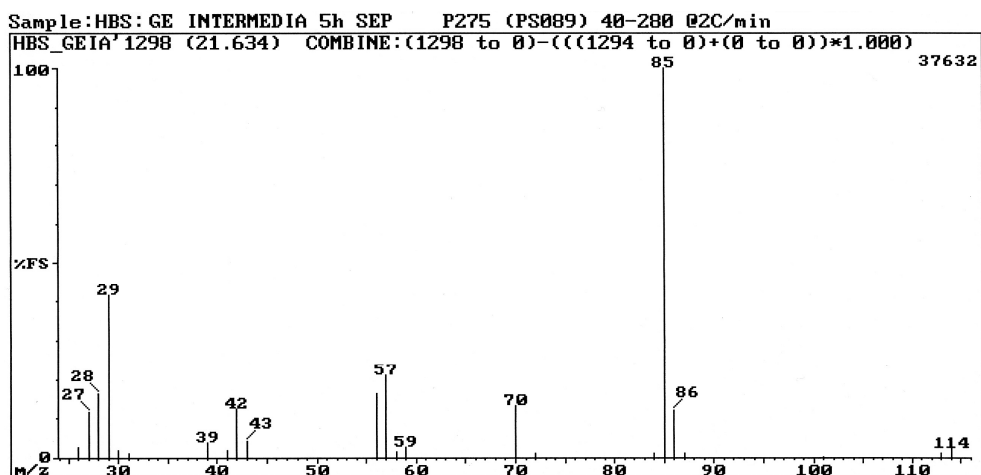


Fig. 3.66: EI mass spectrum of hexan-4-olide (C54).

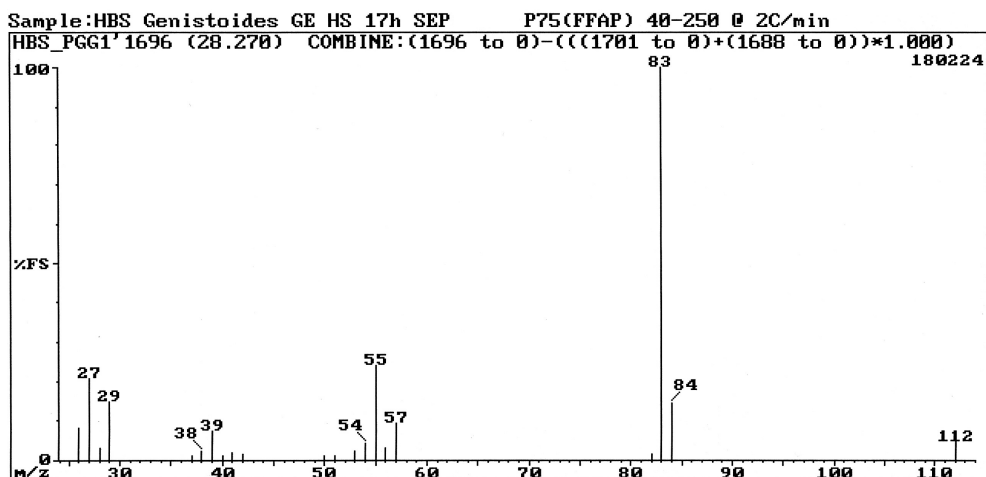


Fig. 3.67: EI mass spectrum of 2-hexen-4-olide (C49).

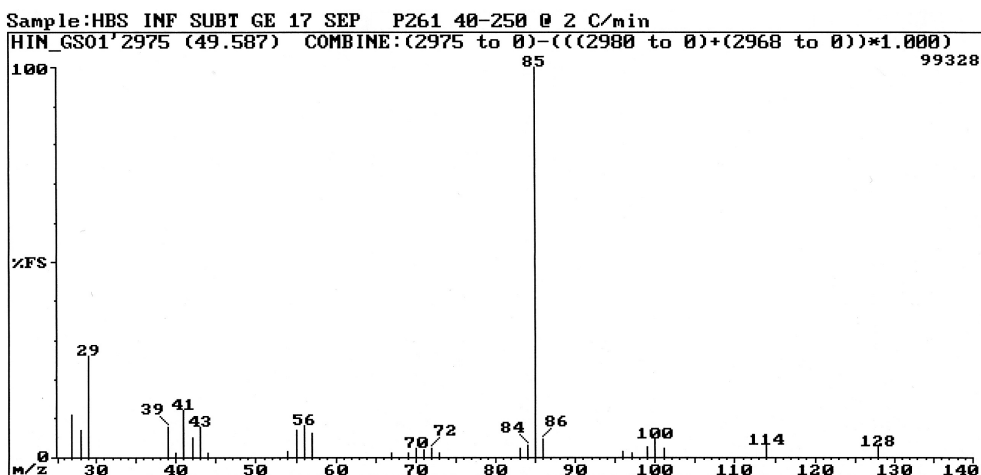


Fig. 3.68: EI mass spectrum of nonan-4-olide (C186).

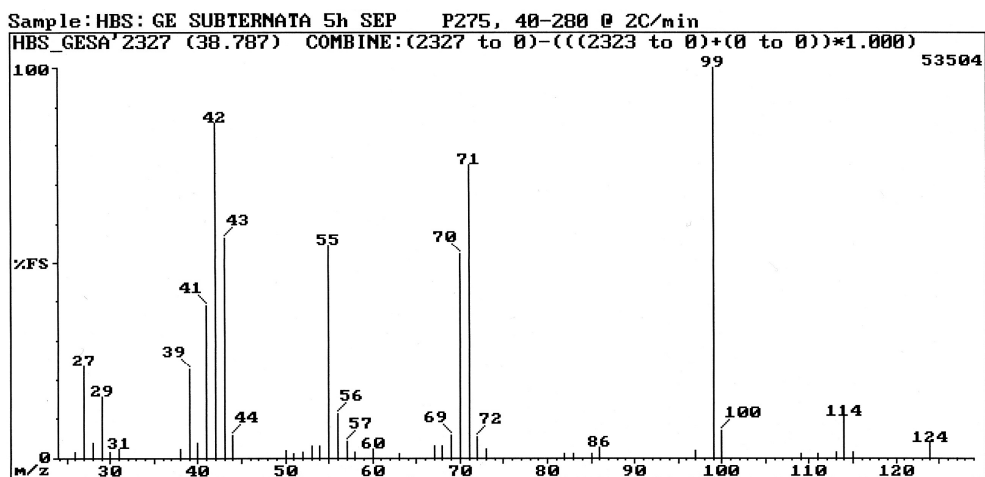


Fig. 3.69: EI mass spectrum of (*R*)-octan-5-olide (**C152**).

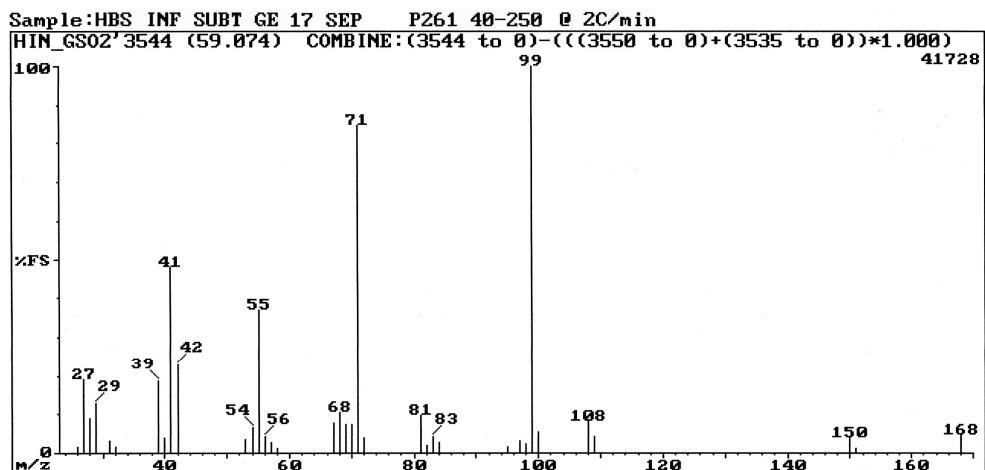


Fig. 3.70: EI mass spectrum of (*S*)-(*Z*)-7-decen-5-olide (**C229**).

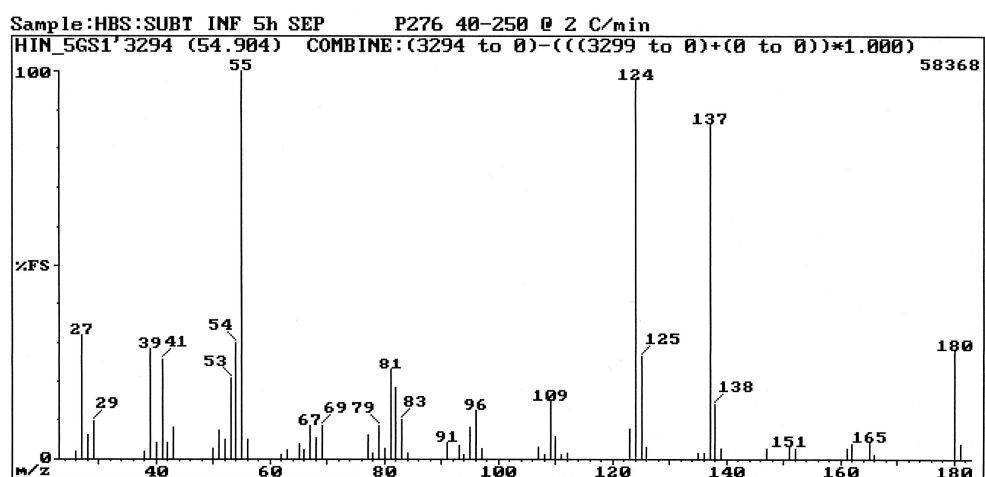


Fig. 3.71: EI mass spectrum of bovalide (**C245**).

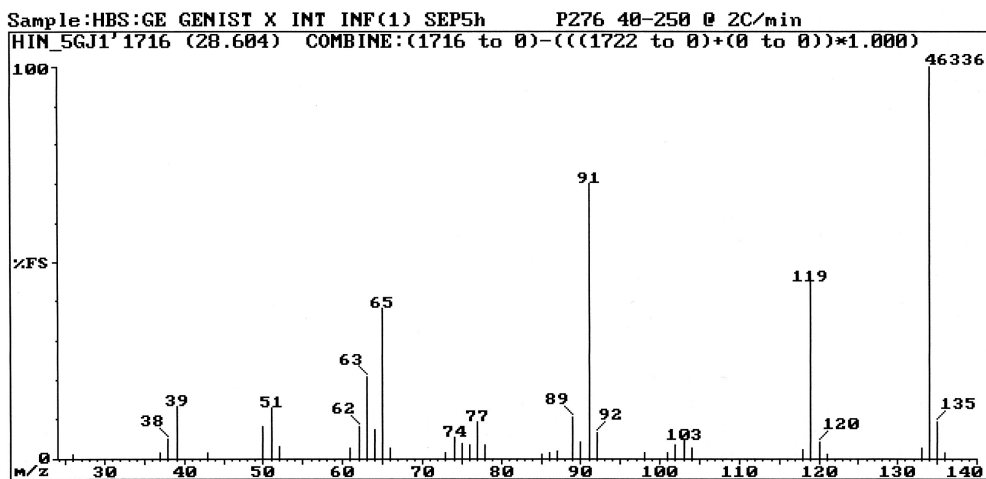


Fig. 3.72: EI mass spectrum of 4-vinylanisole (C100).

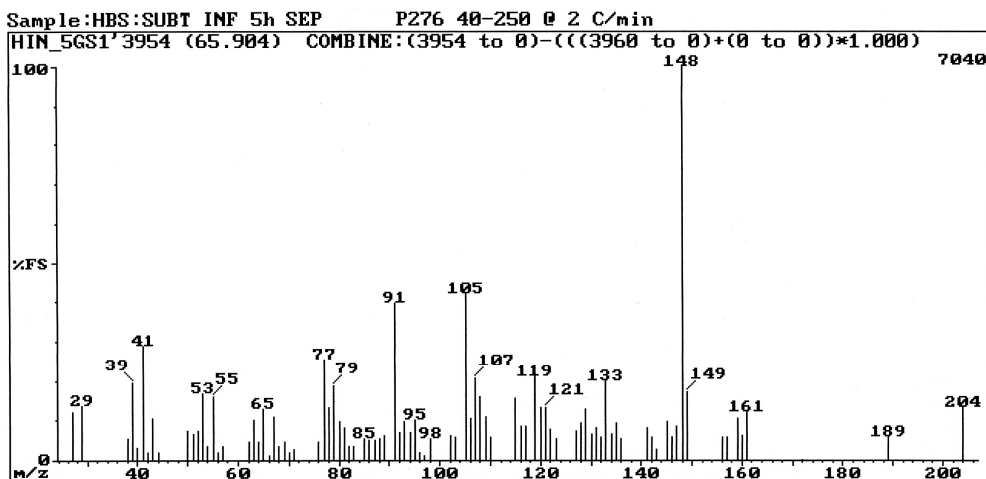


Fig. 3.73: EI mass spectrum of 3,7,7-trimethyl-1-penta-1,3-dienyl-2-oxabicyclo[3.2.0]hept-3-ene (C291).

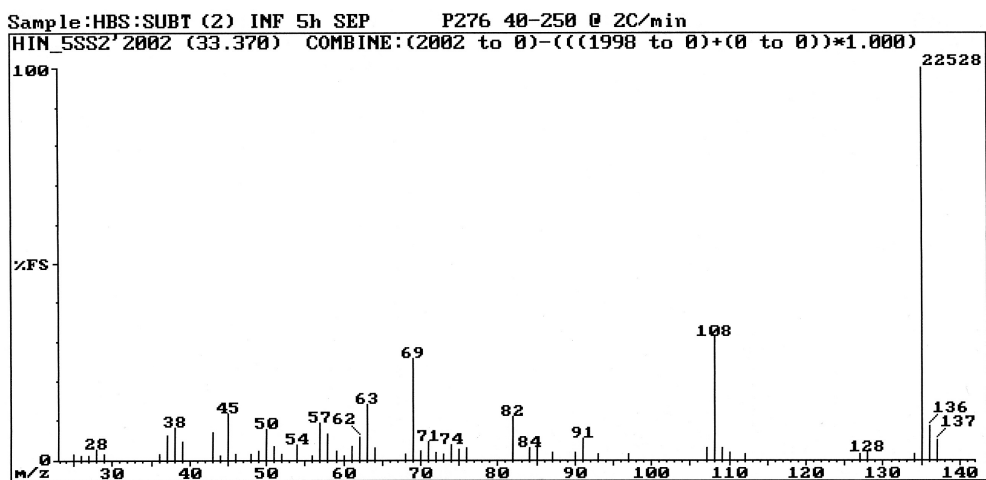


Fig. 3.74: EI mass spectrum of benzothiazole (C127).

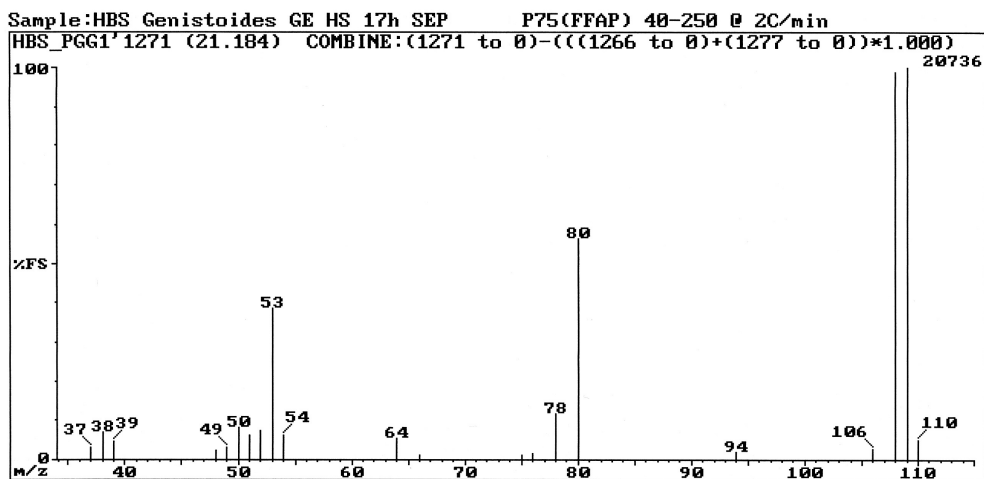


Fig. 3.75: El mass spectrum of 2-formyl-1-methylpyrrole (**C37**).

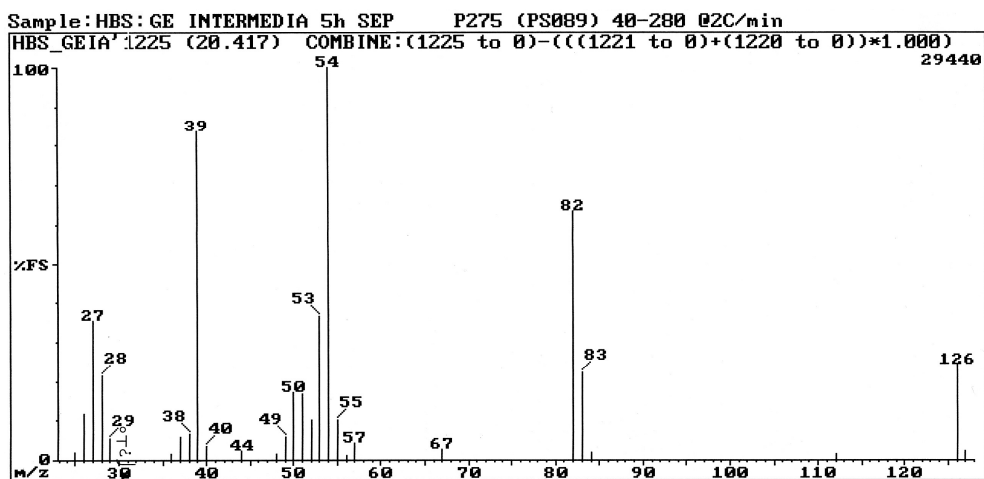


Fig. 3.76: El mass spectrum of 3,4-dimethyl-2,5-furandione (**C48**).

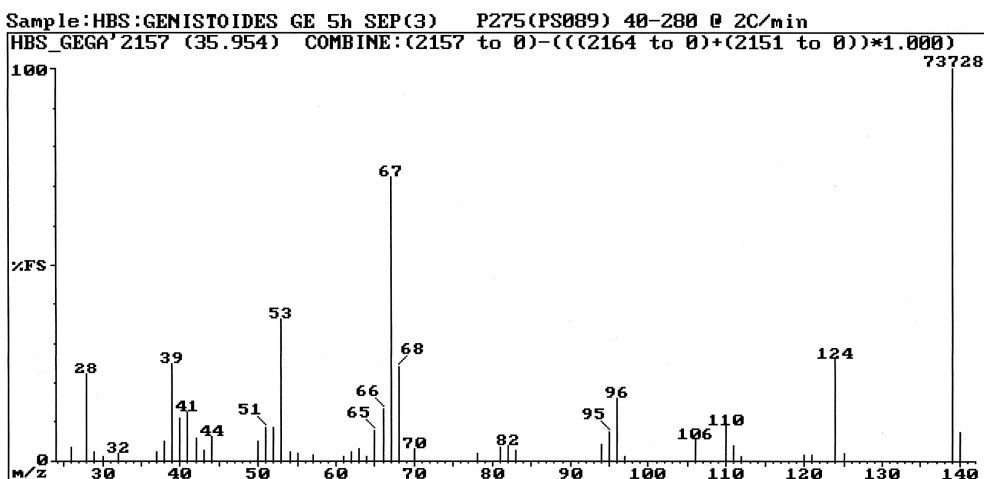


Fig. 3.77: El mass spectrum of 2-ethyl-3-methylmaleimide (**C130**).

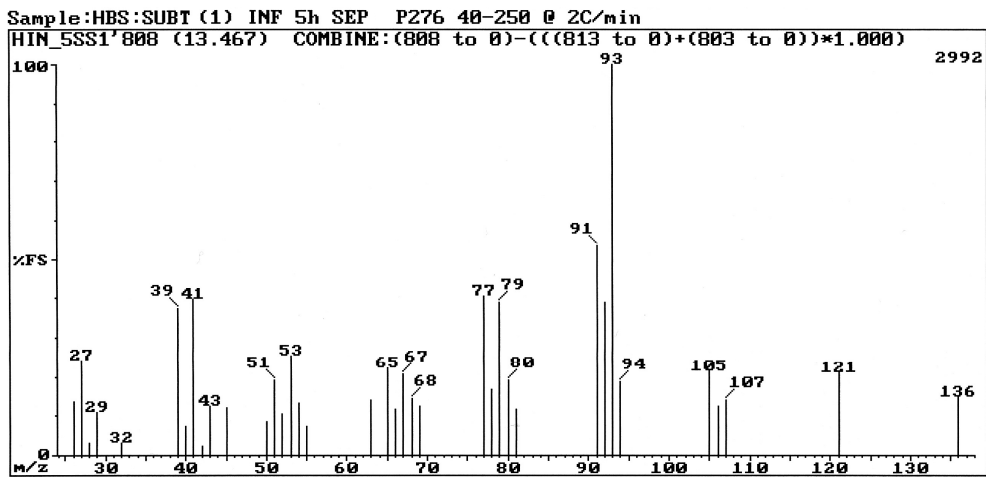


Fig. 3.78: EI mass spectrum of  $\alpha$ -pinene (**C23**).

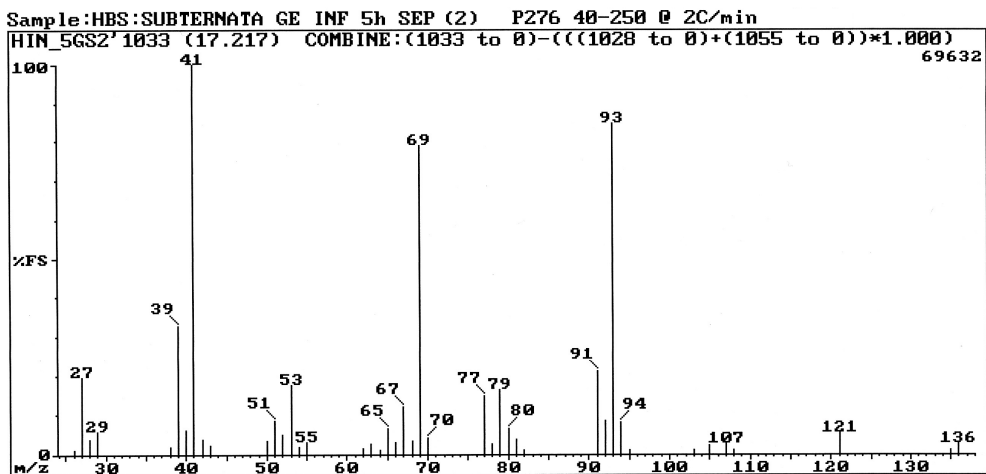


Fig. 3.79: EI mass spectrum of myrcene (**C38**).

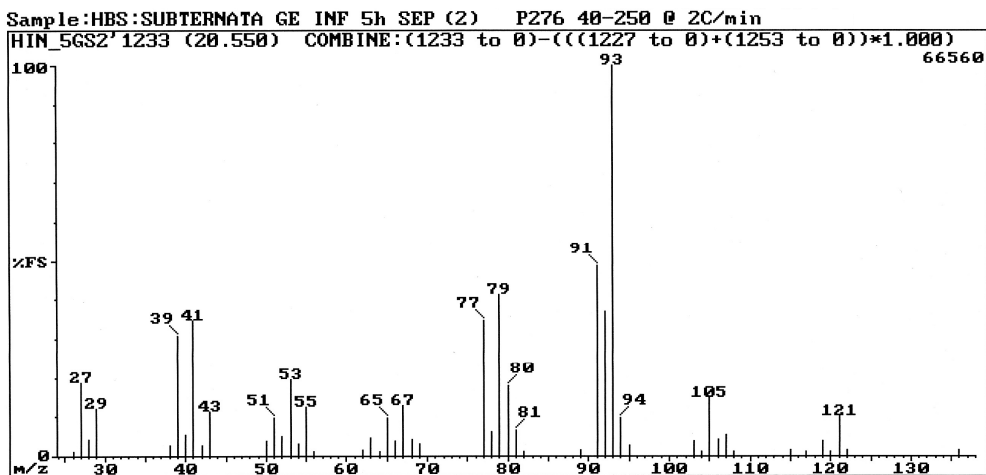


Fig. 3.80: EI mass spectrum of (*Z*)- $\beta$ -ocimene (**C56**).

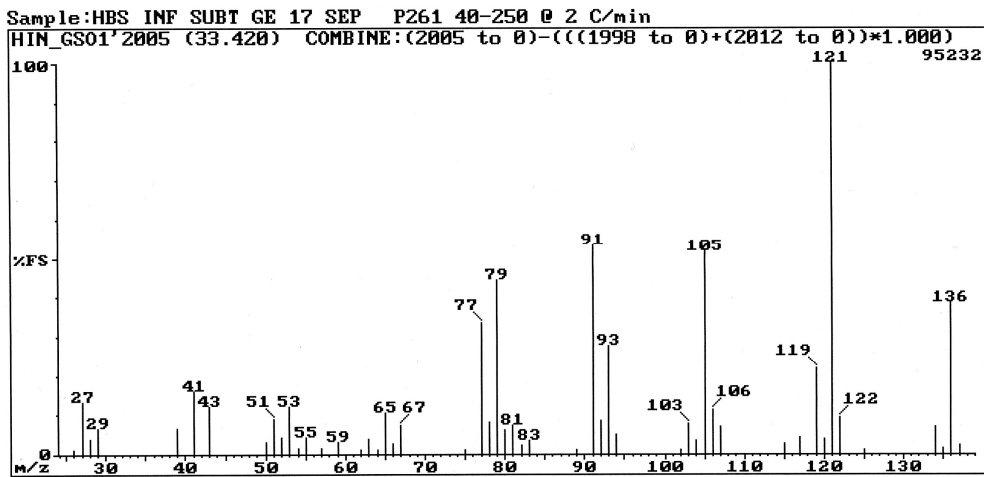


Fig. 3.81: EI mass spectrum of allo-ocimene (C93).

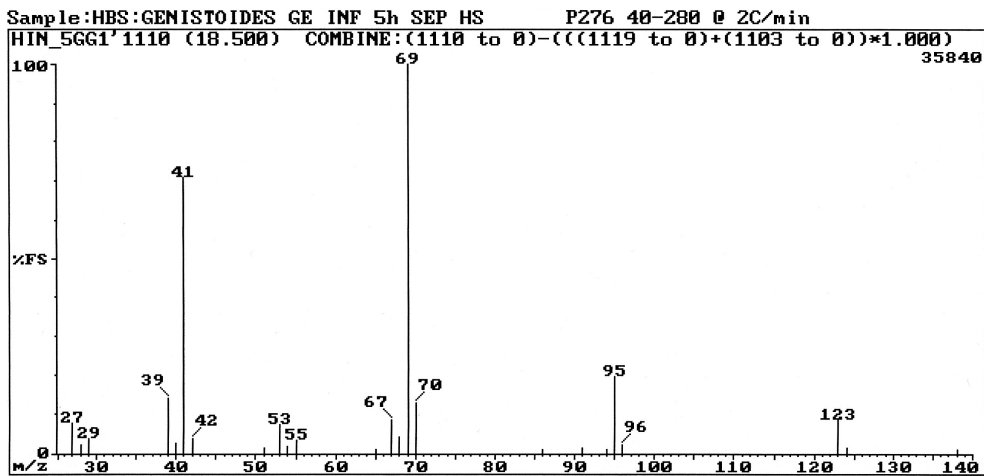


Fig. 3.82: EI mass spectrum of (6E)-2,6-dimethyl-2,6-octadiene (C43).

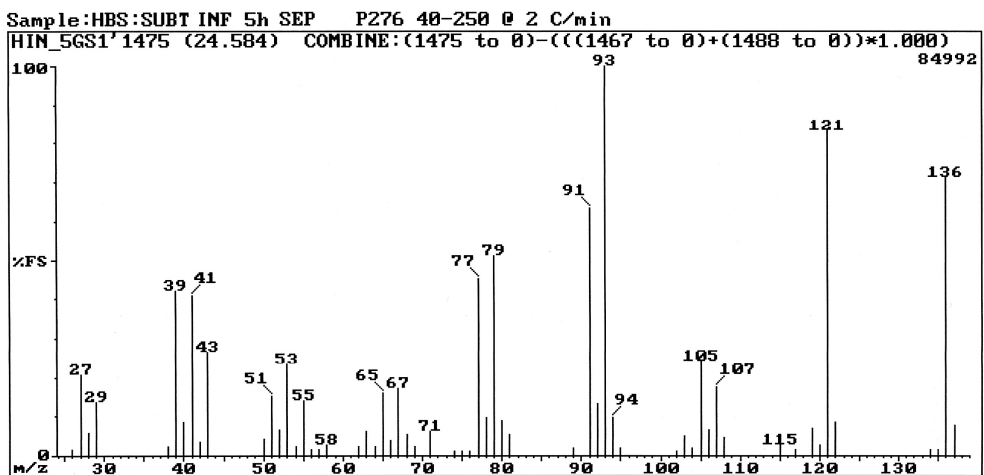


Fig. 3.83: EI mass spectrum of terpinolene (C71).

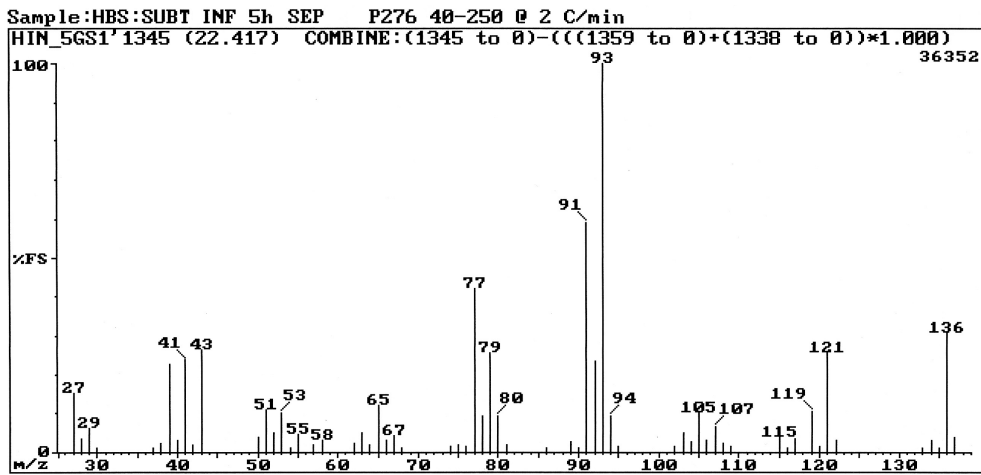


Fig. 3.84: EI mass spectrum of  $\gamma$ -terpinene (C61).

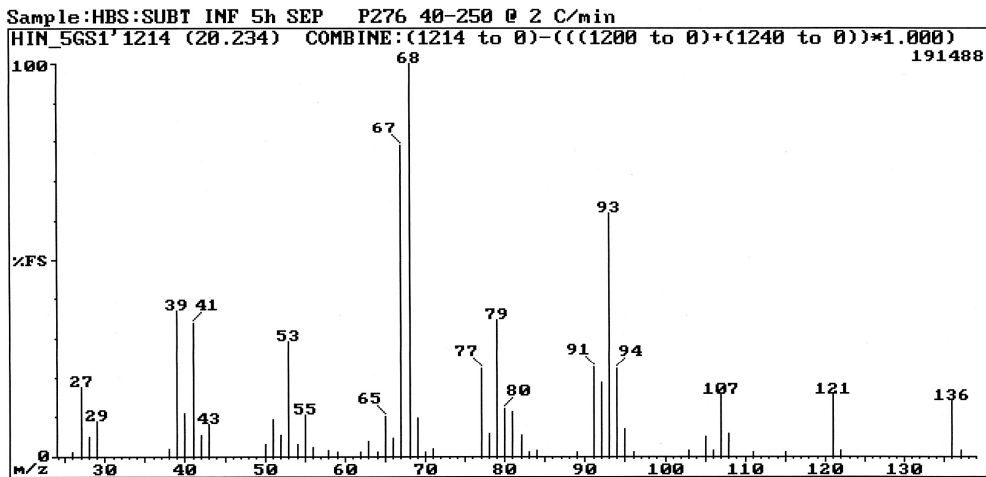


Fig. 3.85: EI mass spectrum of limonene (C52).

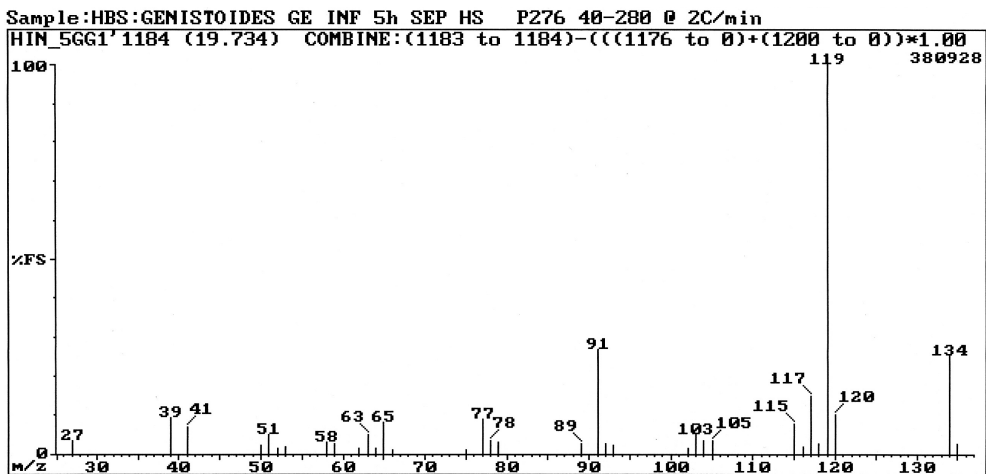


Fig. 3.86: EI mass spectrum of *p*-cymene (C50).



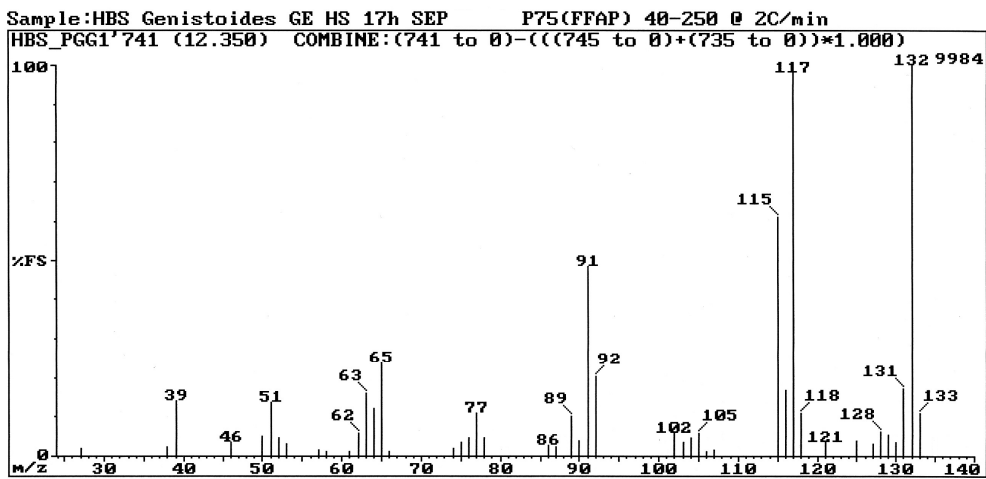


Fig. 3.87: El mass spectrum of *p*-cymenene (C69).

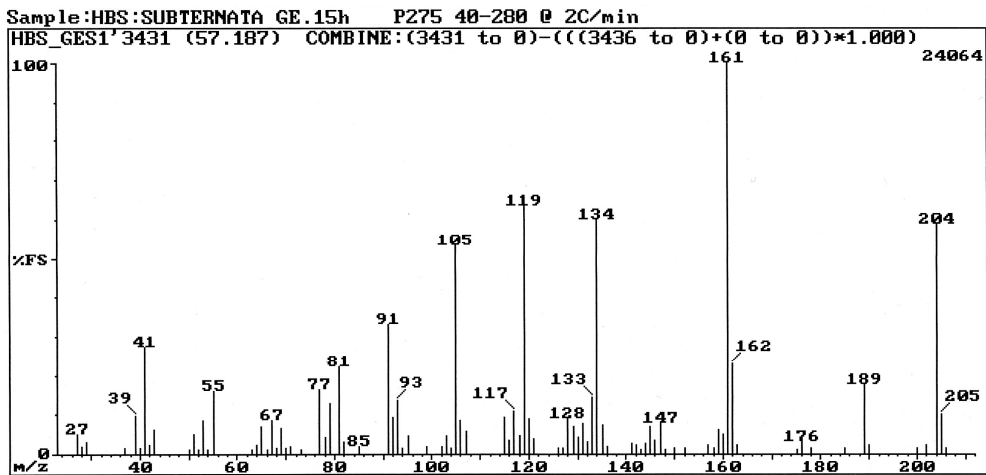


Fig. 3.88: El mass spectrum of  $\delta$ -cadinene (C247).

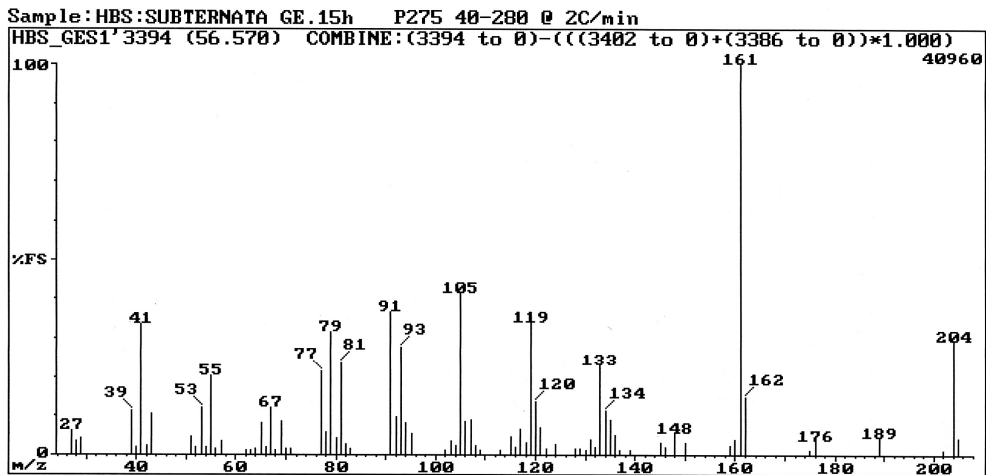


Fig. 3.89: El mass spectrum of  $\gamma$ -cadinene (C244).

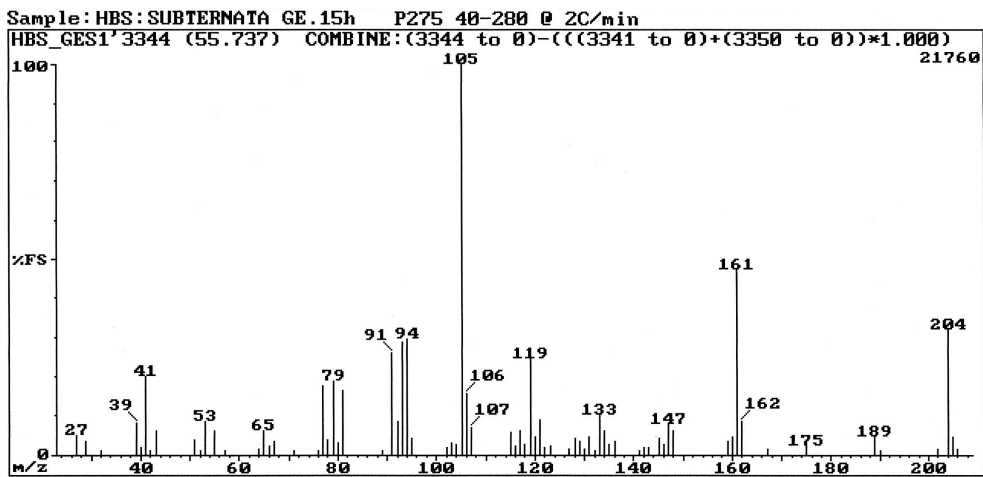


Fig. 3.90: EI mass spectrum of  $\alpha$ -murolene (C240).

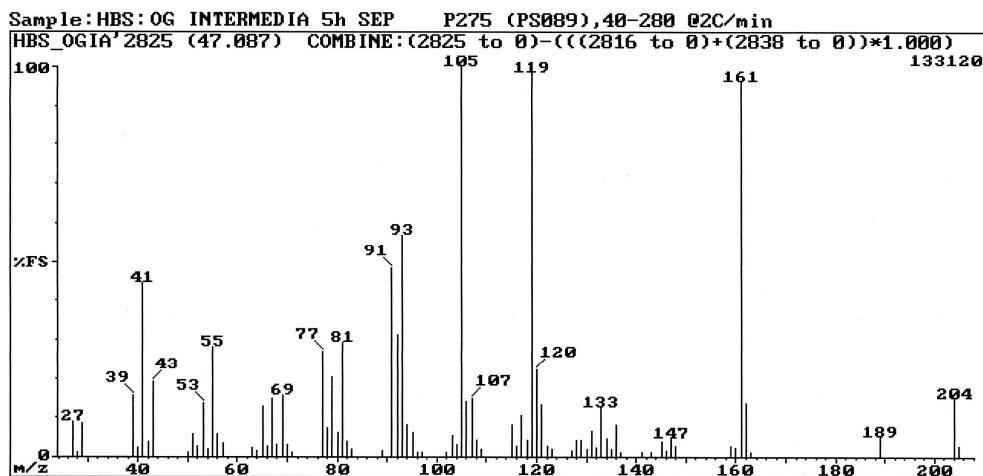


Fig. 3.91: EI mass spectrum of  $\alpha$ -copaene (C205).

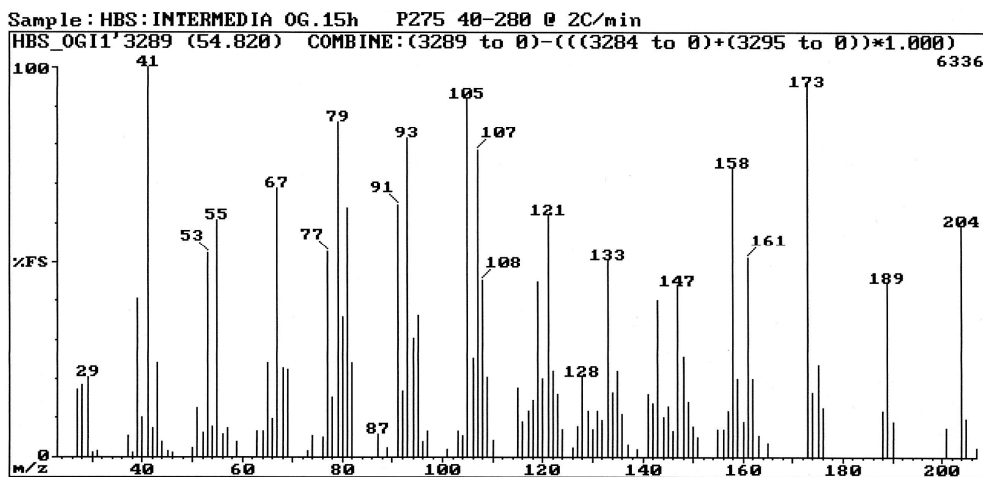


Fig. 3.92: EI mass spectrum of  $\beta$ -selinene (C235).

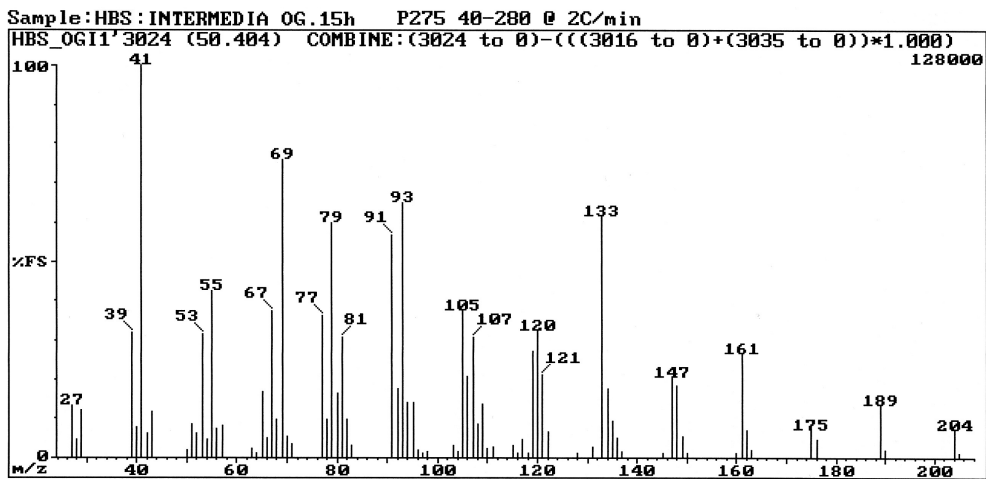


Fig. 3.93: El mass spectrum of (*E*)-caryophyllene (C216).

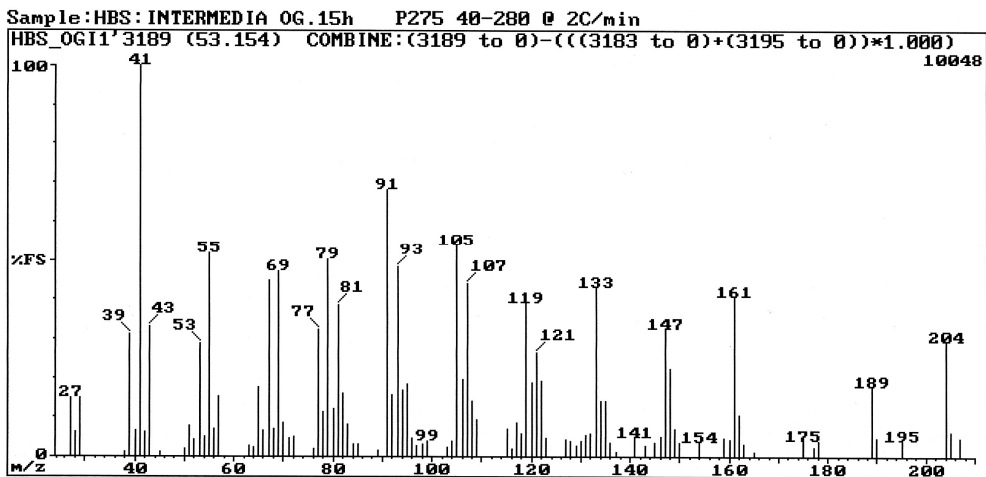


Fig. 3.94: El mass spectrum of 9-*epi*-(*E*)-caryophyllene (C226).

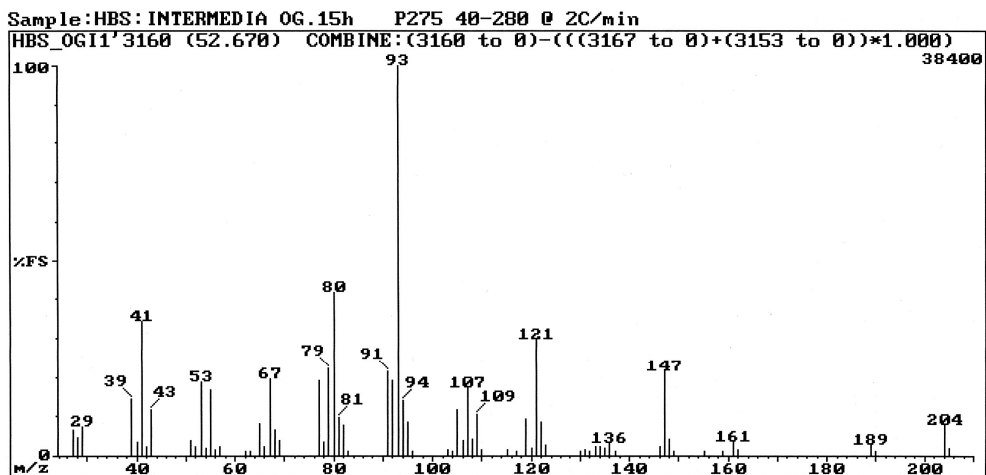


Fig. 3.95: El mass spectrum of  $\alpha$ -humulene (C221).

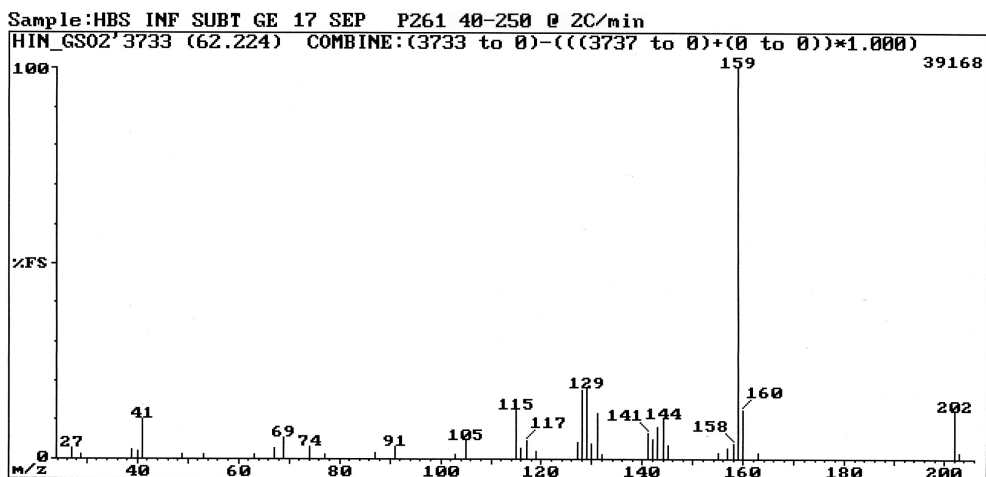


Fig. 3.96: El mass spectrum of *trans*-calamenene (C246).

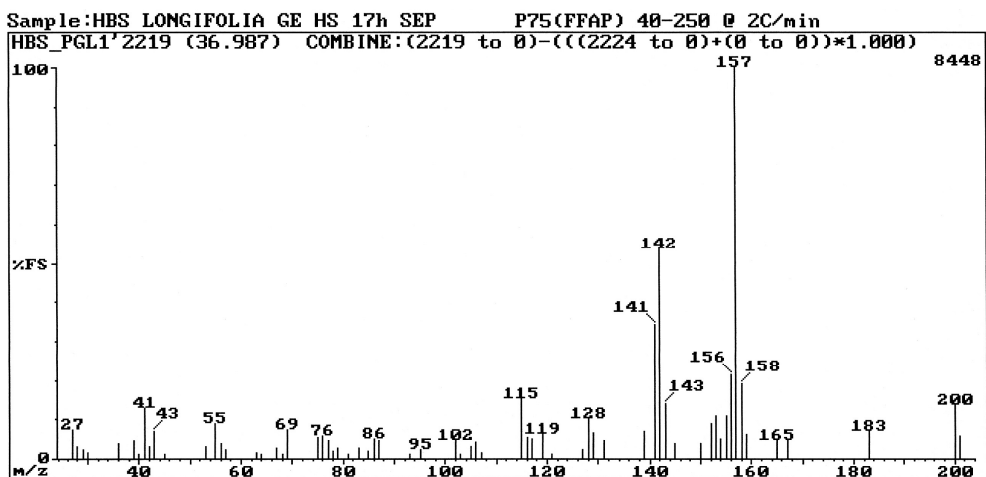


Fig. 3.97: El mass spectrum of  $\alpha$ -calacorene (C252).

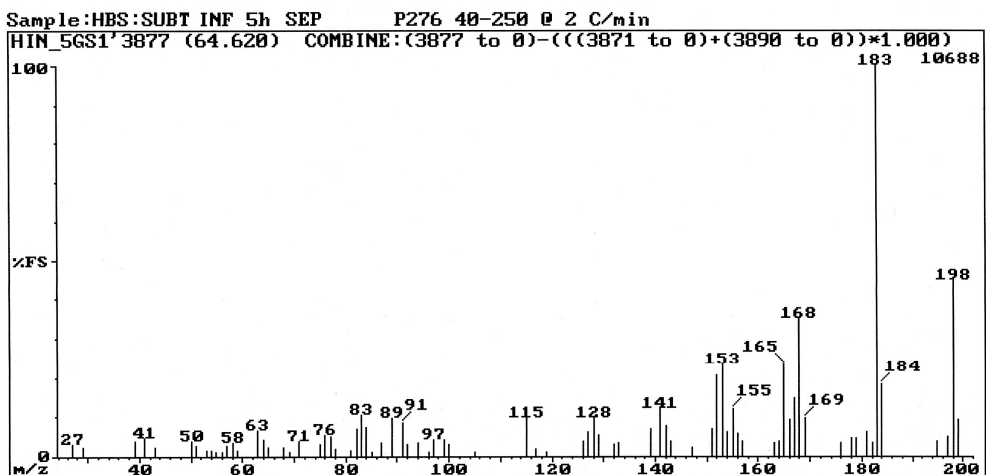


Fig. 3.98: El mass spectrum of cadalene (C290).

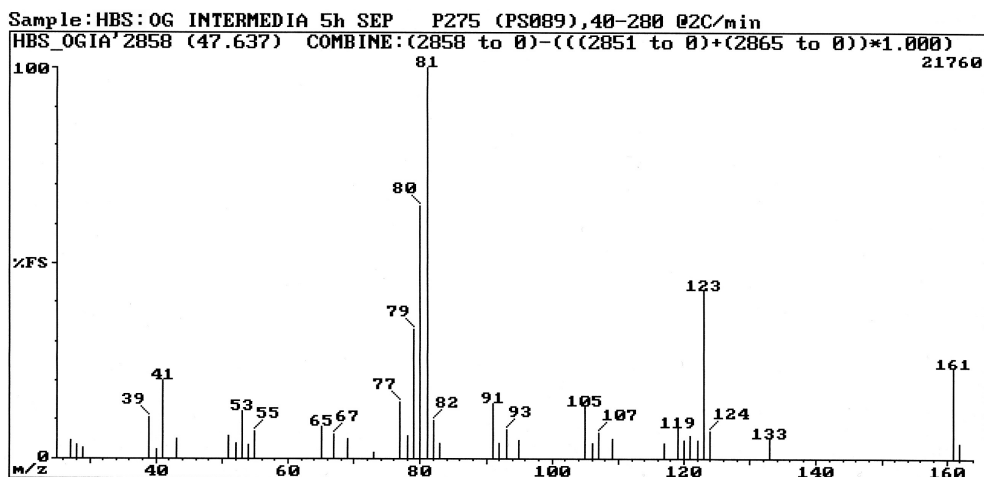


Fig. 3.99: EI mass spectrum of  $\beta$ -bourbonene (C208).

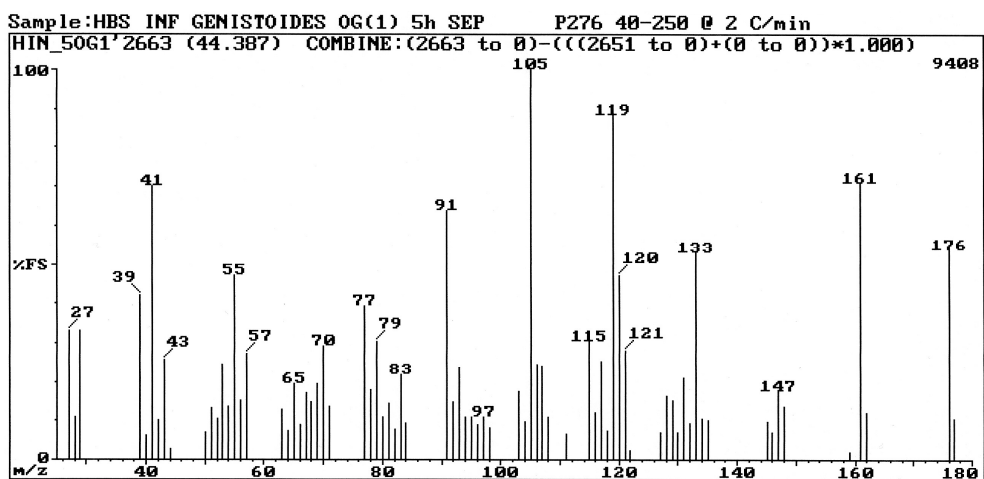


Fig. 3.100: EI mass spectrum of 4,6,8-megastigmatriene (C197).

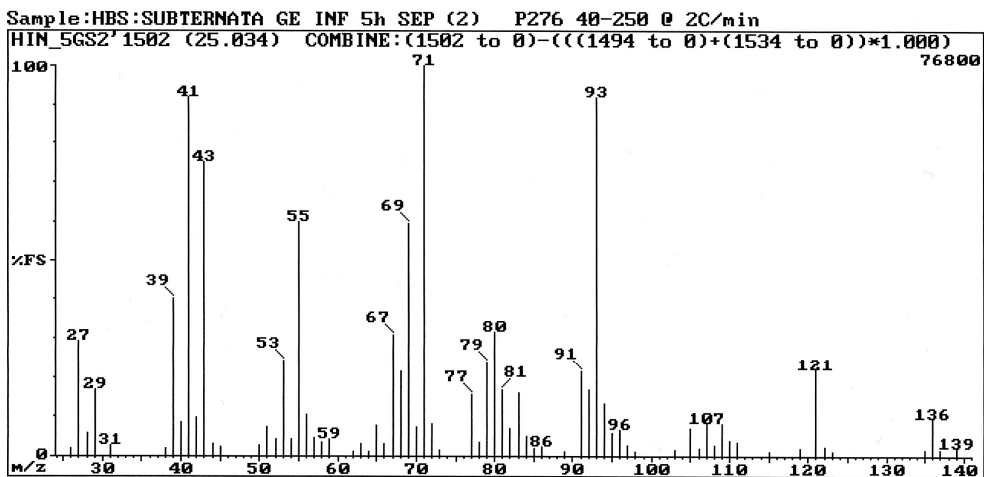


Fig. 3.101: EI mass spectrum of linalool (C76).

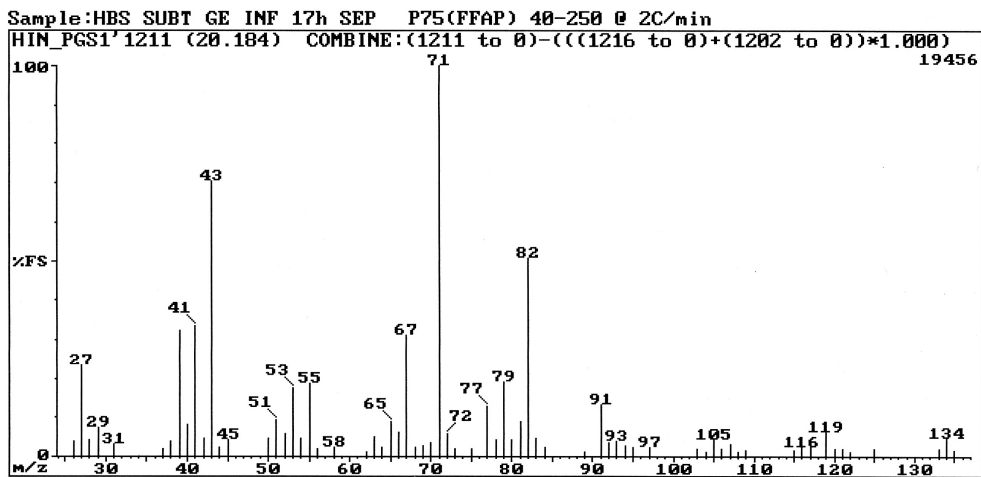


Fig. 3.102: EI mass spectrum of hotrienol (C78).

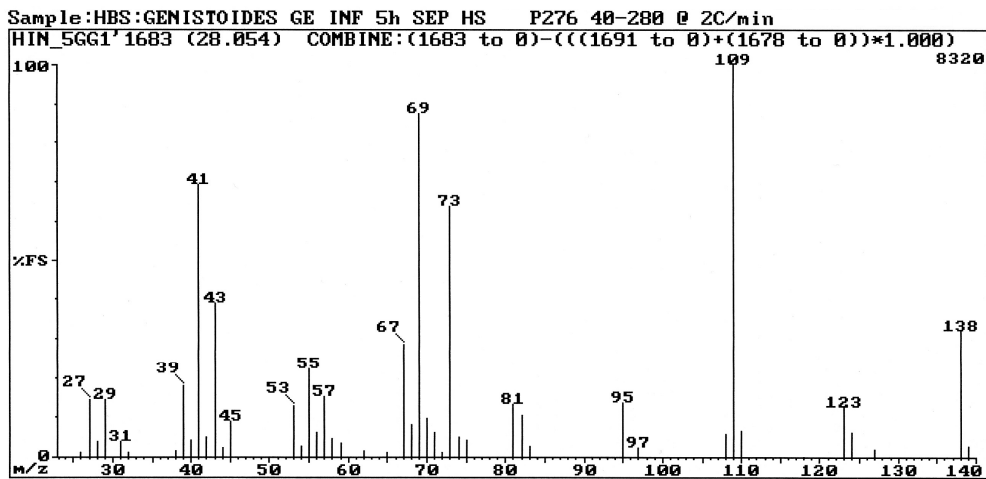


Fig. 3.103: EI mass spectrum of dihydrolinalool (C94).

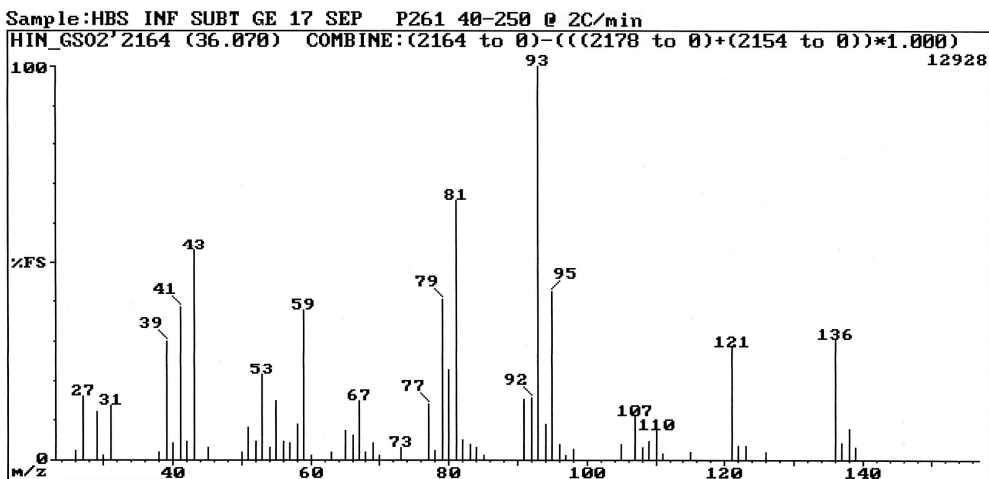


Fig. 3.104: EI mass spectrum of (*E*)-ocimenol (C113).

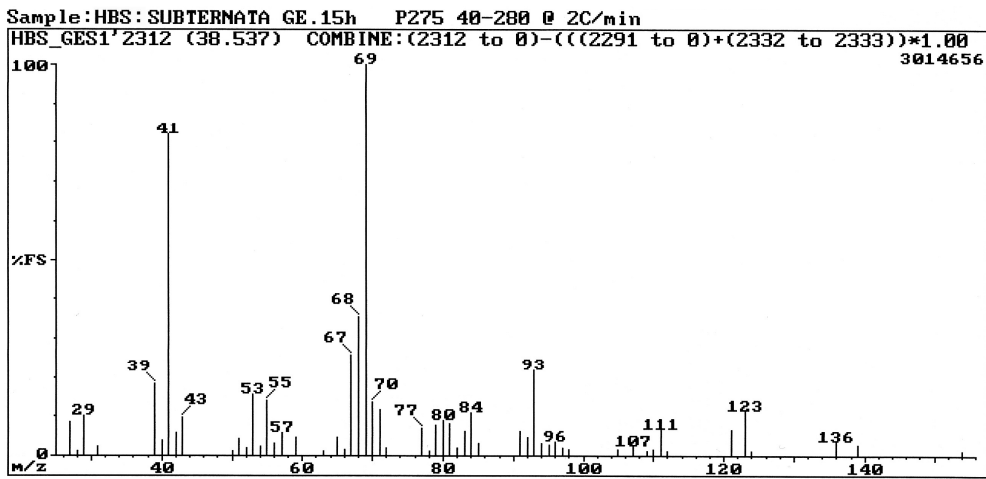


Fig. 3.105: EI mass spectrum of geraniol (C148).

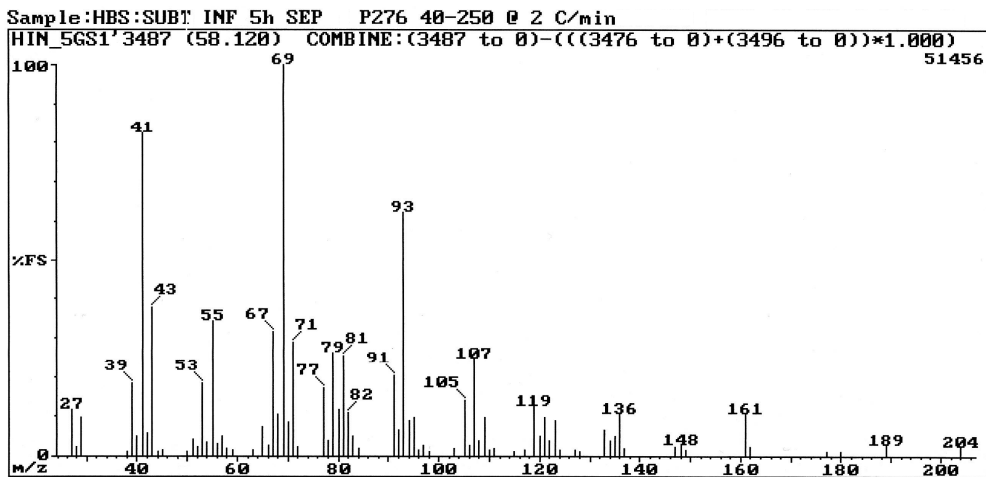


Fig. 3.106: EI mass spectrum of (*E*)-nerolidol (C260).

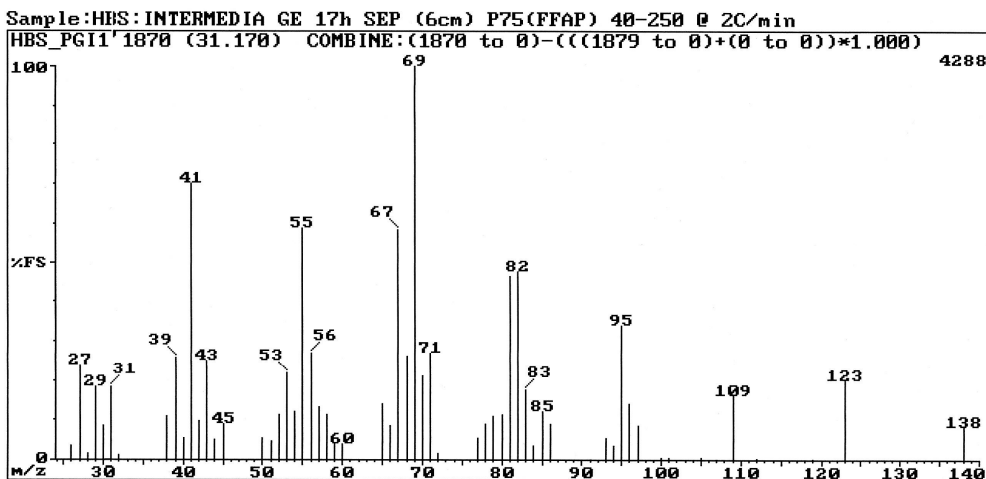


Fig. 3.107: EI mass spectrum of (*R*)- $\beta$ -citronellol (C137).

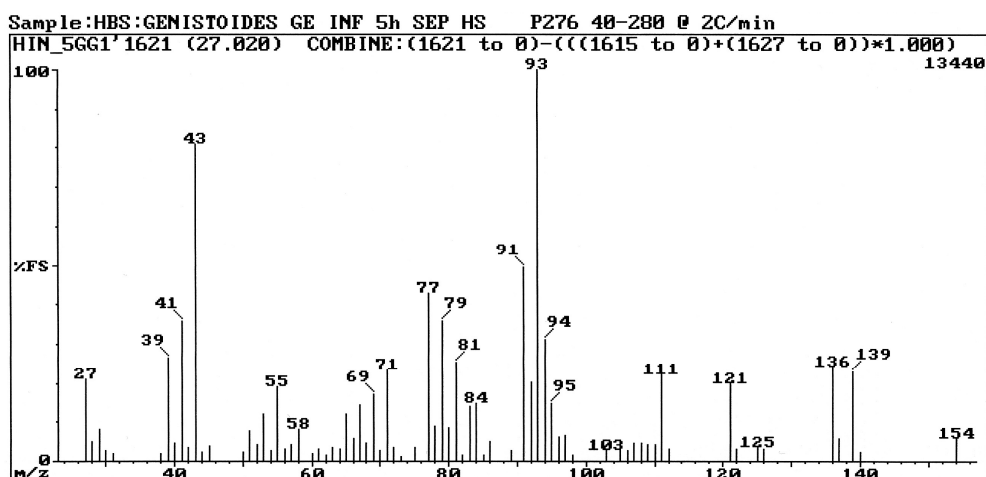


Fig. 3.108: EI mass spectrum of *cis-p*-2-menthen-1-ol (**C86**).

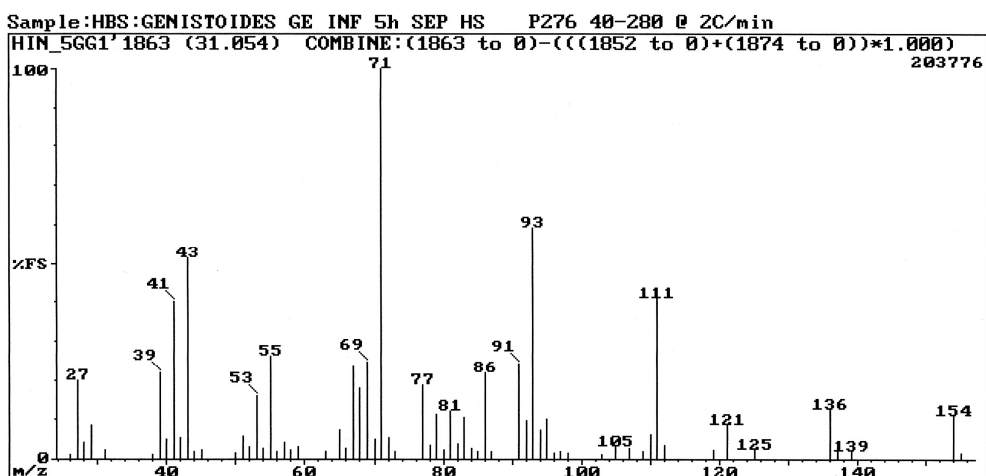


Fig. 3.109: EI mass spectrum of terpinen-4-ol (**C118**).

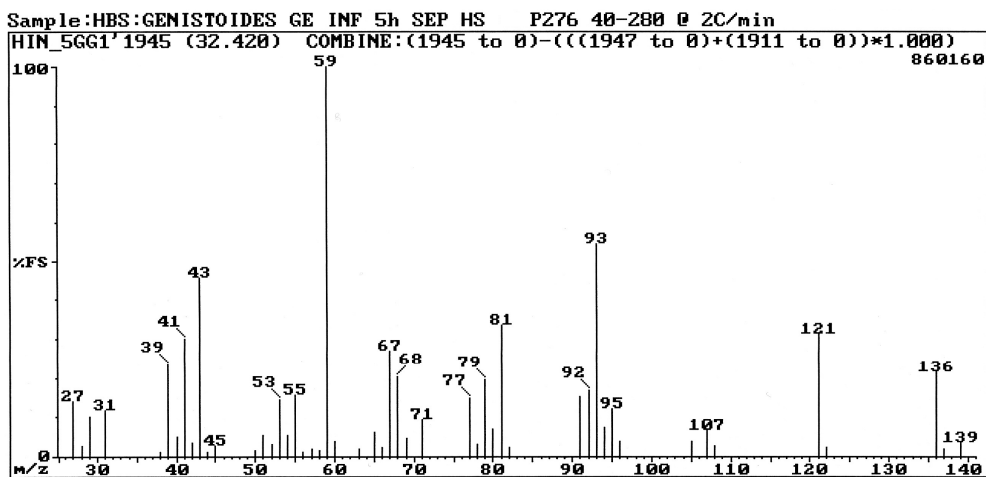


Fig. 3.110: EI mass spectrum of  $\alpha$ -terpineol (**C121**).



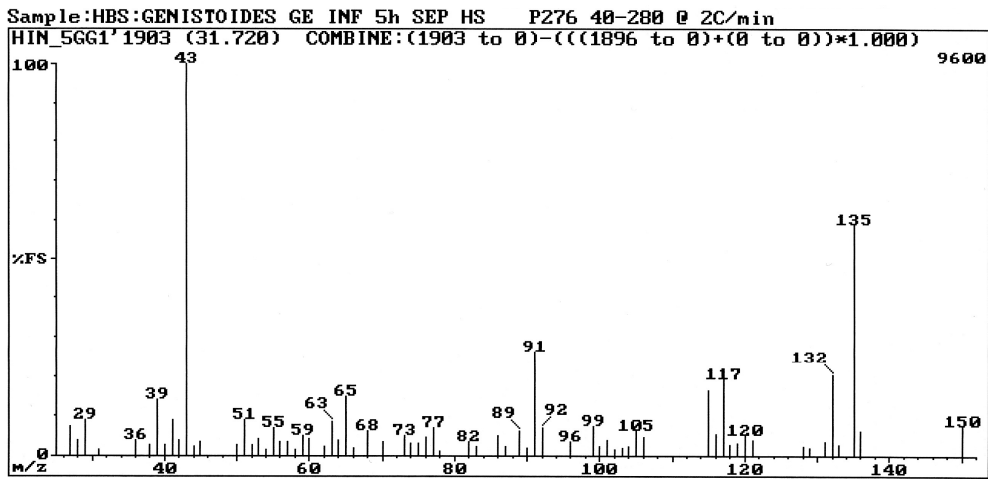


Fig. 3.111: EI mass spectrum of *p*-cymen-8-ol (C120).

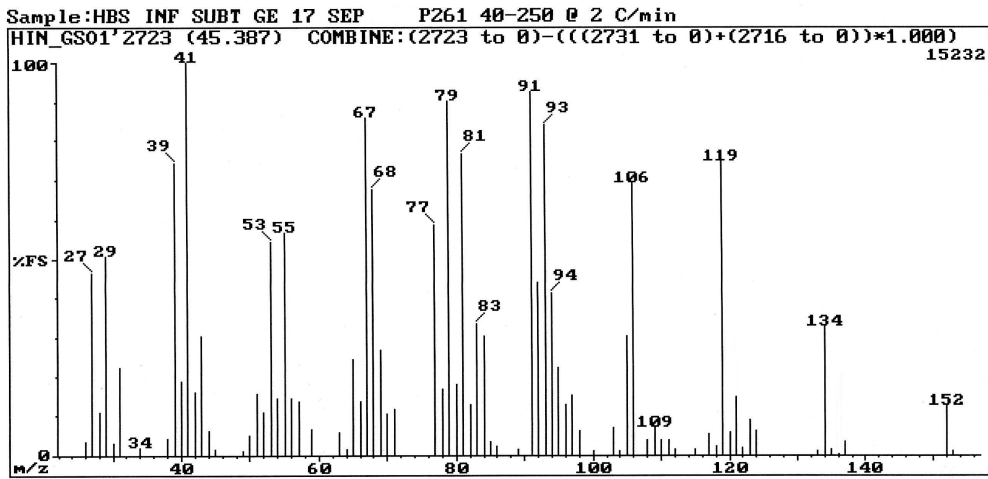


Fig. 3.112: EI mass spectrum of limonen-10-ol (C160).

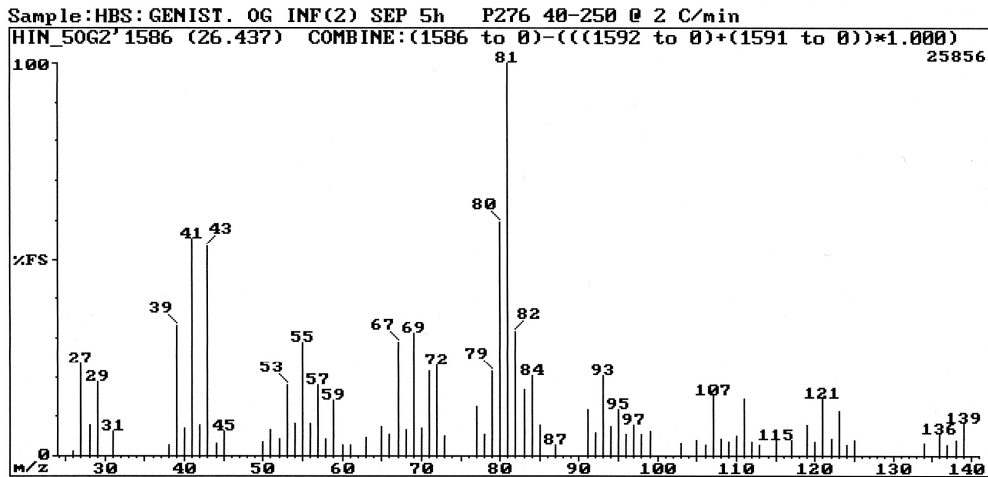


Fig. 3.113: EI mass spectrum of  $\alpha$ -fenchol (C85).

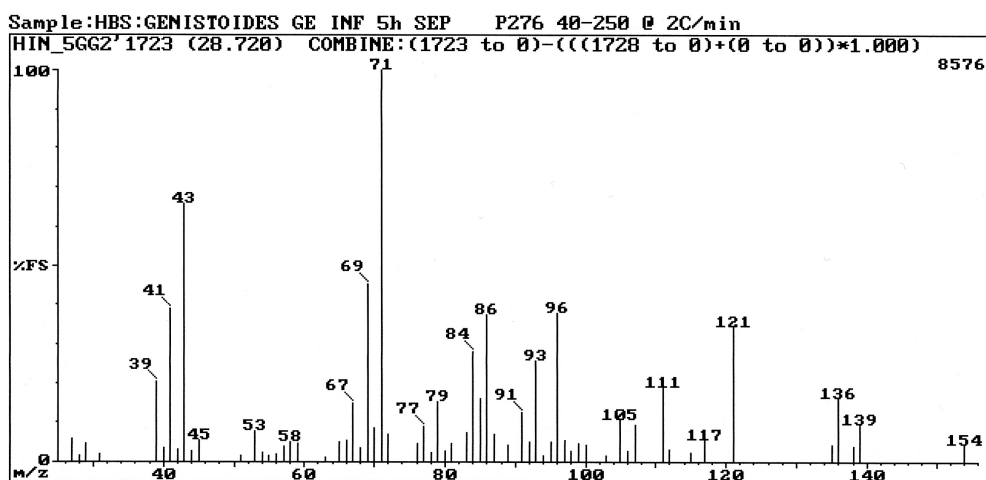


Fig. 3.114: EI mass spectrum of camphene hydrate (C98).

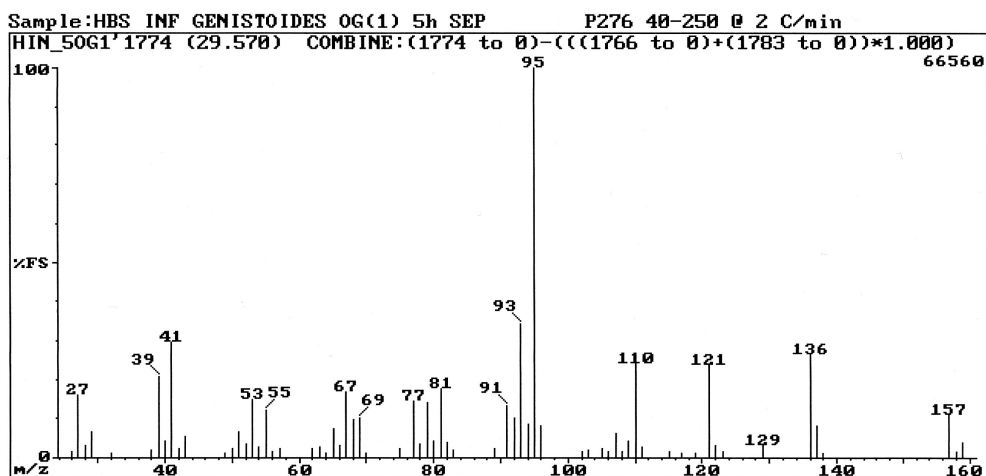


Fig. 3.115: EI mass spectrum of 2-chloro-1,7,7-trimethylbicyclo[2.2.1]heptane (C111).

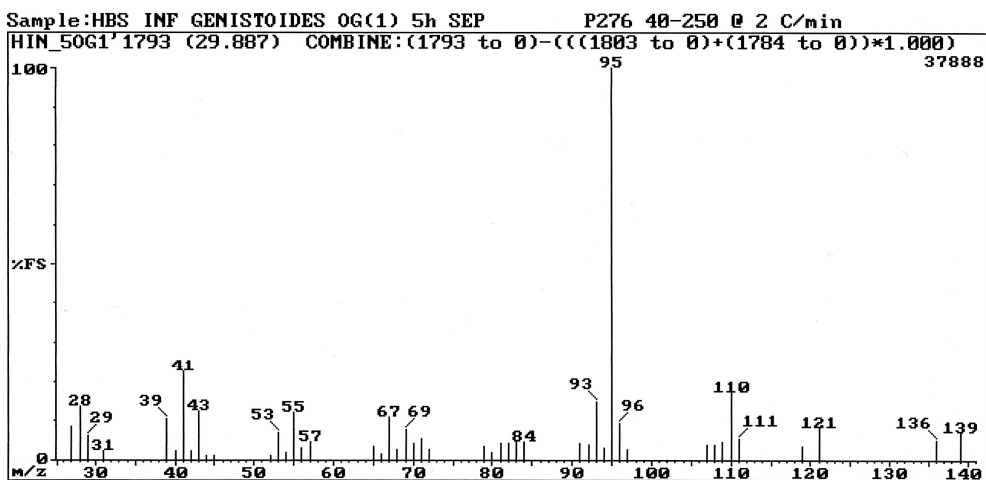


Fig. 3.116: EI mass spectrum of borneol (C112).

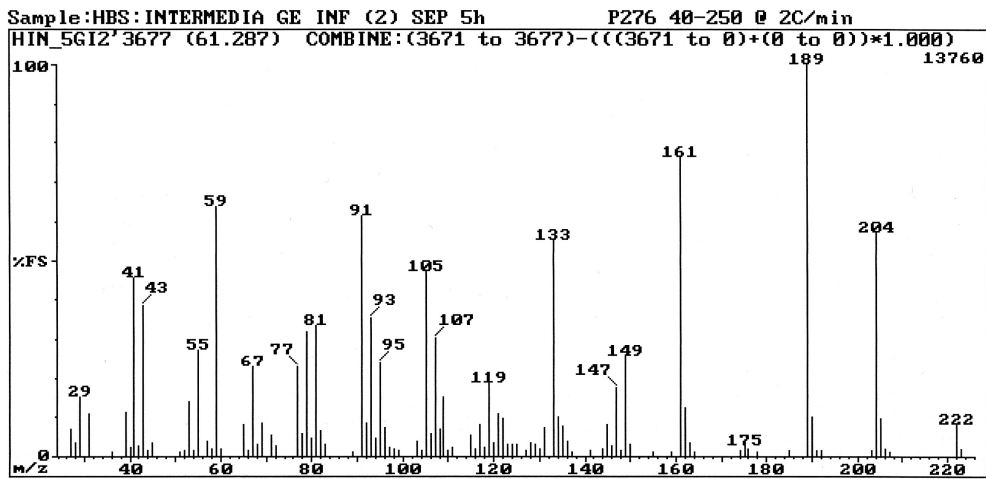


Fig. 3.117: EI mass spectrum of 10-*epi*- $\gamma$ -eudesmol (C278).

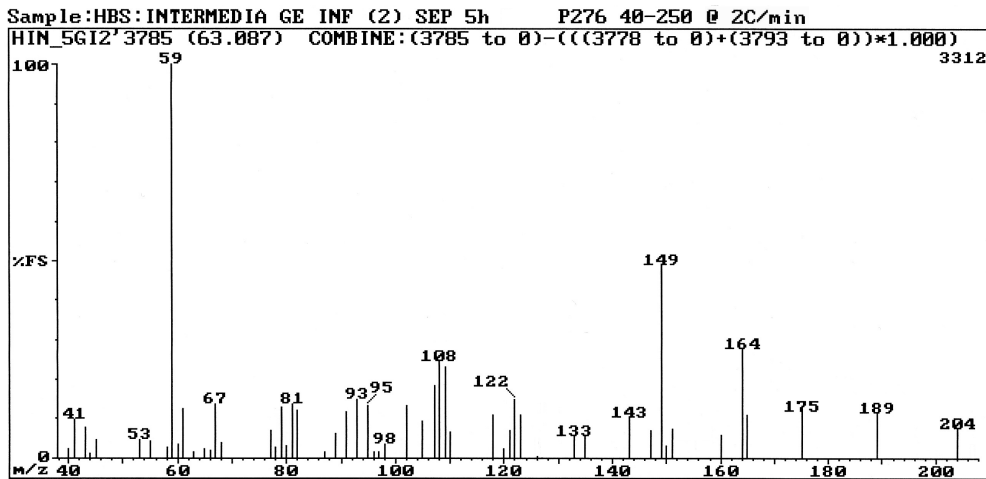


Fig. 3.118: EI mass spectrum of  $\beta$ -eudesmol (C286).

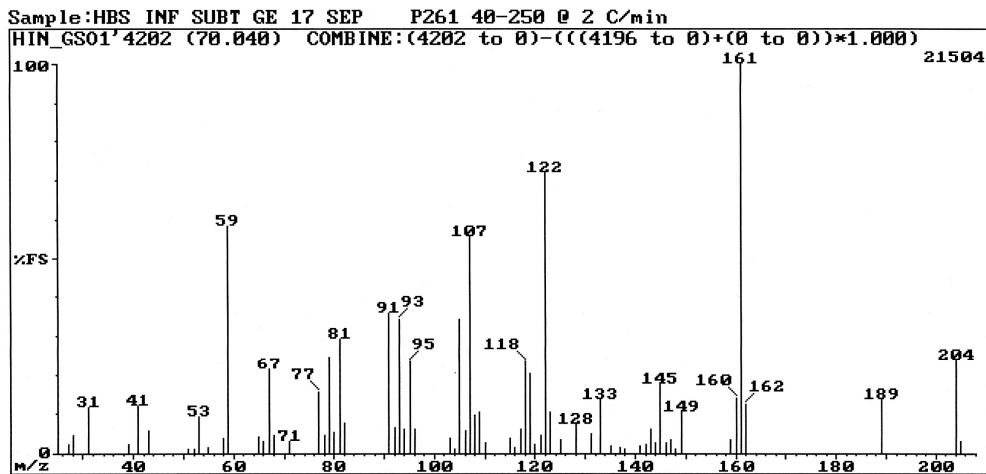


Fig. 3.119: EI mass spectrum of 7-*epi*- $\alpha$ -eudesmol (C289).

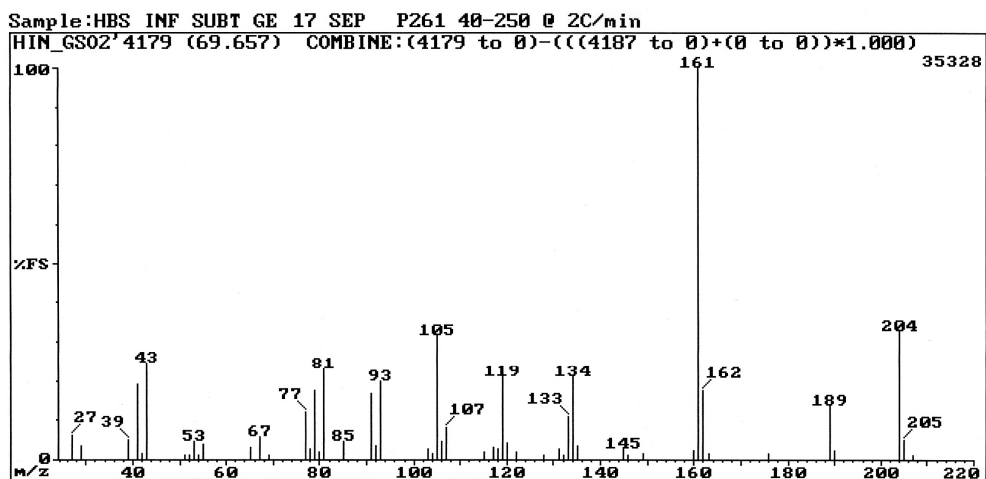


Fig. 3.120: EI mass spectrum of *epi*- $\alpha$ -cadinol (C284).

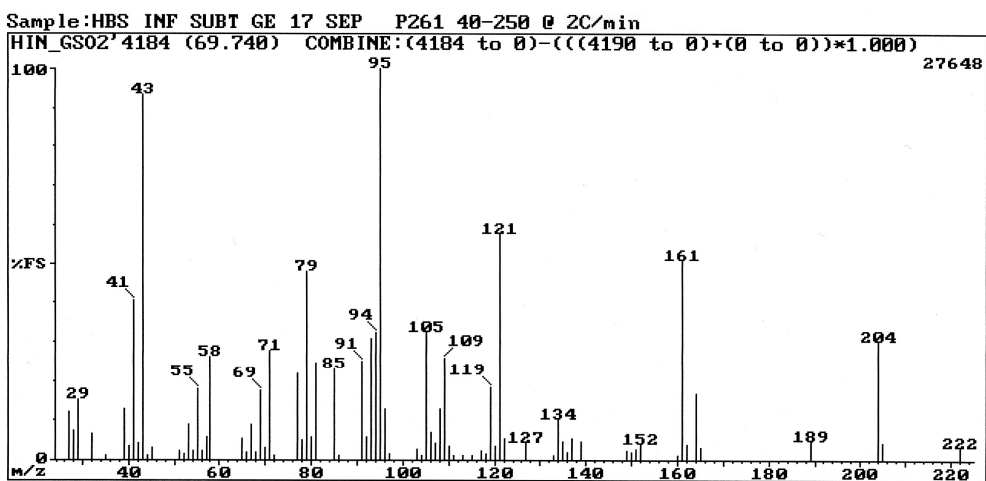


Fig. 3.121: EI mass spectrum of *epi*- $\alpha$ -muurolol (C285).

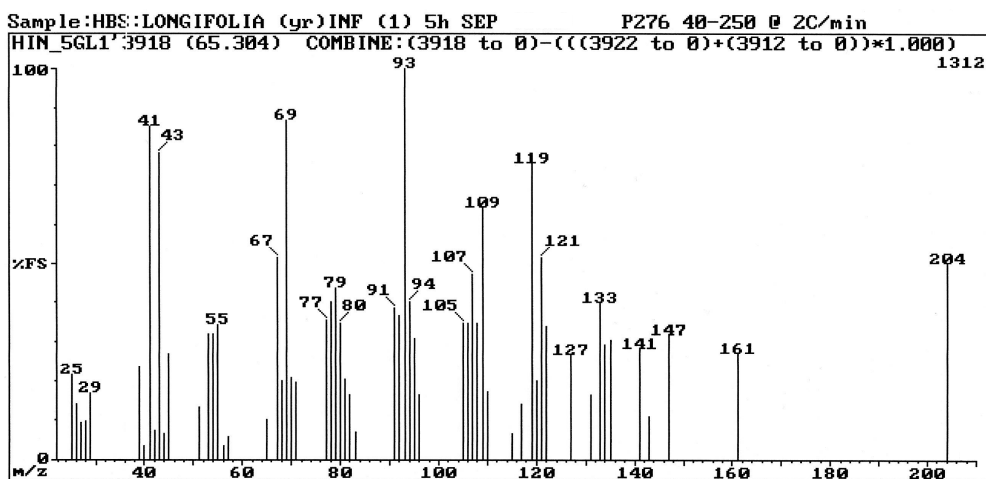


Fig. 3.122: EI mass spectrum of *epi*- $\alpha$ -bisabolol (C292).

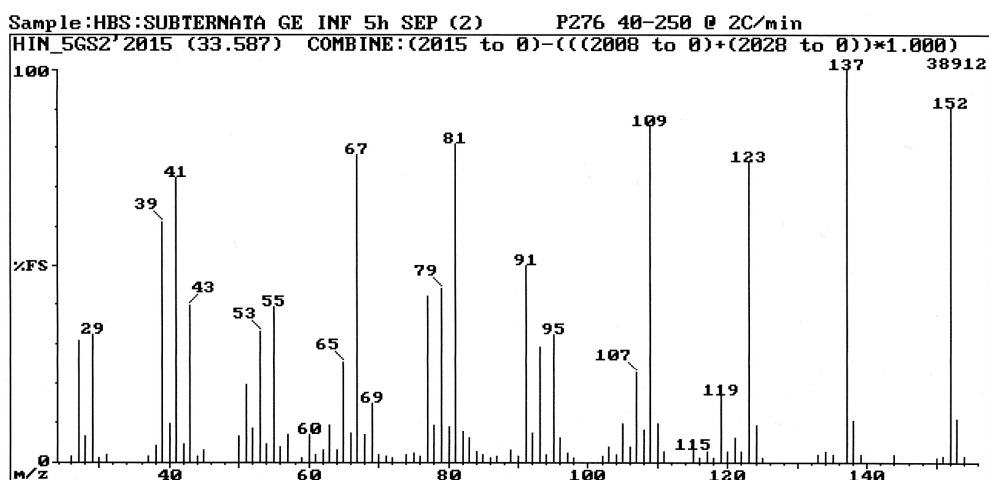


Fig. 3.123: EI mass spectrum of  $\beta$ -cyclosital (C129).

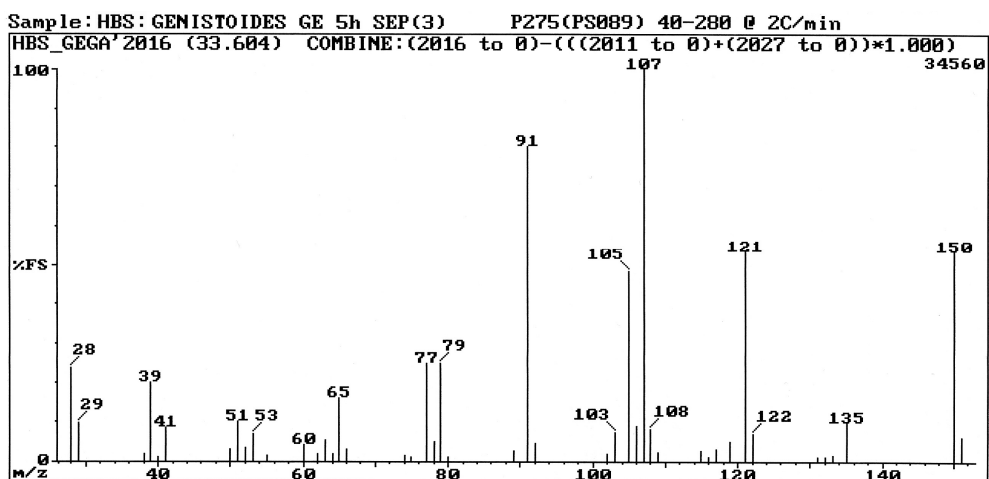


Fig. 3.124: EI mass spectrum of safranal (C122).

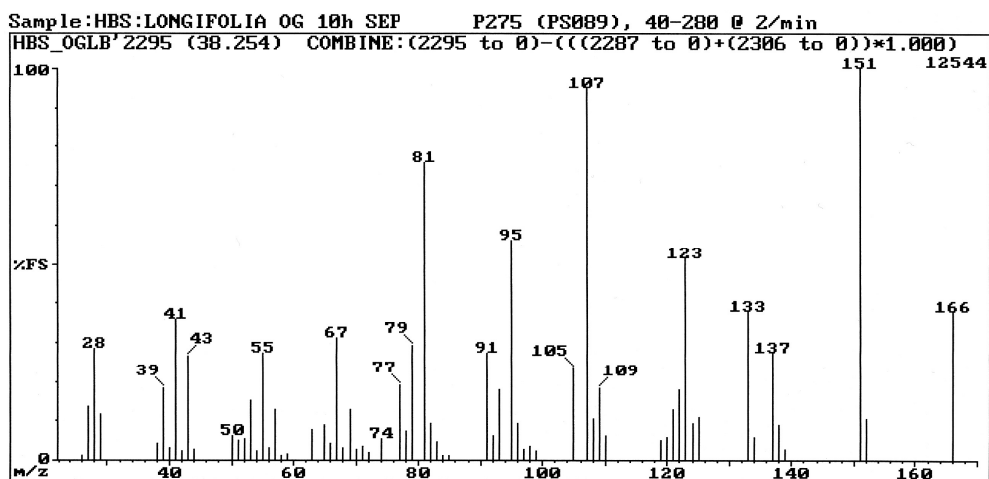


Fig. 3.125: EI mass spectrum of 2,6,6-trimethyl-1-cyclohexene-1-acetaldehyde (C146).

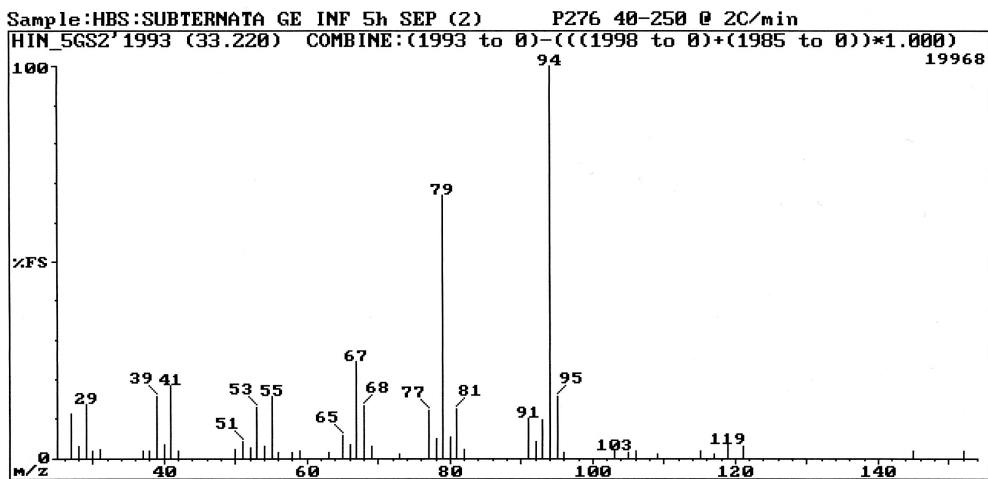


Fig. 3.126: EI mass spectrum of (+)-*p*-menth-1-en-9-al (C125).

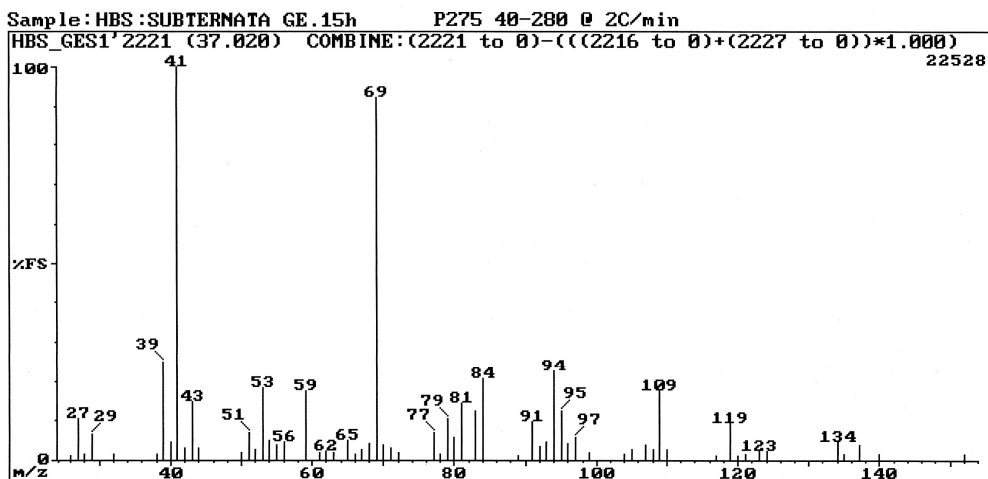


Fig. 3.127: EI mass spectrum of neral (C139).

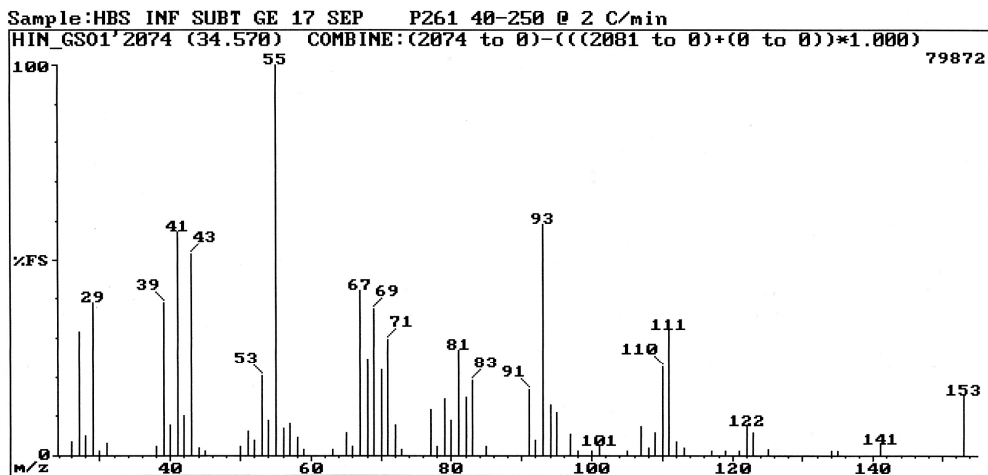


Fig. 3.128: EI mass spectrum of lilac aldehyde (C97).

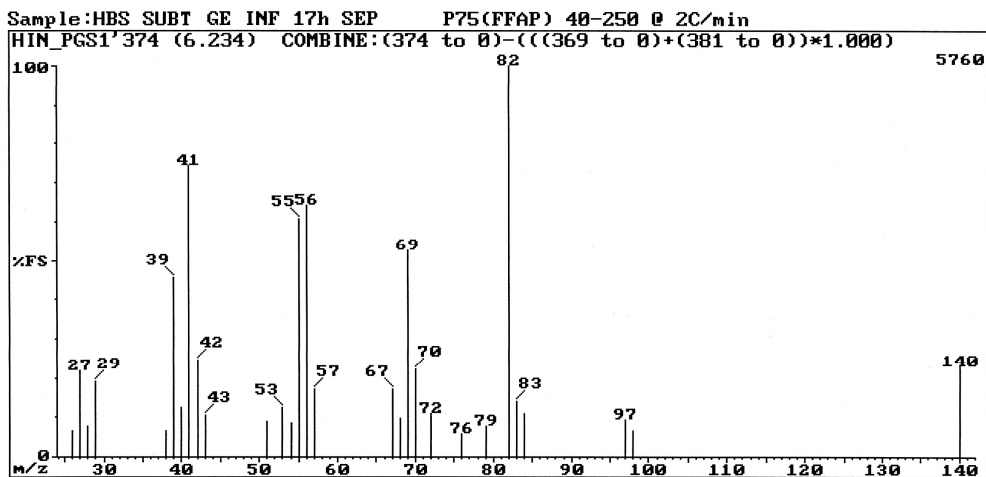


Fig. 3.129: EI mass spectrum of 2,2,6-trimethylcyclohexanone (C51).

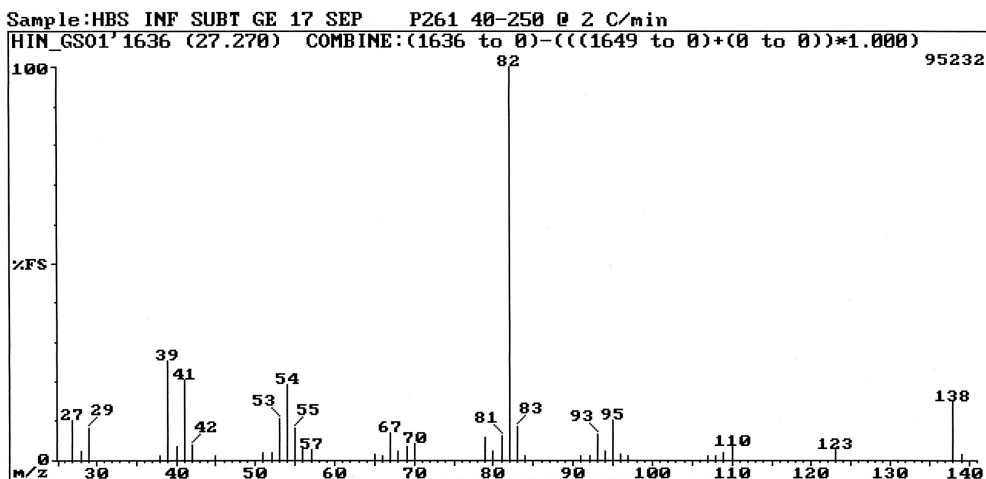


Fig. 3.130: EI mass spectrum of 2,6,6-trimethylcyclohex-2-enone (C59).

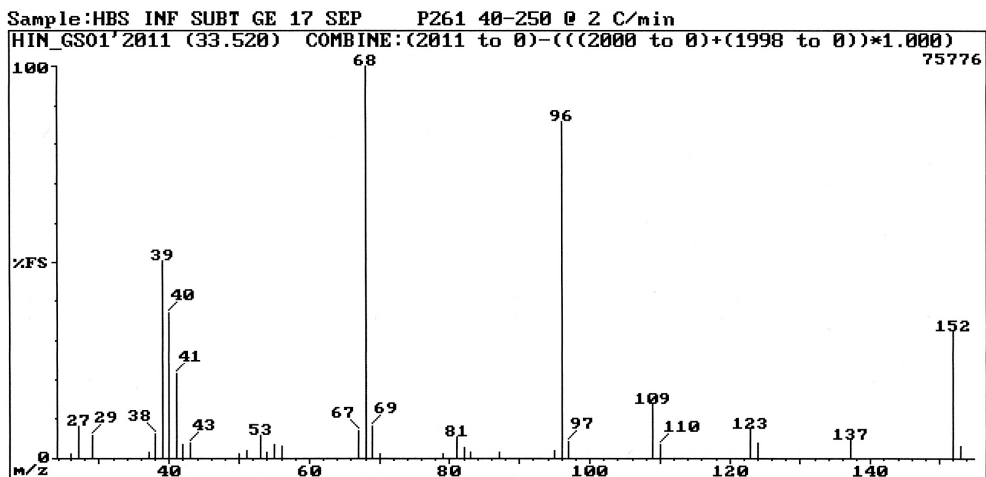


Fig. 3.131: EI mass spectrum of 4-ketoisophorone (C92).

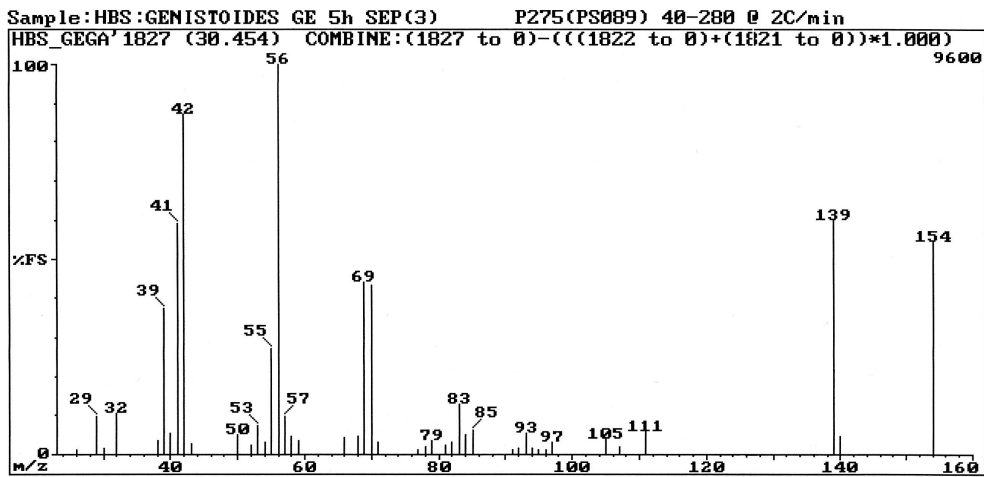


Fig. 3.132: EI mass spectrum of 2,2,6-trimethyl-1,4-cyclohexanedione (**C104**).

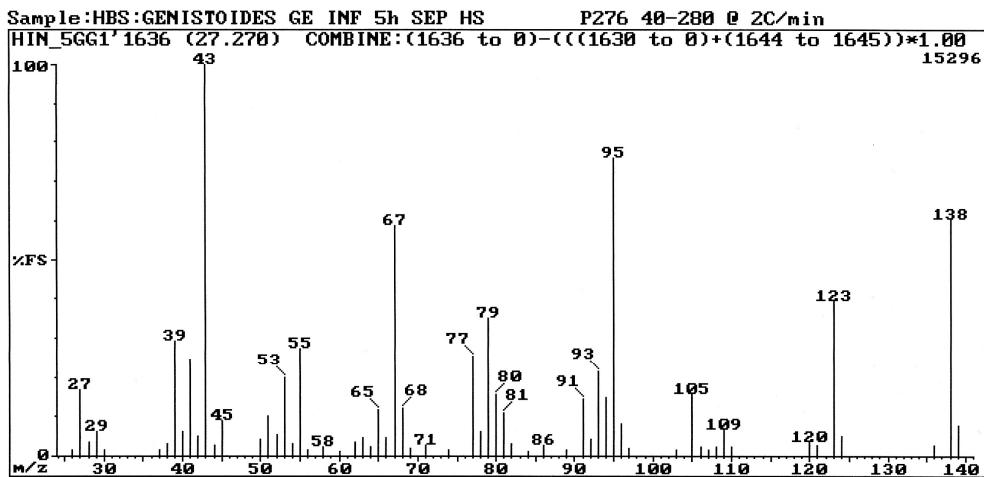


Fig. 3.133: EI mass spectrum of 4-acetyl-1-methylcyclohexene (**C89**).

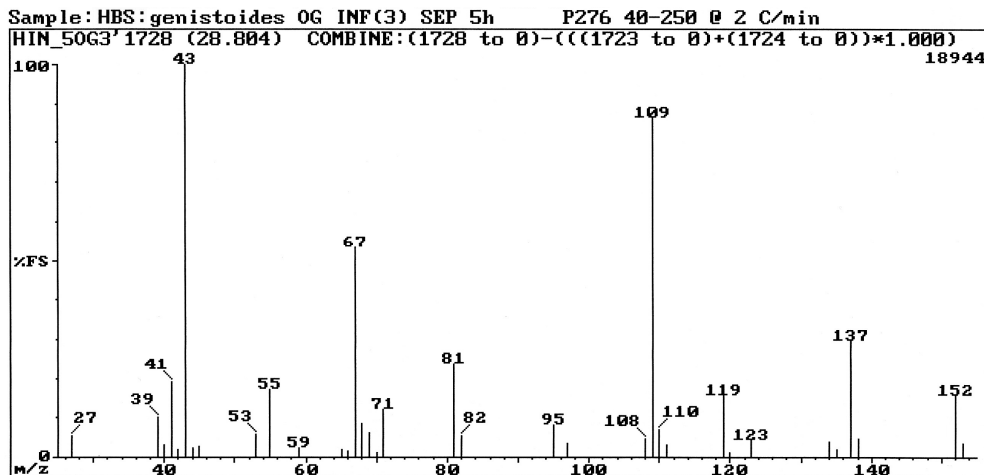


Fig. 3.134: EI mass spectrum of 1-(1,4-dimethyl-3-cyclohexen-1-yl)ethanone (**C99**).



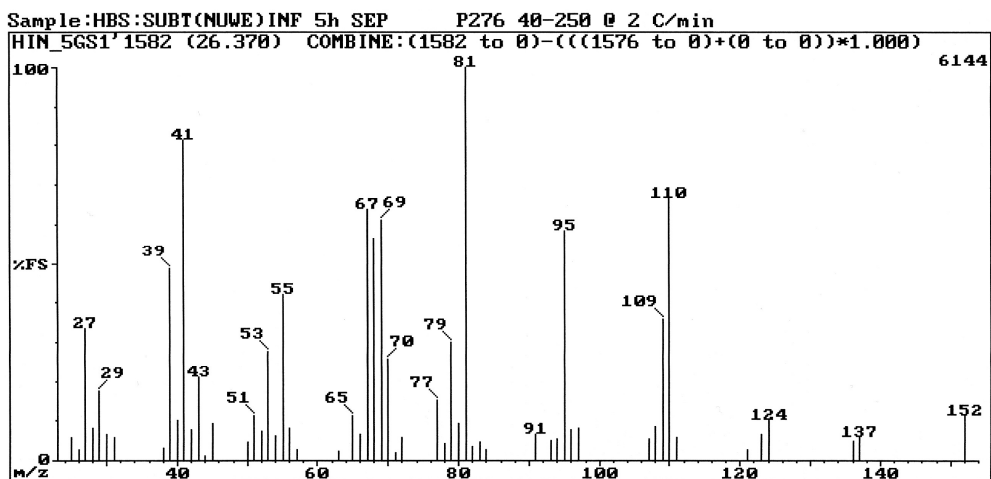


Fig. 3.135: EI mass spectrum of 3-thujanone (C84).

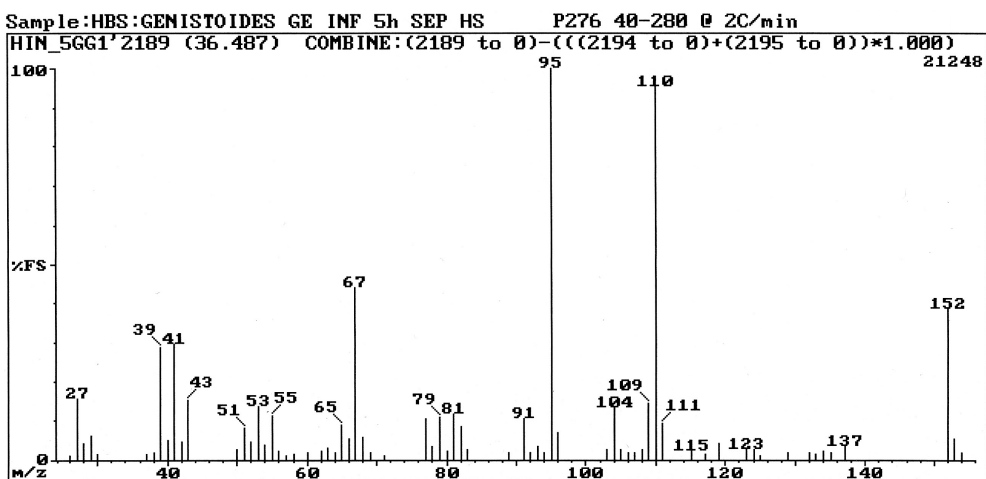


Fig. 3.136: EI mass spectrum of carvenone (C143).

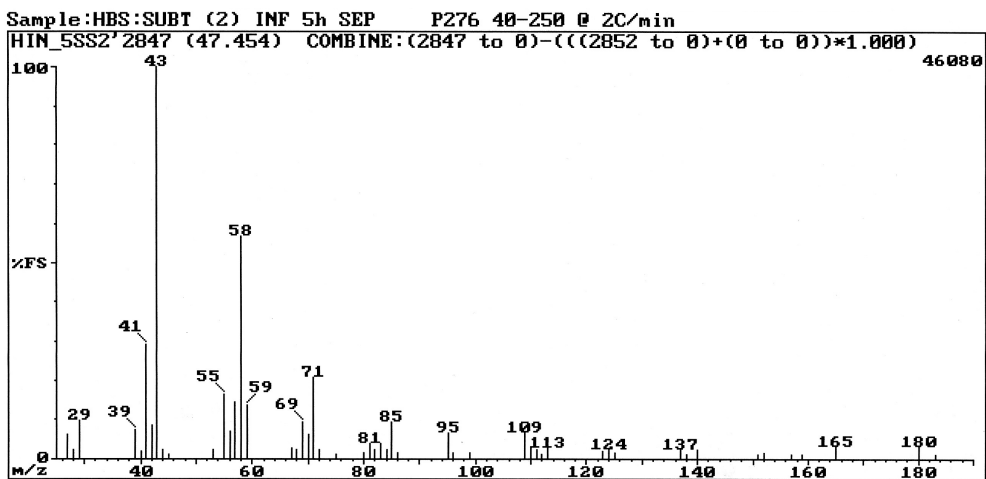


Fig. 3.137: EI mass spectrum of 6,10-dimethyl-2-undecanone (C209).

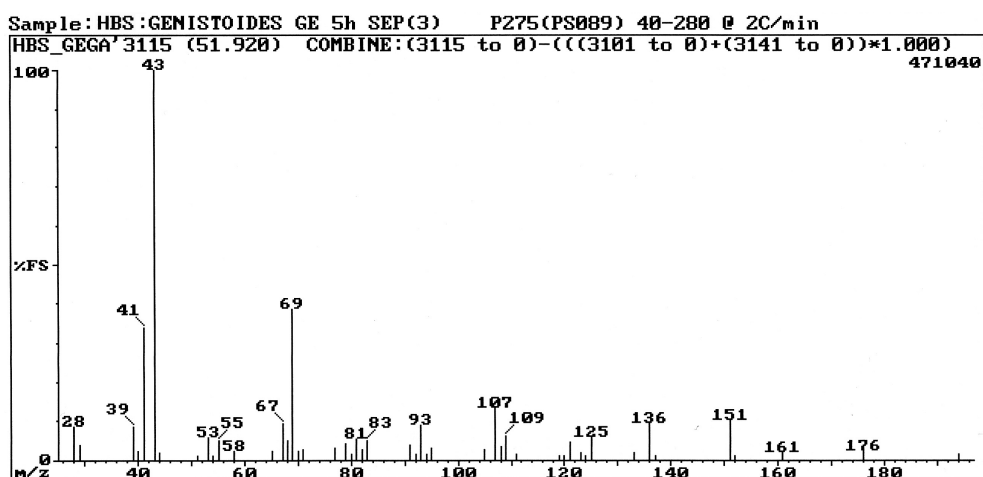


Fig. 3.138: EI mass spectrum of geranylacetone (**C220**).

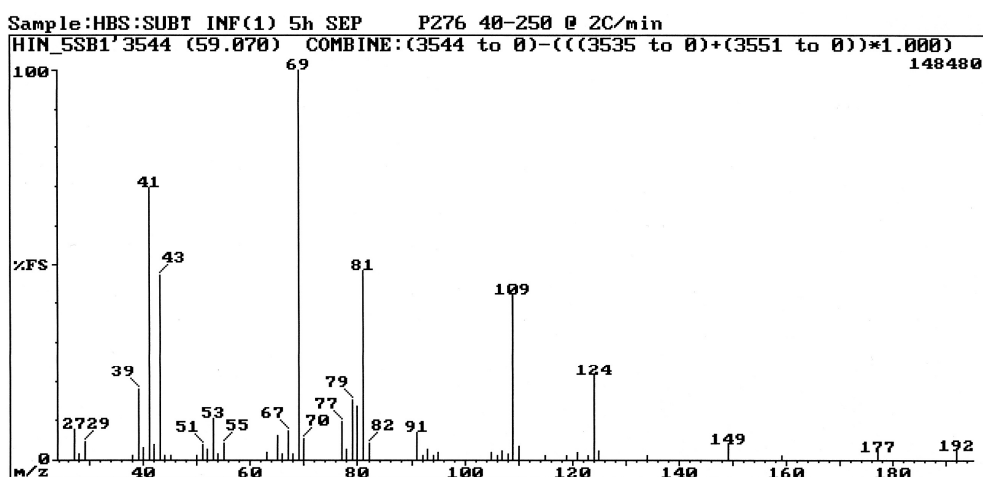


Fig. 3.139: EI mass spectrum of (*E,E*)-pseudoionone (**C266**).

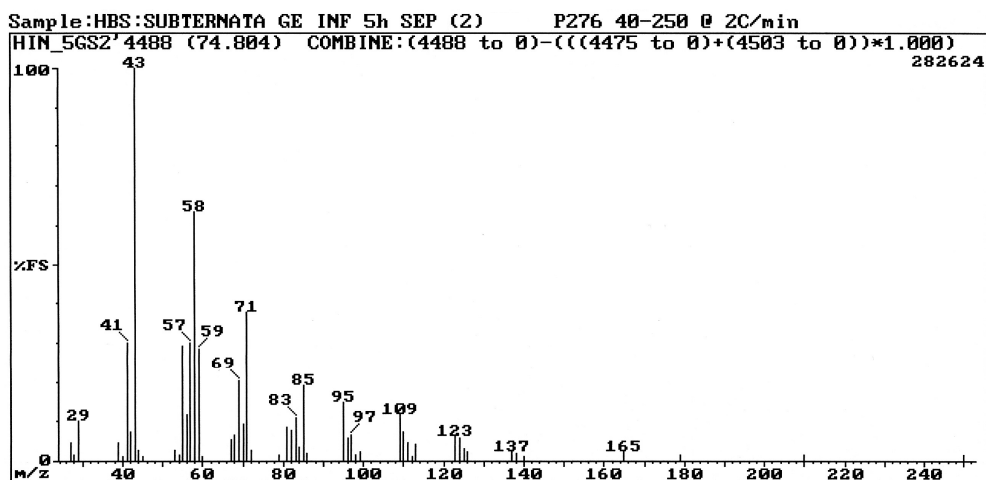


Fig. 3.140: EI mass spectrum of hexahydrofarnesylacetone (**C299**).

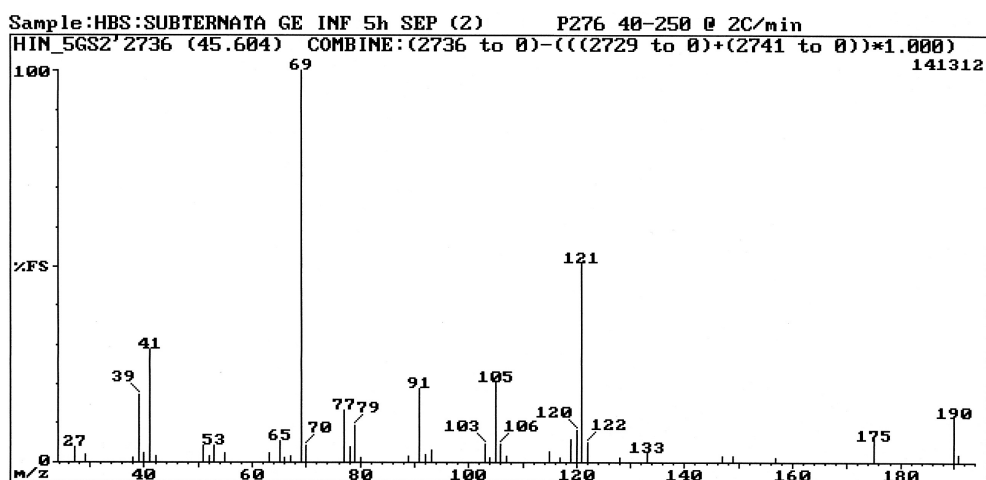


Fig. 3.141: EI mass spectrum of (*E*)-β-damascenone (C204).

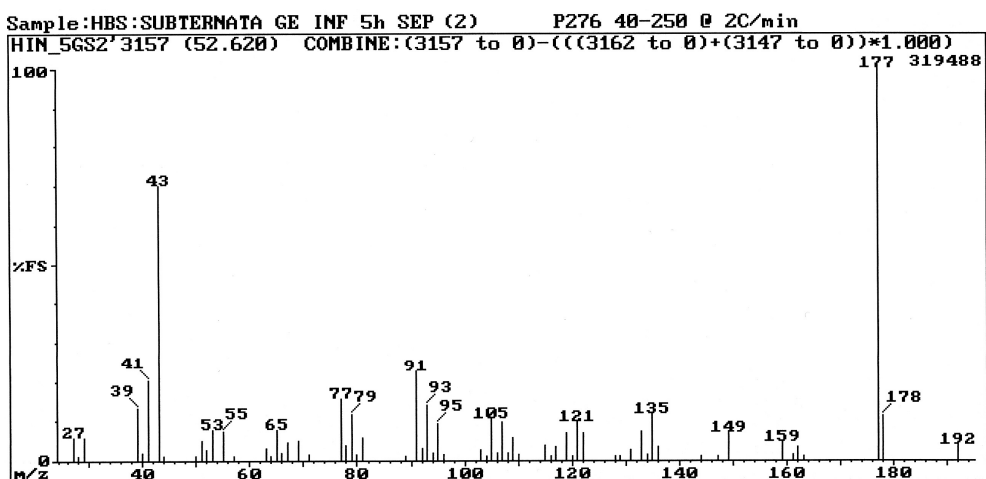


Fig. 3.142: EI mass spectrum of (*E*)-β-ionone (C234).

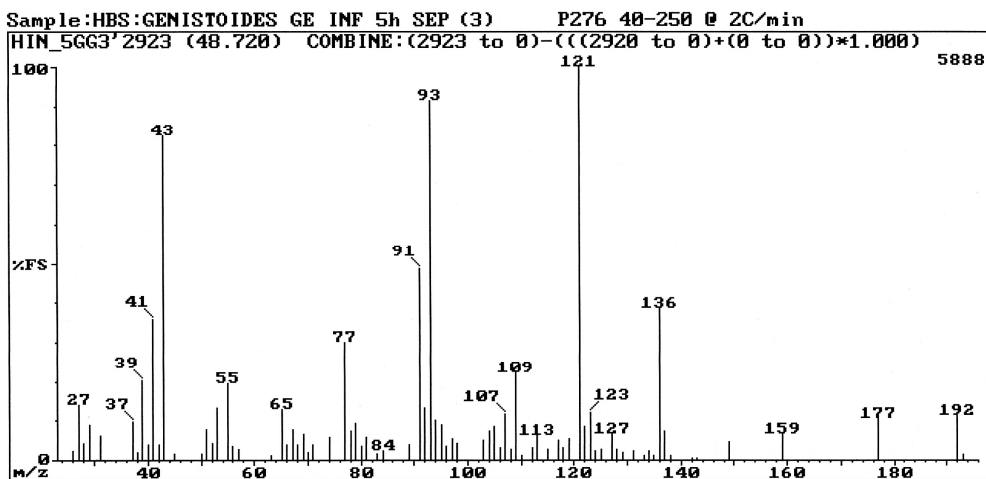


Fig. 3.143: EI mass spectrum of (*R*)-α-ionone (C217).

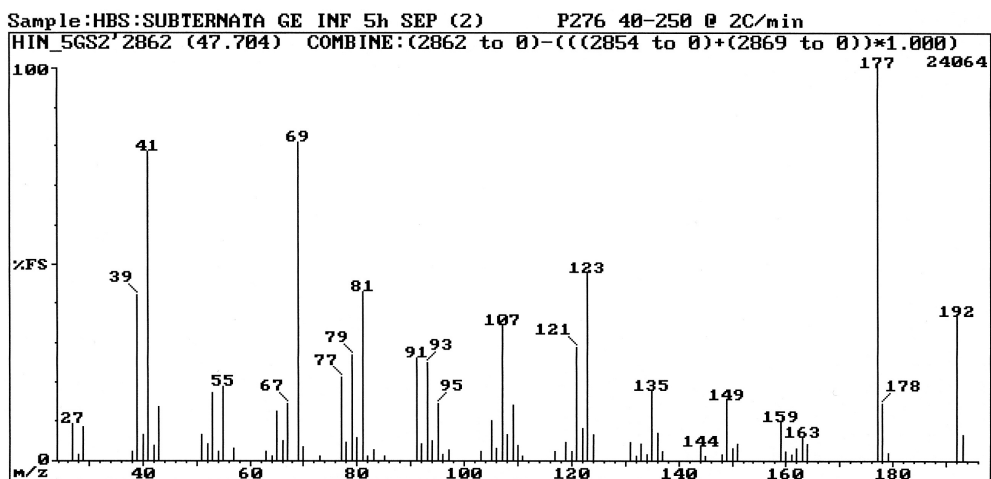


Fig. 3.144: EI mass spectrum of (*E*)- $\beta$ -damascone (C212).

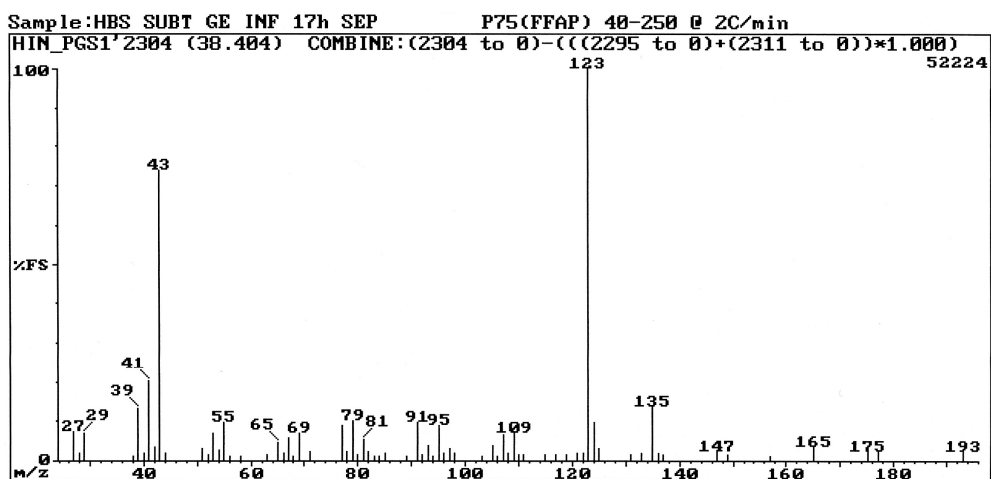


Fig. 3.145: EI mass spectrum of 5,6-epoxy- $\beta$ -ionone (C232).

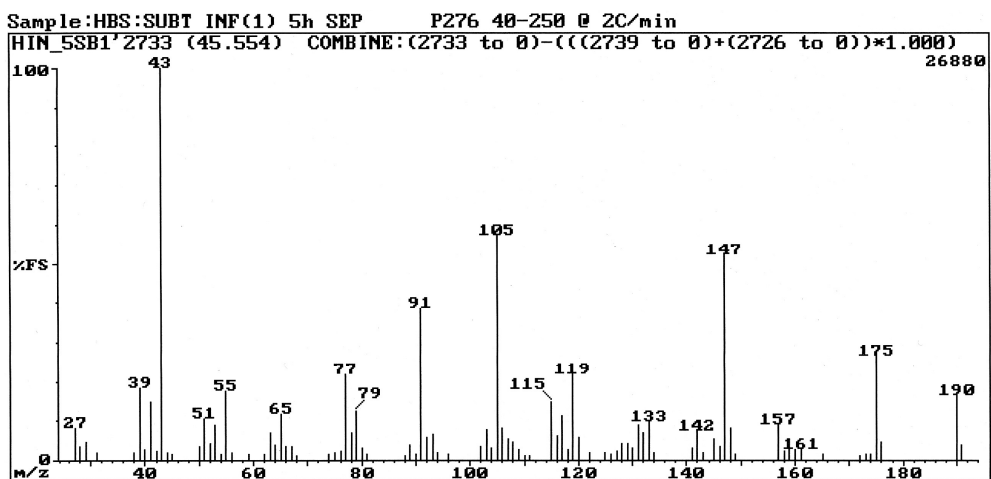


Fig. 3.146: EI mass spectrum of 2,3-dehydro- $\alpha$ -ionone (C203).

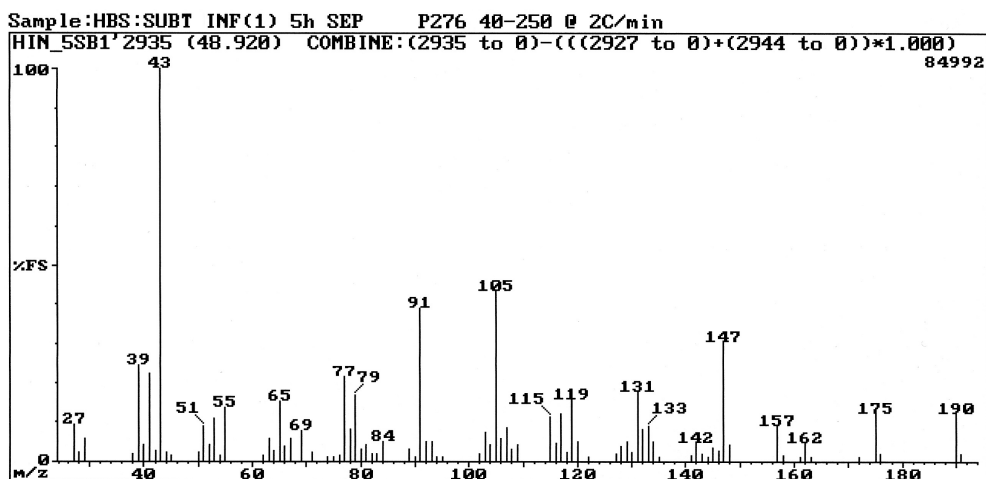


Fig. 3.147: EI mass spectrum of 3,4-dehydro- $\gamma$ -ionone (C218)

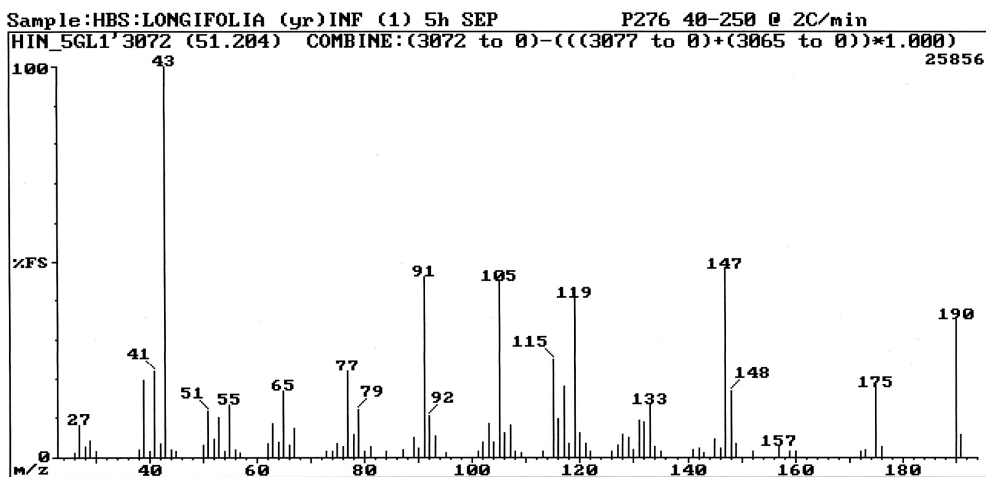


Fig. 3.148: EI mass spectrum of 2,3-dehydro- $\gamma$ -ionone (C222).

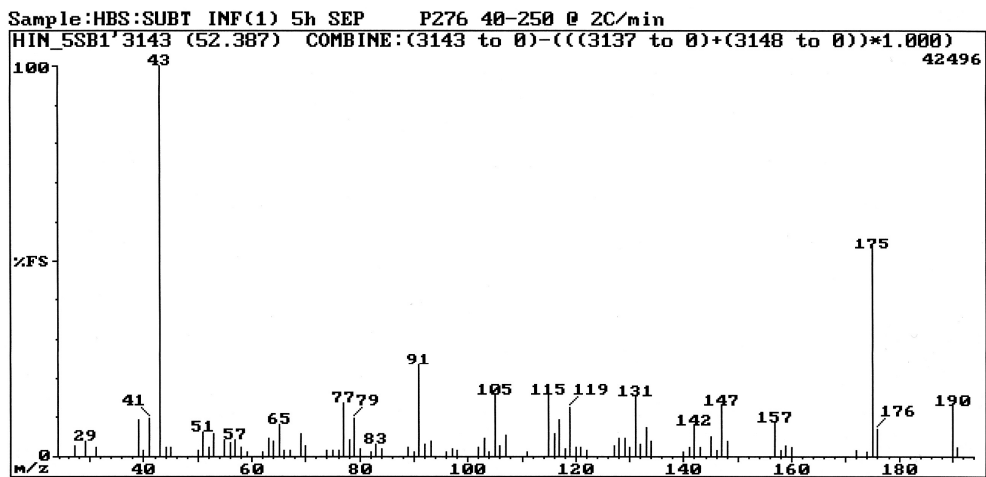


Fig. 3.149: EI mass spectrum of 3,4-dehydro- $\beta$ -ionone (C230).

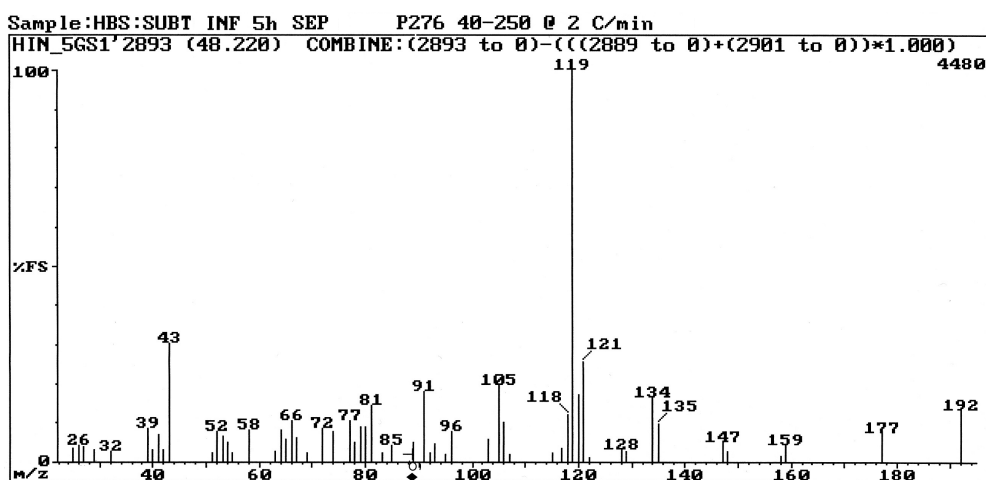


Fig. 3.150: EI mass spectrum of 4-(2,6,6-trimethyl-1,3-cyclohexadien-1-yl)-2-butanone (C214).

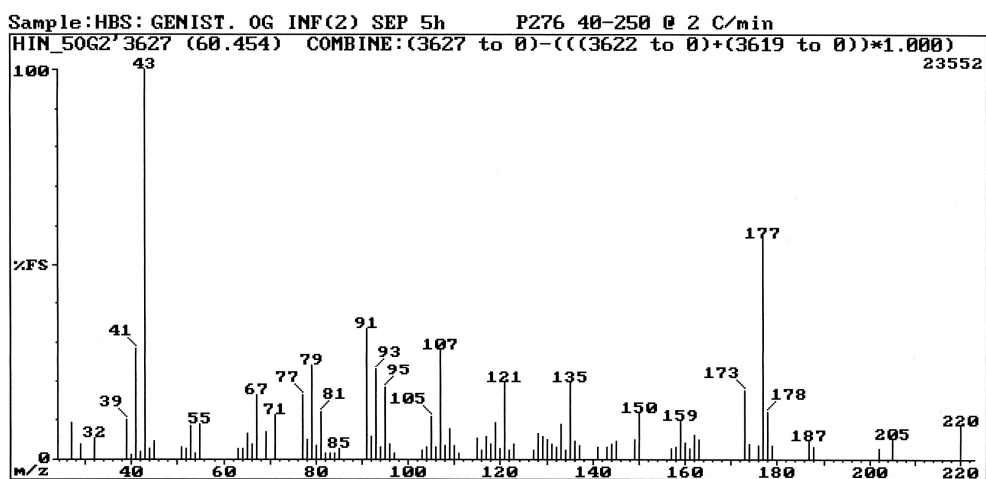


Fig. 3.151: EI mass spectrum of  $\beta$ -oplophenone (C274).

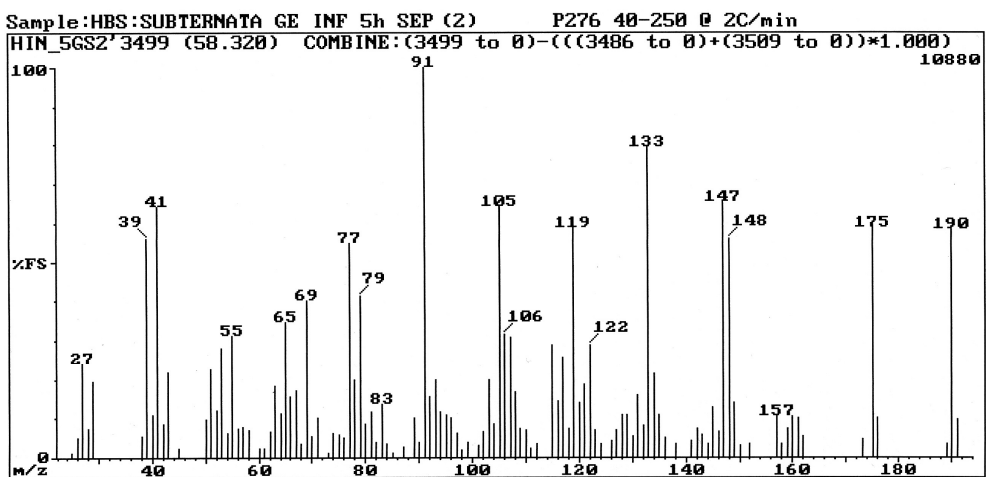


Fig. 3.152: EI mass spectrum of (6Z,8E)-megastigma-4,6,8-trien-3-one (C262).

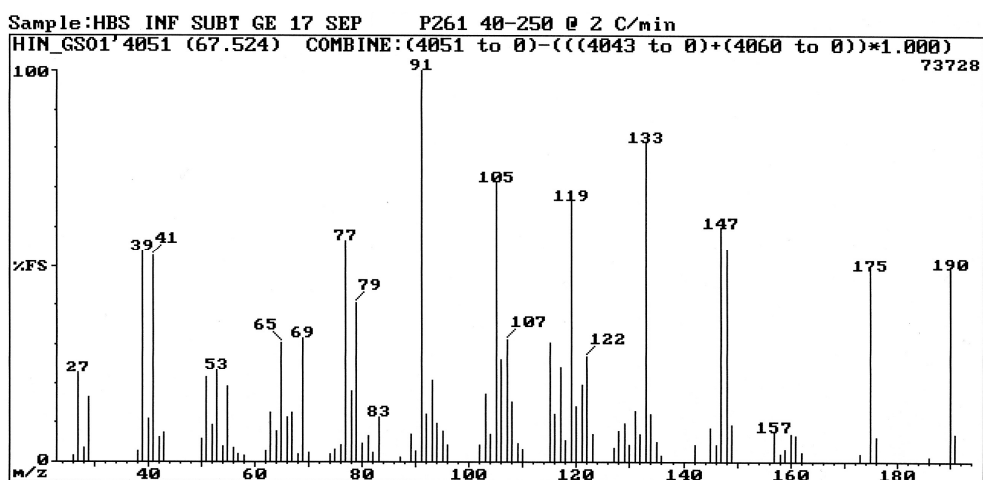


Fig. 3.153: EI mass spectrum of (6*E*,8*E*)-megastigma-4,6,8-trien-3-one (**C277**).

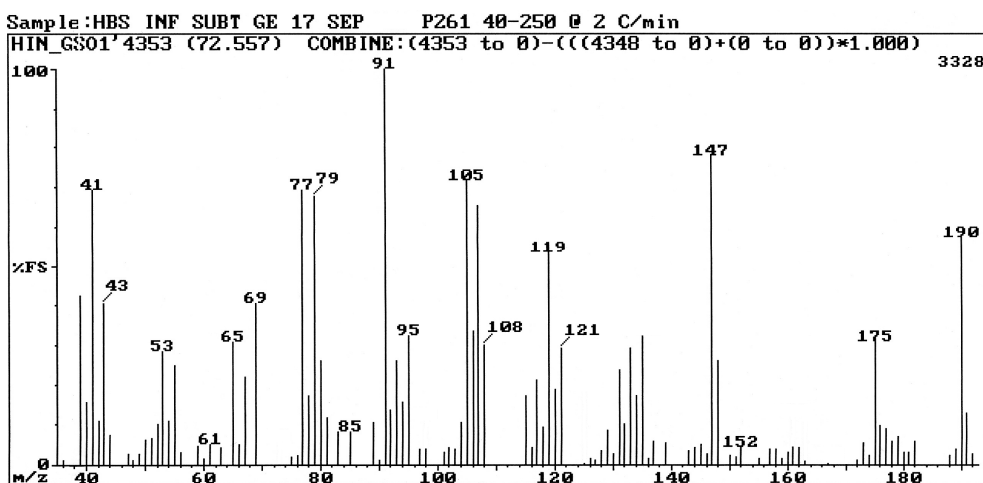


Fig. 3.154: EI mass spectrum of (7*E*)-megastigma-5,7,9-trien-4-one (**C295**).

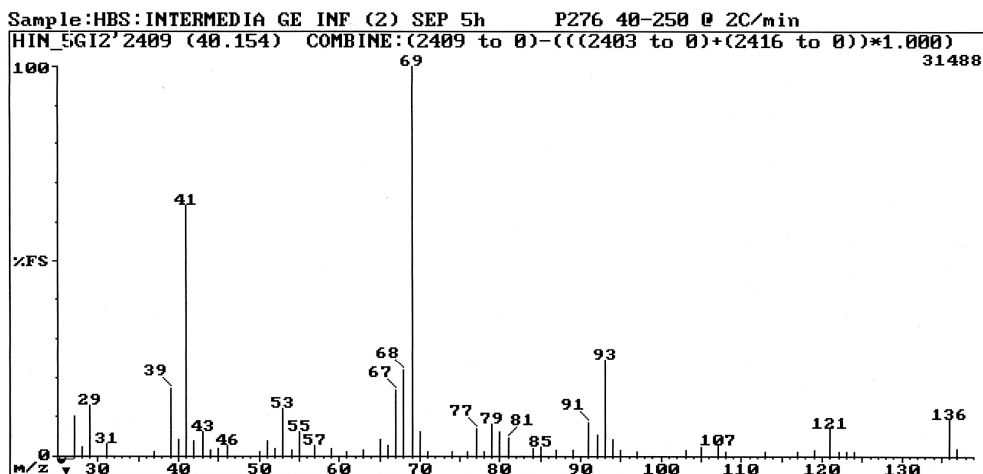


Fig. 3.155: EI mass spectrum of geranyl formate (**C164**).

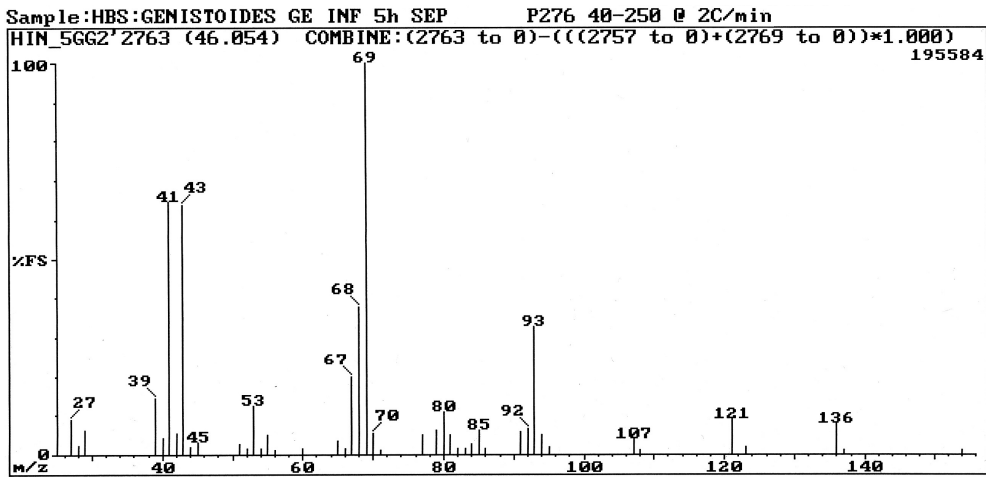


Fig. 3.156: EI mass spectrum of geranyl acetate (C206).

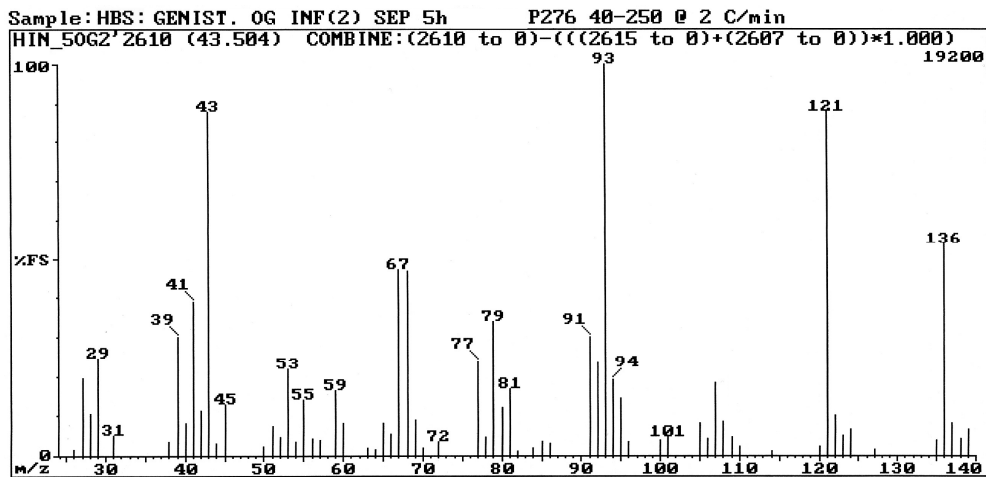


Fig. 3.157: EI mass spectrum of  $\alpha$ -terpinyl acetate (C188).

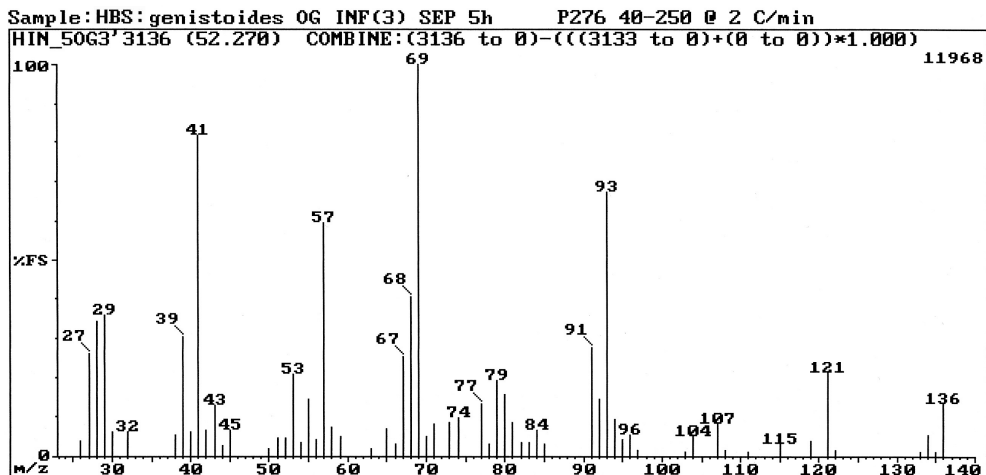


Fig. 3.158: EI mass spectrum of geranyl propanoate (C228).



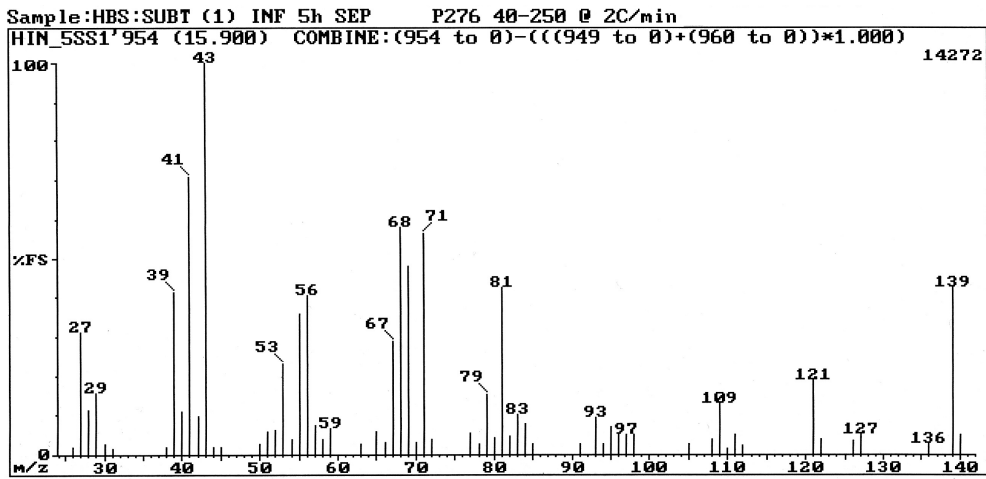


Fig. 3.159: EI mass spectrum of 2,6,6-trimethyl-2-vinyltetrahydropyran (**C29**).

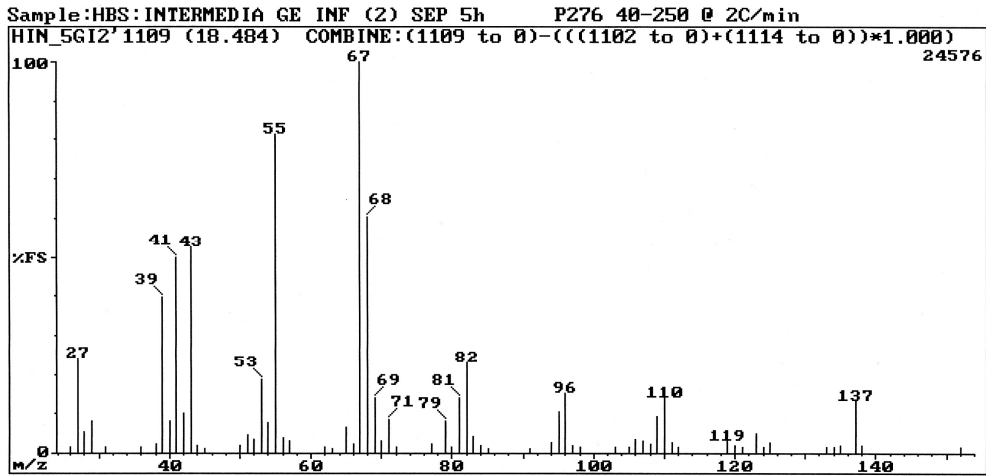


Fig. 3.160: EI mass spectrum of *cis*-dehydroxylinalool oxide (furanoid) (**C45**).

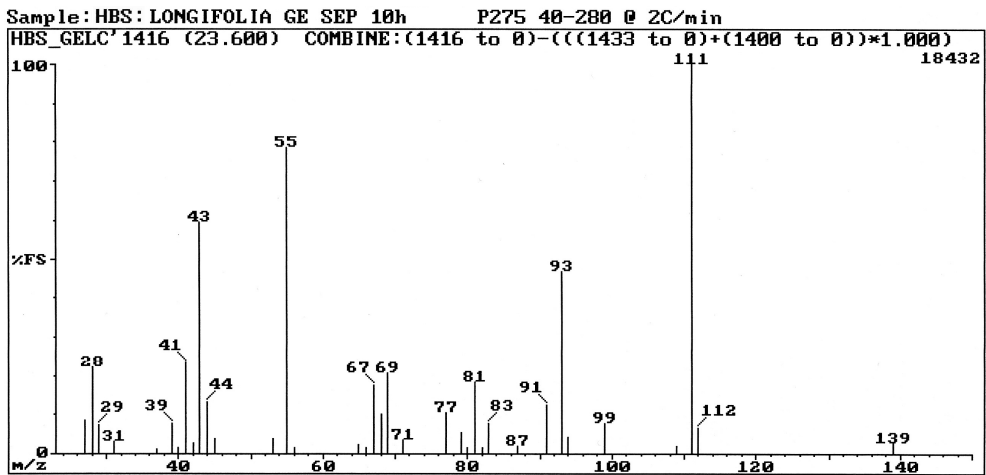


Fig. 3.161: EI mass spectrum of *trans*-arbusculone (**C62**).

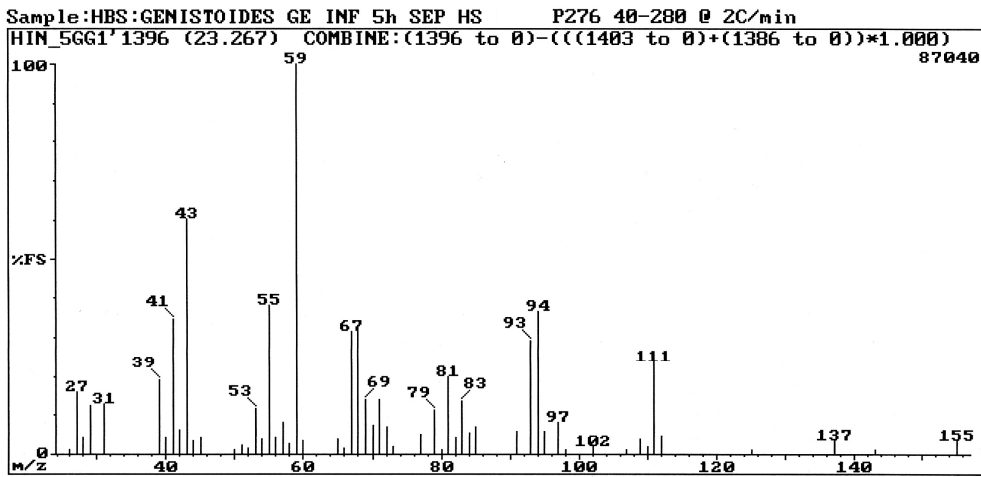


Fig. 3.162: EI mass spectrum of *trans*-linalool oxide (furanoid) (C68).

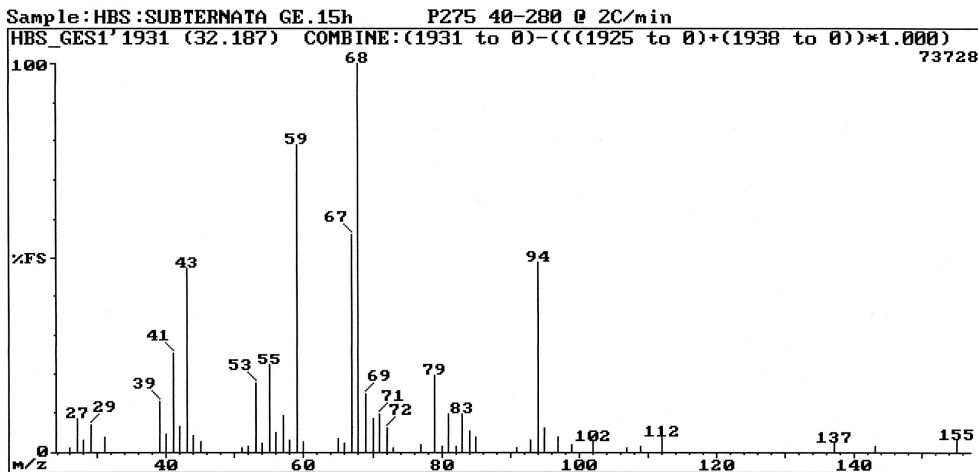


Fig. 3.163: EI mass spectrum of *trans*-pyranoid linalool oxide (C116).

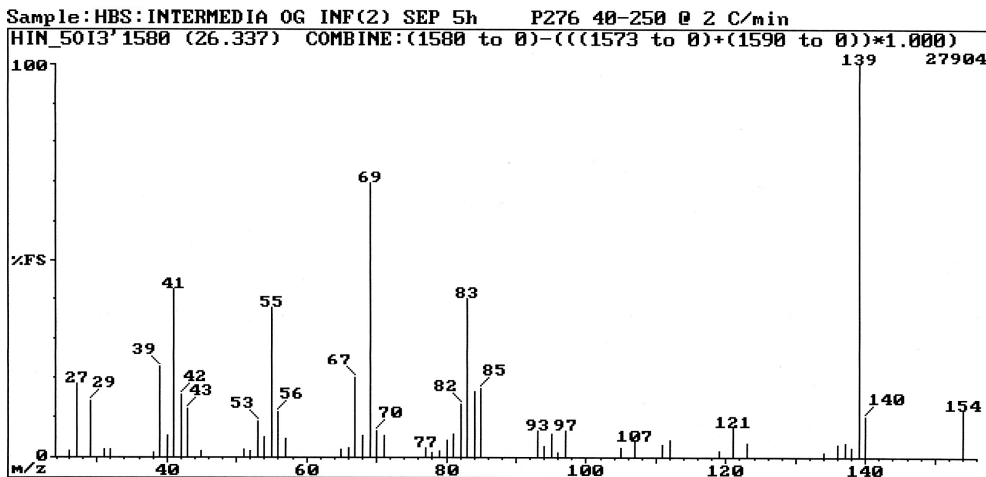


Fig. 3.164: EI mass spectrum of *cis*-rose oxide (C91).

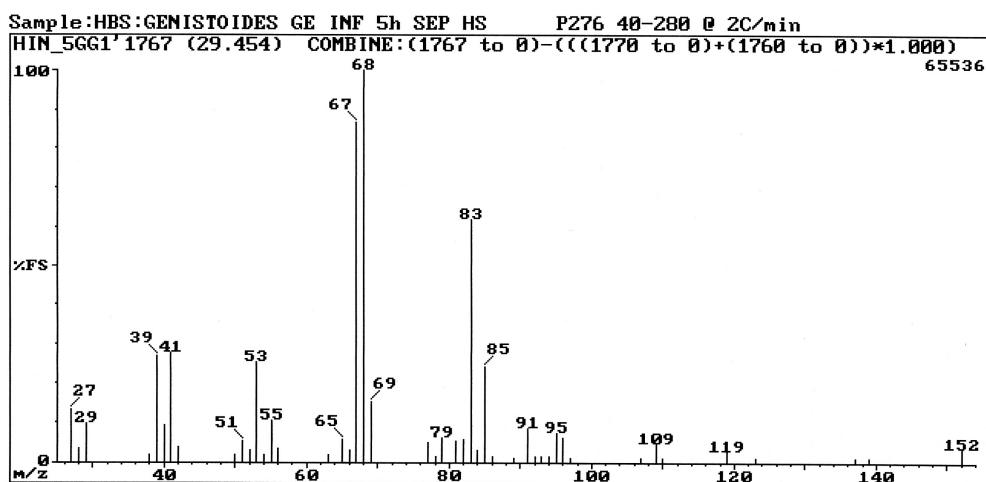


Fig. 3.165: EI mass spectrum of nerol oxide (C106).

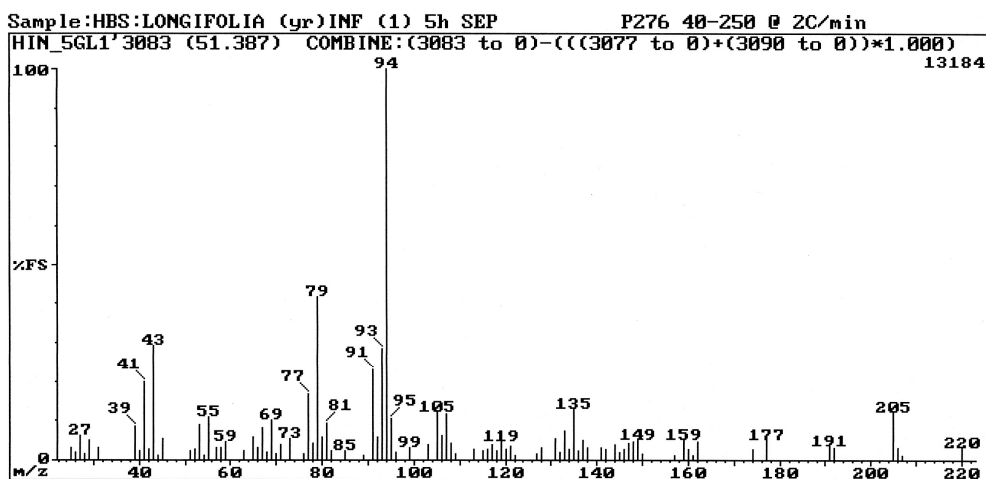


Fig. 3.166: EI mass spectrum of cabreuva oxide B (C225).

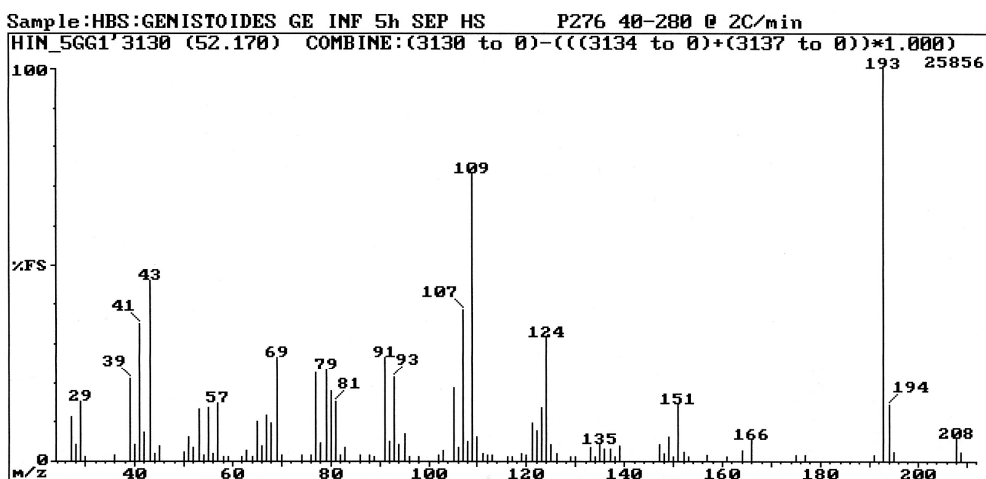


Fig. 3.167: EI mass spectrum of oxo-edulan (C227).

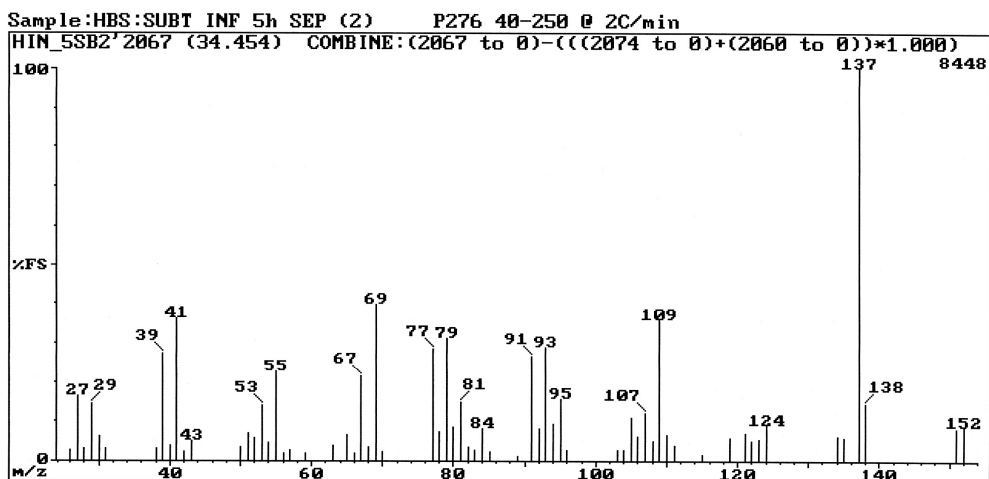


Fig. 3.168: EI mass spectrum of dill ether isomer 1 (C119).

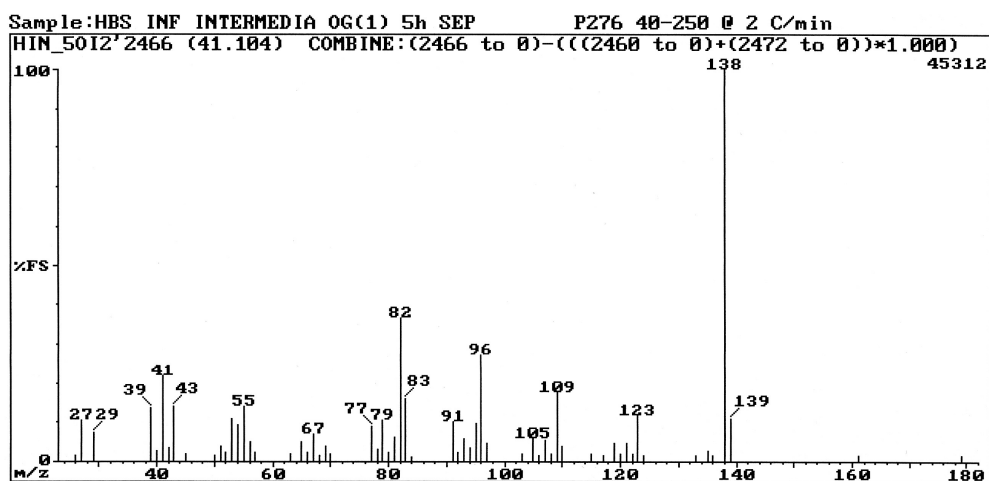


Fig. 3.169: EI mass spectrum of theaspirane isomer 2 (C173).

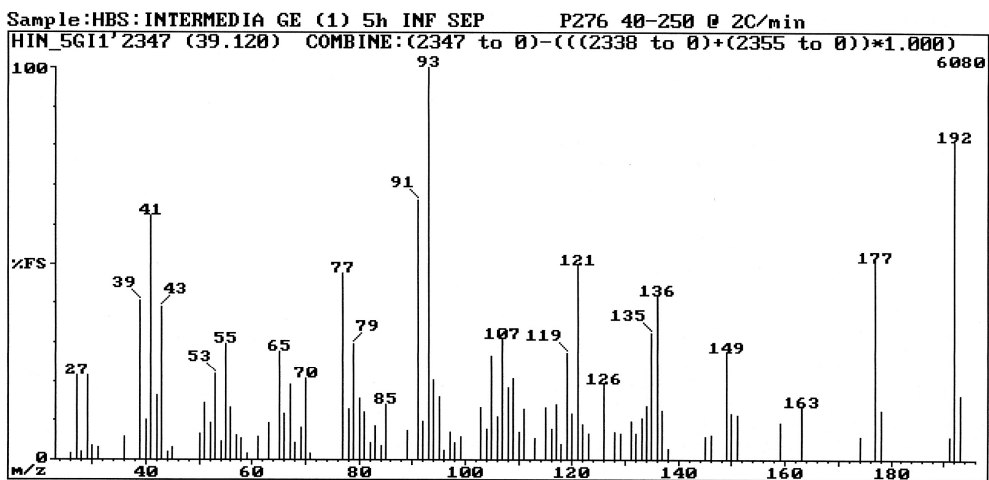


Fig. 3.170: EI mass spectrum of vitispirane (C157).

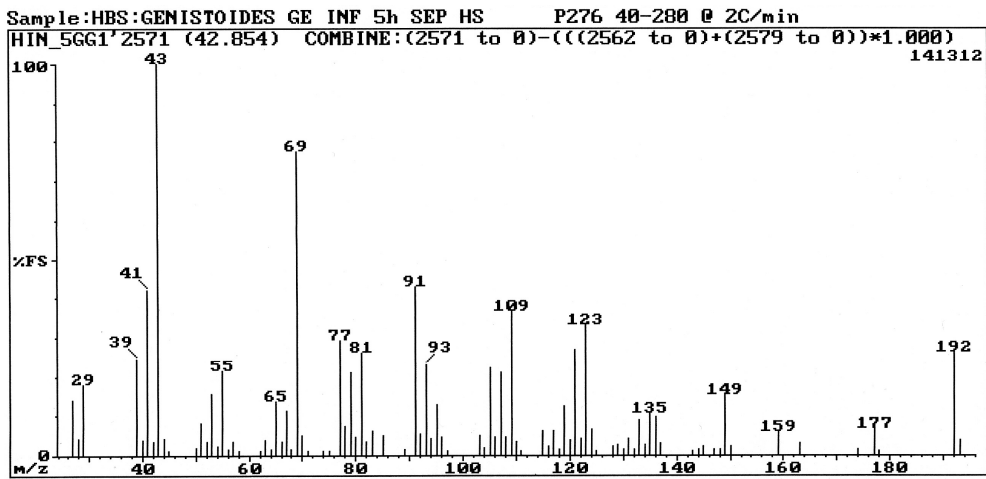


Fig. 3.171: EI mass spectrum of 2,5-epoxymegastigma-6,8-diene (C182).

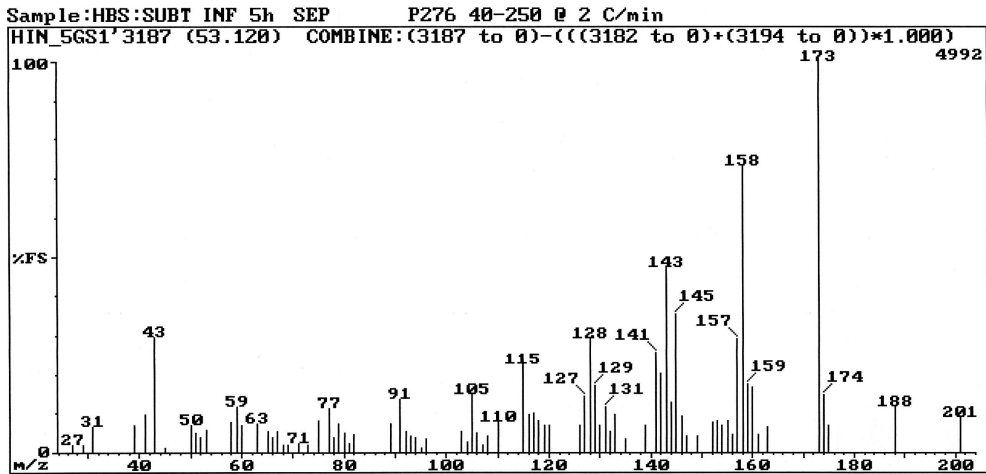


Fig. 3.172: EI mass spectrum of calamenene-1,11-epoxide (C236).

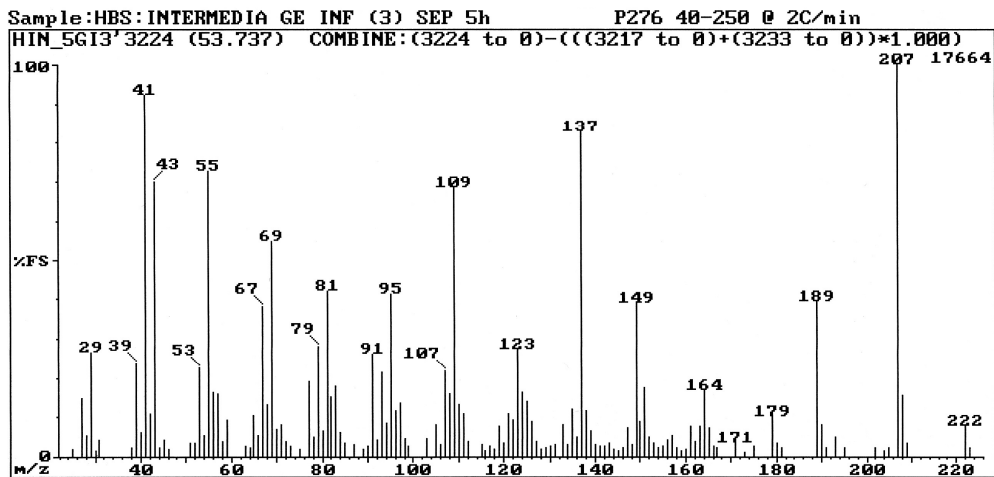


Fig. 3.173: EI mass spectrum of  $\beta$ -dihydroagarofuran (C239).

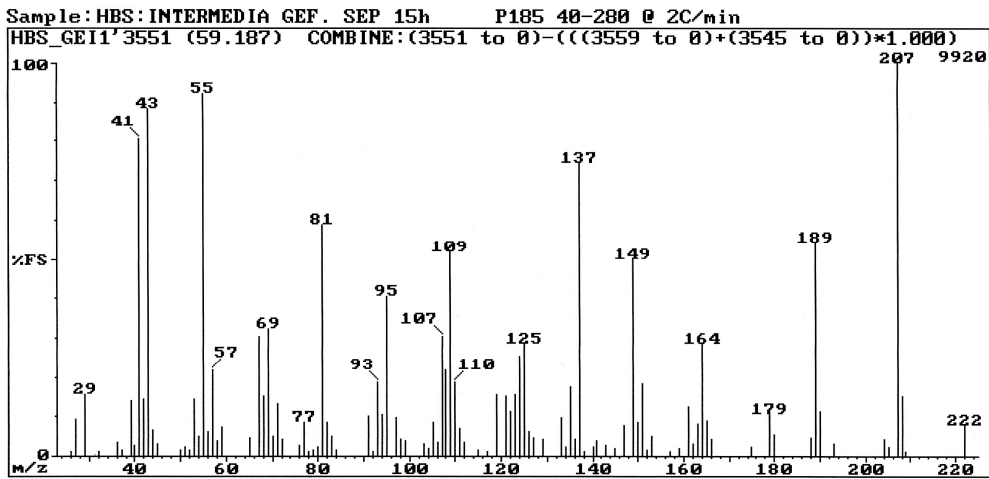


Fig. 3.174: EI mass spectrum of dihydroagarofuran isomer (C258).

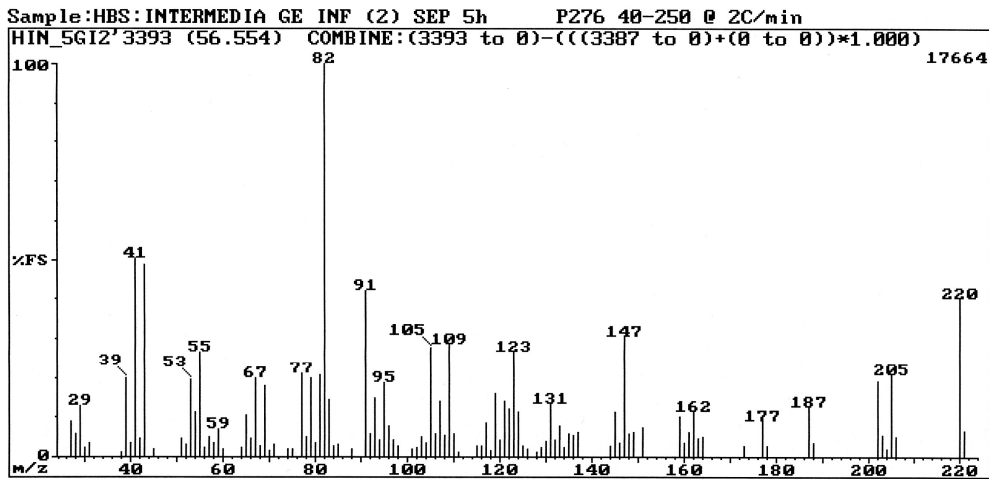


Fig. 3.175: EI mass spectrum of  $\alpha$ -agarofuran (C253).

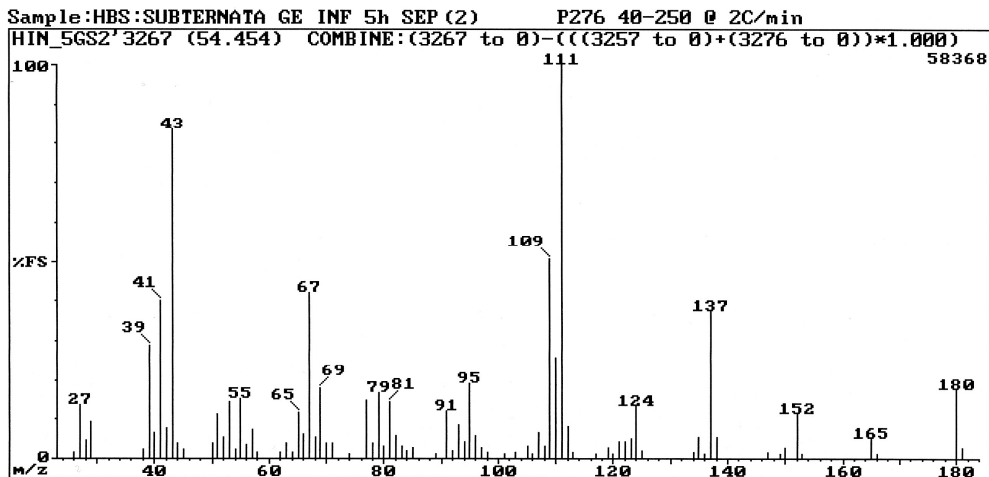


Fig. 3.176: EI mass spectrum of dihydroactinidiolide (C243).

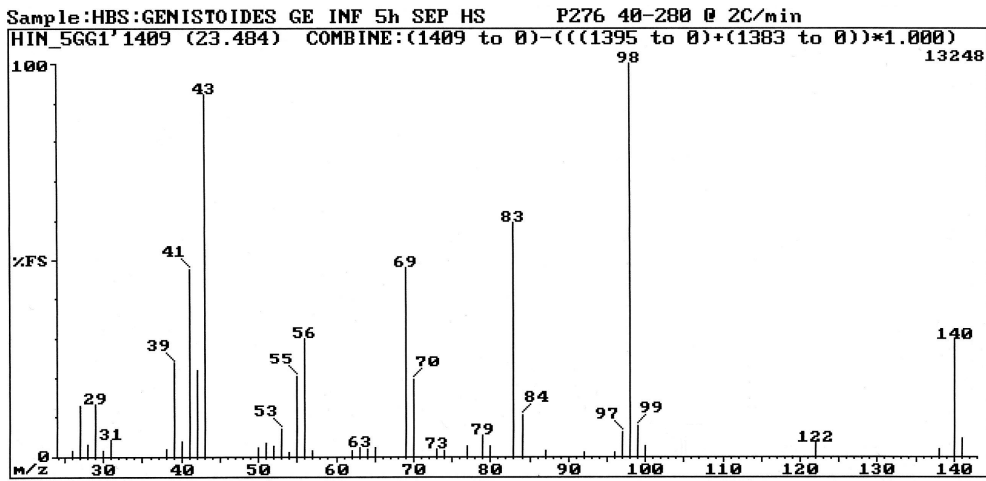


Fig. 3.177: EI mass spectrum of component **C66**.

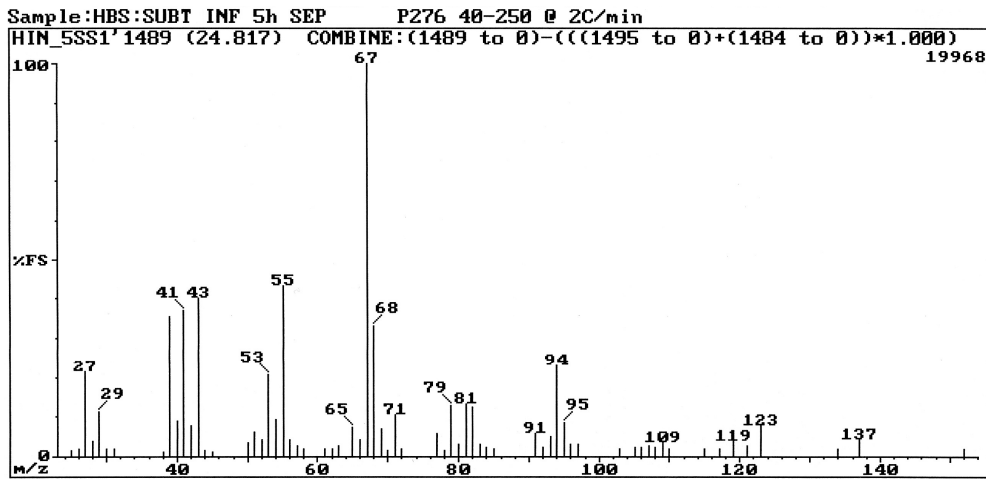


Fig. 3.178: EI mass spectrum of component **C73**.

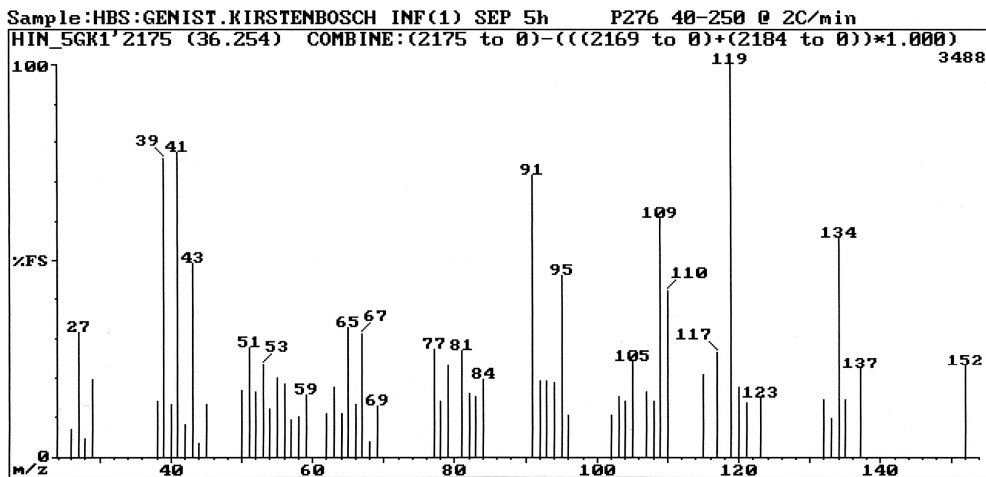


Fig. 3.179: EI mass spectrum of component **C144**.

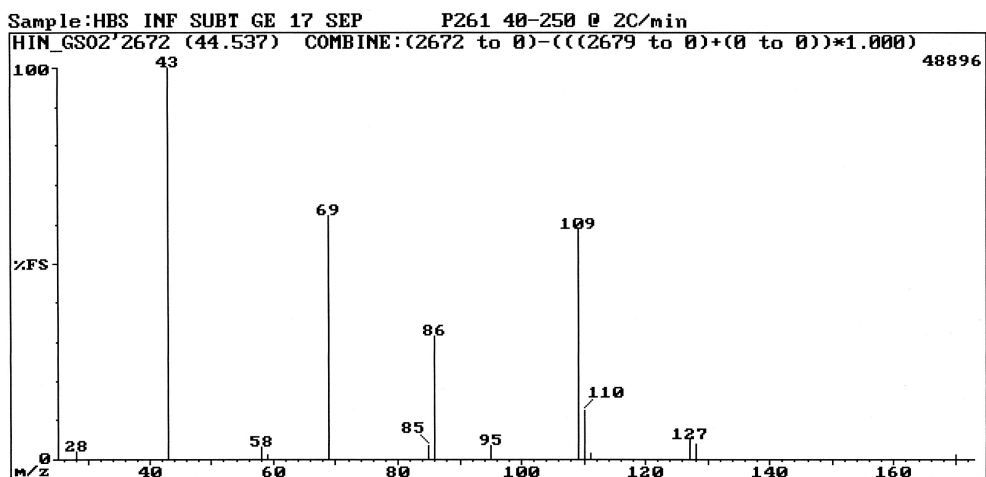


Fig. 3.180: EI mass spectrum of component **C151**.

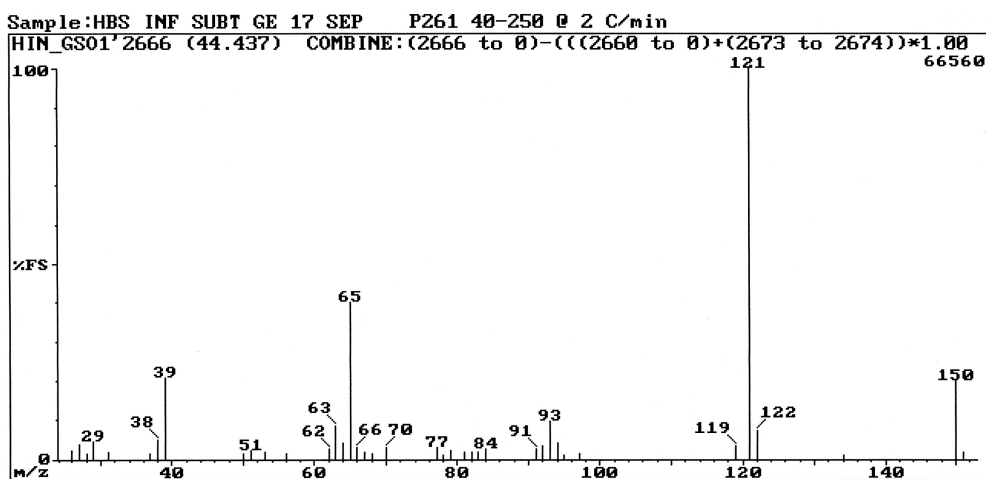


Fig. 3.181: EI mass spectrum of component **C156**.

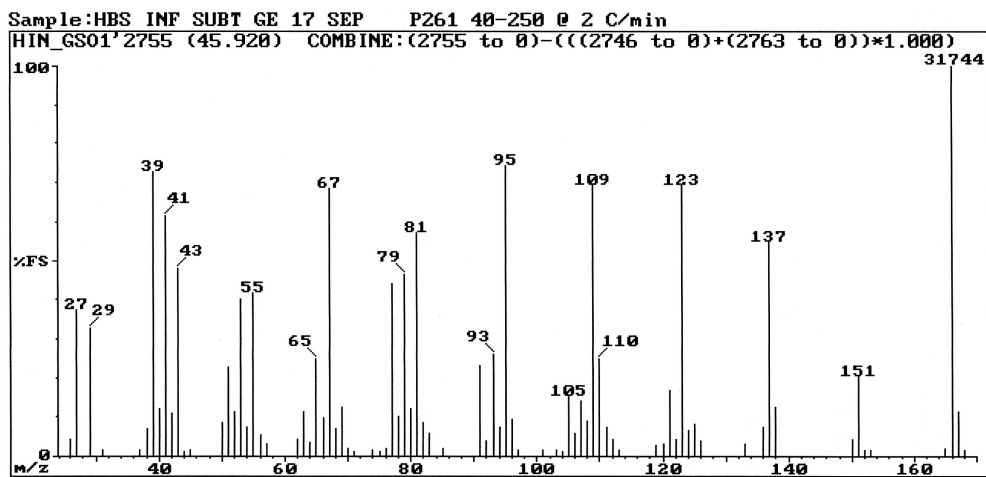


Fig. 3.182: EI mass spectrum of component **C162**.



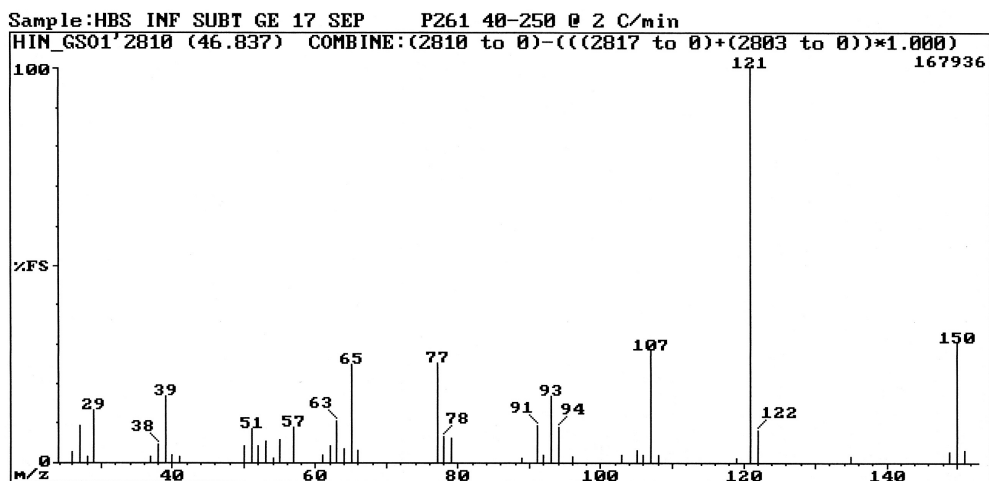


Fig. 3.183: EI mass spectrum of component **C168**.

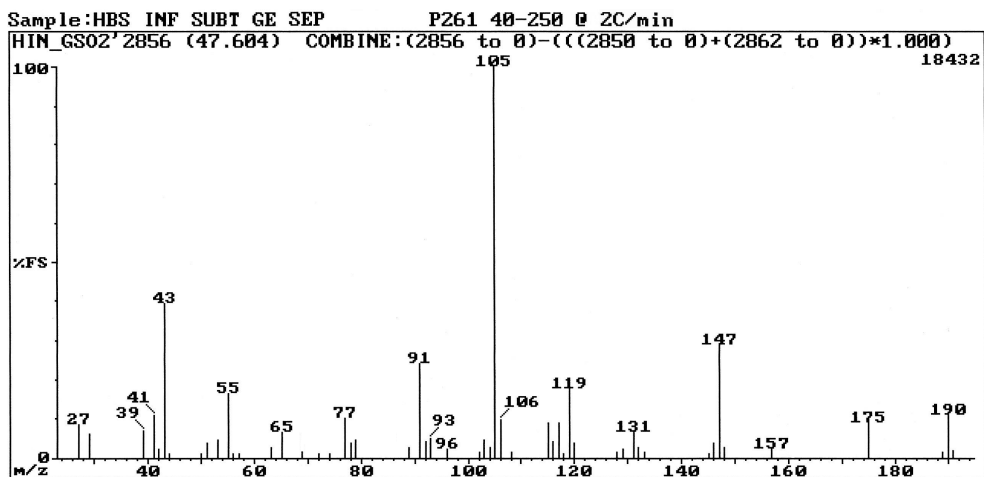


Fig. 3.184: EI mass spectrum of component **C169**.

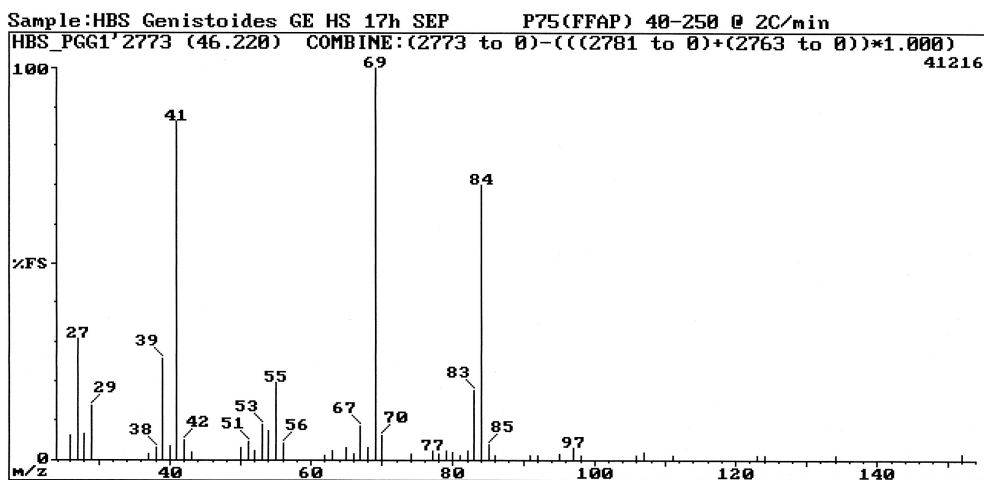


Fig. 3.185: EI mass spectrum of component **C172**.

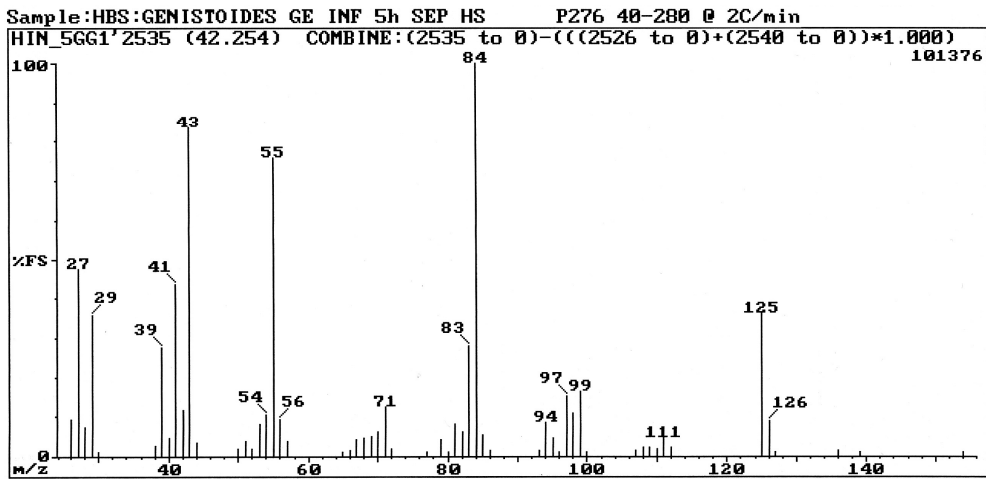


Fig. 3.186: EI mass spectrum of component **C178**.

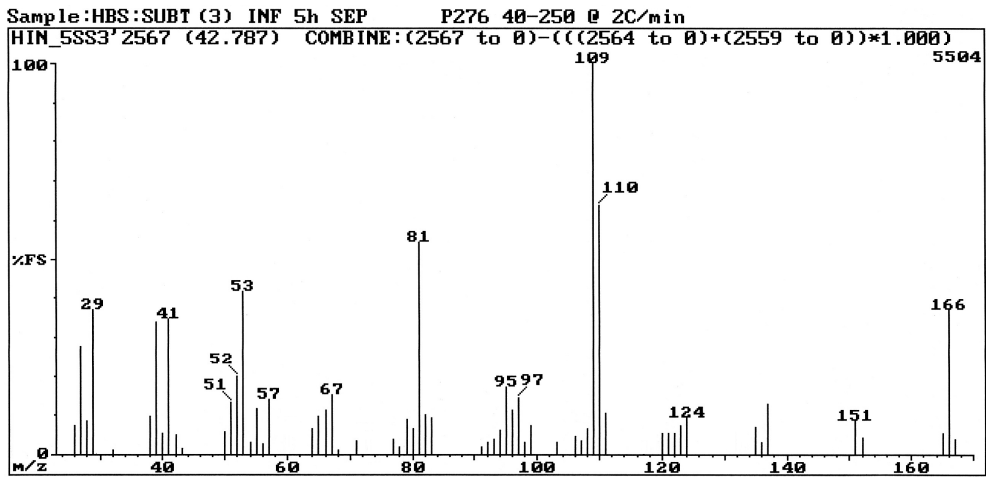


Fig. 3.187: EI mass spectrum of component **C183**.

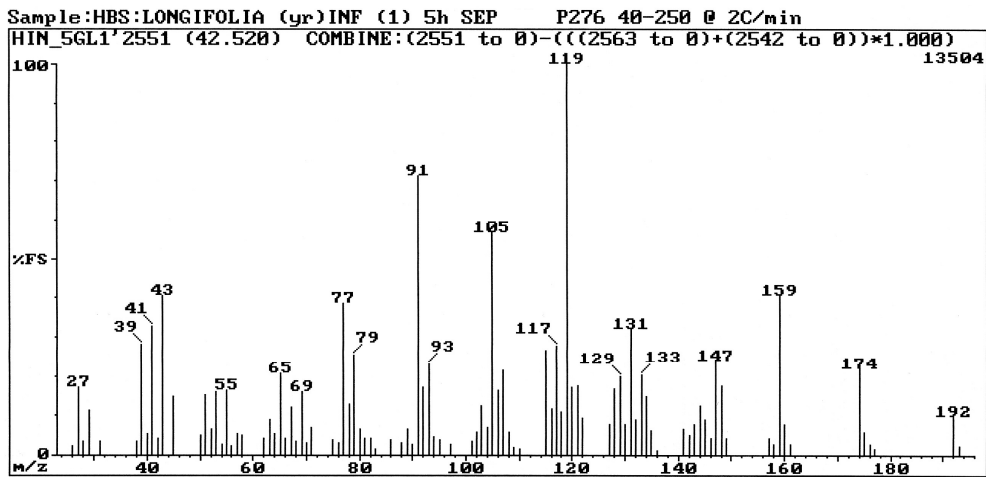


Fig. 3.188: EI mass spectrum of component **C180**.

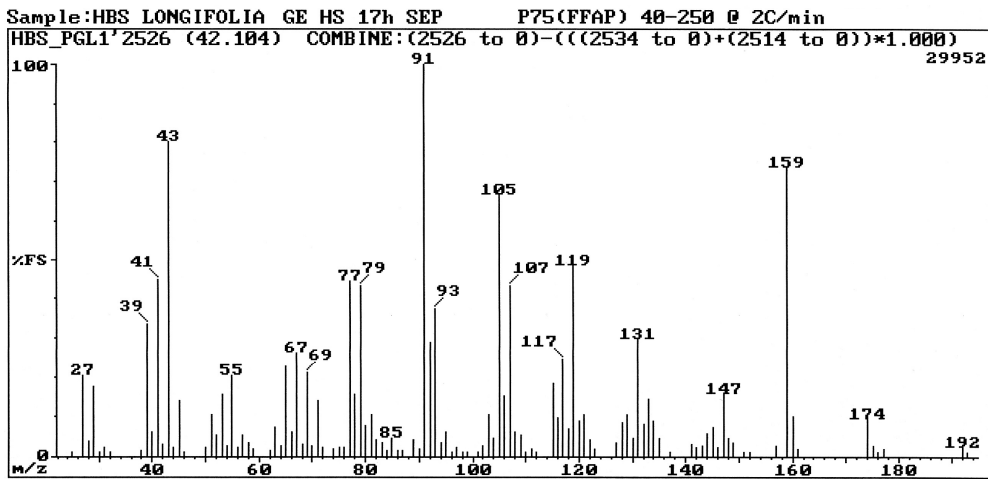


Fig. 3.189: El mass spectrum of component **C207**.

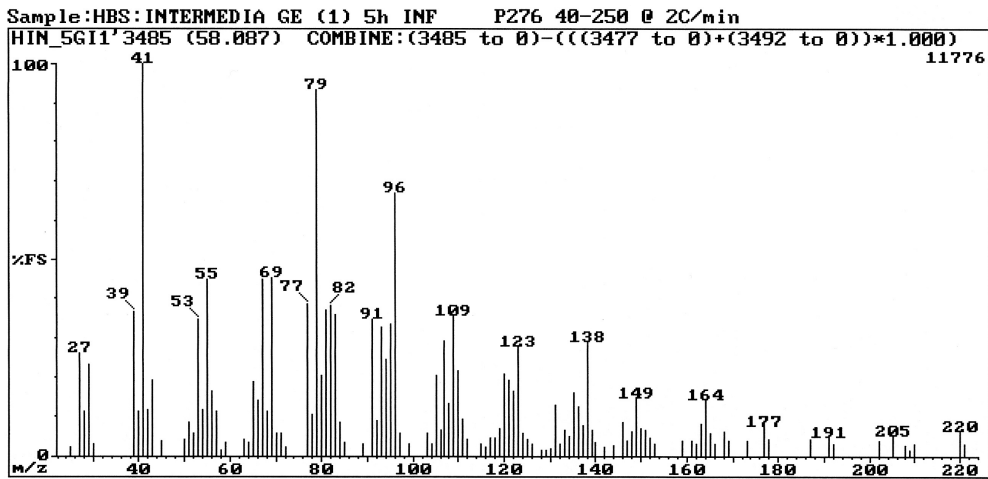


Fig. 3.190: El mass spectrum of component **C254**.

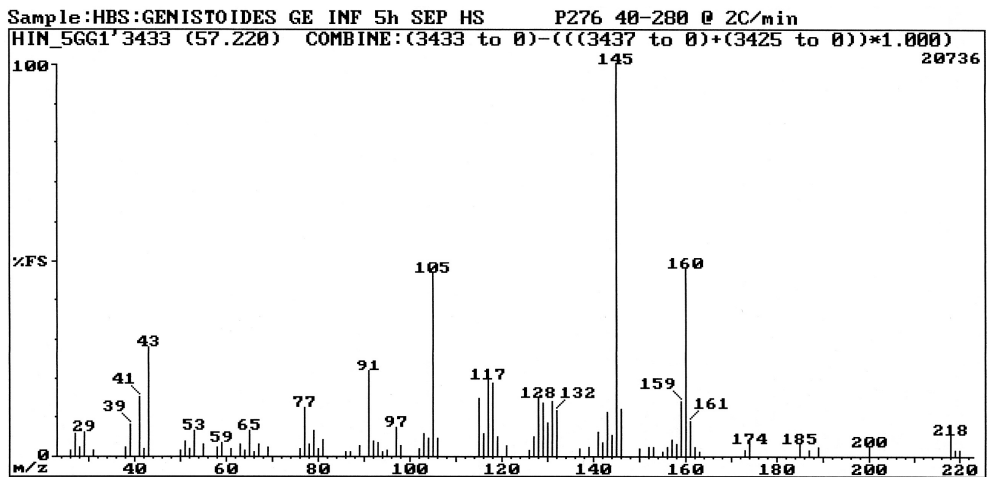


Fig. 3.191: El mass spectrum of component **C255**.

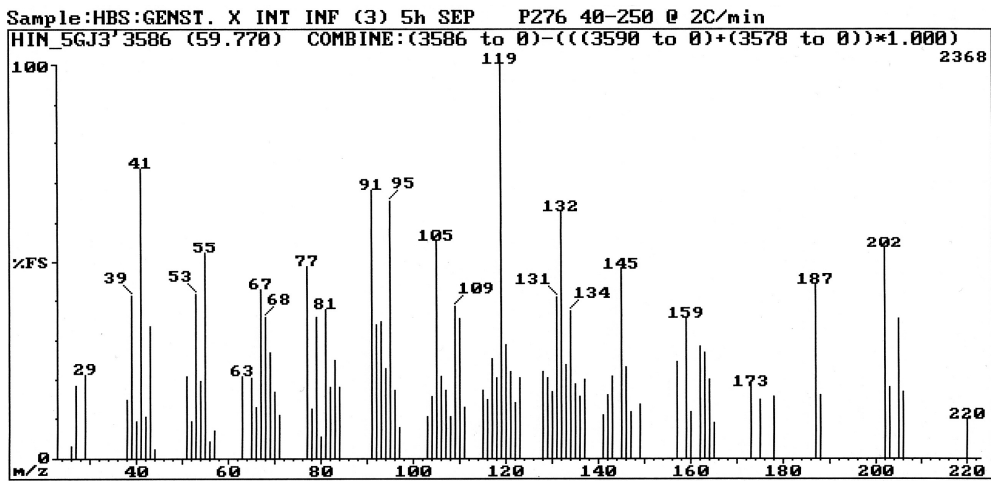


Fig. 3.192: EI mass spectrum of component **C267**.

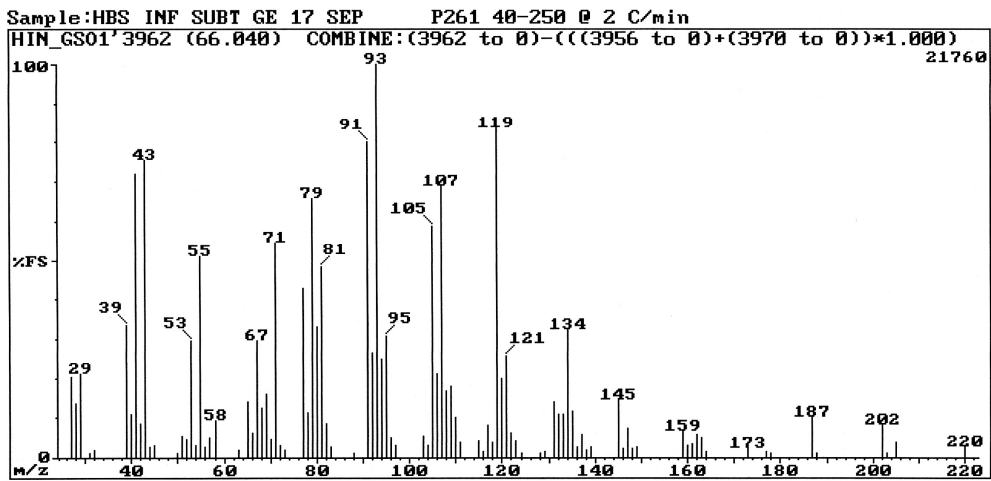


Fig. 3.193: EI mass spectrum of component **C269**.

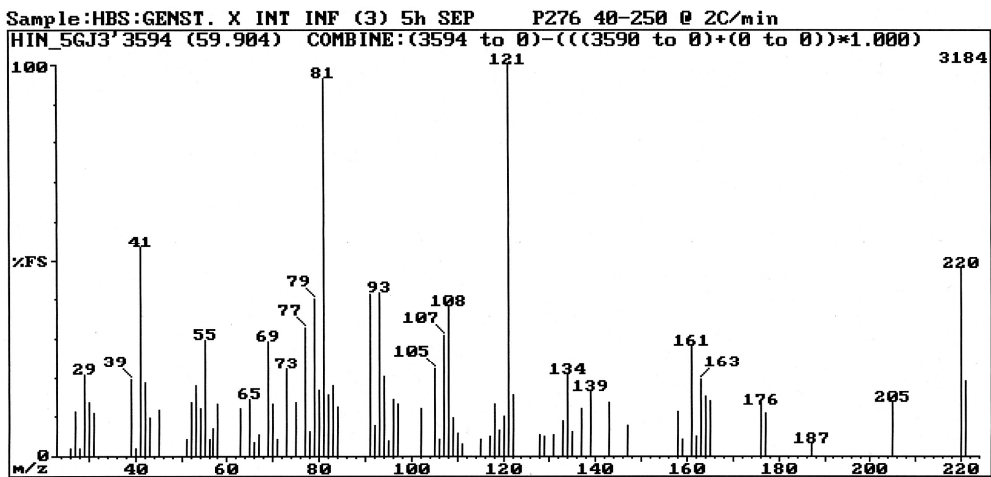


Fig. 3.194: EI mass spectrum of component **C268**.

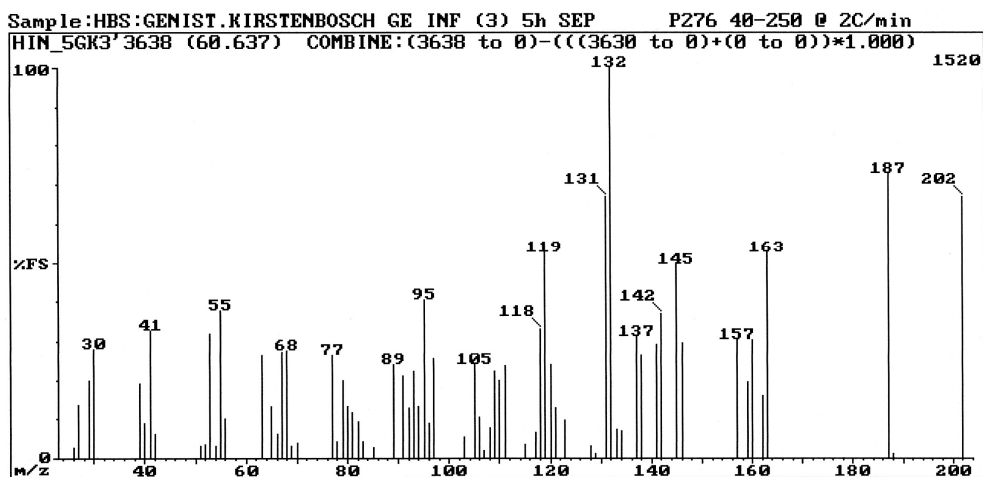


Fig. 3.195: EI mass spectrum of component **C275**.

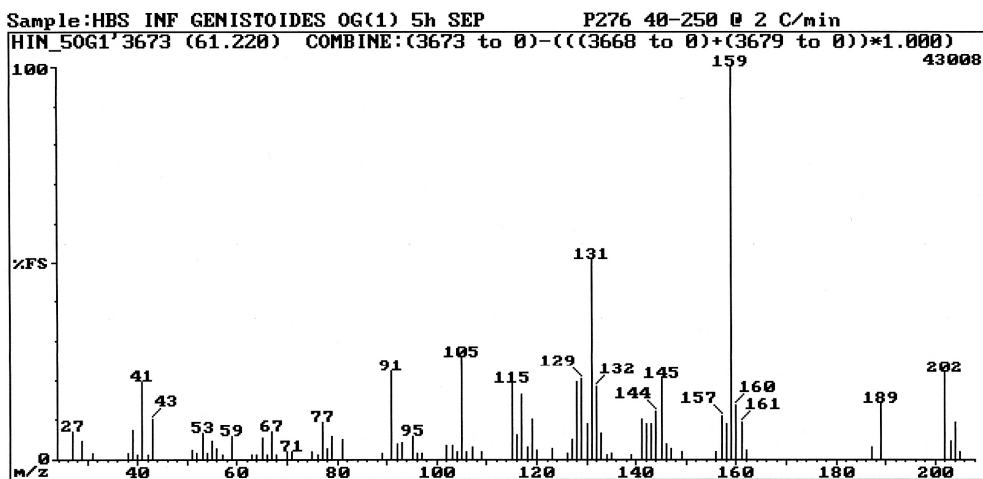


Fig. 3.196: EI mass spectrum of component **C279**.

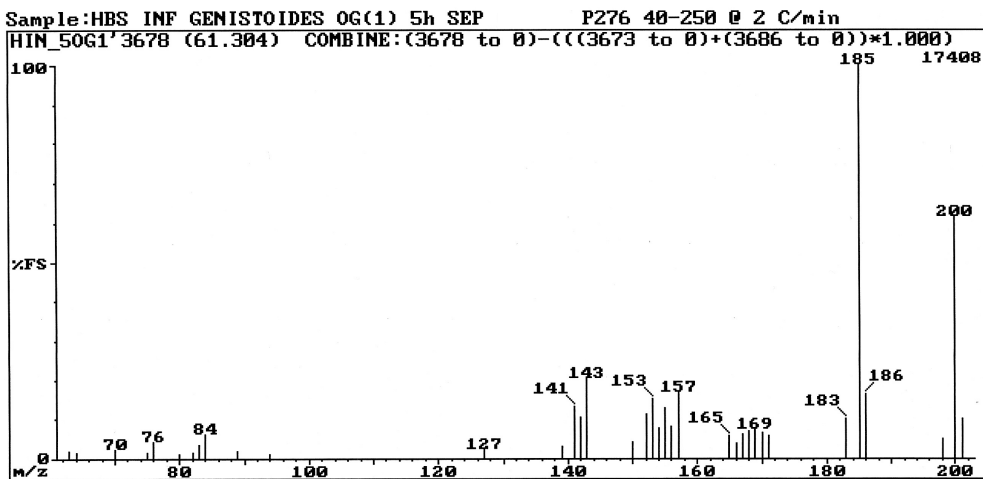


Fig. 3.197: EI mass spectrum of component **C280**.

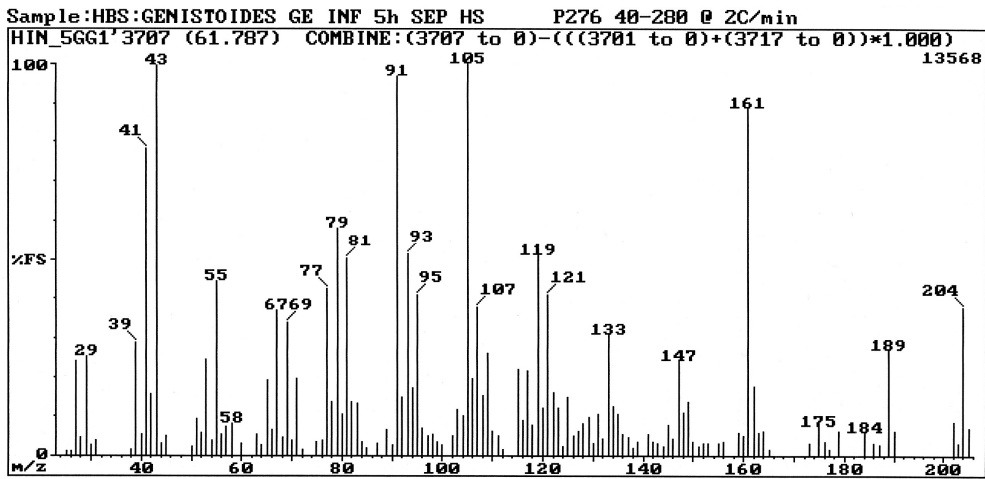


Fig. 3.198: EI mass spectrum of component **C282**.

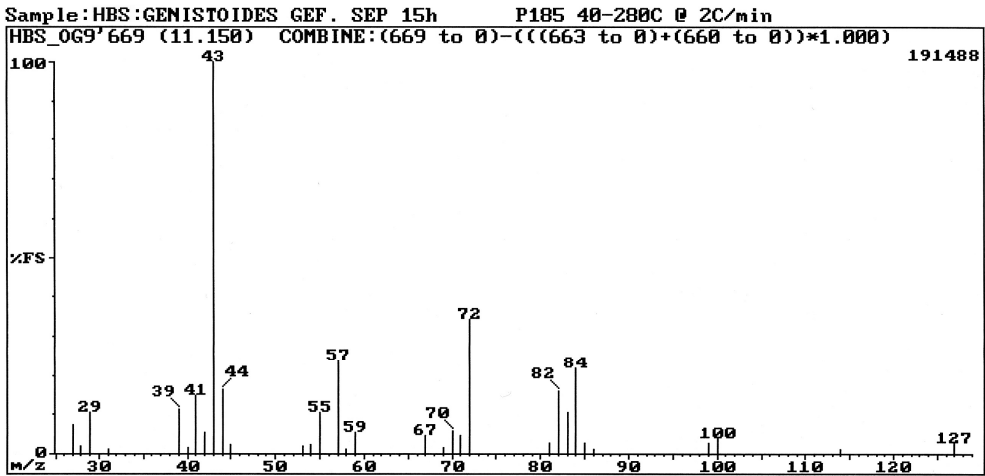


Fig. 3.199: EI mass spectrum of component **C18**.

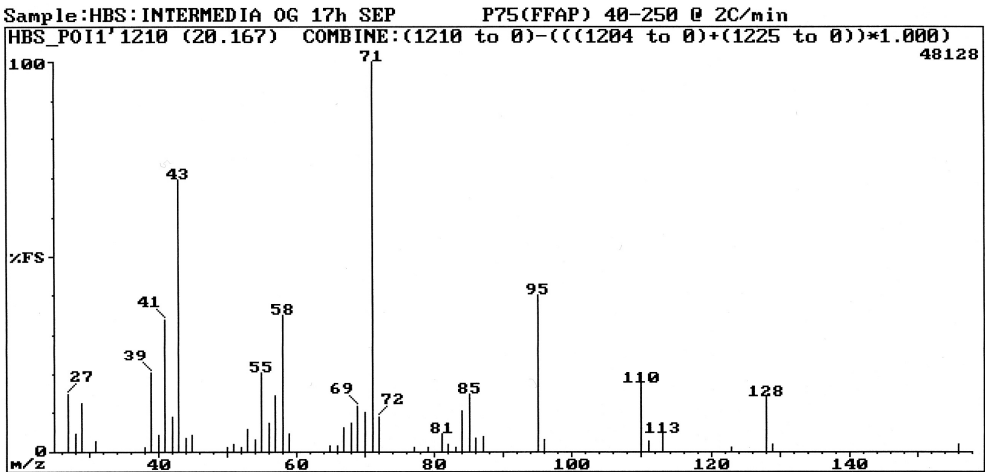


Fig. 3.200: EI mass spectrum of component **C77**.

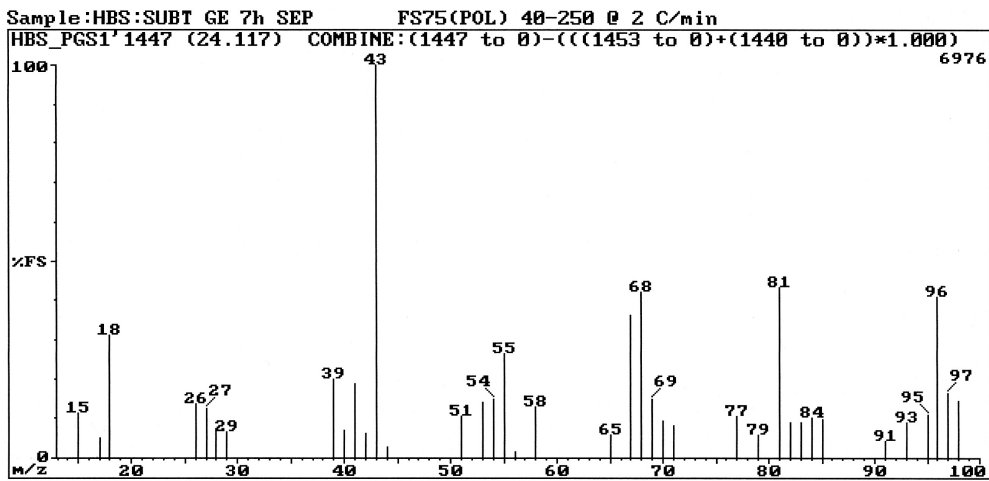


Fig. 3.201: EI mass spectrum of component **C87**.

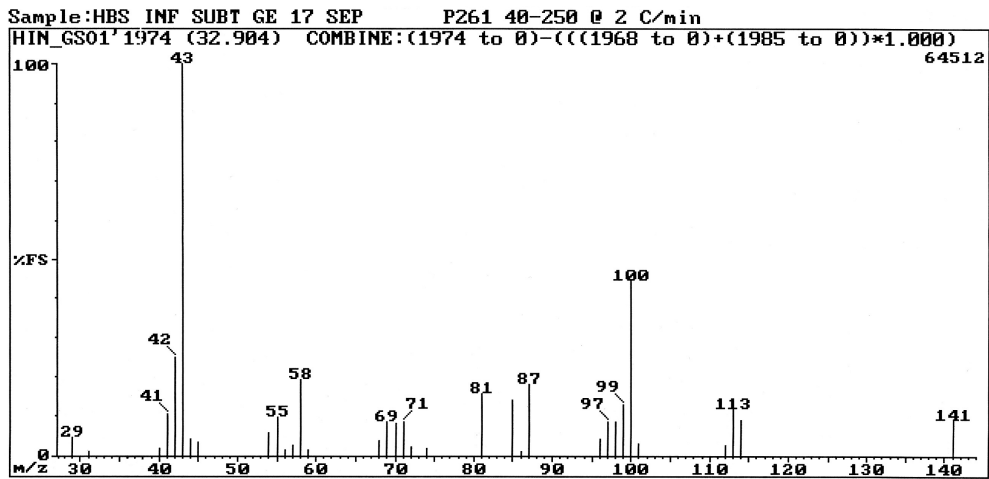


Fig. 3.202: EI mass spectrum of component **C88**.

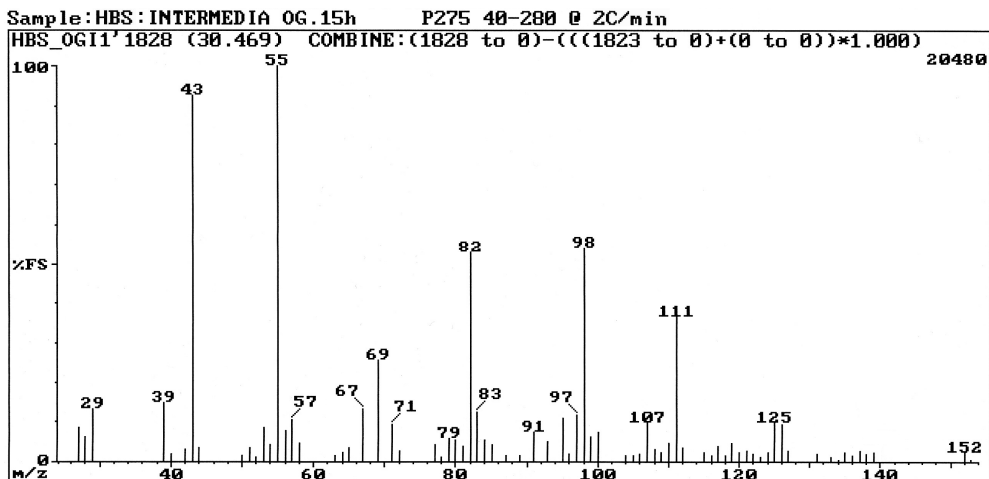


Fig. 3.203: EI mass spectrum of component **C102**.

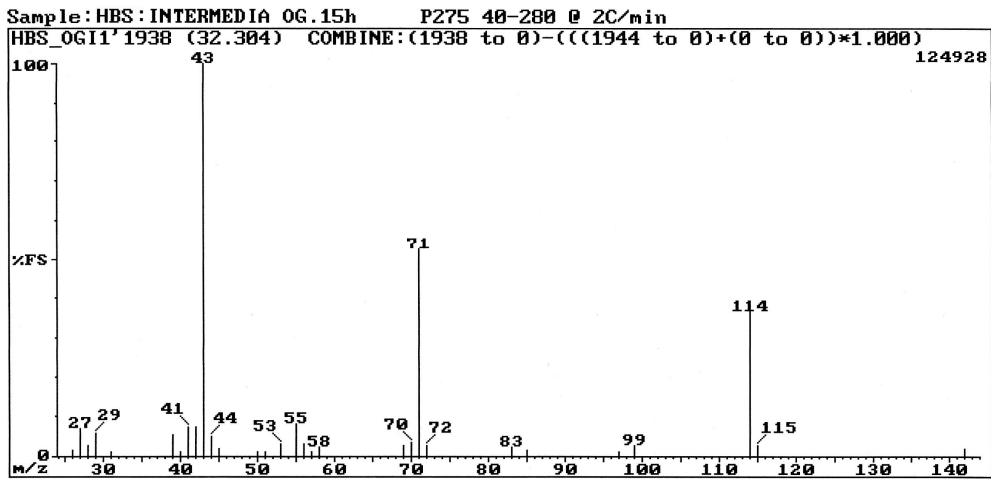


Fig. 3.204: EI mass spectrum of component **C117**.

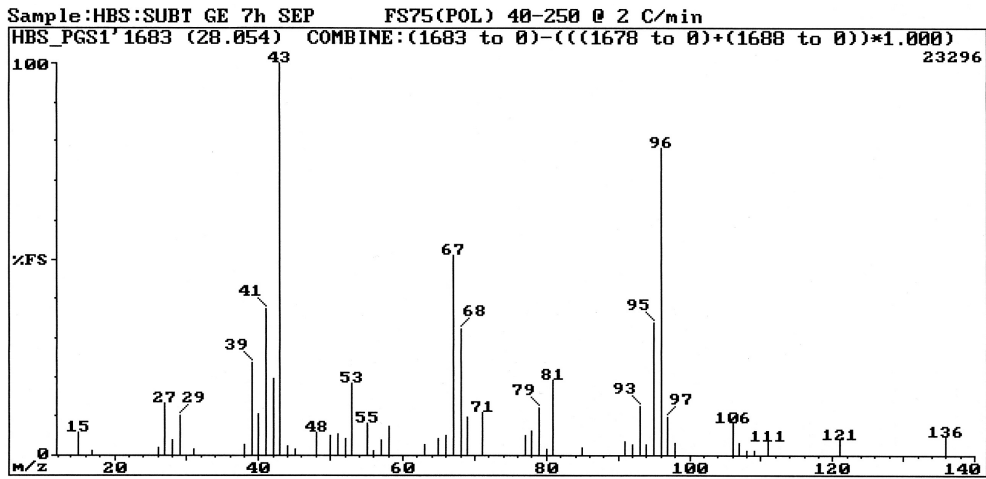


Fig. 3.205: EI mass spectrum of component **C123**.

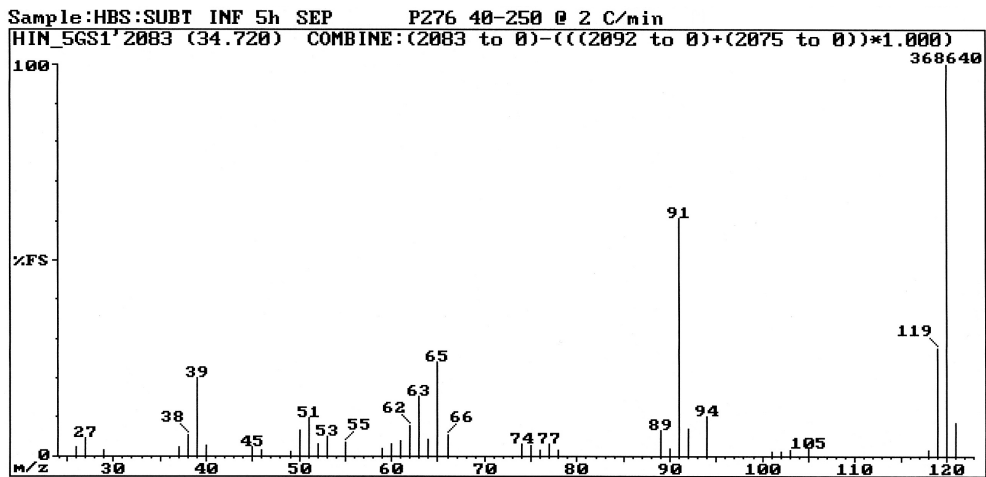


Fig. 3.206: EI mass spectrum of component **C133**.



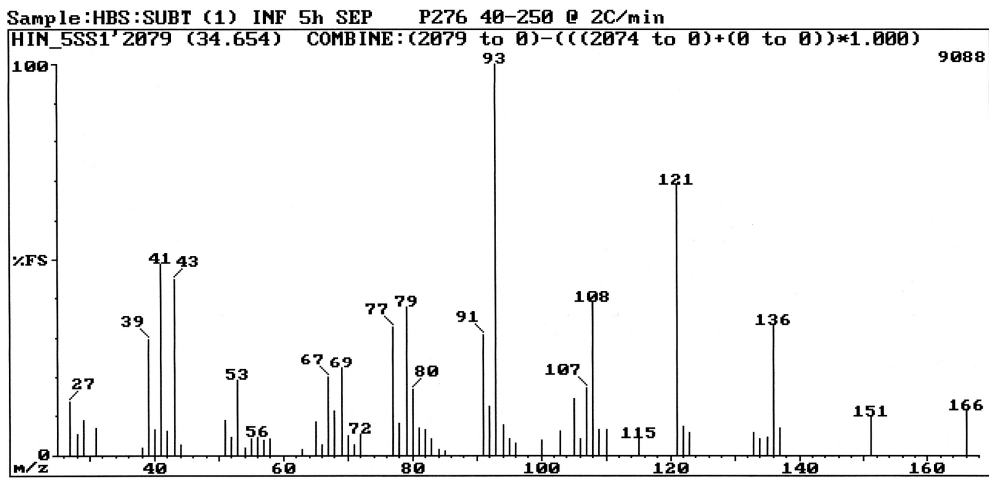


Fig. 3.207: EI mass spectrum of component **C134**.

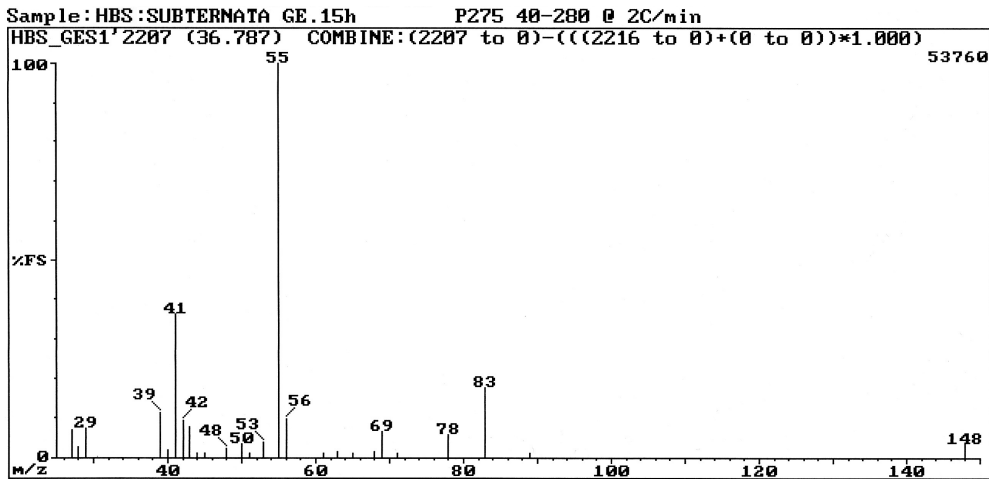


Fig. 3.208: EI mass spectrum of component **C136**.

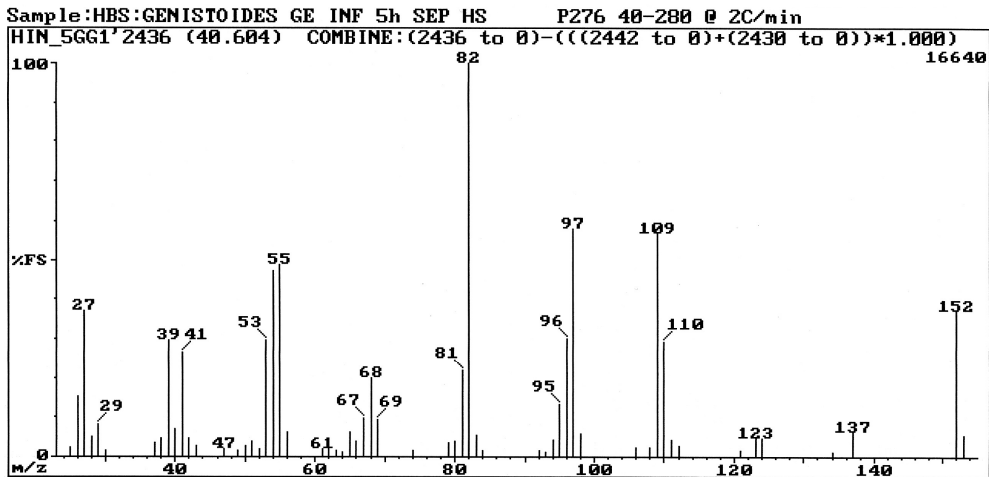


Fig. 3.209: EI mass spectrum of component **C165** and **C185**.

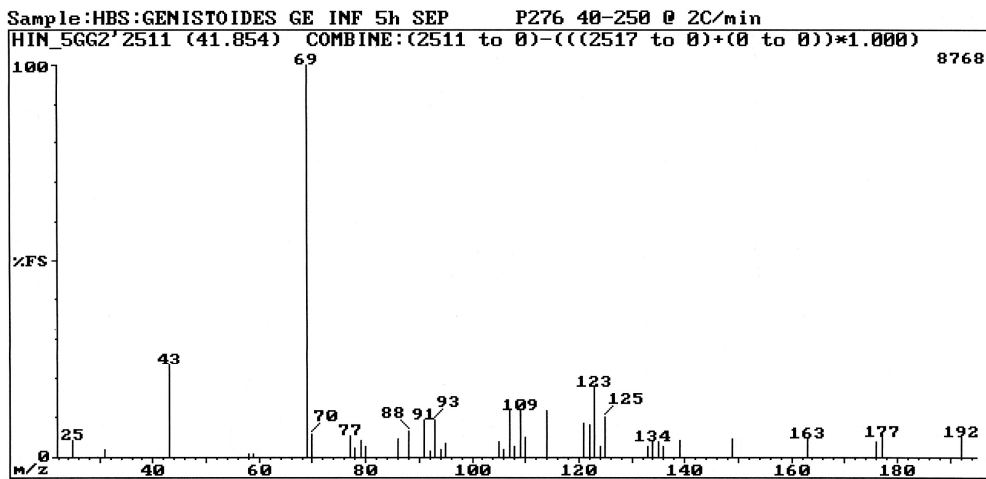


Fig. 3.210: El mass spectrum of component **C174**.

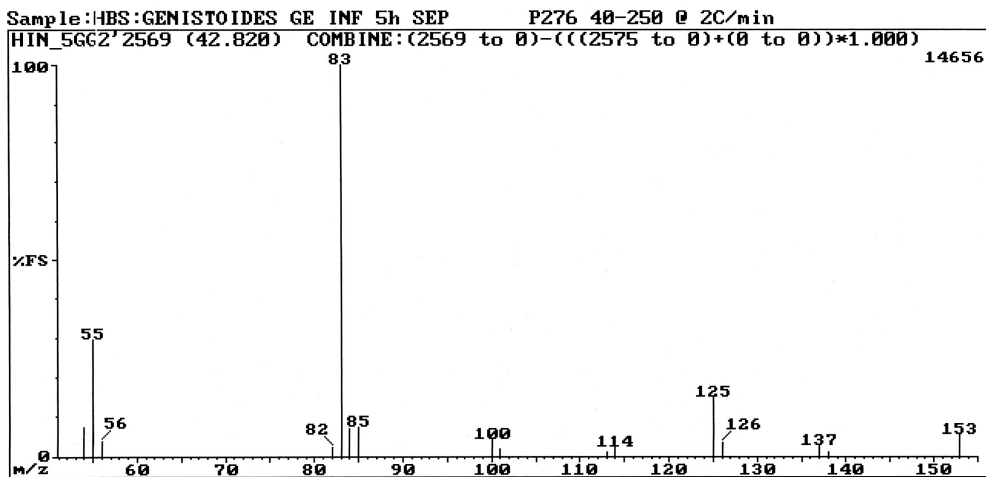


Fig. 3.211: El mass spectrum of component **C181**.

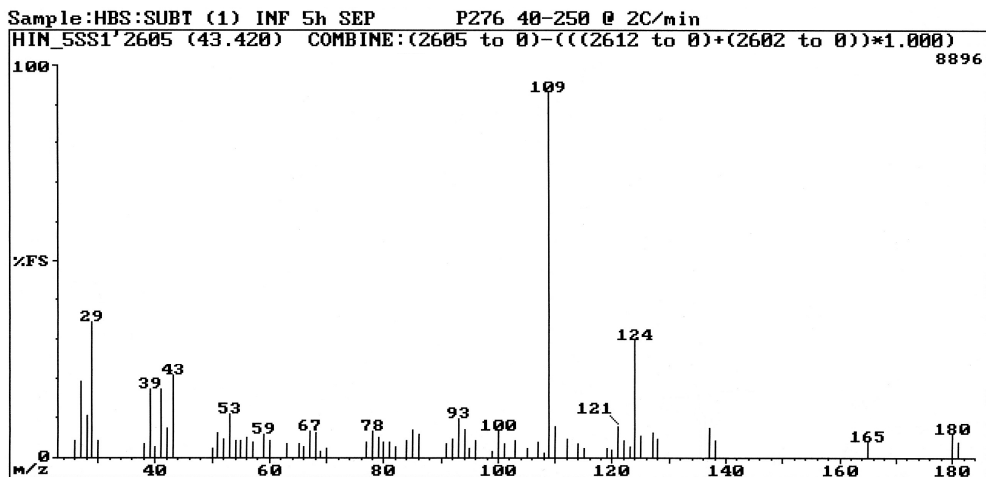


Fig. 3.212: El mass spectrum of component **C187**.

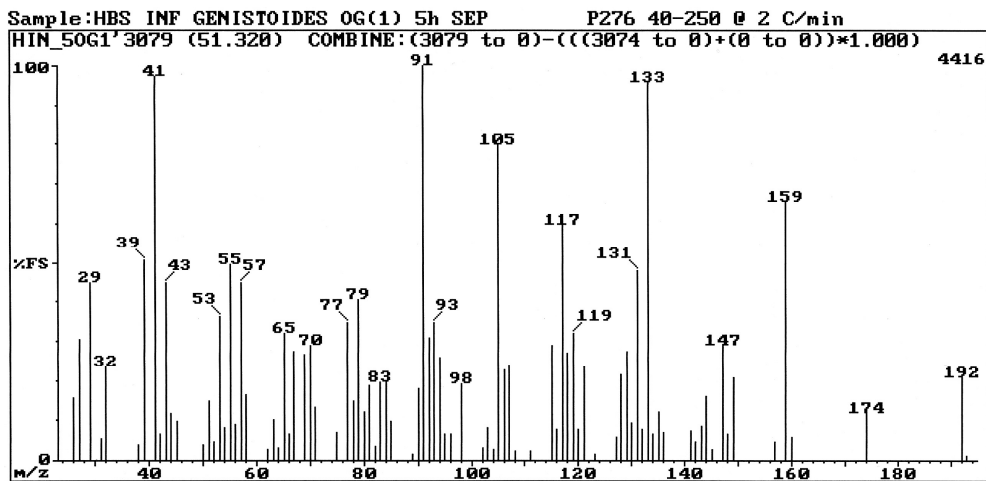


Fig. 3.213: EI mass spectrum of component **C224**.

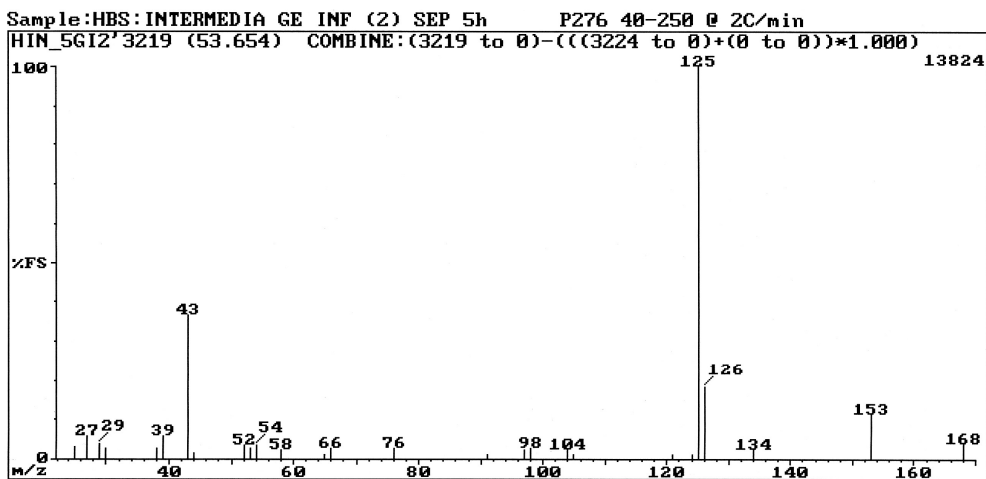


Fig. 3.214: EI mass spectrum of component **C238**.

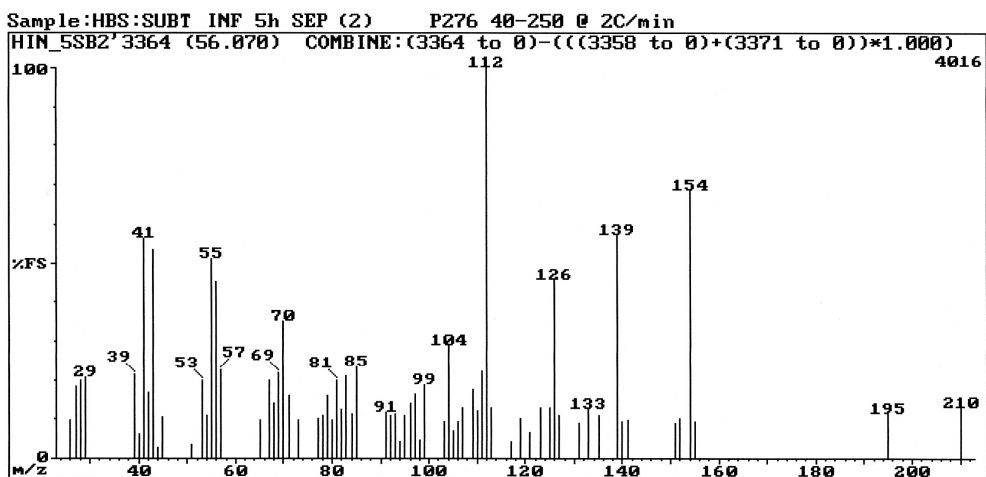


Fig. 3.215: EI mass spectrum of component **C250**.

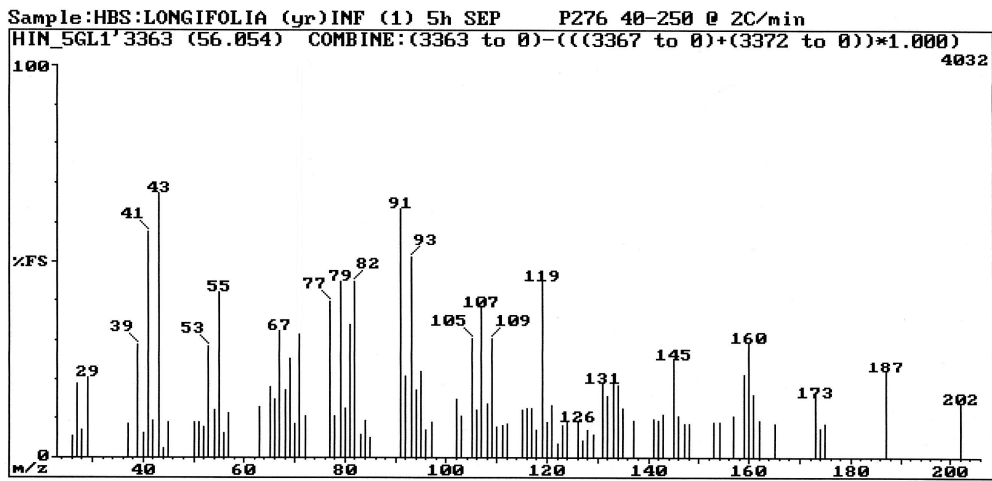


Fig. 3.216: EI mass spectrum of component **C251**.

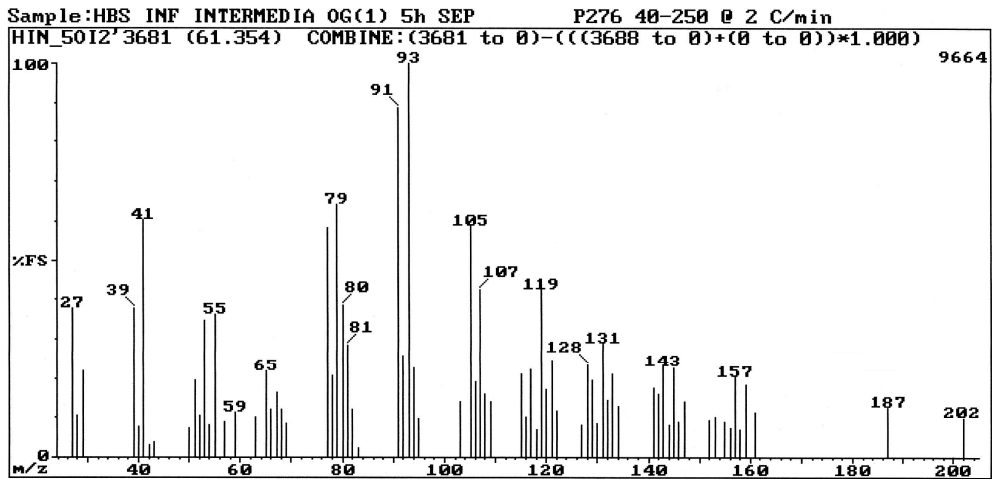


Fig. 3.217: EI mass spectrum of component **C281**.

### 3.4 REFERENCES

- Adams, R.P. 2004. Identification of essential oil components by gas-chromatography/quadropole mass spectrometry. Allured Publishing Corporation, Carol Stream, Illinois, USA.
- Benz, W., Biemann, K. 1964. The specificity of the electron-impact induced elimination of water from alcohols and related reactions in the mass spectrometer. *J. Am. Chem. Soc.* **86**, 2375–2378.
- Berger, R.G. 2007. Flavours and fragrances: Chemistry, bioprocessing and sustainability. Springer, Berlin, Heidelberg.
- Beynon, J.H., Saunders, R.A. Williams, A.E. 1961. The high resolution mass spectra of aliphatic esters. *Anal. Chem.* **33**, 221–225.
- Binder, R.G., Flath, R.A. 1989. Volatile components of pineapple guava. *J. Agric. Food Chem.* **37**, 734–736.
- Black, D.R., McFadden, W.H., Corse, J.W. 1964. Specific rearrangements in the mass spectra of short chain esters. *J. Phys. Chem.* **68**, 1237–1240.
- Boldingh, J., Taylor, R.J. 1962. Trace constituents of butterfat. *Nature* **194**, 909–913.
- Budzikiewicz, H., Djerassi, C., Jackson, A.H., Kenner, G.W., Newman, D.J., Wilson, J.M. 1964a. Pyrroles and related compounds. Part IV. Mass spectrometry in structural and stereochemical problems. Part XXX. Mass spectra of monocyclic derivatives of pyrrole. *J. Chem. Soc.* 1949–1960.
- Budzikiewicz, H., Djerassi, C., Williams, D.H. 1964b. Structure elucidation of natural products by mass spectrometry. Volume II: Steroids, terpenoids, sugars and miscellaneous classes. Holden-Day Inc., San Francisco.
- Budzikiewicz, H., Djerassi, C., Williams, D.H. 1967. Mass Spectrometry of Organic Compounds. Holden-Day Inc., San Francisco.
- Buttery, R.G. 1975. Nona-2,4,6-trienal, an unusual component of blended dry beans. *J. Agric. Food Chem.* **23**, 1003–1004.
- Dias, J.R., Sheikh, Y.M. Djerassi, C. 1972. Mass spectrometry in structural and stereochemical problems. CCVIII. The effect of double bonds upon the McLafferty rearrangement of carbonyl compounds. *J. Am. Chem. Soc.* **94**, 473–481.
- Clarke, G.M., Grigg, R., Williams, D.H. 1966. Studies in mass spectrometry. Part VII. Mass spectra of thiazoles, *J. Chem. Soc. B*, 339–343.
- Demole, E., Enggist, P. 1974. Novel synthesis of 3,5,5-trimethyl-4-(2-butenylidene)-cyclohex-2-en-1-one, a major constituent of Burley tobacco flavour. *Helv. Chim. Acta.* **57**, 2087–2091.
- Djerassi, C., Fenselau, C. 1964. Mass spectrometry in structural and stereochemical problems. LXXXVI. The hydrogen transfer reactions in butyl propionate, benzoate and phthalate. *J. Am. Chem. Soc.* **87**, 5756–5762.
- Dolejs, L., Beran, P., Hradec, J. 1968. Mass spectra of branched long-chain aliphatic alcohols. *Org. Mass Spectrom.* **1**, 563–566.

- Eggers, N.J., Bohna, K., Dooley, B. 2006. Determination of vitispirane in wines by stable isotope dilution assay. *Am. J. En. Vitic.* **57**, 226–232.
- Elmore, J.S., Cooper, S.L., Enser, M., Mottram, D.S., Sinclair, L.A., Wilkinson, R.G., Wood, J.D. 2005. Dietary manipulation of fatty acid composition in lamb meat and its effect on the volatile aroma compounds of grilled lamb. *Meat Science* **69**, 233–242.
- ESO. 2006. The complete database of essential oils, Boelens Aroma Chemical Information Service (BACIS), Leffingwel & Associates (Publisher), Georgia.
- Ethiel, E.L., McCollum, J.D., Meyerson, S., Rylander, P.N. 1961. Organic ions in the gas phase. IX. Dissociation of benzyl alcohol by electron impact. *J. Am. Chem. Soc.* **83**, 2481–2484.
- Fenselau, C., Baum, A., Cowans, D. 1970. Variation of fragmentation with chain length between two functional groups. *Org. Mass Spectrom.* **4**, 229–235.
- Fernández, A., Camacho, A., Fernández, C., Altarejos, J. 2000. Composition of the essential oils from galls and aerial parts of *Pistacia letiscus* L. *J. Essent. Oil Res.* **12**, 19–23.
- Filippi, J.-J., Lanfranchi, D.-A., Prado, S., Baldovini, N., Meierhenrich, U.J. 2006. Composition, enantiomeric distribution, and antibacterial activity of the essential oil of *Achillea ligustica* All. from Corsica. *J. Agric. Food Chem.* **54**, 6308–6313.
- Flamini, G., Cioni, P.L., Morelli, I. 2004. Essential oils of *Galeopsis pubescens* and *G. tetrahit* from Tuscany (Italy). *Flavour Fragr. J.* **19**, 327–329.
- Friedman, L., Long, F.A. 1953. Mass spectra of six lactones. *J. Am. Chem. Soc.* **75**, 2832–2836.
- Friedman, L., Wolf, A.P. 1958. Electron impact dissociation of camphene-8-C<sup>13</sup>. *J. Am. Chem. Soc.* **80**, 2424–2426.
- Giese, B., Haßkerl, T., Lüning, U. 1984. Synthese von  $\gamma$ - und  $\delta$ -lactonen über radikalische CC-verknüpfung. *Chem. Ber.* **117**, 859–861.
- Gomez, E., Ledbetter, C.A., Hartsell, L.H. 1993. Volatile compounds in apricot, plum and their interspecific hybrids. *J. Agric. Food Chem.* **41**, 1669–1676.
- Grigg, R., Jacobsen, H.J., Lawesson, S.-O., Sargent, M.V., Schroll, G., Williams, D.H. 1966. Studies in mass spectrometry. Part IV. Mass spectra of hydroxythiopenes and thiolactones. *J. Chem. Soc. B* 331–335.
- Harrison, A.G., Haynes, P., McLean, S., Meyer, F. 1965. The mass spectra of methyl-substituted cyclopentadienes. *J. Am. Chem. Soc.* **87**, 5099–5105.
- Heydanek, M.G., McGorin, R.J. 1981. Gas chromatography-mass spectroscopy investigations on the flavor chemistry of oat groats. *J. Agric. Food Chem.* **29**, 950–954.
- Horita, H., Hara, T. 1984. Analysis of tea aroma prepared by simultaneous steam distillation and ether extraction method. *Study of Tea* **66**, 41–46.
- Horita, H., Hara, T. 1985. Analysis of headspace volatile components of tea using Tenax TA trapping system. *Study of Tea* **68**, 17–24.
- Horsely, S.B., Cardellina, J.H., Meinwald, J. 1981. Secondary metabolites from a red alga (*Larencia intricata*): Sesquiterpene alcohols. *J. Org. Chem.* **46**, 5033–5035.

- Junge, M., König, W.A. 2003. Selectivity tuning of cyclodextrin derivatives by specific substitution. *J. Sep. Sci.* **26**, 1607–1614.
- Kaiser, R. 1984. (5*R*<sup>\*</sup>, 9*S*<sup>\*</sup>)- and (5*R*<sup>\*</sup>, 9*R*<sup>\*</sup>)-2,2,9-Trimethyl-1,6-dioxaspiro[4.4]non-3-ene and their dihydro derivatives as new constituents of geranium oil. *Helv. Chim. Acta* **67**, 1198–1203.
- Kaiser, R., Lamparsky, D. 1978a. Inhaltsstoffe des *Osmanthus*-absolues. *Helv. Chim. Acta.* **61**, 373–382.
- Kaiser, R., Lamparsky, D. 1978b. Inhaltsstoffe des *Osmanthus*-absolues. *Helv. Chim. Acta.* **61**, 2328–2335.
- Kawakami, M., Chairote, M., Kobayashi, A. 1987. Flavour constituents of pickled tea, Miang, in Thailand. *Agric. Biol. Chem.* **51**, 1683–1687.
- Kawakami, M., Shibamoto, T. 1991. The volatile constituents of piled tea: Toyama Kurocha. *Agric. Biol. Chem* **55**, 1839–1847.
- Kawakami, M., Subhendu, N., Ganguly, J., Banerjee, J. Kobayashi, A. 1995. Aroma composition of Oolong tea and black tea by brewed extraction method and characterizing compounds of Darjeeling tea aroma. *J. Agric. Food Chem.* **43**, 200–207.
- Kawakami, M., Yamanishi, T., Kobayashi, A. 1986. The application of the Pouchong tea process to the leaves of tea plants, *var. assamica* dominant hybrids. *Agric. Biol. Chem.* **50**, 1895–1898.
- Kovats, E. 1958. Gas-chromatographische charakterisierung organischer verbindungen. Teil1: Retentionsindices aliphatischer halogenide, alkohole, aldehyde und ketone. *Helv. Chim. Acta* **41**, 1915–1932.
- Kreck, M., Scharrer, A., Bilke, S., Mosandl, A. 2002. Enantioselective analysis of monoterpene compounds in essential oils by stir bar sorptive extraction (SBSE)-enantio-MDGC-MS. *Flavour Frag. J.* **17**, 32–40.
- Lai, W., Song, C. 1995. Temperature-programmed retention indices for GC and GC-MS analysis of coal- and petroleum-derived liquid fuels. *Fuel* **74**, 1436–1451.
- Lardelli, G., Dijkstra, G., Harkes, P.D., Boldingh, J. 1966. A new  $\gamma$ -lactone found in butter. *Recl. Trav. Chim.* **85**, 43–55.
- Leffingwell and Associates. 1999. Delta-lactones & molecular structures [Online]. Available: <http://www.leffingwell.com/dlacton.htm> [2009, September].
- Liedtke, R.J., Djerassi, C. 1969. Mass spectrometry in structural and stereochemical problems CLXXXIII. A study of the electron impact induced fragmentation of aliphatic aldehydes. *J. Am. Chem. Soc.* **91**, 6814–6821.
- Luan, F., Hampel, D., Mosandl, A., Wüst, M. 2004. Enantioselective analysis of free and glycosidically bound monoterpene polyols in *vitis vinifera* L. Cvs. Morio Muscat and Muscat Ottonel: Evidence for an oxidative monoterpene metabolism in grapes. *J. Agric. Food. Chem.* **52**, 2036–2041.
- Maas, B., Dietrich, A., Mosandl, A. 1994a. Collection of enantiomer separation factors obtained by capillary gas chromatography on chiral stationary phases. *J. High Resolut. Chrom.* **17**, 109–115.

- Maas, B., Dietrich, A., Mosandl, A. 1994b. Collection of enantiomer separation factors obtained by capillary gas chromatography on chiral stationary phases. *J. High Resolut. Chrom.* **17**, 169–173.
- Macoll, A. 1988. Low-energy, low-temperature mass spectra. The McLafferty rearrangement. *Org. Mass Spectrom.* **23**, 381–387.
- Mathias, B., Mosandl, A. 2004. Improved gas chromatographic stereodifferentiation of chiral main constituents from different essential oils using a mixture of chiral stationary phases. *Flavour Fragr. J.* **19**, 515–517.
- McFadden, W.H., Day, E.A., Diamond, M.J. 1965. Correlations and anomalies in mass spectra (lactones). *Anal. Chem.* **37**, 89–92.
- McLafferty, F.W. 1959. Mass spectrometric analysis—molecular rearrangements. *Anal. Chem.* **31**, 82–87.
- McLafferty, F.W. 1973. Interpretation of mass spectra, 2<sup>nd</sup> ed. W.A. Benjamin, Inc., London.
- McLafferty, F.W., Tureček, F. 1993. Interpretation of mass spectra. University Science Books, California.
- Meyerson, S., Rylander, P.N. 1957. Organic ions in the gas phase. III. C<sub>6</sub>H<sub>5</sub><sup>+</sup> ions from benzene derivatives by electron impact. *J. Am. Chem. Soc.* **79**, 1058–1061.
- Meyerson, S., Rylander, P.N., Eliel, E.L., McCollum, J.D. 1959. Organic ions in the gas phase. VII. Tropylium ion from benzyl chloride and benzyl alcohol. *J. Am. Chem. Soc.* **81**, 2606–2610.
- Miyazawa, M., Nagai, S., Oshima, T. 2008. Volatile components of the straw of *Oryza sativa* L. *J. Oleo. Sci.* **57**, 139–143.
- Mo, W-P. 1994. Olfactory communication: Chemical characterization of the preorbital secretion of the oribi, *Ourebia ourebi*. PhD thesis, Stellenbosch University, Stellenbosch, South Africa.
- Näf, R., Jaquier, A. Velluz, A. 1997. A new natural furan and some related compounds. *Flavour Fragr. J.* **12**, 377–380.
- National Institute of Advanced Industrial Science and Technology (AIST). 2010. Spectral database for organic compounds, SDBS [Online]. Available: <http://riodb01.ibase.aist.go.jp/sdbs/> [2009, 19 February].
- NBS database. 1990. VG MassLab, VG Instruments, Manchester, UK.
- NIST/EPA/NIH. 2005. Mass spectral library (version 2.0d), Standard Reference Data: National Institute of Standards and Technology, USA.
- Ohloff, G. 1994. Scent and fragrances: The fascination of odors and their chemical perspectives. Springer-Verlag, Germany.
- Ohloff, G., Giersch, W., Schulte-Elte, K.H., Enggist, P., Demole, E. 1980. Synthesis of (R)- and (S)-4-methyl-6-2'-methylprop-1'-enyl-5,6-dihydro-2H-pyran (nerol oxide) and natural occurrence of its racemate. *Helv. Chim. Acta* **63**, 1582–1588.
- Owuor, O.P., Obanda, M. 1999. The effects of blending clonal leaf on black tea quality. *Food Chemistry* **66**, 147–152.
- Pasto, D.J., Johnson, C.R. 1969. Organic structure determination. Prentice Hall Inc., New Jersey.



- Ramalho, P.S., De Freitas, V.A.P., Macedo, A., Silva, G., Silva, M.S. 1999. Volatile components of *Cistus ladanifer* leaves. *Flavour Frag. J.* **14**, 300–302.
- Radulovic, N., Zlatkovic, D., Zlatkovic, B., Dokovic, D., Stojanovic, G., Palic, R. 2008. Chemical composition of leaf and flower essential oils of *Conium maculatum* from Serbia. *Chem. Nat. Comp.* **44**, 390–392.
- Ryhage, R., Von Sydow, E. 1963. Mass spectrometry of terpenes. I. Monoterpene hydrocarbons. *Acta Chem. Scand.* **17**, 2025–2035.
- Schumacher, J.N., Roberts, D.L. 1966. Tobacco flavours. US patent 3,251,366. *Chem. Abstr.* **65**, 12113b.
- Serra, S., Fuganti, C., Brenna, E. 2006. Synthesis, olfactory evaluation and determination of the absolute configuration of the 3,4-didehydroionone stereoisomers. *Helv. Chim. Acta* **89**, 1110–1122.
- Sharkey, A.G. (jr.), Shultz, J.L., Friedel, R.A. 1956. Mass spectra of ketones. *Anal. Chem.* **28**, 934–940.
- Sharkey, A.G., Schultz, J.L., Friedel, R.A. 1959. Mass spectra of esters-formation of rearrangement ion. *Anal. Chem.* **31**, 87–94.
- Schuh, C., Schieberle, P. 2005. Characterization of (*E,E,Z*)-2,4,6-nonatrienal as a character impact aroma compound of oat flakes. *J. Agric. Food. Chem.* **53**, 8699–8705.
- Sigrist, I.A. 2002. Investigation on aroma active photooxidative degradation products originating from dimethyl pentyl furan fatty acids in green tea and dried green herbs. PhD thesis, Swiss Federal Institute of Technology, Zürich.
- Takazawa, O., Tamura, H., Kogami, K., Hayashi, K. 1982. New synthesis of megastigma-4,6,8-trien-3-ones, 3-hydroxy- $\beta$ -ionol, 3-hydroxy- $\beta$ -ionone, 5,6-epoxy-3-hydroxy- $\beta$ -ionol and 3-oxo- $\alpha$ -ionol. *Bull. Chem. Soc. Jpn.* **55**, 1907–1911.
- Thomas, A.F., Willhalm, B. 1964. Les spectres de masse des hydrocarbures monoterpéniques. *Helv. Chim. Acta* **47**, 475–488.
- Tietze, L.F., Eicher, T. 1981. Reaktionen und synthesen im organisch-chemischen praktikum. Georg Thieme Verlag, Stuttgart, New York.
- Toda, H., Hihara, S., Umamo, K., Shibamoto, T. 1983. Photochemical studies on Jasmin oil. *J. Agric. Food Chem.* **31**, 554–558.
- Van den Dool, H., Kratz, P. DEC. 1963. A generalization of the retention index system including linear temperature programmed gas-liquid partition chromatography. *J. Chromatogr.* **2**, 463–471.
- Weinert, B., Wüst, M., Mosandl, A., Hanssum, H. 1998. Stereoisomeric flavour compounds. LXXVIII. Separation and structure elucidation of the pyranoid linalool oxide stereoisomers using common gas chromatographic phases, modified cyclodextrin phases and nuclear magnetic resonance spectroscopy. *Phytochem. Anal.* **9**, 10–13.
- Wüst, M., Rexroth, A., Beck, T., Mosandl, A. 1997. Structure elucidation of cis- and trans-rose oxide ketone and its enantioselective analysis in geranium oils. *Flav. Frag. J.* **12**, 381–386.

Wüst, M., Mosandl, A. 1999. Important chiral monoterpenoid ethers in flavours and essential oils—enantioselective analysis and biogenesis. *Eur. Food. Res. Technol.* **209**, 3–11.

Yamazaki, Y., Hayashi, Y., Masatoshi, A., Hieda, T., Mikami, Y. 1988. Microbial conversion of  $\alpha$ -ionone,  $\alpha$ -methylionone and  $\alpha$ -isomethylionone. *Appl. Environ. Microbiol.* **54**, 2354–2360.

## CHAPTER 4

# OLFACTOMETRY: IDENTIFICATION OF THE ODOUR-ACTIVE COMPOUNDS PRESENT IN THE AROMA OF FERMENTED HONEYBUSH

### 4.1 GAS CHROMATOGRAPHY-OLFACTOMETRY

In GC-O human assessors are employed as sensitive and selective detectors for odour-active compounds eluting from a GC separation. The human assessor takes the place of a conventional detector, such as a flame ionisation detector (FID) or an MS. Assessors sniff the eluate *via* a specifically designed odour port and report the presence of each odour-active compound detected. The aim of this technique is to determine the odour activity of VOCs in a sample and assign a relative importance to each compound (Delahunty *et al.*, 2006).

The volatile compositions of many natural odours have been studied and the research area has greatly benefited from developments and improvements in instrumental analytical chemistry, especially regarding GC and MS (D' Acampora Zeller *et al.*, 2008). Although the mentioned research has provided much needed information in the areas of food flavour and fragrance quality it was not sufficient, since the initial aim of the research was only to gain information on the profiles of the volatiles of products (D' Acampora Zeller *et al.*, 2008); it did not provide information on how the compounds are perceived at a given concentration. The latter is required to reach a conclusion about the contribution that a compound imparts on the odour quality (Delahunty *et al.*, 2006).

VOCs in complex food and natural fragrances can be recognised and distinguished by the human sense of smell. VOCs have different odour activities that can essentially be ascribed to three important properties of a compound: absolute threshold, intensity as a function of concentration (psychometric function), and quality (Delahunty *et al.*, 2006). Some compounds have very low absolute thresholds whereas others are odourless, and therefore in a complex mixture only a few VOCs contribute to the overall odour. The intensity with which a compound is perceived normally increases when its concentration increases, but for each compound this concentration response is different and it ultimately plays a role in its odour activity. With regard to quality, it is possible that a certain odour sensation might not have a very distinguished quality at its absolute threshold, but it becomes more defined as the concentration increases, and is subject to further change as the concentration changes (Delahunty *et al.*, 2006).

Odours of different quality can mask or suppress one another, or remain distinct, whereas odours that have similar qualities tend to blend and can even produce a new odour quality. It is also possible that synergy can occur between VOCs in a mixture, which could cause certain compounds that are present in concentrations below their odour threshold, or even possess no odour activity

when assessed individually, to contribute to or possess odour activity in a mixture (Day *et al.*, 1963; Delahunty *et al.*, 2006).

So-called electronic noses (e-noses) have been developed in an effort to mimic the human sense of smell. These instruments have applications in the food, cosmetic and pharmaceutical industry, as well as in environmental control and clinical diagnostics. An e-nose consists of broadly tuned sensors that, when exposed to complex odours, generate a characteristic odour fingerprint/smellprint *via* the digital output generated by the e-nose sensors. This digital output is then further analysed by pattern recognition techniques, for example principal component analysis (PCA), to provide useful information (Peris and Escuder-Gilabert, 2009; Wilson and Baietto, 2009). However, it is important to note that e-noses give an indication of the intensity of an odour that is caused by the combined contributions of all the chemicals in the mixture (Bhattacharyya *et al.*, 2007) and are thus not able to identify or determine individual contributions of VOCs in a mixture. The use of human assessors remains the method of choice, although the human sense of smell has its limitations and it is known that it is very difficult to identify individual compounds in even the simplest of mixtures (Delahunty *et al.*, 2006).

GC detector response cannot be used as an accurate representative of odour activity due to the large variations in odour thresholds and psychometric functions of odour-active compounds mentioned above, which means that the largest peak in a GC analysis is not necessarily the most important odorant (Delahunty *et al.*, 2006).

A human assessor can be trained to indicate for each compound eluting from the GC whether the odour is present or not, what the duration of the odour activity is (start to end), what the quality of the perceived odour is, as well as its intensity. Based upon these possible observations, three types of GC-O techniques have been developed: [1] detection frequency (DF) (Linssen *et al.*, 1993; Pollien *et al.*, 1997); [2] dilution to threshold, which includes CharmAnalysis™ (Acree, 1993a; Acree, 1993b; Acree *et al.*, 1984;) and AEDA (Ullrich and Grosch, 1987); [3] direct intensity, which includes the Osme method (Da Silva *et al.*, 1994; Miranda-Lopez *et al.*, 1992) and finger span method (Étiévant, 2002; Étiévant *et al.*, 1999; Guichard *et al.*, 1995).

#### **4.1.1 Detection frequency**

The members of a panel consisting of at least 6–12 assessors are required to sniff the eluate of the same extract and indicate when they detect an odorant. The total number of assessors able to detect an odour at a specific retention time are counted and this number is expressed as a percentage of the total number of assessors (Pollien *et al.*, 1997; van Ruth, 2001; van Ruth and O'Connor, 2001a). Compounds that are detected more frequently are concluded to have a greater relative importance (Plutowska and Wardencki, 2008) and this is assumed to be related to actual odour intensity perceived at the concentration of the compound present in the sample (van Ruth and O'Connor, 2001a). When using this method it is also possible to additionally measure the duration of the odour occurrence, which can be used to calculate a peak area by multiplying it with the number of

odour detections (Ott *et al.*, 1997; Pollien *et al.*, 1997). This results in greater discrimination between compounds (Peterson *et al.*, 2003), but could simultaneously lead to overestimation of broad, partially coeluting peaks, or underestimation of narrow, early-eluting peaks (Peterson *et al.*, 2003). The duration of odour occurrence was not measured in the present study. One of the main attractions of the DF method is its simplicity; intensive assessor training is not required (Delahunty *et al.*, 2006). In theory, this method accounts for the variable sensitivities of the various assessors, it is repeatable, and the results are applicable to a population (Étiévant, 2002; Le Guen *et al.*, 2000; Pollien *et al.*, 1997).

A limitation in the DF method is an 'end-of-scale' effect, where at a particular concentration all assessors may perceive a specific compound. If the concentration is increased, then the odour intensity is also likely to increase, but the DF cannot (Étiévant, 2002; Delahunty *et al.*, 2006; Plutowska and Wardencki, 2008).

#### 4.1.2 Dilution to threshold: Aroma extract dilution analysis

Dilution to threshold methods such as CharmAnalysis™ and AEDA quantify the odour potency of a compound based upon the ratio of its concentration to its odour threshold in air (Acree, 1993b). A dilution series of the sample is prepared (usually by a factor of two or three), and each dilution (usually between eight and 12 in total) is assessed by GC-O to establish a ranked order of potency for individual compounds (Acree, 1993a; Acree *et al.*, 1984). Assessors record when an odour is perceived and, if possible, also give a description for the odour detected (Delahunty *et al.*, 2006). AEDA measures the maximum dilution of a sample that an odour is perceived in, and reports this as the FD (flavour dilution) factor (Ferreira *et al.*, 2002; Grosch, 1993, 1994, 2001; Plutowska and Wardencki, 2008; Ullrich and Grosch, 1987). FD values serve to rank key aroma compounds in order of their potency.

$$FD = R^n$$

where R is the factor by which the dilutions were prepared (typically 2 or 3)  
and n is the last dilution at which the odour was still detected

CharmAnalysis™ differs from AEDA in that the duration of the odours is also recorded, which generates chromatographic peaks where the areas are expressed as unitless "Charm" values (Acree, 1993a; Acree, 1993b; Acree *et al.*, 1984).

Dilution to threshold methods such as AEDA do not measure odour intensity at any of the concentrations evaluated but, as mentioned, rather measure odour potency (Acree, 1997; Acree *et al.*, 1984; Deibler, *et al.*, 1999) and provide reliable results in this regard (Delahunty *et al.*, 2006).

The significant contribution of each individual odorant to the overall aroma can be determined by calculating its odour activity value (OAV) or its relative flavour activity (RFA). The OAV is the ratio of the actual concentration of the compound in the sample to its odour threshold (Grosch, 1994). Compounds with higher OAVs contribute more to the overall aroma (Guth and Grosch, 1999). FD

factors are considered to be proportional to OAVs. The calculation of OAVs is not an easy task, since the determination of threshold values for compounds is time consuming, and they could vary among and within panellist groups (Schieberle *et al.*, 1993). This has led to controversy related to the use of OAVs as indicators of the percent contribution of compounds to the overall intensity of a sample (D'Acampora Zellner *et al.*, 2008). RFA is calculated as an alternative parameter to OAV:

$$\text{RFA} = \log R^n / S^{0.5} \text{ (Song } et al., 2000).$$

where  $\log R^n = \log \text{FD}$

and  $S^{0.5}$  = the square root of the weight percentage (or area %) of the compound

RFA has been used to determine the significant contribution of aroma-active compounds in a variety of citrus cultivars (Choi, 2003; Choi *et al.*, 2001; Dharmawan *et al.*, 2009; Sawamura *et al.*, 2004, 2006, 2001).

A disadvantage of dilution methods is that they are time consuming, requiring analyses of series of dilutions for a single extract, and therefore only one or two assessors are usually used. However, using a low number of assessors makes the results highly susceptible to the large variation in the sensitivities of the individual assessors (Delahunty *et al.*, 2006).

#### 4.1.3 Direct intensity methods

A shortcoming of dilution to threshold methods is that they do not measure the intensity of the perceived stimulus (Da Silva *et al.*, 1994; Frijters, 1978; van Ruth, 2001), whereas in direct intensity methods assessors are required to use a scale to measure the perceived intensity of the compound as it elutes (Delahunty *et al.*, 2006). This can be a single time-averaged measure, e.g. posterior intensity method (Delahunty *et al.*, 2006; van Ruth, 2001b) or it can be dynamic, whereby the onset, maximum intensity and decay of the eluting odour is recorded continuously, e.g. Osme method (Da Silva *et al.*, 1994; Miranda-Lopez *et al.*, 1992).

In the posterior intensity method assessors only rate the maximum odour intensity once the compound has eluted. Although it was found that discrimination between compounds was better for the posterior intensity method compared to the DF method, the results from the two methods were found to be strongly correlated (van Ruth, 2001, 2004; van Ruth and O'Connor, 2001a).

Using the dynamic method, a peak area can be calculated for each odour active compound. In the Osme method odour intensity is assessed by continuously recording the intensity using a horizontal slide bar with a 16-point structured scale. A computerised signal is recorded using a variable resistor (Da Silva *et al.*, 1994). Each sample is replicated by every assessor at a single concentration to produce an individual "Osmegram", in which odour intensity is plotted as a function of retention time, analogous to an FID chromatogram (Da Silva *et al.*, 1994; Miranda-Lopez *et al.*, 1992). A variation of the Osme method in which time-intensity GC-O data is recorded by using cross-modality matching with an assessor's finger span was developed by Étievant *et al.* (1999; 2002).

A potential disadvantage of direct intensity methods is the substantial amount of training that assessors require initially in order to obtain individual reproducibility and agreement with one another. However, once an experienced panel is formed it can be used to rapidly characterise the aroma profiles of samples with excellent precision (Delahunty *et al.*, 2006).

The principles, advantages and disadvantages of the different GC-O methodologies have been discussed and compared by Delahunty *et al.* (2006). Having considered all the available information, it was decided to use DF in combination with AEDA in this study for the identification of the aroma-active components in fermented honeybush.

## 4.2 IDENTIFICATION OF ODOUR-ACTIVE HONEYBUSH VOLATILES

The experimental details of the two GC-O techniques employed in two separate experiments in this study, i.e. the DF method and AEDA, are given in Chapter 8. A panel of 15 assessors participated in the first experiment in which 15 GC-O analyses on the same honeybush infusion (fermented *C. subternata*) were carried out. Each assessor individually sniffed the GC eluate and indicated when an odorant was detected. In order to prevent sensory “fatigue”, each assessor was required to sniff the effluent during alternating first and second halves of consecutive analyses. The total number of assessors able to detect a specific odour at a specific retention time were counted and the number expressed as a percentage of the total number of assessors. Those compounds with the highest DF are presented in a ranked order in Table 4.1.

In a second experiment the AEDA method was applied with one experienced assessor who had conducted a series of honeybush GC-O experiments prior to this study. This assessor sniffed the GC eluate of a series of dilutions of honeybush infusions and for each compound reported the highest dilution at which that specific compound could no longer be detected. FD factors were calculated for individual odorants and are presented in Table 4.1. Although assessors in both experiments also gave general descriptions for certain odours that were readily recognised, these data have not been included in Table 4.1. The reason is that the assessors were not fully trained to assign aroma descriptors and it is not an essential requirement of the two GC-O methods used in this study. However, there was some degree of consensus that the odours of certain components, such as the three megastigmatrienones (C271, C277 and C295), 10-*epi*- $\gamma$ -eudesmol (C278), *epi*- $\alpha$ -muurolol (C284) and *epi*- $\alpha$ -cadinol (C285), are typically honeybush-like. Published aroma descriptors have been included in the table as a matter of interest.

For each aroma-active compound the ratio between its relative concentration (area %) in the honeybush infusion headspace and its odour threshold was calculated to give a value (‘OAV’), which is not identical, but is equivalent to, the OAV defined by Grosch (1994) (see § 4.1.2), and which also incorporates a concept similar to aroma character impact defined by Yang (2008). In addition to DF and FD values, calculated RFA and ‘OAV’ values are also included in Table 4.1. In the case of those compounds for which odour threshold data were not available in the literature, ‘OAV’s were not calculated.

As described in Chapter 3, the honeybush VOCs were identified by means of GC-MS analysis. In order to assign the correct GC retention time to each identified compound in the GC-O analyses most of the compounds listed in Table 4.1 were subjected to retention time comparison with commercially available or synthesised compounds and the identification of most of the compounds was confirmed by GC-MS-O analysis of the honeybush sample.



Table 4.1: Odour-active compounds identified in fermented honeybush (*C. subternata*) aroma by means of GC-O-analysis

No	Compound <sup>a</sup>	Aroma descriptors <sup>b</sup>	I <sup>c</sup>	Conc. <sup>d</sup> (area %)	OT <sup>e</sup> (ppb)	DF <sup>f</sup> (%)	FD <sup>g</sup>	RFA <sup>h</sup>	'OAV' <sup>i</sup>
C76	Linalool	Refreshing, floral-woody	A	23.954	6	100	16384	0.9	4
C101	( <i>E,Z</i> )-2,6-Nonadienal	Green-vegetable, cucumber or violet leaf	B	0.223	0.010	100	32	3.2	22
C108	( <i>E</i> )-2-Nonenal	Green, cucumber, aldehydic and fatty	B	0.128	0.080	100	4	1.7	1.6
C204	( <i>E</i> )- $\beta$ -Damascenone	Woody, sweet, fruity, earthy green-floral	A	0.607	0.002	100	32768	5.8	303
C11	3-Methylbutanoic acid	Acid acrid, cheesy, unpleasant	B	0.034	250	93	8	4.9	$1.3 \times 10^{-4}$
C70	( <i>E,E</i> )-3,5-Octadien-2-one	Fatty, fruity, mushroom	A	0.053	150	93	4	2.6	$3.6 \times 10^{-4}$
C121	$\alpha$ -Terpineol	Floral, sweet, lilac-type	A	14.039	350	93	2	0.1	$4.0 \times 10^{-2}$
C128	(+)- <i>p</i> -Menth-1-en-9-al	Powerful spicy, herbaceous odour	A	0.103	– <sup>j</sup>	93	2	0.9	– <sup>k</sup>
C148	Geraniol	Sweet, floral, rose, citrus-like	A	25.344	40	93	512	0.5	$6.0 \times 10^{-1}$
C212	( <i>E</i> )- $\beta$ -damascone	Fruity (apple-citrus), tea-like with slight minty notes	A	0.249	0.090	93	4096	7.2	2.8
C222	2,3-Dehydro- $\gamma$ -ionone	– <sup>l</sup>	C	0.247	– <sup>j</sup>	87	32	3.0	– <sup>k</sup>
C229	( <i>S</i> )-( <i>Z</i> )-7-Decen-5-olide	Sweet, floral, fruity	A	0.036	2000	87	2	1.6	$1.8 \times 10^{-5}$
C230	3,4-Dehydro- $\beta$ -ionone	Ionone-damascone and saffron-like, fruity and slightly leathery	A	0.104	– <sup>j</sup>	87	64	5.6	– <sup>k</sup>
C233	( <i>R</i> )-Decan-5-olide	Sweet, creamy, nut-like, fruity	A	0.187	100	87	2	0.7	$1.9 \times 10^{-3}$
C234	( <i>E</i> )- $\beta$ -Ionone	Warm, woody, fruity, raspberry-like; resembles cedarwood	A	3.061	0.007	87	512	1.5	437
C71	Terpinolene	Sweet-piney, oily	A	1.116	200	80	1	0.0	$5.6 \times 10^{-3}$
C191	Eugenol	Warm-spicy, dry	B	0.009	6	80	4	6.5	$1.4 \times 10^{-3}$
C245	Bovolide	Celery- and lovage-like, fruity and pleasant	C	0.447	– <sup>j</sup>	80	4	0.9	– <sup>k</sup>
C269	Component C269	–		0.022	– <sup>j</sup>	80	1	0.0	– <sup>k</sup>
C13	( <i>R</i> )-2-Methylbutanoic acid	Cheesy, sweaty, sharp	B	0.011	740	73	2	2.9	$1.5 \times 10^{-5}$
C79	2-Phenylethanol	Mild, warm, rose-honey-like	A	0.010	1100	73	4	6.0	$9.0 \times 10^{-6}$
C97	Lilac aldehyde isomer 1	Sweet, fresh, floral	C	0.009	– <sup>j</sup>	73	1	0.0	– <sup>k</sup>

Table 4.1 *contd.*

No	Compound <sup>a</sup>	Aroma descriptors <sup>b</sup>	I <sup>c</sup>	Conc. <sup>d</sup> (area %)	OT <sup>e</sup> (ppb)	DF <sup>f</sup> (%)	FD <sup>g</sup>	RFA <sup>h</sup>	'OAV' <sup>i</sup>
C32	6-Methyl-5-hepten-2-one	Oily-green, pungent-herbaceous, grassy, with fresh and green-fruity notes	A	0.439	50	67	1	0.0	$8.8 \times 10^{-3}$
C61	$\gamma$ -Terpinene	Refreshing, herbaceous, citrus-like	B	0.283	– <sup>j</sup>	67	1	0.0	– <sup>k</sup>
C89	4-Acetyl-1-methylcyclo- hexene	Spicy	A	0.031	– <sup>j</sup>	67	4	3.4	– <sup>k</sup>
C135	Nerol	Fresh, sweet-rosy	A	6.483	300	67	8	0.4	$2.0 \times 10^{-2}$
C271	(6 <i>E</i> ,8 <i>Z</i> )-Megastigma-4,6,8- trien-3-one	Tobacco-like, woody, balsamic	C	0.027	– <sup>j</sup>	67	2	1.8	– <sup>k</sup>
C50	<i>p</i> -Cymene	Citrus-like, reminiscent of lemon and bergamot	B	0.066	150	60	1	0.0	$4.4 \times 10^{-4}$
C56	( <i>Z</i> )- $\beta$ -Ocimene	Warm-herbaceous, sweet, floral	A	0.475	– <sup>j</sup>	60	4	0.9	– <sup>k</sup>
C150	Geranial	Lemon	A	0.124	32	60	1	0.0	$3.9 \times 10^{-3}$
C152	( <i>R</i> )-Octan-5-olide	Peach, coconut-like, sweet, creamy	A	0.047	400	60	4	2.8	$3.9 \times 10^{-3}$
C178	Component C178	–		0.060	– <sup>j</sup>	60	512	11.1	– <sup>k</sup>
C284	<i>epi</i> - $\alpha$ -Cadinol	Herbaceous, woody	C	0.061	– <sup>j</sup>	60	64	7.3	– <sup>k</sup>
C285	<i>epi</i> - $\alpha$ -Muurolol	Herbaceous, slightly spicy	C	0.034	– <sup>j</sup>	60	64	9.8	– <sup>k</sup>
C295	(7 <i>E</i> )-Megastigma-5,7,9- trien-4-one	Tea-like, spicy and resembling dried fruit		0.002	– <sup>j</sup>	60	512	63.7	– <sup>k</sup>
C6	Hexanal	Fatty-green grassy odour	B	0.329	5	53	1	0.0	$6.0 \times 10^{-2}$
C141	<i>p</i> -Anisaldehyde	Sweet, floral, "hay-like"	B	0.009	200	53	4	6.4	$4.4 \times 10^{-5}$
C272	Geranyl 2-methylbutanoate	Pleasant, sweet		0.026	– <sup>j</sup>	47	8	5.6	– <sup>k</sup>
C129	$\beta$ -Cyclositral	Green, grassy, hay-like	A	0.629	5	40	2	0.4	$1.0 \times 10^{-1}$
C162	Component C162	–		0.022	– <sup>j</sup>	40	2	2.0	– <sup>k</sup>
C277	(6 <i>E</i> ,8 <i>E</i> )-Megastigma-4,6,8- trien-3-one	Tobacco-like, woody, balsamic	C	0.115	– <sup>j</sup>	40	8	2.7	– <sup>k</sup>
C278	10- <i>epi</i> - $\gamma$ -Eudesmol	Woody, floral, sweet	C	0.117	– <sup>j</sup>	40	64	5.3	– <sup>k</sup>
C164	Geranyl formate	Fresh, green-rosy, fruity	B	0.110	200	33	2	0.9	$5.5 \times 10^{-4}$

Table 4.1 *contd.*

No	Compound <sup>a</sup>	Aroma descriptors <sup>b</sup>	I <sup>c</sup>	Conc. <sup>d</sup> (area %)	OT <sup>e</sup> (ppb)	DF <sup>f</sup> (%)	FD <sup>g</sup>	RFA <sup>h</sup>	'OAV' <sup>i</sup>
C171	( <i>E,E</i> )-2,4-Decadienal	Fried, waxy, fatty, orange-like	B	0.035	0.07	33	64	9.7	0.5
C203	2,3-Dehydro- $\alpha$ -ionone	Tobacco-like	C	0.100	– <sup>j</sup>	33	8	2.9	– <sup>k</sup>
C290	Cadalene	–		0.108	– <sup>j</sup>	33	8	2.7	– <sup>k</sup>

<sup>a</sup> In order of decreasing DF values.

<sup>b</sup> Acree and Arn, 2004; Arctander, 1969; Boldingh and Taylor, 1962; Buttery *et al.*, 1979; Demole and Enggist, 1974; JECFA, 2009; Kreck and Mosandl, 2003; Leffingwell, 2002; Mookherjee and Wilson, 1990; Mosciano *et al.*, 1991a, 1991b; Näf and Velluz, 2000; Ohloff, 1994; Oomah and Liang, 2007; Serra *et al.*, 2006; Tachihara *et al.*, 2006; Takahashi *et al.*, 1980; Yamazaki *et al.*, 1988.

<sup>c</sup> Confirmation of GC retention time: A, Confirmation by retention time comparison with commercially available or synthesised compound and by GC-MS-O analysis; B, Confirmation by retention time comparison with commercially available or synthesised compound; C, Confirmation by GC-MS-O analysis.

<sup>d</sup> Average percent peak area calculated from TIC (use of area % TIC discussed in § 5.1.1).

<sup>e</sup> OT – Odour threshold: Buttery *et al.*, 1974; Buttery and Ling, 1995; Buttery *et al.*, 1968; Buttery *et al.*, 1971; Buttery *et al.*, 1990; Buttery *et al.*, 1988; Engel *et al.*, 1988; Ohloff, 1994; Schieberle and Hofmann, 1997; Siegmund and Pöllinger-Zierler, 2006; Takeoka *et al.*, 1990; Tamura *et al.*, 1993.

<sup>f</sup> DF – detection frequency.

<sup>g</sup> FD – flavour dilution factor.

<sup>h</sup> RFA – Relative flavour activity.

<sup>i</sup> 'OAV' – 'Odour activity value'.

<sup>j</sup> OT value not available in literature.

<sup>k</sup> 'OAV' not calculated since odour threshold value not available.

<sup>l</sup> Aroma descriptor not available.

According to the data obtained by means of the DF method the compounds linalool, (*E,Z*)-2,6-nonadienal, (*E*)-2-nonenal and (*E*)- $\beta$ -damascenone could possibly be the most intense individual contributors to the unique aroma of honeybush (DF 100%). (*E*)- $\beta$ -damascenone also has the highest FD factor, which could be ascribed to its very low odour threshold (0.002 ppb). Linalool has the second highest FD factor, but in this case it could rather be attributed to the high concentration of this compound in honeybush aroma (e.g. 24 area % in *C. subternata*) compared to that of (*E*)- $\beta$ -damascenone (0.6 area %) (see Table 4.1 and § 5.1.1). This means that AEDA successfully discriminated between these two compounds, and was instrumental in determining that (*E*)- $\beta$ -damascenone is in fact a more intense honeybush aroma compound than linalool. The DF and AEDA results for linalool and (*E*)- $\beta$ -damascenone are in agreement, i.e. the two compounds with the highest DF also have the highest FD factor. It could therefore be concluded that these two compounds are definitively intense odorants of honeybush aroma.

Other compounds that also have both high DF and FD factors are geraniol, (*E*)- $\beta$ -damascone, (*E*)- $\beta$ -ionone and (*E,Z*)-2,6-nonadienal. Geraniol falls into the same category as linalool, because it is present in a very high concentration in honeybush aroma (25 area %) and therefore will have a high FD factor even if it becomes more diluted. However, its FD value is somewhat less than that of linalool since it has a higher odour threshold (40 ppb) than linalool (6 ppb). (*E*)- $\beta$ -damascone, (*E*)- $\beta$ -ionone and (*E,Z*)-2,6-nonadienal fall in the same category as (*E*)- $\beta$ -damascenone, because their concentrations are also not that high, but, due to their low odour thresholds, even when diluted, they are still detected.

The compounds 3,4-dehydro- $\beta$ -ionone and 2,3-dehydro- $\gamma$ -ionone also have high DFs and relatively high FD factors (64 and 32, respectively) and can thus also be considered important contributors to the aroma of honeybush.

There are other compounds that have lower DFs but high FD factors, such as component C178 and (7*E*)-megastigma-5,7,9-trien-4-one. This phenomenon can be ascribed to the fact that they might be species that have a flat psychometric (concentration) response curve, which implies that for these compounds it is slightly more difficult to obtain unambiguous results when they are perceived by a panel of assessors (Callejón *et al.*, 2008; D' Acampora Zeller *et al.*, 2008). Another possible explanation could be that these compounds, when not diluted and therefore in high concentration, coelute with other compounds, and are not accurately detected by the assessors (Callejón *et al.*, 2008). Apart from the two compounds mentioned, *epi*- $\alpha$ -cadinol, *epi*- $\alpha$ -muurolol, 10-*epi*- $\gamma$ -eudesmol, and (*E,E*)-2,4-decadienal also show a similar pattern, but have somewhat lower FD factors.

(*E*)-2-Nonenal has a DF of 100%, but a low FD factor (4). The reason for this is probably that in the DF experiment it is present in a concentration that is above its threshold, and it probably has a relatively steep psychometric function, so that all assessors could easily detect it (Callejón *et al.*, 2008, D' Acampora Zeller *et al.*, 2008). However, in the AEDA experiment where the component (of which the concentration is relatively low from the onset) is diluted even further, its concentration

becomes too low to be detectable, and as a consequence, it has a low FD factor. Another reason why compounds fall into this last group may be that they have high odour thresholds and so they quickly become insignificant when diluted, even though they might be present in relatively high concentrations, e.g.  $\alpha$ -terpineol. Other compounds that show this trend (high DF but low FD) include 3-methylbutanoic acid, (*E,E*)-3,5-octadien-2-one, *p*-menth-1-en-9-al, (*S*)-(*Z*)-7-decen-5-olide, (*R*)-decan-5-olide, terpinolene, eugenol, boviolide, component C269, 2-methylbutanoic acid, 2-phenylethanol and lilac aldehyde.

A few trends emerge from the RFA and 'OAV' data. (*7E*)-Megastigma-5,7,9-trien-4-one has the highest RFA value, followed by component C178, *epi*- $\alpha$ -muurolol, (*E,E*)-2,4-decadienal, *epi*- $\alpha$ -cadinol and (*E*)- $\beta$ -damascone. Eugenol, *p*-anisaldehyde, 2-phenylethanol, (*E*)- $\beta$ -damascenone, geranyl 2-methylbutanoate, 3,4-dehydro- $\beta$ -ionone and 10-*epi*- $\gamma$ -eudesmol follow, with values between 5 and 7. 'OAV's were calculated for those compounds for which literature odour threshold data were available: (*E*)- $\beta$ -ionone, (*E*)- $\beta$ -damascenone and (*E,Z*)-2,6-nonadienal were found to have the highest 'OAV's. Linalool, (*E*)- $\beta$ -damascone, (*E*)-2-nonenal, geraniol, (*E,E*)-2,4-decadienal and  $\beta$ -cyclositral have 'OAV's between 0.1 and 4 and could also be considered as relatively important. Some compounds have both high RFA and 'OAV' values, e.g. (*E,E*)-2,4-decadienal, (*E*)- $\beta$ -damascone and (*E*)- $\beta$ -damascenone, and can possibly be explained by the low concentration of the compound and its low odour threshold, which relates to high FD factors. Then there are compounds with high 'OAV's but low RFA values, or *vice versa*, such as linalool, (*E*)- $\beta$ -ionone, (*E*)-2-nonenal, (*E,Z*)-2,6-nonadienal, geraniol,  $\beta$ -cyclositral, eugenol, *p*-anisaldehyde and 2-phenylethanol.

In conclusion, those compounds found to be the most intense individual contributors to the honeybush aroma, based on consideration of all the relevant GC-O data (DF, FD, RFA and 'OAV'), are listed in Table 4.2.

No threshold data is available for 2,3-dehydro- $\gamma$ -ionone, therefore no OAV could be calculated. It may be assumed that a compound such as 2,3-dehydro- $\gamma$ -ionone, which does not have a very high concentration but does have a high FD factor, could have a relatively low odour threshold and, as a consequence, should have a relatively high OAV and should therefore make a significant contribution to the aroma of honeybush. Other compounds that are similar to 2,3-dehydro- $\gamma$ -ionone in this respect include component C178, *epi*- $\alpha$ -cadinol, *epi*- $\alpha$ -muurolol, 3,4-dehydro- $\beta$ -ionone and 10-*epi*- $\gamma$ -eudesmol.

A compound not included in Table 4.2 but, which could possibly also make a considerable contribution to the aroma of honeybush on account of its relatively high 'OAV' is  $\beta$ -cyclositral. Eugenol, *p*-anisaldehyde, 2-phenylethanol and geranyl 2-methylbutanoate, all of which are also not included in Table 4.2, have relatively high RFA values and could possibly also make a considerable contribution to the aroma of honeybush.

Table 4.2. The most intense odour-active compounds identified in fermented honeybush (*C. subternata*) aroma by means of GC-O analysis

No	Compound <sup>a</sup>	Aroma descriptors <sup>b</sup>	DF <sup>c</sup>	FD <sup>d</sup>	RFA <sup>e</sup>	'OAV' <sup>f</sup>
C204	( <i>E</i> )- $\beta$ -Damascenone	Woody, sweet, fruity, earthy green-floral	100	32768	5.8	303
C76	Linalool	Refreshing, floral-woody	100	16384	0.9	4
C212	( <i>E</i> )- $\beta$ -Damascone	Fruity (apple-citrus), tea-like with slight minty notes	93	4096	7.2	2.8
C148	Geraniol	Sweet, floral, rose, citrus-like	93	512	0.5	0.6
C234	( <i>E</i> )- $\beta$ -Ionone	Warm, woody, fruity, raspberry-like; resembles cedarwood	87	512	1.5	437
C178	Component C178	– <sup>g</sup>	60	512	11.1	– <sup>h</sup>
C295	(7 <i>E</i> )-Megastigma-5,7,9-trien-4-one	Tea-like, spicy and resembling dried fruit	60	512	63.7	– <sup>h</sup>
C230	3,4-Dehydro- $\beta$ -ionone	Ionone-damascone and saffron-like, fruity and slightly leathery	93	64	5.6	– <sup>h</sup>
C284	<i>epi</i> - $\alpha$ -Cadinol	Herbaceous, woody	60	64	7.3	– <sup>h</sup>
C285	<i>epi</i> - $\alpha$ -Muurolol	Herbaceous, slightly spicy	60	64	9.8	– <sup>h</sup>
C278	10- <i>epi</i> - $\gamma$ -Eudesmol	Woody, floral, sweet	40	64	5.3	– <sup>h</sup>
C171	( <i>E,E</i> )-2,4-Decadienal	Fried, waxy, fatty, orange-like	33	64	9.7	0.5
C222	2,3-Dehydro- $\gamma$ -ionone	– <sup>g</sup>	87	32	3.0	– <sup>h</sup>
C101	( <i>E,Z</i> )-2,6-Nonadienal	Green-vegetable, cucumber or violet leaf	100	32	3.2	22
C108	( <i>E</i> )-2-Nonenal	Green, cucumber, aldehydic and fatty	100	4	1.7	1.6

<sup>a</sup> In order of decreasing FD values.

<sup>b</sup> Acree and Arn, 2004; Arctander, 1969; Demole and Enggist, 1974; Leffingwell, 2002; Mosciano *et al.*, 1991a, 1991b; Ohloff, 1994; Serra *et al.*, 2006; Yamazaki *et al.*, 1988.

<sup>c</sup> DF – detection frequency.

<sup>d</sup> FD – flavour dilution factor.

<sup>e</sup> RFA – Relative flavour activity.

<sup>f</sup> 'OAV' – 'Odour activity value'.

<sup>g</sup> Aroma descriptor not available.

<sup>h</sup> 'OAV' not calculated since odour threshold value not available.

### 4.3 REFERENCES

- Acree, T.E. 1997. GC/Olfactometry. *Anal. Chem.*, **69**, A170–A175.
- Acree, T.E. in: Acree, T.E., Teranishi, R. (Eds.). 1993a. Flavor science: Sensible principles and techniques. American Chemical Society, Washington DC, pp. 1–22.
- Acree, T.E. in: Ho, C.-T., Manley, C.H. (Eds.). 1993b. Flavor measurement (IFT Basic Symposium Series). Marcel Dekker, New York, Vol. 8, pp. 77–94.
- Acree, T., Arn, H. 2004. Flavornet and human odor space [Online]. Available: <http://www.flavornet.org/> [March 2010].
- Acree, T.E., Barnard, J., Cunningham, D.G. 1984. A procedure for the sensory analysis of gas chromatographic effluents. *Food Chem.* **14**, 273–286.
- Arctander, S., 1969. Perfume and flavour chemicals, Vols I and II. Steffen Arctander, Montclair, New Jersey.
- Bhattacharyya, N., Seth, S., Tudu, B., Tamuly, P., Jana, A., Ghosh, D., Bandyopadhyay, R., Bhuyan, M., Sabhapandit, S. 2007. Detection of optimum fermentation time for black tea manufacturing using electronic nose. *Sensors and Actuators B* **122**, 627–634.
- Boldingh, J., Taylor, R.J. 1962. Trace constituents of butterfat. *Nature* **194**, 909–913.
- Buttery, R.G., Black, D.R., Guadagni, D.G., Ling, L.C., Connoly, G., Teranishi, R. 1974. California bay oil. I. Constituents, odor properties. *J. Agric. Food Chem.* **22**, 773–777.
- Buttery, R.G., Black, D.R., Haddon, W.F., Ling, L.C., Teranishi, R., 1979. Identification of additional volatile constituents of carrot roots. *J. Agric. Food Chem.* **27**, 1–3.
- Buttery, R.G., Ling, L.C. 1995. Volatile flavour components of corn tortillas and related products. *J. Agric. Food Chem.* **43**, 1878–1882.
- Buttery, R.G., Seifert, R.M., Guadagni, D.G., Black, D.R., Ling, L.C. 1968. Characterization of some volatile constituents of carrots. *J. Agric. Food Chem.* **16**, 1009–1015.
- Buttery, R.G., Seifert, R.M., Guadagni, D.G., Black, D.R., Ling, L.C. 1971. Characterization of additional volatile components of tomato. *J. Agric. Food Chem.* **19**, 524–529.
- Buttery, R.G., Teranishi, R., Ling, L.C., Turnbaugh, J.G. 1990. Quantitative and sensory studies on tomato paste volatiles. *J. Agric. Food Chem.* **38**, 336–340.
- Buttery, R.G., Turnbaugh, J.G., Ling, L.C. 1988. Contribution of volatiles to rice aroma. *J. Agric. Food Chem.* **36**, 1006–1009.
- Callejón, R.M., Morales, M.L., Troncoso, A.M., Silva Ferreira, A.C. 2008. Targeting key aromatic substances on the typical aroma of sherry vinegar. *J. Agric. Food Chem.* **56**, 6631–6639.
- Choi, H. 2003. Character impact odorants of Citrus Hallabong [(*C. unshiu* Marcov × *C. sinensis* Osbeck) × *C. reticulata* Blanco] cold-pressed peel oil. *J. Agric. Food Chem.* **51**, 2687–2692.
- Choi, H., Kondo, Y., Sawamura, M. 2001. Characterization of odor-active volatiles in citrus Hyuganatsu (*Citrus tamurana* Hort. ex Tanaka). *J. Agric. Food Chem.* **49**, 2404–2408.

- D' Acampora Zeller, B., Dugo, P., Dugo, G., Mondello, L. 2008. Gas chromatography-olfactometry in food flavour analysis. *J. Chromatogr. A* **1186**, 123–143.
- Da Silva, M.A.A.P., Lundahl, D.S., McDaniel, M.R. in: Maarse, H., Van der Heij, D. (Eds.). 1994. Trends in flavour research (Developments in Food Science). Elsevier Science, Amsterdam, Vol. 35, pp. 191–209.
- Day, E.A., Lillard, D.A., Montgomery, M.W. 1963. Autoxidation of milk lipids. III. Effect on flavor of the additive interactions of carbonyl compounds at subthreshold concentrations. *J. Dairy Sci.* **46**, 291–294.
- Deibler, K.D., Acree, T.E., Lavin, E.H. in: Teranishi, R., Wick, E.L., Hornstein, I. (Eds.). 1999. Flavor chemistry: 30 Years of progress. Kluwer Academic/Plenum Publishers, New York, pp. 387–395.
- Delahunty, C.M., Eyres, G., Dufour, J-P. 2006. Gas-chromatography-olfactometry. *J. Sep. Sci.* **29**, 2107–2125.
- Demole, E., Enggist, P. 1974. Novel synthesis of 3,5,5-trimethyl-4-(2-butenylidene)-cyclohex-2-en-1-one, a major constituent of Burley tobacco flavour. *Helv. Chim. Acta.* **57**, 2087–2091.
- Dharmawan, J., Kasapis, S., Sriramula, P., Lear, M.J., Curran, P. 2009. Evaluation of aroma-active compounds in Pontianak orange peel oil (*Citrus nobilis* Lour. Var. *Microcarpa* Hassk.) by gas chromatography-olfactometry, aroma reconstitution, and omission test. *J. Agric. Food Chem.* **57**, 239–244.
- Engel, K.-H., Flath, R.A., Buttery, R.G., Mon, T.R., Ramming, D.W. 1988. Investigation of volatile constituents in nectarines. Analytical and sensory characterization of aroma components in some nectarine cultivars. *J. Agric. Food Chem.* **36**, 549–553.
- Étiévant, P.X., in: Jackson, J., Linskens, H. (Eds.). 2002. Analysis of taste and aroma (Molecular methods of plant analysis). Springer-Verlag, Berlin, Vol. 21, pp. 223–237.
- Étiévant, P.X., Callement, G., Langlois, D., Issanchou, S., Coquibus, N. 1999. Odor intensity evaluation in gas chromatography-olfactometry by finger span method. *J. Agric. Food Chem.* **47**, 1673–1680.
- Ferreira, V., Pet'ka, J., Aznar, M. 2002. Aroma extract dilution analysis. Precision and optimal experimental design. *J. Agric. Food. Chem.* **50**, 1508–1514.
- Frijters, J.E.R. 1978. A critical analysis of the odour unit number and its use. *Chem. Senses* **3**, 227–233.
- Grosch, W. 1993. Detection of potent odorants in foods by aroma extract dilution analysis. *Trends Food Sci Technol.* **4**, 68–73.
- Grosch, W. 1994. Determination of potent odorants in foods by aroma extract dilution analysis (AEDA) and calculation of odour activity values (OAV). *Flavour Fragr. J.* **9**, 147–158.
- Grosch, W. 2001. Evaluation of the key odorants of foods by dilution experiments, aroma models and omission. *Chem. Senses* **26**, 533–545.



- Guichard, H., Guichard, E., Langlois, D., Issanchou, S., Abbott, N. 1995. GC-sniffing analysis: Olfactive intensity measurement by two methods. *Z. Lebensm. Unters. Forsch.* **201**, 344–350.
- Guth, H., Grosch, W, in: Teranishi, R., Wick, E.L., Hornstein, I. (Eds.). 1999. Flavor chemistry: 30 Years of progress. Kluwer Academic/Plenum Publishers, New York, pp. 377–386.
- Joint FAO/WHO Expert Committee on Food Additives (JECFA). 2009. Specifications for flavourings [Online]. Available: <http://www.fao.org/ag/agn/jecfa-flav/index.html?showSynonyms=0> [2009, November].
- Kreck, M., Mosandl, A. 2003. Synthesis, structure elucidation, and olfactometric analysis of lilac aldehyde and lilac alcohol stereoisomers. *J. Agric. Food Chem.* **51**, 2722–2726.
- Leffingwell, J.C. 2002. Leffingwell reports: Tobacco—aroma from carotenoids [Online]. Available: <http://www.leffingwell.com/leffrept.htm> [2010, 10 March].
- Le Guen, S., Prost, C., Demaimay, M. 2000. Critical comparison of three olfactometric methods for the identification of the most potent odorants in cooked mussels (*Mytilus edulis*). *J. Agric. Food Chem.* **48**, 1307–1314.
- Linssen, J.P.H., Janssens, J.L.G.M., Roozen, J.P., Posthumus, M.A. 1993. Combined gas chromatography and sniffing port analysis of volatile compounds of mineral water packed in polyethylene laminated packages. *Food Chem.* **46**, 367–371.
- Miranda-Lopez, R., Libbey, L.M., Watson, B.T., McDaniel, M.R. 1992. Odor analysis of Pinot noir wines from grapes of different maturities by a gas chromatography-olfactometry technique (Osme). *Journal of Food Science* **57**, 985–993, 1019.
- Mookherjee, B.D., Wilson, R.A. 1990. Tobacco constituents. Their importance in flavor and fragrance chemistry. *Perfumer and Flavorist* **15**, 27–49.
- Mosciano, G., Fasano, M., Michalski, J., Sadural, S. 1991a. Organoleptic characteristics of flavor materials. *Perfumer and Flavorist* **16**, 31–33.
- Mosciano, G., Fasano, M., Michalski, J., Sadural, S. 1991b. Organoleptic characteristics of flavor materials. *Perfumer and Flavorist* **16**, 79–81.
- Näf, R., Velluz, A. 2000. The volatile constituents of extracts of cooked spinach leaves (*Spinacia oleracea* L.). *Flavour Fragr. J.* **15**, 329–334.
- Ohloff, G. 1994. Scent and Fragrances. The fascination of odors and their chemical perspectives. Springer-Verlag, Berlin, Germany.
- Oomah, B.D., Liang, L.S.Y. 2007. Volatile compounds of dry beans (*Phaseolus vulgaris* L.). *Plant Foods Hum. Nutr.* **62**, 177–183.
- Ott, A., Fay, L.B., Chaintreau, A. 1997. Determination and origin of the aroma impact compounds of yogurt flavor. *J. Agric. Food Chem.* **45**, 850–858.
- Peris, M., Escuder-Gilabert, L. 2009. A 21st century technique for food control: Electronic noses. *Analytica Chimica Acta* **639**, 1–15.

- Peterson, M.A., Ivanova, D., Møller, P., Bredie, W.L.P. in: Le Quéré, J.L., Étievant, P.X. (Eds.). 2003. Flavour research at the dawn of the twenty-first century, proceedings of the 10<sup>th</sup> Weurman flavour research symposium, pp. 494–499.
- Plutowska, B., Wardencki, W. 2008. Application of gas chromatography-olfactometry (GC-O) in analysis and quality assessment of alcoholic beverages—a review. *Food Chem.* **107**, 449–463.
- Pollien, P., Ott, A., Montigon, F., Baumgartner, M., Muñoz-Box, R., Chaintreau, A. 1997. Hyphenated headspace-gas chromatography-sniffing technique: Screening of impact odorants and quantitative aromagram comparison. *J. Agric. Food Chem.* **45**, 2630–2637.
- Sawamura, M., Nguyen, T.M.T., Onishi, Y., Ogawa, E., Choi, H.S. 2004. Characteristic odor components of Citrus reticulata Blanco (Ponkan) cold-pressed oil. *Biosci. Biotechnol. Biochem.* **68**, 1690–1697.
- Sawamura, M., Onishi, Y., Ikemoto, J., Tu, N.T.M., Phi, N.T.L. 2006. Characteristic odour components of bergamot (*Citrus bergamia* Risso) essential oil. *Flavour Fragr. J.* **21**, 609–615.
- Sawamura, M., Song, H., Choi, H., Sagawa, K., Ukeda, H. 2001. Characteristic aroma components of tosa-buntan (*Citrus grandis* Osbeck forma *Tosa*) fruit. *Food Sci. Technol. Res.* **7**, 45–49.
- Schieberle, P., Gassenmeier, K., Guth, H., Sen, A., Grosch, W. 1993. Character impact odour compounds of different kinds of butter. *Lebensm.-Wiss. u. Technol.* **26**, 347–356.
- Schieberle, P., Hofmann, T. 1997. Evaluation of the character impact odorants in fresh strawberry juice by quantitative measurements and sensory studies on model mixtures. *J. Agric. Food Chem.* **45**, 227–232.
- Serra, S., Fuganti, C., Brenna, E. 2006. Synthesis, olfactory evaluation and determination of the absolute configuration of the 3,4-didehydroionone stereoisomers, *Helv. Chim. Acta* **89**, 1110–1122.
- Siegmund, B., Pöllinger-Zierler, B. 2006. Odor thresholds of microbially induced off-flavor compounds in apple juice. *J. Agric. Food Chem.* **54**, 5984–5989.
- Song, H.S., Sawamura, M., Ito, T., Kawashimo, K., Ukeda, H. 2000. Quantitative determination and characteristic flavour of *Citrus junos* (yuzu) peel oil. *Flavour Fragr. J.* **15**, 245–250.
- Tachihara, T., Hashimoto, H., Ishizaki, S., Komai, T., Fujita, A., Ishikawa, M., Kitahara, T. 2006. Microbial resolution of 2-methylbutyric acid and its application to several chiral flavour compounds. *Dev. Food Sci.* **43**, 97–100.
- Takahashi K., Someya, T., Muraki, S., Yoshida, T. 1980. A new keto-alcohol, (-)-mintlactone, (+)-iso-mintlactone and minor components in peppermint oil. *Agric. Biol. Chem.* **44**, 1535–1543.
- Takeoka, G.R., Flath, R.A., Mon, T.R., Teranishi, R., Guentert, M. 1990. Volatile constituents of apricot (*Prunus armeniaca*). *J. Agric. Food Chem.* **38**, 471–477.

- Tamura, H., Yang, R.-H., Sugisawa, H. in: Teranishi, R., Buttery, R.G., Sugisawa, H. (Eds.). 1993. Bioactive volatile compounds from plants. American Chemical Society, USA, pp. 121–136.
- Ullrich, F., Grosch, W. 1987. Identification of the most intense volatile flavour compounds formed during autoxidation of linoleic acid. *Z. Lebensm. Unters. Forsch.* **187**, 277–282.
- Van Ruth, S.M. 2001. Methods for gas chromatography-olfactometry: A review. *Biomol. Eng.* **17**, 121–128.
- Van Ruth, S.M. 2004. Evaluation of two gas chromatography-olfactometry methods: The detection frequency and perceived intensity method. *J. Chromatogr. A* **1054**, 33–37.
- Van Ruth, S.M., O'Connor, C.H. 2001. Evaluation of three gas-chromatography-olfactometry methods: Comparison of odour intensity-concentration relationships of eight volatile compounds with sensory headspace data. *Food Chem.* **74**, 341–347.
- Van Ruth, S.M., O'Connor, C.H. 2001b. Influence of assessors' qualities and analytical conditions on gas chromatography-olfactometry analysis. *Eur. Food Res. Technol.* **213**, 77–82.
- Wilson, A.D., Baietto, M. 2009. Applications and advances in electronic-nose technologies. *Sensors* **9**, 5099–5148.
- Yamazaki, Y., Hayashi, Y., Arita, M., Hieda, T., Mikami, Y. 1988. Microbial conversion of  $\alpha$ -ionone,  $\alpha$ -methylionone and  $\alpha$ -isomethylionone. *Appl. Environ. Microb.* **54**, 2354–2360.
- Yang, X., 2008. Aroma constituents and alkykamides of red and green Huajiao (*Zanthoxylum bungeanum* and *Zanthoxylum schinifolium*). *J. Agric. Food Chem.* **56**, 1689–1696.

## CHAPTER 5

# QUANTITATIVE ANALYSIS OF THE VOLATILE COMPOUNDS PRESENT IN HONEYBUSH

## 5.1 QUANTITATIVE METHODS

### 5.1.1 Relative quantification

The volatile compounds present in honeybush were quantified by GC-FID and/or GC-MS-analysis of the headspace of either dry or infused honeybush samples. Because honeybush aroma consists of extremely complex mixtures of large numbers of volatile components, the unambiguous assignment of GC peaks in quantitative GC analyses proved to be very difficult. For this reason, quantitative GC-MS analysis was eventually the preferred analytical method in this study, although it is known that quantitative results obtained by GC analysis give a more accurate picture of the quantitative composition of the sample under investigation than obtained by GC-MS analysis. The relative concentrations of the headspace components were computed as percentage areas of the total ion current (area % TIC). The data were calculated as mean values of three analyses of each sample and relatively good RSD values ( $\leq 20\%$ ) were obtained.

### 5.1.2 Absolute quantification

In order to obtain an idea of the actual quantities of the volatile compounds present in the aroma of honeybush, a representative headspace sample was quantified by GC-MS analysis. Standard solutions of all the available pure standards of those compounds identified in honeybush aroma were subjected to GC-MS analysis and an MS response factor was determined for each individual compound. These response factors were then used to calculate absolute quantities (in  $\mu\text{g/ml}$ ) for the respective compounds in the headspace sample, as well as for compounds of similar types but for which no pure standards were available.

## 5.2 COMPARATIVE STUDIES

### 5.2.1 Green (unfermented) vs fermented honeybush

In order to investigate the effect of the fermentation process on the chemical composition of honeybush aroma the quantitative data of 244 volatile compounds identified in green and fermented honeybush infusions by means of HS-GC-MS were compared. *Cyclopia intermedia* was chosen as representative species for this study. The results are presented in Table 5.1. Note that

in this study all the identified volatile components of *C. intermedia* aroma were compared quantitatively, irrespective of whether they are odour-active or not.

Table 5.1: VOCs, identified by HS-GC-MS analysis, in green (unfermented) and fermented honeybush, *Cyclopia intermedia*

No.	Compound <sup>a</sup>	Odour descriptors <sup>b</sup>	Green (area %) <sup>c</sup>	Fermented (area %)	Green (µg/ml)	Fermented (µg/ml)
C1	1-Penten-3-ol		0.0642	0.0291	8.7	4.1
C2	Pentanal		0.0617	0.0497	6.0	5.0
C3	2-Ethylfuran		0.0650	0.0382	4.4	2.6
C4	1-Pentanol		0.0267	0.0352	2.5	3.4
C5	(Z)-2-Penten-1-ol		0.0094	0.0213	1.3	3.0
C6	<b>Hexanal</b>	Fatty-green grassy odour	0.4788	<b>0.9745</b>	47.7	97.7
C7	2-Ethyl-5,5-dimethyl-1,3-cyclopentadiene		0.0326	0.0400	nq <sup>d</sup>	nq <sup>d</sup>
C8	(E)-2-Hexenal		0.2016	0.0947	22.1	9.9
C9	(Z)-3-Hexen-1-ol		0.1761	0.0661	14.1	5.1
C10	1-Hexanol		0.1254	0.0294	7.9	1.8
C11	<b>3-Methylbutanoic acid</b>	Acid acrid, cheesy, unpleasant	<b>0.0101</b>	<b>0.0124</b>	1.3	1.6
C12	1,3,6-Octatriene		0.0381	0.0176	nq <sup>d</sup>	nq <sup>d</sup>
C14	2-Heptanone		0.0442	0.0432	3.3	3.2
C15	(Z)-4-Heptenal		0.0139	0.0149	1.8	2.0
C17	Heptanal		0.0563	0.0689	5.6	6.9
C23	α-Pinene		0.0319	0.0144	2.3	1.1
C24	Camphene		0.2201	0.0397	15.9	2.9
C25	Benzaldehyde		0.3045	0.2188	21.8	15.9
C27	6-Methyl-2-heptanone		0.0498	0.0289	3.6	2.2
C28	5-Methyl-2-furancarboxaldehyde		– <sup>e</sup>	0.0304	– <sup>f</sup>	3.6
C29	2,2,6-Trimethyl-6-vinyltetrahydropyran <sup>†</sup>		0.0136	0.0720	1.1	6.2
C31	1-Octen-3-ol		0.1241	0.0818	10.5	7.0
C32	<b>6-Methyl-5-hepten-2-one*</b>	Oily-green, pungent-herbaceous, grassy, with fresh and green-fruity notes	<b>2.7494</b>	<b>2.8289</b>	234.6	243.7
C33	(E,Z)-2,4-Heptadienal		0.0121	0.0050	1.2	0.5
C34	(6Z)-2,6-Dimethyl-2,6-octadiene		0.1551	0.0560	10.1	3.7
C35	2-Pentylfuran		0.4634	0.5287	31.1	35.8
C36	<i>trans</i> -Dehydroxylinalool oxide (furanoid)		0.1598	0.2808	13.4	23.7
C37	2-Formyl-1-methylpyrrole		0.0194	0.0889	1.5	7.2
C38	Myrcene		0.4311	0.1602	26.8	10.0

Table 5.1: *contd.*

No.	Compound <sup>a</sup>	Odour descriptors <sup>b</sup>	Green (area %) <sup>c</sup>	Fermented (area %)	Green (µg/ml)	Fermented (µg/ml)
C39	Octanal		0.0521	0.0318	4.4	2.8
C40	(2Z)-2-(2-Pentenyl)furan		0.0489	0.0692	3.4	4.8
C41	(E,E)-2,4-Heptadienal		0.2111	0.1525	20.5	14.3
C42	α-Phellandrene		0.3395	0.0640	20.6	4.0
C43	(6E)-2,6-Dimethyl-2,6-octadiene		0.1659	0.0355	10.8	2.4
C44	Hexanoic acid		0.0291	0.0268	5.2	4.6
C45	<i>cis</i> -Dehydroxylinalool oxide (furanoid)		0.1225	0.1884	9.9	15.6
C46	Decane		0.0129	0.0117	0.7	0.6
C47	α-Terpinene		1.3242	0.2130	80.5	13.0
C48	3,4-Dimethyl-2,5-furandione		– <sup>e</sup>	0.0310	– <sup>f</sup>	8.6
C50	<b>p-Cymene</b>	Citrus-like, reminiscent of lemon and bergamot	<b>1.1009</b>	0.4663	65.9	28.3
C51	2,2,6-Trimethylcyclohexanone		0.0901	0.0980	7.0	7.7
C52	Limonene*	Sweet, citrus-like, orange, refreshing, clean, turpentine	8.1664	2.0570	594.0	151.4
C53	(E)-3-Octen-2-one		0.0286	0.0107	2.9	1.0
C55	Benzylalcohol		– <sup>e</sup>	0.0122	– <sup>f</sup>	1.1
C56	<b>(Z)-β-Ocimene</b>	Warm-herbaceous, sweet, floral	<b>0.7798</b>	0.1755	48.4	11.0
C57	2-Methyl-6-methylene-2-octene <sup>†</sup>		0.0757	– <sup>e</sup>	5.0	– <sup>f</sup>
C58	(E)-β-Ocimene		1.0747	0.1814	66.8	11.4
C59	2,6,6-Trimethylcyclohex-2-enone		0.3548	0.3494	21.6	21.6
C60	Acetophenone		0.0330	0.0260	3.4	2.7
C61	<b>γ-Terpinene</b>	Refreshing, herbaceous, citrus-like	<b>1.9083</b>	0.2874	115.9	17.6
C63	(Z,E)-3,5-Octadien-2-one		0.4213	0.4348	39.1	41.1
C64	<i>trans</i> -Linalool oxide (furanoid)		0.0665	0.6085	5.6	51.4
C65	1-Octanol		0.1515	0.0864	13.8	8.0
C67	2,8-Dimethyl-2,6-nonadiene <sup>†</sup>		0.0300	– <sup>e</sup>	nq <sup>d</sup>	– <sup>f</sup>
C68	<i>cis</i> -Linalool oxide (furanoid)		– <sup>e</sup>	0.2920	– <sup>f</sup>	23.9
C69	p-Cymenene		0.1443	0.1418	8.8	8.8
C70	<b>(E,E)-3,5-Octadien-2-one</b>	Fatty, fruity, mushroom	0.2533	<b>0.2707</b>	23.5	25.6
C71	<b>Terpinolene*</b>	Sweet-piney, oily	<b>2.7020</b>	0.5617	194.3	40.8

Table 5.1: *contd.*

No.	Compound <sup>a</sup>	Odour descriptors <sup>b</sup>	Green (area %) <sup>c</sup>	Fermented (area %)	Green (µg/ml)	Fermented (µg/ml)
C72	2-Nonanone		0.2086	0.0593	13.1	3.8
C73	Component C73		0.0203	0.0413	nq <sup>d</sup>	nq <sup>d</sup>
C74	(3 <i>E</i> )-6-Methyl-3,5-heptadien-2-one		0.5185	0.2153	48.3	20.3
C75	Nonanal		0.8398	– <sup>e</sup>	70.0	– <sup>f</sup>
C76	<b>Linalool*</b>	Refreshing, floral-woody	13.158	<b>28.878</b>	1163.2	2584.5
C77	Component C77		0.4549	– <sup>e</sup>	nq <sup>d</sup>	– <sup>f</sup>
C78	Hotrienol		0.1119	0.1032	9.7	9.3
C79	<b>2-Phenylethanol</b>	Mild, warm, rose-honey-like	<b>0.0691</b>	0.0428	5.9	3.7
C81	3,4,4-Trimethyl-2-cyclopenten-1-one		0.1597	0.1397	nq <sup>d</sup>	nq <sup>d</sup>
C82	Isophorone		– <sup>e</sup>	0.0244	– <sup>f</sup>	2.5
C83	(-)- <i>cis</i> -Rose oxide		0.1772	0.0199	nq <sup>d</sup>	nq <sup>d</sup>
C86	<i>cis</i> -2- <i>p</i> -Menthen-1-ol <sup>†</sup>		0.0461	0.0082	2.1	0.4
C89	<b>4-Acetyl-1-methylcyclohexene<sup>†</sup></b>	Spicy	0.0250	<b>0.0911</b>	2.5	9.2
C91	(-)- <i>trans</i> -Rose oxide		0.0600	0.0072	nq <sup>d</sup>	nq <sup>d</sup>
C92	4-Ketoisophorone		0.0297	0.0474	2.1	3.4
C93	Allo-ocimene		0.0595	0.0156	3.6	1.0
C94	Dihydrolinalool <sup>†</sup>		– <sup>e</sup>	0.0102	– <sup>f</sup>	0.9
C95	( <i>E</i> )-3-Nonen-2-one		0.1354	0.0692	10.5	5.4
C96	<i>trans</i> -2- <i>p</i> -Menthen-1-ol <sup>†</sup>		0.0259	– <sup>e</sup>	1.2	– <sup>f</sup>
C98	Camphene hydrate <sup>†</sup>		0.0539	– <sup>e</sup>	7.6	– <sup>f</sup>
C101	<b>(<i>E,Z</i>)-2,6-Nonadienal</b>	Green-vegetable, cucumber or violet leaf	0.0229	<b>0.1235</b>	3.4	18.7
C103	( <i>Z</i> )-Ocimenol		– <sup>e</sup>	0.0224	– <sup>f</sup>	2.0
C105	Isoborneol <sup>†</sup>		0.0218	– <sup>e</sup>	3.1	– <sup>f</sup>
C106	Nerol oxide <sup>†</sup>		0.1021	0.2236	nq <sup>d</sup>	nq <sup>d</sup>
C107	Propiophenone		0.0518	0.0367	3.8	2.8
C108	<b>(<i>E</i>)-2-Nonenal</b>	Green, cucumber, aldehydic and fatty	0.0485	<b>0.1072</b>	5.6	12.6
C109	Benzyl acetate		– <sup>e</sup>	0.0287	– <sup>f</sup>	2.8
C111	2-Chloro-1,7,7-trimethylbicyclo- [2.2.1]heptane <sup>†</sup>		0.0198	– <sup>e</sup>	nq <sup>d</sup>	– <sup>f</sup>
C112	Borneol		0.0256	0.0269	3.8	3.9
C113	( <i>E</i> )-Ocimenol		– <sup>e</sup>	0.0123	– <sup>f</sup>	1.1



Table 5.1: *contd.*

No.	Compound <sup>a</sup>	Odour descriptors <sup>b</sup>	Green (area %) <sup>c</sup>	Fermented (area %)	Green (µg/ml)	Fermented (µg/ml)
C114	A dimethylbenzaldehyde		0.0281	0.0311	nq <sup>d</sup>	nq <sup>d</sup>
C115	<i>cis</i> -Pyranoid Linalool oxide		– <sup>e</sup>	0.0140	– <sup>f</sup>	1.1
C118	Terpinen-4-ol		1.2271	0.5228	54.9	23.7
C119	Dill ether isomer 1 <sup>†</sup>		0.0142	0.0148	nq <sup>d</sup>	nq <sup>d</sup>
C120	<i>p</i> -Cymen-8-ol		0.0472	0.0528	3.9	4.5
C121	<b>α-Terpineol*</b>	Floral, sweet, lilac-type	4.1208	<b>8.7939</b>	194.9	422.9
C122	Safranal		0.1862	0.2530	13.2	18.3
C123	Component C123		0.0386	0.0283	nq <sup>d</sup>	nq <sup>d</sup>
C124	Decanal		0.2125	0.1297	17.4	11.0
C125	(+)- <i>p</i> -Menth-1-en-9-al		0.0554	0.0926	3.9	6.7
C126	Dodecane		0.0076	0.0084	0.4	0.4
C127	Benzothiazole		0.0124	0.0099	1.2	1.0
C128	<b>(+)-<i>p</i>-Menth-1-en-9-al</b>	Powerful spicy, herbaceous odour	0.0549	<b>0.0858</b>	3.9	6.2
C129	<b>β-Cyclosital</b>	Green, grassy, hay-like	<b>0.7457</b>	0.6936	52.9	50.1
C131	Dill ether isomer 2 <sup>†</sup>		– <sup>e</sup>	0.0139	– <sup>f</sup>	nq <sup>d</sup>
C132	Methyl nonanoate		0.0516	0.0145	3.1	0.9
C133	Component C133		1.4759	0.1214	nq <sup>d</sup>	nq <sup>d</sup>
C134	Component C134		0.0461	0.0625	nq <sup>d</sup>	nq <sup>d</sup>
C135	<b>Nerol*</b>	Fresh, sweet-rosy	0.8906	<b>2.8329</b>	75.4	243.4
C137	( <i>R</i> )-β-Citronellol		– <sup>e</sup>	0.0589	– <sup>f</sup>	5.3
C138	( <i>Z</i> )-3-Hexenyl 2-methylbutanoate <sup>†</sup>		0.0415	0.0658	2.8	4.5
C139	Neral		0.2315	0.0917	20.3	8.2
C140	( <i>Z</i> )-3-Hexenyl isovalerate		0.0836	0.0571	6.0	4.2
C141	<b><i>p</i>-Anisaldehyde</b>	Sweet, floral, "hay-like"	0.0376	<b>0.0628</b>	3.0	5.2
C142	2-Phenylethyl acetate		0.0140	0.0160	1.3	1.6
C143	Carvenone <sup>†</sup>		0.0086	0.0135	nq <sup>d</sup>	nq <sup>d</sup>
C146	2,2,6-Trimethyl-1-cyclohexene-1-acetaldehyde		0.0120	0.0112	0.9	0.8
C147	2-(2-Butenyl)-1,3,5-trimethylbenzene <sup>†</sup>		0.0687	0.0301	nq <sup>d</sup>	nq <sup>d</sup>
C148	<b>Geraniol*</b>	Sweet, floral, rose	6.7717	<b>13.8964</b>	753.8	1582.7
C149	( <i>E,E,Z</i> )-2,4,6-Nonatrienal		0.0934	0.0707	13.9	10.8

Table 5.1: *contd.*

No.	Compound <sup>a</sup>	Odour descriptors <sup>b</sup>	Green (area %) <sup>c</sup>	Fermented (area %)	Green (µg/ml)	Fermented (µg/ml)
C150	<b>Geranial</b>	Lemon	<b>0.5004</b>	0.2672	39.8	21.7
C152	<b>(R)-Octan-5-olide</b>	Peach, coconut-like	– <sup>e</sup>	<b>0.0020</b>	– <sup>f</sup>	0.2
C154	4,8-Dimethyl-3,7-nonadien-2-one <sup>†</sup>		0.1553	0.0896	nq <sup>d</sup>	nq <sup>d</sup>
C155	( <i>E,E,E</i> )-2,4,6-Nonatrienal		0.2991	0.4743	44.5	72.3
C156	Component C156		0.0525	0.0177	nq <sup>d</sup>	nq <sup>d</sup>
C157	Vitispirane <sup>†</sup>		– <sup>e</sup>	0.0844	– <sup>f</sup>	5.4
C158	Neryl formate		– <sup>e</sup>	0.0576	– <sup>f</sup>	4.7
C159	Nonanoic acid		0.0215	0.0483	5.1	12.2
C160	Limonen-10-ol <sup>†</sup>		0.0629	– <sup>e</sup>	2.9	– <sup>f</sup>
C161	2-Undecanone		0.0686	0.0422	4.6	2.9
C162	<b>Component C162</b>	–	<b>0.0407</b>	0.0380	nq <sup>d</sup>	nq <sup>d</sup>
C163	Theaspirane isomer 1 <sup>†</sup>		0.2902	0.0490	18.5	3.2
C164	<b>Geranyl formate</b>	Fresh, green-rosy, fruity	0.0167	<b>0.150</b>	1.3	12.2
C165	Component C165		0.0244	0.0462	nq <sup>d</sup>	nq <sup>d</sup>
C166	2,3,4-Trimethylbenzaldehyde		– <sup>e</sup>	0.0174	– <sup>f</sup>	nq <sup>d</sup>
C167	Undecanal		0.0190	0.0160	1.4	1.2
C168	Component C168		0.0554	0.0415	nq <sup>d</sup>	nq <sup>d</sup>
C171	<b>(E,E)-2,4-Decadienal</b>	Fried, waxy, fatty, orange-like	<b>0.0486</b>	0.0428	4.7	4.2
C172	Component C172		0.0420	0.0850	nq <sup>d</sup>	nq <sup>d</sup>
C173	Theaspirane isomer 2 <sup>†</sup>		0.2808	0.0650	17.8	4.2
C174	Component C174		0.1754	0.0588	nq <sup>d</sup>	nq <sup>d</sup>
C175	( <i>Z</i> )-3-Hexenyl ( <i>E</i> )-2-methyl-2-butenolate		0.1153	0.1994	7.0	12.4
C178	<b>Component C178</b>	–	<b>0.4312</b>	0.4238	nq <sup>d</sup>	nq <sup>d</sup>
C179	Hexyl tiglate		– <sup>e</sup>	0.0115	– <sup>f</sup>	0.9
C181	Component C181		0.0218	0.0451	nq <sup>d</sup>	nq <sup>d</sup>
C182	2,5-Epoxymegastigma-6,8-diene <sup>†</sup>		0.0991	0.0446	6.1	2.8
C186	Nonan-4-olide		0.0823	0.0749	14.1	13.2
C188	α-Terpinyol acetate <sup>†</sup>		0.0095	0.0086	nq <sup>d</sup>	nq <sup>d</sup>
C189	1,5,8-Trimethyl-1,2-dihydronaphthalene <sup>†</sup>		0.0281	0.1030	nq <sup>d</sup>	nq <sup>d</sup>
C190	1-(2-Hydroxy-1-methylethyl)-2,2-dimethylpropyl 2-methylpropanoate <sup>†</sup>		0.0213	0.0455	nq <sup>d</sup>	nq <sup>d</sup>

Table 5.1: *contd.*

No.	Compound <sup>a</sup>	Odour descriptors <sup>b</sup>	Green (area %) <sup>c</sup>	Fermented (area %)	Green (µg/ml)	Fermented (µg/ml)
C191	<b>Eugenol</b>	Warm-spicy, dry	0.1537	<b>0.5341</b>	13.2	47.1
C192	2,3-Dihydro-1,1,5,6-tetramethyl-1 <i>H</i> -indene		0.0851	0.0210	nq <sup>d</sup>	nq <sup>d</sup>
C193	α-Ionene		0.0754	0.0973	nq <sup>d</sup>	nq <sup>d</sup>
C195	( <i>Z</i> )-β-Damascenone		0.0237	0.0106	1.1	0.5
C198	Neryl acetate		0.0072	0.0636	0.9	8.1
C200	α-Ylangene <sup>†</sup>		0.0193	0.0069	1.2	0.4
C201	3-Hydroxy-2,4,4-trimethylpentyl 2-methylpropanoate <sup>†</sup>		0.0291	0.0390	nq <sup>d</sup>	nq <sup>d</sup>
C202	2-Butyl-2-octenal <sup>†</sup>		0.0343	0.0428	nq <sup>d</sup>	nq <sup>d</sup>
C203	<b>2,3-Dehydro-α-ionone<sup>†</sup></b>	Tobacco-like	0.0339	<b>0.1126</b>	1.9	6.1
C204	<b>(<i>E</i>)-β-Damascenone*</b>	Woody, sweet, fruity, earthy green-floral	<b>4.4832</b>	1.0417	201.5	47.7
C205	α-Copaene <sup>†</sup>		0.0796	0.0159	4.8	1.0
C206	Geranyl acetate		0.1647	0.2432	20.7	31.0
C207	Component C207 (carene-type comp.)		0.0421	0.0848	nq <sup>d</sup>	nq <sup>d</sup>
C209	6,10-Dimethyl-2-undecanone <sup>†</sup>		0.0627	0.0267	5.2	2.2
C210	Dodecanal		0.0232	— <sup>e</sup>	1.5	— <sup>f</sup>
C211	Tetradecane		0.0253	0.0523	1.2	2.4
C212	<b>(<i>E</i>)-β-Damascone</b>	Fruity (apple-citrus), tea-like with slight minty notes	0.2893	<b>0.7424</b>	17.5	45.9
C213	1,3-Dimethylnaphthalene		0.1143	0.1182	10.0	10.5
C214	4-(2,6,6-Trimethyl-1,3-cyclohexadien-1-yl)-2-butanone		0.0109	0.0063	0.7	0.4
C215	6-Methyl-6-(5-methylfuran-2-yl)heptan-2-one		0.0723	0.0931	nq <sup>d</sup>	nq <sup>d</sup>
C216	( <i>E</i> )-Caryophyllene <sup>†</sup>		0.0157	0.0097	0.9	0.6
C217	( <i>R</i> )-α-Ionone		0.0750	0.0395	4.0	2.1
C218	3,4-Dehydro-γ-ionone <sup>†</sup>		0.0669	0.3717	3.6	20.2
C219	( <i>E</i> )-6-Methyl-6-(5-methylfuran-2-yl)hept-3-en-2-one		0.0148	0.0333	nq <sup>d</sup>	nq <sup>d</sup>
C220	Geranylacetone*	Fresh-floral, sweet-rosy, slightly green, magnolia-like	20.7474	12.2911	1714.5	1037.1

Table 5.1: *contd.*

No.	Compound <sup>a</sup>	Odour descriptors <sup>b</sup>	Green (area %) <sup>c</sup>	Fermented (area %)	Green (µg/ml)	Fermented (µg/ml)
C221	α-Humulene		0.0106	0.0047	0.7	0.3
C222	<b>2,3-Dehydro-γ-ionone</b>	–	0.0448	<b>0.0851</b>	2.6	4.6
C223	5-Methoxy-6,7-dimethylbenzofuran		0.0574	0.0322	nq <sup>d</sup>	nq <sup>d</sup>
C224	Component C224		0.0600	– <sup>e</sup>	nq <sup>d</sup>	– <sup>f</sup>
C225	Cabreuva oxide B <sup>†</sup>		0.0379	0.1188	nq <sup>d</sup>	nq <sup>d</sup>
C226	9- <i>epi</i> -( <i>E</i> )-Caryophyllene <sup>†</sup>		– <sup>e</sup>	0.0446	– <sup>f</sup>	2.7
C227	Oxo-edulan <sup>†</sup>		– <sup>e</sup>	0.0228	– <sup>f</sup>	nq <sup>d</sup>
C229	<b>(S)-(Z)-7-Decen-5-olide</b>	Sweet, floral, fruity	– <sup>e</sup>	<b>0.0047</b>	– <sup>f</sup>	0.4
C230	<b>3,4-Dehydro-β-ionone</b>	Ionone-damascone and saffron-like, fruity and slightly leathery	<b>0.1393</b>	0.1273	9.0	8.4
C231	Cabreuva oxide D <sup>†</sup>		0.0229	0.0698	nq <sup>d</sup>	nq <sup>d</sup>
C232	5,6-Epoxy-β-ionone		0.7761	0.5865	50.2	38.7
C233	<b>(R)-Decan-5-olide</b>	Sweet, creamy, nut-like, fruity	0.0120	<b>0.0242</b>	0.9	1.9
C234	<b>(E)-β-Ionone*</b>	Warm, woody, fruity, raspberry-like; resembles cedarwood	<b>2.2513</b>	1.5161	144.8	99.5
C235	β-Selinene <sup>†</sup>		0.0209	0.0223	1.3	1.4
C236	Calamenene-1,11-epoxide <sup>†</sup>		0.0428	0.0580	nq <sup>d</sup>	nq <sup>d</sup>
C237	Benzyl tiglate		– <sup>e</sup>	0.0206	– <sup>f</sup>	nq <sup>d</sup>
C238	Component C238		0.0372	0.0581	nq <sup>d</sup>	nq <sup>d</sup>
C239	β-Dihydroagarofuran <sup>†</sup>		0.3475	0.4103	nq	nq <sup>d</sup>
C240	α-Murolene <sup>†</sup>		0.0251	0.0134	1.5	0.8
C241	Pentadecane		0.0470	0.0602	1.6	2.0
C243	Dihydroactinidiolide		0.8442	0.6625	nq <sup>d</sup>	nq <sup>d</sup>
C244	γ-Cadinene <sup>†</sup>		0.0763	0.0323	4.6	2.0
C245	<b>Bovolide</b>	Celery- and lovage-like, fruity and pleasant	<b>0.0842</b>	0.0741	nq <sup>d</sup>	nq <sup>d</sup>
C246	<i>trans</i> -Calamenene <sup>†</sup>		0.1095	0.1059	nq <sup>d</sup>	nq <sup>d</sup>
C247	δ-Cadinene <sup>†</sup>		0.0541	0.0215	3.3	1.3
C248	Methyl dodecanoate		0.0643	0.0163	3.0	0.8
C249	Pseudoionone isomer ( <i>E,Z</i> )		0.3284	0.2337	27.2	19.8
C250	Component C250		0.0156	0.0652	nq <sup>d</sup>	nq <sup>d</sup>
C251	Component C251		0.0373	0.0922	nq <sup>d</sup>	nq <sup>d</sup>

Table 5.1: *contd.*

No.	Compound <sup>a</sup>	Odour descriptors <sup>b</sup>	Green (area %) <sup>c</sup>	Fermented (area %)	Green (µg/ml)	Fermented (µg/ml)
C252	α-Calacorene <sup>†</sup>		0.2946	0.0917	nq <sup>d</sup>	nq <sup>d</sup>
C253	α-Agarofuran <sup>†</sup>		0.1906	0.2428	nq <sup>d</sup>	nq <sup>d</sup>
C254	Component C254		0.8604	0.2689	nq <sup>d</sup>	nq <sup>d</sup>
C256	(6 <i>Z</i> ,8 <i>Z</i> )-Megastigma-4,6,8-trien-3-one		– <sup>e</sup>	0.0440	– <sup>f</sup>	2.0
C257	Component C257		0.3573	0.1213	nq <sup>d</sup>	nq <sup>d</sup>
C258	Dihydroagarofuran isomer <sup>†</sup>		0.1977	0.1411	nq <sup>d</sup>	nq <sup>d</sup>
C260	( <i>E</i> )-Nerolidol		0.3550	0.7793	60.5	135.0
C261	( <i>Z</i> )-3-Hexenyl benzoate		0.0938	0.2236	5.8	14.1
C262	(6 <i>Z</i> ,8 <i>E</i> )-Megastigma-4,6,8-trien-3-one		0.0604	0.1832	2.9	8.4
C263	Hexyl benzoate		– <sup>e</sup>	0.0388	– <sup>f</sup>	2.8
C264	Dodecanoic acid		0.0940	– <sup>e</sup>	nq <sup>d</sup>	– <sup>f</sup>
C265	Caryophyllene oxide <sup>†</sup>		0.1190	0.0571	nq <sup>d</sup>	nq <sup>d</sup>
C266	Pseudoionone isomer ( <i>E,E</i> )		1.1167	0.6272	92.5	52.9
C269	<b>Component C269</b> (Bergamotol-type comp.)	–	<b>0.0181</b>	0.0061	nq <sup>d</sup>	nq <sup>d</sup>
C270	1-[2-(Isobutyryloxy)-1-methylethyl]-2,2-dimethylpropyl 2-methylpropanoate <sup>†</sup>		0.0273	0.0206	nq <sup>d</sup>	nq <sup>d</sup>
C271	<b>(6<i>E</i>,8<i>Z</i>)-Megastigma-4,6,8-trien-3-one</b>	Tobacco-like, woody, balsamic	– <sup>e</sup>	<b>0.0342</b>	– <sup>f</sup>	1.6
C273	1-(2,3,6-Trimethylphenyl)-3-buten-2-one		0.0296	0.0264	nq <sup>d</sup>	nq <sup>d</sup>
C274	β-Oplophenone <sup>†</sup>		0.2700	– <sup>e</sup>	nq <sup>d</sup>	– <sup>f</sup>
C276	Hexadecane		– <sup>e</sup>	0.0250	– <sup>f</sup>	0.9
C277	<b>(6<i>E</i>,8<i>E</i>)-Megastigma-4,6,8-trien-3-one</b>	Tobacco-like, woody, balsamic	0.0453	<b>0.1217</b>	2.0	5.6
C278	<b>10-<i>epi</i>-γ-Eudesmol<sup>†</sup></b>	Woody, floral, sweet	0.1758	<b>0.5900</b>	33.8	115.0
C279	Component C279 (Calamenene-type comp.)		0.1784	– <sup>e</sup>	nq <sup>d</sup>	– <sup>f</sup>
C280	Component C280		0.0730	0.0389	nq <sup>d</sup>	nq <sup>d</sup>
C281	Component C281		0.1337	– <sup>e</sup>	nq <sup>d</sup>	– <sup>f</sup>
C282	Component C282		– <sup>e</sup>	0.0323	– <sup>f</sup>	nq <sup>d</sup>
C283	γ-Eudesmol <sup>†</sup>		– <sup>e</sup>	0.0370	– <sup>f</sup>	7.2
C284	<b><i>epi</i>-α-Cadinol<sup>†</sup></b>	Herbaceous, woody	<b>0.1066</b>	0.0630	20.3	12.2
C285	<b><i>epi</i>-α-Muurolol<sup>†</sup></b>	Herbaceous, slightly spicy	<b>0.0505</b>	0.0426	9.7	8.3
C286	β-Eudesmol <sup>†</sup>		– <sup>e</sup>	0.0415	– <sup>f</sup>	8.0
C287	α-Eudesmol <sup>†</sup>		– <sup>e</sup>	0.0368	– <sup>f</sup>	7.2

Table 5.1: *contd.*

No.	Compound <sup>a</sup>	Odour descriptors <sup>b</sup>	Green (area %) <sup>c</sup>	Fermented (area %)	Green (µg/ml)	Fermented (µg/ml)
C288	α-Cadinol <sup>†</sup>		– <sup>e</sup>	0.0445	– <sup>f</sup>	8.7
C289	7- <i>epi</i> -α-Eudesmol <sup>†</sup>		0.0377	0.0850	7.2	16.5
C289	<b>Cadalene</b>	–	0.0952	<b>0.1118</b>	nq <sup>d</sup>	nq <sup>d</sup>
C291	3,7,7-Trimethyl-1-penta-1,3-dienyl-2-oxabicyclo[3.2.0]hept-3-ene isomer 1 <sup>†</sup>		0.0054	0.0106	nq <sup>d</sup>	nq <sup>d</sup>
C292	<i>epi</i> -α-Bisabolol <sup>†</sup>		– <sup>e</sup>	0.0274	– <sup>f</sup>	nq <sup>d</sup>
C293	α-Bisabolol <sup>†</sup>		– <sup>e</sup>	0.0243	– <sup>f</sup>	nq <sup>d</sup>
C294	3,7,7-Trimethyl-1-penta-1,3-dienyl-2-oxabicyclo[3.2.0]hept-3-ene isomer 2 <sup>†</sup>		0.0156	0.0344	nq <sup>d</sup>	nq <sup>d</sup>
C296	Heptadecane		– <sup>e</sup>	0.0393	– <sup>f</sup>	1.4
C297	Octadecane		– <sup>e</sup>	0.0142	– <sup>f</sup>	0.5
C298	Isopropyl myristate		0.0375	0.1481	nq <sup>d</sup>	nq <sup>d</sup>
C299	Hexahydrofarnesylacetone <sup>†</sup>		0.6137	0.3667	62.0	37.9

<sup>a</sup> In order of elution from apolar PS-089 column (DB-5 equivalent). Odour-active compounds in bold-type.

<sup>b</sup> Acree and Arn, 2004; Arctander, 1969; Boldingh and Taylor, 1962; Brenna *et al.* 2003, Buttery *et al.*, 1979; Demole and Enggist, 1974; JECFA, 2009; Kreck and Mosandl, 2003; Leffingwell, 2002; Mookherjee and Wilson, 1990; Mosciano *et al.*, 1991a, 1991b; Näf and Velluz, 2000; Ohloff, 1994; Oomah and Liang, 2007; Serra *et al.*, 2006; Tachihara *et al.*, 2006; Takahashi *et al.* 1980; Yamazaki *et al.*, 1988.

<sup>c</sup> Average percentage area calculated from TIC (n = 3; RSD ≤20%). Higher value in bold type.

<sup>d</sup> Not quantified - reference standard not available.

<sup>e</sup> Not detected, or area % <0.002.

<sup>f</sup> Not detected, or concentration <0.2 µg/ml.

\* 10 Most abundant volatile compounds in *C. intermedia*.

<sup>†</sup> Stereochemistry not determined.

Selected parts of the data given in Table 5.1 are also presented graphically in Fig. 5.1, in which 120 compounds with the highest relative concentrations are compared by means of a bar graph in order to highlight the most obvious quantitative differences between the volatile chemical profiles of green and fermented honeybush. In order to demonstrate the differences between compounds with smaller area percentages, the 10 compounds with the highest area percentages are not included in Fig. 5.1, but are compared separately in Fig. 5.2.

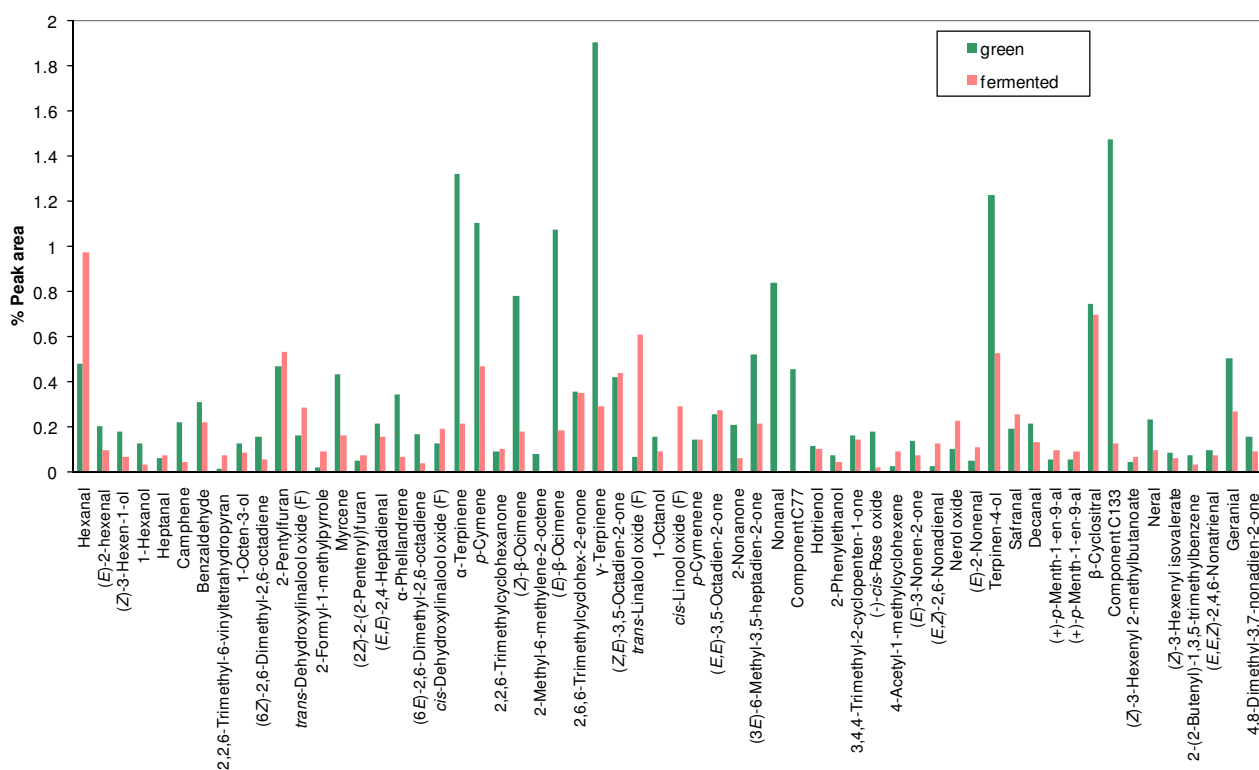


Fig. 5.1: Quantitative comparison of the volatile compounds with highest concentrations (area %) present in the headspace of green and fermented *Cyclopia intermedia*.

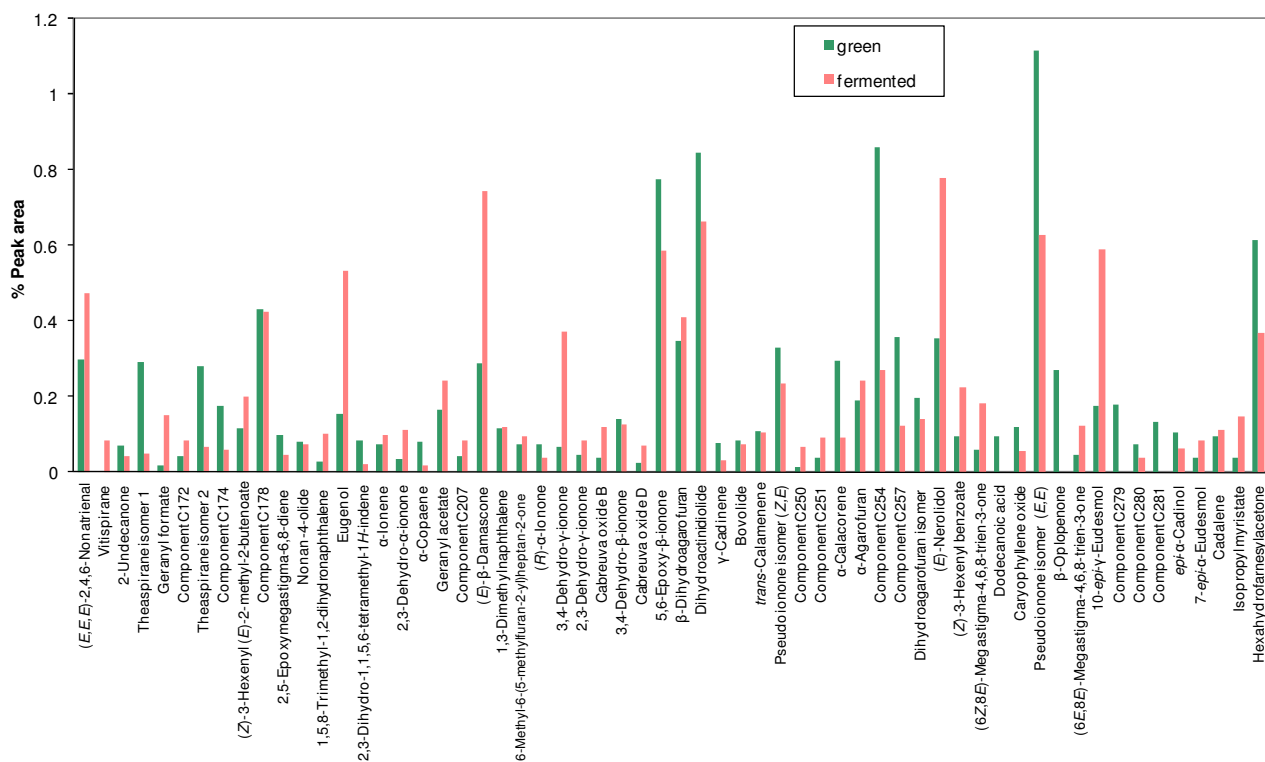


Fig. 5.1: contd.

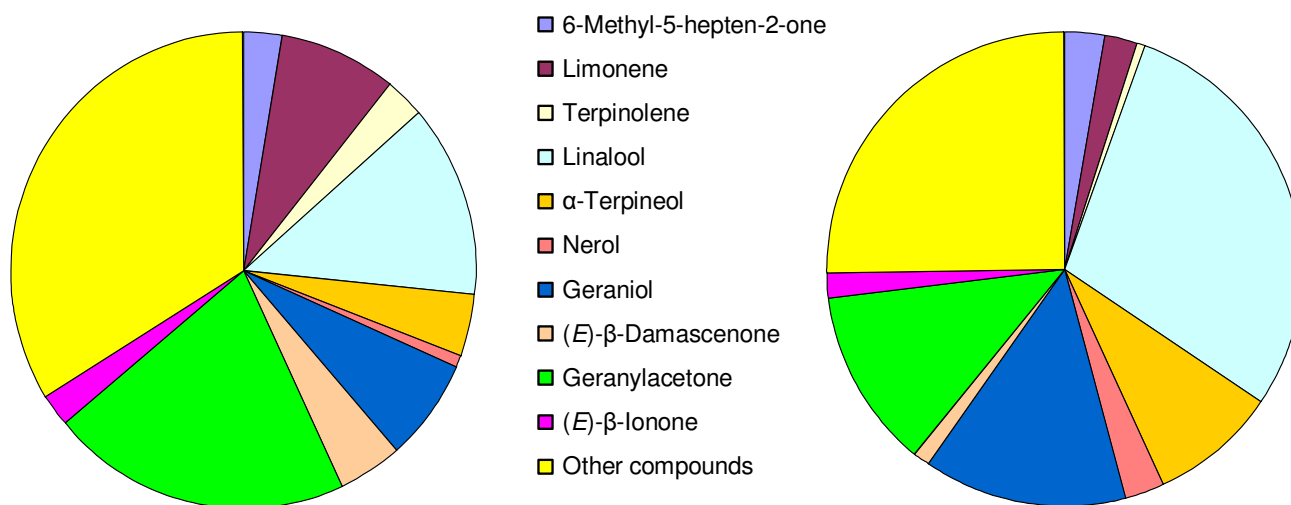


Fig. 5.2: Comparison of the concentrations (area %) of the 10 most abundant compounds in the headspace of green (left) and fermented (right) *Cyclopia intermedia*.

Honeybush plant material contains a variety of volatile and non-volatile compounds that are formed in the plant *via* biogenesis (Sell, 2006: 26). Green (unfermented) honeybush has an overall green-grassy odour which changes during fermentation to a more pleasant and unique honey-like aroma. During the high-temperature fermentation process of the honeybush plant material, oxidative and other chemical reactions occur that are not only responsible for the browning of the leaves but also a change in the composition of the VOCs, which in turn contributes to the



development of the typical honeybush aroma (ARC, 2008). Some of these reactions involve the degradation of  $\alpha$ -amino acids, the thermal degradation of carotenoids, the hydrolysis of terpenoid glycoside precursors, and the oxidative degradation of linolenic and other fatty acids (Yamanishi, 1995). It is interesting to note that many of the compounds, as well as the odour-active compounds, (indicated in bold in Table 5.1) are in most cases already present in the green honeybush, which means that they are formed prior to fermentation. It thus seems that fermentation, to a great extent, only has the effect of either increasing or decreasing the relative concentrations of the VOCs already present in the green honeybush. The effect of different processing techniques on the VOCs present in black tea showed similar results (Ravichandran and Parthiban, 1998). It was found that the VOCs were already present in the fresh green leaves before processing commenced. After the different processing stages quantitative differences in the VOCs were observed and a delicate balance between the relative concentrations of these compounds is responsible for the final quality of the tea aroma (Ravichandran and Parthiban, 1998).

The overall impression gained from the organoleptic descriptors of compounds that have higher relative concentrations (Table 5.1) in the green honeybush than in the fermented honeybush is that these compounds are mainly citrus-like, herbaceous, camphoraceous and, in some cases, green and woody, whereas the descriptors of compounds with higher concentrations in the fermented honeybush are mostly sweet, floral, fruity and, in some cases, woody.

Referring to Fig. 5.2 (10 compounds with the highest concentrations), the compounds linalool, geraniol,  $\alpha$ -terpineol and nerol are present in higher concentrations in the fermented than in the green honeybush and belong to the group of odour-active compounds typically described as floral and sweet. These compounds are therefore expected to contribute to the unique aroma of fermented honeybush. On the other hand, (*E*)- $\beta$ -damascenone and terpinolene (both odour-active) have higher relative concentrations in the green honeybush. Although the aroma of (*E*)- $\beta$ -damascenone is described as sweet and fruity it also contains some green-floral notes and, as can be seen from Table 5.1, it is present in a higher concentration in the green than in the fermented honeybush. The same can also be said of terpinolene with its sweet-piney odour. The relative quantities of 6-methyl-5-hepten-2-one and (*E*)- $\beta$ -ionone (both odour-active) do not differ significantly in the green and fermented honeybush. Geranylacetone and limonene occur in higher concentrations in green than in fermented honeybush—although their concentrations in the latter are also relatively high—but these two compounds were not identified as odour-active compounds in the fermented honeybush.

### 5.2.2 Comparison of seven *Cyclopia* samples

Seven *Cyclopia* samples, namely *C. genistoides*(a) (Albertinia), *C. genistoides*(b) (Pearly Beach), *C. genistoides* x *C. intermedia*, *C. intermedia*, *C. longifolia*, *C. subternata*(a) (Bredasdorp),

and *C. subternata*(b) (Genadendal), were analysed by subjecting the infused, fermented plant material of each sample to HS-GC-MS analysis. The identified volatile compounds were quantified, and the results are compared in Table 5.2 and Figs. 5.3–5.4p. In Table 5.2 only the odour-active compounds are listed and compared, while in Fig. 5.3 (which consists of five bar graphs because of the large number of components) all compounds present in the headspace of the infusions in concentrations of more than 0.1% (area %), irrespective of odour activity, are compared. All of the odour-active compounds were also included in the bar graphs. In some of the bar graphs the scale of the y-axis was minimised so that compounds with a smaller area % could be more clearly visible. Each bar graph of Fig. 5.3 is followed by a short discussion focussing on variations between the different samples, particularly with respect to the odour-active compounds as listed in Table 4.1. These variations are then also depicted graphically in the form of a pie chart for each of the most intense odour-active compounds (Figs. 5.4a–5.4p).

Table 5.2: Comparison of the odour-active compounds identified in seven *Cyclopia* samples

No	Compound <sup>a</sup>	Aroma descriptors <sup>b</sup>	<i>Cyclopia</i> samples <sup>c</sup>							
			<i>gen(a)</i>	<i>gen(b)</i>	<i>gen × int</i>	<i>int</i>	<i>long</i>	<i>subt(a)</i>	<i>subt(b)</i>	
C6	Hexanal	Fatty-green grassy odour	✓ <sup>d</sup>	✓	✓	✓	✓	✓	✓	✓
C11	3-Methylbutanoic acid	Acid acrid, cheesy, unpleasant	✓			✓	✓	✓	✓	✓
C13	( <i>R</i> )-2-Methylbutanoic acid	Cheesy, sweaty, sharp					✓	✓		
C32	6-Methyl-5-hepten-2-one	Oily-green, pungent-herbaceous, grassy, with fresh and green-fruity notes	✓	✓	✓	✓	✓	✓	✓	✓
C50	<i>p</i> -Cymene	Citrus-like, reminiscent of lemon and bergamot	✓	✓	✓	✓	✓	✓	✓	✓
C56	( <i>Z</i> )-β-Ocimene	Warm-herbaceous, sweet, floral	✓	✓	✓	✓	✓	✓	✓	✓
C61	γ-Terpinene	Refreshing, herbaceous, citrus-like	✓	✓	✓	✓	✓	✓	✓	✓
C70	( <i>E,E</i> )-3,5-Octadien-2-one	Fatty, fruity, mushroom	✓	✓	✓	✓	✓	✓	✓	✓
C71	Terpinolene	Sweet-piney, oily	✓	✓	✓	✓	✓	✓	✓	✓
C76	Linalool*	Refreshing, floral-woody	✓	✓	✓	✓	✓	✓	✓	✓
C79	2-Phenylethanol	Mild, warm, rose-honey-like	✓	✓		✓	✓	✓	✓	✓
C89	4-Acetyl-1-methyl-cyclohexene	Spicy	✓	✓	✓	✓	✓	✓	✓	✓
C97	Lilac aldehyde isomer 1	Sweet, fresh, floral							✓	✓
C101	( <i>E,Z</i> )-2,6-Nonadienal*	Green-vegetable, cucumber or violet leaf	✓	✓	✓	✓	✓	✓	✓	✓
C108	( <i>E</i> )-2-Nonenal*	Green, cucumber, aldehydic and fatty	✓	✓	✓	✓	✓	✓	✓	✓
C121	α-Terpineol	Floral, sweet, lilac-type	✓	✓	✓	✓	✓	✓	✓	✓
C128	(+)- <i>p</i> -Menth-1-en-9-al	Powerful spicy, herbaceous odour	✓	✓	✓	✓	✓	✓	✓	✓
C129	β-Cyclositral	Green, grassy, hay-like	✓	✓	✓	✓	✓	✓	✓	✓
C135	Nerol	Fresh, sweet-rosy	✓	✓	✓	✓	✓	✓	✓	✓
C141	<i>p</i> -Anisaldehyde	Sweet, floral, "haylike"	✓	✓	✓	✓	✓	✓	✓	✓
C148	Geraniol*	Sweet, floral, rose	✓	✓	✓	✓	✓	✓	✓	✓
C150	Geranial	Lemon	✓	✓	✓	✓	✓	✓	✓	✓
C152	( <i>R</i> )-Octan-5-olide	Peach, coconut-like				✓	✓	✓	✓	✓
C162	Component C162	– <sup>e</sup>	✓	✓	✓	✓	✓	✓	✓	✓
C164	Geranyl formate	Fresh, green-rosy, fruity	✓	✓	✓	✓	✓	✓	✓	✓
C171	( <i>E,E</i> )-2,4-Decadienal*	Fried, waxy, fatty, orange-like	✓	✓	✓	✓	✓	✓	✓	✓
C178	Component C178*	–	✓	✓	✓	✓	✓	✓	✓	✓
C191	Eugenol	Warm-spicy, dry	✓	✓	✓	✓	✓	✓	✓	✓

Table 5.2: *contd.*

No	Compound <sup>a</sup>	Aroma descriptors <sup>b</sup>	<i>Cyclopia</i> samples <sup>c</sup>						
			<i>gen(a)</i>	<i>gen(b)</i>	<i>gen × int</i>	<i>int</i>	<i>long</i>	<i>subt(a)</i>	<i>subt(b)</i>
C203	2,3-Dehydro- $\alpha$ -ionone	Tobacco-like	✓	✓	✓	✓	✓	✓	✓
C204	( <i>E</i> )- $\beta$ -Damasconone*	Woody, sweet, fruity, earthy green-floral	✓	✓	✓	✓	✓	✓	✓
C212	( <i>E</i> )- $\beta$ -Damascone*	Fruity (apple-citrus), tea-like with slight minty notes	✓	✓	✓	✓	✓	✓	✓
C222	2,3-Dehydro- $\gamma$ -ionone*	–	✓	✓	✓	✓	✓	✓	✓
C229	( <i>S</i> )-( <i>Z</i> )-7-Decen-5-olide	Sweet, floral, fruity				✓	✓	✓	✓
C230	3,4-Dehydro- $\beta$ -ionone*	Ionone-damascone and saffron-like, fruity and slightly leathery	✓	✓	✓	✓	✓	✓	✓
C233	( <i>R</i> )-Decan-5-olide	Sweet, creamy, nut-like, fruity	✓	✓	✓	✓	✓	✓	✓
C234	( <i>E</i> )- $\beta$ -Ionone*	Warm, woody, fruity, raspberry-like; resembles cedarwood	✓	✓	✓	✓	✓	✓	✓
C245	Bovolide	Celery- and lovage-like, fruity and pleasant	✓	✓	✓	✓	✓	✓	✓
C269	Component C269	–	✓			✓	✓	✓	
C271	(6 <i>E</i> ,8 <i>Z</i> )-Megastigma-4,6,8-trien-3-one	Tobacco-like, woody, balsamic	✓	✓	✓	✓	✓	✓	✓
C272	Geranyl 2-methylbutanoate	Pleasant, sweet	✓					✓	✓
C277	(6 <i>E</i> ,8 <i>E</i> )-Megastigma-4,6,8-trien-3-one	Tobacco-like, woody, balsamic	✓	✓	✓	✓	✓	✓	✓
C278	10- <i>epi</i> - $\gamma$ -Eudesmol*	Woody, floral, sweet	✓	✓	✓	✓	✓	✓	✓
C284	<i>epi</i> - $\alpha$ -Cadinol*	Herbaceous, woody	✓	✓	✓	✓	✓	✓	✓
C285	<i>epi</i> - $\alpha$ -Muurolol*	Herbaceous, slightly spicy	✓	✓	✓	✓	✓	✓	✓
C290	Cadalene	–	✓	✓	✓	✓	✓	✓	✓
C295	(7 <i>E</i> )-Megastigma-5,7,9-trien-4-one*	Tea-like, spicy and resembling dried fruit	✓	✓				✓	✓

<sup>a</sup> In order of elution from apolar PS-089 column (DB-5 equivalent). \*Most intense odour-active compounds (See § 4.2 pp. 238–239).

<sup>b</sup> Acree and Arn, 2004; Arctander, 1969; Boldingh and Taylor, 1962; Buttery *et al.*, 1979; Demole and Enggist, 1974; JECFA, 2009; Kreck and Mosandl, 2003; Leffingwell, 2002; Mookherjee and Wilson, 1990; Mosciano *et al.*, 1991a, 1991b; Näf and Velluz, 2000; Ohloff, 1994; Oomah and Liang, 2007; Serra *et al.*, 2006; Tachihara *et al.*, 2006; Takahashi *et al.*, 1980; Yamazaki *et al.*, 1988.

<sup>c</sup> *Cyclopia* samples: *C. genistoides*(a) (Albertinia); *C. genistoides*(b) (Pearly Beach); *C. genistoides* × *C. intermedia*; *C. intermedia*; *C. longifolia*; *C. subternata*(a) (Bredasdorp); *C. subternata*(b) (Genadendal).

<sup>d</sup> Compound detected in GC-MS analysis in area %  $\geq 0.001$  ( $n = 3$ ; RSD  $\leq 20\%$ ).

<sup>e</sup> Aroma descriptor not available.

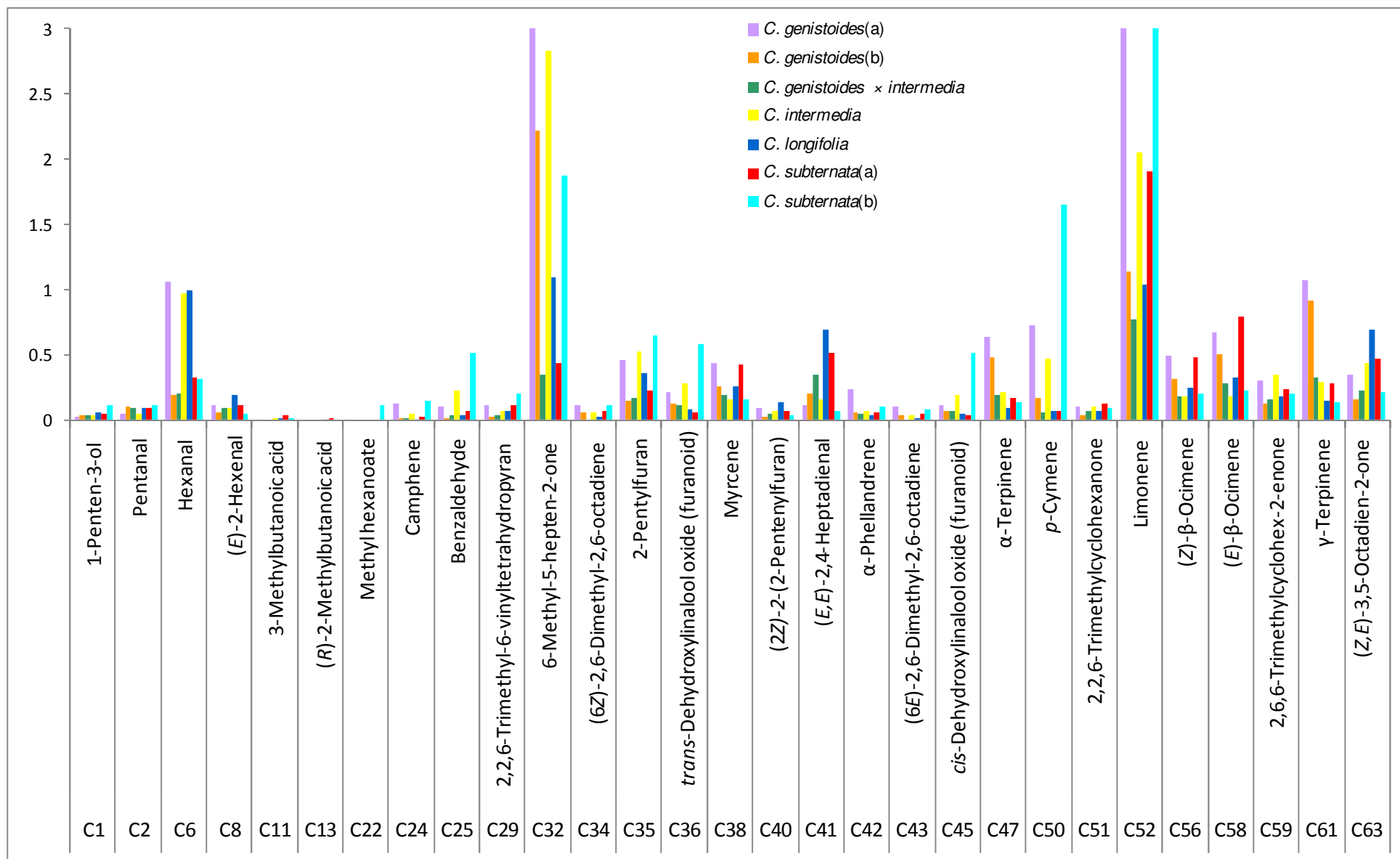


Fig. 5.3: Comparison of the VOCs, identified by HS-SEP-GC-MS analysis, in seven *Cylcopia* samples (area % >0.1%).

In the first of the series of bar graphs (Fig. 5.3) **hexanal** is very prominent in *C. genistoides*(a), *C. intermedia* and *C. longifolia*, whereas **p-cymene** is very prominent in the *C. subternata*(b) sample. The relative concentrations of **6-methyl-5-hepten-2-one** in *C. subternata*(a), *C. genistoides* × *C. intermedia*, and to a lesser extent in *C. longifolia*, are much lower than in the other samples. **γ-Terpinene** is very prominent in both samples of *C. genistoides*, while **(Z)-**and **(E)-β-ocimene** are more prominent in *C. genistoides*(a), *C. subternata*(a) and *C. genistoides*(b) than in the other honeybush samples.

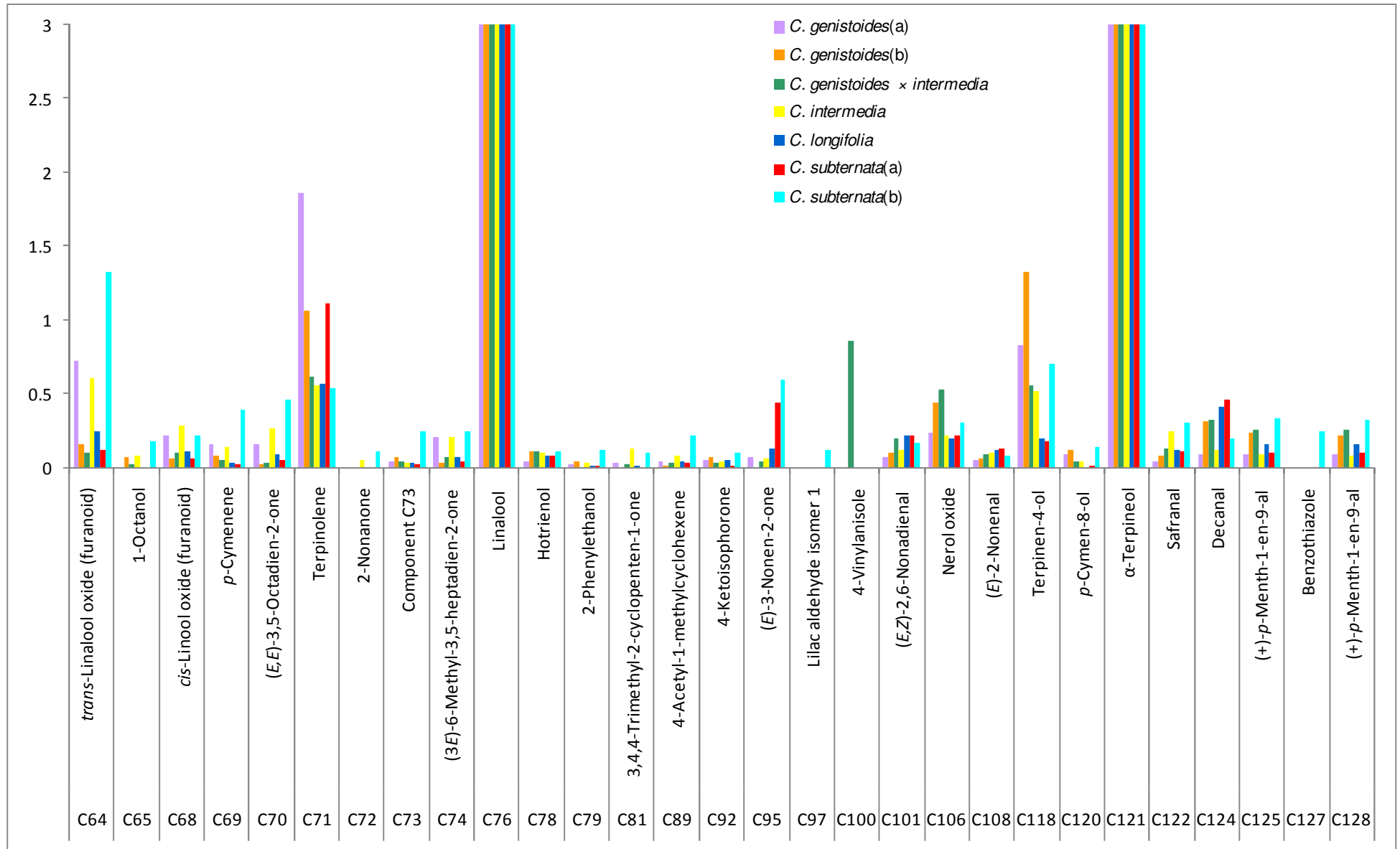


Fig. 5.3: contd.

The second bar graph shows that **(E,E)-3,5-octadien-2-one** is prominent in *C. genistoides*(a), *C. intermedia* and *C. subternata*(b), whereas **terpinolene** is more prominent in the two *C. genistoides* samples and *C. subternata*(a). **Linalool** occurs in all seven honeybush samples in more or less the same relative concentrations, although somewhat lower in *C. longifolia*, and *C. subternata*(b). **2-Phenylethanol**, **4-acetyl-1-methylcyclohexene**, **lilac aldehyde isomer 1** and both diastereomers of **p-menth-1-en-9-al** are present in *C. subternata*(b) in greater quantities than in the other samples. **(E,Z)-2,6-nonadienal** is present in smaller quantities in the two *C. genistoides* samples and *C. intermedia* and the quantity of **(E)-2-nonenal** is more or less the same in the majority of the honeybush samples, but somewhat smaller in the two *C. genistoides* samples.

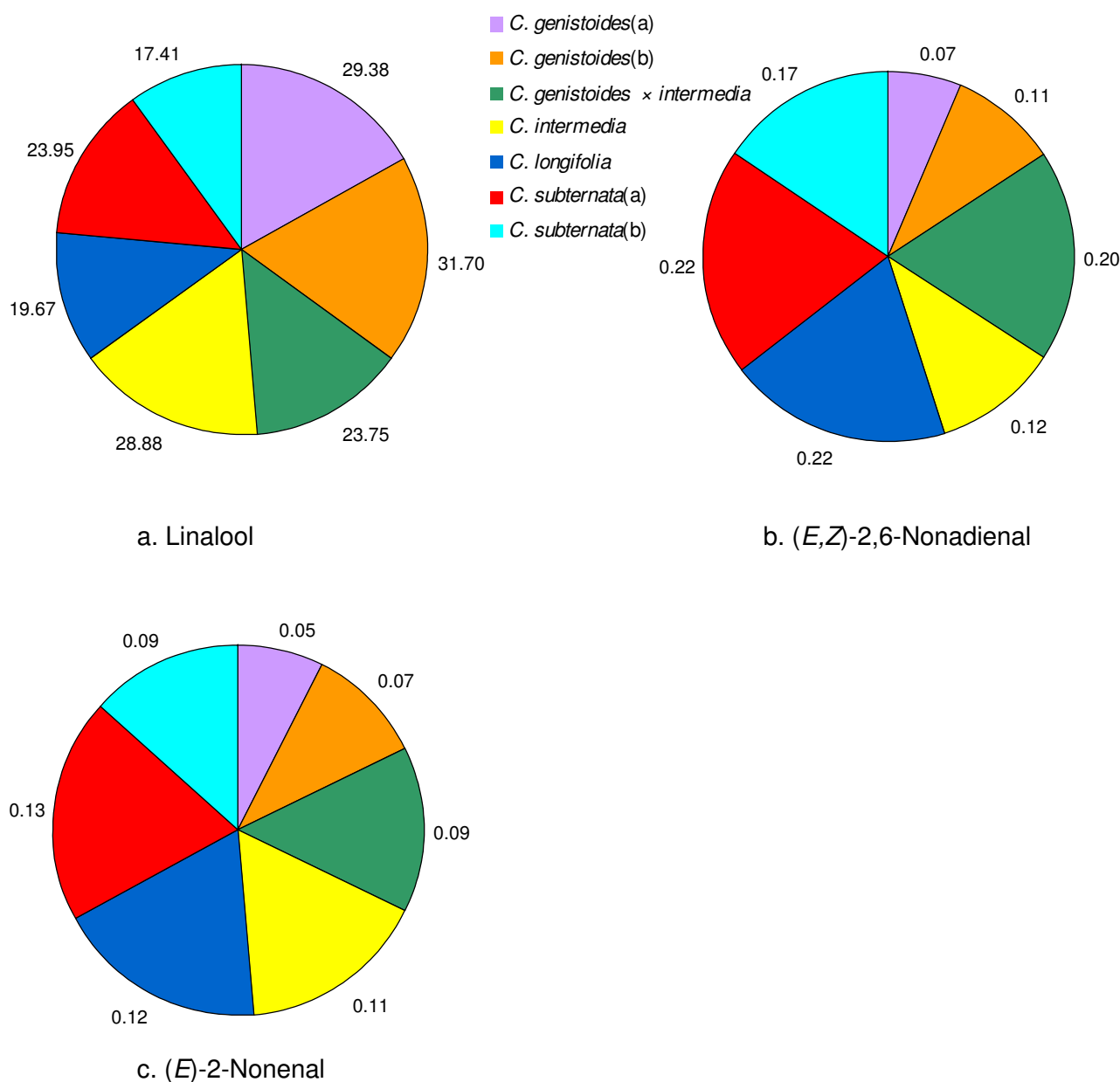


Fig. 5.4: Comparison of the relative concentrations (area %) of the most intense odour-active compounds identified in seven *Cyclopiya* samples.



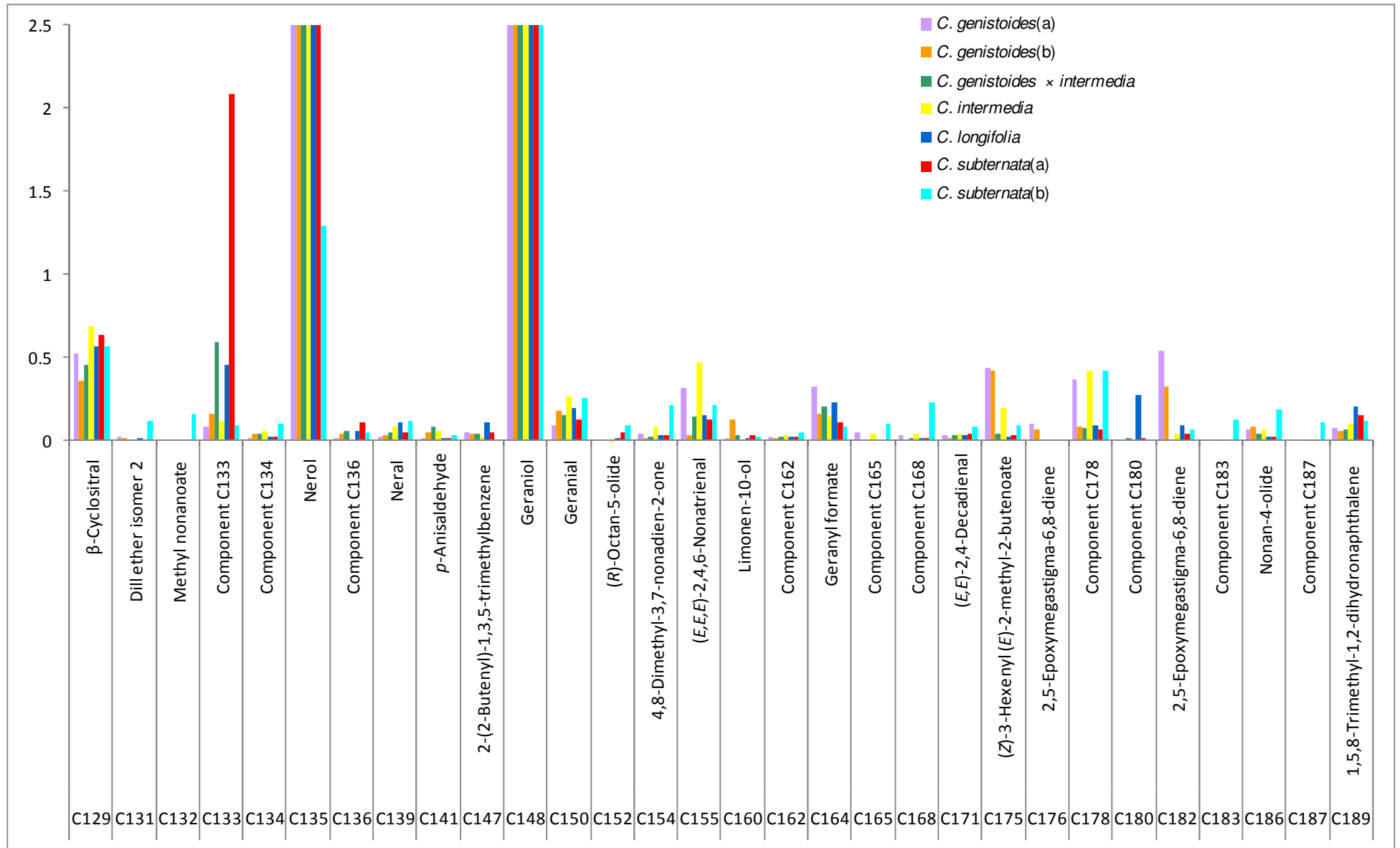


Fig. 5.3: contd.

Although  **$\beta$ -cyclositral** has the highest area % in *C. intermedia* there is not a very significant variation between the seven honeybush samples. **(R)-Octan-5-olide** is only prominent in four of the seven samples. The concentrations of both **nerol** and **geraniol** are relatively low in *C. subternata(b)*, as shown in Figs. 5.4(f) and 5.4(g). **(E,E)-2,4-Decadienal** is present in higher quantities in *C. subternata(b)* and **component C178** is especially prominent in *C. genistoides*, *C. intermedia* and *C. subternata(b)*.

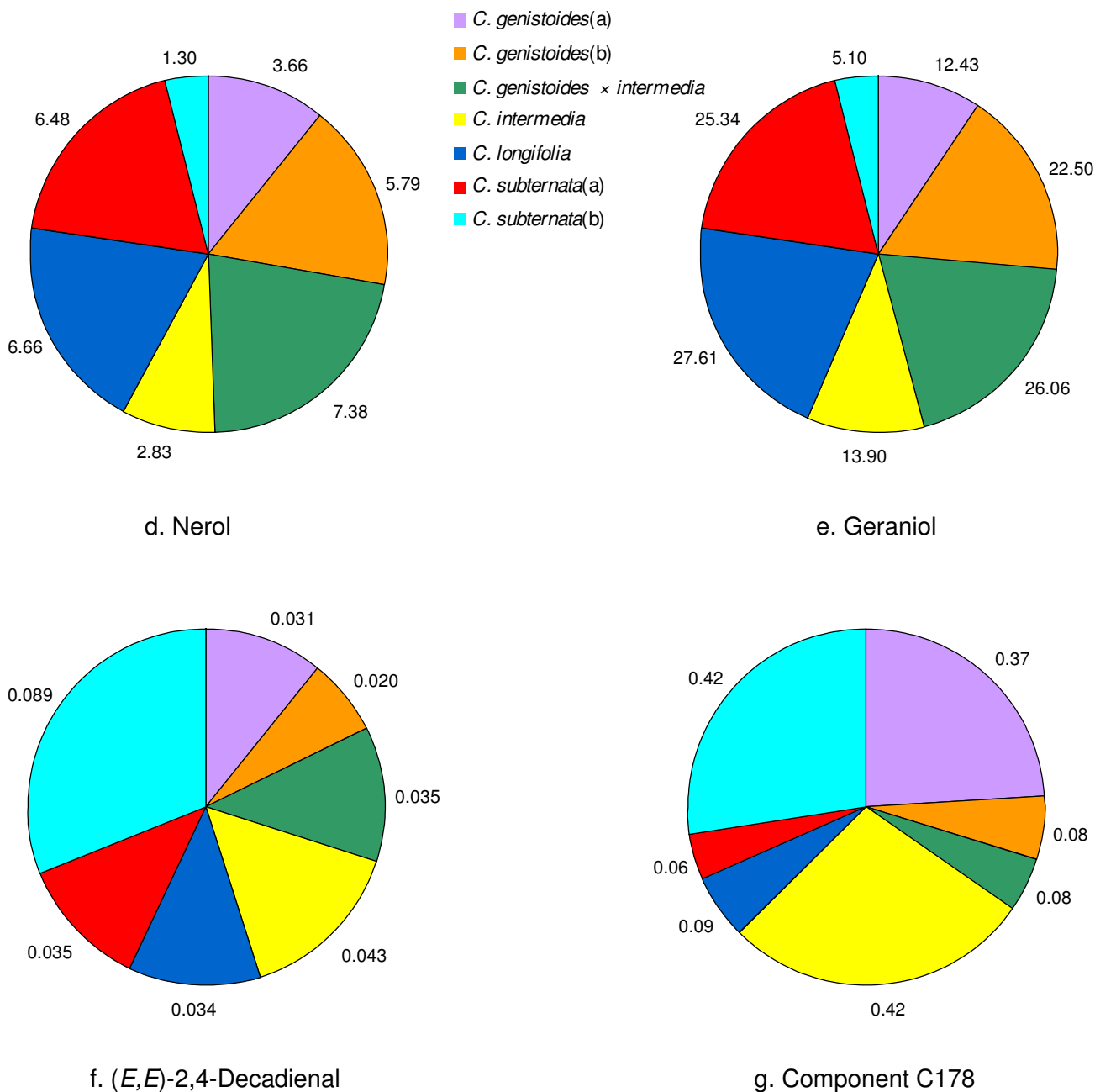


Fig. 5.4: Comparison of the relative concentrations (area %) of the most intense odour-active compounds identified in seven *Cyclopiya* samples.

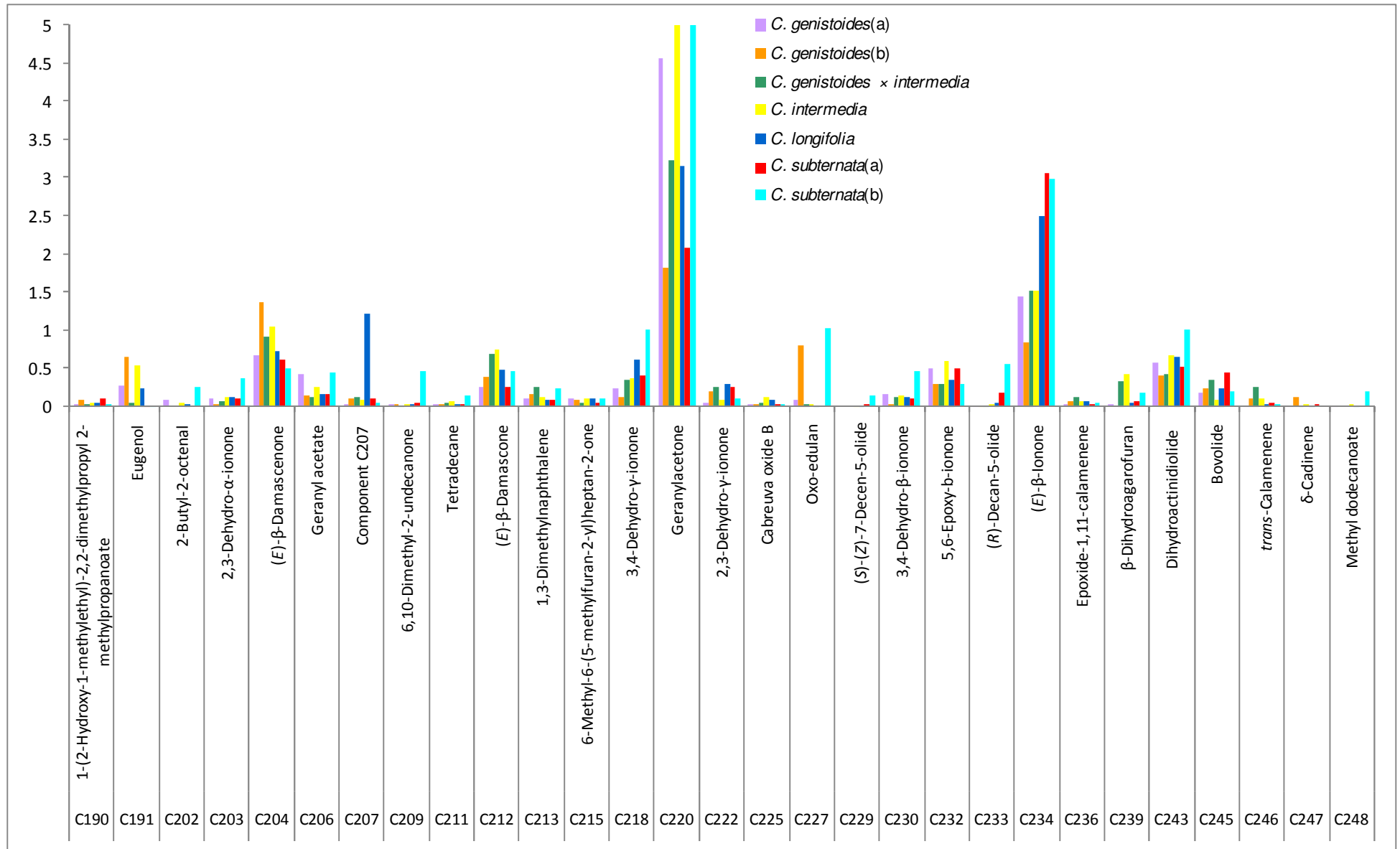
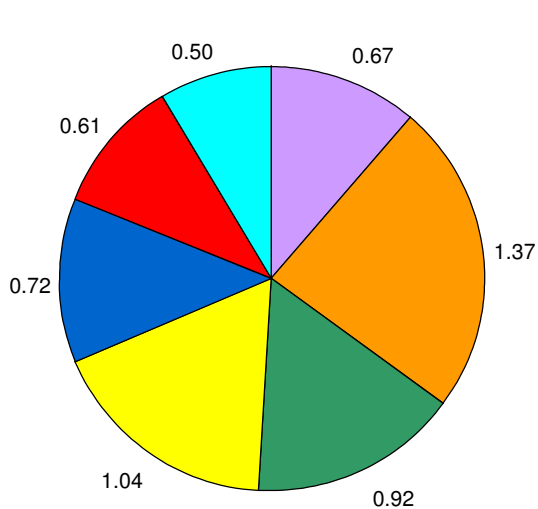
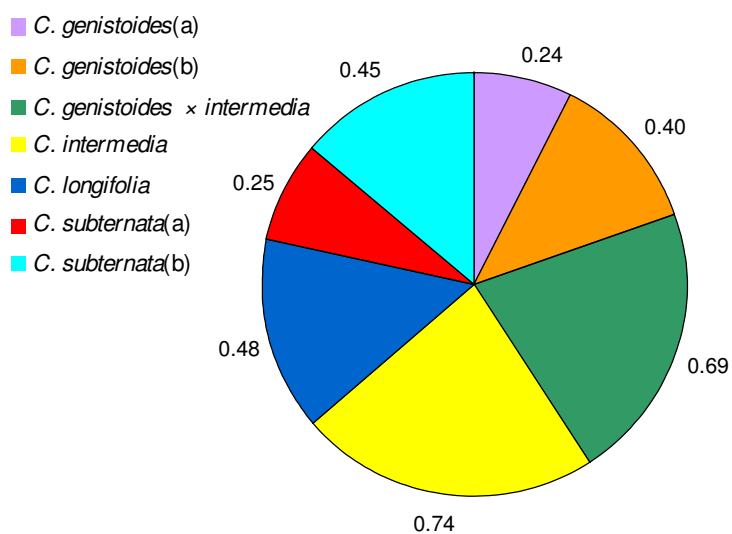


Fig. 5.3: *contd.*

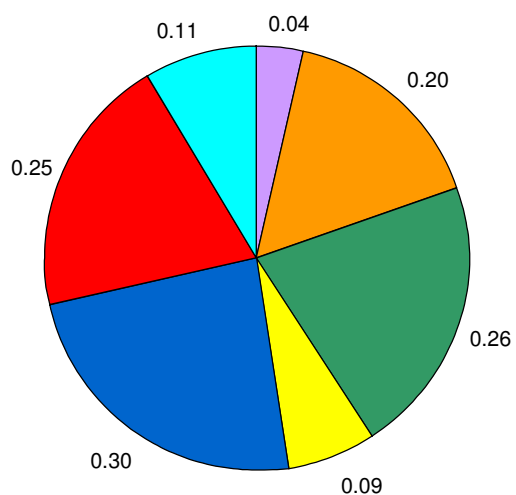
**Eugenol** and **(E)- $\beta$ -damascenone** are more prominent in *C. genistoides*(b) and *C. intermedia*, while **(E)- $\beta$ -damascone** is more prominent in *C. genistoides*  $\times$  *C. intermedia* and *C. intermedia*. The compound **2,3-dehydro- $\gamma$ -ionone** is present in higher concentrations in *C. subternata*(a), *C. genistoides*(b), *C. genistoides*  $\times$  *C. intermedia* and *C. longifolia* than in the other honeybush samples. *C. genistoides*(b) and *subternata*(b) have the highest concentrations of **(S)- $\beta$ -ionone**, **(Z)-7-decen-5-olide**, **(R)-decan-5-olide** and **3,4-dehydro- $\beta$ -ionone**. *C. subternata*(a), *C. subternata*(b), and *C. longifolia* have higher relative quantities of **(E)- $\beta$ -ionone**. The compound **bovolide** is more prominent in *C. subternata*(a).



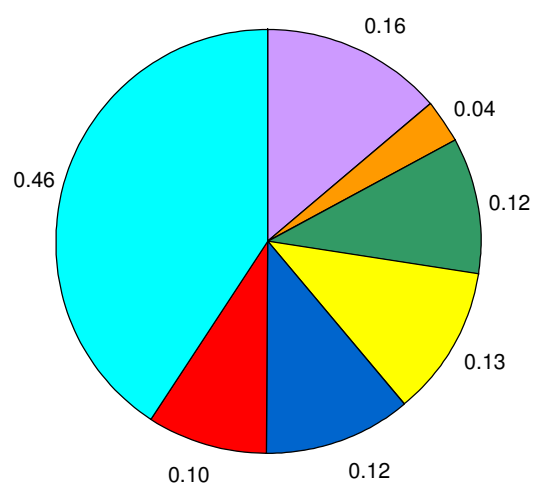
h. (E)- $\beta$ -damascenone



i. (E)- $\beta$ -damascone



j. 2,3-Dehydro- $\gamma$ -ionone



k. 3,4-Dehydro- $\beta$ -ionone

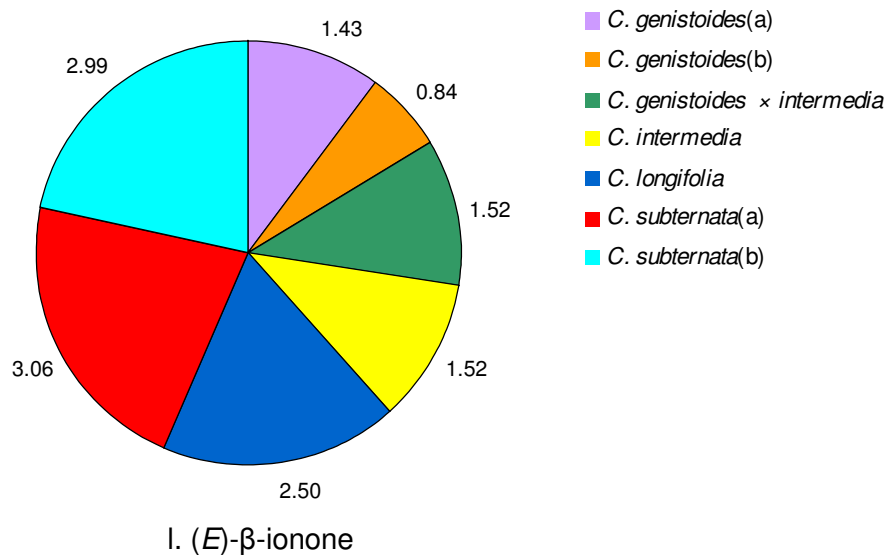


Fig. 5.4: Comparison of the relative concentrations (area %) of the most intense odour-active compounds identified in seven *Cyclopiea* samples.

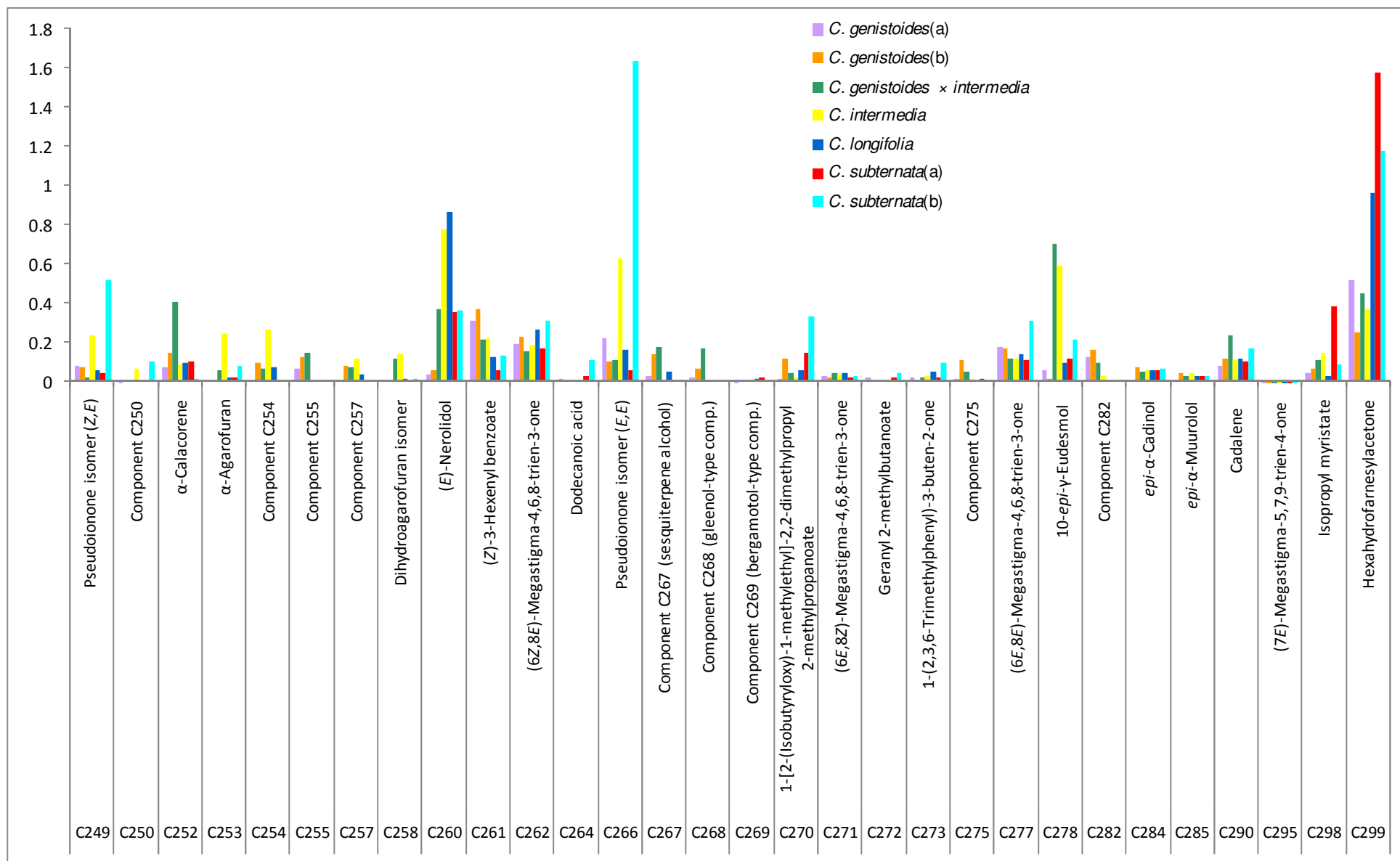


Fig. 5.3: contd.

Both isomers of **megastigma-4,6,8-trien-3-one** are more prominent in *C. subternata*(b). **Cadalene** is prominent in *C. genistoides* × *C. intermedia* and **10-*epi*- $\gamma$ -eudesmol** is prominent not only in this sample, but also in *C. intermedia*. ***epi*- $\alpha$ -Cadinol** and ***epi*- $\alpha$ -muurolol** are present in more or less the same relative concentrations in six of the seven honeybush samples, but markedly less in *C. genistoides*(a). In three samples, i.e. *C. genistoides* × *C. intermedia*, *C. intermedia* and *C. longifolia*, **(7*E*)-megastigma-5,7,9-trien-4-one** is barely detectable, whereas in the remaining three samples the concentrations, although very low, are more or less similar.

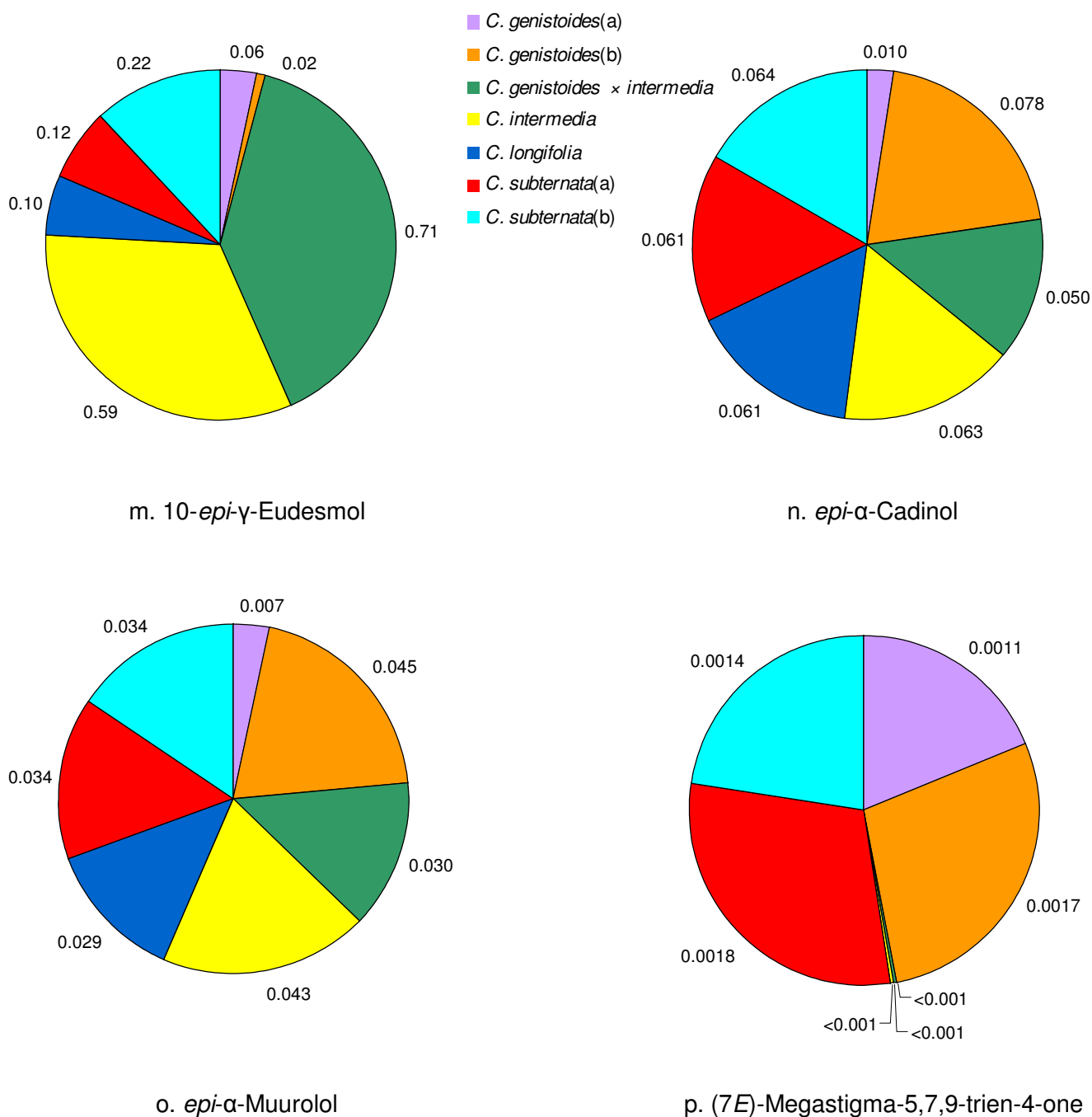


Fig. 5.4: Comparison of the relative concentrations (area %) of the most intense odour-active compounds identified in seven *Cyclopiya* samples.

From the above discussion it is evident that the seven honeybush samples are qualitatively very similar, but there are, however, important quantitative differences.

### 5.3 REFERENCES

- Acree, T., Arn, H. 2004. Flavornet and human odor space [Online]. Available: <http://www.flavornet.org/> [March 2010].
- Agricultural Research Council. 2008. Website of honeybush research programme, ARC, South Africa [Online]. Available: <http://www.arc.agric.za/home.asp?pid=4053> [2010, 5 February].
- Arctander, S., 1969. Perfume and flavour chemicals, Vols I and II. Steffen Arctander, Montclair, New Jersey.
- Boldingh, J., Taylor, R.J. 1962. Trace constituents of butterfat. *Nature* **194**, 909–913.
- Brenna, E., Fuganti, C., Serra, S. 2003. Enantioselective perception of chiral odorants. *Tetrahedron: Asymm.* **14**, 1–42.
- Buttery, R.G., Black, D.R., Haddon, W.F., Ling, L.C., Teranishi, R., 1979. Identification of additional volatile constituents of carrot roots. *J. Agric. Food Chem.* **27**, 1–3.
- Demole, E., Enggist, P. 1974. Novel synthesis of 3,5,5-trimethyl-4-(2-butenylidene)-cyclohex-2-en-1-one, a major constituent of Burley tobacco flavour. *Helv. Chim. Acta.* **57**, 2087–2091.
- Eggers, N.J., Bohna, K., Dooley, B. 2006. Determination of vitispirane in wines by stable isotope dilution assay. *Am. J. Enol. Vitic.* **57**, 226–232.
- Joint FAO/WHO Expert Committee on Food Additives (JECFA). 2009. Specifications for flavourings [Online]. Available: <http://www.fao.org/ag/agn/jecfa-flav/index.html?showSynonyms=0> [2009, November].
- Kreck, M., Mosandl, A. 2003. Synthesis, structure elucidation, and olfactometric analysis of lilac aldehyde and lilac alcohol stereoisomers. *J. Agric. Food Chem.* **51**, 2722–2726.
- Leffingwell, J.C. 2002. Leffingwell reports: Tobacco—aroma from carotenoids [Online]. Available: <http://www.leffingwell.com/leffrept.htm> [2010, 10 March].
- Mookherjee, B.D., Wilson, R.A. 1990. Tobacco constituents. Their importance in flavour and fragrance chemistry. *Perfumer and Flavorist* **15**, 27–49.
- Mosciano, G., Fasano, M., Michalski, J., Sadural, S. 1991a. Organoleptic characteristics of flavor materials. *Perfumer and Flavorist* **16**, 31–33.
- Mosciano, G., Fasano, M., Michalski, J., Sadural, S. 1991b. Organoleptic characteristics of flavor materials. *Perfumer and Flavorist* **16**, 79–81.
- Näf, R., Velluz, A. 2000. The volatile constituents of extracts of cooked spinach leaves (*Spinacia oleracea* L.). *Flavour Fragr. J.* **15**, 329–334.
- Ohloff, G. 1994. Scent and fragrances. The Fascination of odors and their chemical perspectives. Springer-Verlag, Berlin, Germany.
- Oomah, B.D., Liang, L.S.Y. 2007. Volatile compounds of dry beans (*Phaseolus vulgaris* L.). *Plant Foods Hum. Nutr.* **62**, 177–183.



- Ravichandran, R., Parthiban, R. 1998. The impact of processing techniques on tea volatiles. *Food Chem.* **62**, 347–353.
- Sell, S. 2006. The chemistry of fragrances. The Royal Society of Chemistry, Cambridge.
- Serra, S., Fuganti, C., Brenna, E. 2006. Synthesis and olfactory evaluation, and determination of the absolute configuration of the 3,4-didehydroionone stereoisomers. *Helv. Chim. Acta* **89**, 1110–1122.
- Tachihara, T., Hashimoto, H., Ishizaki, S., Komai, T., Fujita, A., Ishikawa, M., Kitahara, T. 2006. Microbial resolution of 2-methylbutyric acid and its application to several chiral flavour compounds. *Dev. Food Sci.* **43**, 97–100.
- Takahashi K., Someya, T., Muraki, S., Yoshida, T. 1980. A new keto-alcohol, (–)-mintlactone, (+)-*iso*-mintlactone and minor components in peppermint oil. *Agric. Biol. Chem.* **44**, 1535–1543.
- Yamanishi, T. 1995. Chemical composition of tea. *Food Rev. Int.* **11**, 435–456.
- Yamazaki, Y., Hayashi, Y., Arita, M., Hieda, T., Mikami, Y. 1988. Microbial conversion of  $\alpha$ -ionone,  $\alpha$ -methylionone and  $\alpha$ -isomethylionone. *Appl. Environ. Microb.* **54**, 2354–2360.

## CHAPTER 6

# SENSORY AROMA ATTRIBUTES OF HONEYBUSH TEA

### 6.1 INTRODUCTION

Of the many sectors of consumer product industries, the food and beverage sectors provided much early support for an interest in sensory analysis. A wide spectrum of attributes drive food quality as well as food preference. Research has shown that adequate nutrition does not always guarantee food acceptance and that the flavour of a product can be regarded as one of the most important drivers of food quality and preference. In the past many consumer product industries, including the food industry, had a company “expert” who, through years of accumulated experience, evaluated the manufactured products and set standards of quality. These “experts” included the perfumer, flavourist, brewmaster, winemaker, and coffee and tea tasters. In the early years of the food industry such evaluation procedures by experts were very useful, but became increasingly difficult to maintain by a few experts because the food industry showed enormous growth and new measurement techniques for sensory analysis were developed. As a result, companies turned to sensory analysis, previously known as “organoleptic analysis” (Stone and Sidel, 2004: 7–9).

Sensory analysis can be defined as “a scientific discipline used to evoke, measure, analyse and interpret reactions to those characteristics of foods and materials as they are perceived by the senses of sight, smell, taste, touch and hearing” (Anonymous, 1975; Stone and Sidel, 2004: 13). After analysis by a group of individuals, specifically trained in perceiving the required characteristic of the food/material, the data are subjected to statistical analysis in order to determine whether the responses from the group are sufficiently similar or represent a random occurrence (Stone and Sidel, 2004: 111). Different sensory test methods are used to profile a product sensorially, and these include discrimination testing, descriptive analysis and acceptance testing (Stone and Sidel, 2004: 145, 201, 248). Of these three methods, descriptive sensory analysis is the most sophisticated (Lawless and Heymann, 1999: 341). It involves the detection (discrimination) and description of the qualitative and quantitative sensory components of a product by a trained panel of judges (Meilgaard *et al.*, 2006: 173). Using descriptive analysis, it is possible to determine relationships between descriptive sensory and other types of analyses, e.g. instrumental and/or consumer preference measurements, which allows for product optimisation and the establishment of validated models between descriptive sensory tests and the relevant instrumental and/or preference measures (Murray *et al.*, 2001).

Descriptive sensory analyses are used for quality control purposes, to compare product prototypes, for sensory mapping and product matching (Gacula, 1997: 1; Murray *et al.*, 2001). It can also be used to follow the change of a product over time in order to establish the effects of shelf-life

and packaging and to establish the possible effects of certain ingredients or processing variables on the final sensory quality of a product (Murray *et al.*, 2001).

The first step in the process of descriptive analysis is the selection of a panel of judges. A vast array of literature describing the process of screening and selection is available (Stone and Sidel, 2004: 50–61). After the selection phase, the panellists are trained in a common sensory ‘language’ which comprehensively and accurately describes the attributes of the product under investigation (Murray *et al.*, 2001). Once the product attributes have been established, the panellists are trained with reference standards to align the concepts of each participant as to the types of experiences referred to by a given attribute. Each panellist is then able to provide an intensity rating for each attribute to reflect the perceived intensity of that characteristic in the product (Lawless, 1999).

In this study, eight different honeybush samples were analysed for a spectrum of sensory aroma attributes (orthonasal) by trained panellists using the descriptive sensory analysis technique. The panel established six sensory aroma attributes associated with honeybush tea before the aroma of the eight honeybush samples were analysed and the data subjected to statistical analysis. The eight honeybush samples consisted of four honeybush species and variant species thereof, as well as a sample of one of the chosen species (*C. subternata*) which had been harvested and fermented with its flowers.

## 6.2 RESULTS AND DISCUSSION

### 6.2.1 Sensory aroma attributes of honeybush tea, using univariate analyses

Analysis of variance (ANOVA) is a statistical procedure used to partition all the sources of variability in a test, in order to provide a more precise estimate of the variable being studied (Stone and Sidel, 2004: 123). It is an appropriate method for the analyses of the scaled responses obtained from a descriptive sensory test (Stone and Sidel, 2004: 223).

Table 6.1 lists the mean values of the sensory aroma attributes of the eight respective honeybush samples as scored by the panel of judges, in order to determine whether the mean scores for a specific attribute differ significantly from one another (Stone and Sidel, 2004: 230). The results in Table 6.1 are also presented graphically in Fig. 6.1. The results indicate that the honeybush tea samples differed significantly ( $P \leq 0.05$ ) with regard to the respective sensory aroma attributes. Fig. 6.2 is another visual presentation (spider webs) incorporating the scores obtained for all the sensory aroma attributes of the respective honeybush samples. Table 6.2 is a summary of the two main and minor sensory aroma attributes associated with each honeybush sample, i.e. the four attributes for which the highest scores were obtained as listed in Table 6.1.

Table 6.1: Sensory aroma attributes of eight honeybush samples

	Honeybush aroma	Sweet aroma	Plant-like aroma	Rooibos aroma	Lemon aroma	Earl Grey aroma
Product 1: <i>C. genistoides</i> (a) (Albertinia)	59.7 <sup>ab</sup>	60.1 <sup>b</sup>	9.1 <sup>ef</sup>	6.1 <sup>c</sup>	7.1 <sup>ab</sup>	25.6 <sup>a</sup>
Product 2: <i>C. genistoides</i> (b) (Pearly Beach)	53.6 <sup>c</sup>	52.6 <sup>c</sup>	23.4 <sup>a</sup>	6.9 <sup>c</sup>	7.5 <sup>a</sup>	4.7 <sup>b</sup>
Product 3: <i>C. genistoides</i> × <i>C. intermedia</i>	58.2 <sup>bc</sup>	58.2 <sup>bc</sup>	6.9 <sup>f</sup>	17.7 <sup>b</sup>	4.7 <sup>bc</sup>	6.4 <sup>b</sup>
Product 4: <i>C. intermedia</i>	59.4 <sup>ab</sup>	59.0 <sup>b</sup>	5.1 <sup>f</sup>	15.6 <sup>b</sup>	2.6 <sup>cd</sup>	0.5 <sup>c</sup>
Product 5: <i>C. longifolia</i>	64.5 <sup>a</sup>	59.4 <sup>b</sup>	10.4 <sup>de</sup>	28.7 <sup>a</sup>	4.9 <sup>bc</sup>	0.3 <sup>c</sup>
Product 6: <i>C. subternata</i> (a) (Bredasdorp)	60.1 <sup>ab</sup>	59.2 <sup>b</sup>	19.8 <sup>ab</sup>	29.0 <sup>a</sup>	6.6 <sup>ab</sup>	0.1 <sup>c</sup>
Product 7: <i>C. subternata</i> (b) – flower (Genadendal)	58.9 <sup>abc</sup>	63.4 <sup>ab</sup>	14.6 <sup>cd</sup>	4.2 <sup>c</sup>	0.9 <sup>d</sup>	0.2 <sup>c</sup>
Product 8: <i>C. subternata</i> (c) + flower (Genadendal)	61.9 <sup>ab</sup>	67.9 <sup>a</sup>	16.1 <sup>bc</sup>	6.8 <sup>c</sup>	2.6 <sup>cd</sup>	0.4 <sup>c</sup>
<b>LSD<sup>a</sup> (P = 0.05)</b>	<b>5.71</b>	<b>6.01</b>	<b>4.31</b>	<b>4.88</b>	<b>2.62</b>	<b>3.22</b>

<sup>a</sup> LSD (Least significant difference).

<sup>a-f</sup> Means with different superscripts in the same column differ significantly at the 5% level.

■ Product 1: *C. genistoides*(a)   
 ■ Product 2: *C. genistoides*(b)   
 ■ Product 3: *C. genistoides* × *C. intermedia*   
 ■ Product 4: *C. intermedia*  
■ Product 5: *C. longifolia*   
 ■ Product 6: *C. subternata*(a)   
 ■ Product 7: *C. subternata*(b)   
 ■ Product 8: *C. subternata*(c)

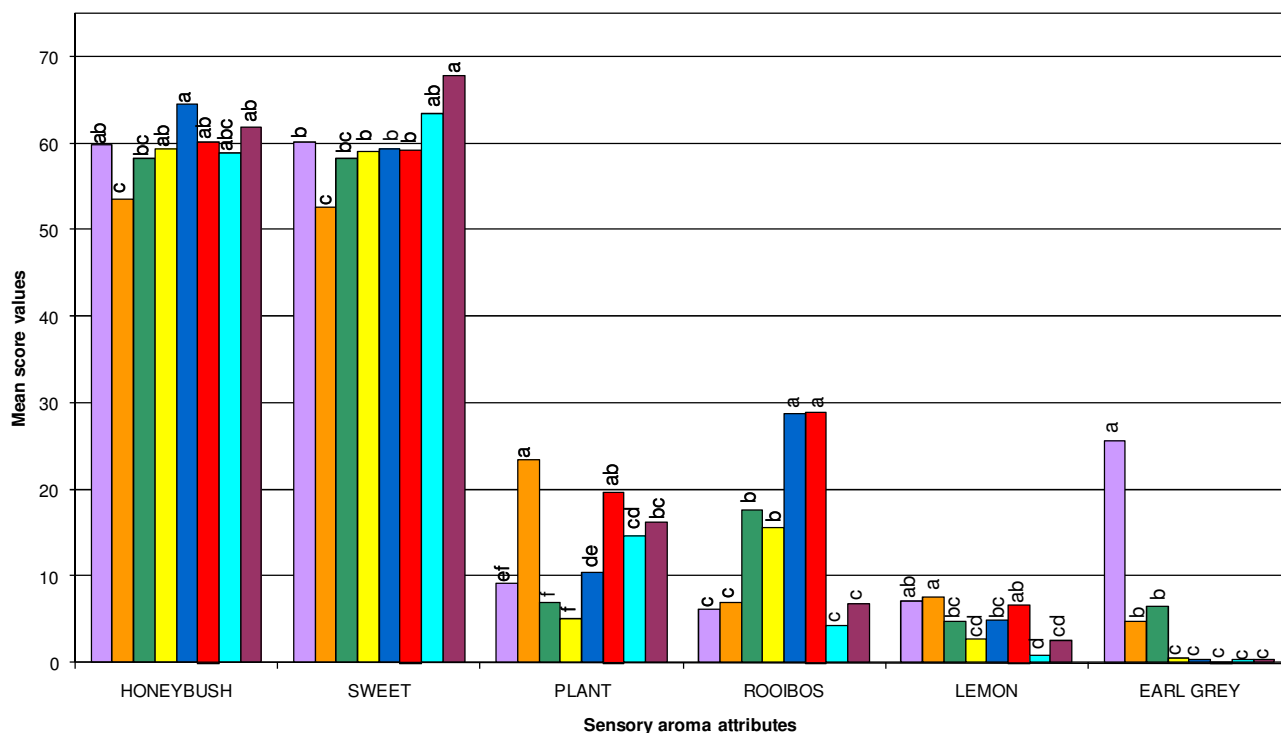


Fig. 6.1: Sensory aroma attributes of eight honeybush samples.

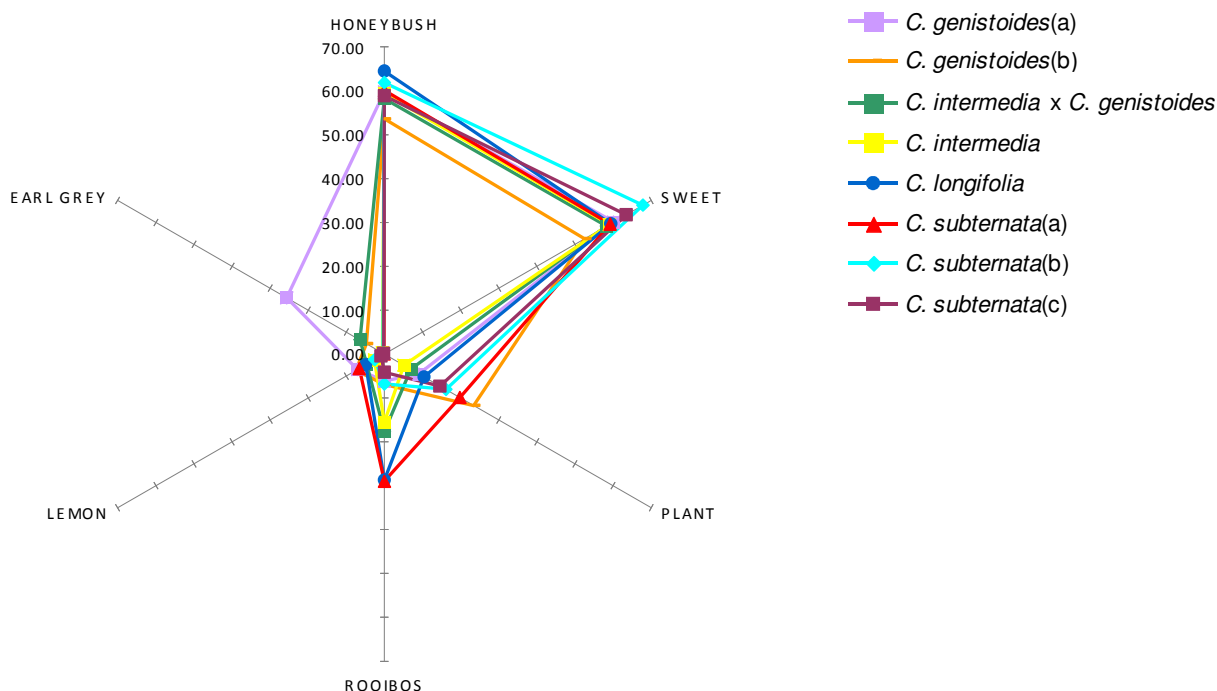


Fig. 6.2: Presentation (spider web) of the sensory aroma attributes of eight honeybush samples.

### 6.2.1.1 Honeybush aroma

All the samples had a moderately strong honeybush aroma. Products 6, 7 and 8, (*C. subternata*) had a honeybush aroma of similar strengths ( $P > 0.05$ ). Product 5 (*C. longifolia*) had the strongest honeybush aroma, significantly more ( $P \leq 0.05$ ) than that of product 2 [*C. genistoides*(b)]. The panellists were of the opinion that product 5 had a typical (generic) honeybush aroma and that it was of a similar strength to that of the reference standard (infusion of Woolworths Organic Honeybush tea) used during the training sessions.

### 6.2.1.2 Sweet aroma

All the samples had a moderately strong sweet aroma. The sweet aroma was distinctly different from the honeybush aroma and thus rated separately. Product 8 (*C. subternata* + flower) and product 7 (*C. subternata* – flower) had the strongest sweet aroma ( $P > 0.05$ ). Some of the judges also indicated that product 8 had a prominent pot-pourri-like aroma; this attribute was, however, not analysed. The sweet aroma of products 2 to 6 was significantly less strong ( $P \leq 0.05$ ) than that of products 7 and 8. Product 2 [*C. genistoides*(b)] had the lowest degree of sweetness.

### 6.2.1.3 Plant-like, rooibos, lemon and Earl Grey aroma

The plant-like, rooibos, lemon and Earl Grey aromas were more subtle and were not equally strongly associated with all the honeybush tea samples. Product 2 [*C. genistoides*(b)] and product 6 [*C. subternata*(a)] had a notable plant-like (vegetative, fynbos) aroma. Both teas prepared from

young regrowths [product 6: *C. subternata(a)*; product 5: *C. longifolia*] had a slight rooibos aroma, significantly more than that of the other samples ( $P \leq 0.05$ ). A slight lemon aroma, significantly more than in any of the other samples ( $P \leq 0.05$ ), was associated with products 2 [*C. genistoides(b)*], 1 [*C. genistoides(a)*] and 6 [*C. subternata(a)*]. Only product 1 [*C. genistoides(a)*], had a slight but notable Earl Grey aroma—an aroma similar to that of bergamot. The other two *C. genistoides*-associated teas, product 3 (*C. genistoides* × *C. intermedia*) and product 2 [*C. genistoides(b)*], had a significantly less notable Earl Grey aroma ( $P \leq 0.05$ ).

Table 6.2: Summary of the main and minor sensory aroma attributes associated with eight samples of honeybush tea

Species	Main aroma attribute	Minor aroma attribute
<i>C. genistoides(a)</i>	Sweet, honeybush	Earl grey, plant, lemon
<i>C. genistoides(b)</i>	Honeybush, sweet	Plant, lemon, rooibos
<i>C. genistoides</i> × <i>C. intermedia</i>	Sweet, honeybush	Rooibos, plant, Earl Grey
<i>C. intermedia</i>	Honeybush, sweet	Rooibos, plant, lemon
<i>C. longifolia</i>	Honeybush, sweet	Rooibos, plant, lemon
<i>C. subternata(a)</i>	Honeybush, sweet	Rooibos, plant, lemon
<i>C. subternata(b)</i> (– flower)	Sweet, honeybush	Plant, rooibos, lemon
<i>C. subternata(c)</i> (+ flower)	Sweet, honeybush	Plant, rooibos, lemon

## 6.2.2 Sensory aroma attributes of honeybush tea, using multivariate analyses

PCA was performed in order to show the relationship between sensory aroma attributes and to investigate sample patterns (Guchu *et al.*, 2006). Figs. 6.3(a) and 6.3(b) are PCA bi-plots indicating the overall association between the scores (products 1–8) and loadings or sensory aroma attributes (honeybush, sweet, lemon, Earl Grey, plant-like, rooibos). In both bi-plots, Factors 1 and 2 explain approximately 60% of the variance. Note that the PCA in Fig. 6.3(a) is based on the overall means, whereas the PCA in Fig. 6.3(b) is based on the product × replicate means.

According to Fig. 6.3(a) the two sensory aroma attributes honeybush and sweet are closely associated with products 4 (*C. intermedia*), 7 [*C. subternata(b)*] and 8 [*C. subternata(c)*], while product 6 [*C. subternata(a)*] and product 5 (*C. longifolia*) are closely associated with rooibos aroma. The sensory aroma attributes lemon, plant-like and Earl Grey are not very dominant attributes. The plant-like aroma associates with products 2 [*C. genistoides(b)*], 3 (*C. genistoides* × *C. intermedia*) and 6 [*C. subternata(a)*], while lemon aroma associates with products 2 [*C. genistoides(b)*], 1 [*C. genistoides(a)*], 6 [*C. subternata(a)*] and 3 (*C. genistoides* × *C. intermedia*). The prominence of Earl Grey aroma in product 1 [*C. genistoides(a)*] is also shown in Fig. 6.3(a). Fig. 6.3(b), with the product × replicate means, depicts a pattern similar to that illustrated in Fig. 6.3(a), however, there is a slight change as one can argue that by using the overall means a degree of statistical variation is removed in Fig. 6.3(a).

Discriminant analysis (DA), just like PCA, is a multivariate statistical technique that can be used to generate a perceptual map by using the attribute ratings of products generated by descriptive sensory analysis (Lawless and Heymann, 1999: 611). DA indicates to what extent the respective sensory attributes can be used to point out differences or similarities between different samples. Thus, the objective of DA is to identify different categories/groups and to determine which attributes are responsible for these categories/groups (Lawless and Heymann, 1999: 588, 611). The DA-plot (Fig. 6.4) indicates that the sensory attributes could discriminate effectively between product 1 and the other products. Product 1 [*C. genistoides*(a)], which had a slight, but notable, Earl Grey aroma, was thus different from the other samples. The centroids of products 2, 3, 4, 5, 6, 7 and 8 overlap, indicating that the respective sensory aroma attributes do not differentiate effectively between samples 2 to 8.

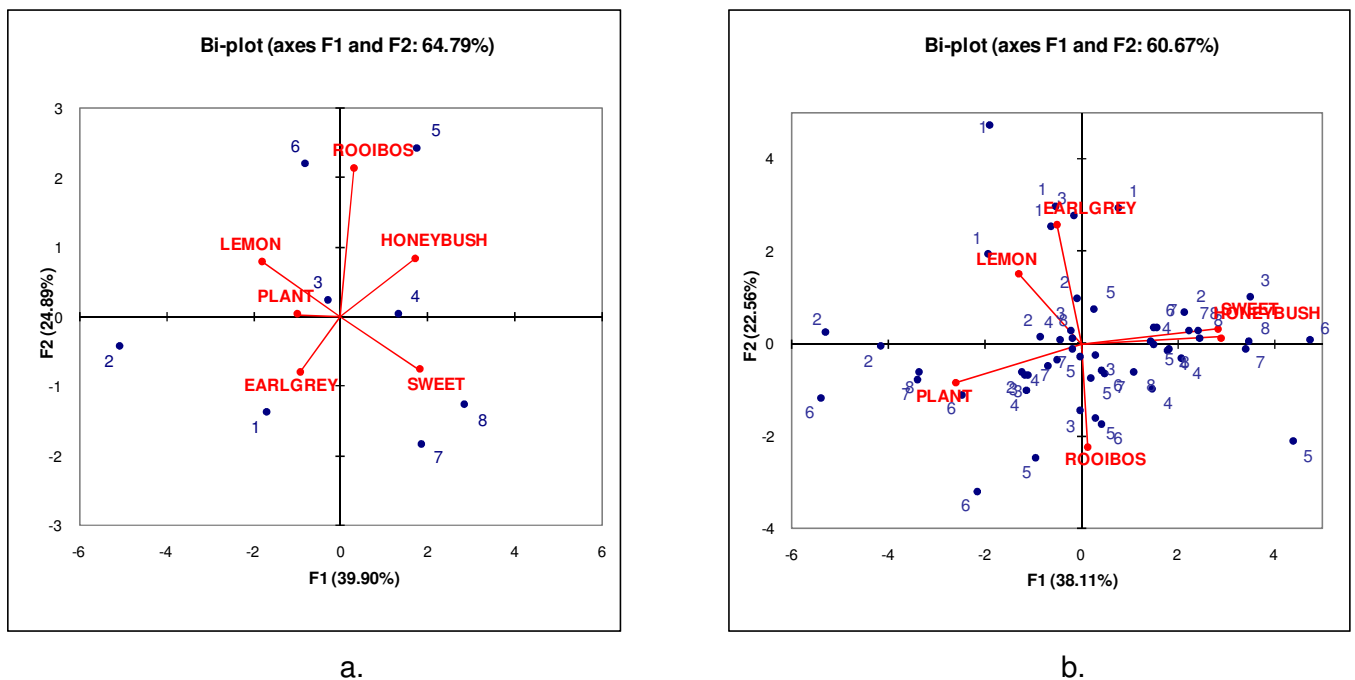


Fig. 6.3: PCA bi-plots indicating the association between sensory aroma attributes (loadings) and products 1–8 (scores): (a) based on overall means, (b) based on product  $\times$  replicate means.

[Product 1: *C. genistoides*(a) (Albertinia); Product 2: *C. genistoides*(b) (Pearly Beach); Product 3: *C. genistoides*  $\times$  *C. intermedia*; Product 4: *C. intermedia*; Product 5: *C. longifolia*; Product 6: *C. subternata*(a) (Bredasdorp); Product 7: *C. subternata*(b) (Genadendal; – flower); Product 8: *C. subternata*(c) (Genadendal; + flower)].

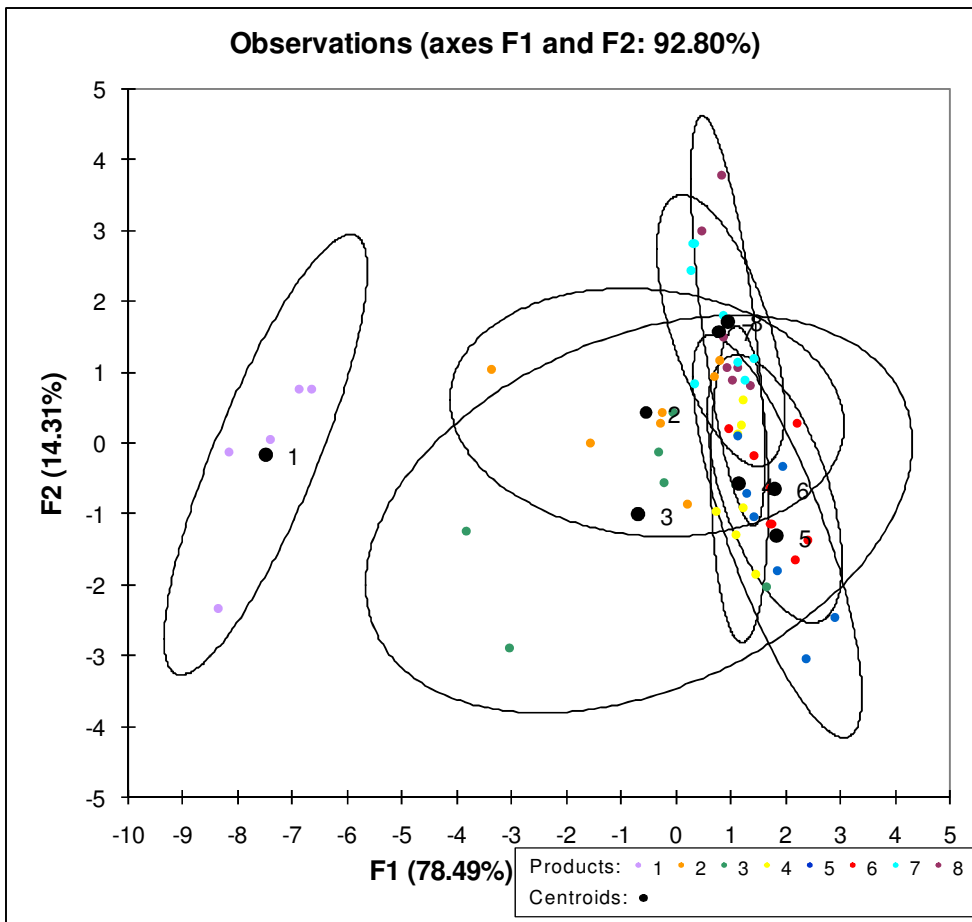


Fig. 6.4: DA plot indicating the overall discrimination between products using a spectrum of aroma attributes.

[Product 1: *C. genistoides*(a) (Albertinia); Product 2: *C. genistoides*(b) (Pearly Beach); Product 3: *C. genistoides* × *C. intermedia*; Product 4: *C. intermedia*; Product 5: *C. longifolia*; Product 6: *C. subternata*(a) (Bredasdorp); Product 7: *C. subternata*(b) (Genadendal; – flower); Product 8: *C. subternata*(c) (Genadendal; + flower)].

### 6.3 SUMMARY

It is clear that all the samples have both a prominent honeybush and sweet aroma. The latter aromas can be classified as generic aromas, i.e. typical of all honeybush species. However, the Earl Grey, lemon, plant-like and roibos aromas are slight, and not found in all honeybush samples: they can therefore be classified as species-specific aromas. The results of this investigation can however only be regarded as broad indicators. Further research is required since there are many factors that could have contributed to the variation in the results, e.g. sample size, harvesting date, production area, fermentation time, etc. An in-depth study, using a large number of samples of each species, should be carried out to profile the sensory aroma attributes of different species and to develop a valid flavour lexicon for honeybush.



## 6.4 REFERENCES

- Anonymous. 1975. Minutes of division business meeting. Institute of Food Technologists—sensory evaluation division, IFT, Chigago, IL.
- Gacula, M.C. 1997. Descriptive sensory analysis in practice. Food and Nutrition Press, Connecticut, USA.
- Guchu, E., Díaz-Maroto, M.C., Pérez-Coello, M.A., González-Viñas, M.A., Cabezudo Ibáñez, M.D. 2006. Volatile composition and sensory characteristics of Chardonnay wines treated with American and Hungarian oak chips. *Food Chem.* **99**, 350–359.
- Lawless, H.T. 1999. Descriptive analysis of complex odors: Reality, model or illusion? *Food Quality and Preference* **10**, 325–332.
- Lawless, H.T., Heyman, H. 1999. Sensory evaluation of food: Principles and practices. Chapman and Hall, USA.
- Meilgaard, M.C., Civille, G.V., Carr, B.T. 2006. Sensory evaluation techniques. CRC Press, USA.
- Murray, J.M., Delahunty, C.M., Baxter, I.A. 2001. Descriptive sensory analysis: Past, present and future. *Food Res. Int.* **34**, 461–471.
- Stone, H., Sidel, J.L. 2004. Sensory evaluation practices. Elsevier Academic press.

## CHAPTER 7

# STATISTICAL DATA ANALYSIS: CORRELATION OF CHEMICAL AND SENSORY DATA OF HONEYBUSH SAMPLES

### 7.1 INTRODUCTION

PCA, a multivariate statistical technique, is a very useful tool for identifying patterns in data sets so that similarities and differences therein can be highlighted (Rencher, 2002). It was applied to the different variables obtained for the odour-active compounds identified in honeybush in combination with sensory profiling data. PCA finds patterns and correlations in data sets and substitutes a new variable, called a factor, for the group of original attributes that were correlated. The analysis then finds a second and third group of attributes and derives a factor for each which is based on the variance left over at each step after the variance accounted for by the previous factor is removed. What essentially happens is that a new set of fewer axes or dimensions in space is found to replace the  $N$ -dimensional space of the original data set. The original data set will have a correlation with the new dimensions, which is called a factor loading, and the products will have values on the new dimensions, called factor scores. The factor loadings are useful for interpreting the dimensions whereas the factor scores show the relative position of the products in the map or picture, and ultimately highlight similarities and differences (Lawless and Heymann, 1999: 608–609).

### 7.2 PRINCIPAL COMPONENT ANALYSIS OF HONEYBUSH DATA

#### 7.2.1 Principal component analysis based on concentration data

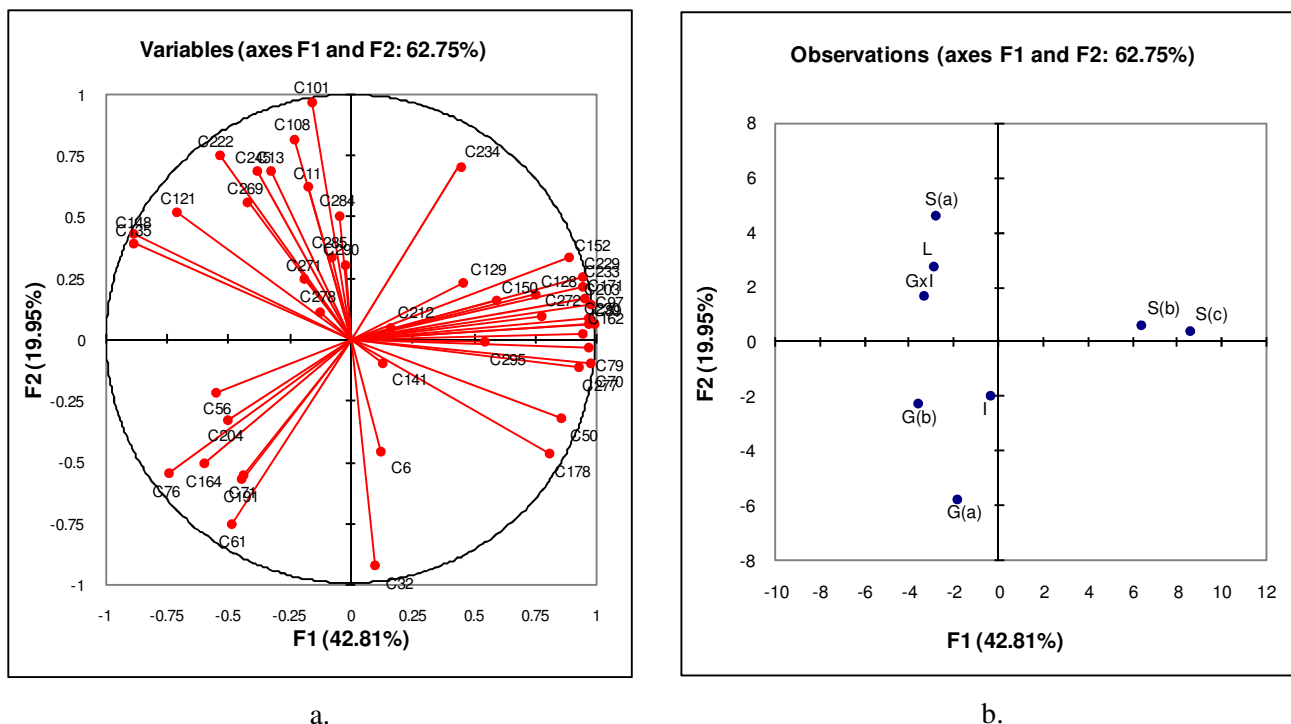
In a first study, a PCA was performed on the relative concentrations (area % TIC) obtained for the odour-active compounds (Chapter 4: § 4.2) of eight honeybush samples. Two factors that represent 62.75% of the variability in the data were considered and a map with axes F1 and F2, depicting the projection of the initial variables in the factor space, was constructed (Fig. 7.1a).

The map provides useful information on how to interpret the meaning of the axes. To establish whether a variable is well linked with the corresponding axis the squared cosines of the variables should be considered. The greater the squared cosines are the greater the link between the variable and the corresponding axis. Therefore, after considering the map as well as the squared cosine values for the variables (those greater than 0.5) Table 7.1 could be composed; it shows which compounds are correlated best with one of the two axes. When the squared cosine value of a variable is close to zero that particular variable does not contribute significantly to the variance explained by the corresponding axis and the interpretation of results in terms of trends on the axis is not very clear and a sensible conclusion will not easily be established.

Table 7.1: Correlation of components (squared cosine values >0.5) with axes F1 or F2

<b><u>Compound No.</u></b>		<b><u>Compound No.</u></b>	
<b>Horizontal axis F1</b>	<b>Squared cosine</b>	<b>Vertical axis F2</b>	<b>Squared cosine</b>
C50	0.734	C32	0.857
C70	0.953	C61	0.575
C76	0.549	C101	0.931
C79	0.943	C108	0.662
C89	0.987	C222	0.564
C97	0.947		
C128	0.562		
C135	0.774		
C148	0.780		
C152	0.792		
C162	0.895		
C171	0.907		
C178	0.657		
C203	0.958		
C229	0.897		
C230	0.948		
C233	0.895		
C272	0.608		
C277	0.868		

These correlations will be useful in interpreting the two-dimensional map (Fig. 7.1b) that shows the distribution of honeybush samples that share common characteristics. The driving force behind this distribution is in fact the variance in the relative concentrations obtained for these components in the analyses of eight honeybush samples, which are now transferred onto these newly defined axes.



a.

b.

Fig. 7.1: PCA loadings and scores plots of the relative concentrations of the odour-active compounds in eight honeybush samples: (a) loadings plot; (b) scores plot. [G(a): *C. genistoides*(a) (Albertinia); G(b): *C. genistoides*(b) (Pearly Beach); GxI: *C. genistoides* × *C. intermedia*; I: *C. intermedia*; L: *C. longifolia*; S(a): *C. subternata*(a) (Bredasdorp); S(b): *C. subternata*(b) (Genadendal; – flower); S(c): *C. subternata*(c) (Genadendal; + flower)].

From Fig. 7.1b it is evident that *C. longifolia*, *C. subternata*(a) and the *C. genistoides* × *C. intermedia* cross-species show some similarities. *Cyclopia genistoides*(a) and *C. genistoides*(b) are mutually similar and the same can be said of *C. subternata*(b) and *C. subternata*(c). What is important to note is that a PCA based on the sensory aroma attributes (Chapter 6: Figs. 6.3a and 6.3b) gave a similar distribution of the eight honeybush samples than depicted in the PCA of Fig. 7.1b. This indicates that the sensory data and the concentration data of the odour-active compounds associate similarly with the respective samples.

## 7.2.2 Principal component analysis based on combined concentration and sensory data

In a second study, PCA was applied to the data obtained from the sensory analysis of eight honeybush samples as well as the concentration of the odour-active compounds. In this analysis the first two factors (F1 and F2) represent 61.64% of the initial variability of the data. These factors were chosen since the inclusion of more factors did not describe significantly more variability. The first map (Fig. 7.2a), with axes F1 and F2, shows the projection of the initial variables in the factor space. When two variables are far from the centre they can be either close to each other, orthogonal, or on opposite sides of the centre. This respectively, signifies a strong positive correlation ( $r$  close to 1), no

correlation ( $r$  close to 0) or a strong negative correlation ( $r$  close to  $-1$ ). When variables are close to the centre it means that some of the information is carried on other axes, and therefore their interpretation in the context of the selected factors/principal components may not be reliable. Table 7.2 lists the compounds that have a relatively strong positive or negative correlation ( $r \geq \pm 0.5$ ) to the respective sensory aroma attributes. Aroma descriptors obtained from literature sources, associated with these compounds, are also provided. In statistics, the probability value (or P-value) is used to assess the significance of observed effects or variations; a small P-value means that the risk of mistakenly concluding that the observed effect is real is very low (Ghasemi, *et al.*, 2007). If a P-value is  $\leq 0.05$  the observed effect is probably not due to random variations or chance, and is concluded to be significant (Ghasemi, *et al.*, 2007). The P-values are thus also given in Table 7.2 to show which correlations are in fact significant ( $P \leq 0.05$ ). Table 7.2 shows that the correlation between sensory aroma attributes and compounds are significant when  $r > 0.7$ .

Fig. 7.2b is a two-dimensional presentation of the data and the bi-plot map Fig. 7.2c is a final summary of all the maps combined.



Table 7.2: Correlation of odour-active compounds with the respective sensory aroma attributes determined by PCA

<b>Aroma attributes</b>	<b>Comp. no.<sup>a</sup></b>	<b>Compound name</b>	<b>Aroma descriptors<sup>b</sup></b>	<b>Correlation factor (r)</b>	<b>P-value</b>	
<b><u>Roobos</u></b>	C269	Component C269 (bergamotol type)	–	0.897	0.003	
	C108	( <i>E</i> )-2-Nonenal	Green, cucumber, aldehydic and fatty	0.832	0.010	
	C101	( <i>E,Z</i> )-2,6-Nonadienal	Green-vegetable, reminiscent of cucumber or violet leaf	0.806	0.016	
	C13	( <i>R</i> )-2-Methylbutanoic acid	Cheesy, sweaty, sharp	0.791	0.019	
	C148	Geraniol	Sweet, floral, rose, citrus-like	0.765	0.027	
	C222	2,3-Dehydro- $\gamma$ -ionone	–	0.752	0.031	
	C11	3-Methylbutanoic acid	Acid acrid, cheesy, unpleasant	0.726	0.042	
	C121	$\alpha$ -Terpineol	Floral, sweet, lilac-type	0.716	0.046	
	C135	Nerol	Fresh, sweet-rosy	0.691	0.058	
	C245	Bovolide	Celery- and lovage-like, fruity and pleasant	0.538	0.169	
	C50	<i>p</i> -Cymene	Citrus-like, reminiscent of lemon and bergamot	–0.733	0.039	
	C277	(6 <i>E</i> ,8 <i>E</i> )-Megastigma-4,6,8-trien-3-one	Tobacco-like, woody, balsamic	–0.677	0.065	
	C178	Component C178	–	–0.648	0.082	
	C79	2-Phenylethanol	Mild, warm, rose-honey-like	–0.619	0.102	
	C32	6-Methyl-5-hepten-2-one	Oily-green, pungent-herbaceous, grassy, with fresh and green-fruity notes	–0.595	0.120	
	C70	( <i>E,E</i> )-3,5-Octadien-2-one	Fatty, fruity, mushroom	–0.527	0.180	
	C97	Lilac aldehyde isomer 1	Sweet, fresh, floral	–0.512	0.195	
	<b><u>Plant</u></b>	C295	(7 <i>E</i> )-Megastigma-5,7,9-trien-4-one	Tea-like, spicy and resembling dried fruit	0.764	0.027
		C271	(6 <i>E</i> ,8 <i>Z</i> )-Megastigma-4,6,8-trien-3-one	Tobacco-like, woody, balsamic.	–0.733	0.038
C278		10- <i>epi</i> - $\gamma$ -Eudesmol	Woody, floral, sweet	–0.693	0.057	
C6		Hexanal	Fatty-green grassy odour	–0.585	0.128	
C212		( <i>E</i> )- $\beta$ -Damascone	Fruity (apple-citrus), tea-like with slight minty notes	–0.574	0.137	
<b><u>Honeybush</u></b>		C129	$\beta$ -Cyclositral	Green, grassy hay-like	0.642	0.086
	C234	( <i>E</i> )- $\beta$ -Ionone	Warm, woody, fruity, raspberry-like; resembles cedarwood	0.615	0.104	
	C269	Component C269 (bergamotol type)	–	0.591	0.123	
	C6	Hexanal	Fatty-green grassy odour	0.550	0.158	
	C271	(6 <i>E</i> ,8 <i>Z</i> )-Megastigma-4,6,8-trien-3-one	Tobacco-like, woody, balsamic	0.531	0.175	
	C204	( <i>E</i> )- $\beta$ -Damasconone	Woody, sweet, fruity, earthy green-floral	–0.697	0.055	
	C76	Linalool	Refreshing, floral-woody	–0.640	0.087	
	C61	$\gamma$ -Terpinene	Refreshing, herbaceous, citrus-like	–0.580	0.132	

Table 7.2: contd.

Aroma attributes	Comp. no. <sup>a</sup>	Compound name	Aroma descriptors <sup>b</sup>	Correlation factor (r)	P-value
	C191	Eugenol	Warm-spicy, dry and almost sharp odour	-0.522	0.184
<b>Sweet</b>	C203	2,3-Dehydro- $\alpha$ -ionone	Tobacco-like	0.915	0.001
	C230	3,4-Dehydro- $\beta$ -ionone	Ionone-damascone and saffron-like note, with fruity and slightly leathery aspects	0.914	0.001
	C162	Component C162	–	0.907	0.002
	C89	4-Acetyl-1-methylcyclohexene	Spicy	0.872	0.005
	C70	( <i>E,E</i> )-3,5-Octadien-2-one	Fatty, fruity, mushroom	0.872	0.005
	C171	( <i>E,E</i> )-2,4-Decadienal	Fried, waxy, fatty, orange-like	0.858	0.006
	C233	( <i>R</i> )-Decan-5-olide	Sweet, creamy, nut-like, fruity	0.853	0.007
	C229	( <i>S</i> )-( <i>Z</i> )-7-Decen-5-olide	Sweet, floral, fruity	0.847	0.008
	C97	Lilac aldehyde isomer 1	Sweet, fresh, floral	0.845	0.008
	C152	( <i>R</i> )-Octan-5-olide	Peach, coconut-like, sweet, creamy	0.840	0.009
	C272	Geranyl 2-methylbutanoate	Pleasant, sweet .	0.749	0.032
	C277	(6 <i>E</i> ,8 <i>E</i> )-Megastigma-4,6,8-trien-3-one	Tobacco-like, woody, balsamic	0.746	0.034
	C79	2-Phenylethanol	Mild, warm, rose-honey-like	0.737	0.037
	C178	Component C178	–	0.726	0.042
	C50	<i>p</i> -Cymene	Citrus-like, reminiscent of lemon and bergamot	0.687	0.060
	C129	$\beta$ -Cyclositral	Green, grassy hay-like .	0.645	0.084
	C234	( <i>E</i> )- $\beta$ -Ionone	Warm, woody, fruity, raspberry-like; resembles cedarwood	0.596	0.119
	C128	(+)- <i>p</i> -Menth-1-en-9-al	Powerful spicy, herbaceous odour	0.561	0.148
	C76	Linalool	Refreshing, floral-woody	-0.831	0.011
	C204	( <i>E</i> )- $\beta$ -Damascenone	Woody, sweet, fruity, earthy green-floral	-0.767	0.026
	C148	Geraniol	Sweet, floral, rose, citrus-like	-0.721	0.044
	C135	Nerol	Fresh, sweet-rosy	-0.704	0.051
	C191	Eugenol	Warm-spicy, dry and almost sharp odour	-0.692	0.057
	C61	$\gamma$ -Terpinene	Refreshing, herbaceous, citrus-like	-0.559	0.150
<b>Earl Grey</b>	C71	Terpinolene	Sweet-piney, oily	0.848	0.008
	C164	Geranyl formate	Fresh, green-rosy, fruity	0.816	0.013
	C61	$\gamma$ -Terpinene	Refreshing, herbaceous, citrus-like	0.806	0.016
	C32	6-Methyl-5-hepten-2-one	Oily-green, pungent-herbaceous, grassy, with fresh and green-fruity notes	0.770	0.025
	C56	( <i>Z</i> )- $\beta$ -Ocimene	Warm-herbaceous, sweet, floral	0.602	0.115
	C284	<i>epi</i> - $\alpha$ -Cadinol	Herbaceous, woody	-0.855	0.007
	C285	<i>epi</i> - $\alpha$ -Muurolol	Herbaceous, slightly spicy	-0.770	0.025
	C150	Geranial	Lemon	-0.723	0.043



Table 7.2: *contd.*

Aroma attributes	Comp. no. <sup>a</sup>	Compound name	Aroma descriptors <sup>b</sup>	Correlation factor (r)	P-value
	C101	( <i>E,Z</i> )-2,6-Nonadienal	Green-vegetable, reminiscent of cucumber or violet leaf	-0.607	0.110
	C108	( <i>E</i> )-2-Nonenal	Green, cucumber, aldehydic and fatty	-0.548	0.160
<b>Lemon</b>	C56	( <i>Z</i> )- $\beta$ -Ocimene	Warm-herbaceous, sweet, floral	0.786	0.021
	C61	$\gamma$ -Terpinene	Refreshing, herbaceous, citrus-like	0.734	0.038
	C71	Terpinolene	Sweet-piney, oily	0.732	0.039
	C135	Nerol	Fresh, sweet-rosy	0.688	0.059
	C76	Linalool	Refreshing, floral-woody	0.666	0.071
	C148	Geraniol	Sweet, floral, rose, citrus-like	0.647	0.083
	C164	Geranyl formate	Fresh, green-rosy, fruity	0.547	0.161
	C121	$\alpha$ -Terpineol	Floral, sweet, lilac-type	0.515	0.192
	C171	( <i>E,E</i> )-2,4-Decadienal	Fried, waxy, fatty, orange-like	-0.878	0.004
	C150	Geranial	Lemon	-0.828	0.011
	C89	4-Acetyl-1-methylcyclohexene	Spicy	-0.803	0.016
	C70	( <i>E,E</i> )-3,5-Octadien-2-one	Fatty, fruity, mushroom	-0.797	0.018
	C203	2,3-Dehydro- $\alpha$ -ionone	Tobacco-like	-0.754	0.031
	C79	2-Phenylethanol	Mild, warm, rose-honey-like	-0.721	0.043
	C162	Component C162	–	-0.704	0.051
	C230	3,4-Dehydro- $\beta$ -ionone	Ionone-damascone and saffron-like note, with fruity and slightly leathery aspects	-0.700	0.053
	C97	Lilac aldehyde isomer	Sweet, fresh, floral	-0.690	0.058
	C178	Component C178	–	-0.672	0.068
	C50	<i>p</i> -Cymene	Citrus-like, reminiscent of lemon and bergamot	-0.675	0.066
	C229	( <i>S</i> )-( <i>Z</i> )-7-Decen-5-olide	Sweet, floral, fruity	-0.668	0.070
	C233	( <i>R</i> )-Decan-5-olide	Sweet, creamy, nut-like, fruity	-0.638	0.089
	C212	( <i>E</i> )- $\beta$ -Damascone	Fruity (apple-citrus), tea-like with slight minty notes	-0.591	0.123
	C277	(6 <i>E</i> ,8 <i>E</i> )-Megastigma-4,6,8-trien-3-one	Tobacco-like, woody, balsamic	-0.589	0.124
	C152	( <i>R</i> )-Octan-5-olide	Peach, coconut-like, sweet, creamy	-0.570	0.141
	C129	$\beta$ -Cyclositral	Green, grassy hay-like	-0.546	0.162
	C128	(+)- <i>p</i> -Menth-1-en-9-al	Powerful spicy, herbaceous odour	-0.540	0.167

<sup>a</sup> In order of decreasing positive and negative correlation factors.

<sup>b</sup> Acree and Arn, 2004; Arctander, 1969; Boldingh and Taylor, 1962; Buttery *et al.*, 1979; Demole and Enggist, 1974; JECFA, 2009; Kreck and Mosandl, 2003; Leffingwell, 2002; Mookherjee and Wilson, 1990; Mosciano *et al.*, 1991a, 199b; Näf and Velluz, 2000; Ohloff, 1994; Oomah and Liang, 2007; Serra *et al.*, 2006; Tachihara *et al.*, 2006; Takahashi *et al.*, 1980; Yamazaki *et al.*, 1988.

During the sensory analysis of honeybush tea the samples that have more of a **rooibos aroma** were not considered by the panel to be those with the most typical overall honeybush aroma,

because the rooibos aroma, although not unpleasant, seems to partially mask the honeybush aroma. Some of the compounds associated with rooibos aroma, such as (*E*)-2-nonenal (C108), 3-methylbutanoic acid (C11), (*R*)-2-methylbutanoic acid (C13) and (*E,Z*)-2,6-nonadienal (C101), do not typically have very pleasant associated descriptors, whereas compounds such as nerol (C135), geraniol (C148) and boviolide (C245) are decidedly more pleasant. There are also a few compounds with a relatively strong negative correlation with rooibos aroma, and which most likely do not contribute to the rooibos aroma. These include *p*-cymene (C50), (6*E*,8*E*)-megastigma-4,6,8-trien-3-one (C277), component C178, 2-phenylethanol (C79) and 6-methyl-5-hepten-2-one (C32).

As found for the rooibos aroma, the **plant aroma** did not contribute positively to the overall honeybush aroma, but rather downgraded the typical honeybush aroma. (7*E*)-Megastigma-5,7,9-trien-4-one (C295) had a positive correlation with the plant aroma, whereas (6*E*,8*Z*)-megastigma-4,6,8-trien-3-one (C271), 10-*epi*- $\gamma$ -eudesmol (C278), hexanal (C6) and (*E*)- $\beta$ -damascone (C212) had a relatively strong negative correlation, and the negative correlation of the first compound (C271) was the most significant ( $P \leq 0.05$ ). The plant sensory aroma variable, as well as some compounds such as *p*-anisaldehyde (C141), (*E*)- $\beta$ -damascone (C212), (6*E*,8*Z*)-megastigma-4,6,8-trien-3-one (C271), 10-*epi*- $\gamma$ -eudesmol (C278) and cadalene (C290), are very close to the centre of the loadings plot and have squared cosine values that are close to zero for axes F1 and F2. This makes the interpretation of these variables very difficult, because some information might be carried on other axes. A second group of variables falls into the same category as the variables mentioned above, i.e. they have relatively close association with the centre of the loadings plot and low squared cosine values. However, the situation is not as critical as for the first group. These variables include the honeybush sensory aroma variable, hexanal (C6),  $\beta$ -cyclositral (C129), *epi*- $\alpha$ -cadinol (C284), *epi*- $\alpha$ -muurolol (C285) and (7*E*)-megastigma-5,7,9-trien-4-one (C295). A third group of variables, although not close to the centre, have relatively low squared cosine values and should also be interpreted with a degree of caution. These include eugenol (C191) and (*E*)- $\beta$ -damascenone (C204). Therefore, the mentioned positive and negative correlations of the five components associated with the plant sensory aroma attribute cannot be interpreted sensibly. This might, for example, explain why (7*E*)-megastigma-5,7,9-trien-4-one (C295), which could be expected to contribute to the typical honeybush aroma, is not associated with the honeybush sensory aroma attribute, but rather with the plant sensory aroma attribute, and why a compound such as hexanal (C6), with a typical plant/green aroma, is associated with the honeybush sensory aroma attribute instead.

The two most important sensory aroma attributes associated with the different honeybush samples were honeybush and sweet, and samples that had the highest scores for these sensory aroma attributes were considered the best representatives of a typical and desirable honeybush aroma. Only a few compounds have a positive association with the **honeybush aroma**. Two of these compounds do not have typically pleasant descriptors, namely  $\beta$ -cyclositral (C129) and hexanal (C6), whereas (*E*)- $\beta$ -ionone (C234) and (6*E*,8*Z*)-megastigma-4,6,8-trien-3-one (C271) have more pleasant aroma descriptors. The components (*E*)- $\beta$ -damascenone (C204), linalool (C76),  $\gamma$ -terpinene (C61) and eugenol (C191) have a negative correlation with the honeybush sensory aroma attribute. Bearing

in mind that the interpretation of some of the correlations between variables should be treated with some caution for the components mentioned in the previous paragraph, this might explain the somewhat unexpected association of  $\beta$ -cyclositral (C129) and hexanal (C6) with honeybush aroma. The negative correlation of the very intense aroma-active compound (*E*)- $\beta$ -damascenone (C204) to the honeybush sensory aroma attribute is somewhat surprising. However, C204 is also one of those components whose interpretation should be treated with some caution, and therefore an understanding of this association is more complicated.

Many compounds show strong association with the **sweet aroma** and many of them have sweet and floral characteristics and an overall pleasant aroma.  $\beta$ -Cyclositral (C129) and (*E*)- $\beta$ -ionone (C234) are two compounds associated with both the honeybush and the sweet aroma. Six compounds show a negative correlation towards the sweet aroma. The negative association of (*E*)- $\beta$ -damascenone (C204) (also negatively correlated to honeybush aroma) is not that easy to explain, since its aroma descriptors could easily fit with the sweet sensory aroma attribute as well, but then the same reason could apply as in the case of its negative correlation to the honeybush sensory aroma attribute. The negative correlation of geraniol (C148), nerol (C135), eugenol (C191) and  $\gamma$ -terpinene (C61) with the sweet sensory aroma attribute would be somewhat easier to explain, since some of the descriptors associated with these compounds include citrus-like/fresh (geraniol and nerol), spicy (eugenol) and herbaceous and citrus-like in the case of  $\gamma$ -terpinene.

The **Earl Grey** and **lemon sensory aroma** attributes are minor attributes and were only slightly prominent in a few samples. Many compounds, such as terpinolene (C71), geranyl formate (C164),  $\gamma$ -terpinene (C61) and (*Z*)- $\beta$ -ocimene (C56), associate with both the Earl Grey and lemon aroma. The two compounds nerol (C135) and geraniol (C148), which associate with the lemon aroma, do have somewhat typical citrus-like and fresh aroma descriptors. The compound geraniol, with its lemon aroma descriptor, might also fit with the lemon sensory aroma attribute, but it somehow has a negative correlation. Many compounds have a negative correlation with the lemon aroma. All of them, except for (*E*)- $\beta$ -damascone (C212), were associated positively with the sweet sensory aroma attribute, which is the result of a relatively strong negative correlation between the sweet and lemon sensory aroma attributes. The two compounds *epi*- $\alpha$ -cadinol (C284) and *epi*- $\alpha$ -muurolol (C285) have a strong negative correlation with the Earl Grey aroma, which is somewhat unexpected considering their associated descriptors (herbaceous, woody and spicy). However, they also form part of the small group of components that are relatively close to the centre of the correlation circle, which therefore renders their association with other variables and axes to be approached with more caution.

In Fig. 7.2b, a two-dimensional presentation of the data, the same distribution of the eight honeybush samples is observed as seen in Fig. 7.1b. The bi-plot map (Fig. 7.2c) indicates that the species *C. subternata*(a), *C. longifolia* and *C. intermedia*  $\times$  *C. genistoides* associate with rooibos aroma, while *C. intermedia*  $\times$  *C. genistoides* also has some association with the plant-like aroma as well as the lemon aroma. The two *C. subternata* samples, S(b) and S(a), associate with sweet and honeybush, aroma, while the two *C. genistoides* samples, G(a) and G(b), associate with lemon and

Earl Grey aroma. *Cyclopia intermedia* has some association with both the lemon and plant aromas. Approximately the same pattern was observed when a PCA was performed on the sensory data (see Fig. 6.3a).

### 7.2.3 Principal component analysis based on combined 'odour activity' and sensory data

Relative 'OAV's calculated for those odour-active compounds for which literature threshold values were available (see Table 4.1), were subjected to a third PCA in combination with the sensory aroma attributes obtained during the sensory analysis of the eight honeybush samples. The first two factors (F1 and F2) represent 61.63% of the initial variability and the following two graphs were constructed: a loadings plot (Fig. 7.3a) and scores plot (two-dimensional map) (Fig. 7.3b).

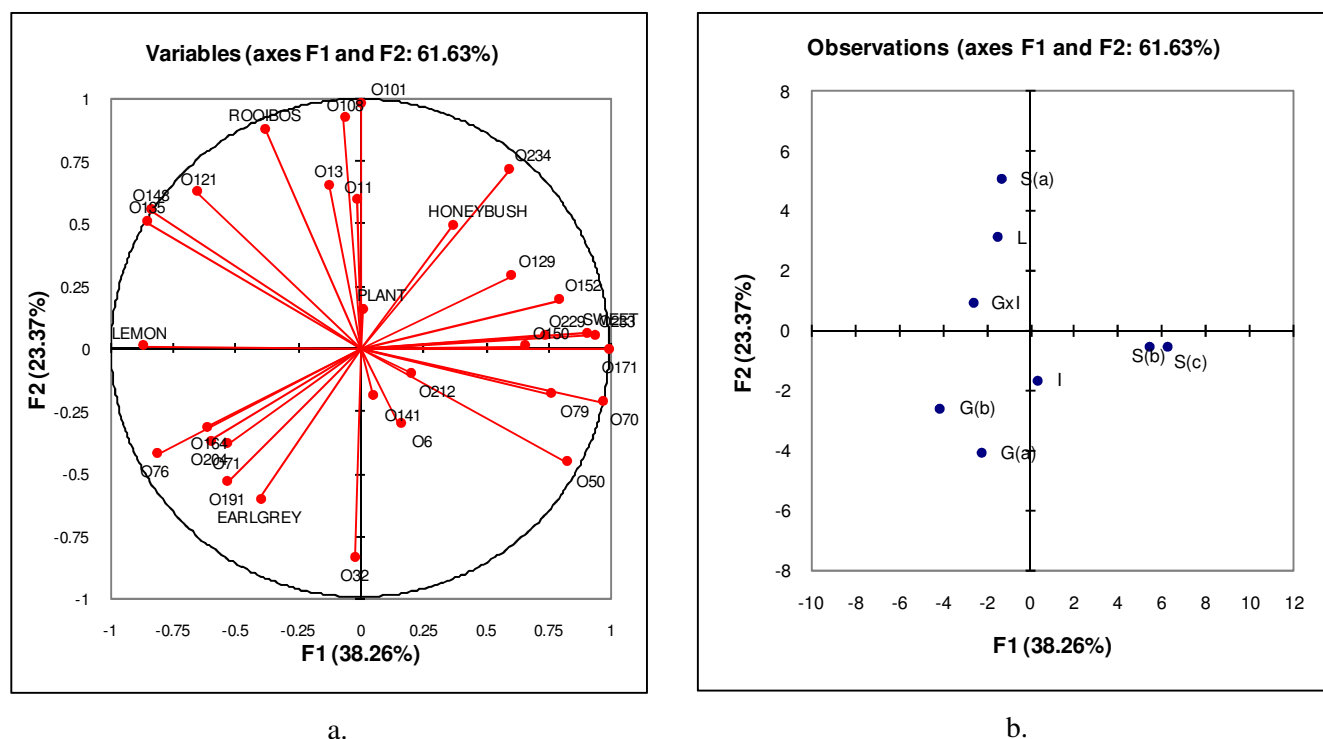


Fig. 7.3: Loadings plot (a) and scores plot (b) constructed by PCA using the relative 'OAV's and sensory aroma attributes obtained during sensory analysis of honeybush samples. [G(a): *C. genistoides*(a) (Albertinia); G(b): *C. genistoides*(b) (Pearly Beach); Gxl: *C. genistoides* × *C. intermedia*; I: *C. intermedia*; L: *C. longifolia*; S(a): *C. subternata*(a) (Bredasdorp); S(b): *C. subternata*(b) (Genadendal; – flower); S(c): *C. subternata*(c) (Genadendal; + flower)].

The two-dimensional map shows a similar distribution of the honeybush samples that was observed in the PCA of the combined concentration and sensory data (Fig. 7.2b), and therefore the association of the samples with the respective sensory aroma attributes is the same as already discussed. Table 7.2 is therefore also representative of the results obtained with 'OAV' data.

The strong correlation between the two PCA analyses could be explained by the correlation between the relative 'OAV's and the concentrations of the compounds, since the latter values were used to calculate the relative 'OAV's.

Table 7.3 is a summary of the most intense odour-active compounds identified by means of GC-O and their strongest correlation ( $r > 0.55$ ) with the respective sensory aroma attributes, whether it be a positive (+) or negative correlation (-).

Table 7.3: Most intense odour-active compounds and their association with the sensory aroma attributes

Compound no. <sup>a</sup>	Compound name	Sensory aroma attributes <sup>b</sup>		
		1 <sup>st</sup>	2 <sup>nd</sup>	3 <sup>rd</sup>
C204	( <i>E</i> )- $\beta$ -Damascenone	- Sweet	- Honeybush	
C76	Linalool	- Sweet	+ Lemon	- Honeybush
C212	( <i>E</i> )- $\beta$ -Damascone	- Lemon	- Plant	
C148	Geraniol	+ Rooibos	- Sweet	+ Lemon
C234	( <i>E</i> )- $\beta$ -Ionone	+ Honeybush	+ Sweet	
C178	Component C178	+ Sweet	- Lemon	- Rooibos
C295	(7 <i>E</i> )-Megastigma-5,7,9-trien-4-one	+ Plant		
C230	3,4-Dehydro- $\beta$ -ionone	+ Sweet	- Lemon	
C284	<i>epi</i> - $\alpha$ -Cadinol	- Earl Grey		
C285	<i>epi</i> - $\alpha$ -Muurolol	- Earl Grey		
C278	10- <i>epi</i> - $\gamma$ -Eudesmol	- Plant		
C171	( <i>E,E</i> )-2,4-Decadienal	- Lemon	+ Sweet	
C222	2,3-Dehydro- $\gamma$ -ionone	+ Rooibos		
C101	( <i>E,Z</i> )-2,6-Nonadienal	+ Rooibos	- Earl Grey	
C108	( <i>E</i> )-2-Nonenal	+ Rooibos	- Earl Grey	

<sup>a</sup> In order of decreasing FD factors (see Table 4.2).

<sup>b</sup> Ranked according to strongest correlation ( $r > 0.55$ ).

### 7.3 SUMMARY

PCA was used to identify and highlight patterns and correlations in the different data sets subjected to this multivariate statistical technique. It revealed interesting correlations between certain compounds and sensory aroma attributes, some of which can be sensibly interpreted and others that are more complex.

## 7.4 REFERENCES

- Acree, T., Arn, H. 2004. Flavornet and human odor space [Online]. Available: <http://www.flavornet.org/> [March 2010].
- Arctander, S., 1969. Perfume and flavour chemicals, Vols I and II. Steffen Arctander, Montclair, New Jersey.
- Boldingh, J., Taylor, R.J. 1962. Trace constituents of butterfat. *Nature* **194**, 909–913.
- Buttery, R.G., Black, D.R., Haddon, W.F., Ling, L.C., Teranishi, R., 1979. Identification of additional volatile constituents of carrot roots. *J. Agric. Food Chem.* **27**, 1–3.
- Demole, E., Enggist, P. 1974. Novel synthesis of 3,5,5-trimethyl-4-(2-butenylidene)-cyclohex-2-en-1-one, a major constituent of Burley tobacco flavour. *Helv. Chim. Acta.* **57**, 2087–2091.
- Gashemi, J., Saaidpour, S., Brown, S.D. 2007. QSPR study for estimation of acidity constants of some aromatic acids derivatives using multiple linear regression (MLR) analysis. *J. Mol. Struc.: THEOCHEM.* **805**, 27–32.
- Joint FAO/WHO Expert Committee on Food Additives (JECFA). 2009. Specifications for flavourings [Online]. Available: <http://www.fao.org/ag/agn/jecfa-flav/index.html?showSynonyms=0> [2009, November].
- Kreck, M., Mosandl, A. 2003. Synthesis, structure elucidation, and olfactometric analysis of lilac aldehyde and lilac alcohol stereoisomers. *J. Agric. Food Chem.* **51**, 2722–2726.
- Lawless, H.T., Heyman, H. 1999. Sensory evaluation of food: Principles and practices. Chapman and Hall, USA.
- Leffingwell, J.C. 2002. Leffingwell reports: Tobacco—aroma from carotenoids [Online]. Available: <http://www.leffingwell.com/leffrept.htm> [2010, 10 March].
- Mookherjee, B.D., Wilson, R.A. 1990. Tobacco constituents. Their importance in flavour and fragrance chemistry. *Perfumer and Flavorist* **15**, 27–49.
- Mosciano, G., Fasano, M., Michalski, J., Sadural, S. 1991a. Organoleptic characteristics of flavor materials. *Perfumer and Flavorist* **16**, 31–33.
- Mosciano, G., Fasano, M., Michalski, J., Sadural, S. 1991b. Organoleptic characteristics of flavor materials. *Perfumer and Flavorist* **16**, 79–81.
- Näf, R., Velluz, A. 2000. The volatile constituents of extracts of cooked spinach leaves (*Spinacia oleracea* L.). *Flavour Fragr. J.* **15**, 329–334.
- Ohloff, G. 1994. Scent and fragrances: The fascination of odors and their chemical perspectives. Springer-Verlag, Germany.
- Oomah, B.D., Liang, L.S.Y. 2007. Volatile compounds of dry beans (*Phaseolus vulgaris* L.). *Plant Foods Hum. Nutr.* **62**, 177–183.
- Rencher, A.C. 2002. Methods of multivariate analysis (2<sup>nd</sup> Edition), John Wiley and Sons.
- Serra, S., Fuganti, C., Brenna, E. 2006. Synthesis, olfactory evaluation and determination of the absolute configuration of the 3,4-didehydroionone stereoisomers. *Helv. Chim. Acta* **89**, 1110–1122.

- Tachihara, T., Hashimoto, H., Ishizaki, S., Komai, T., Fujita, A., Ishikawa, M., Kitahara, T. 2006. Microbial resolution of 2-methylbutyric acid and its application to several chiral flavour compounds. *Dev. Food Sci.* **43**, 97–100.
- Takahashi K., Someya, T., Muraki, S., Yoshida, T. 1980. A new keto-alcohol, (-)-mintlactone, (+)-*iso*-mintlactone and minor components in peppermint oil. *Agric. Biol. Chem.* **44**, 1535–1543.
- Yamazaki, Y., Hayashi, Y., Arita, M., Hieda, T., Mikami, Y. 1988. Microbial conversion of  $\alpha$ -ionone,  $\alpha$ -methylionone and  $\alpha$ -isomethylionone. *Appl. Environ. Microb.* **54**, 2354–2360.

## CHAPTER 8

# EXPERIMENTAL

### 8.1 GENERAL

All Pyrex glassware used for the handling of samples was thoroughly washed with distilled water and heated in an annealing oven at 400 °C to remove all traces of adsorbed organic material. DCM (Merck Residue Analysis Grade, Darmstadt, Germany) was used for extraction purposes and for the preparation of solutions of reference compounds. A sample (1 ml) of DCM was concentrated to 10 µl in a nitrogen atmosphere as described in § 8.3.3, analysed for impurities, and found to be adequately pure for the purpose of trace analysis. Microlitre syringes were cleaned by flushing with DCM and the plungers and outside of the needles were thoroughly rinsed with the same solvent.

### 8.2 SAMPLE PREPARATION METHODS

#### 8.2.1 Collection, fermentation and drying of honeybush plant material

Honeybush plant material from all of the species, except for *Cyclopia intermedia*, was harvested from plantations on different farms in the South Western Cape of South Africa. *Cyclopia genistoides* was harvested on Reins farm near Albertinia, while a different *C. genistoides* population (ex Kirstenbosch) was harvested on Koksrivier farm in the Pearly Beach area. *Cyclopia subternata* was harvested on Kanetberg in the Barrydale region, on the farm Toekomst near Bredasdorp and in the Genadendal region. *Cyclopia longifolia* was harvested on Kanetberg and on Toekomst, and a *C. intermedia-genistoides* cross-species was also obtained from the latter farm. *Cyclopia intermedia* was harvested from the wild on Nooitgedacht farm in the Kouga mountains of the Eastern Cape (see Addendum 1).

All the plants were harvested before flowering could occur, except for *C. subternata* from the Genadendal region, which was harvested with and without its flowers. The plants of *C. genistoides* and *C. intermedia* were harvested by cutting them to the ground whereas about only two thirds of the shoot lengths were removed from *C. longifolia* and *C. subternata* plants. The shoots were shredded to 2–3 mm lengths using a mechanised fodder cutter. The plant material of each species was divided into two batches. One batch was used to prepare unfermented tea by drying it immediately, in a thin layer, to a moisture content of about 10% on 30 mesh stainless steel drying racks at 40 °C for 6 h in a temperature-controlled dehydration tunnel with a cross-flow air movement of 3 m/s. Deionised water was added to the other batch to wet the leaves superficially. The wet leaves were placed in a stainless steel container covered with aluminium foil and allowed to ferment (oxidise) in a laboratory oven at 90 °C for 16 h. After fermentation the tea was dried by the same method as described for the drying of the green tea. The dried tea was sieved, using a 1.4 mm Endecotts sieve. The fractions



smaller than 1.4 mm in size were collected and stored in sealed glass jars at room temperature (22 °C) until subjected to analysis of the headspace volatiles of the dry plant material or of infusions of the plant material.

## 8.2.2 Preparation of honeybush infusions

**Standard** infusions of fermented and unfermented honeybush plant material were prepared by adding boiling filtered water (130 ml) to 20 g of the dry tea in an insulated flask, sealing it immediately and allowing the tea to brew for 15 min while swirling the contents of the flask. The leaves and twigs were then removed by filtering. For each analysis, a volume of 50 ml of tea infusion was subjected to headspace sampling.

**Concentrated** infusions were prepared for GC-O analyses using the AEDA method. Boiling filtered water (220 ml) was added to 30 g of fermented tea in a 500-ml round-bottom flask. The flask was heated at 100 °C for a few minutes until the tea began to boil lightly. The temperature was reduced to 90 °C, the flask was covered, and the tea allowed to brew for 9 h. The leaves and twigs were removed by filtering. Two 100-ml glass bottles were then filled each with 50 ml of the concentrated infusion. The headspace of one infusion sample was sampled directly while the other sample was subjected to stepwise dilution (1 + 1 by volume) with boiled filtered water before the headspace of each dilution was sampled. Similar concentrated infusions were also prepared for GC-MS-O and GC-TOF-HRMS analyses.

## 8.3 SAMPLING METHODS

### 8.3.1 Enrichment of headspace volatiles by the sample enrichment probe technique

#### 8.3.1.1 Sample enrichment probe sampling of dry honeybush plant material

Individual samples (8 g) of fermented and unfermented *C. genistoides*, *C. intermedia*, *C. subternata* and *C. longifolia* were placed in 100-ml glass bottles with adapted caps (Burger *et al.*, 2006) and the VOCs present in the headspace were collected by means of a SEP (MasChrom Analisetegniek, Stellenbosch, South Africa). This was done by exposing the sorptive phase of a SEP30 (30 mm PDMS tubing, containing 28 mg of the rubber) to the headspace of a honeybush sample at 40 °C for a period of 5 h. The analytes were thermally desorbed at 230 °C in the injector of a GC or GC-MS, and the probe was left in the injector until completion of the analysis (Burger *et al.*, 2006). Sampling of the headspace volatiles of dry honeybush plant material for analyses on chiral or polar columns was also carried out in the manner described above, but the headspace sampling periods were varied.

### **8.3.1.2 Sample enrichment probe sampling of honeybush infusions**

Infusions of fermented and unfermented honeybush were prepared as described above (§ 8.2.2), and for each analysis 50 ml of tea infusion was transferred to a 100-ml glass bottle with adapted cap, sealed and incubated at 50 °C for 30 min, after which the headspace volatiles of the infusion were enriched by means of a SEP30 at 50 °C for 5 h. Longer enrichment periods and SEP60 tubing (60 mm PDMS tubing, containing 56 mg of the rubber) were used for GC-O (17 h) and GC-TOF-HRMS analyses (17 h), with thicker SEP60 tubing (0.37 g rubber) for GC-MS-O analyses (3 weeks). Standard or concentrated infusions, in combination with varying enrichment periods, were used for analyses on chiral and polar columns in order to obtain the best results.

### **8.3.2 Increased-capacity sample enrichment probe**

An attempt was made to improve the extraction of volatiles from the headspace of plant material and infusions by using a high-capacity sample enrichment device. The device was made by coiling PDMS tubing (Dow Corning, Midland MI; USA, 1 m x 0.64 mm inner diameter (i.d.) x 1.19 mm outer diameter.) tightly around a support (4.5 cm diameter) consisting of four parallel glass rods fused together at their tips. The rubber tubing was kept in place by a cotton thread. Before use, any soluble organic material was thoroughly extracted from the PDMS rubber with DCM for 2 h in a Soxhlet extractor, after which the device was dried in a stream of pure nitrogen. A standard honeybush infusion (§ 8.2.2) was transferred to a 150-ml Erlenmeyer flask with a glass encapsulated magnetic follower, and the enrichment device was suspended in the headspace for 42 h while stirring the infusion in a water bath at 50 °C. After the 42 h enrichment period the volatiles trapped in the rubber were extracted in a Soxhlet apparatus using the smallest possible volume of DCM (approximately 10 ml). The extract was concentrated in a nitrogen atmosphere to less than 1 ml, as described in § 8.3.3.

Two alternative enrichments were carried out using dry tea instead of an infusion. For the first of these two enrichments 14 g of dry fermented tea was weighed into a 250-ml Erlenmeyer flask, and for the second enrichment 50 g of ground dry fermented tea was used. The Erlenmeyer flasks were placed in an oven at 60 °C and the headspace sampled with the enrichment device for 2 and 5 days, respectively. After enrichment, the extraction and concentration steps were carried out as described above.

### **8.3.3 Conventional sample extraction**

Dry honeybush plant material (14 g) was extracted with DCM (35 ml) in a 100-ml round-bottom flask at room temperature (22 °C) for 14 days. The DCM extract was removed with a Pasteur pipette and the plant material was rinsed with DCM (2 x 1.4 ml) and the washings combined with the previous extract. The solvent was evaporated by placing the extract in a 50-ml flask which in turn was placed in a 250-ml beaker, which was covered with aluminium foil, and the solvent vapour was

purged from the beaker with a slow stream of nitrogen without directing the nitrogen flow directly onto the extract. When the volume of the extract had decreased to 4 ml it was transferred to a 5-ml Reacti-Vial and the concentration process continued until approximately 0.2–0.5 ml of the extract remained (Reiter *et al.*, 2003). Another extraction was carried out by stirring the honeybush plant material (14 g) with DCM (35 ml) for 2 h. The extract was concentrated following the procedure described above.

## 8.4 ANALYTICAL TECHNIQUES

### 8.4.1 Gas chromatography

GC analyses were carried out with a Carlo Erba HRGC gas chromatograph equipped with an FID and a Grob split-splitless sample inlet. GC data were acquired with a DELTA Chromatography Data System, Version 5.0 (Digital Solutions, Brisbane, Australia). The capillary columns used in this study were manufactured by the Laboratory for Ecological Chemistry (LECUS, Stellenbosch University) and were provided with integrated retention gaps of 1 to 2 m. Column A [glass, 40 m × 0.25 mm i.d., coated with 0.25 µm of PS-089-OH (DB-5 equivalent)], column B [glass, 40 m × 0.25 mm i.d., coated with 0.25 µm of the polar stationary phase AT-1000 (FFAP equivalent)], enantioselective column C [glass, 30 m × 0.3 mm i.d., coated with 0.25 µm of OV-1701-OH containing 10% heptakis(2,3-di-*O*-methyl-6-*O*-tert-butyl-dimethylsilyl)-β-cyclodextrin] and enantioselective column D [glass, 30 m × 0.3 mm i.d., coated with 0.25 µm of OV-1701-OH containing 10% heptakis(2,3-di-*O*-acetyl-6-*O*-tert-butyl-dimethylsilyl)-β-cyclodextrin]. Hydrogen was used as carrier gas at a linear velocity of 50 cm/s (at column temperature 40 °C). The injector was operated at 220 °C and the FID at 280 °C. Samples were injected in the split mode at a column temperature below 30 °C. The column temperature was then ballistically increased to 40 °C, after which temperature programs of 2 °C/min from 40 °C to 280 °C and 2 °C/min from 40 °C to 250 °C were used for columns A and B, respectively. The final temperature was held for 20 min at either 250 °C or 280 °C. The enantioselective columns C and D were programmed at 1 °C/min from 40 °C to 240 °C and 200 °C, respectively.

### 8.4.2 Gas chromatography-mass spectrometry

GC-LRMS was performed on a Carlo Erba QMD 1000 GC-MS system (Milan, Italy) using the columns A and B and the GC conditions mentioned in § 8.4.1: helium as carrier gas at a linear velocity of 28.6 cm/s at 40 °C. The line-of-sight interface was kept at 250 °C, while the ion-source temperature was set at 180 °C. Mass spectra were recorded at 70 eV at a scan rate of 0.9 s/scan, with an interscan time of 0.1 s. The components were tentatively identified using an online reference library of mass spectrometric data (NBS, 1990), as well as two offline libraries (Adams, 2004; NIST, 2005).

### **8.4.3 Gas chromatography-time-of-flight-high-resolution mass spectrometry**

GC-TOF-HRMS was performed on a Waters GCT Premier benchtop orthogonal acceleration time-of-flight instrument (Waters, Massachusetts, USA), using an Agilent HP5MS (30 m x 0.25 mm i.d, coated with 0.25  $\mu\text{m}$  5% phenylmethylpolysiloxane) column (Agilent JW Scientific, Folsom, USA). Headspace volatiles were sampled either by means of SPME, using a Supelco Stableflex divinylbenzene/carboxen/polydimethylsiloxane fibre, or by means of the SEP. The SPME fibre was exposed to the headspace of dry fermented honeybush (3.8 g) for 15 min at 80  $^{\circ}\text{C}$  prior to GC-MS analysis, while the SEP was exposed to the headspace of honeybush infusions for 17 h. The injector temperature was set at 260  $^{\circ}\text{C}$  and operated in the splitless mode. Helium was used as carrier gas at a flow rate of 1 ml/min, with the ion source temperature set at 180  $^{\circ}\text{C}$ . Data was acquired in centroid mode, scanning from 35–650 amu, and using perfluorotri-*N*-butylamine as reference for accurate mass determination. Mass spectra were recorded at 70 eV at a scan rate of 0.2 s/scan, with an interscan time of 0.05 s. The temperature program used was the same as described in § 8.4.1.

### **8.4.4 Enantioselective gas chromatographic-mass spectrometric analyses with $\beta$ -cyclodextrin columns as chiral selectors**

GC-LRMS was performed on a Fisons MD800 GC-MS system (Rodano, Milan, Italy), using the two enantioselective columns C and D described in § 8.4.1. Helium was used as carrier gas at a linear velocity of 28.6 cm/s at 40  $^{\circ}\text{C}$ . The line-of-sight interface was kept at 250  $^{\circ}\text{C}$ , while the ion-source temperature was set at 180  $^{\circ}\text{C}$ . Mass spectra were recorded at 70 eV at a scan rate of 0.9 s/scan with an interscan time of 0.1 s, using a temperature program of 1  $^{\circ}\text{C}/\text{min}$  from 40  $^{\circ}\text{C}$  to 240  $^{\circ}\text{C}$  for column C, and 1  $^{\circ}\text{C}/\text{min}$  from 40  $^{\circ}\text{C}$  to 200  $^{\circ}\text{C}$  for column D.

### **8.4.5 Gas chromatographic-mass spectrometric retention index determination**

GC-MS RIs of honeybush volatile constituents, determined relative to the  $\text{C}_5$  to  $\text{C}_{18}$  *n*-alkanes, were compared with those of authentic reference compounds that were obtained commercially or were synthesised for this purpose and confirmed with RI values recorded in reference libraries of retention indices (Adams, 2004; ESO, 2006; Hochmuth, 2006). These databases were also used to identify components for which standard reference compounds were not available.

### **8.4.6 Quantitative gas chromatography and gas chromatography-mass spectrometry**

Quantitative GC analyses of dry honeybush samples were carried out on a Thermo Electron Corporation Trace 2DGC gas chromatograph (Milan, Italy) fitted with a split/splitless injector and FID. Processing of results was done using Chrom-Card software version 2.4.0 (2006). The instrument was operated in the single-dimensional mode. The sorbed volatiles were thermally desorbed from the

SEP at an injector temperature of 230 °C without cryotrapping, and were analysed on capillary column A, using a temperature program of 2 °C/min from 40 to 280 °C. Hydrogen was used as carrier gas at a constant pressure of 100 kPa. The injector was operated in the split mode with a split flow of 10 ml/min. All quantitative GC and GC-MS analyses were carried out in triplicate and the relative concentrations of the volatile constituents were computed as percentage areas of the total integrated area.

Absolute quantitation of the honeybush aroma constituents was carried out by GC-MS analysis on the instrumentation and under the conditions described in § 8.4.2. In order to calculate individual MS response factors, 17 mixtures of representative reference compounds (commercial or synthesised), each containing 7 of the compounds (neat), were prepared. Standard solutions of these mixtures were prepared for GC-MS analysis by diluting 1 µl of each of the 17 mixtures in DCM (1 ml) (Table 8.1).

Table 8.1: Composition of standard solutions of reference compounds used for quantitation of honeybush aroma compounds

<b>Std sol.</b>	<b>Compounds</b>	<b>Conc. (mg/ml)</b>	<b>Std sol.</b>	<b>Compounds</b>	<b>Conc. (mg/ml)</b>
<b>Mix 1</b>	2-Acetylfuran	0.156	<b>Mix 2</b>	Propiophenone	0.144
	6-Methyl-5-hepten-2-one	0.121		2-Undecanone	0.118
	Isophorone	0.131		( <i>E</i> )-6-Methyl-3,5-heptadien-2-one	0.128
	2,2,6-Trimethylcyclohexanone	0.128		α-Pinene	0.123
	( <i>E</i> )-3-Octen-2-one	0.121		Limonene	0.120
	Acetophenone	0.146		<i>p</i> -Cymenene	0.129
	( <i>E,E</i> )-3,5-Octadien-2-one	0.090		Geraniol	0.126
<b>Mix 3</b>	Hexanal	0.119	<b>Mix 4</b>	2-Methylbutanoic acid	0.134
	( <i>E</i> )-2-Hexenal	0.121		Nonanoic acid	0.129
	5-Methylfurfural	0.158		Benzyl acetate	0.151
	Octanal	0.117		Hexyl benzoate	0.140
	2-Formyl-1-methylpyrrole	0.145		Hexan-4-olide	0.146
	Decanal	0.119		Decan-5-olide	0.136
	<i>p</i> -Anisaldehyde	0.160		α-Humulene	0.127
<b>Mix 5</b>	( <i>Z</i> )-3-Hexen-1-ol	0.121	<b>Mix 6</b>	2-Pentylfuran	0.127
	1-Octen-3-ol	0.119		4-Vinylanisole	0.144
	Benzylalcohol	0.149		( <i>E</i> )-2-Nonenal	0.121
	2-Phenylethanol	0.146		Nerol	0.125
	Eugenol	0.152		Undecanal	0.118

Table 8.1 *contd.*

Std sol.	Compounds	Conc. (mg/ml)	Std sol.	Compounds	Conc. (mg/ml)
	4-Ketoisophorone	0.147		<i>cis</i> -3-Hexenyl-( <i>E</i> )-2-methyl-2-butenoate	0.136
	( <i>E</i> )- $\beta$ -Ionone	0.135		( <i>Z</i> )-3-Hexenyl benzoate	0.143
<b>Mix 7</b>	$\alpha$ -Cubebene	0.134	<b>Mix 8</b>	1-Pentanol	0.111
	( <i>Z</i> )-3-Hexenyl isovalerate	0.125		Nonanal	0.113
	( <i>Z</i> )-2-Penten-1-ol	0.122		<i>trans</i> Linalool oxide (furanoid)	0.129
	( <i>Z</i> )-4-Heptenal	0.121		<i>cis</i> Linool oxide (furanoid)	0.129
	$\gamma$ -Terpinene	0.121		Hexyl tiglate	0.122
	( <i>E</i> )-3-Nonen-2-one	0.121		Hexahydrofarnesylacetone	0.121
	( <i>E,Z</i> )-2,6-Nonadienal	0.125			
<b>Mix 9</b>	Decane	0.104	<b>Mix 10</b>	Methyl dodecanoate	0.121
	1-Octanol	0.118		1-Hexanol	0.113
	2-Nonanone	0.117		2,6,6-Trimethylcyclohex-2-enone	0.126
	Methyl octanoate	0.125		$\alpha$ -Ionone	0.128
	Dodecane	0.107		( <i>E</i> )- $\beta$ -Damascenone	0.111
	Methyl nonanoate	0.125		$\beta$ -Pinene	0.120
	Tetradecane	0.109		Terpinen-4-ol	0.129
<b>Mix 11</b>	<i>p</i> -Cymene	0.114	<b>Mix 12</b>	(6 <i>Z</i> )-2,6-Dimethyl-2,6-octadiene	0.111
	Linalool	0.115		Butyl benzoate	0.136
	Allocimene	0.108		( <i>Z</i> )-3-Hexenyl 2-methylbutanoate	0.119
	Benzothiazole	0.165		( <i>E</i> )-Nerolidol	0.119
	Theaspirane isomer 1	0.124		$\gamma$ -Butyrolactone	0.152
	Theaspirane isomer 2	0.114		$\beta$ -Cyclositral	0.129
	Geranyl acetate	0.121		( <i>E</i> )- $\beta$ -Damascone	0.128
<b>Mix 13</b>	Pentadecane	0.102	<b>Mix 14</b>	Geranyl formate	0.152
	Dodecanal	0.109		( <i>E,E</i> )-2,4-Decadienal	0.144
	3-Methylbutanoic acid	0.122		( <i>E</i> )-Caryophyllene	0.149
	$\alpha$ -Terpineol	0.123		Neral	0.084
	Benzaldehyde	0.138		Geranial	0.143
	Hexanoic acid	0.123		( <i>E</i> )-2-Heptenal	0.143
	Isopropyl myristate	0.112			

Table 8.1 *contd.*

Std sol.	Compounds	Conc. (mg/ml)	Std sol.	Compounds	Conc. (mg/ml)
<b>Mix 15</b>	Methyl decanoate	0.129	<b>Mix 16</b>	( <i>E,E</i> )-2,4-Heptadienal	0.115
	( <i>Z</i> )- $\beta$ -Ocimene	0.119		Terpinolene	0.112
	(+)- <i>p</i> -Menth-1-en-9-al	0.080		4-Acetyl-1-methyl- cyclohexene	0.121
	(+)- <i>p</i> -Menth-1-en-9-al	0.070		<i>p</i> -Cymen-8-ol	0.126
	6-Methyl-2-heptanone	0.126		( <i>E</i> )-2-Undecenal	0.111
	6,10-Dimethyl-2- undecanone	0.121		$\alpha$ -Copaene	0.119
	Nonan-4-olide	0.143		Isopropyl myristate	0.110
<b>Mix 17</b>	3,4-Dimethyl-2,5-furandione	0.359			
	Isoborneol	0.344			
	2,6-Dimethylnaphthalene	0.323			
	5,6-Epoxy- $\beta$ -ionone	0.352			
	Dodecanoic acid	0.394			
	$\beta$ -Eudesmol	0.168			
	Borneol	0.350			

#### 8.4.7 Gas chromatography-olfactometry

GC-O was performed on a Carlo Erba HR gas chromatograph with a split/splitless injector and an FID operated at 220 °C and 250 °C, respectively. The capillary column was connected to a glass effluent splitter with two deactivated fused silica tubing outlets of equal lengths conducting the column effluent to the FID and a sample collection device or an electroantennographic detector (EAD) according to the basic design described by Burger *et al.* (2008). The most important feature of this set-up is a heated interface, which delivers the hot effluent at about 250 °C to, for example, the EAD, without conducting appreciable heat to the EAD or any other device. For GC-O the set-up was adapted as follows: medical air was purified by passing it through a column of activated charcoal and humidified by bubbling the air at about 20 ml/min through a wash bottle containing clean deionised water at room temperature. The humidified air conduit was connected to the leg of a small funnel that was formed using a glass blower's torch in such a way as to allow the evaluator to smell the column effluent without breathing in too much of the ambient air. One of the fused silica arms of the effluent splitter, which is normally used for preparative GC or for gas chromatography-electroantennographic detector analyses, was inserted through a small hole into the leg of the funnel, mounted on the side of the GC in such a position and at such a height as to subject the assessor to as little physical strain as possible.

The sorbed volatiles were thermally desorbed from the SEP at an injector temperature of 230 °C without cryotrapping. They were analysed on column A, using the temperature program described

in § 8.4.1. Helium was used as carrier gas at a linear flow velocity of 28.6 cm/s, measured at an oven temperature of 40 °C. The injector was operated in the split mode with a split flow of 10 ml/min.

#### **8.4.7.1 Detection frequency method**

The headspace volatiles of infused (§ 8.2.2) *C. subternata(a)* were sampled by means of a SEP, thermally desorbed in the GC injector, and analysed as described in § 8.4.1. Members of a panel of 15 volunteer assessors were required to sniff the GC effluent and results were reported according to the DF method.

In order to prevent sensory “fatigue”, each assessor was required to sniff the effluent for about 35 min after which a second person took over and sniffed for the remaining 35 min of the analysis. Each person participated in the sniffing of both the first and the second 35-min session during two consecutive analyses. Assessors verbally announced when they were able to smell a compound as it eluted from the GC. Each positive response was marked on the chromatogram at the corresponding retention time. The total number of panel members able to positively detect an aroma at a specific retention time was expressed as a percentage of the total number of assessors (15). A compound was considered to be aroma active if it was positively detected by more than half (i.e. 60%) of the assessors (Áslaug and Rouseff, 2003).

#### **8.4.7.2 Dilution to threshold method: aroma extract dilution analysis**

A concentrated honeybush infusion of *C. subternata(a)* was prepared and subjected to stepwise-dilution (1:1) as described in § 8.2.2. The individual dilutions were analysed by GC-O. The trained assessor was required to sniff the effluent of each consecutive dilution and report which odorants could still be detected and which odorants were no longer detected. Sniffing of the series of dilutions proceeded until no odorant could be detected by the assessor, and the previous dilution was then recorded as the final dilution. A FD factor was then calculated for each odorant by means of the formula  $FD = R^n$ , where n is the last dilution in which the odorant was still detectable, and R is the rate at which the sample was sequentially diluted (in this case R = 2) (Delahunty *et al.*, 2006; Ferreira *et al.*, 2002; Grosch, 1993, 1994; Plutowska and Wardencki, 2008).

#### **8.4.8 Gas chromatography-mass spectrometry-olfactometry**

GC-MS-O was performed on a Hewlett-Packard 5890 Series II gas chromatograph (Hewlett-Packard, Waldbronn, Germany), connected to a 5972 Series mass spectrometer (Hewlett-Packard, Waldbronn, Germany), and equipped with an olfactometric port. The sorbed volatiles were thermally desorbed from the SEP at an injector temperature of 250 °C and then analysed on a Supelcowax-10™ column (60 m × 0.32 mm i.d., coated with 0.5 µm Carbowax 20M phase), using a temperature program of 2 °C/min from 40 to 220 °C with a solvent delay of 10 min. Helium was used as carrier gas at a linear flow rate of 3 ml/min, at 40 °C. The injector was used in the splitless mode (2 min). A four-way effluent splitter (Gerstel GmbH, Mülheim a/d Ruhr, Germany) connected to the end of the



capillary column, split the effluent in a 3:1 ratio before it was transferred to the sniff port and the mass spectrometer *via* two fused silica capillaries. The sniffing port is a glass cone with a small aperture through which the capillary can fit, mounted on the door of the gas chromatograph and held at a temperature of 280 °C. The effluent was diluted in a stream of humidified air obtained by bubbling air through water via a fused silica capillary.

Mass spectra were recorded at 70 eV at a scan rate of 2.36 scans/s, scanning from 30 to 350 amu. The structures of the compounds were assigned by comparing their mass spectra to those obtained from an on-line Wiley 275 reference library (Wiley & Sons Inc., New York).

#### **8.4.9 Nuclear magnetic resonance spectrometry**

<sup>1</sup>H and <sup>13</sup>C NMR spectra were recorded in CDCl<sub>3</sub> on Varian VnmrS 300, Unity *INOVA* 400 and UNITY *INOVA* 600 NMR instruments (Varian, Palo Alto, USA). Chemical shifts are given in parts per million ( $\delta$ ) relative to chloroform (7.26 and 77.04 ppm for <sup>1</sup>H and <sup>13</sup>C NMR, respectively).

### **8.5 REFERENCE COMPOUNDS**

#### **8.5.1 Commercial standards**

Reference compounds were purchased from Fluka Chemical Co. and Sigma-Aldrich Chemical Co. and an extensive collection of reference standard compounds, collected from previous studies in LECUS, was also available for GC-MS RI comparison purposes. Those compounds that were not commercially or locally available were synthesised from authentic starting materials, obtained from the South African distributors of the products of Sigma-Aldrich, Merck, Saarchem, NT Laboratories and BDH.

#### **8.5.2 Synthetic standards**

##### **8.5.2.1 2,6,6-Trimethylcyclohex-2-enone**

###### *8.5.2.1.a 2-Bromo-2,6,6-trimethylcyclohexanone*

Following the protocol of Tietze and Eicher (1981: 261–262) for the  $\alpha$ -bromination of an  $\alpha$ -substituted ketone, a solution of bromine (0.57 g; 3.57 mmol; 0.18 ml) in CCl<sub>4</sub> (5 ml) was added dropwise over a period of 15 min to a magnetically stirred solution of 2,2,6-trimethylcyclohexanone (0.5 g; 3.57 mmol) in CCl<sub>4</sub> (10 ml) in a round-bottom flask fitted with a cooler and dropping funnel. After addition of the bromine, ether (10 ml) was added and the reaction mixture was washed once with water (10 ml) and dried on anhydrous MgSO<sub>4</sub>. The drying agent was filtered off and the solvent removed on a rotary evaporator to yield 2-bromo-2,6,6-trimethylcyclohexanone (0.72 g; 92%) in a purity of 98% (GC-MS).

#### 8.5.2.1.b 2,6,6-Trimethylcyclohex-2-enone

2-Bromo-2,6,6-trimethylcyclohexanone (0.35 g; 1.6 mmol) was heated to 170 °C in 2,4,6-trimethylpyridine (collidine) (1.4 ml) for 70 min, after which the reaction mixture was cooled to 0 °C. Ether (2.8 ml) was added to the reaction mixture, which was left to stand for 1 h. The collidinium hydrobromide was filtered off, washed with ether (3 x 2 ml) and the combined filtrate and ether washings washed consecutively with 4 M HCl solution (2 ml), water (2 ml) and 5% NaOH solution (2 ml), and dried on anhydrous MgSO<sub>4</sub>. Since GC-MS analysis of the product mixture indicated that dehydrohalogenation was not yet complete, a further volume of collidine (0.5 ml) was added and the mixture heated for another hour. The work-up procedure described above was followed and 2,6,6-trimethylcyclohex-2-enone (0.156 g; 71%) was obtained in a purity of 96% (GC-MS).

MS (70 eV): *m/z* (%): 138 (M<sup>+</sup>, 9), 123 (1), 110 (5), 95 (5), 82 (100), 67 (6), 54 (56), 39 (36).

<sup>1</sup>H NMR (CDCl<sub>3</sub>, 300 MHz): δ = 1.096 (s, 6H, 6-CH<sub>3</sub>s), 1.75 (dd, 3H, J = 2.0 Hz, J = 3.4 Hz, 2-CH<sub>3</sub>), 1.81 (t, 2H, J = 6.1 Hz, 5-CH<sub>2</sub>), 2.28-2.36 (m, 2H, 4-CH<sub>2</sub>), 6.624 (br s, 1H, 3-CH).

<sup>13</sup>C NMR (CDCl<sub>3</sub>, 300 MHz): δ = 16.46 (q, C-2a), 23.05 (s, C-6), 24.30 (q, C-6a & C-6b), 36.65 (t, C-4), 41.21 (t, C-5), 133.74 (d, C-3), 143.50 (s, C-2), 204.74 (s, C-1).

#### 8.5.2.2 (E,E)- and (Z,E)-3,5-Octadien-2-one

Following an adapted version of the protocol described by Heydanek and McGorin (1981) a solution of (E)-2-pentenal (1.013 g; 12 mmol) in THF (5 ml) was added dropwise to a solution of sodium hydride (122 mg; 3.1 mmol; 60% NaH) and acetone (3.017 g; 52 mmol) in THF (30 ml) over a period of 2.5 h, while cooling the reaction mixture to a temperature between 10–15 °C. After completion of the addition the solution was stirred for 1 h at room temperature, quenched with 20% HCl (1 ml) and the solvent removed on a rotary evaporator. Ether (40 ml) was added to the oily yellow residue. The ether solution was then washed with water (3 x 10 ml) and dried on anhydrous Na<sub>2</sub>SO<sub>4</sub>. Evaporation of the solvent yielded a yellow oil (1.31 g; 79%) which consisted of a 99:1 mixture of (E,E)- and (Z,E)-3,5-octadien-2-one with 90% purity (GC-MS).

MS (70 eV): *m/z* (%): 124 (M<sup>+</sup>, 29), 109 (12), 96 (7), 95 (100), 81 (44), 79 (26), 77 (8), 65 (8), 53 (24), 43 (35), 41(13), 39 (15).

<sup>1</sup>H NMR (CDCl<sub>3</sub>, 400 MHz): δ = 1.03 (t, 3H, J = 7.4 Hz, 8-CH<sub>3</sub>), 2.15-2.26 (m, 2H, 7-CH<sub>2</sub>), 2.23 (s, 3H, 1-CH<sub>3</sub>), 6.03 (d, 1H, J = 15.8 Hz, 3-CH), 6.12-6.25 (m, 2H, 5- and 6-CH), 7.08 (dd, 1H, J = 9.6 Hz, J = 15.6 Hz, 4-CH).

<sup>13</sup>C (CDCl<sub>3</sub>, 400 MHz): δ = 13.06 (q, C-8), 26.37 (t, C-7), 27.30 (q, C-1), 128.07 (d, C-3), 128.97 (d, C-5), 144.41 (d, C-6), 147.33 (d, C-4), 199.14 (s, C-2).

#### 8.5.2.3 5,6-Epoxy-β-ionone

*m*-Chloroperbenzoic acid (*m*CPBA; 70%) (9.1 mmol) was slowly added in small portions, to a magnetically stirred solution of β-ionone (1.93 g; 10 mmol) in a biphasic solvent system of DCM (100 ml) and 0.05 M NaHCO<sub>3</sub> (30 ml) (Anderson and Veysoglu, 1973). After addition of the *m*CPBA the solution was stirred at room temperature for a further 2 h. The two phases were separated and the

organic phase was washed consecutively with 1 M NaOH (30 ml) and water (30 ml), and dried on anhydrous Na<sub>2</sub>SO<sub>4</sub>. GC-MS analysis of the product mixture at this stage indicated the presence of approximately 80% 5,6-epoxy-β-ionone and 20% unepoxidised β-ionone. The synthesis was repeated with half of the product mixture, using the amount of *m*CPBA necessary to epoxidise the remaining β-ionone, but no further epoxidation took place. The second half of the crude product (1 g) was chromatographed on a 25-cm column of Kieselgel 60 (230–400 mesh), and the pure (GC-MS) 5,6-epoxy-β-ionone (0.46 g, 22%) was eluted with ether:petroleum ether (25:75).

MS (70 eV): *m/z* (%) 208 (M<sup>+</sup>, <0.1), 193 (3), 165 (3), 135 (33), 124 (25), 123 (100), 43 (83), 41 (32).

<sup>1</sup>H NMR (CDCl<sub>3</sub>, 400 MHz)<sup>1</sup>: δ = 0.895 (s, 3H, 5-CH<sub>3</sub>), 1.11 (s, 6H, 1-CH<sub>3</sub>s), 1.35–1.91 (m, 6H, 2,3,4-CH<sub>2</sub>), 2.24 (s, 3H, 10-CH<sub>3</sub>), 6.25 (d, 1H, J = 15.6 Hz, 8-CH), 6.98 (d, 1H, J = 15.6 Hz, 7-CH).

<sup>13</sup>C (CDCl<sub>3</sub>, 300 MHz)<sup>1</sup>: δ = 16.86 (t, C-3), 20.81 (q, C-5a), 25.81 and 25.87 (q, C-1a and C-1b), 28.23 (q, C-10), 29.74 (t, C-4), 33.52 (s, C-1), 35.46 (t, C-2), 65.84 (s, C-5), 70.57 (s, C-6), 132.45 (d, C-8), 142.63 (d, C-7), 197.49 (s, C-9).

#### 8.5.2.4 Hexyl tiglate

A solution of tiglic acid (5 g; 0.05 mol) and 1-hexanol (1.7 g; 0.0167 mol) in benzene (30 ml) was refluxed with Amberlyst 15 ion-exchange catalyst granules (1 g), using a Dean-Stark water separator. The reaction mixture was washed with NaOH solution (1.332 g in 10 ml water) and dried on anhydrous MgSO<sub>4</sub>. The drying agent was filtered off and the solvent evaporated to yield hexyl tiglate (2.34 g; 73%) in a purity of 96% (GC-MS).

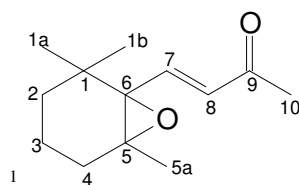
MS (70 eV): *m/z* (%) 181 (M<sup>+</sup>, 0), 111 (4), 101 (100), 100 (15), 83 (45), 69 (9), 56 (24), 55 (81), 43 (42), 41 (36), 39 (25).

<sup>1</sup>H NMR (CDCl<sub>3</sub>, 400 MHz): δ = 0.89 (t, 3H, J = 6.9 Hz, 11-CH<sub>3</sub>), 1.27–1.43 (m, 6H, 8,9,10-CH<sub>2</sub>), 1.62–1.70 (m, 2H, 7-CH<sub>2</sub>), 1.77–1.80 (m, 3H, 4-CH<sub>3</sub>), 1.82–1.85 (m, 3H, 5-CH<sub>3</sub>), 4.12 (t, 2H, J = 6.7 Hz, 6-CH<sub>2</sub>), 6.82–6.89 (qq, 1H, J = 1.4 Hz, J = 7.0 Hz, 3-CH).

<sup>13</sup>C NMR (CDCl<sub>3</sub>, 300 MHz): δ = 11.99 (q, C-5), 13.97 (q, C-11), 14.27 (q, C-4), 22.53 (t, C-10), 25.69 (t, C-8), 28.66 (t, C-9), 31.45 (t, C-7), 64.56 (t, C-6), 128.78 (s, C-2), 136.76 (d, C-3), 168.21 (s, C-1).

#### 8.5.2.5 Benzyl tiglate

Tiglic acid (2 g; 0.02 mol) was added to thionyl chloride (3.57 g, 0.03 mol) in a round-bottom flask at room temperature. The apparatus was set up as if for a distillation procedure with a pear flask as collecting vessel. The pear flask was connected to a CaCl<sub>2</sub> drying tube leading to a water bath by



means of rubber tubing. A funnel fitted at the end of the rubber tube was positioned on the surface of the water in order to follow the reaction by monitoring the formation of SO<sub>2</sub>(g) and HCl(g). The reaction mixture was stirred for 2 h at room temperature and then heated to 110 °C to distill off any excess thionyl chloride in a fume hood. The mixture was left to cool to room temperature. Benzyl alcohol (1.5 g; 0.014 mol) was then added and the mixture stirred at room temperature overnight. The mixture was then heated for an hour at 80 °C, allowed to cool, and diluted with ether (20 ml). The ether solution was washed with water (8 x 20 ml) and dried on anhydrous Na<sub>2</sub>SO<sub>4</sub>. Evaporation of the solvent yielded benzyl tiglate (1.97 g; 75%) in a purity of 84% (GC-MS).

MS (70 eV): *m/z* (%) 190 (M<sup>+</sup>, 3), 172 (23), 145 (28), 129 (5), 107 (7), 91 (100), 83 (61), 65 (20), 55 (42), 39 (17).

<sup>1</sup>H NMR (CDCl<sub>3</sub>, 400 MHz)<sup>2</sup>: δ = 1.79–1.81 (m, 3H, 4-CH<sub>3</sub>), 1.86–1.88 (m, 3H, 5-CH<sub>3</sub>), 5.19 (s, 2H, 6-CH<sub>2</sub>), 6.89–6.96 (qq, 1H, J = 1.4 Hz, J = 7.1 Hz, 3-CH), 7.28–7.39 (m, 5H, 8,9,10-CH).

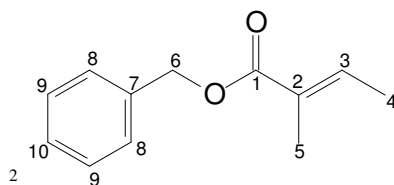
<sup>13</sup>C (CDCl<sub>3</sub>, 300 MHz)<sup>2</sup>: δ = 12.30 (q, C-5), 14.59 (q, C-4), 66.39 (t, C-6), 128.19 (d, C-8), 128.24 (d, C-10), 128.72 (d, C-9), 128.73 (s, C-2), 137.87 (d, C-3), 140.04 (s, C-7), 168.12 (s, C-1).

### 8.5.2.6 3,4-Dehydro-β-ionone

NaHCO<sub>3</sub> (3.28 g; 0.039 mol), CaO (2.62 g; 0.047 mol) and NBS (7 g; 0.039 mol) were added to β-ionone (6 g; 0.031 mol) in CCl<sub>4</sub> (40 ml) in a round-bottom flask equipped with a condenser, magnetic follower and thermometer, and the reaction mixture was heated to boiling point (Surmatis and Thommen, 1967). The external heat source was removed and the mixture was allowed to boil vigorously for at least 10 min, after which the exothermic reaction began to subside. The temperature was then reduced to 40 °C and dimethyl aniline (9 ml) was added. The succinimide that formed in the reaction was filtered off and washed with CCl<sub>4</sub>. After evaporation of the solvent and heating the mixture in a nitrogen atmosphere for 2 h pyridine (3 ml) was added and heating continued for 1 h. After the mixture had cooled it was poured into cold water (40 ml) and extracted with petroleum ether (3 x 40 ml). The combined extracts were washed consecutively with 2% H<sub>2</sub>SO<sub>4</sub> (50 ml), water (50 ml) and a 2% NaHCO<sub>3</sub> (50 ml), and then dried on Na<sub>2</sub>SO<sub>4</sub>. After evaporation of the solvent, vacuum distillation yielded 3,4-dehydro-β-ionone in a purity of 88% (GC-MS) (3.69 g; 62%); bp 90–95 °C (0.3 mmHg).

MS (70 eV): *m/z* (%) 190 (M<sup>+</sup>, 14), 175 (47), 157 (8), 147 (15), 131 (19), 115 (19), 105 (17), 91 (21), 77 (10), 43 (100).

<sup>1</sup>H NMR (CDCl<sub>3</sub>, 300 MHz): δ = 1.08 (s, 6H, 1,1-CH<sub>3</sub>), 1.91 (s, 3H, 5-CH<sub>3</sub>), 2.12 (d, 2H, J = 2.2 Hz, 2-CH<sub>2</sub>), 2.31 (s, 3H, 10-CH<sub>3</sub>), 5.89 (s, 2H, 3,4-CH), 6.21 (d, 1H, J = 16.4 Hz, 8-CH), 7.28 (d, 1H, J = 16.4 Hz, 7-CH).



$^{13}\text{C}$  ( $\text{CDCl}_3$ , 300 MHz):  $\delta$  = 20.34 (q, C-5a), 26.56 (q, C1a, C1b), 27.36 (q, C-10), 34.04 (s, C-1), 39.98 (t, C-2), 128.25 (d), 129.61 (d), 130.36 (s), 132.75 (d, C-8), 135.94 (s), 141.76 (d, C-7), 198.40 (s, C-9).

#### 8.5.2.7 Octan-5-olide

Mercury(II) acetate (9.1 g; 25.56 mmol) and 1-pentene (2g; 28.57 mmol) were added to a mixture of THF (70 ml) and water (30 ml) (Giese *et al.*, 1984). After stirring the mixture for 1 h, acrylonitrile (4.54 g; 85.71 mmol), 2 M NaOH (30 ml) and a solution of  $\text{NaBH}_4$  (2.16 g; 57.14 mmol) dissolved in 2 M NaOH (110 ml) were added, and the reaction mixture stirred for another 30 min. The product was extracted with DCM, dried on anhydrous  $\text{Na}_2\text{SO}_4$ , and the solvent evaporated to give 5-hydroxyoctanenitrile. NaOH (2 M; 28 ml) was added to the nitrile and the mixture extracted with ether (6 x 5 ml) to remove any unsaponified material. The water layer was acidified with  $\text{H}_2\text{SO}_4$  (50% solution), extracted with ether (6 x 5 ml), and the combined extracts were washed with water and dried on  $\text{MgSO}_4$ . Evaporation of the solvent yielded octan-5-olide (0.80 g; 30%) in a purity of 86% (GC-MS) as a slightly yellow liquid with a distinctly pleasant smell.

MS (70 eV):  $m/z$  (%) 142 ( $\text{M}^+$ , <0.7), 124 (3), 114 (9), 99 (100), 71 (60), 70 (39), 55 (45), 42 (69).

$^1\text{H}$  NMR ( $\text{CDCl}_3$ , 300 MHz):  $\delta$  = 0.93 (t, 3H,  $J$  = 7.2 Hz, 8- $\text{CH}_3$ ), 1.37–1.46 (m, 1H), 1.46–1.6 (m, 3H), 1.66–1.74 (m, 1H), 1.84–1.94 (m, 3H), 2.42 (ddd, 1H,  $J$  = 1.6 Hz,  $J$  = 8.7 Hz,  $J$  = 17.3 Hz, 2-CH), 2.56–2.63 (m, 1H, 2-CH), 4.24–4.34 (m, 1H, 5-CH).

$^{13}\text{C}$  ( $\text{CDCl}_3$ , 300 MHz):  $\delta$  = 13.81 (q, C-8), 18.15 (t, C-7), 18.44 (t, C-3), 27.75 (t, C-4), 29.43 (t, C-2), 37.85 (t, C-6), 80.41 (d, C-5), 172.28 (s, C-1).

#### 8.5.2.8 Hexahydrofarnesylacetone

A solution of farnesylacetone (0.53 g; 0.2 mmol) in absolute ethanol (15 ml) was hydrogenated in a conventional hydrogenation apparatus (Furniss *et al.*, 1989: 89–91) using platinum on activated charcoal (0.04 g; 10% Pt/C) as catalyst. The hydrogenation was carried out at approximately atmospheric pressure and the consumption of hydrogen was monitored. The reaction was allowed to run to completion. A total volume of 138.6 ml (6.2 mmol) hydrogen was taken up. Most of the ethanol was then evaporated using a slow stream of nitrogen. Petroleum ether (20 ml) was added to the residue consisting of the product and catalyst, and the catalyst was filtered off through a layer of magnesium sulphate. The petroleum ether was evaporated to afford hexahydrofarnesylactone (0.42 g; 79%) in a purity of 90% (GC-MS).

MS (70 eV):  $m/z$  (%) 268 ( $\text{M}^+$ , <0.5), 250 (6), 210 (3), 179 (4), 165 (5), 137 (5), 124 (9), 109 (17), 95 (17), 85 (20), 71 (39), 58 (74), 43 (100), 41 (31).

$^1\text{H}$  NMR ( $\text{CDCl}_3$ , 400 MHz)<sup>3</sup>:  $\delta$  = 0.827–0.880 (m, 12 H), 1.04–1.17 (m, 6H), 1.22–1.31 (m, 7H), 1.32–1.44 (m, 3H), 1.45–1.64 (m, 3H), 2.13 (s, 3H, 1- $\text{CH}_3$ ), 2.40 (t, 2H,  $J$  = 7.5 Hz, 3- $\text{CH}_2$ ).

$^{13}\text{C}$  ( $\text{CDCl}_3$ , 300 MHz)<sup>3</sup>:  $\delta$  = 19.51 (q, C-17), 19.67 (q, C-16), 21.44 (t, C-4), 22.62 (q, C-18/15), 22.72 (q, C18/15), 24.42 (t, C-12), 24.81 (t, C-8), 27.97 (d, C-14), 29.83 (q, C-1), 32.65 (d, C-6), 32.76 (d, C-10), 36.49 (t, C-7), 36.58 (t, C-11), 37.23 (t, C-5), 37.38 (t, C-13), 39.37 (t, C-9), 44.13 (t, C-3), 209.32 (s, C-2).

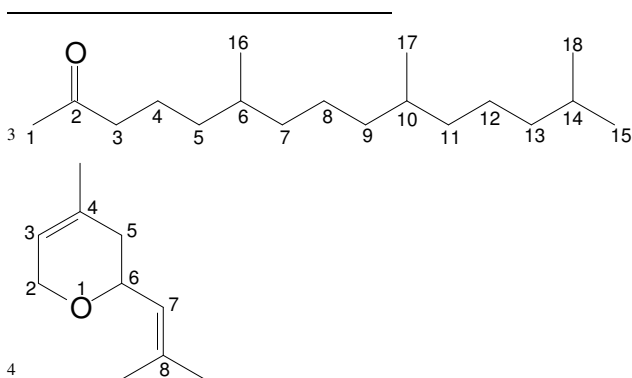
### 8.5.2.9 Nerol oxide

Nerol oxide was prepared according to the procedure of Gupta *et al.* (2007), by adding nerol (15 g; 0.0974 mol) to anhydrous methanol (50 ml) in a round-bottom flask fitted with a magnetic follower, thermometer and gas inlet. 1,3-Dibromo-5,5-dimethylhydantoin (DDH) (15 g; 0.0525 mol) was added in small portions to the nerol solution under a nitrogen atmosphere, while keeping the temperature at 5–10 °C. The mixture was then poured into cold water (25 ml) and extracted with ethyl acetate (3 x 25 ml). The combined organic layers were washed consecutively with 5%  $\text{Na}_2\text{CO}_3$  (3 x 15 ml) and water (3 x 15 ml), dried on anhydrous  $\text{Na}_2\text{SO}_4$ , and the solvent evaporated. The crude product (22.22 g) was dissolved in methanol (60 ml), containing 10.5 g of KOH, and heated under reflux for 9 h. Most of the solvent was then evaporated under reduced pressure before the reaction mixture was poured into cold water (20 ml) and extracted with  $\text{CHCl}_3$  (4 x 25 ml). The combined organic layers were washed with water (3 x 15 ml) and dried on  $\text{CaCl}_2$ . The drying agent was filtered off and the solvent removed under reduced pressure. GC-MS analysis of the crude product at this stage indicated that nerol oxide was present as the main product (50% purity, GC-MS). It was distilled to give nerol oxide (0.96 g; 23%) in a purity of 87% (GC-MS); bp 88–92 °C (20 mmHg).

MS (70 eV):  $m/z$  (%) 152 ( $\text{M}^+$ , 11), 137 (2), 109 (11), 96 (17), 85 (28), 83 (77), 68 (100), 67 (94), 55 (32), 53 (52), 41 (79), 39 (61).

$^1\text{H}$  NMR ( $\text{CDCl}_3$ , 400 MHz)<sup>4</sup>:  $\delta$  = 1.70, 1.703 (2s, 6H, 8- $\text{CH}_3$ s), 1.74 (s, 3H, 4- $\text{CH}_3$ ), 2.04 (m, 2H, 5- $\text{CH}_2$ ), 4.15–4.24 (m, 3H, 2- $\text{CH}_2$ ; 6-CH), 5.22 (tdd, 1H,  $J$  = 1.4 Hz,  $J$  = 2.8 Hz,  $J$  = 8.1 Hz, 7-CH), 5.41 (br. s, 1H, 3-CH).

$^{13}\text{C}$  ( $\text{CDCl}_3$ , 300 MHz)<sup>4</sup>:  $\delta$  = 18.34 (q), 22.94 (q), 25.7 (q), 35.95 (t, C-5), 65.52 (t, C-2), 70.68 (d, C-6), 119.66 (d, C-3), 125.68 (d, C-7), 131.82 (s, C-8), 136.01 (s, C-4).



### 8.5.2.10 (+)-*p*-Menth-1-en-9-al

Following the procedure of Slusarchyk *et al.* (1978), (+)-*p*-menth-1-en-9-ol (3 g; 19.5 mmol) in DCM (20 ml) was added to a vigorously stirred solution of pyridinium chlorochromate (PCC) (6.3 g; 0.0292 mol) in DCM (60 ml). After stirring the reaction mixture for 2 h the reaction mixture was diluted with ether (60 ml) and stirred for another hour. The reaction mixture was then filtered through Florosil (Merck Chemical Co.), the solvent evaporated under reduced pressure, and the resultant residue distilled to give two diastereomers of (+)-*p*-menth-1-en-9-al (0.38 g, 13%); bp 82–85 °C (8 mmHg) in a purity of 93% (GC-MS).

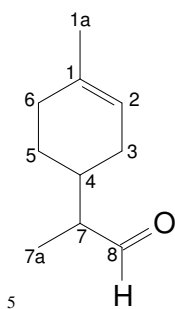
MS (70 eV):  $m/z$  (%) 152 ( $M^+$ , <1), 105 (3), 95 (16), 94 (100), 93 (10), 79 (46), 67 (14), 55 (13), 53 (12), 41 (18), 39 (17).

$^1\text{H}$  NMR ( $\text{CDCl}_3$ , 600 MHz)<sup>5</sup>:  $\delta$  = 1.07 (dd, 3H,  $J$  = 7.0 Hz,  $J$  = 7.8 Hz, 7- $\text{CH}_3$ ), 1.60–2.32 (m, 11H), 5.36 (br. s, 1H, 2-CH), 9.67 (dd, 1H,  $J$  = 2.5 Hz,  $J$  = 7.8 Hz, 8-CHO).

$^{13}\text{C}$  ( $\text{CDCl}_3$ , 600 MHz)<sup>5</sup>:  $\delta$  = 10.54 and 10.45 (q, C-7a, C-7a'), 23.60 (q, C-1a, C-1a'), 25.65 (t, C-5), 27.51 (t, C-3), 28.27 (t, C-5'), 29.87 (t, C-3'), 30.35 and 30.19 (t, C-6, C-6'), 34.55 and 34.48 (d, C-4, C-4'), 51.18 and 50.87 (d, C-7, C-7'), 120.15 and 120.08 (d, C-2, C-2'), 134.27 and 134.23 (s, C-1, C-1'), 205.72 and 205.64 (s, C-8, C-8').

### 8.5.2.11 *cis*- and *trans*-Dehydroxylinalool oxide

Linalool oxide (1.018 g; 5.99 mmol) was dissolved in hexamethylphosphoric triamide (HMPT) (30 g; 0.168 mol) (Monson and Priest, 1971) and refluxed for 1 h. The reaction mixture was allowed to cool and pentane (25 ml) was added. The solution was washed with brine (3 x 60 ml), dried on anhydrous  $\text{Na}_2\text{SO}_4$ , and the solvent removed to yield a product (0.23 g, 25%) which, according to GC-MS analysis, consisted of 42% *cis*- and *trans*-dehydroxylinalool oxide (in a ratio of 66:34) and 58% of an unknown compound. The *cis*- and *trans*-dehydroxylinalool oxide was further purified by dissolving a quarter of the crude product (0.2 ml) in an equal volume of DCM. This solution was then striped on a 20 x 20 cm silica (2 mm thickness) glass plate (Kieselgel 60 F<sub>254</sub>, Merck) and developed with ether:petroleum ether (3:1) as mobile phase. After separation, one of the bands was scraped from the plate, extracted with deuteriochloroform (5 ml) in a 25-ml flask, and filtered. The purity of the dehydroxy isomers relative to the unknown compound had improved to 75:25, according to GC-MS analysis. The identity of the compound was confirmed by comparison of published  $^1\text{H}$  NMR (Ohloff *et al.*, 1964) and MS (Adams, 2004) data with the experimental data (only  $^{13}\text{C}$  NMR data reported below).



MS (70 eV):  $m/z$  (%) 152 ( $M^+$ , 4), 137 (14), 119 (10), 110 (22), 109 (18), 105 (9), 96 (28), 91 (19), 82 (27), 81 (20), 79 (16), 68 (59), 67 (100), 55 (47), 53 (15), 43 (56), 41 (47), 39 (37).

$^{13}\text{C}$  ( $\text{CDCl}_3$ , 600 MHz)<sup>6</sup>:  $\delta$  = 18.08 (*cis*) and 18.31 (*trans*) (q, C-6), 26.84 and 26.46 (q, C-5), 30.65 and 31.0 (t, C-8), 36.97 and 37.33 (t, C-7), 81.97 and 82.16 (d, C-3), 83.24 and 82.84 (s, C-9), 110.23 and 110.39 (t, C-4), 111.46 and 111.44 (t, C-2), 143.85 and 144.50 (d, C-1), 146.09 and 145.62 (s, C-10).

## 8.6 SENSORY ANALYSIS

Eight honeybush samples (Table 8.2) were tested for a spectrum of sensory aroma attributes (Table 8.3). A trained sensory panel conducted orthonasal aroma perception experiments using the descriptive sensory analysis technique.

Table 8.2: Honeybush samples tested by a sensory panel

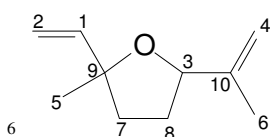
---

Product 1: <i>C. genistoides</i> (a) (Albertinia)
Product 2: <i>C. genistoides</i> (b) (Pearly Beach)
Product 3: <i>C. genistoides x intermedia</i>
Product 4: <i>C. intermedia</i>
Product 5: <i>C. longifolia</i>
Product 6: <i>C. subternata</i> (a) (Bredasdorp)
Product 7: <i>C. subternata</i> (b) – flower (Genadendal)
Product 8: <i>C. subternata</i> (c) + flower (Genadendal)

---

The panel consisted of eight judges with substantial experience in sensory analysis. The judges were trained (three sessions of 2 hours per session) in the consensus method (Lawless and Heymann, 1999), primarily to analyse the respective aromas of eight samples of honeybush tea. During the training sessions various reference standards were used to familiarise the panel with the spectrum of aromas associated with the respective honeybush tea samples: honeybush aroma (infusion of *Woolworths Organic Honeybush tea*); rooibos aroma (infusion of *Woolworths Organic Rooibos tea*), and plant-like aroma (infusion of *Five Roses Rooibos Select tea*); Earl Grey aroma (infusion of *Twinings Earl Grey tea*) and lemon aroma (infusion of *Freshpak Green Rooibos & Lemongrass*). Each reference standard was prepared in such a way so as to simulate a prominent aroma in terms of strength and aroma.

In the final test phase the panel used a 100-mm unstructured line scale to analyse the eight samples for the respective sensory attributes (Table 8.3). Each sample was replicated three times in





three sessions on two consecutive days. An infusion was made of each sample (5.8 g tea in 300 ml distilled water; infusion time 5 min) and kept at boiling point in a stainless steel thermos flask (Woolworths, 1 L). The eight samples were presented in a completely randomised order and served in two sets: Samples 5, 6, 7 and 8 in Set 1, and samples 1, 2, 3 and 4 in Set 2. This procedure was followed to ensure that the samples were all at a temperature of 75–80 °C for effective aroma analysis. Each sample (50 ml per judge) was served in pre-heated fine bone china porcelain mugs (Woolworths, South Africa) and each sample was coded with a three digit random code. All analyses were conducted in a light- and temperature-controlled room (21 °C).

Table 8.3: Descriptors for the respective sensory aroma attributes

Sensory aroma attributes	Descriptors
Honeybush aroma	0 = None; 100 = Prominent honeybush aroma
Rooibos aroma	0 = None; 100 = Prominent rooibos aroma
Plant-like aroma	0 = None; 100 = Prominent plant-like aroma
Earl Grey aroma	0 = None; 100 = Prominent Earl Grey aroma
Lemon aroma	0 = None; 100 = Prominent lemon aroma
Sweet aroma	0 = None; 100 = Prominent sweet aroma

## 8.7 STATISTICAL METHODS

### 8.7.1 Univariate analysis of data

For descriptive sensory analysis a randomised complete block design was used with eight samples and three replications. All data were subjected to test–retest ANOVA using SAS<sup>®</sup> software (Version 9; SAS<sup>®</sup> Institute Inc, Cary, USA) to test for reliability, i.e. temporal stability (Judge\*Replication interaction) and internal consistency (Judge\*Level interaction) (SAS<sup>®</sup>, 2002). The Shapiro-Wilk test was used to test for non-normality (Shapiro and Wilk, 1965). If non-normality was significant ( $P \leq 0.05$ ), and caused by skewness, the outliers were identified and removed until the data were normal or symmetrically distributed (Glass *et al.*, 1972). Using SAS<sup>®</sup> line plots indicating temporal stability and internal consistency, single odd judges were identified and removed. PanelCheck software (Version 1.3.1, Nofima, Norway) was used to substantiate the latter results, thereby testing for panel reliability. The final ANOVA was performed after the above-mentioned procedures had taken place. Student's t-LSD was calculated at the 5% significance level to compare sample means.

### 8.7.2 Multivariate statistical techniques

The above-mentioned pre-processed dataset, i.e. normalised data, was used for performing PCAs and DA using the XLSTAT software package (Version 7.5.2, Addinsoft, Paris, 2008). PCA was

performed to illustrate the relationship between the chemical compounds and/or the sensory aroma attributes, and their association with the different honeybush samples. DA was used to perceptually map the replication means of the sensory aroma attributes to ascertain to what extent the respective sensory aroma attributes can be used to point out differences or similarities between the different samples (Lawless and Heymann, 1999) during the sensory analysis.

## 8.8 REFERENCES

- Adams, R.P. 2004. Identification of essential oil components by gas chromatography/quadropole mass spectrometry. Allured Publishing Corporation, Carol Stream, Illinois, USA.
- Anderson, W.K., Veysoglu, T. 1973. A simple procedure for the epoxidation of acid-sensitive olefinic compounds with *m*-chloroperbenzoic acid in an alkaline biphasic solvent system. *J. Org. Chem.* **38**, 2267–2268.
- Áslaug, H., Rouseff, R.L. 2003. Identification of aroma active compounds in orange essence oil using gas-chromatography-olfactometry and gas-chromatography-mass spectrometry. *J. Chromatogr. A* **998**, 201–211.
- Burger, B.V., Marx, B., le Roux, M., Burger, W.J.G. 2006. Simplified analysis of organic compounds in headspace and aqueous samples by high-capacity sample enrichment probe. *J. Chromatogr. A* **1121**, 259–267.
- Burger, B.V., Petersen, W.G.B., Ewig, B.T., Neuhaus, J., Tribe, G.D., Spies, H.S.C., Burger W.J.G. 2008. Semiochemicals of the Scarabaeinae. VIII: Identification of active constituents of the abdominal sex-attracting secretion of the male dung beetle, *Kheper bonellii*, using gas chromatography with flame ionization and electroantennographic detection in parallel. *J. Chromatogr. A* **1186**, 245–253.
- Delahunty, C.M, Eyres, G., Dufour, J. 2006. Gas-chromatography-olfactometry. *J. Sep. Sci.* **29**, 2107–2125.
- ESO. 2006. The complete database of essential oils. Boelens Aroma Chemical Information Service (BACIS), Leffingwel & Associates (Publisher), Georgia.
- Ferreira, V., Pet'ka, J., Aznar, M. 2002. Aroma extract dilution analysis. Precision and optimal experimental design. *J. Agric. Food. Chem.* **50**, 1508–1514.
- Furniss, B.S., Hannaford, A.J., Smith, P.W., Thatchell, A.R. 1989. Vogel's textbook of practical and organic chemistry. Longman Scientific & Technical, United States.
- Giese, B., Haßkerl, T., Lüning, U. 1984. Synthese von  $\gamma$ - und  $\delta$ -lactonen über radikalische CC-verknüpfung. *Chem. Ber.* **117**, 859–861.
- Glass, G.V., Peckham, P.D., Sanders, J.R. 1972. Consequences of failure to meet assumptions underlying the fixed effects analyses of variance and covariance. *Rev. Educ. Res.* **42**, 237–288.

- Grosch, W. 1993. Detection of potent odorents in foods by aroma extract dilution analysis. *Trends Food Sci. Technol.* **4**, 68–73.
- Grosch, W. 1994. Determination of potent odorants in foods by aroma extract dilution analysis (AEDA) and calculation of odour activity values (OAVs). *Flavour Fragr. J.* **9**, 147–158.
- Gupta, P., Sethi, V.K., Taneja, S.C., Shah, B.A., Andotra, S.S., Koul, S., Chimni, S.S., Qazi, G.N. 2007. Odiferous cyclic ethers via co-halogenation reaction: Facile preparation of nerol oxide Florol<sup>®</sup>, Florol<sup>®</sup> methyl ether and Pityol<sup>®</sup> methyl ether. *Helv. Chim. Acta* **90**, 196–204.
- Heydanek, M.G., McGorin, R.J. 1981. Gas chromatography-mass spectroscopy investigations on the flavor chemistry of oat groats. *J. Agric. Food Chem.* **29**, 950–954.
- Hochmuth, D.H. 2006. MassFinder 3 software (incorporating W.A. König, D. Joulain, D.H. Hochmuth, GC-MS Library: Terpenoids and related constituents of essential oils). Dr. Hochmuth Scientific Consulting, Hamburg, Germany.
- Lawless, H.T., Heyman, H. 1999. Sensory evaluation of food: Principles and practices. Chapman and Hall, USA.
- Monson, R.S., Priest, D.N. 1971. Dehydration of secondary alcohols by hexamethylphosphoric triamide. *J. Org. Chem.* **36**, 3826–3828.
- NBS Database. 1990. VG Masslab. VG Instruments, Manchester, UK.
- NIST/EPA/NIH. 2005. Mass spectral library (Version 2.0d), Standard reference data: National Institute of Standards and Technology, USA.
- Ohloff, G., Schulte-Elte, K.H., Wilhalm, B. 1964. Zur darstellung von Tetrahydropyran- und Tetrahydrofuran-derivaten aus 1,7- bzw. 1,6-Allyldiolen durch dehydratation in der allylstellung. *Helv. Chim. Acta* **47**, 602–626.
- Plutowska, B., Wardencki, W. 2008. Application of gas chromatography-olfactometry (GC-O) in analysis and quality assessment of alcoholic beverages—a review. *Food Chem.* **107**, 449–463.
- Reiter, B., Burger, B.V., Dry, J. 2003. Mammalian exocrine secretions. XVIII: Chemical characterization of interdigital secretion of red hartebeest, *Alcelaphus buselaphus caama*. *J. Chem. Ecol.* **29**, 2235–2252.
- SAS<sup>®</sup>. 2002. SAS/STAT<sup>®</sup> user's guide, Version 9, 1<sup>st</sup> printing, volume 2, Cary, USA: SAS<sup>®</sup> Institute, Inc.
- Shapiro, S.S., Wilk, M.B. 1965. An analysis of variance test for normality (complete samples). *Biometrika* **52**, 591–611.
- Slusarchyk, W.A., Applegate, H.E., Cimarusti, C.M., Dolfini, J.E., Funke, P., Puar, M. 1978. Synthesis of mercury mercaptide azetidinones via 2- and 4-methylthio-substituted cephalosporins. *J. Am. Chem. Soc.* **100**, 1883–1886.
- Surmatis, J.D., Thommen, R. 1967. A total synthesis of astaxanthin dimethyl ether. *J. Org. Chem.* **32**, 180–184.
- Tietze, L.F., Eicher, T. 1981. Reaktionen und synthesen im organisch-chemischen praktikum. Georg Thieme Verlag Stuttgart, New York.

**Addendum 1: Specific information on selected species**

<b>Species</b>	<b>Details</b>
<i>C. genistoides</i> (a)	Harvested: 5/2/08 Farm/area: Reins farm (Albertinia) Fermented: 90 °C/16 h Dried: 40 °C / 6 h
<i>C. genistoides</i> (b) (ex Kirstenbosch)	Harvested: 21/01/09 Farm/area: Koksrivier (Pearly Beach) Fermented : 90 °C/16 h Dried: 40 °C / 6 h
<i>C. intermedia</i> × <i>C. genistoides</i>	Harvested: 28/10/08 Farm/area: Toekomst (Bredasdorp) Fermented: 90 °C/16 h Dried: 40 °C/6 h
<i>C. intermedia</i>	Harvested: 5/2/08 Farm/area: Nooitgedacht (Kouga mountains) Fermented: 90 °C/16 h Dried: 40 °C/6 h
<i>C. longifolia</i> (young regrowth)	Harvested: 18/10/08 Farm/area: Toekomst (Bredasdorp) Fermented: 90 °C/16 h Dried: 40 °C/6 h
<i>C. subternata</i> plain(a) (young regrowth)	Harvested: 28/16/08 Farm/area: Toekomst (Bredasdorp) Fermented: 90 °C/16 h Dried: 40 °C/6 h
<i>C. subternata</i> (a)	Harvested: 5/2/08 Farm/area: Kanetberg (Barrydale) Fermented: 90 °C/16 h Dried: 40 °C/6 h
<i>C. subternata</i> – flower(b)	Harvested: 15/1/98 Farm/area: Genadendal Fermented: 70 °C/72 h Dried: 40 °C/12 h Samples: 1–16 (combined)
<i>C. subternata</i> + flower(c)	Harvested: 22/9/97 Farm/area: Genadendal Fermented: 70 °C/72 h Dried: 40 °C/12 h Samples: 1–16 (combined)

## CHAPTER 9

# CONCLUSION

### 9.1 SUMMARY OF RESULTS

As stated in Chapter 1 the main broad goal of this study was the chemical characterisation of all the volatile organic compounds (VOCs) present in unfermented and fermented honeybush. This was indeed the most challenging and time-consuming part of the project. The identification of particularly the odour-active VOCs in fermented honeybush was important in the sense that it added value to the entire research project by enabling the combination of chemical and sensory data. The research would otherwise have been a purely analytical chemical study. The objectives that were originally formulated in order to achieve this goal were all met successfully:

- In order to sample and analyse the VOCs present in the headspace of honeybush samples in extremely low concentrations, a high-capacity sample enrichment probe (SEP) was developed in the Laboratory for Ecological Chemistry (LECUS) and applied successfully in this study. The SEP was used for the headspace sampling of both dry plant material and honeybush infusions. Better results were obtained with the SEP than with conventional solid-phase microextraction.
- The complete chemical characterisation of all the VOCs in unfermented and fermented honeybush presented a major challenge. Not only do the honeybush volatiles occur in extremely complex mixtures, but most of these compounds were also found to be terpenoids. The interpretation of the mass spectra of terpenoids is difficult because there are many terpenoids with almost indistinguishable mass spectra. Nevertheless, 255 compounds, of which 54% are terpenoids, were identified in unfermented and fermented honeybush by means of low- and high-resolution gas chromatography-mass spectrometry analysis and retention index correlation, using commercial and synthesised reference standards as well as published retention index data. The new information gained in the present study with respect to the mass spectra of terpenoids constitutes a considerable contribution to the bank of mass spectrometric data accumulated in LECUS during the past 30 years.
- The compounds identified in unfermented and fermented honeybush were quantified for one representative species, namely *C. intermedia*, and comparison of these two sets of data made it possible to gain information as to which compounds increased or decreased in concentration during the fermentation process. It was found that the volatile compound profiles in unfermented and fermented honeybush are qualitatively similar, but quantitatively different.

- Before embarking on the identification of the odour-active compounds in fermented honeybush, a detailed study was made of existing gas chromatography-olfactometry (GC-O) methods and it was decided to use the detection frequency method in combination with aroma extract dilution analysis. A total of 46 VOCs were successfully identified as odour-active, of which 15 compounds were singled out as the most intense individual contributors to honeybush aroma, based on all the relevant GC-O data.
- In the next phase of the research, the identified VOCs in seven honeybush samples (including four different species and variants thereof) were quantified and the data compared, with special emphasis on the odour-active compounds. Significant quantitative differences were found.
- Finally, the sensory aroma attributes for eight different honeybush samples (including four different species and variants thereof) were determined. By using suitable statistical analytical methods, these attributes were combined with the quantitative data obtained for the odour-active compounds and a few interesting correlations were found.

## 9.2 RECOMMENDATIONS

As the flavour of a herbal tea is only as good as the inherent flavour potential of the plant, researchers involved in the comprehensive honeybush research programme conducted at ARC Infruitec-Nietvoorbij, are now utilising plant selection, propagation and the application of certain horticultural practices as methods of improving product quality. Large numbers of samples generated during the course of the plant selection programme have to be evaluated in terms of several criteria, such as growth and production parameters, composition, bioactivity and sensory characteristics, as determined by the eventual use of the plant material. With regard to sensory characteristics, it is envisaged that the present study could supply the necessary analytical and chemical information to serve as a basis for the development of a rapid analytical device and protocol suitable for the large scale screening of honeybush tea for quality control purposes and for the selection of those species that show potential as far as optimum flavour development is concerned. Such a screening method would be preferred above sensory analysis, which is not a viable option due to its inherent drawbacks such as the lack of trained panellists and panel continuity, panellist sensory “fatigue” during testing sessions, limited number of samples tested per session and the time-consuming nature of panellist training and sensory testing sessions.

Another aspect that would be worth investigating is the formation of especially the odour-active VOCs from precursor molecules, and to follow their development during the processing of honeybush plant material. Some glycosidic aroma precursors and enzymes involved in the formation of VOCs have been identified and studied in Oolong and black tea. Comparison of green and fermented *C. intermedia* in the present study showed that most of the VOCs are already present in the green honeybush, and that changes in the relative concentrations of the VOCs are most likely responsible

for the development of the pleasant sweet and honey-like aroma rather than the formation of new compounds during fermentation.